(19) DANMARK

(10) DK/EP 3364997 T5

(12) Rettet oversættelse af europæisk patentskrift

Patent- og Varemærkestyrelsen

(51) Int.Cl.: *A 61 K 38/50 (2006.01)* *A 61 K 48/00 (2006.01)* *A 61 P 25/28 (2006.01)*
C 12 N 7/00 (2006.01) *C 12 N 15/00 (2006.01)* *C 12 N 15/86 (2006.01)*
G 01 N 33/50 (2006.01)

(45) Oversættelsen bekendtgjort den: **2024-09-30**

(80) Dato for Den Europæiske Patentmyndigheds bekendtgørelse om meddelelse af patentet: **2024-01-17**

(86) Europæisk ansøgning nr.: **16858331.8**

(86) Europæisk indleveringsdag: **2016-10-21**

(87) Den europæiske ansøgnings publiceringsdag: **2018-08-29**

(86) International ansøgning nr.: **US2016058197**

(87) Internationalt publikationsnr.: **WO2017070525**

(30) Prioritet: **2015-10-22 US 201562245213 P**
2016-04-13 US 201662322101 P
2016-04-15 US 201662323558 P

(84) Designerede stater: **AL AT BE BG CH CY CZ DE DK EE ES FI FR GB GR HR HU IE IS IT LI LT LU LV MC MK MT NL NO PL PT RO RS SE SI SK SM TR**

(73) Patenthaver: **University of Massachusetts, One Beacon Street, 31st Floor, Boston, MA 02108, USA**

(72) Opfinder: **Gao, Guangping, 4 Edward Dunn Way, Westborough, MA 01581, USA**
GESSLER, Dominic, 11 Winco Road, Worcester, MA 01605, USA

(74) Fuldmægtig i Danmark: **RWS Group, Europa House, Chiltern Park, Chiltern Hill, Chalfont St Peter, Bucks SL9 9FG, Storbritannien**

(54) Benævnelse: **ASPARTOACYLASE GENTERAPI TIL BEHANDLING AF CANAVANS SYGDOM**

(56) Fremdragne publikationer:
EP-A1- 2 261 242
WO-A2-2015/127128
US-A1- 2010 183 570
US-A1- 2013 023 488
US-A1- 2013 323 229
US-A1- 2014 142 152
US-A1- 2014 335 054
US-B1- 6 620 800

DESCRIPTION

Description

BACKGROUND

[0001] Disorders of the central nervous system (CNS) are a huge financial burden for society with increasing incidence and prevalence in populations across the world. Neurodegenerative disorders are a subgroup of CNS disorders that are caused by a variety of genetic and nongenetic factors with variable disease onset, e.g., Canavan Disease, Alzheimer Disease, multiple sclerosis (MS). A subgroup of neurodegenerative disorders are leukodystrophies, which are diseases which target the white matter of the CNS. The white matter of the CNS is comprised of oligodendrocytes that form myelin, wrapping around neuronal axons. One function of oligodendrocytes is to facilitate axon potential propagation.

[0002] WO 2015/127128 describes recombinant adeno-associated viruses (rAAVs) having distinct tissue targeting capabilities, including AAV capsid proteins and the use of the rAAVs for gene transfer methods. US 2014/335054 relates to rAAVs useful for targeting transgenes to the CNS, e.g. for treating CNS-related disorders. US 2014/142152 describes methods and compositions for treating cancer, including cancers in which aspartocylase (ASPA) and/or N-acetylaspartate (NAA) expression or activity is decreased. US 2013/0023488 provides compounds for reducing lipid accumulation in a cell which are useful for the treatment of lipid/glycogen disorders. EP 2261242 relates to the identification of the NAA-forming aspartate-N-acetyltransferase enzyme and its use in diagnostic and drug screening e.g. in neurological disorders.

SUMMARY

[0003] The invention is set out in the appended claims.

[0004] The disclosure relates, in some aspects, to compositions and methods useful for the diagnosis and treatment of neurodegenerative diseases. In some aspects, the disclosure relates to the discovery that disturbance of N-acetylaspartate (NAA) metabolism or aspartoacylase (ASPA) deficiency shifts energy metabolism in the CNS away from glycolysis and toward beta oxidation (*e.g.*, fatty acid metabolism) in subjects having white matter diseases (*e.g.*, Canavan's disease), or other neurodegenerative disorders such as Alzheimer's disease and traumatic brain injury. Without wishing to be bound by any particular theory, methods and compositions described herein identify and/or correct metabolic imbalances in

the CNS of a subject having a neurodegenerative disease.

[0005] Aspects of the disclosure relate to methods for treating leukodystrophy in a subject in need thereof. Methods may comprise administering to the subject an N-acetylaspartate (NAA)-depleting agent. It may have been determined that the leukodystrophy is associated with a metabolic imbalance comprising a shift from glycolysis to beta-oxidation in the subject. Methods may further comprise detecting the metabolic imbalance by evaluating levels of one or more glycolysis and/or beta-oxidation factors (e.g., by evaluating levels of an informative molecule or set of molecules of a metabolic pathway, for example, any one or more of those listed in FIG. 57). Levels of one or more glycolysis and/or beta-oxidation factors may be determined using CNS fluid obtained from the subject.

[0006] Treating a leukodystrophy may comprise obtaining CNS fluid from a subject; detecting increased beta-oxidation in the CNS fluid; and based on the detected increase in beta-oxidation, administering to the subject an N-acetylaspartate (NAA)-depleting agent. The NAA-depleting agent may be ASPA.

[0007] Treating a leukodystrophy may comprise measuring a metabolic profile of a biological sample obtained from a subject; identifying a metabolic imbalance associated with the leukodystrophy based upon the metabolic profile; and, administering to the subject an N-acetylaspartate (NAA)-depleting agent. The metabolic imbalance may comprise a shift from glycolysis to beta-oxidation.

[0008] A leukodystrophy may be associated with a condition selected from the group consisting of Canavan disease, adrenomyeloneuropathy, Alexander disease, cerebrotendineous xanthomatosis, Krabbe disease, metachromic leukodystrophy, adrenoleukodystrophy, Pelizaeur disease, and Refum disease. In some embodiments, a leukodystrophy is associated with Canavan disease.

[0009] Measuring the metabolic profile may comprise assaying the biological sample using liquid chromatography (LC), mass spectrometry (MS), or liquid chromatography/mass spectrometry (LC/MS). Measuring the metabolic profile may comprise assaying the biological sample using Ultrahigh Performance Liquid Chromatography-Tandem Mass Spectroscopy (UPLC-MS/MS).

[0010] The biological sample may comprise CNS tissue or cerebrospinal fluid (CSF). The CNS tissue may be brain tissue.

[0011] A metabolic profile may comprise a level of a first biomarker selected from the group consisting of glucose, glucose-6-phosphate, 3-phosphoglycerate, pyruvate, lactate, and phosphoenolpyruvate. A metabolic profile may comprise a level of a second biomarker selected from the group consisting of carnitine, malonylcarnitine, myristoylcarnitine, palmitoylcarnitine, malonylcarnitine, and beta-hydroxybutyrate. A metabolic profile may further comprise a level of one or more additional biomarkers indicating a reduction in glycolysis of the

subject. The metabolic profile may further comprise a level of one or more additional biomarkers indicating an increase in beta-oxidation of the subject.

[0012] A NAA-depleting agent may be selected from the group consisting of a small molecule, a protein, and a nucleic acid. In some embodiments, a NAA-depleting agent is administered using an recombinant adeno-associated virus (rAAV). In some embodiments, the rAAV comprises: a capsid protein; and, a nucleic acid comprising a promoter operably linked to a transgene, e.g., a transgene that encodes aspartoacylase (ASPA). In some embodiments, the promoter is an astrocyte-specific promoter. In some embodiments, the astrocyte-specific promoter is glial fibrillary acidic protein (GFAP) promoter.

[0013] In some embodiments, a capsid protein has a serotype AAV9.

[0014] In some embodiments, the rAAV is administered via injection. In some embodiments, the injection is selected from the group consisting of intravenous injection, intravascular injection and intraventricular injection. In some embodiments, the administration results in expression of the gene in peripheral tissue. In some embodiments, the administration results in expression of the gene in CNS tissue. In some embodiments, administration results in astrocyte-restricted expression of the gene.

[0015] Methods provided herein may further comprise administering a small molecule metabolic modulator to the subject. Methods provided herein may further comprise prescribing to the subject a dietary intervention, wherein the dietary intervention promotes glycolysis and/or reduces beta-oxidation in the subject. Methods provided herein may further comprise administering an immune-suppressing agent to the subject. The immune-suppressing agent may comprise prednisone or a corticosteroid. The immune-suppressing agent may be administered to the subject prior to the administration of the rAAV.

[0016] Aspects of the disclosure relate to methods for treating a neurodegenerative disease. Methods may comprise: measuring a metabolic profile of a biological sample obtained from a subject; identifying a metabolic imbalance associated with the neurodegenerative disease based upon the metabolic profile; and, administering to the subject an N-acetylaspartate (NAA)-increasing agent. The metabolic imbalance may comprise a decrease in N-acetylaspartate (NAA) level. Methods may involve evaluating levels of an informative molecule or set of molecules of a metabolic pathway to establish a metabolic profile. Neurodegenerative diseases may be selected from the group consisting of Alzheimer's disease, traumatic brain injury (TBI), bipolar disorder, catalepsy, epilepsy (e.g., seizures), migraine, Huntington's disease, attention deficit disorder (ADD), attention deficit/hyperactivity disorder (e.g., ADHD), autism spectrum disorder (*e.g.*, Asperger's disease, autism, *etc.*), Parkinson's disease, Tourette's syndrome, clinical depression, multiple sclerosis, and autoimmune disease (*e.g.*, CNS demyelinating disease, Myastenia gravis, *etc.*). Measuring the metabolic profile may comprise assaying the biological sample using liquid chromatography (LC), mass spectrometry (MS), or liquid chromatography/mass spectrometry (LC/MS). Measuring the metabolic profile may comprise assaying the biological sample using Ultrahigh Performance Liquid

Chromatography-Tandem Mass Spectroscopy (UPLC-MS/MS). The biological sample may comprise CNS tissue or cerebrospinal fluid (CSF). The CNS tissue may be brain tissue.

[0017] The metabolic imbalance may not be caused by an ASPA-deficiency. The metabolic profile may comprise a level of one or more biomarkers indicating a change in glycolysis of the subject. The metabolic profile may comprise a level of one or more biomarkers indicating a change in beta-oxidation of the subject.

[0018] In some methods described herein, an N-acetylaspartate (NAA)-increasing agent may be selected from the group consisting of a small molecule, a protein, and a nucleic acid. The N-acetylaspartate(NAA)-increasing agent may be administered using an recombinant adeno-associated virus (rAAV). The rAAV may comprise: (a) a capsid protein; and, (b) a nucleic acid comprising a promoter operably linked to a transgene, *e.g.*, a transgene that encodes N-acetylaspartate synthetase (NAT8L). The capsid protein may have a serotype selected from the group consisting of AAV1, AAV2, AAV3, AAV4, AAV5, AAV6, AAV6.2, AAV7, AAV8, AAV9 and AAV.rh10. The rAAV may be administered via injection. The injection may be selected from the group consisting of intravenous injection, intravascular injection and intraventricular injection. Administration may result in the ubiquitous expression of the transgene. Administration may result in expression of the gene in peripheral tissue. Administration may result in expression of the gene in CNS tissue. Methods may further comprises administering a small molecule metabolic modulator to the subject.

[0019] Further aspects of the disclosure relate to methods of increasing ATP production in a subject. The methods may involve administering to a subject a recombinant adeno-associated virus (rAAV) comprising a transgene encoding ASPA enzyme, or NAT8L enzyme. In some aspects, the subject does not have an ASPA deficiency or a neurodegenerative disease.

BRIEF DESCRIPTION OF DRAWINGS

[0020]

FIG. 1 shows data illustrating that rAAV-ASPA gene therapy restores the thalamocortical tract, as measured by diffusion tensor imaging (DTI) for brain water flow.

FIG. 2 shows data illustrating that Canavan disease (CD) causes increased oxygen consumption for functional neuro-connectivity, as measured by resting state functional MRI (RS-fMRI).

FIG. 3 shows data illustrating that Canavan disease (CD) causes increased oxygen consumption for cortical-subcortical connectivity.

FIGs. 4A-4B show statistical analysis of whole brain metabolome in wild-type (WT) and ASPA knockout (KO) mice. Treated mice were administered rAAV-ASPA via intravenous injection at P1. Neuormetabolome data was analyzed at P25; N=8. FIG. 4A shows a Principle Component

Analysis (PCA) of WT (untreated/treated) and KO (untreated/treated) mice. FIG. 4B shows Hierarchical Clustering Analysis of WT (untreated/treated) and KO (untreated/treated) mice. Both FIG. 4A and 4B show clustering of WT and KO(treated) mice, indicating that rAAV-ASPA treatment rescues metabolic phenotype in CD mice.

FIG. 5 shows representative data relating to levels of glucose metabolism biomarkers in WT (untreated and treated) and KO (untreated and treated) mice. Treated mice were administered rAAV-ASPA.

FIG. 6 shows representative data relating to levels of beta-oxidation biomarkers in WT (untreated and treated) and KO (untreated and treated) mice. Treated mice were administered rAAV-ASPA.

FIG. 7 shows representative data illustrating down-regulation of O_2 radical scavengers (e.g., anserine) and their precursor molecules (e.g., cysteine) in CD mice (KO). Treatment with rAAV-ASPA restores anserine and cysteine levels in KO mice.

FIG. 8 shows data illustrating that CNS-restricted (intraventricular, ICV) and systemic (intravenous, IV) administration of rAAV-ASPA result in comparable therapeutic outcomes in P1 treated CD mice. Mice were assessed at P26.

FIG. 9 shows data illustrating that administration of rAAV-ASPA restores mobility of Nur7 (a model of mild CD) mice. Mice were administered rAAV-ASPA at various time points (e.g., 1 month of age, 2.5 months of age, 6.5 months of age). Psychomotor function was assessed by rotarod and balance beam tests.

FIG. 10 shows data illustrating that cognitive function (e.g., working/spatial memory) is restored in Nur7 mice intravenously administered rAAV-ASPA at P1 and at 3 months.

FIG. 11 shows data illustrating the rapid and efficient elimination of spongy degeneration of the CNS in Nur7 mice receiving intravenous administration of rAAV-ASPA at P1. Neuropathology was assessed at P25.

FIG. 12 shows data illustrating that administration of rAAV-ASPA rapidly reduces NAA in the brain of Nur7 mouse. Nur7 mice were treated with rAAV-ASPA at 6 weeks of age and monitored at 7 weeks and 10 weeks of age by neuroimaging.

FIG. 13 shows data illustrating that rAAV-ASPA treatment restores the myelin-lipid profile in CD mice. Compared to WT mice, KO mice have significantly reduced levels of sphingolipids and other myelin components. CD mice treated with rAAV-ASPA show a significant increase in myelin components, such as sphinganine.

FIG. 14 shows weight loss/gain patterns in wild-type (WT) and CD model (Nur7) mice. Nur7 mice treated with i.v. administered 3rd generation rAAV-hASPA (FKzhAspA-Opt) at P1 show growth similar to WT mice. Male and female mice show the same pattern of weight loss/gain.

FIG. 15 shows improvement in overall health of Nur7 mice treated with rAAV-hASPA. Nur7

mice were treated with rAAV-hASPA at p1, p42, p84, or p168 and weighed. Treated mice were compared to a wild-type (WT) mouse control. All treatment groups show normalization/improvement in weight.

FIG. 16 shows data related to the expanded therapeutic window for treatment of CD using rAAV-hASPA. Nur7 mice treated with rAAV-hASPA at p1, p42, p84 and p168, and motor function was assessed by rotarod. Mice treated at 6 weeks of age recovered completely within 4 weeks post-injection.

FIG. 17 shows data related to the expanded therapeutic window for treatment of CD using rAAV-hASPA. Nur7 mice treated with rAAV-hASPA at p1, p42, and p84, and motor function was assessed by balance beam.

FIG. 18 shows data related to assessment of cognitive function of Nur7 mice treated with rAAV-hASPA. At p70, Nur7 mice treated with rAAV-hASPA outperformed wild-type (WT) mice with respect to total distance travelled and total distance travelled in the periphery.

FIG. 19 shows normalization of T2 signal and NAA levels in the brains of Nur7 mice treated with rAAV-hASPA, as shown by magnetic resonance imaging (MRI), magnetic resonance spectroscopy (MRS) and measurement of NAA aciduria.

FIG. 20 shows normalization of brain morphology at p25 in Nur7 mice treated with rAAV-hASPA at p1.

FIG. 21 shows complete normalization of T2 signal intensities and MRS in one-year old Nur7 mice that were treated with rAAV-hASPA at p42.

FIG. 22 shows improvement in overall health, as measured by weight gain, in CD KO mice treated with astrocyte-restricted rAAV-hASPA. The astrocyte-specific expression of ASPA was produced by using a glial fibrillary acidic protein (GFAP) promoter to drive hASPA expression. The lifespan of CD KO mice treated with astrocyte-restricted rAAV-hASPA extended beyond the 28 day lifespan of untreated KO mice and was not significantly different from the lifespan of wild-type (WT) mice.

FIG. 23 shows astrocyte-restricted expression of hASPA results in normalization of motor function in CD KO mice. CD KO mice were administered astrocyte-restricted rAAVhASPA and motor function was measured at p27 and p90. Data show that astrocyte-restricted expression of hASPA resulted in restoration of motor function in treated CD KO mice compared to wild-type (WT) mice. At p90, treated CD KO mice outperformed WT mice in a rotarod test.

FIG. 24 shows astrocyte-restricted expression of hASPA results in normalization of motor function in CD KO mice. CD KO mice were administered astrocyte-restricted rAAVhASPA and motor function was measured by a balance beam test at p27 and p90. Data show that astrocyte-restricted expression of hASPA resulted in restoration of motor function in treated CD KO mice compared to wild-type (WT) mice.

FIG. 25 shows astrocyte-restricted expression of hASPA normalizes NAA levels, as measured

by MRS.

FIGs. 26A-26C show optimized gene expression cassette rescues normal ASPA and NAA protein levels in CD KO mice. FIG. 26A shows three expression cassettes were cloned carrying either half (HKz) or full Kozak (FKz) sequence and the wild-type (WT) human aspartoacylase (hASPA) cDNA or a codon-optimized (Opt) hASPA; 3rd generation construct comprises full FKz and Opt hASPA. FIG. 26B shows mice were treated at p1 via facial vein with 4×10^{11} genome copies (GC) of rAAV9 carrying either 1st, 2nd, or 3rd generation expression cassette. WB of the brains 42 days post-treatment shows relative ASPA expression normalized to actin and WT; due to early lethality, untreated CD KO mice were used at p25 as control (n=3 each). FIG. 26C shows cerebral NAA levels of treated CD KO mice were quantified using magnet resonance spectroscopy (MRS) in living mice at p42; untreated CD KO mice were used at p25 as control. Displayed are total NAA (tNAA) over total creatine (tCr). Error bars indicate mean ± SD; n=3; * $p<0.05$, ** $p<0.01$, *** $p<0.001$, **** $p<0.0001$.

FIG. 27 shows weights of full-dose treatment groups comparing 1st, 2nd, and 3rd generation gene replacement therapy. Mice were treated at p1 with 4×10^{11} GC of the three different generation vectors. Weights were taken every other day for the first 32 days and biweekly afterwards (n=10 each). Error bars indicate mean ± SD; * $p < 0.05$; ** $p < 0.01$; ns = non-significant.

FIG. 28 shows magnetic resonance imaging (MRI) T2 sequence at p28/42. Mice treated at p1 with either 1st, 2nd, or 3rd generation gene therapy were imaged by MRI (n=3 per group). Shown is the T2 sequence, which emphasizes signals derived from water. Treated and wild-type (WT) mice were imaged at p42. Due to early lethality, untreated (knock-out; KO) mice were imaged at p28. KO mice display strong hyperintensity (white signals) in striatum, cortex, thalamus, midbrain, and cerebellum/pons. A gradual reduction of hyerintense signals can be seen in the different treatment groups. 3rd generation treated mice show the same signal pattern as WT mice, indicating reversal of MRI T2 pathologic signals.

FIG. 29 shows treatment of CD KO mice with 3rd generation gene therapy leads to rescue of neuropathology at p25. Mice (n=3 per group) were treated at P1 with 4×10^{11} GC via facial vein and sacrificed at p25 for neuropathology. Untreated (KO) mice show extensive vacuolization across the brain. 1st generation treated mice show less vacuole formation, but still display substantial defects. 3rd generation treated mice are indistinguishable from wild-type (WT). Cx = cortex; St = striatum; DG = dentate gyrus; CA3 = cornu ammonis 3; Th = thalamus; Po = pons; Ce = cerebellum. Images are x10, insets are x40.

FIGs. 30A-30C show optimized gene replacement therapy normalizes motor function in CD KO mice. Each assay was performed with an independent group of CD KO mice. Mice were treated at p1 with 4×10^{11} GC into the facial vein using the 2nd or 3rd generation gene therapy (total n=24 per vector group). Shown are testing time points at p27 and p365. FIG. 30A shows accelerated rotarod data. FIG. 30B shows balance beam tests for deficits in equilibrium sense

and for ataxia. Cut-off time point was 300 seconds. FIG. 30C shows muscle/grip strength was tested on inverted screen for up to 300 seconds. Error bars indicate mean ± SD; for all motor assays, n=6-8 atP27 and n=8 at p375. *** p<0.001; **** p<0.0001.

FIG. 31 shows treatment of CD KO mice with 2nd or 3rd generation gene therapy rescues motor function at p27, p90, p180, and p365. Mice treated at p1 with 4×10^{11} GC by facial vein delivery of 2nd or 3rd generation gene therapy were tested on rotarod, balance beam, and inverted screen over the course of 1 year. All four testing time points are shown, demonstrating rescue of the motor function phenotype. Error bars indicate mean ± SD; n=6-8; * p<0.05; ** p<0.01; *** p<0.001; **** p<0.0001; ns = non-significant.

FIG. 32 shows data for the T maze at 1 year. P1 treated CD KO mice and WT mice were tested on T maze for spatial/working memory and compared to untreated WT mice. Each mouse was tested 11 times with 20 seconds retention time between each run. Error bars indicate mean ± SD; n=6-8; ns=not significant.

FIGs. 33A-33D show optimized gene replacement therapy leads to sustained rescue of neuropathology and biomarker expression. Mice were treated at p1 intravenously with 4×10^{11} GC of 1st, 2nd, or 3rd generation vector. Data from 1 year after treatment are shown in comparison to wild-type (WT). FIG. 33A shows MRI imaging comparing WT and all three vector generations. FIG. 33B shows H&E staining shows degree of neuropathologic changes. FIG. 33C shows Magnetic resonance spectroscopy (MRS) analysis of brain total NAA levels normalized against total creatine at 1 year of age. FIG. 33D shows NAA levels of urine normalized against creatinine at 1 year of age as quantified by mass spectrometry. Error bars indicate mean ± SD; n=3; **** p<0.0001; ns = non-significant.

FIG. 34 shows treatment of CD KO mice with 3rd generation gene therapy leads to sustained rescue of neuropathology at 1 year of age. Mice were treated with 4×10^{11} GC of 1st, 2nd, or 3rd generation gene therapy. Mice were sacrificed at 1 year of age and subjected to H&E staining. Shown are 10X images with 40X insets. Cx = cortex, St = striatum, DG = dentate gyrus, CA3 = cornu ammonis 3, Th = thalamus, Po = pons, Ce = cerebellum, CSC = cervical spinal cord, TSC = thoracic spinal cord, LSC = lumbar spinal cord.

FIG. 35 shows rotarod comparing wild-type versus treated wild-type mice. Mice were treated at p1 intravenously with 4×10^{11} GC of 3rd generation gene therapy. Shown are testing time-points p27, p90, p180, and p365. Error bars indicate mean ± SD; n=8 ; * p<0.05; ** p<0.01; *** p<0.001; **** p<0.0001; ns = non-significant

FIGs. 36A-36I show astrocyte-restricted hASPA expression rescues motor function, neuropathology, and biomarker expression in CD KO mice. Mice were treated intravenously at p1 with 4×10^{11} GC of 3rd generation gene therapy containing either a ubiquitous or a partial human glial fibrillary acid protein (phGFAP) promoter. FIGs. 36A-36B show brain sections with astrocyte-restricted EGFP expression that co-localizes with GFAP (red in H) positive cells but not with Myelin basic protein (MBP) positive cells (n=3). FIG. 36C shows weights of wild-type

mice vs. mice treated with ubiquitous or astrocyte-restricted hASPA expression (n=8-10). FIG. 36D shows motor function (accelerated rotarod, balance beam, and inverted screen) and cognitive (T maze; FIG. 36E) tests of mice with astrocyte-restricted hASPA expression (n=6-8). FIG. 36F shows MRI shows T2 signal pattern of ubiquitous vs. astrocyte-restricted hASPA expression in comparison to wild-type and untreated mice (n=3). FIGs. 36G-36H show MRS and WB of brain NAA levels and ASPA expression (n=3). FIG. 36I shows luxol fast blue staining of myelin shows a reduction of myelin fibers (light arrows) and the presence of vacuoles (black arrows) in the cerebellar white matter of CD KO mice vs. mice treated with ubiquitous or astrocyte-restricted hASPA expression (n=3). ML = molecular layer, PK = Purkinje cell layer, GR = granular layer, WM = white matter. Error bars indicate mean ± SD; * $p<0.05$, ** $p<0.01$, *** $p<0.001$, **** $p<0.0001$.

FIG. 37 shows rAAV dose-dependent weights. Shown are weights by day (inset) and week of CD KO mice treated at p1 with either full, 3- or 10-fold lower dose of the 3rd generation gene therapy construct. For comparison, CD KO mice were treated with the 1st generation gene therapy at 3-fold lower dose. Mice treated with 10-fold lower dose are only shown for the first four weeks. For weights by week of CD KO mice treated with full dose 3rd generation, see Fig. S1. Error bars indicate mean ± SD; n=8-10, except for 0.3X 1st gen after 24 weeks because animals started to die; **** $p<0.0001$.

FIGs. 38A-38D show dose reduction of 3rd generation therapy achieves efficacious disease rescue in CD KO mice. CD KO mice were treated at p1 via facial vein with either 4×10^{10}, 1.33×10^{11}, or 4×10^{11} GC of 3rd generation gene replacement therapy. FIG. 38A shows MRI T2 sequences of different brain regions are shown with wild-type (WT) and untreated (KO) control mice. All mice were imaged at p25 (n=3). FIG. 38B shows total NAA levels of the same mice as in FIG. 38A were quantified by MRS at p25 and normalized against total creatine (n=3). FIG. 38C shows dose-dependent H&E neuropathology of mice at p25 treated with 3rd generation or full dose 1st generation vectors. WT and KO were used as controls (n=3). FIG. 38D shows dose-dependent motor function was assessed on rotarod, balance beam, and inverted screen at p27 and p90 (n=6-8). Error bars indicate mean ± SD; * $p<0.05$; ** $p< 0.01$; *** $p<0.001$; **** $p<0.0001$.

FIG. 39 shows dose-dependent neuropathology. CD KO pups were treated intravenously at p1 with either 4×10^{11}, 1.33×10^{11}, or 4×10^{10} GC of 3rd generation gene therapy. Mice were sacrificed at p25 and subjected to H&E staining and microscopy. Shown are 10X magnification of 7 different brain regions. Wild-type (WT) and untreated (KO) mice were used as controls. See FIG. 29 for legend.

FIG. 40 shows rAAV vector genome copy numbers vary among brain regions of treated CD KO mice. 11 different regions of the CNS were analyzed for rAAV9 vector genome copy number per cell. Displayed is a schematic drawing of a sagittal section of mouse brain with 11 brain regions, including spinal cord, labeled and highlighted. Vector genome copy number is shown per diploid cell (rAAV genome/cell) for WT control, and 1-year-old CD KO mice treated with full

dose 1st generation, and full and 3-fold lower dose 3rd generation gene therapy. On the left side, a ranking of the rAAV genome/cell of the 3rd generation treated are shown. CBL = cerebellum, LMN = lamina tecti, MB = midbrain, OB = olfactory bulb, LSC = lumbar spinal cord, TSC = thoracic spinal cord, BS = brain stem, CSC = cervical spinal cord, TH = thalamus and hypothalamus, HPC = hippocampus, Cx = cortex. Error bars indicate mean ± SD; n=3-4; * p<0.05; ** p<0.01; *** p<0.001; **** p<0.0001; ns = non-significant.

FIG. 41 shows luxol fast blue staining and astrocytic ASPA expression. CD KO mice were treated at p1 via facial vein with either 4×10^{11} GC of 3rd generation gene therapy or GFAPhASPA-Opt in rAAV9. Shown are 5 brain regions of p25 mice vs. wild-type (WT) and untreated (KO) control mice. Shown are 10X magnifications. See FIG. 29 for legend.

FIGs. 42A-42F show high-field imaging non-invasively evaluates therapy outcomes. Male mice were treated at p1 and imaged at p25, comparing untreated (UT) CD KO mice, wild-type (WT) mice, and treated (Tx) CD KO mice (n=8-10 each). FIG. 42A shows representative images for tractography of the corpus callosum. FIG. 42B shows representative images for the fractional anisotropy (FA) values for left and right external capsule (EC) and corpus callosum (CC). FIG. 42C shows 19 brain regions were selected to analyze resting state-functional magnetic resonance imaging (rs-fMRI) results and mapped on a sagittal brain map. Light and black dots indicate cortical and sub-cortical brain regions, respectively. Light lines display all connections that involve cortical regions and darker lines show sub-cortical connections only. FIG. 42D shows T score statistics of rs-fMRI are shown that indicate differences between corresponding brain regions and overall brain activity (displayed in FIG. 42C). FIG. 42E shows total N-acetylaspartate (NAA) normalized against total creatine (tCr) was measured in all mice that underwent DTI and rs-fMRI imaging. FIG. 42F shows overall functional connectivity (untreated 31, wild-type 21, treated 19) was correlated to the average accelerated rotarod performance in seconds (FIG. 33A, p27) and analyzed via linear regression analysis (R^2 = 0.89). Error bars indicate mean ± SD; n=8-10; p<0.05; ** p<0.01; *** p<0.001; **** p<0.0001; ns = non-significant.

FIG. 43 shows resting state functional magnet resonance imaging (rs-fMRI) regions of interest. 19 regions of interest (ROI) were selected to represent regions of motor and cognitive function. N=9-10 mice per group were imaged while anesthetized to acquire rs-fMRI.

FIG. 44 shows NAA levels correlate with T2 Signal Intensities.

FIG. 45 shows restoration of myelin 4-weeks post-treatment with hASPA construct.

FIG. 46 shows rotarod assay data for male mice. Data indicates an expanded therapeutic window for ASPA gene therapy. Mice were assayed at 4 weeks, 10 weeks, 16 weeks, 28 weeks and 52 weeks.

FIG. 47 shows rotarod assay data for female mice. Data indicates an expanded therapeutic window for ASPA gene therapy. Mice were assayed at 4 weeks, 10 weeks, 16 weeks, 28 weeks and 52 weeks.

FIG. 48 shows T maze data indicating that working/spatial memory is restored in Nur7 mice

after treatment with the 3rd generation hASPA gene therapy construct. Cognitive function of Nur7 mice treated at Neonatal, Juvenile or Adult age was tested at 1 Year of Age.

FIG. 49 shows gait analysis data indicating a therapeutic benefit for mice treated with 3rd generation ASPA gene therapy at 6 months and earlier.

FIG. 50 shows gait analysis data indicating that mice treated at mature adult age (p168) still benefit from the 3rd generation ASPA gene therapy treatment.

FIG. 51 shows Mito Stress Test data comparing ASPA deficient HEK cells to wild-type HEK cells (*e.g.*, non ASPA deficient cells).

FIG. 52 shows mitochondrial profiling data for ASPA deficient HEK cells (HEK293 KO) compared to wild-type HEK cells (HEK293 WT).

FIG. 53 shows data indicating that ASPA deficient cells use more Fatty acids and Glutamine for energy production. Data relating to the dependency, flexibility and capacity of wild-type or ASPA deficient cells to use glucose (GLC), glutamine (GLN) or fatty acids (FA) for energy production is shown.

FIG. 54 shows data indicating that Nur7 mice treated with the 3rd generation ASPA gene therapy construct have a significantly lower g-ratio than untreated Nur7 mice, indicating an increase in myelin thickness due to re-myelination.

FIG. 55 shows data relating to measurement of beta-oxidation in untreated ASPA deficient mice, wild-type mice, treated control mice, and 3rd generation ASPA gene therapy construct treated mice.

FIG. 56 shows decreased glycolysis in ASPA deficient brain and restoration upon ASPA reconstitution.

FIG. 57 shows additional data representative data for whole brain metabolome analysis in wild-type (WT) and ASPA knockout (KO) mice.

DETAILED DESCRIPTION

[0021] Aspects of the disclosure relate to methods for treating neurodegenerative disease (*e.g.*, leukodystrophies) in a subject in need thereof. Methods provided herein involve modulating N-acetylaspartate (NAA) levels in a subject. NAA has been identified as the second most abundant molecule in the central nervous system (CNS). NAA synthesis may take place in neurons. In some instances, NAA is not synthesized in cells or organs outside the CNS. NAA is metabolized by the enzyme aspartoacylase (ASPA) into acetate and L-aspartate. ASPA may be expressed in the CNS (*e.g.*, in oligodendrocytes). ASPA may be expressed in peripheral

organs, such as kidney, small intestines and others. Neurodegenerative diseases may demonstrate disturbance of NAA metabolism. Accordingly, NAA may be used as a disease marker for a wide range of CNS disorders, *e.g.*, Canavan Disease, Alzheimer disease, traumatic brain injury, and psychiatric disorders. Further examples of neurodegenerative diseases include but are not limited to Alzheimer's disease, traumatic brain injury (TBI), bipolar disorder, catalepsy, epilepsy (*e.g.*, seizures), migraine, Huntington's disease, attention deficit disorder (ADD), attention deficit/hyperactivity disorder (*e.g.*, ADHD), autism spectrum disorder (*e.g.*, Asperger's disease, autism, *etc.*), Parkinson's disease, Tourette's syndrome, clinical depression, multiple sclerosis, and autoimmune disease (*e.g.*, CNS demyelinating disease, Myasthenia gravis, *etc.*).

[0022] Methods for treating leukodystrophy in a subject in need thereof are provided that involve administering to the subject an N-acetylaspartate (NAA)-depleting agent. As used herein, term "NAA-depleting agent" refers to an agent (*e.g.*, nucleic acid, protein, small molecule) that depletes NAA levels directly or indirectly. It may has been determined that the leukodystrophy is associated with a metabolic imbalance comprising a shift from glycolysis to beta-oxidation in the subject.

[0023] Other aspects of the disclosure relate to methods for treating neurodegenerative disease in a subject in need thereof in which the methods involve administering to the subject an N-acetylaspartate (NAA)-increasing agent. As used herein, term "NAA-increasing agent" refers to an agent (*e.g.*, nucleic acid, protein, small molecule) that increases NAA levels directly or indirectly. In some embodiments, it has been determined that the neurodegenerative disease is associated with a metabolic imbalance comprising an NAA deficiency. *e.g.*, delivering siRNA/shRNA or miRNA, *e.g.*, that inhibits expression of ASPA. As used herein, "metabolic imbalance" refers to a dysregulated or abnormal metabolic state in a subject. For example, CNS cells of a healthy subject may display a preference for glycolysis as a major mode of energy *(e.g.,* ATP production); in subjects having certain neurodegenerative diseases (*e.g.*, diseases associated with leukodystrophy, e.g., Canavan disease), CNS cells may display a preference for fatty acid metabolism. Such a shift away from glycolysis and towards beta-oxidation can be referred to as a "metabolic imbalance".

[0024] Methods disclosed herein may involve comparing biomarkers (e.g., beta-oxidation, glycolysis) with an appropriate control. An "appropriate control" refers a level of a particular biomarker (e.g., beta-oxidation, glycolysis) that is indicative of a known metabolic status. Such levels can be determined experimentally or can be pre-existing reference levels. In some embodiments, an appropriate control may be a biomarker level indicative of the presence of a metabolic imbalance. For example, an appropriate control may be level of a factor (e.g., beta-oxidation, glycolysis) in a control subject. A control subject may not have a metabolic imbalance. However, a control subject may have a metabolic imbalance.

Recombinant Adeno-associated Viruses (rAAVs)

[0025] In some aspects, the disclosure provides isolated AAVs that are useful for delivering transgenes that encode NAA-modulating agents (e.g., an NAA-depleting agent, an NAA-increasing agent). As used herein with respect to AAVs, the term "isolated" refers to an AAV that has been artificially produced or obtained. Isolated AAVs may be produced using recombinant methods. Such AAVs are referred to herein as "recombinant AAVs". Recombinant AAVs (rAAVs) preferably have tissue-specific targeting capabilities, such that a nuclease and/or transgene of the rAAV will be delivered specifically to one or more predetermined tissue(s). The AAV capsid is an important element in determining these tissue-specific targeting capabilities. Thus, an rAAV having a capsid appropriate for the tissue being targeted can be selected.

[0026] In some aspects, the disclosure provides an rAAV having a capsid appropriate for targeting central nervous system (CNS) tissue or other tissue (e.g., a peripheral tissue). The capsid may have a serotype selected from the group consisting of AAV1, AAV2, AAV5, AAV6, AV6.2, AAV7, AAV8, AAV9 and AAVrh.10. An rAAV may comprise variants of AAV1, AAV2, AAV5, AAV6, AV6.2, AAV7, AAV8, AAV9, and AAVrh.10 serotype capsid proteins. Capsid proteins may comprise an amino acid sequence that is at least 70%, at least 80%, at least 90%, at least 95% , or at least 99% identical to any one of the recited capsids.

[0027] Appropriate methods may be used for obtaining recombinant AAVs having a desired capsid protein. (See, for example, US 2003/0138772). Typically the methods involve culturing a host cell which contains a nucleic acid sequence encoding an AAV capsid protein; a functional *rep* gene; a recombinant AAV vector composed of, AAV inverted terminal repeats (ITRs) and a transgene; and sufficient helper functions to permit packaging of the recombinant AAV vector into the AAV capsid proteins. Capsid proteins may be structural proteins encoded by the cap gene of an AAV. AAVs comprise three capsid proteins, virion proteins 1 to 3 (named VP1, VP2 and VP3), all of which are transcribed from a single cap gene via alternative splicing. In some embodiments, the molecular weights of VP1, VP2 and VP3 are respectively about 87 kDa, about 72 kDa and about 62 kDa. Upon translation, capsid proteins may form a spherical 60-mer protein shell around the viral genome. The functions of the capsid proteins may be to protect the viral genome, deliver the genome and interact with the host. In some aspects, capsid proteins deliver the viral genome to a host in a tissue specific manner.

[0028] The components to be cultured in the host cell to package a rAAV vector in an AAV capsid may be provided to the host cell in *trans.* Alternatively, any one or more of the required components (e.g., recombinant AAV vector, rep sequences, cap sequences, and/or helper functions) may be provided by a stable host cell which has been engineered to contain one or more of the required components using methods known to those of skill in the art. Most suitably, such a stable host cell will contain the required component(s) under the control of an inducible promoter. However, the required component(s) may be under the control of a constitutive promoter. Examples of suitable inducible and constitutive promoters are provided herein, in the discussion of regulatory elements suitable for use with the transgene. In still another alternative, a selected stable host cell may contain selected component(s) under the control of a constitutive promoter and other selected component(s) under the control of one or

more inducible promoters. For example, a stable host cell may be generated which is derived from 293 cells (which contain E1 helper functions under the control of a constitutive promoter), but which contain the rep and/or cap proteins under the control of inducible promoters. Still other stable host cells may be generated by one of skill in the art.

[0029] The instant disclosure relates to a host cell containing a nucleic acid that comprises a coding sequence encoding a gene associated with a neurodegenerative disease (e.g., a leukodystrophy). The instant disclosure may relates to a composition comprising the host cell described above. The composition comprising the host cell above may further comprise a cryopreservative.

[0030] The recombinant AAV vector, rep sequences, cap sequences, and helper functions required for producing the rAAV of the disclosure may be delivered to the packaging host cell using any appropriate genetic element (vector). The selected genetic element may be delivered by any suitable method, including those described herein. The methods used to construct any embodiment of this disclosure are known to those with skill in nucleic acid manipulation and include genetic engineering, recombinant engineering, and synthetic techniques. See, e.g., Sambrook et al, Molecular Cloning: A Laboratory Manual, Cold Spring Harbor Press, Cold Spring Harbor, N.Y. Similarly, methods of generating rAAV virions are well known and the selection of a suitable method is not a limitation on the present disclosure. See, e.g., K. Fisher et al, J. Virol., 70:520-532 (1993) and U.S. Pat. No. 5,478,745.

[0031] Recombinant AAVs may be produced using the triple transfection method (described in detail in U.S. Pat. No. 6,001,650). Typically, the recombinant AAVs are produced by transfecting a host cell with an recombinant AAV vector (comprising a transgene) to be packaged into AAV particles, an AAV helper function vector, and an accessory function vector. An AAV helper function vector encodes the "AAV helper function" sequences (i.e., rep and cap), which function in *trans* for productive AAV replication and encapsidation. Preferably, the AAV helper function vector supports efficient AAV vector production without generating any detectable wild-type AAV virions (i.e., AAV virions containing functional rep and cap genes). Non-limiting examples of vectors suitable for use with the present disclosure include pHLP19, described in U.S. Pat. No. 6,001,650 and pRep6cap6 vector, described in U.S. Pat. No. 6,156,303. The accessory function vector encodes nucleotide sequences for non-AAV derived viral and/or cellular functions upon which AAV is dependent for replication (*i.e.*, "accessory functions"). The accessory functions include those functions required for AAV replication, including, without limitation, those moieties involved in activation of AAV gene transcription, stage specific AAV mRNA splicing, AAV DNA replication, synthesis of cap expression products, and AAV capsid assembly. Viral-based accessory functions can be derived from any of the known helper viruses such as adenovirus, herpesvirus (other than herpes simplex virus type-1), and vaccinia virus.

[0032] In some aspects, the disclosure provides transfected host cells. The term "transfection" is used to refer to the uptake of foreign DNA by a cell, and a cell has been "transfected" when exogenous DNA has been introduced inside the cell membrane. A number of transfection

techniques are generally known in the art. See, e.g., Graham et al. (1973) Virology, 52:456, Sambrook et al. (1989) Molecular Cloning, a laboratory manual, Cold Spring Harbor Laboratories, New York, Davis et al. (1986) Basic Methods in Molecular Biology, Elsevier, and Chu et al. (1981) Gene 13:197. Such techniques can be used to introduce one or more exogenous nucleic acids, such as a nucleotide integration vector and other nucleic acid molecules, into suitable host cells.

[0033] A "host cell" refers to any cell that harbors, or is capable of harboring, a substance of interest. Often a host cell is a mammalian cell. A host cell may be used as a recipient of an AAV helper construct, an AAV minigene plasmid, an accessory function vector, or other transfer DNA associated with the production of recombinant AAVs. The term includes the progeny of the original cell which has been transfected. Thus, a "host cell" as used herein may refer to a cell which has been transfected with an exogenous DNA sequence. It is understood that the progeny of a single parental cell may not necessarily be completely identical in morphology or in genomic or total DNA complement as the original parent, due to natural, accidental, or deliberate mutation.

[0034] As used herein, the term "cell line" refers to a population of cells capable of continuous or prolonged growth and division *in vitro.* Often, cell lines are clonal populations derived from a single progenitor cell. It is further known in the art that spontaneous or induced changes can occur in karyotype during storage or transfer of such clonal populations. Therefore, cells derived from the cell line referred to may not be precisely identical to the ancestral cells or cultures, and the cell line referred to includes such variants.

[0035] As used herein, the terms "recombinant cell" refers to a cell into which an exogenous DNA segment, such as DNA segment that leads to the transcription of a biologically-active polypeptide or production of a biologically active nucleic acid such as an RNA, has been introduced.

[0036] As used herein, the term "vector" includes any genetic element, such as a plasmid, phage, transposon, cosmid, chromosome, artificial chromosome, virus, virion, *etc.,* which is capable of replication when associated with the proper control elements and which can transfer gene sequences between cells. Thus, the term includes cloning and expression vehicles, as well as viral vectors. Useful vectors are contemplated to be those vectors in which the nucleic acid segment to be transcribed is positioned under the transcriptional control of a promoter. A "promoter" refers to a DNA sequence recognized by the synthetic machinery of the cell, or introduced synthetic machinery, required to initiate the specific transcription of a gene. The phrases "operatively positioned," "under control" or "under transcriptional control" means that the promoter is in the correct location and orientation in relation to the nucleic acid to control RNA polymerase initiation and expression of the gene. The term "expression vector or construct" means any type of genetic construct containing a nucleic acid in which part or all of the nucleic acid encoding sequence is capable of being transcribed. Expression may includes transcription of the nucleic acid, for example, to generate a biologically-active polypeptide product or functional RNA (*e.g.*, shRNA, miRNA) from a transcribed gene.

[0037] The foregoing methods for packaging recombinant vectors in desired AAV capsids to produce the rAAVs of the disclosure are not meant to be limiting and other suitable methods will be apparent to the skilled artisan.

Isolated Nucleic Acids

[0038] A "nucleic acid" sequence refers to a DNA or RNA sequence. Proteins and nucleic acids of the disclosure may be isolated. As used herein, the term "isolated" means artificially produced. As used herein with respect to nucleic acids, the term "isolated" means: (i) amplified *in vitro* by, for example, polymerase chain reaction (PCR); (ii) recombinantly produced by cloning; (iii) purified, as by cleavage and gel separation; or (iv) synthesized by, for example, chemical synthesis. An isolated nucleic acid is one which is readily manipulable by recombinant DNA techniques well known in the art. Thus, a nucleotide sequence contained in a vector in which 5' and 3' restriction sites are known or for which polymerase chain reaction (PCR) primer sequences have been disclosed is considered isolated but a nucleic acid sequence existing in its native state in its natural host is not. An isolated nucleic acid may be substantially purified, but need not be. For example, a nucleic acid that is isolated within a cloning or expression vector is not pure in that it may comprise only a tiny percentage of the material in the cell in which it resides. Such a nucleic acid is isolated, however, as the term is used herein because it is readily manipulable by standard techniques known to those of ordinary skill in the art. As used herein with respect to proteins or peptides, the term "isolated" refers to a protein or peptide that has been isolated from its natural environment or artificially produced (e.g., by chemical synthesis, by recombinant DNA technology, *etc.).*

[0039] Conservative amino acid substitutions may be made to provide functionally equivalent variants, or homologs of the capsid proteins. In some aspects the disclosure embraces sequence alterations that result in conservative amino acid substitutions. As used herein, a conservative amino acid substitution refers to an amino acid substitution that does not alter the relative charge or size characteristics of the protein in which the amino acid substitution is made. Variants can be prepared according to methods for altering polypeptide sequence known to one of ordinary skill in the art such as are found in references that compile such methods, *e.g.*, Molecular Cloning: A Laboratory Manual, J. Sambrook, et al., eds., Second Edition, Cold Spring Harbor Laboratory Press, Cold Spring Harbor, New York, 1989, or Current Protocols in Molecular Biology, F.M. Ausubel, et al., eds., John Wiley & Sons, Inc., New York. Conservative substitutions of amino acids include substitutions made among amino acids within the following groups: (a) M, I, L, V; (b) F, Y, W; (c) K, R, H; (d) A, G; (e) S, T; (f) Q, N; and (g) E, D. Therefore, one can make conservative amino acid substitutions to the amino acid sequence of the proteins and polypeptides disclosed herein.

Recombinant AAV Vectors (rAA V Vectors)

[0040] "Recombinant AAV (rAAV) vectors" of the disclosure are typically composed of, at a minimum, a transgene and its regulatory sequences, and 5' and 3' AAV inverted terminal repeats (ITRs). It is this recombinant AAV vector which is packaged into a capsid protein and delivered to a selected target cell. In some embodiments, the transgene is a nucleic acid sequence, heterologous to the vector sequences, which encodes a polypeptide, protein, functional RNA molecule (*e.g.*, shRNA, miRNA) or other gene product, of interest. The nucleic acid coding sequence is operatively linked to regulatory components in a manner which permits transgene transcription, translation, and/or expression in a cell of a target tissue.

[0041] In some embodiments, the instant disclosure relates to a recombinant AAV (rAAV) vector comprising a nucleic acid sequence including a promoter operably linked to a transgene, wherein the transgene is a gene associated with a neurodegenerative disease (*e.g.*, leukodystrophy). A rAAV vector may further comprises nucleic acid sequences encoding one or more AAV inverted terminal repeat sequences (ITRs), for example AAV2 ITRs. A rAAV vector may further comprises nucleic acid sequences encoding one or more AAV ITRs selected from the group consisting of AAV2, AAV3, AAV4, AAV5, and AAV6.

[0042] The AAV sequences of the vector typically comprise the cis-acting 5' and 3' inverted terminal repeat sequences (See, *e.g.*, B. J. Carter, in "Handbook of Parvoviruses", ed., P. Tijsser, CRC Press, pp. 155 168 (1990)). The ITR sequences are about 145 bp in length. Preferably, substantially the entire sequences encoding the ITRs are used in the molecule, although some degree of minor modification of these sequences is permissible. The ability to modify these ITR sequences is within the skill of the art. (See, *e.g.*, texts such as Sambrook et al, "Molecular Cloning. A Laboratory Manual", 2d ed., Cold Spring Harbor Laboratory, New York (1989); and K. Fisher et al., J Virol., 70:520 532 (1996)). An example of such a molecule employed in the present disclosure is a "cis-acting" plasmid containing the transgene, in which the selected transgene sequence and associated regulatory elements are flanked by the 5' and 3' AAV ITR sequences. The AAV ITR sequences may be obtained from any known AAV, including presently identified mammalian AAV types (*e.g.*, AAV2, AAV3, AAV4, AAV5, or AAV6 ITR sequences).

[0043] The rAAVs of the present disclosure may be pseudotyped rAAVs. Pseudotyping is the process of producing viruses or viral vectors in combination with foreign viral envelope proteins. The result is a pseudotyped virus particle. With this method, the foreign viral envelope proteins can be used to alter host tropism or an increased/decreased stability of the virus particles. In some aspects, a pseudotyped rAAV comprises nucleic acids from two or more different AAVs, wherein the nucleic acid from one AAV encodes a capsid protein and the nucleic acid of at least one other AAV encodes other viral proteins and/or the viral genome. A pseudotyped rAAV may refer to an AAV comprising an inverted terminal repeats (ITRs) of one AAV serotype and an capsid protein of a different AAV serotype. For example, a pseudotyped AAV vector containing the ITRs of serotype X encapsidated with the proteins of Y will be designated as AAVX/Y (*e.g.*, AAV2/1 has the ITRs of AAV2 and the capsid of AAV1). Pseudotyped rAAVs may be useful for combining the tissue-specific targeting capabilities of a capsid protein from one AAV serotype with the viral DNA from another AAV serotype, thereby

allowing targeted delivery of a transgene to a target tissue.

[0044] In addition to the major elements identified above for the recombinant AAV vector, the vector also includes control elements necessary which are operably linked to the transgene in a manner which permits its transcription, translation and/or expression in a cell transfected with the plasmid vector or infected with the virus produced by the disclosure. As used herein, "operably linked" sequences include both expression control sequences that are contiguous with the gene of interest and expression control sequences that act in trans or at a distance to control the gene of interest.

[0045] Expression control sequences include appropriate transcription initiation, termination, promoter and enhancer sequences; efficient RNA processing signals such as splicing and polyadenylation (polyA) signals; sequences that stabilize cytoplasmic mRNA; sequences that enhance translation efficiency (*i.e.*, Kozak consensus sequence); sequences that enhance protein stability; and when desired, sequences that enhance secretion of the encoded product. A great number of expression control sequences, including promoters which are native, constitutive, inducible, ubiquitous, and/or tissue-specific, are known in the art and may be utilized.

[0046] As used herein, a nucleic acid sequence (*e.g.*, coding sequence) and regulatory sequences are said to be "operably" linked when they are covalently linked in such a way as to place the expression or transcription of the nucleic acid sequence under the influence or control of the regulatory sequences. If it is desired that the nucleic acid sequences be translated into a functional protein, two DNA sequences are said to be operably linked if induction of a promoter in the 5' regulatory sequences results in the transcription of the coding sequence and if the nature of the linkage between the two DNA sequences does not (1) result in the introduction of a frame-shift mutation, (2) interfere with the ability of the promoter region to direct the transcription of the coding sequences, or (3) interfere with the ability of the corresponding RNA transcript to be translated into a protein. Thus, a promoter region would be operably linked to a nucleic acid sequence if the promoter region were capable of effecting transcription of that DNA sequence such that the resulting transcript might be translated into the desired protein or polypeptide. Similarly two or more coding regions are operably linked when they are linked in such a way that their transcription from a common promoter results in the expression of two or more proteins having been translated in frame. Operably linked coding sequences may yield a fusion protein. Operably linked coding sequences may yield a functional RNA (e.g., shRNA).

[0047] For nucleic acids encoding proteins, a polyadenylation sequence generally is inserted following the transgene sequences and before the 3' AAV ITR sequence. A rAAV construct useful in the present disclosure may also contain an intron, desirably located between the promoter/enhancer sequence and the transgene. One possible intron sequence is derived from SV-40, and is referred to as the SV-40 T intron sequence. Another vector element that may be used is an internal ribosome entry site (IRES). An IRES sequence is used to produce more than one polypeptide from a single gene transcript. An IRES sequence would be used to

produce a protein that contain more than one polypeptide chains. Selection of these and/or other vector elements may be performed, as appropriate, and many such sequences are available [see, e.g., Sambrook et al, and references cited therein at, for example, pages 3.18 3.26 and 16.17 16.27 and Ausubel et al., Current Protocols in Molecular Biology, John Wiley & Sons, New York, 1989]. In some embodiments, a Foot and Mouth Disease Virus 2A sequence is included in polyprotein; this is a small peptide (approximately 18 amino acids in length) that has been shown to mediate the cleavage of polyproteins (Ryan, M D et al., EMBO, 1994; 4: 928-933; Mattion, N M et al., J Virology, November 1996; p. 8124-8127; Furler, S et al., Gene Therapy, 2001; 8: 864-873; and Halpin, C et al., The Plant Journal, 1999; 4: 453-459). The cleavage activity of the 2A sequence has previously been demonstrated in artificial systems including plasmids and gene therapy vectors (AAV and retroviruses) (Ryan, M D et al., EMBO, 1994; 4: 928-933; Mattion, N M et al., J Virology, November 1996; p. 8124-8127; Furler, S et al., Gene Therapy, 2001; 8: 864-873; and Halpin, C et al., The Plant Journal, 1999; 4: 453-459; de Felipe, P et al., Gene Therapy, 1999; 6: 198-208; de Felipe, P et al., Human Gene Therapy, 2000; 11: 1921-1931.; and Klump, H et al., Gene Therapy, 2001; 8: 811-817).

[0048] The precise nature of the regulatory sequences needed for gene expression in host cells may vary between species, tissues or cell types, but shall in general include, as necessary, 5' non-transcribed and 5' non-translated sequences involved with the initiation of transcription and translation respectively, such as a TATA box, capping sequence, CAAT sequence, enhancer elements, and the like. Especially, such 5' non-transcribed regulatory sequences will include a promoter region that includes a promoter sequence for transcriptional control of the operably joined gene. Regulatory sequences may also include enhancer sequences or upstream activator sequences as desired. The vectors of the disclosure may optionally include 5' leader or signal sequences. The choice and design of an appropriate vector is within the ability and discretion of one of ordinary skill in the art.

[0049] Examples of constitutive promoters include, without limitation, the retroviral Rous sarcoma virus (RSV) LTR promoter (optionally with the RSV enhancer), the cytomegalovirus (CMV) promoter (optionally with the CMV enhancer) [see, e.g., Boshart et al, Cell, 41:521-530 (1985)], the SV40 promoter, the dihydrofolate reductase promoter, the β-actin promoter, the phosphoglycerol kinase (PGK) promoter, and the EF1α promoter [Invitrogen]. In some embodiments, a promoter is an enhanced chicken β-actin promoter. In some embodiments, a promoter is an astrocyte specific promoter. In some embodiments, a promoter is an oligodendrocyte specific promoter. In some embodiments, a promoter is an CNS-specific promoter.

[0050] Inducible promoters allow regulation of gene expression and can be regulated by exogenously supplied compounds, environmental factors such as temperature, or the presence of a specific physiological state, *e.g.*, acute phase, a particular differentiation state of the cell, or in replicating cells only. Inducible promoters and inducible systems are available from a variety of commercial sources, including, without limitation, Invitrogen, Clontech and Ariad. Many other systems have been described and can be readily selected by one of skill in the art. Examples of inducible promoters regulated by exogenously supplied promoters include

the zinc-inducible sheep metallothionine (MT) promoter, the dexamethasone (Dex)-inducible mouse mammary tumor virus (MMTV) promoter, the T7 polymerase promoter system (WO 98/10088); the ecdysone insect promoter (No et al, Proc. Natl. Acad. Sci. USA, 93:3346-3351 (1996)), the tetracycline-repressible system (Gossen et al, Proc. Natl. Acad. Sci. USA, 89:5547-5551 (1992)), the tetracycline-inducible system (Gossen et al, Science, 268:1766-1769 (1995), see also Harvey et al, Curr. Opin. Chem. Biol., 2:512-518 (1998)), the RU486-inducible system (Wang et al, Nat. Biotech., 15:239-243 (1997) and Wang et al, Gene Ther., 4:432-441 (1997)) and the rapamycin-inducible system (Magari et al, J. Clin. Invest., 100:2865-2872 (1997)). Still other types of inducible promoters which may be useful in this context are those which are regulated by a specific physiological state, e.g., temperature, acute phase, a particular differentiation state of the cell, or in replicating cells only.

[0051] The native promoter for the transgene may be used. The native promoter may be preferred when it is desired that expression of the transgene should mimic the native expression. The native promoter may be used when expression of the transgene must be regulated temporally or developmentally, or in a tissue-specific manner, or in response to specific transcriptional stimuli. In a further embodiment, other native expression control elements, such as enhancer elements, polyadenylation sites or Kozak consensus sequences may also be used to mimic the native expression.

[0052] Regulatory sequences may impart tissue-specific gene expression capabilities. In some cases, the tissue-specific regulatory sequences bind tissue-specific transcription factors that induce transcription in a tissue specific manner. Such tissue-specific regulatory sequences (e.g., promoters, enhancers, *etc.)* are well known in the art. Exemplary tissue-specific regulatory sequences include, but are not limited to the following tissue specific promoters: a liver-specific thyroxin binding globulin (TBG) promoter, an insulin promoter, a glucagon promoter, a somatostatin promoter, a pancreatic polypeptide (PPY) promoter, a synapsin-1 (Syn) promoter, a creatine kinase (MCK) promoter, a mammalian desmin (DES) promoter, a α-myosin heavy chain (a-MHC) promoter, or a cardiac Troponin T (cTnT) promoter. Other exemplary promoters include Beta-actin promoter, hepatitis B virus core promoter, Sandig et al., Gene Ther., 3:1002-9 (1996); alpha-fetoprotein (AFP) promoter, Arbuthnot et al., Hum. Gene Ther., 7:1503-14 (1996)), bone osteocalcin promoter (Stein et al., Mol. Biol. Rep., 24:185-96 (1997)); bone sialoprotein promoter (Chen et al., J. Bone Miner. Res., 11:654-64 (1996)), CD2 promoter (Hansal et al., J. Immunol., 161:1063-8 (1998); immunoglobulin heavy chain promoter; T cell receptor α-chain promoter, neuronal such as neuron-specific enolase (NSE) promoter (Andersen et al., Cell. Mol. Neurobiol., 13:503-15 (1993)), neurofilament light-chain gene promoter (Piccioli et al., Proc. Natl. Acad. Sci. USA, 88:5611-5 (1991)), and the neuron-specific vgf gene promoter (Piccioli et al., Neuron, 15:373-84 (1995)), among others which will be apparent to the skilled artisan. The promoter may be an oligodendrocyte-specific promoter, for example the myelin basic protein (MBP) promoter (Chen et al., J. Neurosci, Res., 55(4); 504-13 (1999)).

[0053] Aspects of the disclosure relate to the discovery that astrocyte-specific (e.g., astrocyte-restricted) expression of hASPA results has a positive therapeutic effect (e.g., survival,

normalized growth, restoration of normal motor function and cognitive function) in mouse models of Canavan Disease. Therefore, in some embodiments, the transgene of an rAAV described by the disclosure is operably-linked to an astrocyte-specific promoter. Examples of astrocyte-specific promoters include but are not limited to glial fibrillary acidic protein (GFAP) (Brenner et al., J. Neurosci, 14(3, Pt 1); 1030-7 (1994)), aldehyde dehydrogenase 1 family, member L1 (ALDH1L1) promoter (Cahoy et al., J. Neurosci. 28, 264-278 (2008)), and glutamate transporter promoter EAAT1 (Colin et al., Glia 57, 667-679 (2009)). In some embodiments, the astrocyte-specific promoter is the glial fibrillary acidic protein (GFAP) promoter.

[0054] One or more bindings sites for one or more of miRNAs may be incorporated in a transgene of a rAAV vector, to inhibit the expression of the transgene in one or more tissues of an subject harboring the transgene. The skilled artisan will appreciate that binding sites may be selected to control the expression of a transgene in a tissue specific manner. For example, binding sites for the liver-specific miR-122 may be incorporated into a transgene to inhibit expression of that transgene in the liver. The target sites in the mRNA may be in the 5' UTR, the 3' UTR or in the coding region. Typically, the target site is in the 3' UTR of the mRNA. Furthermore, the transgene may be designed such that multiple miRNAs regulate the mRNA by recognizing the same or multiple sites. The presence of multiple miRNA binding sites may result in the cooperative action of multiple RISCs and provide highly efficient inhibition of expression. The target site sequence may comprise a total of 5-100, 10-60, or more nucleotides. The target site sequence may comprise at least 5 nucleotides of the sequence of a target gene binding site.

Recombinant AA VAdministration Methods

[0055] The rAAVs may be delivered to a subject in compositions according to any appropriate methods. The rAAV, e.g., suspended in a physiologically compatible carrier (*i.e.*, in a composition), may be administered to a subject, *i.e.* host animal, such as a human, mouse, rat, cat, dog, sheep, rabbit, horse, cow, goat, pig, guinea pig, hamster, chicken, turkey, or a nonhuman primate (*e.g.*, Macaque). In some cases, a host animal does not include a human.

[0056] The compositions of the disclosure may comprise an rAAV alone, or in combination with one or more other viruses (e.g., a second rAAV encoding having one or more different transgenes). A composition may comprises 1, 2, 3, 4, 5, 6, 7, 8, 9, 10, or more different rAAVs each having one or more different transgenes.

[0057] In some cases, administration of an rAAV to a subject elicits an immune response against the rAAV capsid protein in the subject. Without wishing to be bound by any particular theory, suppressing the immune system of a subject prior to administration of an rAAV results, in some embodiments, in increased therapeutic effect of the rAAV. Therefore, a subject may be administered one or more *(e.g.,* 2, 3, 4, 5, or more) immune-suppressing agents prior to administration of an rAAV as described by the disclosure. An "immune-suppressing agent" is

any composition *(e.g.,* a protein, nucleic acid, small molecule, *etc.)* that reduces the immune response of a subject to an rAAV. An immune-suppressing agent can reduce the innate immune response, adaptive immune response, cellular immune response, humoral immune response, or any combination of the foregoing, in a subject.

[0058] Examples of biological immune-suppressing agents include but are not limited to monoclonal antibodies, such as monoclonal antibodies that block the co-stimulatory pathway (e.g., appropriate antibodies against CTLA4, ICOS, CD80, OX40, or other targets), interfering RNA *(e.g.,* siRNA, dsRNA, shRNA, miRNA, *etc.)* targeting immunostimulatory molecules *(e.g.,* cytokines), and proteins *(e.g.,* proteasome inhibitors).

[0059] Examples of small molecule immune-suppressing molecules include but are not limited to glucocorticoids (e.g., cortisol, cortisone, prednisone, prednisolone, methylprednisolone, dexamethasone, betamethasone, triamcinolone, beclomethasone, fludrocortisone, deoxy corticosterone (DOCA), and aldosterone), cytostatics (e.g., cyclophosphamide, nitrosoureas, platinum compounds, methotrexate, azathioprine, mercaptopurine, fluorouracil, dactinomycin, *etc.),* immunophilin-targeting drugs *(e.g.,* cyclosporine, tacrolimus, sirolimus, rapamycin, *etc.),* interferons (e.g., IFN-β), mycophenolate, fingolimod, and myriocin.

[0060] An immune-suppressing agent can be administered to a subject at between about one week and one minute prior to administration of an rAAV as described by the disclosure. In some embodiments, an immune-suppressing agent is administered to a subject between about 5 days, about 1 day, about 12 hours, about 2 hours, about 1 hour, about 30 minutes, about 10 minutes, about 5 minutes, or about 1 minute prior to administration of an rAAV. A subject may be administered an immune-suppressing agent on multiple (*e.g.* 2, 3, 4, 5, 6, 7, 8, 9, 10, or more) occasions prior to administration of an rAAV to the subject.

[0061] A composition may further comprise a pharmaceutically acceptable carrier. Suitable carriers may be readily selected by one of skill in the art in view of the indication for which the rAAV is directed. For example, one suitable carrier includes saline, which may be formulated with a variety of buffering solutions (e.g., phosphate buffered saline). Other exemplary carriers include sterile saline, lactose, sucrose, calcium phosphate, gelatin, dextran, agar, pectin, peanut oil, sesame oil, and water. The selection of the carrier is not a limitation of the present disclosure.

[0062] Optionally, the compositions of the disclosure may contain, in addition to the rAAV and carrier(s), other pharmaceutical ingredients, such as preservatives, or chemical stabilizers. Suitable exemplary preservatives include chlorobutanol, potassium sorbate, sorbic acid, sulfur dioxide, propyl gallate, the parabens, ethyl vanillin, glycerin, phenol, and parachlorophenol. Suitable chemical stabilizers include gelatin and albumin.

[0063] The rAAVs are administered in sufficient amounts to transfect the cells of a desired tissue *(e.g.,* CNS tissue) and to provide sufficient levels of gene transfer and expression without undue adverse effects. Examples of pharmaceutically acceptable routes of

administration include, but are not limited to, direct delivery to the selected organ (e.g., intrathecal, intracerebral), oral, inhalation (including intranasal and intratracheal delivery), intraocular, intravenous, intramuscular, subcutaneous, intradermal, intratumoral, and other parental routes of administration. Routes of administration may be combined, if desired.

[0064] The dose of rAAV virions required to achieve a particular "therapeutic effect," *e.g.*, the units of dose in genome copies/per kilogram of body weight (GC/kg), will vary based on several factors including, but not limited to: the route of rAAV virion administration, the level of gene or RNA expression required to achieve a therapeutic effect, the specific disease or disorder being treated, and the stability of the gene or RNA product. One of skill in the art can readily determine a rAAV virion dose range to treat a patient having a particular disease or disorder based on the aforementioned factors, as well as other factors.

[0065] An effective amount of an rAAV is an amount sufficient to target infect an animal, target a desired tissue. An effective amount of an rAAV may be an amount sufficient to produce a stable somatic transgenic animal model. The effective amount will depend primarily on factors such as the species, age, weight, health of the subject, and the tissue to be targeted, and may thus vary among animal and tissue. For example, an effective amount of the rAAV is generally in the range of from about 1 ml to about 100 ml of solution containing from about 10^9 to 10^{16} genome copies (gc). A dosage between about 10^{10} and 10^{15} genome copies may be appropriate. In some cases, a dosage between about 10^{11} to 10^{13} rAAV genome copies is appropriate. In certain cases, 10^{11} or 10^{12} rAAV genome copies is effective to target CNS tissue. A dosage of an rAAV may be calculated based upon the weight of the subject to which the rAAV is being administered. For example, a dosage between 1.0×10^{10} gc/kg and 1.0×10^{15} gc/kg may be appropriate. A dosage of 2.0×10^{10} gc/kg, 2.0×10^{11} gc/kg , 2.0×10^{12} gc/kg , 2.0×10^{13} gc/kg , 2.0×10^{14} gc/kg , or 2.0×10^{15} gc/kg may be appropriate. In some cases, stable transgenic animals are produced by multiple doses of an rAAV.

[0066] A dose of rAAV may be administered to a subject no more than once per calendar day (e.g., a 24-hour period). A dose of rAAV may be administered to a subject no more than once per 2, 3, 4, 5, 6, or 7 calendar days. A dose of rAAV may be administered to a subject no more than once per calendar week (e.g., 7 calendar days). A dose of rAAV may be administered to a subject no more than bi-weekly (e.g., once in a two calendar week period). A dose of rAAV may be administered to a subject no more than once per calendar month (e.g., once in 30 calendar days). A dose of rAAV may be administered to a subject no more than once per six calendar months. A dose of rAAV may be administered to a subject no more than once per calendar year (e.g., 365 days or 366 days in a leap year).

[0067] rAAV compositions may be formulated to reduce aggregation of AAV particles in the composition, particularly where high rAAV concentrations are present (e.g., ~10^{13} GC/ml or more). Appropriate methods for reducing aggregation of may be used, including, for example, addition of surfactants, pH adjustment, salt concentration adjustment, *etc.* (See, *e.g.*, Wright

FR, et al., Molecular Therapy (2005) 12, 171-178.

[0068] Formulation of pharmaceutically-acceptable excipients and carrier solutions is well-known to those of skill in the art, as is the development of suitable dosing and treatment regimens for using the particular compositions described herein in a variety of treatment regimens. Typically, these formulations may contain at least about 0.1% of the active compound or more, although the percentage of the active ingredient(s) may, of course, be varied and may conveniently be between about 1 or 2% and about 70% or 80% or more of the weight or volume of the total formulation. Naturally, the amount of active compound in each therapeutically-useful composition may be prepared is such a way that a suitable dosage will be obtained in any given unit dose of the compound. Factors such as solubility, bioavailability, biological half-life, route of administration, product shelf life, as well as other pharmacological considerations will be contemplated by one skilled in the art of preparing such pharmaceutical formulations, and as such, a variety of dosages and treatment regimens may be desirable.

[0069] rAAVs in suitably formulated pharmaceutical compositions disclosed herein may be delivered directly to target tissue, e.g., direct to CNS tissue. However, in certain circumstances it may be desirable to separately or in addition deliver the rAAV-based therapeutic constructs via another route, e.g., subcutaneously, intraopancreatically, intranasally, parenterally, intravenously, intramuscularly, intrathecally, or orally, intraperitoneally, or by inhalation. The administration modalities as described in U.S. Pat. Nos. 5,543,158; 5,641,515 and 5,399,363 may be used to deliver rAAVs.

[0070] The pharmaceutical forms suitable for injectable use include sterile aqueous solutions or dispersions and sterile powders for the extemporaneous preparation of sterile injectable solutions or dispersions. Dispersions may also be prepared in glycerol, liquid polyethylene glycols, and
mixtures thereof and in oils. Under ordinary conditions of storage and use, these preparations contain a preservative to prevent the growth of microorganisms. In many cases the form is sterile and fluid to the extent that easy syringability exists. It must be stable under the conditions of manufacture and storage and must be preserved against the contaminating action of microorganisms, such as bacteria and fungi. The carrier can be a solvent or dispersion medium containing, for example, water, ethanol, polyol (e.g., glycerol, propylene glycol, and liquid polyethylene glycol, and the like), suitable mixtures thereof, and/or vegetable oils. Proper fluidity may be maintained, for example, by the use of a coating, such as lecithin, by the maintenance of the required particle size in the case of dispersion and by the use of surfactants. The prevention of the action of microorganisms can be brought about by various antibacterial and antifungal agents, for example, parabens, chlorobutanol, phenol, sorbic acid, thimerosal, and the like. In many cases, it will be preferable to include isotonic agents, for example, sugars or sodium chloride. Prolonged absorption of the injectable compositions can be brought about by the use in the compositions of agents delaying absorption, for example, aluminum monostearate and gelatin.

[0071] For administration of an injectable aqueous solution, for example, the solution may be

suitably buffered, if necessary, and the liquid diluent first rendered isotonic with sufficient saline or glucose. These particular aqueous solutions are especially suitable for intravenous, intramuscular, subcutaneous and intraperitoneal administration. In this connection, a suitable sterile aqueous medium may be employed. For example, one dosage may be dissolved in 1 ml of isotonic NaCl solution and either added to 1000 ml of hypodermoclysis fluid or injected at the proposed site of infusion, (see for example, "Remington's Pharmaceutical Sciences" 15th Edition, pages 1035-1038 and 1570-1580). Some variation in dosage will necessarily occur depending on the condition of the host. The person responsible for administration will, in any event, determine the appropriate dose for the individual host.

[0072] Sterile injectable solutions are prepared by incorporating the active rAAV in the required amount in the appropriate solvent with various of the other ingredients enumerated herein, as required, followed by filtered sterilization. Generally, dispersions are prepared by incorporating the various sterilized active ingredients into a sterile vehicle which contains the basic dispersion medium and the required other ingredients from those enumerated above. In the case of sterile powders for the preparation of sterile injectable solutions, the preferred methods of preparation are vacuum-drying and freeze-drying techniques which yield a powder of the active ingredient plus any additional desired ingredient from a previously sterile-filtered solution thereof.

[0073] The rAAV compositions disclosed herein may also be formulated in a neutral or salt form. Pharmaceutically-acceptable salts, include the acid addition salts (formed with the free amino groups of the protein) and which are formed with inorganic acids such as, for example, hydrochloric or phosphoric acids, or such organic acids as acetic, oxalic, tartaric, mandelic, and the like. Salts formed with the free carboxyl groups can also be derived from inorganic bases such as, for example, sodium, potassium, ammonium, calcium, or ferric hydroxides, and such organic bases as isopropylamine, trimethylamine, histidine, procaine and the like. Upon formulation, solutions will be administered in a manner compatible with the dosage formulation and in such amount as is therapeutically effective. The formulations are easily administered in a variety of dosage forms such as injectable solutions, drug-release capsules, and the like.

[0074] As used herein, "carrier" includes any and all solvents, dispersion media, vehicles, coatings, diluents, antibacterial and antifungal agents, isotonic and absorption delaying agents, buffers, carrier solutions, suspensions, colloids, and the like. The use of such media and agents for pharmaceutical active substances is well known in the art. Supplementary active ingredients can also be incorporated into the compositions. The phrase "pharmaceutically-acceptable" refers to molecular entities and compositions that do not produce an allergic or similar untoward reaction when administered to a host.

[0075] Delivery vehicles such as liposomes, nanocapsules, microparticles, microspheres, lipid particles, vesicles, and the like, may be used for the introduction of the compositions of the present disclosure into suitable host cells. In particular, the rAAV vector delivered trangenes may be formulated for delivery either encapsulated in a lipid particle, a liposome, a vesicle, a nanosphere, or a nanoparticle or the like.

[0076] Such formulations may be preferred for the introduction of pharmaceutically acceptable formulations of the nucleic acids or the rAAV constructs disclosed herein. The formation and use of liposomes is generally known to those of skill in the art. Recently, liposomes were developed with improved serum stability and circulation half-times (U.S. Pat. No. 5,741,516). Further, various methods of liposome and liposome like preparations as potential drug carriers have been described (U.S. Pat. Nos. 5,567,434; 5,552,157; 5,565,213; 5,738,868 and 5,795,587).

[0077] Liposomes have been used successfully with a number of cell types that are normally resistant to transfection by other procedures. In addition, liposomes are free of the DNA length constraints that are typical of viral-based delivery systems. Liposomes have been used effectively to introduce genes, drugs, radiotherapeutic agents, viruses, transcription factors and allosteric effectors into a variety of cultured cell lines and animals. In addition, several successful clinical trials examining the effectiveness of liposome-mediated drug delivery have been completed.

[0078] Liposomes are formed from phospholipids that are dispersed in an aqueous medium and spontaneously form multilamellar concentric bilayer vesicles (also termed multilamellar vesicles (MLVs). MLVs generally have diameters of from 25 nm to 4 μm. Sonication of MLVs results in the formation of small unilamellar vesicles (SUVs) with diameters in the range of 200 to 500 .ANG., containing an aqueous solution in the core.

[0079] Alternatively, nanocapsule formulations of the rAAV may be used. Nanocapsules can generally entrap substances in a stable and reproducible way. To avoid side effects due to intracellular polymeric overloading, such ultrafine particles (sized around 0.1 μm) should be designed using polymers able to be degraded *in vivo.* Biodegradable polyalkyl-cyanoacrylate nanoparticles that meet these requirements are contemplated for use.

EXAMPLES

Example 1: Pathomechanism of Canavan's Disease

Experimental design

[0080] Global biochemical profiles were determined in mouse brain tissue collected from postnatal day 25 (P25) mice representing treatment groups shown below in Table 1.

Table 1: Treatment groups

Group	n	Description
WT	8	Wild type mouse

Group	n	Description
KO	8	Aspartoacylase gene knockout mouse
rAAV Ctrl	8	Aspartoacylase gene knockout mouse, treated with virus with a promoter-less expression construct
rAAV Tx	8	Aspartoacylase gene knockout mouse, treated with virus encoding the human ASPA gene

Metabolomics of healthy and Canavan disease mouse brains

[0081] Results of resting state functional MRI (RS-fMRI) indicate that Canavan disease causes increased oxygen consumption for functional neuro-connectivity (FIG. 2). Further, Canavan disease causes increased oxygen consumption for cortical/sub-cortical connectivity (FIG. 3). These data indicate that Canavan disease may be characterized by an altered metabolic state in the CNS.

[0082] The molecular phenotype of brains of mice having Canavan disease was investigated by using a whole brain metabolomics approach. Canavan disease were treated with intravenous (IV) injection of rAAV-ASPA at p1. Healthy and CD mouse brains (both untreated and treated groups) were homogenized and subjected to metabolic analysis. Over 452 metabolites were quantified in each wild-type, untreated, treated and treatment control groups (Table 2). This large data set revealed several crucial and entirely new aspects about Canavan disease pathomechanism, its gene therapy, CNS metabolism and novel function of AspA in general.

Table 2: Metabolomics analysis results

Significantly Altered Biochemicals	Total Biochemicals $p \leq 0.05$	Biochemicals (↑|↓)	Total Biochemicals $0.05 < p < 0.10$	Biochemicals (↑|↓)
KO ***WT***	273	681205	32	7|25
rAAV Tx ***rAAV Ctrl***	286	190196	29	14|15
rAAV Ctrl ***WT***	293	811212	30	12|18
rAAV Tx ***WT***	88	20168	41	9|32
rAAV Ctrl ***KO***	44	26118	32	16|16
rAAV Tx ***KO***	257	184|73	41	21|20

Statistical Analysis

[0083] Principal component analysis (PCA) transforms a large number of metabolic variables into a smaller number of orthogonal variables (Component 1, Component 2, *etc.)* in order to analyze variation between groups and to provide a high-level overview of the dataset. In the PCA (FIG. 4A), samples formed into two populations; interestingly, rather than reflecting the genetic background, these two populations appeared to reflect disease state: WT and rAAV Tx formed the left-most population, with KO and rAAV Ctrl forming the right population, consistent with a "rescue" of disease by treatment.

[0084] The hierarchical clustering analysis (HCA) analyzes similarities between groups (FIG. 4B); consistent with observations in the PCA, the top-level separation of the dendrogram distinguished between WT and rAAV Tx samples (on the left) and KO and rAAV samples (on the right), with sub-clusters forming by individual samples by group. It is striking that both the PCA and HCA grouped the WT and rAAV Tx samples together. A high-level assessment of patterns of metabolic changes in the HCA indicates that WT and rAAV Tx tended to show similar trends in a number of metabolites, indicating that rAAV Tx was effective at modulating disease. Many of the observed changes in KO (compared to WT) trended in the opposite direction in rAAV (Tx vs Ctrl), consistent with "rescue" of disease-associated phenotypes. Consistent with the metabolic analysis, FIG. 1 shows that rAAV-ASPA gene therapy restores the thalmo-cortical tract of CD mice, as measured by diffusion tensor imaging for brain water flow.

Neurotransmitter biosynthesis

[0085] Aspartoacylase (ASPA) is responsible for the breakdown of N-acetylaspartate (producing acetate and aspartate). Consistently, N-acetylaspartate (NAA) was increased in KO (compared to WT); treatment with rAAV-expressing ASPA resulted in a decrease in NAA (and increases in aspartate). Curiously, while NAA levels were increased (KO vs WT), the neuropeptide N-acetyl-aspartyl-glutamate (NAAG) was not significantly changed (which could reflect changes in demand or regulation of steady-state pools/pool size). Gamma-aminobutyrate (GABA) was decreased (KO vs WT), which could reflect changes in GABA-mediated signaling (GABA increased in rAAV Tx, compared to rAAV Ctrl).

[0086] Several other neurotransmitters were also detected in the dataset; while acetylcholine and serotonin were not significantly changed in KO (compared to WT), serotonin did show increases in rAAV Tx (compared to Ctrl), which could reflect changes in serotonergic signaling.

Glucose metabolism

[0087] In the absence of disease, energetics in the brain is thought to focus on glycolytic use, with acetyl CoA input into the TCA cycle to support oxidative metabolism and macromolecule biosynthesis. Increases in glucose, glucose 6-phosphate, and an isobar of sugar diphosphates (fructose 1,6-diphosphate, glucose 1,6-diphosphate, myo-inositol 1,4 or 1,3-diphosphate) could indicate changes in glucose use or increased availability.

[0088] Glucose and related molecules (fructose, mannose and myo-inositol) were elevated, though nucleotide sugars (e.g., UDP-glucose, UDP-galactose) were decreased, which could indicate changing biosynthetic demand (KO vs WT). Three-carbon glycolytic intermediates 3-phosphoglycerate (3-PG) and phosphoenolpyruvate (PEP) were also increased; pools for these biochemicals tend to increase as glycolytic use declines.

[0089] Consistent with decreasing glycolytic use, lactate was decreased (with non-significant decrease in pyruvate). Glycogen metabolites (maltotetraose, maltotriose, and maltose) were also increased, reflecting decreased glycolytic use. Changes in energetics reflect declining energy demand (potentially associated with increased neuronal cell death or senescence) or may reflect metabolic effects of NAA accumulation in the brain.

[0090] In rAAV (Tx vs Ctrl), decreases in glucose and related molecules, with increases in lactate, were indicative of increasing glycolytic use. Interestingly, DHAP was elevated in rAAV (Tx vs Ctrl), which could reflect changing use for triglyceride biosynthesis (potentially related to a restoration of lipid biosynthesis, TAGs can be used as a precursor for phospholipids). Representative data relating to glucose metabolism is provided in FIG. 5.

Lipid Metabolism

[0091] Complex lipids, sphingolipids, diacylglycerols, monoacylglycerols, and plasmalogens were all decreased, with decreases in lysolipids, long-chain (e.g., palmitate, palmitoleate, and stearate) and polyunsaturated fatty acids, and longer acylcarnitines (e.g., myristoylcarnitine, palmitoylcarnitine) indicative of changing availability or use to support beta-oxidation (KO vs WT). The ketone body 3-hydroxybutyrate (BHBA) was also elevated in KO (compared to WT), with decreases in malonylcarnitine (a surrogate reporter for malonyl CoA) indicative of a shift toward increased fatty acid beta-oxidation. Increases in BHBA may also reflect changes in liver ketogenesis (or increased brain ketone uptake to supplement energetics).

[0092] Increases in carnitine, deoxycarnitine, and changes in coenzyme A precursors (increases in pantothenate with decreases in 3'-dephosphocoenzyme A and coenzyme A) could reflect changing demand or use (KO vs WT). N-acetylaspartate has been indicated as a key carrier of 2-carbon units to oligodendrocytes for lipid biosynthesis; decreases in lipids could reflect increased demand related to decreased biosynthesis.

[0093] Interestingly, in rAAV (Tx vs Ctrl), increases in malonylcarnitine could imply shifts toward increased fatty acid biosynthesis; metabolites related to phospholipid biosynthesis and

remodeling (e.g., choline, CDP-choline, phosphoethanolamine) were also elevated. Finally, decreases in sphingolipids (e.g., sphinganine, sphingosine, and sphingomyelins) in KO (compared to WT), with increases in serine and threonine, could reflect changing availability for myelin biosynthesis, which has been indicated as one cause of neuronal cell death in Canavan disease; rAAV (Tx vs Ctrl) showed increases in these biochemicals. Representative data relating to lipid metabolism is provided in FIG. 6.

Redox homeostasis

[0094] Changes in metabolites related to glutathione biosynthesis (e.g., methionine, cystathionine, and cysteine) could indicate alterations in redox homeostasis in KO (compared to WT) (FIG. 7). Glutathione (either oxidized or reduced) was decreased, as were related oxidized products (S-methylglutathione and S-lactoylglutathione), likely reflecting decreased glutathione availability. Finally, gamma-glutamyl amino acids tended to decrease as a class (potentially reflecting decreased glutathione and/or amino acid availability); decreases in 5-oxoproline could indicate declining exchange of gamma-glutamyl amino acids to regenerate glutathione. Changes in KO (compared to WT) were indicative of a less robust redox environment; however, significant differences in oxidized lipids (e.g. 4-hydroxy-nonenal-glutathione, 9/13-HODE) and products of methionine or cysteine oxidation (methionine sulfoxide, cysteine sulfinic acid) were not observed. Given the overall decrease in parent metabolites, "similar" levels in KO compared to WT may reflect a relative increase in these products (as a result of increasing oxidative stress). Changes in endogenous antioxidants, such as decreases in vitamin C metabolites (ascorbate, dehydroascorbate and threonate) and dipeptide products of histidine with antioxidant function (anserine (FIG. 7), homocarnosine), and increases in taurine and N-acetyltaurine, could reflect use to balance changes in redox homeostasis. Finally, changes in rAAV (Tx vs Ctrl) were consistent with decreasing oxidative stress (essentially showing inverse changes as those observed in KO vs WT).

Gene therapy in Canavan disease

[0095] While gene therapy in CD patients using intraparenchymal injections of ASPA expression systems was considered safe, it failed to show clinically significant improvements. Similar results were found using acetate replacement.

[0096] Data described herein demonstrate that either intraventricular (e.g., direct injection) or intravenous injection (e.g., systemic) of recombinant adeno-associated virus (rAAV) expressing ASPA can cure Canavan Disease. CD mice administered rAAV expressing ASPA by either intraventricular injection show similar improvement of motor function (FIG. 8). Systemic (e.g., IV) injection of rAAV-ASPA also expands the treatment window. Experimental data indicate that rAAV-ASPA administered intravenously to Nur7 mice (a model of mild CD) as late as 3 months of age results in restoration of mobility (FIG. 9) and improvement of cognitive function (FIG.

10). Further, intravenous delivery of rAAV-ASPA results in rapid and efficient elimination of spongy degeneration of the CNS (FIG. 11) in Nur7 mice receiving treatment at P1. Importantly, intravenous administration of rAAV-ASPA results in rapid reduction of NAA in the brain of Nur7 mice (FIG. 12). Mice were treated at 6 weeks and monitored at 7 and 10 weeks by neuroimaging. Treatment of CD mice with rAAV-ASPA also restores the myelin lipid profile, as evidenced by measurement of sphingolipids in treated and control mice (FIG. 13).

[0097] A crucial finding is that high ubiquitous ASPA expression enhances motor performance in treated CD mice over wild-type mice. This may be the result of enhanced energy metabolism due to direct intervention in the ASPA-mediated metabolism of NAA.

[0098] The results from this global metabolomic study compare WT or aspartoacylase (ASPA) KO brain samples, or KO mice treated with recombinant AAV (to express ASPA or not, as control), including changes in metabolites related to energetics (carbohydrate and lipid metabolism), neurotransmitter production, inflammation, and redox homeostasis. In the principal component analysis (PCA), samples split into two groups, with WT and rAAV Tx in one, and KO and rAAV Ctrl in the other, indicating that rAAV Tx-mediated "rescued" metabolomic effects of ASPA deficiency. Consistent with loss of ASPA function, N-acetylaspartate (NAA) accumulated in brain (KO vs WT), while levels decreased following ASPA re-expression (rAAV Tx vs Ctrl). Lipids tended to show decreases across all classes, which could reflect changes in beta-oxidation and/or biosynthesis (KO vs WT); rAAV Tx (compared to rAAV Ctrl) showed increases in a marker of lipid biosynthesis, with increases in a number of lipid classes. Evidence of declining glycolytic use in KO (compared to WT) was reversed in rAAV Tx (compared to rAAV Control). Finally, changes in the dataset pointed to increasing inflammation and oxidative stress in KO (compared to WT), with decreases in rAAV Tx (compared to Ctrl).

Summary of results

Regarding gene therapy:

[0099] Gene Therapy reverses the metabolic changes in Canavan disease brains.

Regarding Canavan disease pathomechanism and CNS energy metabolism:

[0100]

1. 1. Glucose metabolism in Canavan brains
    1. a. Substrates for glycolysis are abundant in Canavan mouse brains
        1. i. Substrates of glycolysis accumulate (e.g. glucose, glucose-6-phosphate,

3-phosphoglycerate, phosphoenolpyruvate) indicating a decreased rate of glycolysis.

2. ii. Increased phosphoenolpyruvate inhibits the enzyme "triosephosphate isomerase" which decreases the efficacy of glycolysis by utilizing only 50% of each glucose molecule for energy production.
3. iii. Glycogen, the glucose storage system of cells, is being broken down despite the abundancy of glucose in Canavan mouse brains. In a physiologic state, increased glucose leads to glycogen synthesis not break down.

2. b. Products of glycolysis are unchanged or decreased in Canavan mouse brains
    1. i. Pyruvate is unchanged despite the abundancy of glycolysis substrates, which is paralleled by an decrease in lactate. Both indicates that the glycolytic rate is decreased.

2. 2. Fatty acid metabolism in Canavan brains
    1. a. Products of fatty acid break down are changed to favor beta-oxidation (use of fatty acids for energy production).
        1. i. Carnitine is increased in Canavan brains. The transport into mitochondria is the rate limiting step in beta-oxidation. This transport is conducted by Carnitine palmitoyltransferase 1 and 2 (CPT1 and CPT2). Fatty acids need to be bound to carnitine in order to be transported into mitochondria. An increase in carnitine usually facilitates the esterification of fatty acids and carnitine supported fatty acid transport into mitochondria.
        2. ii. Several carnitine esters are increased, decreased or unchanged indicating consumption of fatty acids in Canavan brains.
        3. iii. Several fatty acids are decreased as well in Canavan brains, which might be because of fatty acid consumption for energy production, e.g. ATP or other energy equivalents.
        4. iv. Malonylcarnitine, a surrogate marker for malonyl-CoA is decreased which facilitates fatty acid transport into mitochondria for beta-oxidation (Malonyl-CoA inhibits CPT1 and thus reduces fatty acid transport into mitochondria; a reduction in malonyl-CoA removed this inhibitory stimulus). Malonyl-CoA is also a precursor for fatty acid synthesis and thus mediates between fatty acid break down and fatty acid synthesis. The fact that malonylcarnitine is decreased points towards fatty acid break down.

3. 3. Ketone bodies in Canavan brains
    1. a. The ketone body beta-hydroxybutyrate is increased, which is directly broken down to acetate and feed into the TCA cycle.
    2. b. Beta-hydroxybutyrate also mediates between metabolism and transcription.

4. 4. Acetate in Canavan brains
    1. a. Acetyl-CoA is not changed in the CD neurometabolome, which argues against the "acetate deficiency hypothesis". In addition, it might also explain why acetate supplementation failed to cure Canavan disease in patients.
    2. b. Acetylcarnitine, which has been reported to be crucial in energy production is highly increased and thus facilitates energy production.

5. 5. Antioxidants
    1. a. Some antioxidants were decreased, some increased, which could support the oxidative stress hypothesis. However, there was a significant reduction in metabolites for the synthesis of antioxidants, indicating that the decreased in some antioxidants is an issue of supply rather than demand. This argues against the oxidative stress hypothesis as a primary disease causing factor.

[0101] NAA accumulation and/or ASPA deficiency disrupt the CNS energy metabolism by favoring fatty acids over glucose/lactate for energy production, causing "self-consumption" of fatty acids, critical components of myelin and thus white matter vacuolations and disease pathology.

[0102] NAA metabolic deficiency and/or its causative ASPA deficiency might promote fatty acid over glucose/lactate consumption for energy production.

[0103] NAA metabolism with its associated proteins such as AspA, might be a key player in regulating and communication between metabolic pathways and monitoring metabolic homeostasis of cells and organs, which is demonstrated by the fact that despite the abundancy of glucose, fatty acid metabolism is favored, glycogen is broken down and ketone bodies are formed, which are highly detrimental processes in a physiologic system but not in a state of altered NAA/ASPA metabolism. Also, in addition to be involved in NAA metabolism, AspA may play critical roles in energy metabolism.

[0104] These conclusions are further supported by the fact that rAAV mediated delivery of ASPA corrects these observed changes.

Example 2: Nur7 Mouse Model of Canavan Disease

[0105] A single intravenous (i.v.) injection of recombinant adeno-associated virus (rAAV) expressing human ASPA (hASPA) rescues early lethality and partially restores motor function (1^{st} generation gene therapy) in a CD knock-out (CD KO) mouse, which resembles the congenital sub-form of CD and displays the severest phenotype of all available CD mouse models, with early death at around post-natal day (p) 28.

[0106] This example describes a 3^{rd} generation rAAV expressing hASPA (also referred to as FKzhAspA-Opt), which comprises the sequence represented by SEQ ID NO: 1 and cures disease in a CD KO mouse model. Interestingly, the 3^{rd} generation gene therapy turns CD KO mice into "supermice", that outperform wild-type (WT) mice on rotarod motor function test. This rescue is persistent- treated mice assessed at 1.5 years of age still show no signs of disease reoccurrence. CNS pathology and magnet resonance imaging (MRI) at p25 and p365 show

complete normalization.

[0107] To further support the efficacy of the 3rd generation gene therapy, neurometabolome profiling was performed. Data indicate that over 400 characterized metabolites that showed reversal of the Canavan disease related metabolic changes including myelin associated lipids. Transcriptomic profiling was also performed.

[0108] To further evaluate the potency of the 3rd generation gene therapy, different doses and routes of administration were tested. Of note, 200-fold lower doses intraventricularly (ICV) administered rAAV still rescues lethality, while mice treated ICV with 20-fold reduced dose draw even with WT mice on motor function testing.

[0109] Next, the Nur7 mouse model, which resembles infantile and juvenile sub-form of CD, was tested. This model displays a similar disease pattern as the CD KO mouse with respect to growth curve and neurologic symptoms but eventually re-gains weight and shows survival similar to wild-type mice (FIG. 14). Again, mice received a single i.v. dose of rAAVhASPA at p1 (gold standard positive control) and subsequent groups were dosed at 6, 12, and 24 weeks of age with a dose 10-fold higher than that for neonates to determine the therapeutic window. Of note, mice treated at 6 weeks of age recovered within 4 weeks post-treatment. Mice treated later than 6 weeks require more time to recover but still showed significant improvement over Nur7 mutants (FIG. 15). This recovery was also correlated by CNS pathology and MRI.

[0110] Motor function was tested for all mice 4 weeks after treatment and subsequent intervals up to one year of age for direct comparison (FIGs. 16 and FIG. 17). Generally, the earlier mice were treated, the better the therapeutic outcome. Surprisingly, juvenile mice at 6 weeks of age recovered completely within 4 weeks post-injection (FIG. 16 and FIG. 17). Although mice treated at 3 months of age and older did not respond immediately within the first 4 weeks post-treatment, they eventually showed significant improvements over Nur7 mutant control mice. Cognitive function was also tested; representative data are shown in FIG. 18. Of note, cognitive function testing revealed that treated mice recover cognitively before motor function improves; this was even true for late treatment time points. Furthermore, response to rAAVhASPA gene therapy was confirmed via MRS for N-acetyaspartate, MRI, and neuropathology (FIGs. 19-21).

[0111] Overall, data demonstrate that rAAV mediated hASPA expression of the 3rd generation gene therapy vector not only prevents but also rescues the clinical manifestation and pathology of the juvenile and adult model of Canavan disease at an unprecedented level, which might have implications for other CNS disorders that require treatment in later stages of life. In addition, this is confirmed on different levels of cellular complexity by MRI, fMRI, CNS pathology, and neurometabolic profiling.

Example 3: Astrocyte-restricted hASPA expression in CD KO mice (severe phenotype)

[0112] Several tissue/cell-specific expression cassettes configured for restricting hASPA expression to either astrocytes, neurons, oligodendrocytes, liver, heart, or muscle were produced. For example, a rAAV-hASPA construct comprising an astrocyte-specific glial fibrillary acidic protein (GFAP) promoter was produced. Tissue-restricted rAAV were administered to Canavan disease knock-out (CD KO) mice. Surprisingly, mice expressing hASPA restricted to peripheral organs showed extended survival and normalization of the growth curve at later time points, indicating a contribution of peripheral organs to the disease pathomechanism.

[0113] Astrocyte-restricted hASPA expression produced the strongest disease recovery matching the performance of wild-type (WT) mice (FIGs. 22-24). FIG. 22 shows astrocyte-restricted expression of hASPA results in survival and growth of treated CD KO mice compared to untreated control mice. FIG. 23 shows astrocyte-restricted expression of hASPA results in restoration of motor function in treated CD KO mice, as measured by rotarod test at p27 and p90. FIG. 24 shows astrocyte-restricted expression of hASPA results in restoration of motor function in treated CD KO mice, as measured by balance beam test at p27 and p90.

[0114] A lower dose of rAAV-hASPA was administered to mice via localized brain injections. Data indicates localized T2 hyper-intensity signal clearance on MRI was well correlated with reduction of NAA levels by MRS (FIG. 25). In other words, the further away from the injection site, the higher the NAA levels, which supports the idea of drainage and hydrolytic activity of NAA towards the injection side. Currently, we are investigating this metabolic sink theory in more detail by creating a functional map of therapeutic gene transfer in the brain by mass spectrometry quantification of NAA, and vector genome and ASPA transcripts analyses in different anatomic regions.

[0115] Overall, data indicate that hASPA expression does not have to be restored in oligodendrocytes in order to rescue lethality and Canavan disease phenotype.

Example 4: High-field in Vivo Neuroimaging

[0116] Gene therapy targeting the central nervous system (CNS) is one of the most challenging gene therapies due to the blood-brain barrier (BBB). One obstacle in the monitoring and evaluation of CNS gene therapy is the non-invasive evaluation of therapeutic outcome. While biopsies and sections of the CNS are the gold-standard to assess brain pathology and response to CNS gene therapy, the invasiveness and potentially associated complications limit its frequent use in pre-clinical as well as clinical studies.

[0117] This example describes high-field *in vivo* neuroimaging to monitor intravenously (i.v.) and intracerebroventricularly (i.c.v.) administered rAAV-based CNS directed gene therapy in a mouse model of Canavan disease (CD). Characteristically, Canavan disease presents with a very high NAA peak detected by magnet resonance spectrometry (MRS) and hyper intensity on T2-weighted anatomic images using magnet resonance imaging (MRI). Consequently, the

efficacy of i.v. and i.c.v. gene therapy by those two means was evaluated. In congruence with motor function and pathology data described elsewhere in the disclosure, both MRI and MRS alterations have been entirely normalized by gene therapy.

[0118] Another characteristic neuropathological change on Canavan brain sections is the loss of white matter tracts, which is thought to explain neurological symptoms seen in Canavan disease patients. The ability of diffusion tensor imaging (DTI) to enable the assessment of white matter tract degeneration and recovery upon gene therapy without brain biopsies was investigated. Selecting thalamus and corpus callosum as regions of interest (ROI), DTI shows a recovery of brain white matter integrity when utilizing 3rd generation Canavan gene therapy (e.g., FKzhAspA-Opt, SEQ ID NO: 1). Furthermore, the 3rd generation gene therapy converts this CD mouse model with the severest phenotype into "supermouse", outperforming wild-type mouse on motor function testing.

[0119] Functional connectivity identifies brain regions that not only show response to treatment but also indicates possible explanations for this enhanced phenotype. Using resting-state functional MRI (rs-fMRI), it was shown that treated CD mice have a functional connectivity pattern that is more similar to, or even enhanced beyond, what is seen in WT brain. This indicates facilitated inter-brain-region functional connectivity, might provide a neural mechanism that sub-serves the observed enhanced motor function.

[0120] In summary, imaging data show that high-field *in vivo* neuroimaging is a valuable tool to monitor pre-clinical CNS gene therapy and pathology in detail, that it can provide insights into pathophysiology and that it has potential implications for the use in clinical trial outcome prediction and assessment.

Example 5: Redirecting N-acetylaspartate metabolism in the central nervous system normalizes myelination and rescues Canavan disease.

Materials and Methods

Animal procedures

[0121] Heterozygous Aspa +/- mice in a Sv129 background were bred and newborns were genotyped on the day of birth. Briefly, 1 mm tail tips were cut and genomic DNA was extracted according to manufacturer's protocol using either manual QIAamp DNA mini kit or QIAcube robot (Qiagen, Hilden, Germany). DNA extraction was followed by quantitative PCR (qPCR). Injections were performed on P1 via the right facial vein at either 4×10^11 (~ 2.6×10^14 vg/kg; based on average 1.5g weight), 1.33×10^11 (~ 8.8×10^13 vg/kg; based on average 1.5g weight) or 4×10^10 (~ 2.6×10^13 vg/kg; based on average 1.5g weight) genome copy (GC)

number. After every procedure, pups were cleaned with 70% ethanol and rubbed with bedding material. The parent animal was returned after brief nose numbing with 70% ethanol. Vg = viral genomes

Viral production and vector design

[0122] Recombinant adeno-associated virus (rAAV) was produced by transient HEK 293 cell transfection and Cesium-chloride (CsCl) sedimentation. Vector preparations were titered by quantitative PCR, and purity was assessed by 4-12% SDS-acrylamide gel electrophoresis and silver staining (Invitrogen, Carlsbad, CA). Morphological integrity of virions was assessed by transmission electron microscopy of negative stained rAAV. Due to packaging size restrictions, single stranded rAAV genome was used for the phGFAP-hASPA and phGFAP-EGFP constructs. All other vectors were self-complementary (sc) AAV vectors (scAAV).

Western blot

[0123] Protein was extracted using RIPA buffer. Protein quantification was performed by BCA assay (Pierce Biotechnologies, Rockford, IL, USA) and 10-20 µg of total protein mixed with 4X Laemmli buffer (BioRad, Hercules, CA, USA) were loaded onto a 10-12% Tris-HCl acrylamide gel (BioRad, Hercules, CA, USA). After electrophoresis, protein was blotted on a nitrocellulose membrane (BioRad, Hercules, CA, USA) with the Trans-Blot Turbo Transfer System (BioRad, Hercules, CA, USA). Subsequently, membranes were subjected to blocking at room temperature for at least one hour with Odyssey Blocking Buffer (Licor, Lincoln, NE, USA). Next, membranes were incubated with primary (anti-ASPA, 1:2000, ab 97454; anti-Actin, 1:5000, ab8224) antibody at 4°C overnight and incubated with secondary antibody (Licor, Lincoln, NE, USA) the next day. The membranes were analyzed with Odyssey analyzer (Licor, Lincoln, NE, USA). Quantification was performed using ImageJ.

Isolation of brain regions and DNA and RNA extraction

[0124] Mice were anesthetized with isofluorane and transcardially perfused with ice-cold phosphate buffered saline (PBS). Next, brains were removed and divided in half along the interhemispheric cleft. One brain half at a time was placed on an RNase free and ice-cooled plate under a dissection microscope. First, the olfactory bulb was removed using a cold razor blade. Next, the brain stem/midbrain was removed along the line between the cortex/thalamus and the lamina tecti. The brainstem was further subdivided into midbrain, lamina tecti, cerebellum, and brain stem. Furthermore, the thalamus/hypothalamus was removed using Wecker Micro Dissecting Spatula (Roboz Surgical Instruments Inc., Gaithersburg, MD, USA). The hippocampus was removed. Finally, part of the cortex was removed with a fresh razor blade. All samples were snap frozen immediately after removal.

[0125] DNA and RNA were extracted using the Qiagen Allprep DNA/RNA Mini kit (Qiagen, Hilden, Germany) and RNA samples were subjected to on column DNase treatment before RT-PCR. DNA was subjected to viral genome copy number determination and total RNA for RT-PCR (High Capacity cDNA Reverse Transcription kit, Applied Biosystems).

Droplet digital PCR (ddPCR)

[0126] Multiplex ddPCR was performed on a QX200 ddPCR system (Bio-Rad, Hercules, CA). All assays were based on TaqMan probes, where the gene of interest probes were labelled with FAM and the reference gene as VIC. Bio-Rad ddPCR mastermix with no dUTP was used (BioRad 1863024) for all ddPCR reactions.

Vector genome copy number

[0127] DNA was digested with BamHI at >10U/µg of DNA at 37C for 1 hour. The BamHI digest ensured single copies of rAAV genomes. All vectors contained a RBG sequence, which was targeted for viral genome quantification. Viral genome numbers were normalized to the number of diploid cells by using transferrin receptor (Tfrc) as the reference gene (Invitrogen, 4458367).

Motor function and spatial memory testing

[0128] Mouse motor performance was assessed using accelerated rotarod for motor function and endurance, balance beam for vestibular function and ataxia, and inverted screen for grip strength. For each motor function test, n=8 mice were injected and tested independently.

Accelerated rotarod

[0129] Mice were trained two days before the testing day for three runs each. On the testing day, mice were placed on the rotarod to acclimate for 1 minute. Each mouse was tested three times and the best value was used for analysis. The acceleration and timing was set to 4 - 40 rpm over 5 minutes.

Balance beam

[0130] To increase the stringency of this test, the cut-off time was increased from 3 minutes to

5 minutes. Mice were placed in the middle of the balance beam and the latency until drop off was measured. Again, the best value was counted.

Inverted screen

[0131] Mice were placed in the center of a grid (30 cm2 with 25 mm2 holes) in horizontal position and allowed to acclimate for 1 minute. Grid was turned slowly within 15 seconds to 125 degrees so that the mouse was hanging upside-down. Time was measured until drop off. The cut-off for p28 testing was 3 minutes. At all other time points, the cut-off was 5 minutes to increase the stringency of the test.

T maze

[0132] T-maze testing was done in a spontaneous, unrewarded manner, with all arms of the T-maze open during testing. Mice were placed within the initial chamber with the door down, and the side-arm doors open for 10s, upon which the initial chamber's door was opened, and the mice were allowed to enter and explore the T-maze. Upon the complete entry of the mouse into one of the side arms, defined as all four of the paws having passed through the edge of the arm, all doors of the T-maze were closed, and the mouse was returned to the initial chamber for a 10s resting time. During this 10s, the side arm doors were re-opened. This process was repeated 10 times, which provides the mouse with a total of 10 opportunities to alternate their side-arm choice. The final result is expressed as a ratio of the number of alternations over 10.

H&E and Luxolfast blue staining

[0133] Mice were euthanized and perfused transcardially with ice-cold PBS and 4% paraformaldehyde (PFA). Tissues were removed and sliced using an Alto brain or spinal cord matrix (Roboz Surgical Instruments Inc., Gaithersburg, MD, USA). Subsequently, mouse tissues were stored in PFA at 4°C overnight. Paraffin embedding, Hematoxilin & Eosin (H&E), and Luxol fast blue staining was performed. Stained sections were analyzed and pictures taken with an Axioscope 50 (Zeiss, Jena, Germany) using a DMC2900 camera (Leica Microsystems, Wetzlar, Germany).

Magnetic resonance imaging (MRS) and spectroscopy (MRS)

[0134] Mice were anesthetized with 2% isofluorane and constantly monitored for vital signs during the entire time of imaging. P42 mice were imaged with a 4.7T/40cm horizontal magnet (Oxford, UK) equipped with a Biospec Avance Bruker console (Bruker, Germany). Experiments

for all other imaging was performed using a 4.7T/40cm horizontal magnet (Oxford, UK) equipped with a Biospec Avance III HD Bruker console (Bruker, Germany). A ^{1}H radiofrequency mouse head coil (Bruker, Germany) with inner diameter of 23mm was used for the experiments.

[0135] T1-weighted anatomical images were acquired using FLASH sequence with the following parameters: repetition time (TR) = 280.86ms, echo time (TE) = 4.5ms, matrix size = 384x384, field of view (FOV) = 18×18mm^2, slice number = 15, slice thickness = 0.5mm, flip angle = 40°, number of averages = 8. T2-weighted images were acquired using TurboRARE sequence with TR = 2200ms, TE=36ms, echo spacing = 12ms, 8 averages, and rare factor = 8. ^{1}H magnetic resonance spectroscopy data were acquired using single voxel PRESS (Pont Resolved Spectroscopy Sequence) (repetition time = 2,500 ms, echo time = 16 ms, number of averages = 512, voxel size = 3×3×3mm). Functional MRI images were acquired for 10 minutes using echo planar imaging (EPI) sequence, with TR=1000ms, TE=18ms, matrix size = 96x96, FOV = 18×18mm^2, slice number = 15, slice thickness = 0.5mm, number of repetitions = 600. Diffusion tensor imaging (DTI) data were acquired from 30 directions with B value of 650/0, TR=2300ms, TE=21ms, number of averages = 4, with the same geometry parameters as EPI.

^{1}H magnetic resonance imaging and spectroscopy study.

[0136] Proton spectra were fit using LCModel (Version 6.2-2B) which analyzed *in vivo* proton spectrum as a linear combination of model *in vitro* spectra from individual metabolite solutions (Provencher, 2001) and generated data as absolute fits (in institutional units) and SD%. SD was used as a measure of the reliability of the fit. The spectral inclusion criteria were SD <20% for NAA, creatine, and inositol.

Resting state functional connectivity (rsFC) analysis

[0137] EPI images were preprocessed using Medical Image Visualization and Analysis (MIVA, http://ccni.wpi.edu/) and Matlab 2010b (the Mathworks Inc.). All EPI images were first registered to a standard anatomy, where seed regions were defined. After registration, all EPIs went through motion correction, spatial smoothing (full-width-half maximum = 1mm), and 0.002-0. 1Hz band-pass filtering. Seed-based rsFC was calculated using previously demonstrated algorithm.

Diffusion Tensor Imaging (DTI)

[0138] DTI data were analyzed using DTIstudio (www.mristudio.org/, Susumi Mori and Hangyi Jiang, Johns Hopkins University), including eddy current correction, motion correction, and

generation of all tensor metrics (FA and eigen decomposition of the voxel-wise diffusion tensor). FA values in particular regions of interest (ROIs) were extracted from manually drawn ROIs.

[0139] For all imaging results, group comparisons were carried out by one way ANOVA, with a significance threshold of $p<0.05$.

Immunohistology

[0140] Mice were perfused transcardially with 4% paraformaldehyde (PFA) and kept in PFA overnight at 4°C. The next day, brains were extracted and subjected to gradient sucrose steps (10, 20 and 30%) overnight at 4°C. Brains were mounted in O.T.C. compound (Fisher HealthCare, Houston, TX, USA) and stored at -80°C until cryosectioning (Cryostar NX70, Thermo Fisher Scientific, Walldorf, Germany). Floating brain slices were washed in 1XPBS 3X for 5 min each. Cells were permeabilized with 1XPBS and 0.5% Triton-X 100 at room temperature for 1 hr, with subsequent blocking for 1 hr at room temperature with 5% serum (10% normal goat serum, Life technologies, 50062Z). Brain slices were incubated with primary antibodies (anti-GFAP, EMD Millipore, 1:1000, MAB360; anti-MBP, Abeam, 1:1000, ab40390) in 1.5% serum overnight at 4°C, washed the next day (1xPBS, x3, 5 min each), and stained with secondary antibody in 1.5% serum at room temperature for 1 hr (anti-mouse or rabbit; Invitrogen, A-11031 or A-11011). Slices were mounted using Vectashield with 4', 6-diamidino-2-phenylindole (Vector Laboratories, Burlingame, CA).

[0141] Brain sections were imaged and recorded using DM 5500B Upright microscope (Leica Microsystems, Wetzlar, Germany) and Leica DFC365 FX digital camera.

Software and statistics

[0142] Image analysis and displaying was done using Imaris 8.2 Software (Bitplane Inc., South Windsor, CT, USA). Western blots were quantified using ImageJ (National Institute of Health, USA). Graphs were analyzed and statistical calculations were performed in GraphPad Prism 7 (GraphPad Software, Inc., La Jolla, CA, USA). Correlation between overall functional connectivity on fMRI to mean of accelerated rotarod performance was calculated and linear regression analysis was performed using GraphPad Prism 7. Statistics were performed using GraphPad Prism 7, two-way ANOVA with multi-comparison correction (Turkey) for weights, and one-way ANOVA with multi-comparison correction for all other statistics, if not stated otherwise. If not otherwise states at least n=3 mice were analyzed.

Transgene cassette optimization achieves a rapid therapeutic response in Canavan mice

[0143] To overcome the challenge of efficacy and sustainability of a 1st generation gene therapy, hASPA expression from the vector genome was increased without changing the parameters of administration route, vector dose, or serotype. Comparing the effect of Kozak sequence and cDNA optimization, two new expression cassettes with either a half or full Kozak sequence and a codon-optimized cDNA were designed and named 2nd and 3rd generation vectors (FIG. 26A; hereafter referred to as 2nd or 3rd generation), respectively. In order to test the translatability *in vivo*, each of the expression cassettes was packaged into the highly CNS-tropic rAAV9 vector for intravenous gene delivery to the CNS. Untreated and 1st generation treated mice displayed the characteristic low weight at around p14-16 (FIG. 27). However, 2nd and 3rd generation treated mice (n=10 each) paralleled wild-type (WT) weight gain, indicating a more rapid onset of therapeutic transgene expression levels (FIG. 27). To evaluate neuropathology in the living mice, MRI was performed at p42 for treated and p28 for untreated animals. While untreated and 1st generation treated mice showed strong hyperintense signals (white signals) on T2 sequence, particularly in deeper brain regions, the signals appeared isotense (unremarkable) in the 2nd and 3rd generation vector treated groups (FIG. 28), indicating normalization of brain edema. This therapeutic effect was corroborated by normalized NAA levels in the 2nd and 3rd generation treatment groups on MRS, which also coincided with ASPA protein expression levels (FIGs. 26B-26C). Finally, mice were assessed for neurohistopathology at p25. Again, the 1st generation treated mice still showed vacuolization of the CNS, although to a lesser extent than untreated mice. In contrast, 2nd and 3rd generation treated mouse brains were indistinguishable from WT, demonstrating that the improved gene therapy effectively mitigates neuropathology (FIG. 29).

3rd generation treated Canavan mice sustainably outperform control animals

[0144] CD KO mice recapitulate the clinical phenotype of Canavan patients, presenting with ataxia, dysbalance, muscle weakness, and cognitive impairment within the first month of life. It was observed that at 1 month of age, 2nd generation treated CD mice performed as well as WT controls on accelerated rotarod (FIG. 30A). The 3rd generation treatment group displayed a "supermouse" phenotype, significantly outperforming WT mice for the entire 1 year duration of the study (FIG. 30A and FIG. 31). In order to assess ataxia and the ability to balance, 2nd and 3rd generation treated mice were evaluated on balance beam, showing full recovery as well (FIG. 30B and FIG. 31). This was paralleled by the performance on inverted screen and was persistent throughout the study (FIG. 30C and FIG. 31). Finally, to determine the long-term ability to rescue spatial/working memory, mice were tested on T maze at 1 year, performing as well as WT control mice (FIG. 32).

Efficient hASPA gene delivery to the CNS persistently eliminates neuropathology and

normalizes NAA levels

[0145] To determine if the phenotypic rescue of psychomotor function was supported by brain pathology and NAA biomarker levels, living mice from all three treatment groups were assessed at 1 year of age. First, T2 MRI showed strong hyperintensities of 1st generation treated mice, particularly in the thalamus, midbrain, and cerebellum (FIG. 33A). In contrast, 2nd generation treated mice showed mild increased T2 signals in the midbrain, appearing otherwise similar to WT mice. Importantly, comparison between WT and 3rd generation treated mice revealed no difference on T2 MRI, which was also supported by neuropathology analysis (FIG. 33B). While some regions of the CNS (e.g., thoracic spinal cord) showed similar patterns between WT and all three treatment groups, the brain regions with the strongest T2 signal also corresponded with the most severe vacuolization in the brain sections of 1st generation treated mice (FIGs. 33A-33B and FIG. 34). When 1-year-old mice of all treatment groups were subjected to MRS for NAA quantification, 1st generation treated mice showed a significantly higher NAA signal than WT mice, while NAA levels of 2nd and 3rd generation treated mice were normalized (FIG. 33C). This strongly indicates that the new generation gene therapies are significantly more efficacious and are able to normalize NAA biomarker levels, a finding which is further supported by normalized NAA levels in urine, as measured by mass spectrometry (FIG. 33D).

Astrocyte-specific ASPA expression is sufficient for generating the "super-mouse phenotype"

[0146] The way in which the 3rd generation gene therapy accomplished performance enhancement beyond WT control animals was investigated. No reported phenotypic differences were observed between patients who are heterozygous or homozygous for the WT ASPA allele, implying that oligodendroglial ASPA and its associated NAA catabolism might not cause dose-dependent behavioral variations within the physiological range. In addition, most rAAVs including rAAV9 poorly transduce oligodendrocytes. Thus, in some embodiments, hASPA transgene expression from non-oligodendrocyte glial cells contributes to the "super-mouse" phenomenon seen on accelerated rotarod. To test whether WT mice respond to ASPA supplementation with increased motor performance, WT animals were treated with 3rd generation gene therapy. Initially, treated WT mice showed no difference on accelerated rotarod at p28, but began significantly outperforming untreated WT controls at p90 to 1 year of age, indicating that supplementing the non-ASPA-expressing cells with ASPA by gene transfer contributes to the observed "enhanced" phenotype (FIG. 35).

[0147] To further define the CNS cell type contributing to the "super-mouse" phenotype, the 3rd generation hASPA construct was paired with a partial human glial fibrillary acidic protein

(phGFAP) promoter. First, the astrocyte specificity of the phGFAP promoter was confirmed by expressing enhanced green fluorescence protein (EGFP), which showed co-localization with glial fibrillary acidic protein (GFAP) positive cells, but not with myelin basic protein (MBP) positive cells (FIGs. 36A-36B). Next, neonatal CD KO mice were treated with rAAVphGFAP-*hASPA*-Opt. Treated mice displayed the same growth curve as the group treated with ubiquitously expressed 3rd generation gene therapy (FIG. 36C). The performance of these mice on accelerated rotarod was significantly increased over WT mice at all testing time points (e.g., p27 and p90), similar to what was seen with the 3rd generation vector for ubiquitous hASPA expression (FIG. 36D). This data indicates that astrocyte-restricted hASPA expression contributes substantially to the enhanced performance on accelerated rotarod. It was observed that other less stringent motor function tests did not show a difference compared to WT mice (FIG. 36D). Importantly, rAA VphGFAP-*hASPA*-Opt treated mice performed better than untreated control mice on T maze, but showed no difference in spatial/working memory function vs. WT animals (FIG. 36E and FIG. 32). This indicates that mice with increased motor performance have normal spatial/working memory function on T maze testing. In addition, MRI and MRS showed normalization of T2 signals and NAA levels in the brains of mice receiving astrocyte-specific gene therapy (FIGs. 36E-36F), indicating that astrocyte-restricted hASPA expression alone is capable of creating an alternative metabolic sink for NAA and is rescuing neuropathology and biomarker expression in the CD mice. To corroborate that astrocyte-restricted hASPA expression can indeed rescue neuropathology, e.g., improve myelination, brain sections were stained with Luxol fast blue for myelin sheaths. The staining pattern was indistinguishable between WT, astrocyte-restricted, and ubiquitously expressed 3rd generation gene therapy treated animals, and in all cases myelination was recovered compared to untreated CD KO mice (FIG. 36I).

Optimized gene therapy achieves efficacious rescue of the Canavan phenotype at lower doses

[0148] One important aspect in translating gene therapy into the clinic is the vector dose, which is relevant to manufacturing burden, costs, and safety. Based on the performance of mice treated with a full-dose of hASPA construct, *e.g.,* 4×10^{11} genome copies (GCs)/animal, 3rd generation gene therapy, 3-fold (1.33×10^{11} GC) and 10-fold (4×10^{10} GC) lower doses were then tested to compare their therapeutic outcomes. Within the first 4 weeks of life, 3- and 10-fold lower 3rd generation treated mice showed significantly better weight gain than full-dose and 3-fold lower 1st generation treated mice (FIG. 27 and FIG. 37). This was further shown over the course of the entire study period for the 3-fold lower dose 3rd generation group, which paralleled the weights of WT animals. In contrast, 3-fold lower dose 1st generation treated mice declined starting at 16 weeks of age (FIG. 37). Again, the study mice were subjected to MRI and MRS for *in vivo* CNS assessment, but at an earlier time point (p25). T2 sequences showed hyperintensities particularly in thalamus, midbrain, cerebellum, and brain stem of untreated mice (FIG. 38A). This signal was reduced in a dose-dependent manner with the 3-fold lower

dosing group showing the least hyperintense signal. As a control, WT and full-dose treated CD mice showed normalized T2 signals and were indistinguishable from each other (FIG. 38A). The MRI findings from the dose down-escalation study were also reflected in the NAA quantification by MRS (FIG. 38B). This was further supported by neuropathology analysis, showing a dose-dependent distribution of vacuoles with a similar pattern in 1st generation full-dose treated mice and 10-fold lower 3rd generation treated mice (FIG. 38C and FIG. 39). Finally, mice were tested on accelerating rotarod, balance beam, and inverted screen. At p27, 10-fold lower 3rd generation treated mice performed as well as WT mice on rotarod and balance beam, but not as well on inverted screen test (Fig. 38D). Over time, this low-dose treatment group showed deterioration of motor function by p90. In contrast, at p27, 3-fold lower dose could restore the motor functions of CD KO mice to the levels of WT mice, as measured by all three aforementioned tests. By p90, these mice were still performing as well as WT mice on accelerating rotarod and balance beam, but not on inverted screen (FIG. 38D). These data indicate that the 3rd generation gene therapy is significantly more potent, even at lower doses, than our 1st generation gene therapy.

CNS region specific rAAV genome distribution profile coincides with regional neuropathology

[0149] Since it was observed that expression cassette optimization correlates with higher hASPA protein expression (FIG. 26B), 11 CNS regions were analyzed to obtain further insight into CNS region specific pathology and rAAV transduction. No significant differences in vector GC number per diploid cell between full-dose 1st and 3rd generation treatment groups were detected, indicating that increased hASPA protein expression from the optimized expression cassette, but not improved vector genome delivery, was responsible for the significant therapeutic improvement of the 3rd generation treated mice (FIG. 26B and FIG. 40). When regional distribution of vector genome was ranked, cortex showed the highest and cerebellum the lowest rAAV GC number per cell (FIG. 40). In relation to neuropathology, this indicates that certain brain regions have different therapeutic thresholds to achieve complete mitigation (FIG. 33A-33D and FIG. 34). Particularly the cerebellum showed minimal response comparing full-dose 1st generation to 10- and 3-fold lower dose 3rd generation gene therapy (FIG. 39). However, upon full-dose 3rd generation treatment, complete rescue was achieved with rAAV GC numbers lower than in any other CNS region (FIG. 39 and FIG. 40).

High field neuroimaging enables noninvasive monitoring and prediction of therapeutic outcomes

[0150] One aspect of CD is the loss of myelin structures in the CNS. The myelin stain luxol fast blue showed widespread vacuoles and reduced myelin in untreated CD KO mice (FIG. 41). In

contrast, myelin structures in WT and full-dose 3rd generation treated mice were indistinguishable (FIG. 41). To evaluate if these findings can be monitored in the living mouse, high-field DTI was applied to assess myelin fiber tracts in the corpus callosum (CC) and the external capsule (EC). Tractography to obtain an overall assessment of fiber tract morphology showed substantially altered and shortened interhemispheric tracts of the CC in untreated mice, whereas WT and 3rd generation treated mice were indistinguishable (FIG. 42A). For quantitative assessment, fractional anisotropy (FA) values of the CC and right and left EC were compared between groups. While there was no significant difference between WT and treated mice, untreated mice differed significantly, supporting the tractography data and indicating the value of DTI for non-invasive CNS gene therapy assessment (FIG. 42B).

[0151] Resting state-functional MRI (rs-fMRI) was performed on groups of WT, untreated, and treated male mice to determine whether ubiquitous ASPA expression changes functional connectivity. A total of 19 different brain regions were analyzed (FIG. 43). Based on T score analysis, the most active brain regions were observed in untreated mice, with decreasing activity in WT and treated mice, indicating that the ASPA-deficient brain might have to engage more brain regions at baseline (FIGs. 42C-42D). Thus in some embodiments, ubiquitous ASPA expression in the brain facilitates the communication between brain regions and thus engages fewer brain regions at baseline (FIGs. 42C-42D). Correlation analysis between the average number of active brain regions and accelerated rotarod results revealed a negative correlation between overall functional connectivity and accelerated rotarod motor function, indicating that rs-fMRI supports the correlation between treatment and motor performance (R^2 = 0.89; FIGs. 42D-42F).

Example 6: NAA levels correlate with T2 Signal Intensities

[0152] Mice were treated IV at Juvenile Age and monitored for four weeks by MRI/MRS. Brain NAA levels and corresponding T2 MRI sequences indicate that hyperintense signal decrease when NAA levels decrease in mice treated at 6 weeks of age (FIG. 44). This indicates that neuroradiologic correlates of pathology can be reversed when treated after the onset of pathology.

Example 7: Restoration of myelin after hASPA gene therapy treatment

[0153] Six-week old ASPA deficient mice (juvenile) show a disrupted axon and myelin structure (FIG. 45, left). Four weeks after treatment, treated mice show a axon pattern and myelination indistinguishable to wild-type mice, indicating reversal of neuropathology (FIG. 45, right).

[0154] Mice were treated at 6 weeks of age and sacrificed at 7 or 10 weeks of age for electron microscopy analysis of the anterior commissure. G-ratio is describes the ratio of inner over outer axon diameter and is indicative of myelin and axon thickness. The lower the value, the

more myelin is present. Data indicates that at 7 weeks of age untreated mice (Nur7) have a significantly higher g-ratio than wild-type mice; this is also found for mice one week after treatment (FIG. 54). After 4 weeks of treatment (10 weeks of age), treated mice show a significantly lower g-ratio than untreated mice suggesting an increase in myelin thickness, most likely due to re-myelination (FIG 54).

Example 8: Expanded Therapeutic Window Data

[0155] FIGs. 46 and 47 show data relating to the expanded therapeutic window for treatment of a mouse model of CD in males (FIG. 46) and females (FIG. 47). Improved performance on the rotarod was observed in treated Nur7 mice compared to untreated Nur7 mice at 52 wks of age, indicating that ASPA gene therapy is capable of reversing CD pathology.

[0156] FIG. 48 shows that working/spatial memory is restored after treatment with the 3rd generation hASPA gene therapy construct in Nur7 mice.

Example 9: Gait analysis data

[0157] CatWalk testing was conducted with the CatWalk XT system from Noldus, in a darkened room. Mice were placed within the CatWalk system, and allowed to freely walk towards the other end of the CatWalk tunnel. The attached computer records the paw prints and their associated time of contact with the illuminated floor, which are then used for the various calculations that generates the data presented. The mice are required to run for at least 5 complete runs within the CatWalk, and in between each run, the mice are able to turn around for the next run.

[0158] Gait analysis data indicates a therapeutic benefit for mice treated with ASPA gene therapy at 6 months and earlier (FIG. 49). Furthermore, gait analysis reveals that mice treated at mature adult age (p168) still benefit from gene therapy treatment (FIG. 50).

Example 10: Additional metabolomics data

[0159] This example describes real-time analysis of increased metabolic activity and oxygen consumption of ASPA deficient cells (HEK). Data were generated on a Seahorse XF24 system (Agilent) using about 50,000 cell/well. Each samples was run as triplicate or quadruplet. For metabolic analysis the XF Mito Fuel Flex Test (Agilent) or XF Cell Mito Stress Test (Agilent) were performed.

[0160] The Mito Stress test was performed on WT on CRISPR-generated ASPA deficient HEK cells. Data indicates that the overall metabolic activity is increased in ASPA deficient cells

(FIGs. 51 and 52). Increased basal respiration, which indicates increased oxygen consumption was observed (see Table 3).

Table 3

	ASPA -/-	ASPA -/%	WT	WT %	Oligo WT	Oligo WT %
Basal respiration	356.1	25.9	240.1	26.9	409.2	20
ATP Production	181.9	13.2	139.1	15.6	335.7	16.4
Maximal Respiration	391.6	28.5	254.9	28.6	676	33.1
Proton Leak	174.2	**12.7**	35.5	4	73.5	3.6
Non-Mitochondrial Respiration	237.1	**17.2**	103.6	11.6	283.9	13.9
Spare Capacity	35.4	**2.6**	118.4	13.3	266.8	13

In addition, it was observed that ASPA deficient cells produce more ATP. For example, FIG. 52 shows data of the Mito stress test comparing ASPA deficient and wild-type HEK cells and human oligodendrocytes. The data indicates that oligodendrocyte wild-type cells have a similar percentage energy production profile as HEK wild-type cells. For example, HEK ASPA deficient cells have an reduced percentage of "spare capacity" or an increased percentage of "proton leak". In contrast, HEK wild-type and oligodendrocytes show a much more similar pattern. Interestingly, ASPA deficient cells have increased non-mitochondrial respiration, indicating that metabolic processed outside the mitochondria are increased as well. All data point shown are statistically significant with at least n=3 biological replicates.

[0161] A Mito flex test was also performed. FIG. 53 shows data indicating that ASPA deficient cells use more Fatty acids and Glutamine for energy production. FIG. 53 also shows data relating to the dependency, flexibility and capacity of wild-type or ASPA deficient cells to use glucose (GLC), glutamine (GLN) or fatty acids (FA) for energy production. Data indicates that ASPA deficient cells rely less on glucose for energy production than non-ASPA deficient cells. In contrast, ASPA deficient cells depend more on fatty acid oxidation to generate energy. Interestingly, the flexibility to use either glucose or FA is higher in ASPA deficient cells. However, the capacity to use glucose is reduced in ASPA deficient cells overall. Finally, ASPA deficient cells rely on glutamine for energy generation.

[0162] In general, these data are consistent with the metabolome data of mouse brain (described in Example 1 and in FIGs. 55 and 56), where ASPA deficient brains rely on FA oxidation to generate energy but do not utilize glucose to the extent of wild-type brains, and that glutamine is an important source of energy for the ASPA deficient brain (e.g., glutamine is reduced in the ASPA deficient brain).

SEQUENCES

[0163]

> SEQ ID NO: 1- Codon-optimized human aspartoacylase (hASPA) cDNA (full Kozak sequence underlined)

GCCACCATGACAAGCTGCCACATCGCCGAGGAGCACATCCAGAAAGTCGCCATTTT
TGGGGGAACTCACGGTAACGAACTCACAGGGGTCTTCCTGGTGAAGCACTGGCTCG
AGAACGGCGCAGAAATCCAGAGAACCGGACTGGAGGTGAAACCCTTCATTACAAA
TCCTCGGGCCGTCAAGAAATGCACTCGCTACATCGACTGTGATCTGAACCGGATTTT
TGATCTGGAAAATCTCGGCAAGAAAATGTCCGAGGACCTGCCATACGAAGTGAGGA
GAGCTCAGGAGATCAACCACCTCTTCGGACCCAAGGACAGCGAAGATTCCTATGAC
ATCATTTTTGATCTGCATAACACCACATCAAATATGGGGTGCACCCTGATCCTCGAG
GACAGCCGCAACAATTTCCTGATCCAGATGTTTCACTATATTAAGACAAGTCTGGCA
CCACTCCCCTGTTACGTGTATCTGATTGAGCATCCCTCTCTCAAGTACGCTACTACCC
GAAGTATCGCAAAATATCCTGTGGGGATTGAAGTCGGTCCTCAGCCACAGGGAGTC
CTGCGAGCCGATATCCTCGACCAGATGAGGAAGATGATCAAACATGCTCTGGATTT
CATTCACCACTTCAACGAGGGCAAGGAGTTCCCCCCTTGCGCCATCGAGGTGTACA
AGATCATTGAAAAAGTCGATTATCCTCGGGACGAGAACGGCGAAATTGCCGCTATC
ATTCACCCAAATCTGCAGGACCAGGATTGGAAGCCCCTCCATCCTGGGGATCCAAT
GTTCCTGACACTCGACGGTAAAACTATCCCACTGGGCGGAGACTGTACCGTGTACC
CCGTGTTTGTCAATGAGGCAGCCTACTATGAGAAGAAAGAAGCTTTCGCCAAAACA
ACAAAACTCACTCTCAATGCTAAATCTATTCGGTGCTGCCTCCACTGA

> SEQ ID NO: 2- Codon-optimized human aspartoacylase (hASPA)

MTSCHIAEEHIQKVAIFGGTHGNELTGVFLVKHWLENGAEIQRTGLEVKPFITNPRAVK
KCTRYIDCDLNRIFDLENLGKKMSEDLPYEVRRAQEINHLFGPKDSEDSYDIIFDLHNTT
SNMGCTLILEDSRNNFLIQMFHYIKTSLAPLPCYVYLIEHPSLKYATTRSIAKYPVGIEVG
PQPQGVLRADILDQMRKMIKHALDFIHHFNEGKEFPPCAIEVYKIIEKVDYPRDENGEIA
AIIHPNLQDQDWKPLHPGDPMFLTLDGKTIPLGGDCTVYPVFVNEAAYYEKKEAFAKT
TKLTLNAKSIRCCLH

>SEQ ID NO:3- Codon-optimized human NAT8L cDNA (full Kozak sequence underlined)

GCCACCATGCACTGCGGGCCACCTGATATGGTCTGTGAAACTAAGATTGTCGCTGCC
GAGGATCACGAGGCTCTGCCTGGAGCTAAAAAAAGATGCTCTGCTGGCCGCCGCCGG

CGCCATGTGGCCCCCTCTGCCAGCAGCACCAGGACCAGCAGCAGCACCACCCGCCC
CTCCACCCGCCCCTGTGGCCCAGCCACACGGCGGCGCCGGCGGCGCCGGCCCTCCA
GGCGGCCGGGGCGTGTGCATCCGGGAGTTCAGAGCAGCAGAGCAGGAGGCAGCAA
GGAGAATCTTTTATGACGGCATCATGGAGCGGATCCCCAACACCGCCTTCAGGGGA
CTGAGGCAGCACCCTAGAGCACAGCTGCTGTACGCACTGCTGGCCGCCCTGTGCTTT
GCCGTGAGCAGGTCCCTGCTGCTGACCTGTCTGGTGCCCGCCGCCCTGCTGGGACTG
AGGTACTATTACAGCCGGAAAGTGATCAGAGCCTATCTGGAGTGCGCCCTGCACAC
AGACATGGCCGATATCGAGCAGTATTACATGAAGCCCCCTGGCTCCTGTTTCTGGGT
GGCCGTGCTGGACGGAAACGTGGTGGGAATCGTGGCAGCAAGGGCACACGAGGAG
GACAATACCGTGGAGCTGCTGCGCATGTCTGTGGATAGCAGGTTCCGCGGCAAGGG

AATCGCAAAGGCCCTGGGAAGGAAGGTGCTGGAGTTTGCCGTGGTGCACAATTACT
CTGCCGTGGTGCTGGGCACCACAGCAGTGAAGGTGGCAGCCCACAAGCTGTATGAG
TCCCTGGGCTTTAGGCACATGGGCGCCTCTGATCACTACGTGCTGCCTGGCATGACA
CTGTCCCTGGCCGAGAGACTGTTCTTCCAGGTCCGCTACCATAGATATAGACTGCAG
CTGAGGGAGGAGTGA

> SEQ ID NO:4- Codon-optimized human NAT8L
MHCGPPDMVCETKIVAAEDHEALPGAKKDALLAAAGAMWPPLPAAPGPAAAPPAPPP
APVAQPHGGAGGAGPPGGRGVCIREFRAAEQEAARRIFYDGIMERIPNTAFRGLRQHPR
AQLLYALLAALCFAVSRSLLLTCLVPAALLGLRYYYSRKVIRAYLECALHTDMADIEQY
YMKPPGSCFWVAVLDGNVVGIVAARAHEEDNTVELLRMSVDSRFRGKGIAKALGRKV
LEFAVVHNYSAVVLGTTAVKVAAHKLYESLGFRHMGASDHYVLPGMTLSLAERLFFQ
VRYHRYRLQLREE

REFERENCES CITED IN THE DESCRIPTION

Cited references

This list of references cited by the applicant is for the reader's convenience only. It does not form part of the European patent document. Even though great care has been taken in compiling the references, errors or omissions cannot be excluded and the EPO disclaims all liability in this regard.

Patent documents cited in the description

- WO2015127128A [0002]
- US2014335054A [0002]
- US2014142152A [0002]
- US20130023488A [0002]
- EP2261242A [0002]
- US20030138772A [0027]
- US5478745A [0030]
- US6001650A [0031] [0031]
- US6156303A [0031]
- WO9810088A [0050]
- US5543158A [0069]

- US5641515A [0069]
- US5399363A [0069]
- US5741516A [0076]
- US5567434A [0076]
- US5552157A [0076]
- US5565213A [0076]
- US5738868A [0076]
- US5795587A [0076]

Non-patent literature cited in the description

- **SAMBROOK et al.**Molecular Cloning: A Laboratory ManualCold Spring Harbor Press [0030]
- **K. FISHER et al.**J. Virol, 1993, vol. 70, 520-532 [0030]
- **GRAHAM et al.**Virology, 1973, vol. 52, 456- [0032]
- **SAMBROOK et al.**Molecular Cloning, a laboratory manualCold Spring Harbor Laboratories19890000 [0032]
- **DAVIS et al.**Basic Methods in Molecular BiologyElsevier19860000 [0032]
- **CHU et al.**Gene, 1981, vol. 13, 197- [0032]
- Molecular Cloning: A Laboratory ManualCold Spring Harbor Laboratory Press19890000 [0039]
- Current Protocols in Molecular BiologyJohn Wiley & Sons, Inc [0039]
- **B. J. CARTERP. TIJSSER**Handbook of ParvovirusesCRC Press19900000155-168 [0042]
- **SAMBROOK et al.**Molecular Cloning. A Laboratory ManualCold Spring Harbor Laboratory19890000 [0042]
- **K. FISHER et al.**J Virol.19960000vol. 70, 520-532 [0042]
- **AUSUBEL et al.**Current Protocols in Molecular BiologyJohn Wiley & Sons19890000 [0047]
- **RYAN, M D et al.**EMBO, 1994, vol. 4, 928-933 [0047] [0047]
- **MATTION, N M et al.**J Virology, 1996, 8124-8127 [0047] [0047]
- **FURLER, S et al.**Gene Therapy, 2001, vol. 8, 864-873 [0047] [0047]
- **HALPIN, C et al.**The Plant Journal, 1999, vol. 4, 453-459 [0047] [0047]
- **DE FELIPE, P et al.**Gene Therapy, 1999, vol. 6, 198-208 [0047]
- **DE FELIPE, P et al.**Human Gene Therapy, 2000, vol. 11, 1921-1931 [0047]
- **KLUMP, H et al.**Gene Therapy, 2001, vol. 8, 811-817 [0047]
- **BOSHART et al.**Cell, 1985, vol. 41, 521-530 [0049]
- **NO et al.**Proc. Natl. Acad. Sci. USA, 1996, vol. 93, 3346-3351 [0050]
- **GOSSEN et al.**Proc. Natl. Acad. Sci. USA, 1992, vol. 89, 5547-5551 [0050]
- **GOSSEN et al.**Science, 1995, vol. 268, 1766-1769 [0050]

- **HARVEY et al.**Curr. Opin. Chem. Biol., 1998, vol. 2, 512-518 [0050]
- **WANG et al.**Nat. Biotech, 1997, vol. 15, 239-243 [0050]
- **WANG et al.**Gene Ther., 1997, vol. 4, 432-441 [0050]
- **MAGARI et al.**J. Clin. Invest, 1997, vol. 100, 2865-2872 [0050]
- **SANDIG et al.**Gene Ther., 1996, vol. 3, 1002-9 [0052]
- **ARBUTHNOT et al.**Hum. Gene Ther, 1996, vol. 7, 1503-14 [0052]
- **STEIN et al.**Mol. Biol. Rep, 1997, vol. 24, 185-96 [0052]
- **CHEN et al.**J. Bone Miner. Res., 1996, vol. 11, 654-64 [0052]
- **HANSAL et al.**J. Immunol., 1998, vol. 161, 1063-8 [0052]
- **ANDERSEN et al.**Cell. Mol. Neurobiol., 1993, vol. 13, 503-15 [0052]
- **PICCIOLI et al.**Proc. Natl. Acad. Sci. USA, 1991, vol. 88, 5611-5 [0052]
- **PICCIOLI et al.**Neuron, 1995, vol. 15, 373-84 [0052]
- **CHEN et al.**J. Neurosci, Res, 1999, vol. 55, 4504-13 [0052]
- **BRENNER et al.**J. Neurosci, 1994, vol. 14, 31030-7 [0053]
- **CAHOY et al.**J. Neurosci, 2008, vol. 28, 264-278 [0053]
- **COLIN et al.**Glia, 2009, vol. 57, 667-679 [0053]
- **WRIGHT FR et al.**Molecular Therapy, 2005, vol. 12, 171-178 [0067]
- Remington's Pharmaceutical Sciences1035-10381570-1580 [0071]

Patentkrav

1. Rekombinant adeno-associeret virus (rAAV) til anvendelse i en fremgangsmåde til behandling af Canavan sygdom, hvor rAAV omfatter:
(a) et capsidprotein; og
(b) en nukleinsyre omfattende en promotor, der er operabelt forbundet til et transgen, hvor transgenet koder for aspartoacylase (ASPA), og hvor transgenet omfatter SEQ ID NO:1.

2. rAAV til anvendelse ifølge krav 1, hvor rAAV administreres via injektion, hvor administrationen resulterer i ekspression af genet i perifert væv, eller hvor administrationen resulterer i ekspression af genet i CNS-væv.

3. rAAV til anvendelse ifølge krav 2, hvor injektionen er valgt fra gruppen bestående af intravenøs injektion, intravaskulær injektion og intraventrikulær injektion.

4. rAAV til anvendelse ifølge krav 1 eller 2, hvor rAAV administreres intrathecalt eller intracerebralt.

5. rAAV til anvendelse ifølge et hvilket som helst af kravene 1 til 4, hvor promotoren er en astrocytspecifik promotor, eventuelt glialfibrillært syreholdig protein- (GFAP) promoter.

6. rAAV til anvendelse ifølge et hvilket som helst af kravene 1 til 4, hvor promotoren er en forstærket kylling β-actin promoter.

7. rAAV til anvendelse ifølge et hvilket som helst af kravene 1 til 6, hvor transgenet koder for ASPA omfattende SEQ ID NO:2.

8. rAAV til anvendelse ifølge et hvilket som helst af kravene 1 til 7, hvor capsidproteinet har serotypen AAV9.

DRAWINGS

Drawing

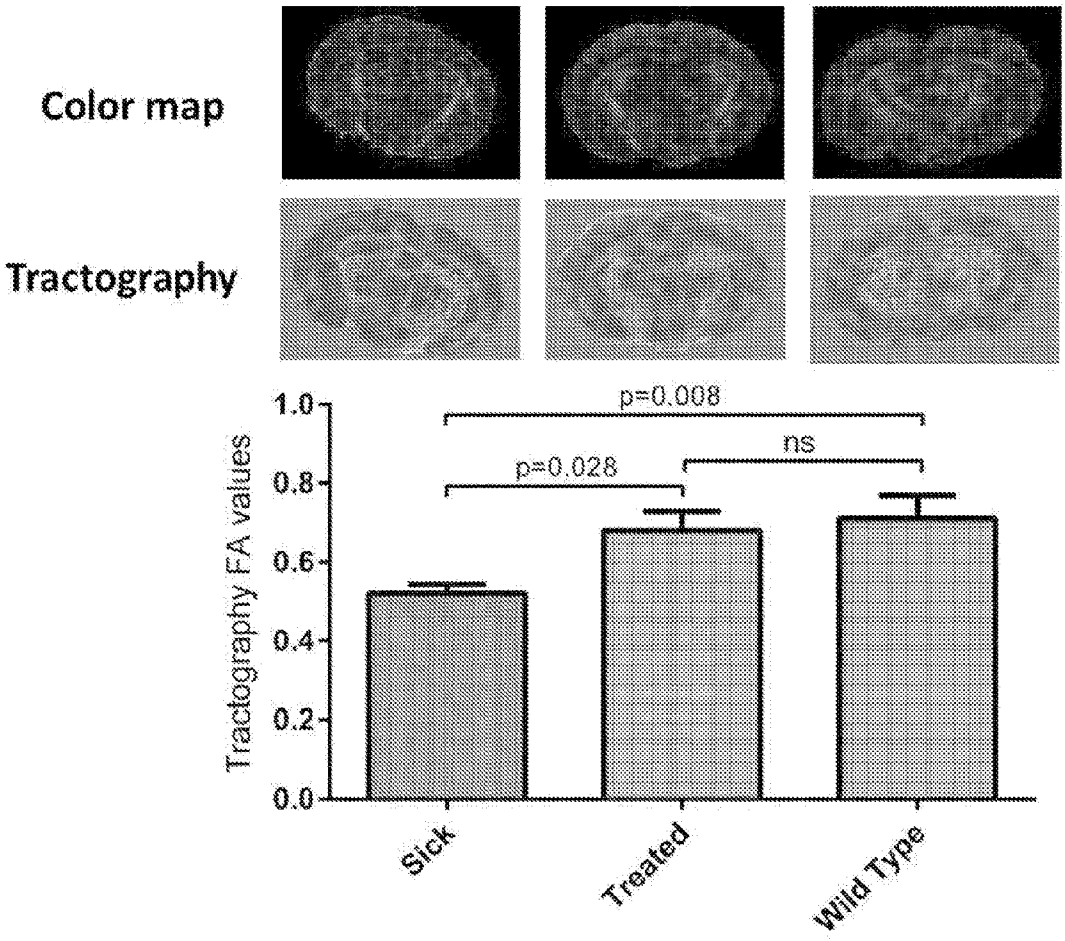

FIG. 1

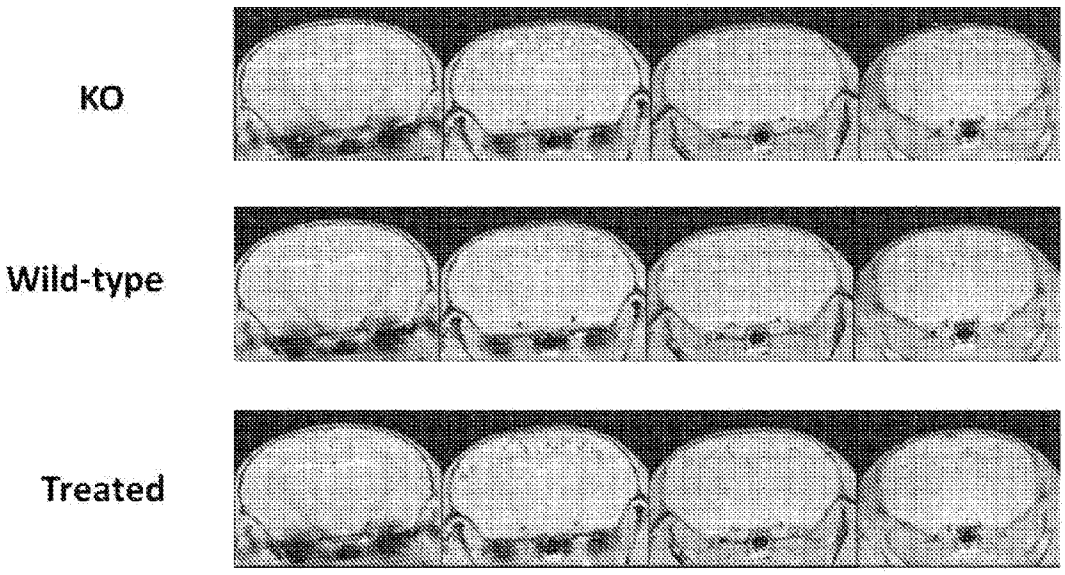

FIG. 2

FIG. 3

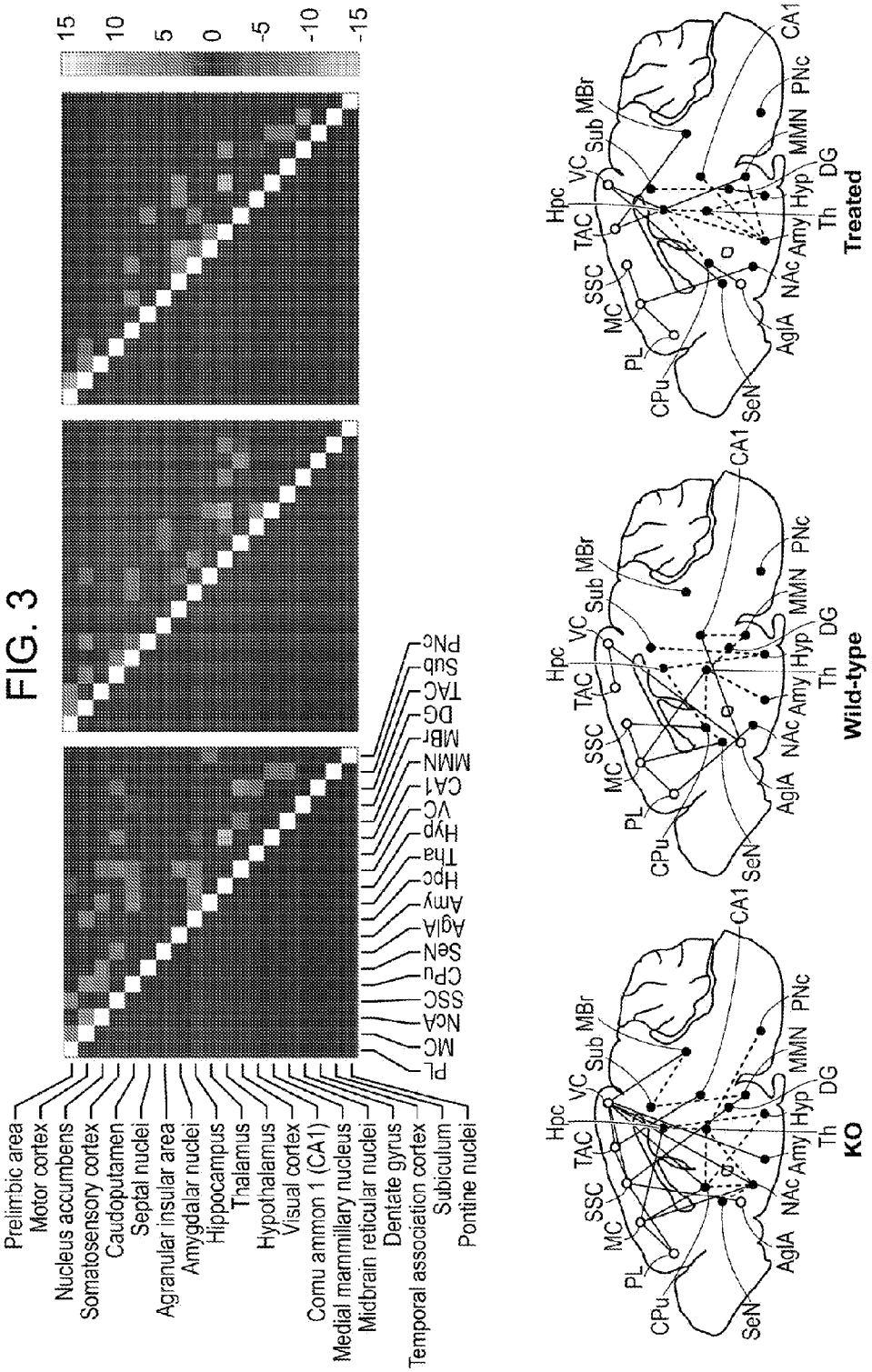
15
10
5
0
-5
-10
-15
Prelimbic area
Motor cortex
Nucleus accumbens
Somatosensory cortex
Caudoputamen
Septal nuclei
Agranular insular area
Amygdalar nuclei
Hippocampus
Thalamus
Hypothalamus
Visual cortex
Comu ammon 1 (CA1)
Medial mammillary nucleus
Midbrain reticular nuclei
Dentate gyrus
Temporal association cortex
Subiculum
Pontine nuclei
PL
MC
NcA
SSC
CPu
SeN
AgIA
Amy
Hpc
Tha
Hyp
VC
CA1
MMN
MBr
DG
TAC
Sub
PNc
Hpc
VC
Sub
MBr
TAC
SSC
MC
PL
CPu
SeN
AgIA
NAc
Amy
Hyp
Th
MMN
PNc
CA1
DG
KO
Wild-type
Treated

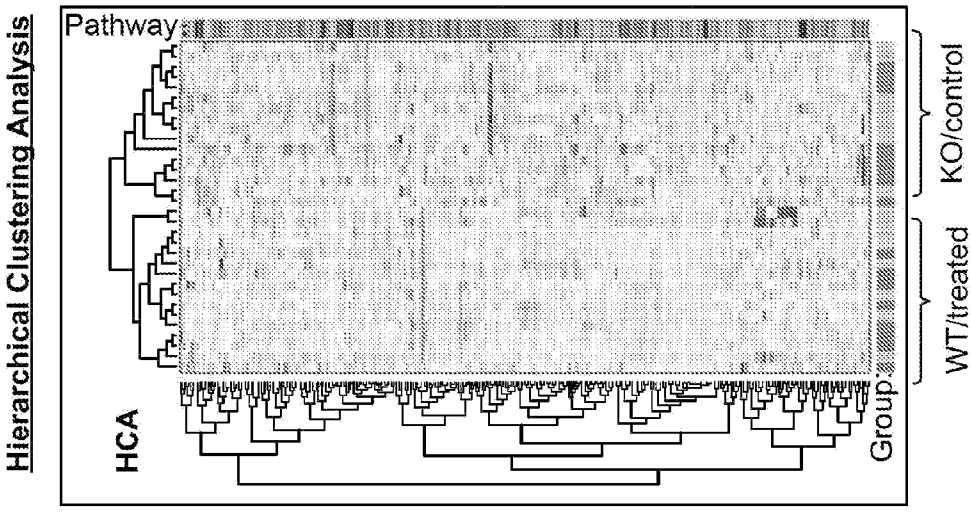

FIG. 4B

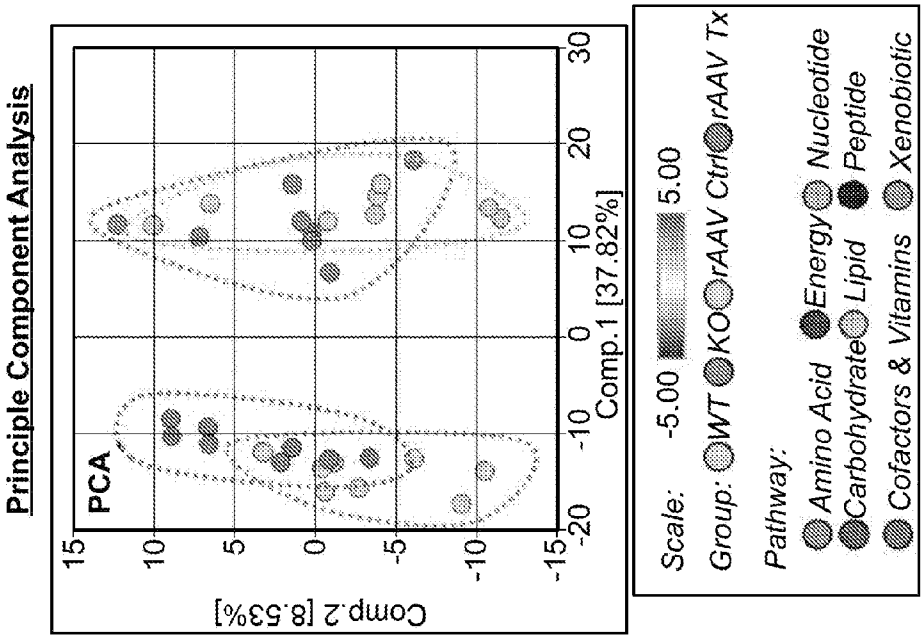

PCA = Principal component analysis
HCA = hierarchical clustering analysis

FIG. 4A

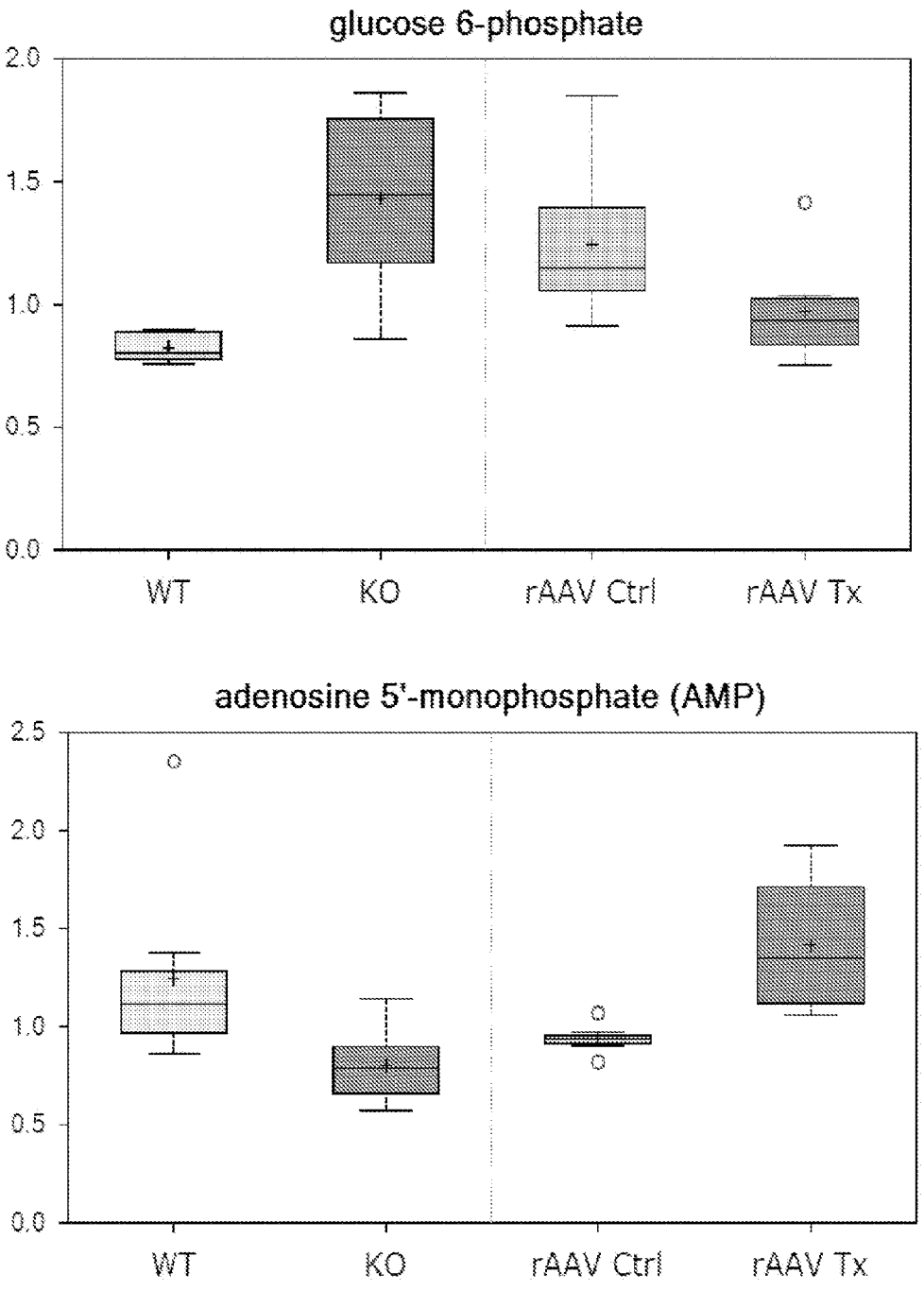
glucose 6-phosphate
2.0
1.5
1.0
0.5
0.0
WT
KO
rAAV Ctrl
rAAV Tx
adenosine 5'-monophosphate (AMP)
2.5
2.0
1.5
1.0
0.5
0.0
WT
KO
rAAV Ctrl
rAAV Tx

FIG. 5

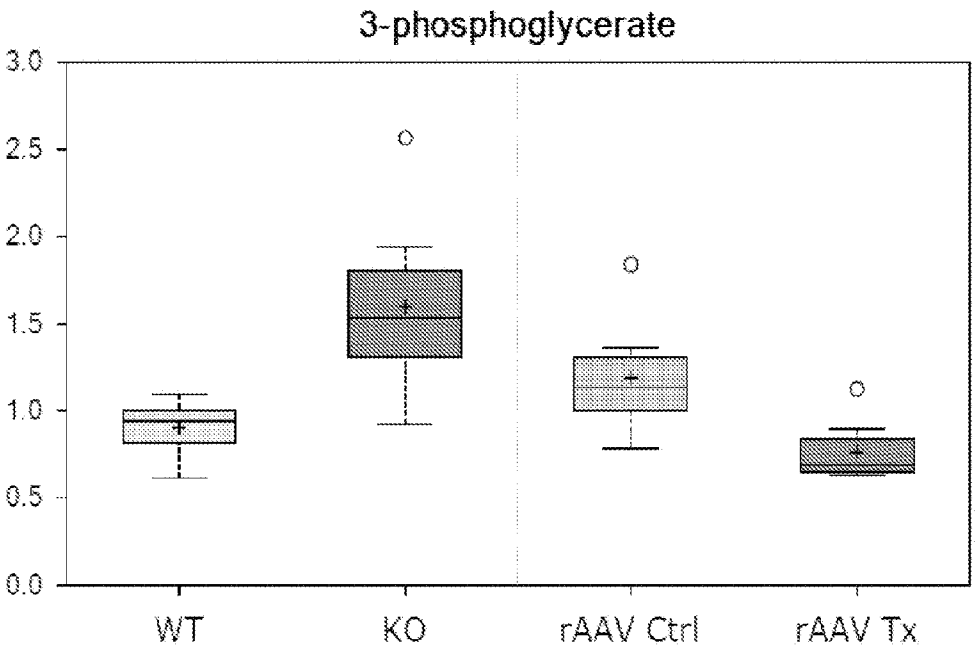
3-phosphoglycerate
3.0
2.5
2.0
1.5
1.0
0.5
0.0
WT
KO
rAAV Ctrl
rAAV Tx

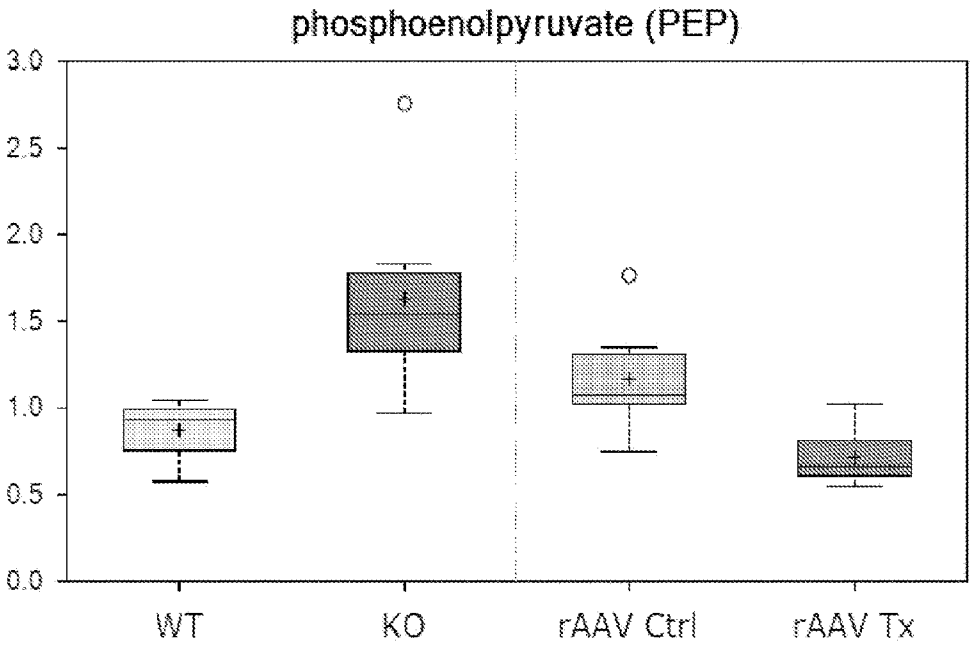
phosphoenolpyruvate (PEP)
3.0
2.5
2.0
1.5
1.0
0.5
0.0
WT
KO
rAAV Ctrl
rAAV Tx

FIG. 5 cont.

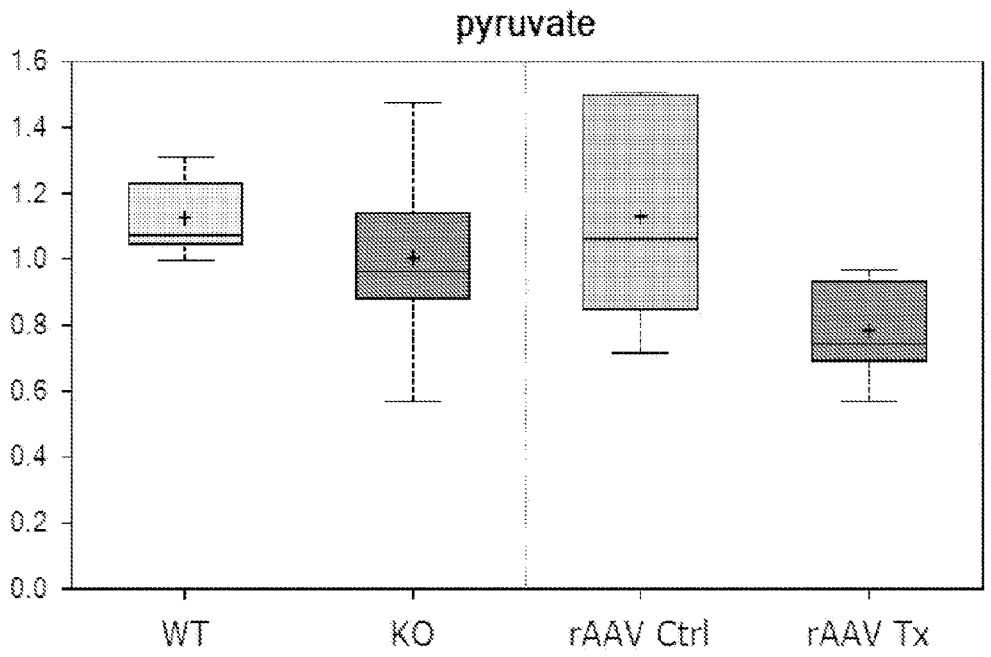
pyruvate
1.6
1.4
1.2
1.0
0.8
0.6
0.4
0.2
0.0
WT
KO
rAAV Ctrl
rAAV Tx

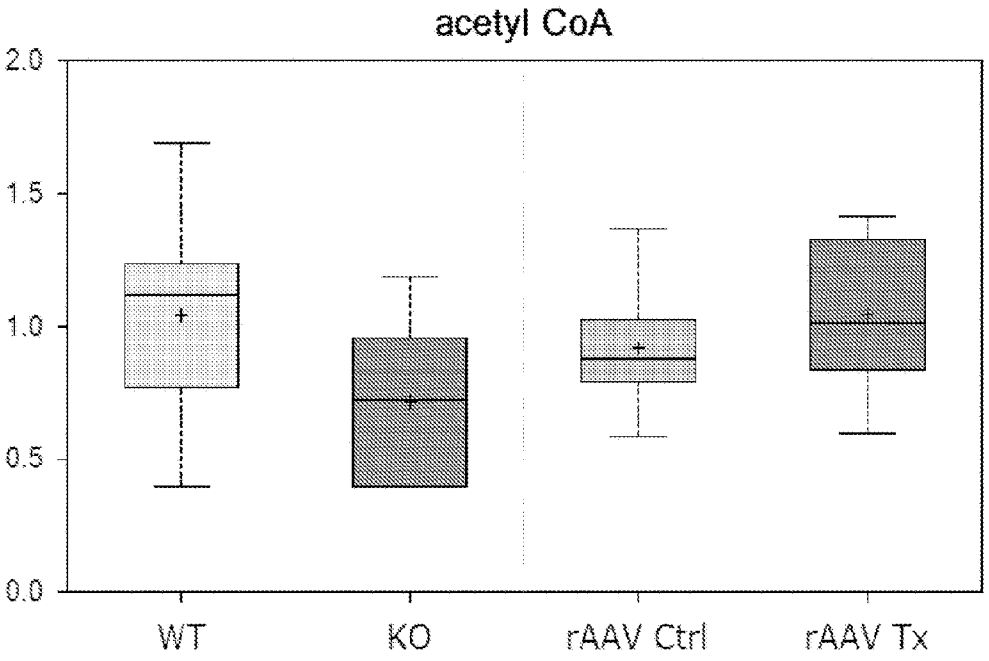
acetyl CoA
2.0
1.5
1.0
0.5
0.0
WT
KO
rAAV Ctrl
rAAV Tx

FIG. 5 cont.

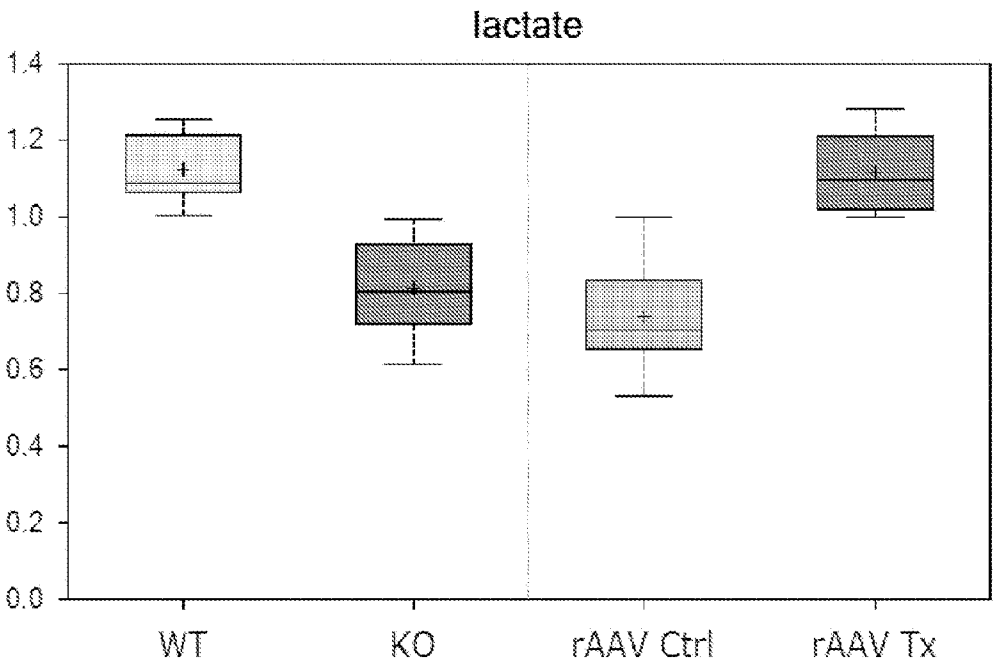
lactate
1.4
1.2
1.0
0.8
0.6
0.4
0.2
0.0
WT
KO
rAAV Ctrl
rAAV Tx

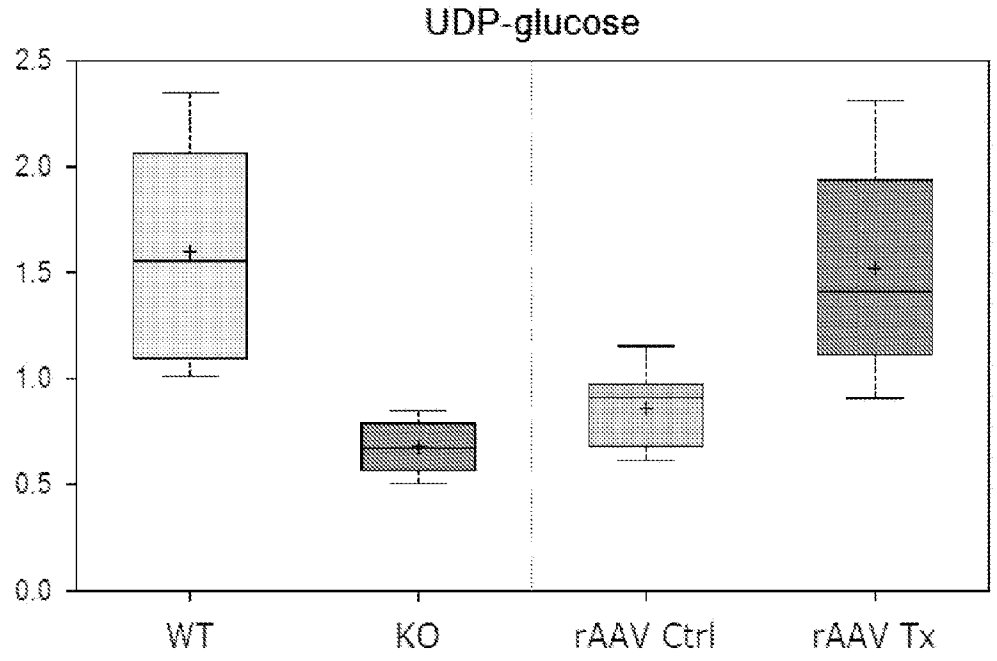
UDP-glucose
2.5
2.0
1.5
1.0
0.5
0.0
WT
KO
rAAV Ctrl
rAAV Tx

FIG. 5 cont.

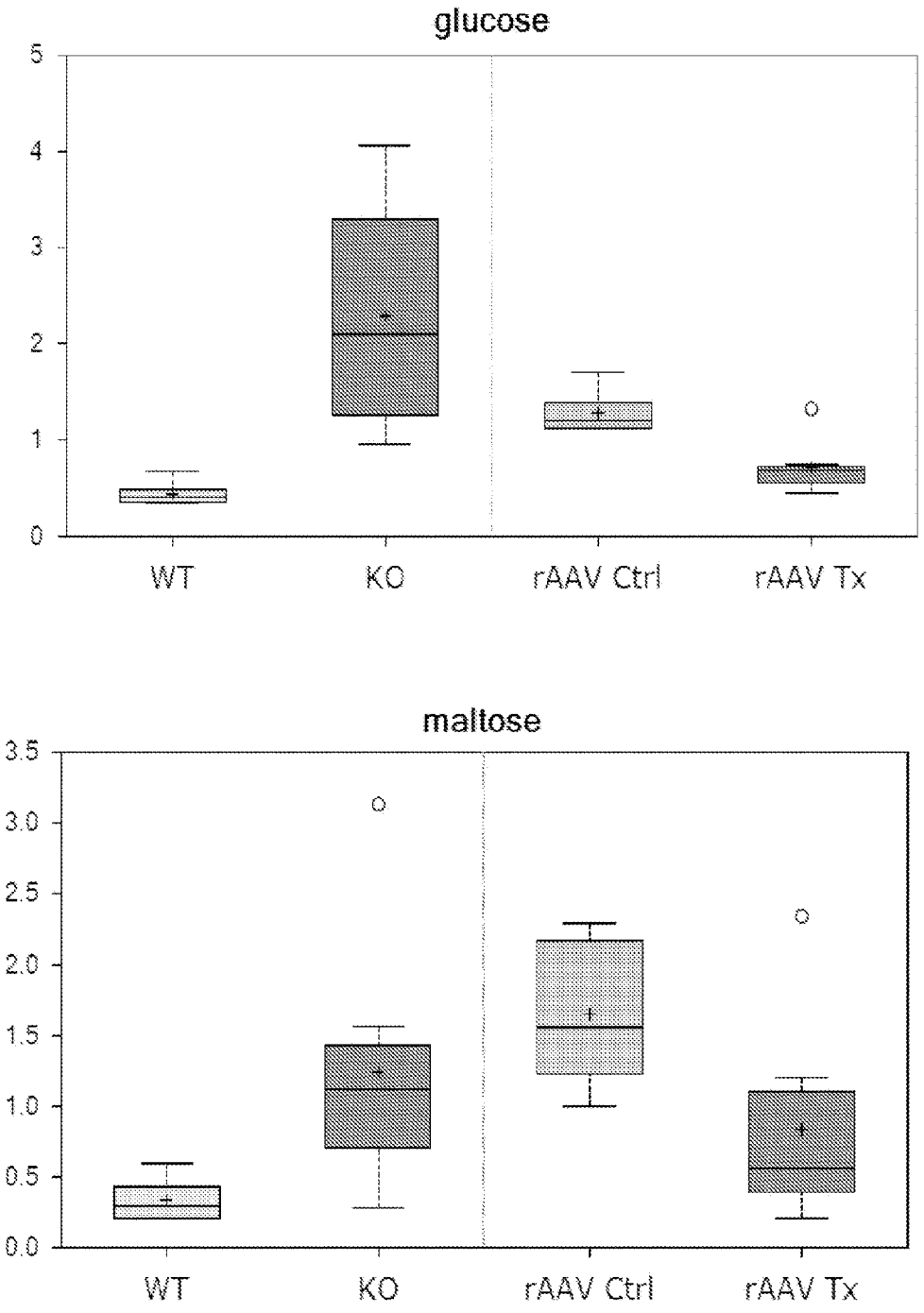
glucose
5
4
3
2
1
0
WT
KO
rAAV Ctrl
rAAV Tx
maltose
3.5
3.0
2.5
2.0
1.5
1.0
0.5
0.0
WT
KO
rAAV Ctrl
rAAV Tx

FIG. 5 cont.

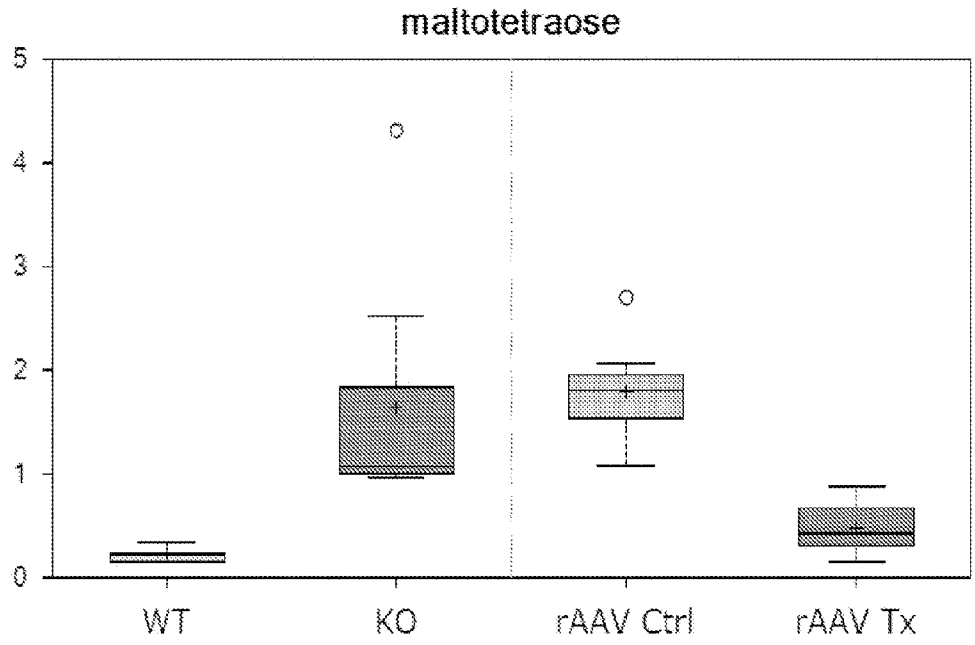
maltotetraose
5
4
3
2
1
0
WT
KO
rAAV Ctrl
rAAV Tx

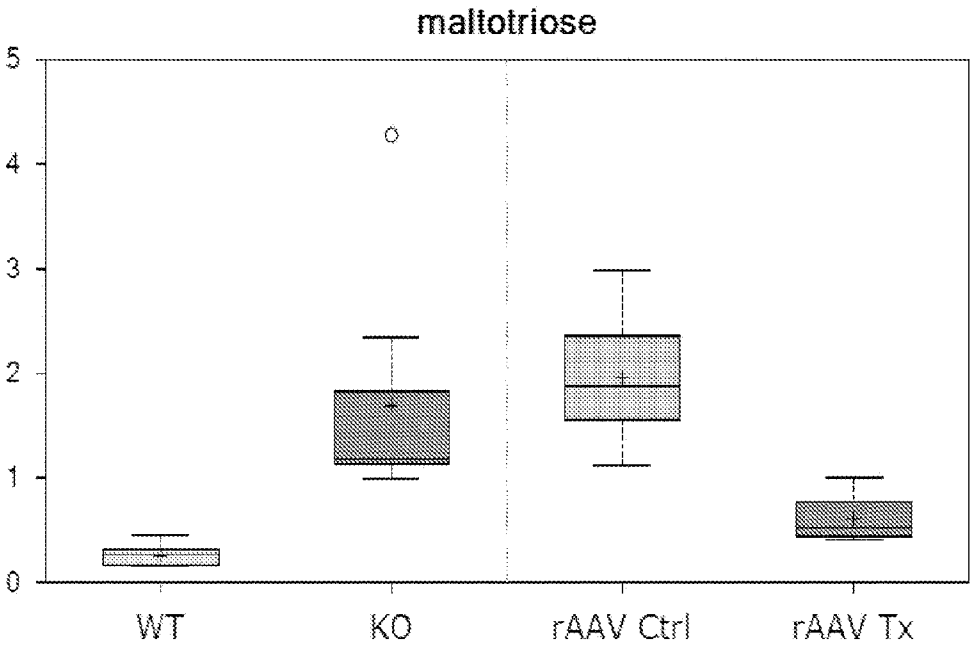
maltotriose
5
4
3
2
1
0
WT
KO
rAAV Ctrl
rAAV Tx

FIG. 5 cont.

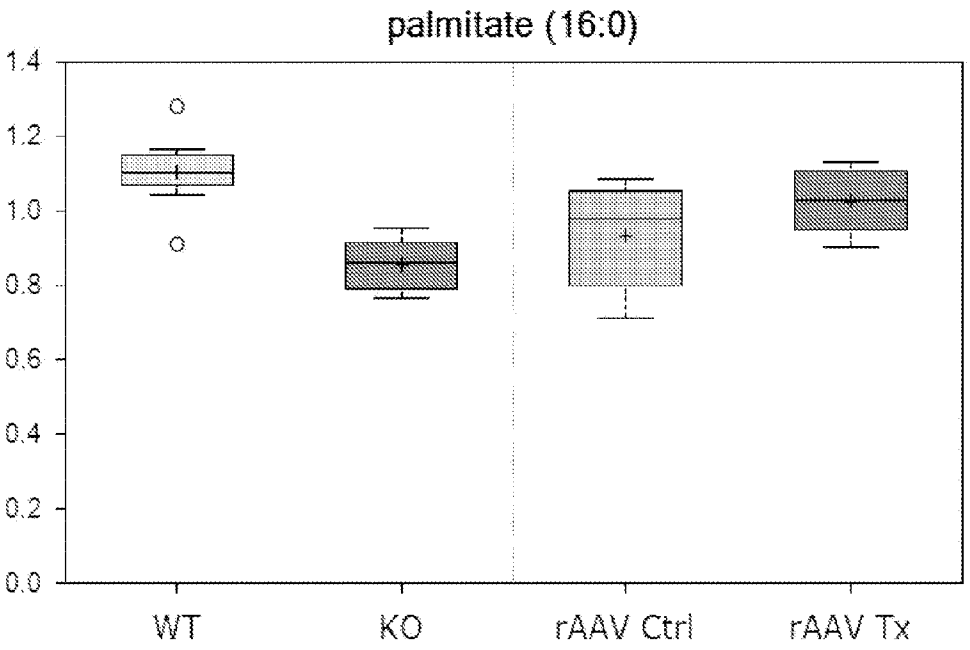
palmitate (16:0)
1.4
1.2
1.0
0.8
0.6
0.4
0.2
0.0
WT
KO
rAAV Ctrl
rAAV Tx

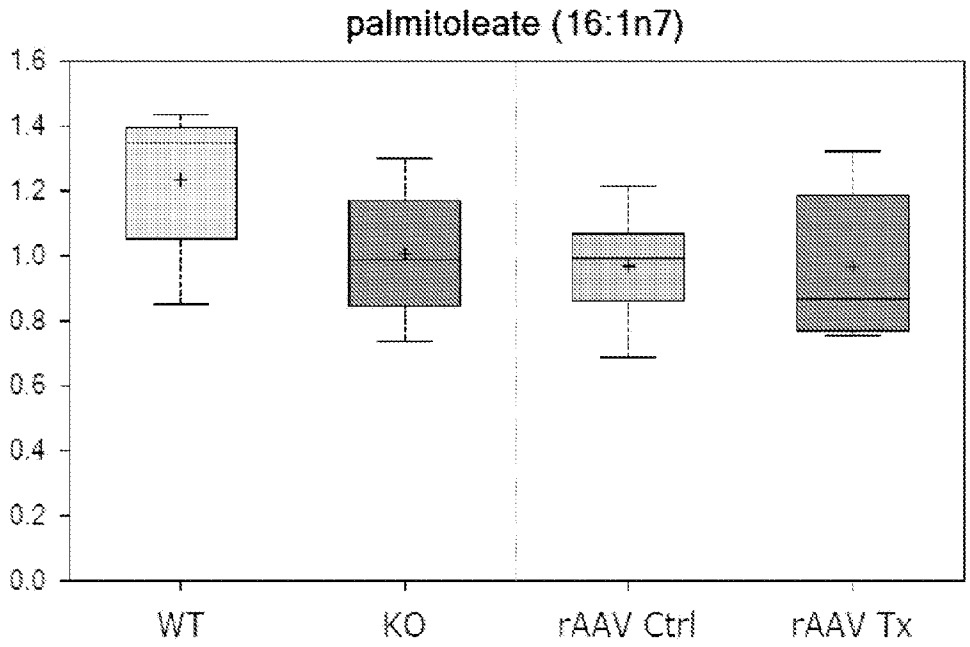
palmitoleate (16:1n7)
1.6
1.4
1.2
1.0
0.8
0.6
0.4
0.2
0.0
WT
KO
rAAV Ctrl
rAAV Tx

FIG. 6

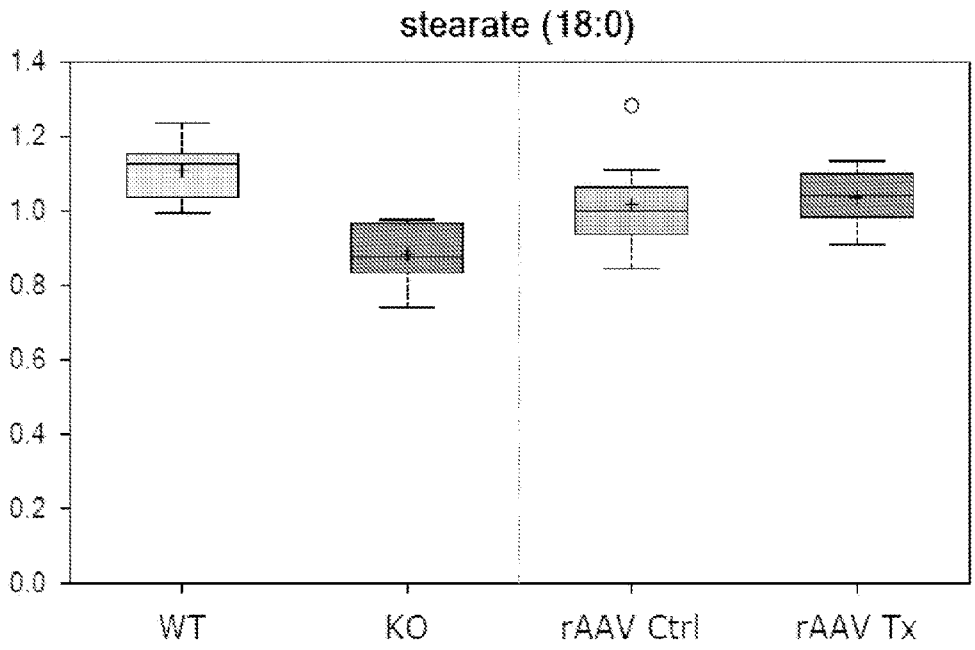
stearate (18:0)
1.4
1.2
1.0
0.8
0.6
0.4
0.2
0.0
WT
KO
rAAV Ctrl
rAAV Tx

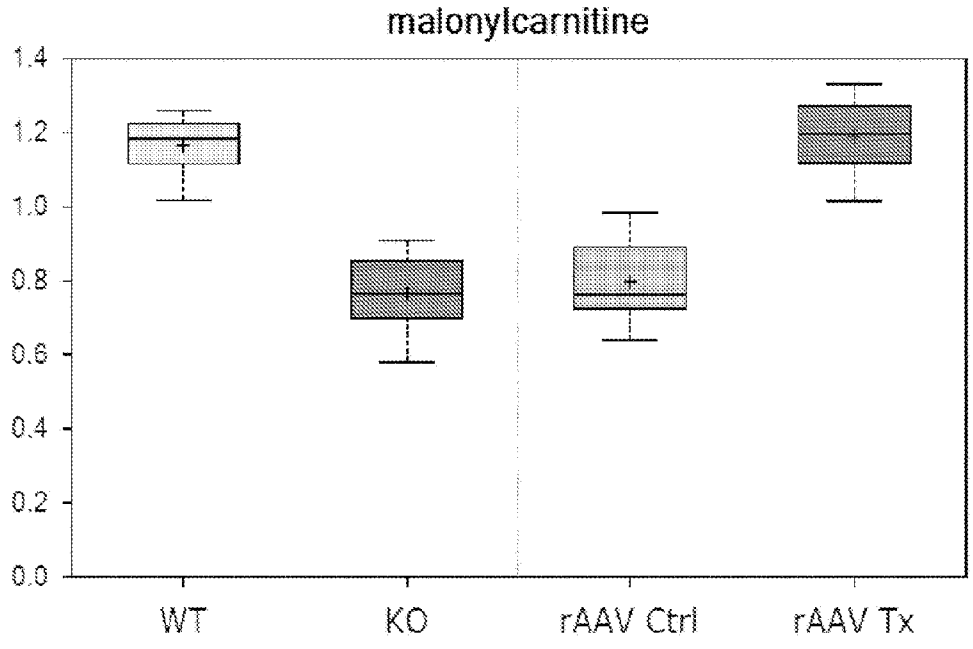
malonylcarnitine
1.4
1.2
1.0
0.8
0.6
0.4
0.2
0.0
WT
KO
rAAV Ctrl
rAAV Tx

FIG. 6 cont.

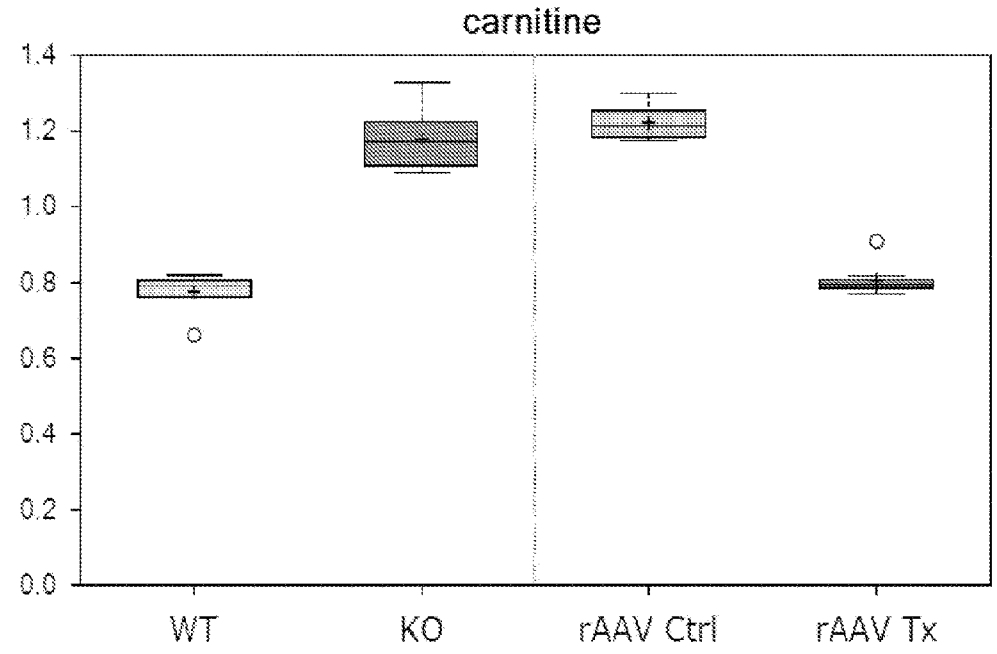
carnitine
1.4
1.2
1.0
0.8
0.6
0.4
0.2
0.0
WT
KO
rAAV Ctrl
rAAV Tx

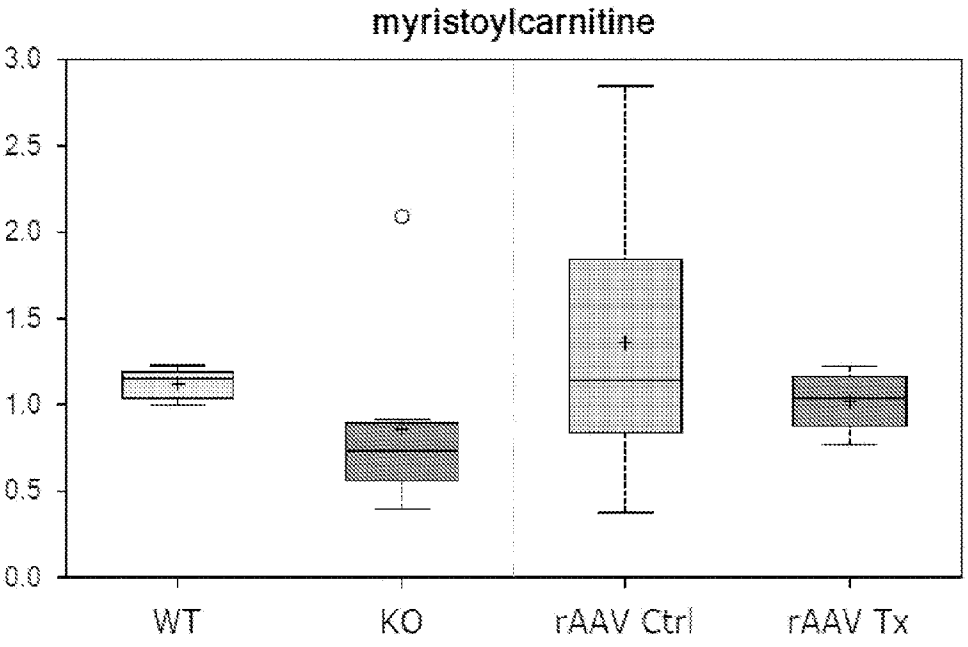
myristoylcarnitine
3.0
2.5
2.0
1.5
1.0
0.5
0.0
WT
KO
rAAV Ctrl
rAAV Tx

FIG. 6 cont.

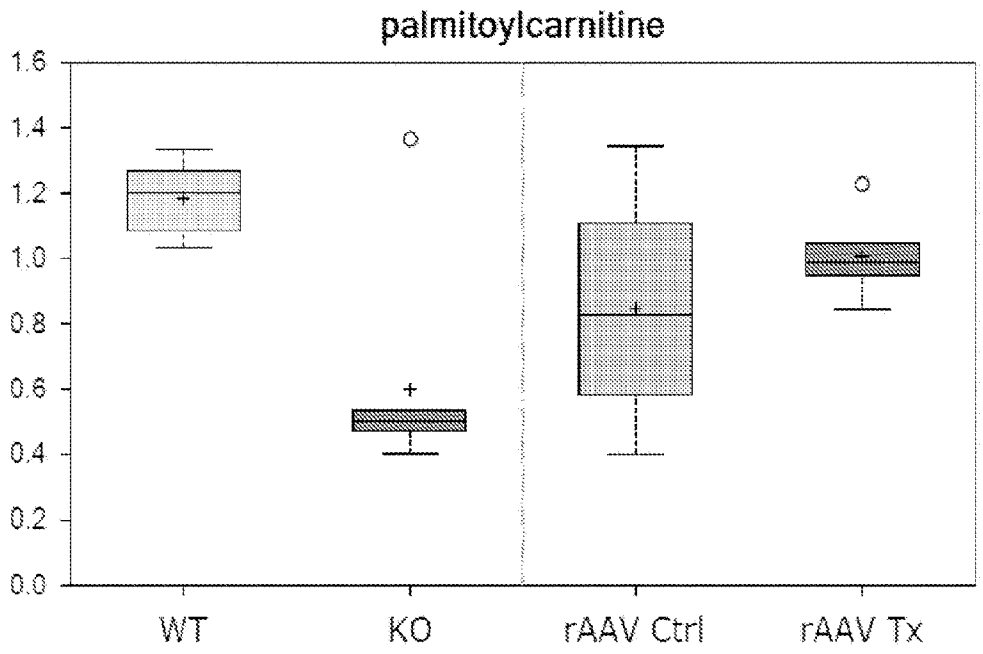
palmitoylcarnitine
1.6
1.4
1.2
1.0
0.8
0.6
0.4
0.2
0.0
WT
KO
rAAV Ctrl
rAAV Tx

FIG. 6 cont.

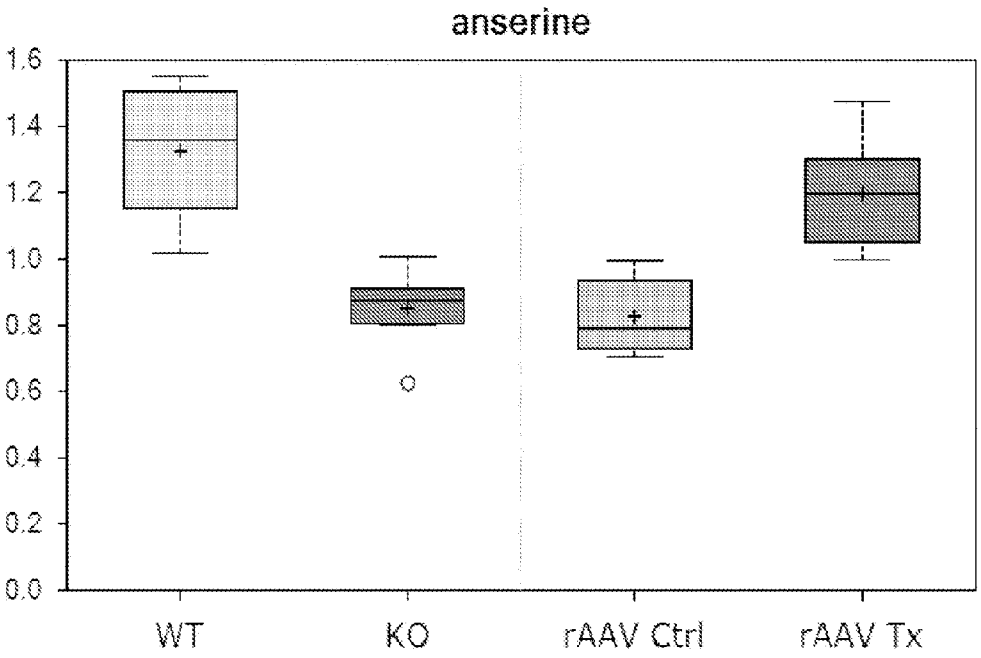
anserine
1.6
1.4
1.2
1.0
0.8
0.6
0.4
0.2
0.0
WT
KO
rAAV Ctrl
rAAV Tx

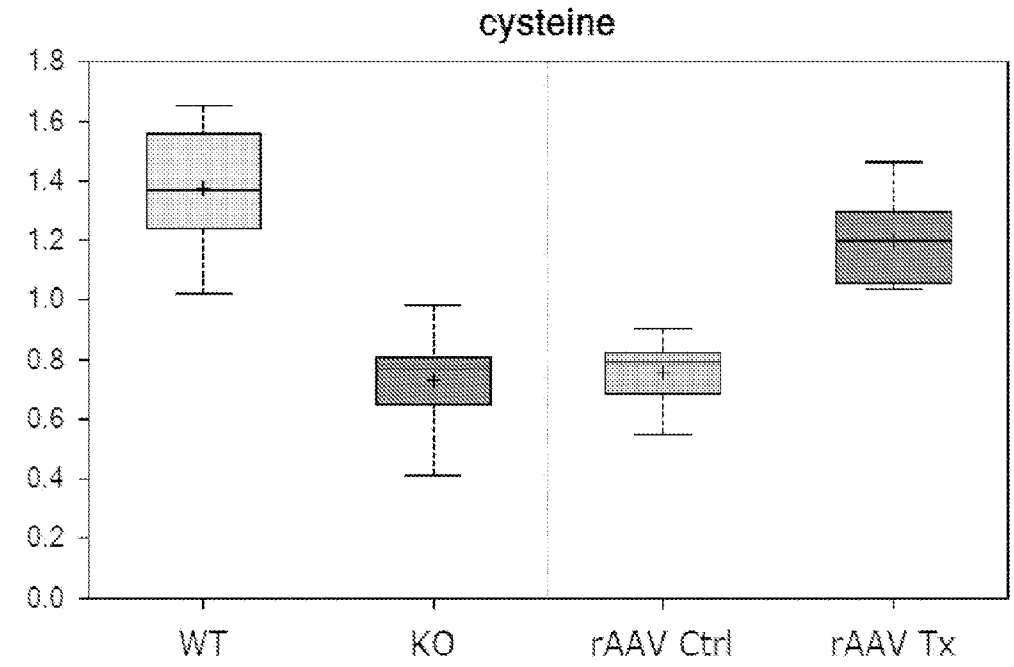
cysteine
1.8
1.6
1.4
1.2
1.0
0.8
0.6
0.4
0.2
0.0
WT
KO
rAAV Ctrl
rAAV Tx

FIG. 7

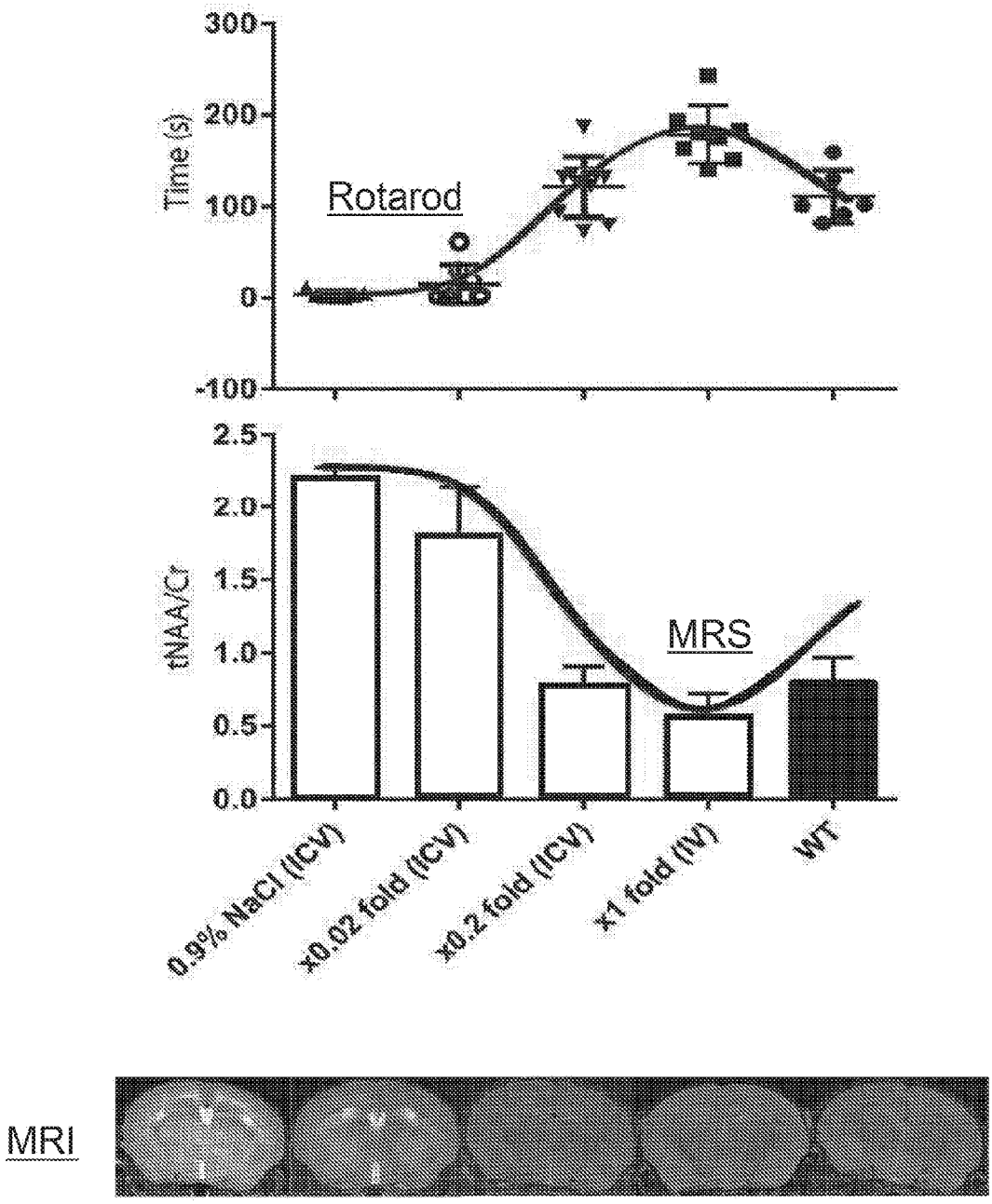
Rotarod
Time (s)
300
200
100
0
-100
MRS
tNAA/Cr
2.5
2.0
1.5
1.0
0.5
0.0
0.9% NaCl (ICV)
x0.02 fold (ICV)
x0.2 fold (ICV)
x1 fold (IV)
WT
MRI

FIG. 8

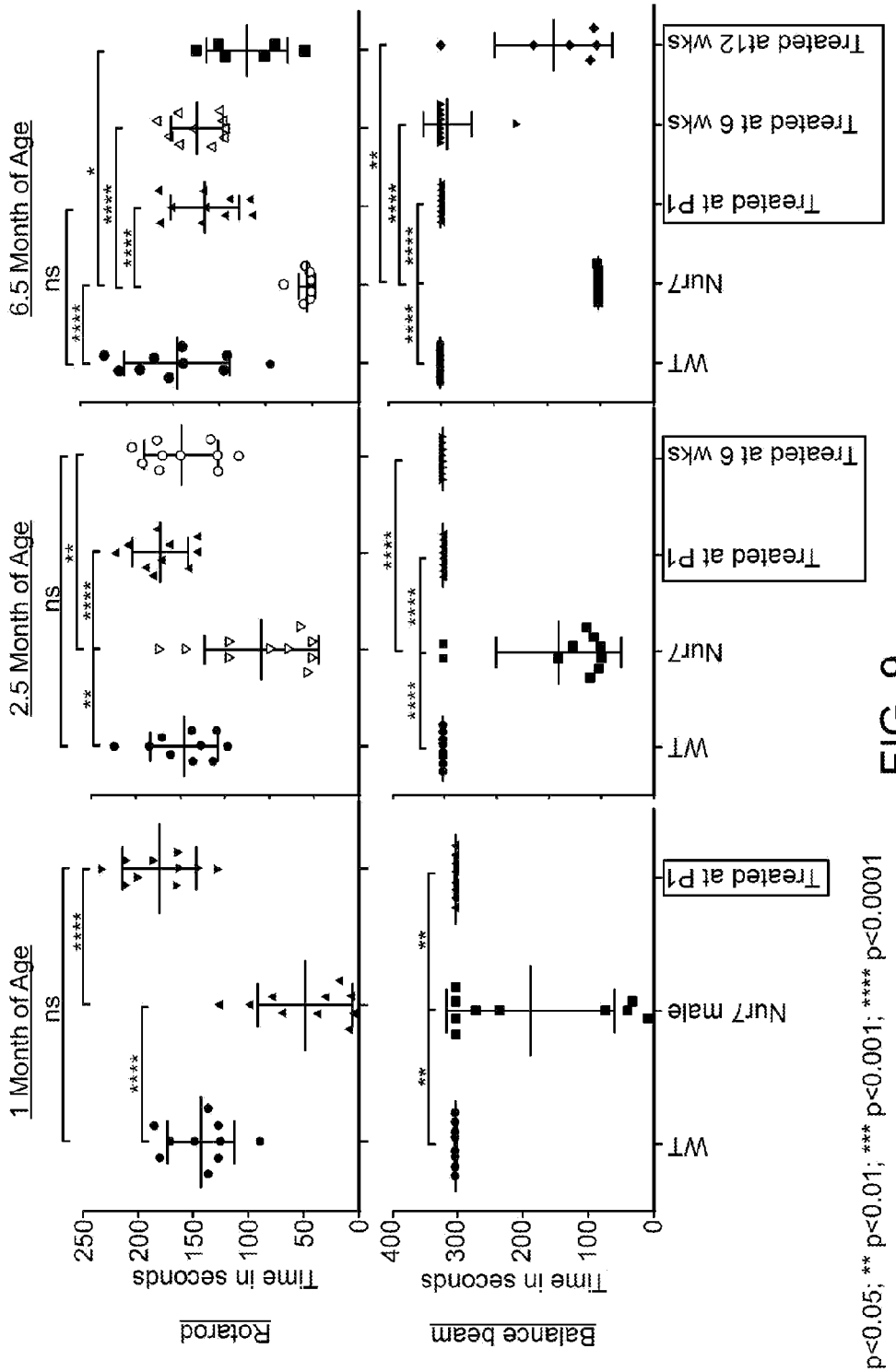

FIG. 9

* p<0.05; ** p<0.01; *** p<0.001; **** p<0.0001

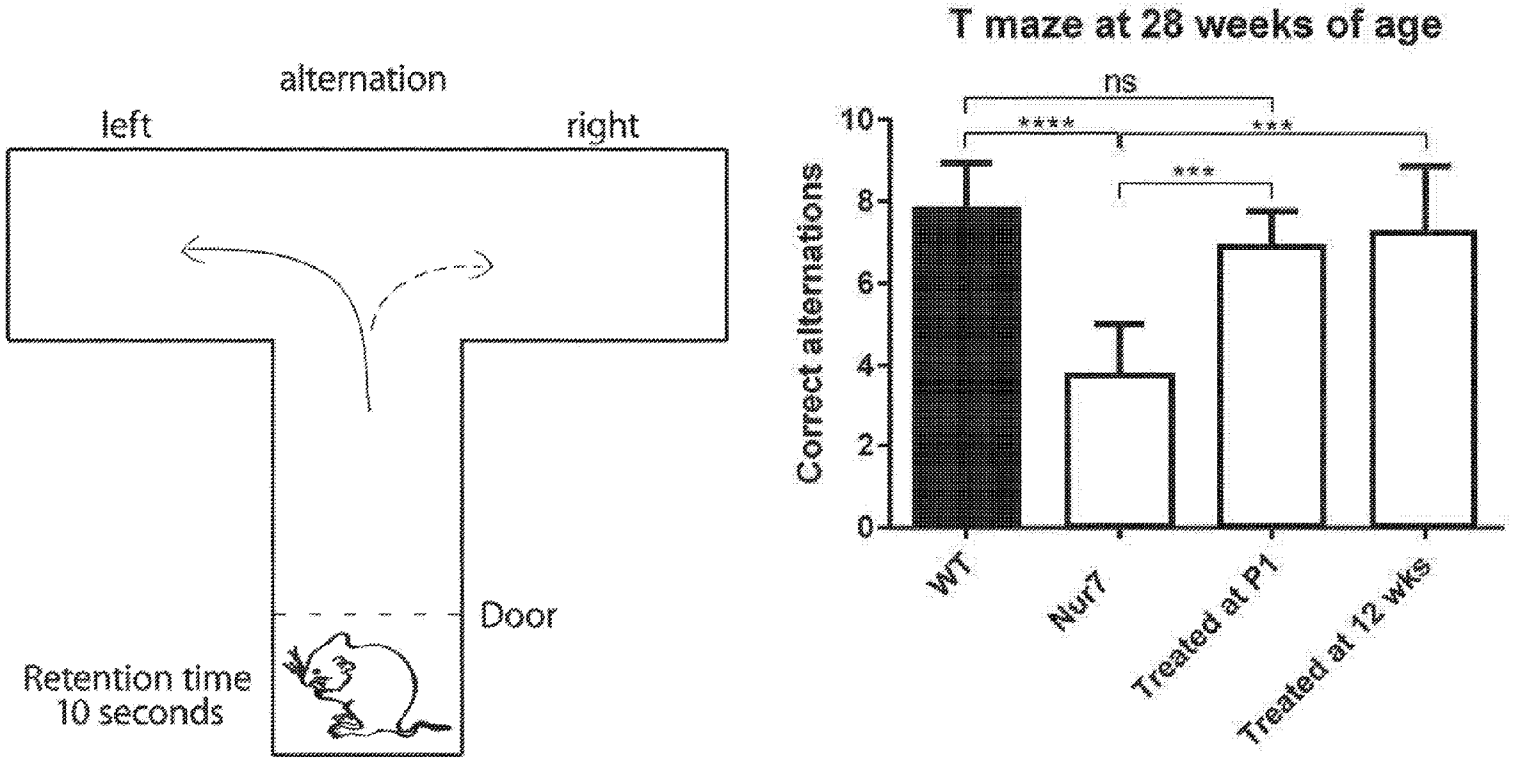

* p<0.05; ** p<0.01; *** p<0.001; **** p<0.0001

FIG. 10

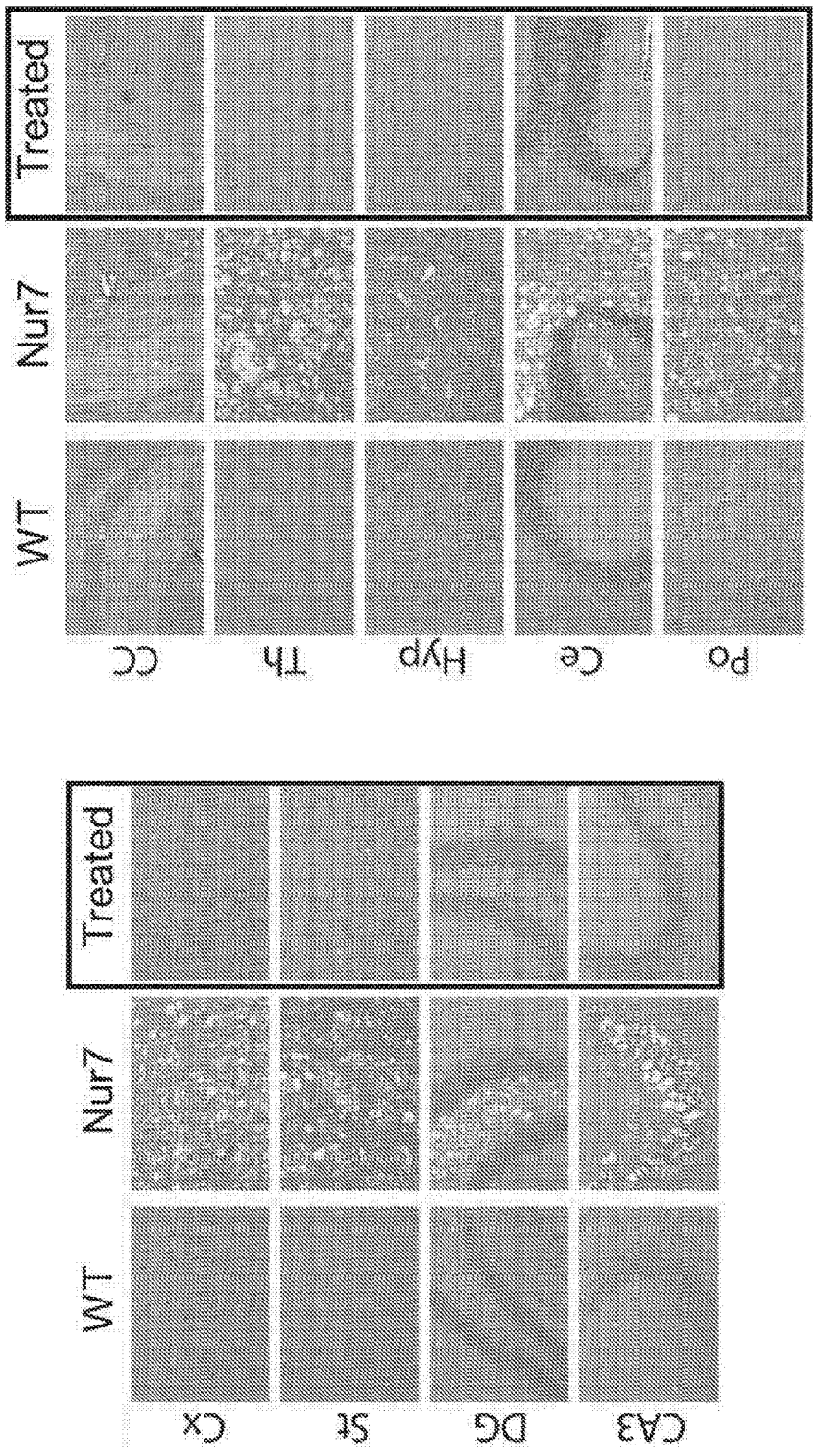

Neuropathology at postntal day 25

FIG. 11

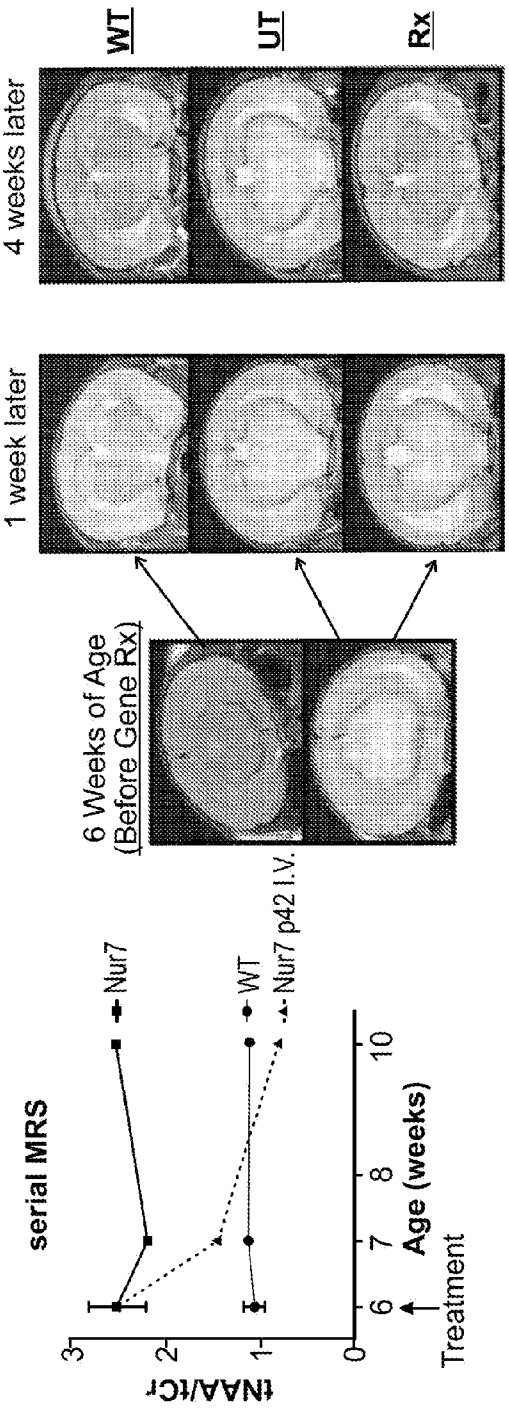
serial MRS
tNAA/tCr
3
2
1
0
Nur7
WT
Nur7 p42 I.V.
6
7
8
10
Age (weeks)
Treatment
6 Weeks of Age
(Before Gene Rx)
1 week later
4 weeks later
WT
UT
Rx

FIG. 12

sphingomyelins	KO/WT	rAAV (Tx/Ctrl)
palmitoyl sphingomyelin (d18:1/16:0)	0.59	1.22
stearoyl sphingomyelin (d18:1/18:0)	0.84	1.16
sphingomyelin (d18:1/18:1, d18:2/18:0)	0.97	1.05
sphingomyelin (d18:1/14:0, d16:1/16:0)*	0.5	1.01
sphingomyelin (d18:1/24:1, d18:2/24:0)*	0.56	1.95
sphingomyelin (d18:2/16:0, d18:1/16:1)*	0.47	0.82
sphingomyelin (d18:1/20:1, d18:2/20:0)*	0.82	0.87
behenoyl sphingomyelin (d18:1/22:0)*	0.56	1.56
sphingomyelin (d18:1/22:1, d18:2/22:0, d	0.59	1.62
sphingomyelin (d18:1/20:0, d16:1/22:0)*	0.9	1.09
palmitoyl dihydrosphingomyelin (d18:0/16	0.37	2.09
sphingomyelin (d18:1/15:0, d16:1/17:0)*	0.26	0.95
sphingomyelin (d18:1/21:0, d17:1/22:0, d	0.6	1.19
sphingomyelin (d18:2/23:0, d18:1/23:1, d	0.6	1.79
sphingomyelin (d18:2/24:1, d18:1/24:2)*	0.76	1.38
tricosanoyl sphingomyelin (d18:1/23:0)*	0.83	0.87
sphingomyelin (d18:1/17:0, d17:1/18:0,d	0.72	1.28

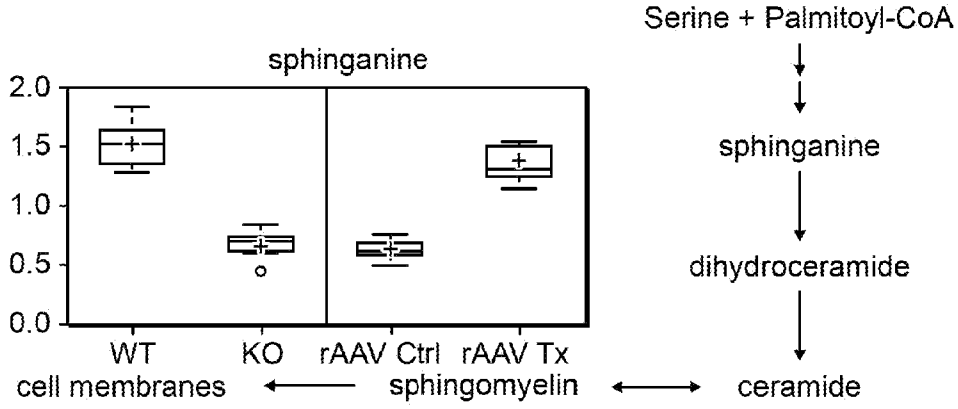

FIG. 13

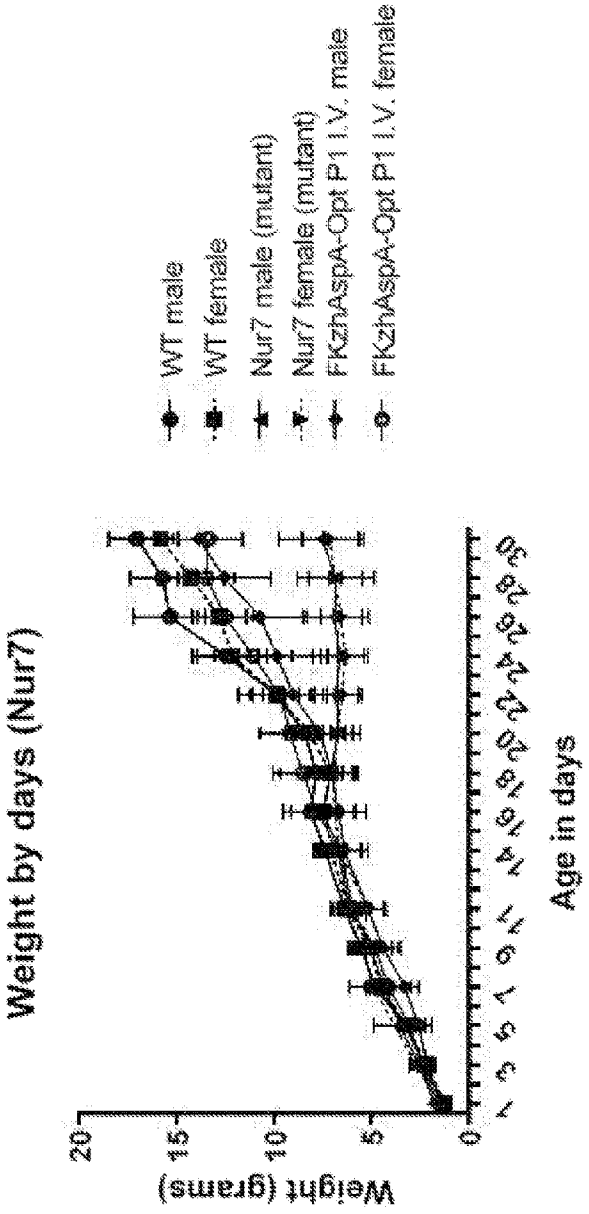
Weight by days (Nur7)
WT male
WT female
Nur7 male (mutant)
Nur7 female (mutant)
FKphAspA-Opt P1 I.V. male
FKphAspA-Opt P1 I.V. female
Weight (grams)
20
15
10
5
0
1
3
5
7
9
11
13
15
17
19
21
23
25
27
29
Age in days

FIG. 14

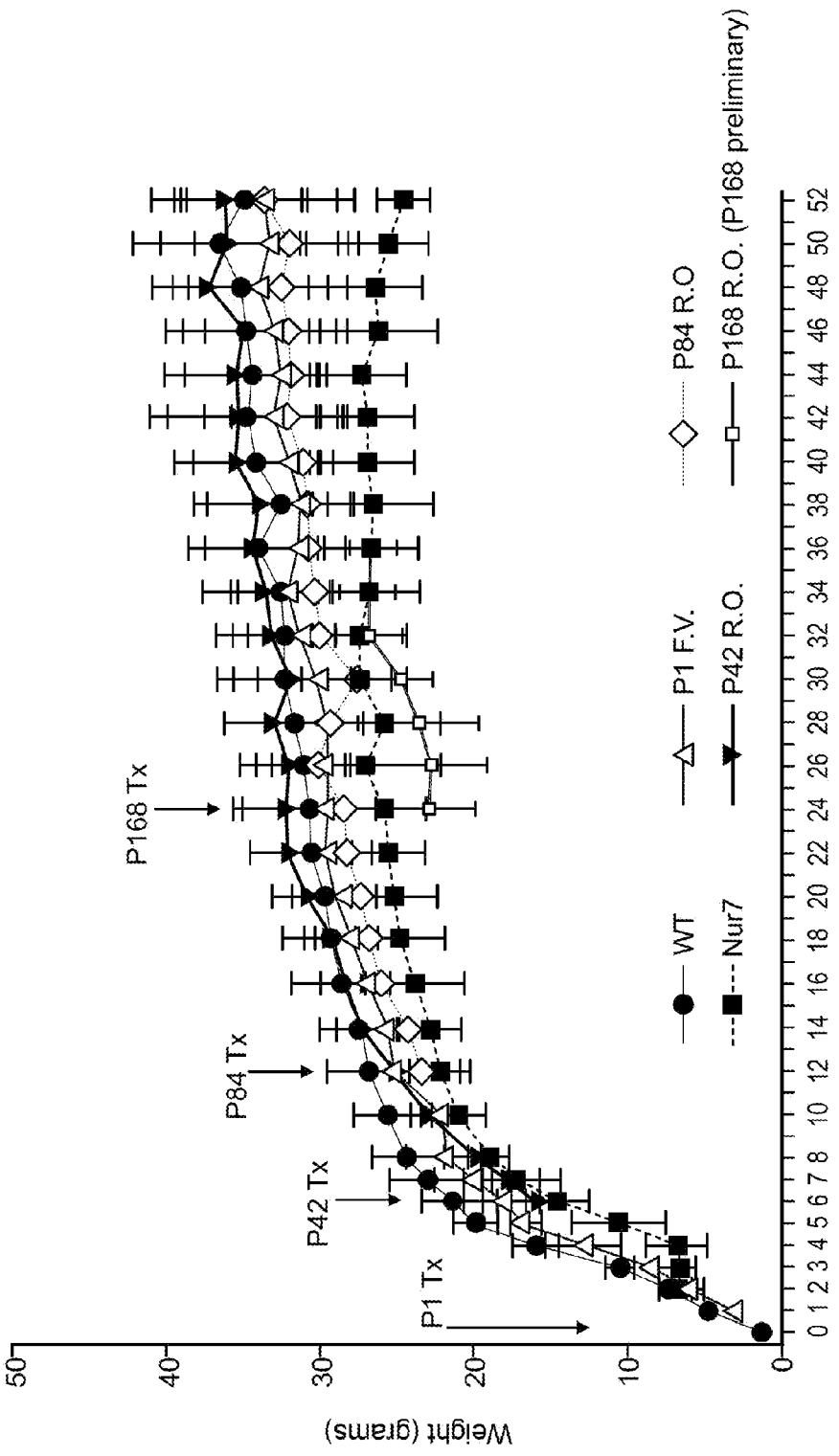
Weight (grams)
50
40
30
20
10
0
P168 Tx
P84 Tx
P42 Tx
P1 Tx
0 1 2 3 4 5 6 7 8 10 12 14 16 18 20 22 24 26 28 30 32 34 36 38 40 42 44 46 48 50 52
Age in weeks
WT
Nur7
P1 F.V.
P42 R.O.
P84 R.O
P168 R.O. (P168 preliminary)

FIG. 15

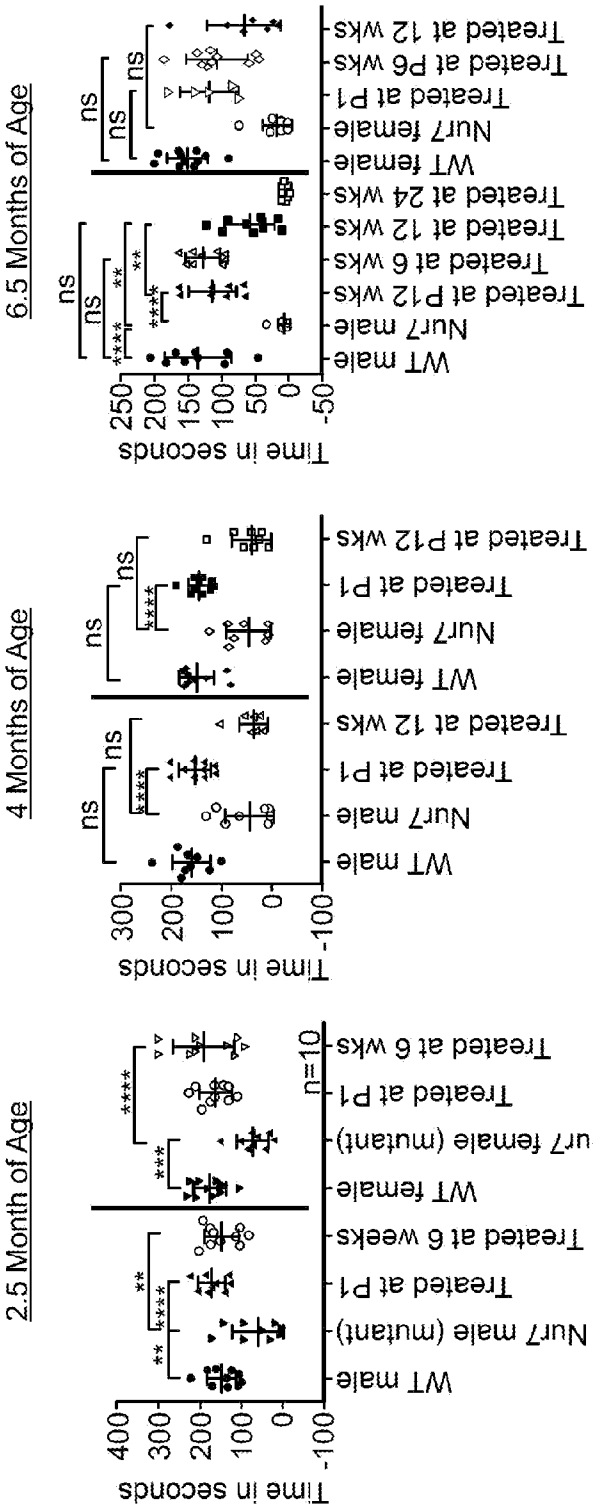
2.5 Month of Age
4 Months of Age
6.5 Months of Age
Time in seconds
WT male
Nur7 male (mutant)
Treated at P1
Treated at 6 weeks
WT female
Nur7 female (mutant)
Treated at P1
Treated at 6 wks
Nur7 male
Treated at P12 wks
Treated at 12 wks
Treated at 24 wks
Nur7 female
Treated at P6 wks
n=10
ns
* p<0.05; ** p<0.01; *** p<0.001; **** p<0.0001

FIG. 16

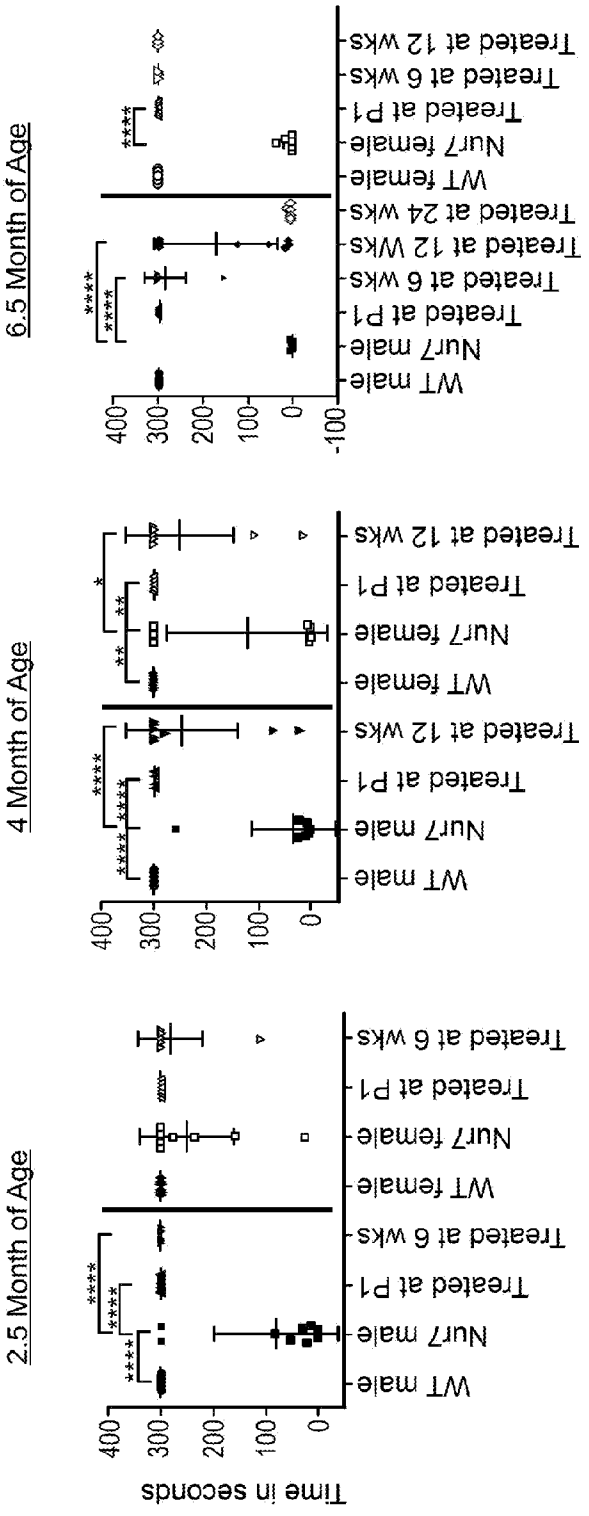
2.5 Month of Age
4 Month of Age
6.5 Month of Age
Time in seconds
400
300
200
100
0
-100
WT male
Nur7 male
Treated at P1
Treated at 6 wks
Treated at 12 Wks
Treated at 24 wks
WT female
Nur7 female
Treated at P1
Treated at 6 wks
Treated at 12 wks
****
**
*

FIG. 17

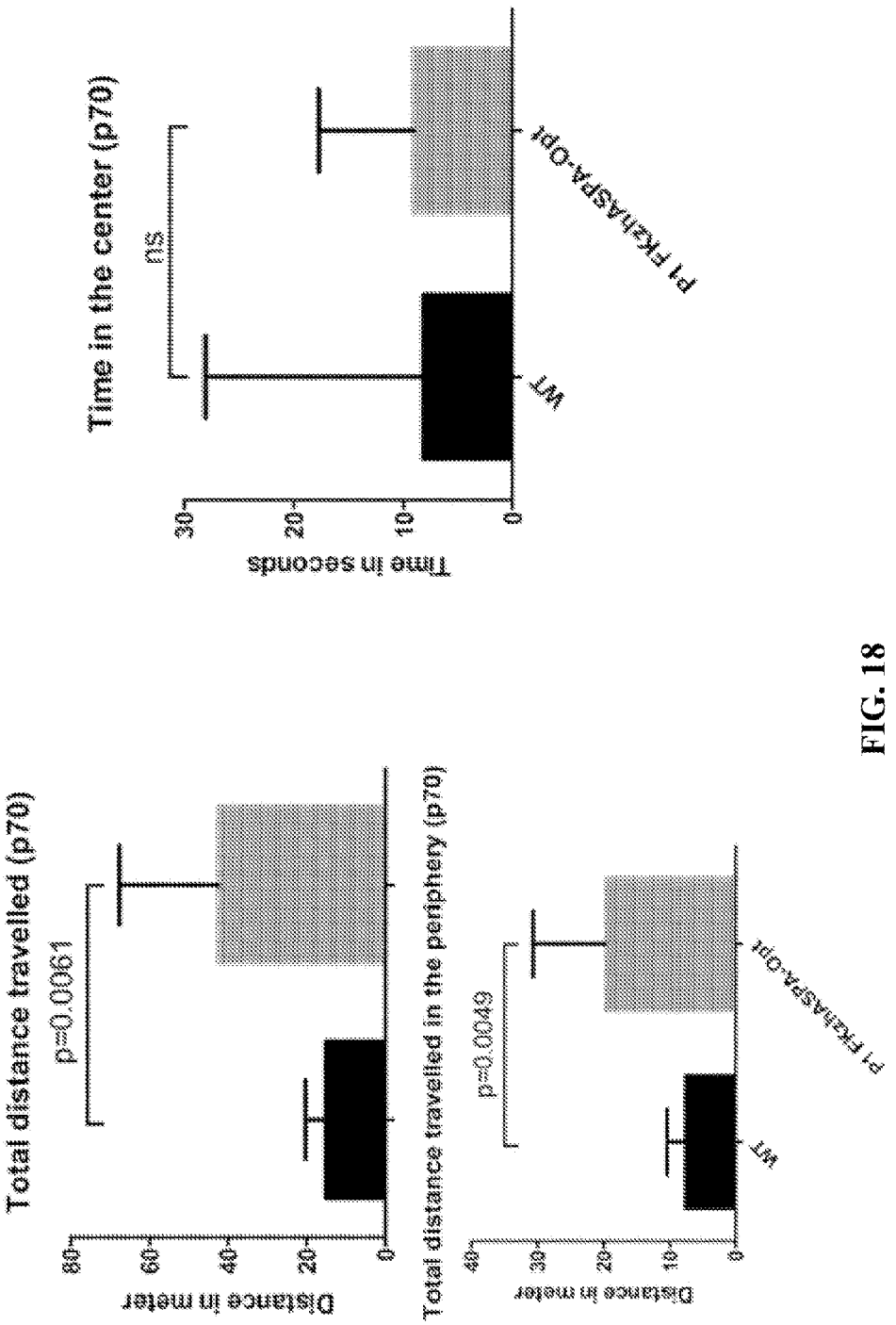
Time in the center (p70)
NS
Time in seconds
0
10
20
30
WT
Pi FKBP5ASPA-Opt
Total distance travelled (p70)
p=0.0061
Distance in meter
0
20
40
60
80
Total distance travelled in the periphery (p70)
p=0.0049
Distance in meter
0
10
20
30
40
WT
Pi FKBP5ASPA-Opt

FIG. 18

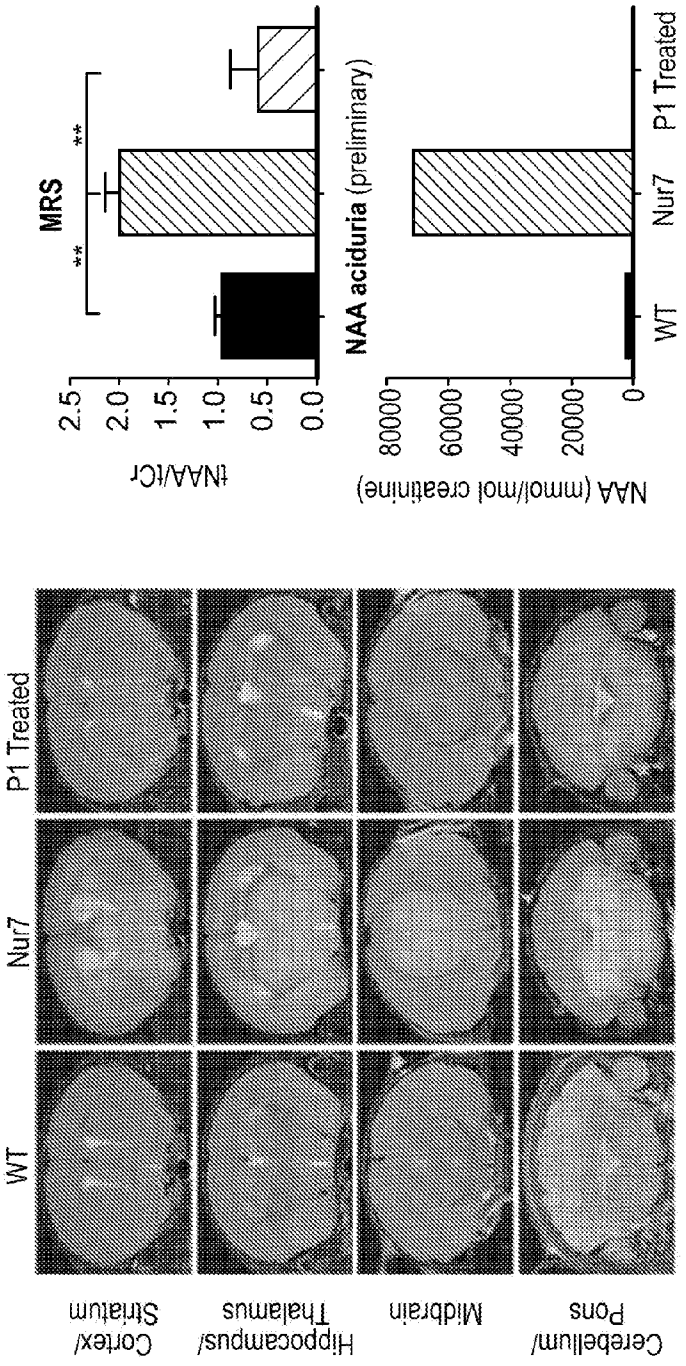
MRS
**
**
tNAA/tCr
2.5
2.0
1.5
1.0
0.5
0.0
NAA aciduria (preliminary)
NAA (mmol/mol creatinine)
80000
60000
40000
20000
0
WT
Nur7
P1 Treated
WT
Nur7
P1 Treated
Cerebellum/ Pons
Midbrain
Hippocampus/ Thalamus
Cortex/ Striatum

FIG. 19

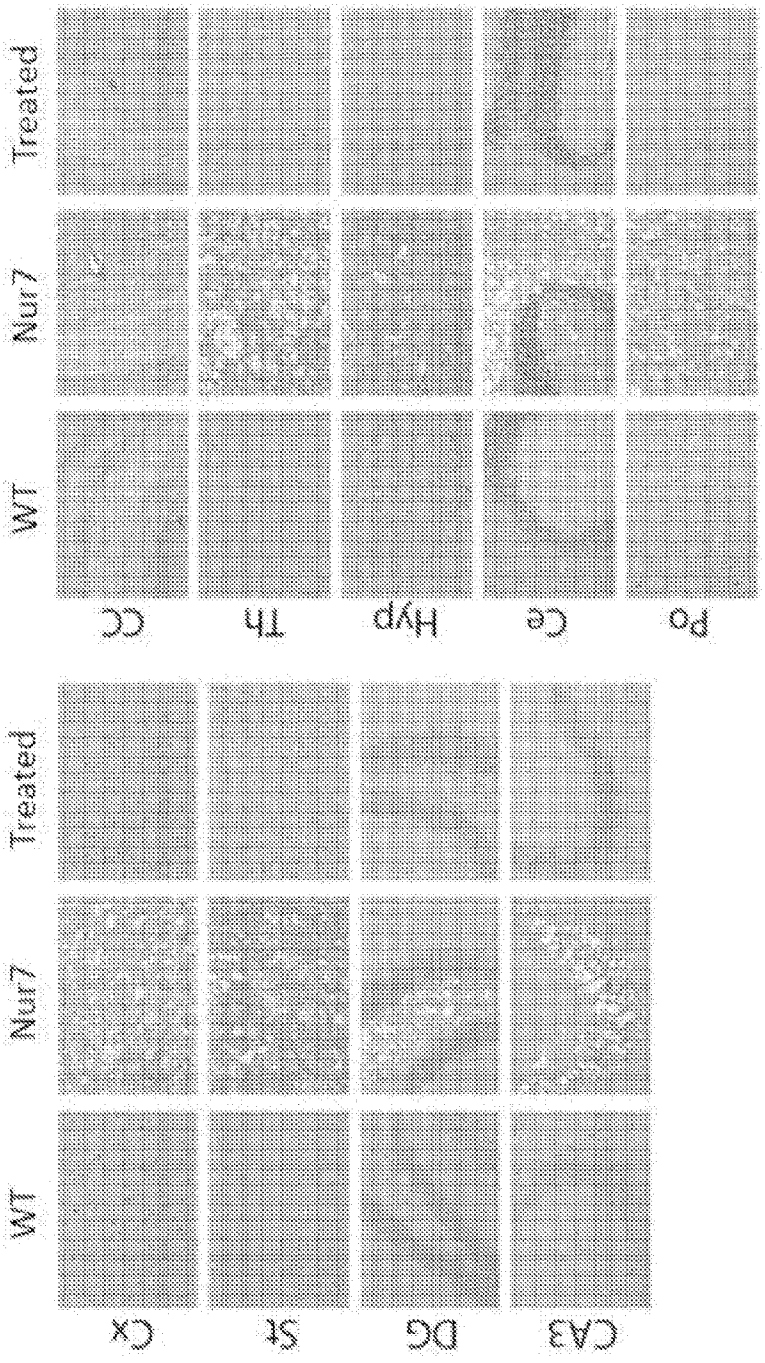

FIG. 20

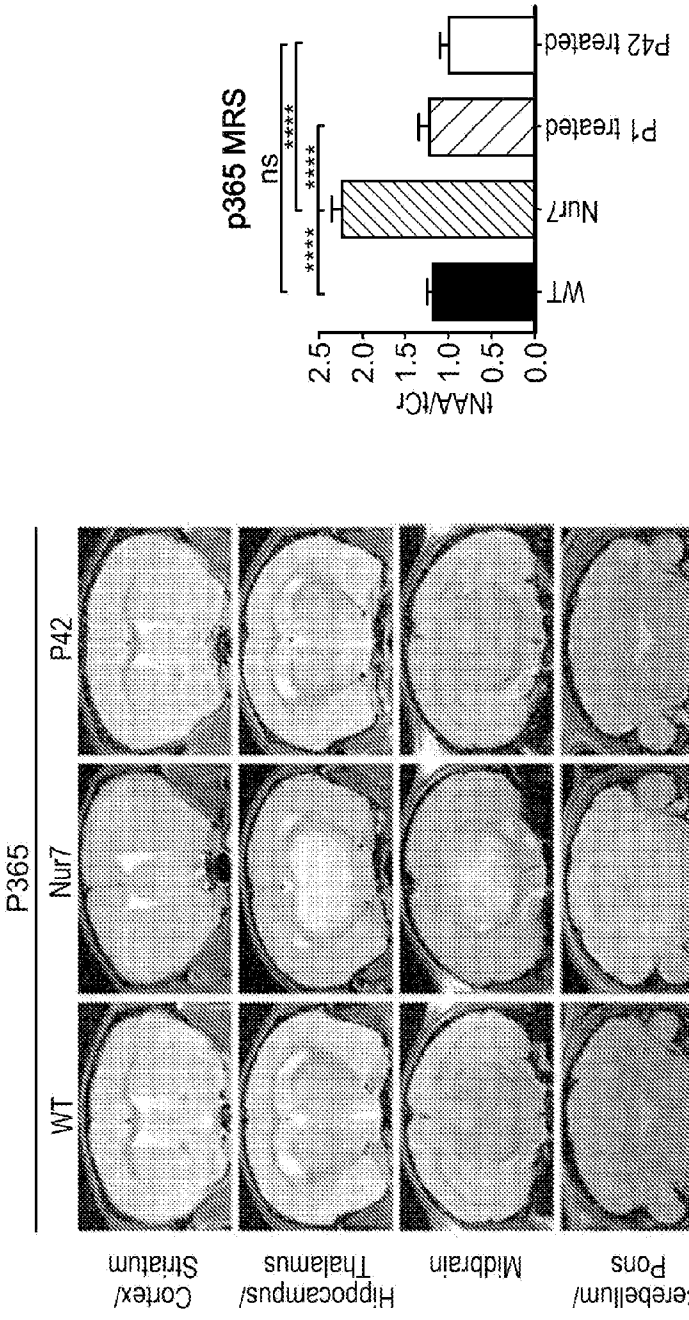
P365
WT
Nur7
P42
Cortex/
Striatum
Hippocampus/
Thalamus
Midbrain
Cerebellum/
Pons
p365 MRS
tNAA/tCr
2.5
2.0
1.5
1.0
0.5
0.0
WT
Nur7
P1 treated
P42 treated
ns
****
****
****

FIG. 21

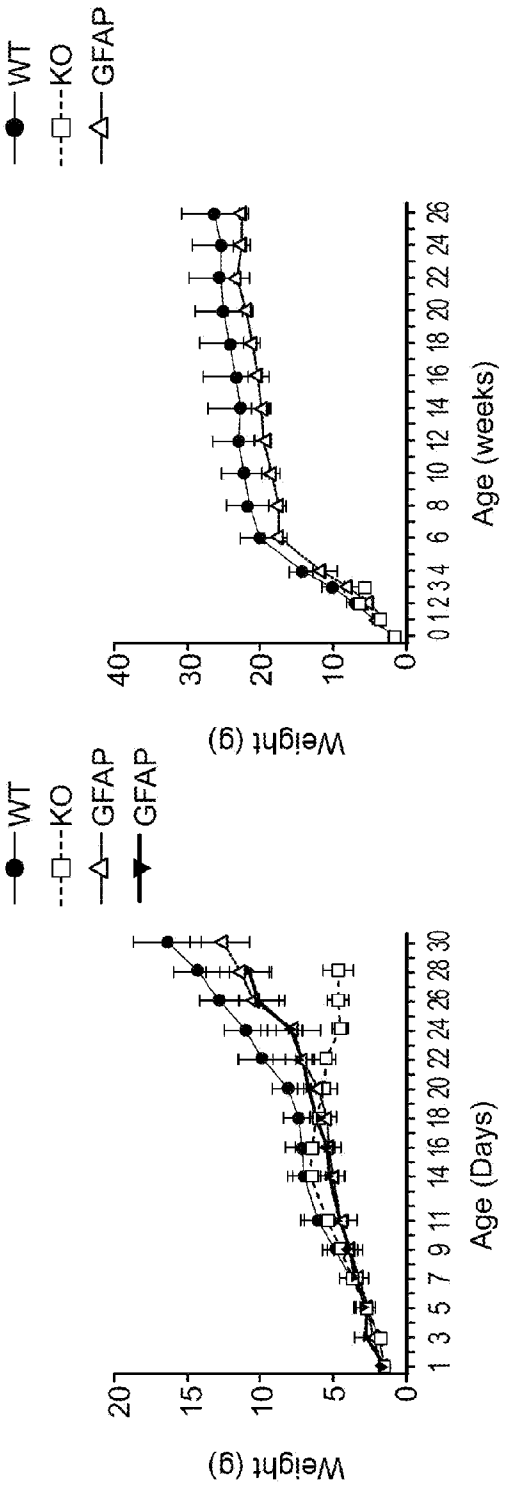
WT
KO
GFAP
GFAP
Weight (g)
0
5
10
15
20
1 3 5 7 9 11 14 16 18 20 22 24 26 28 30
Age (Days)
WT
KO
GFAP
Weight (g)
0
10
20
30
40
0 1 2 3 4 6 8 10 12 14 16 18 20 22 24 26
Age (weeks)

FIG. 22

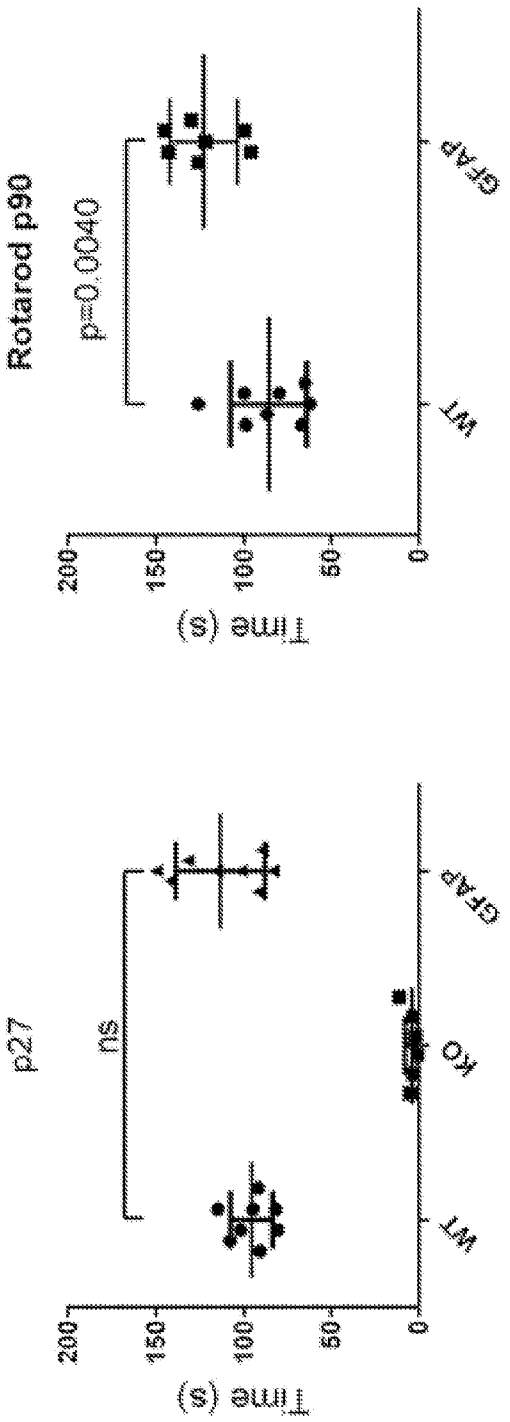
Rotarod p90
p=0.0040
Time (s)
200
150
100
50
0
WT
GFAP
p27
ns
Time (s)
200
150
100
50
0
WT
KO
GFAP

FIG. 23

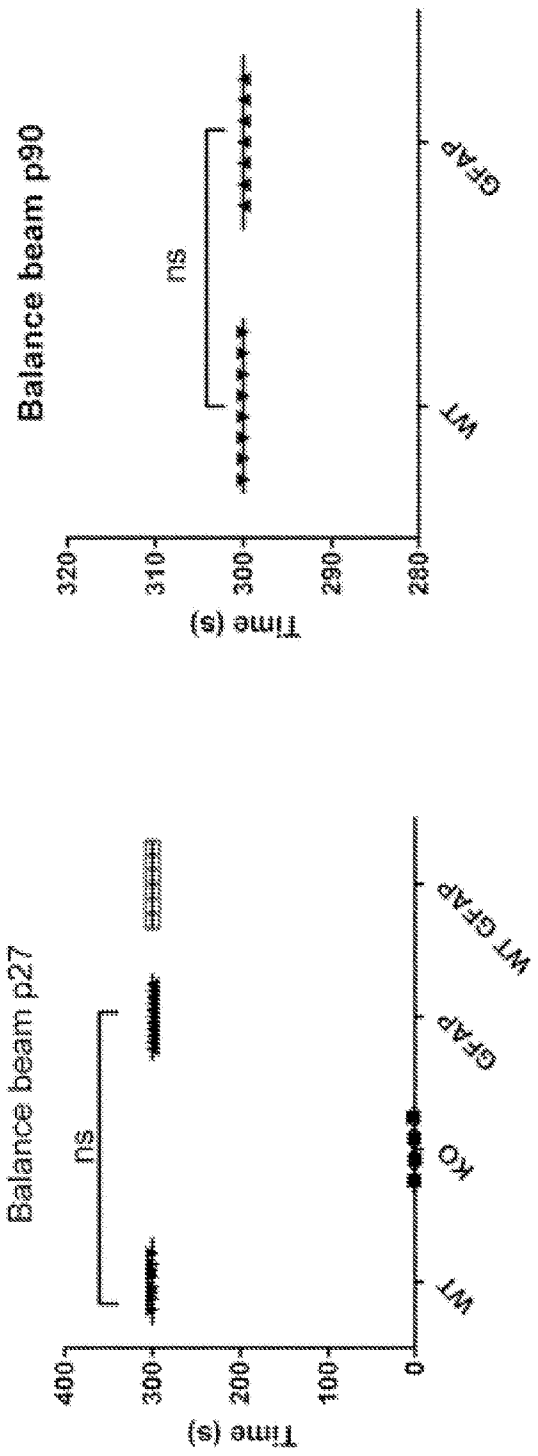
Balance beam p90
ns
Time (s)
320
310
300
290
280
WT
GFAP
Balance beam p27
ns
Time (s)
400
300
200
100
0
WT
KO
GFAP
WT GFAP

FIG. 24

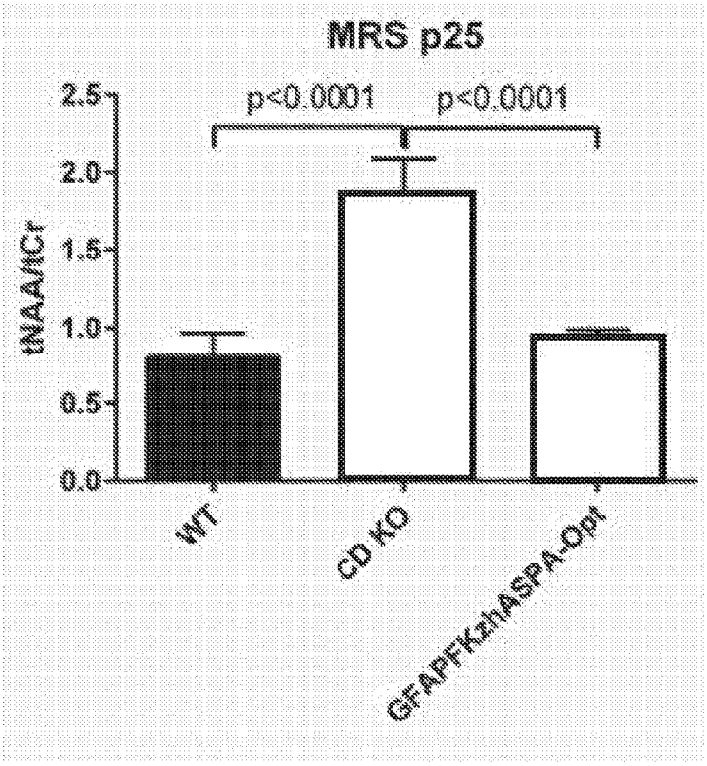
MRS p25
p<0.0001
p<0.0001
tNAA/tCr
2.5
2.0
1.5
1.0
0.5
0.0
WT
CD KO
GFAPFKzhASPA-Opt

FIG. 25

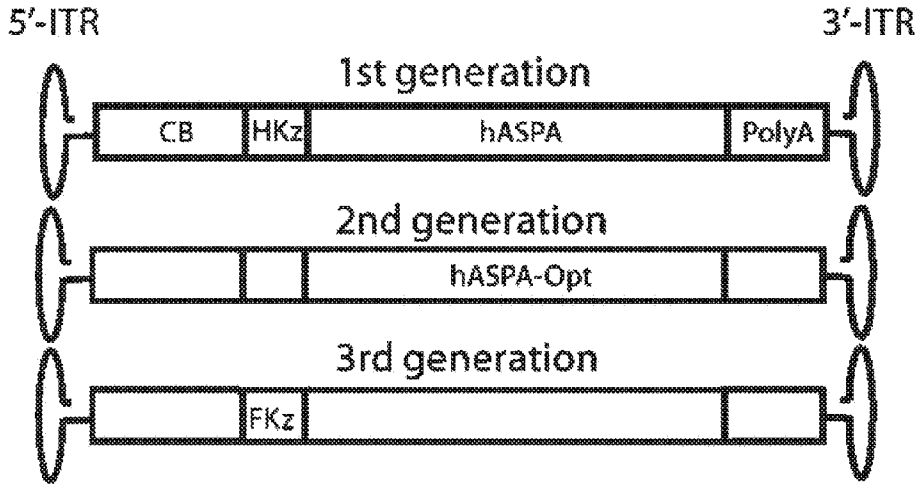

FIG. 26A

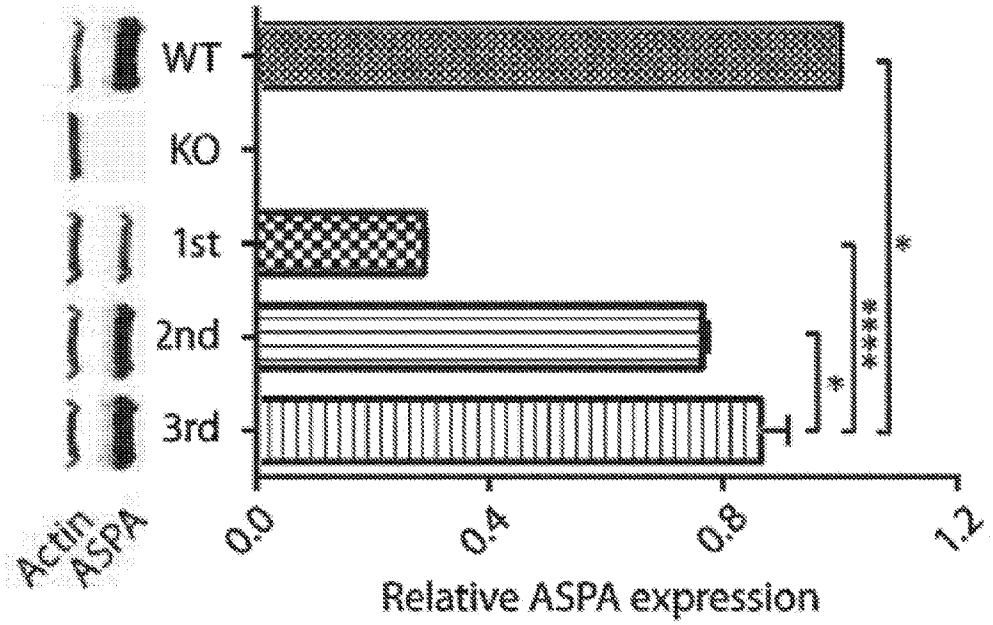

FIG. 26B

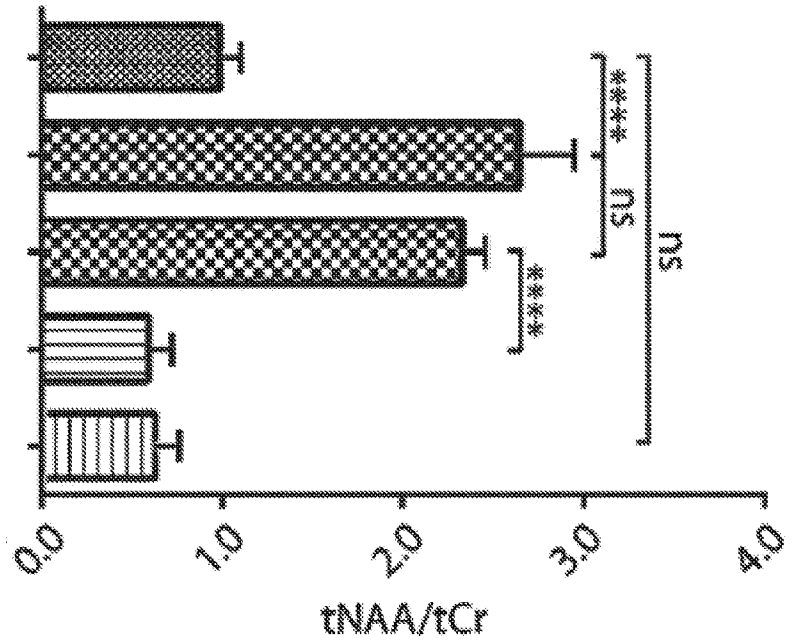

FIG. 26C

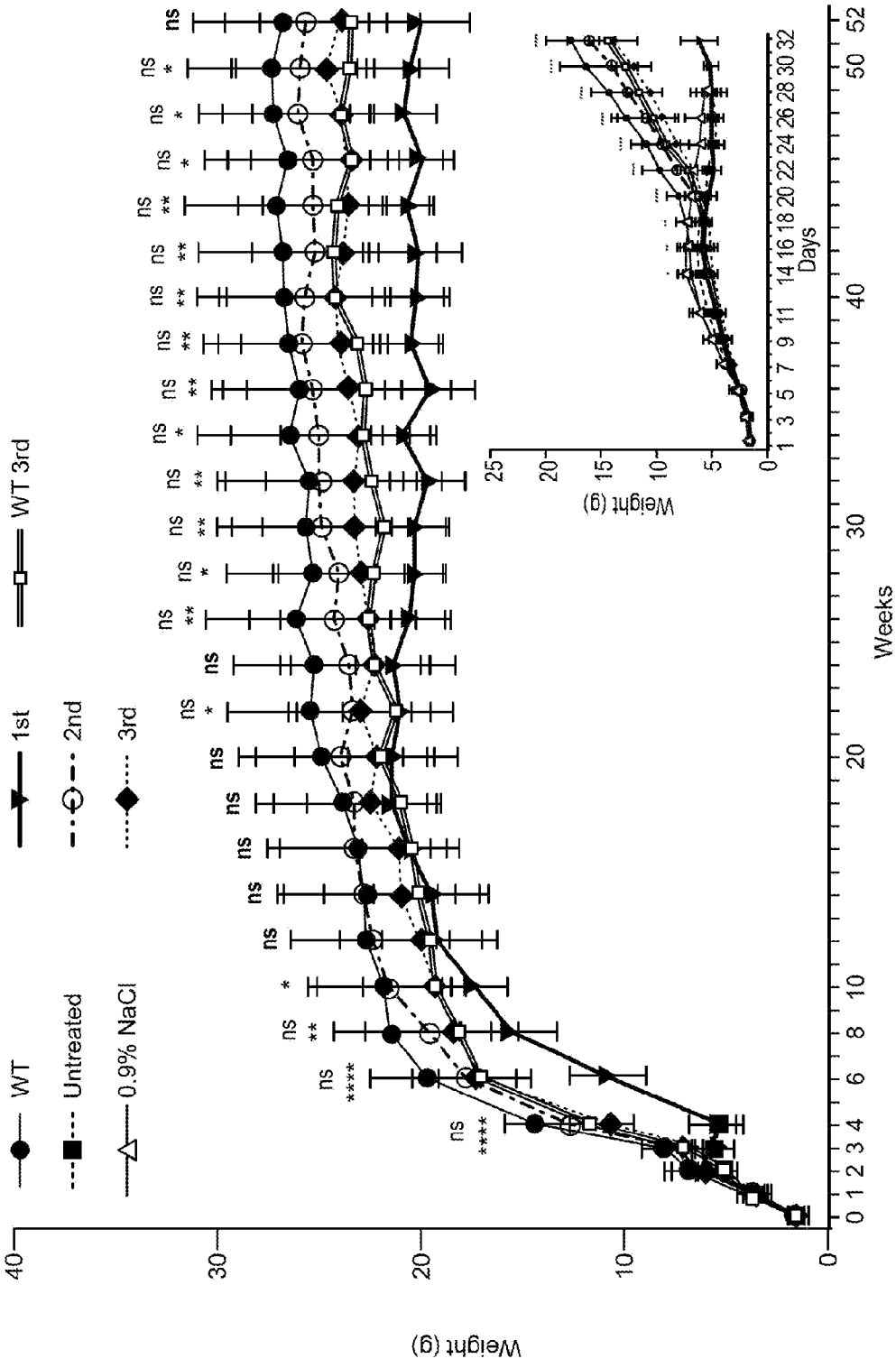
WT
Untreated
0.9% NaCl
1st
2nd
3rd
WT 3rd
Weight (g)
Weeks
Days
Weight (g)

FIG. 27

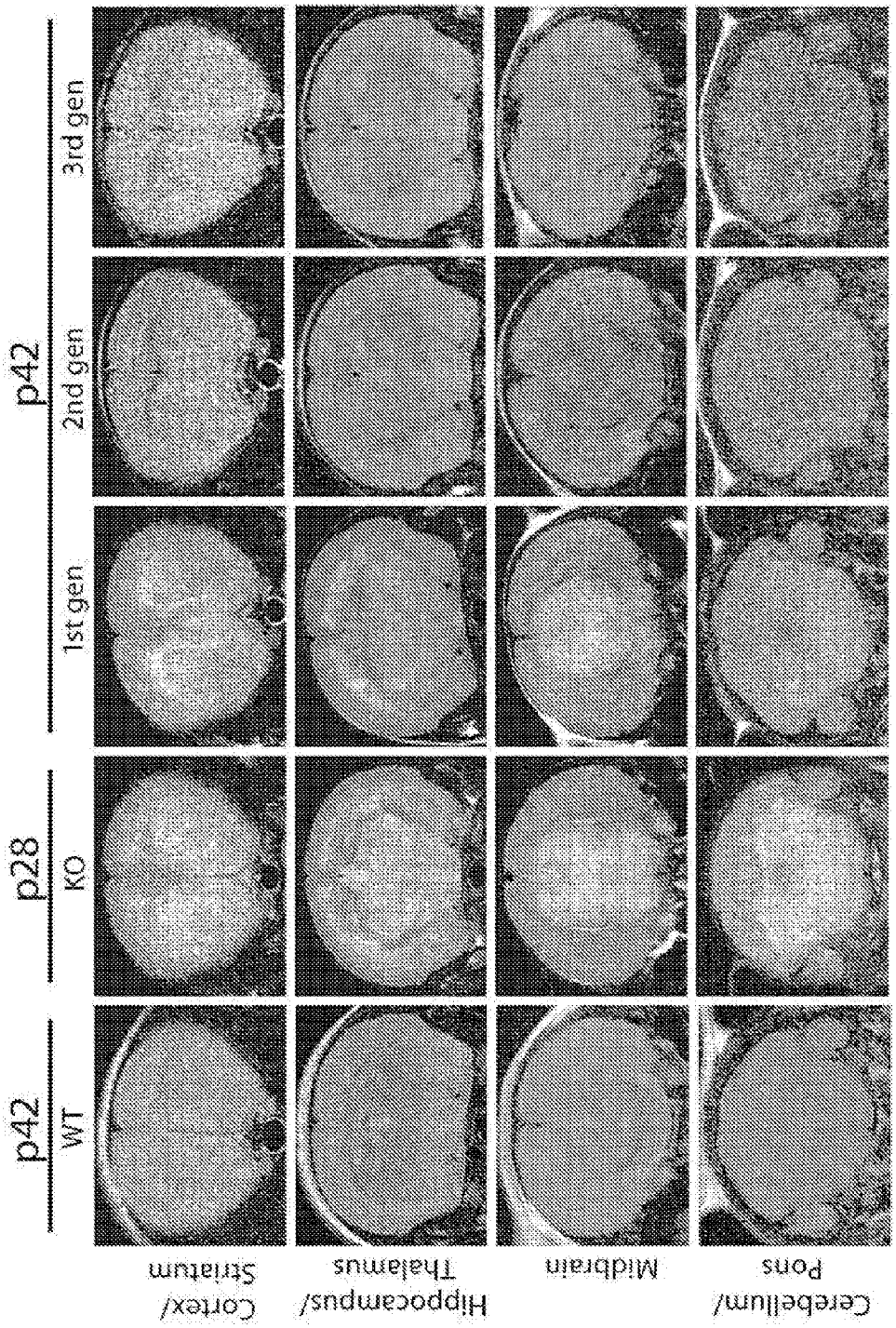
p42
WT
p28
KO
p42
1st gen
2nd gen
3rd gen
Cortex/
Striatum
Hippocampus/
Thalamus
Midbrain
Cerebellum/
Pons

FIG. 28

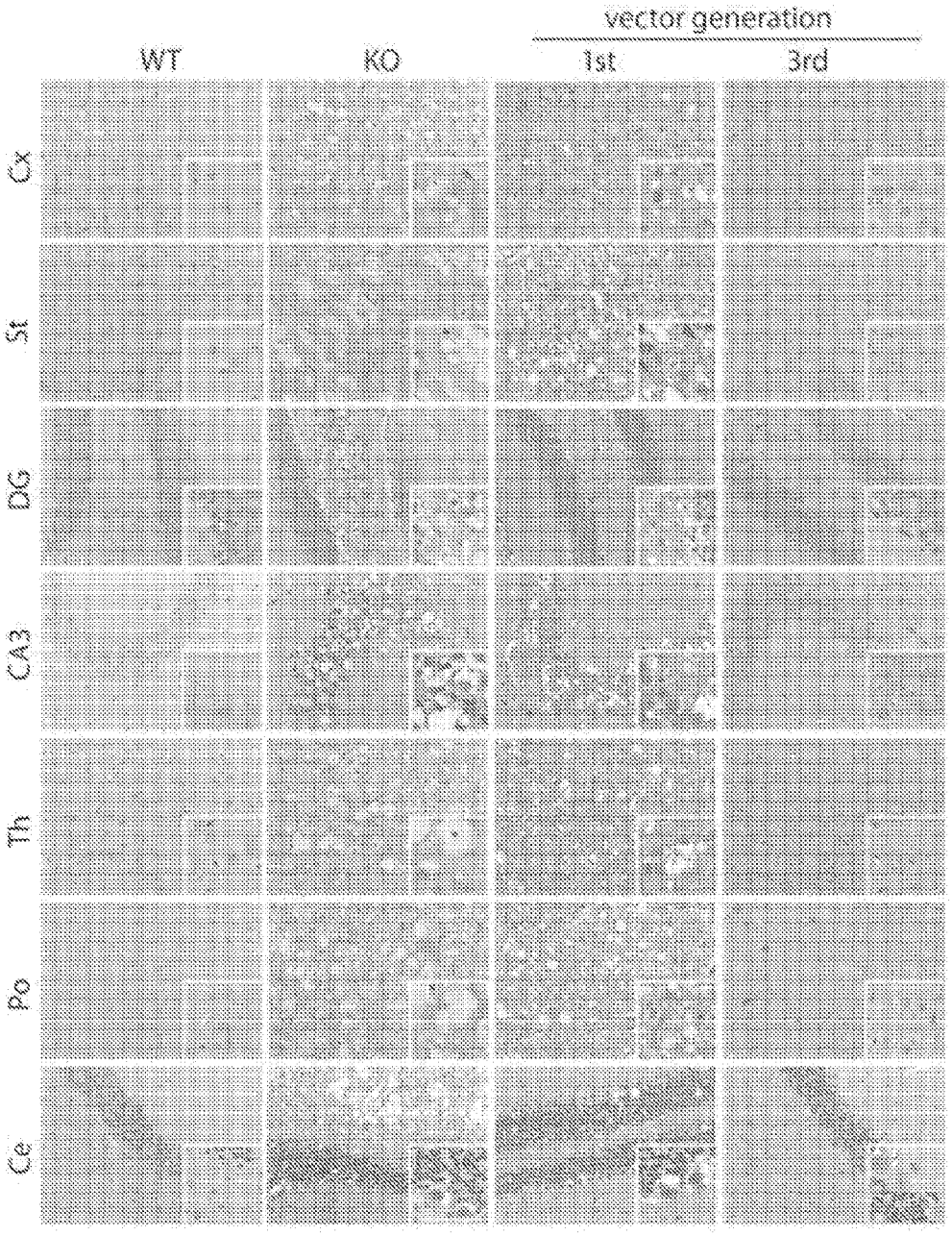

FIG. 29

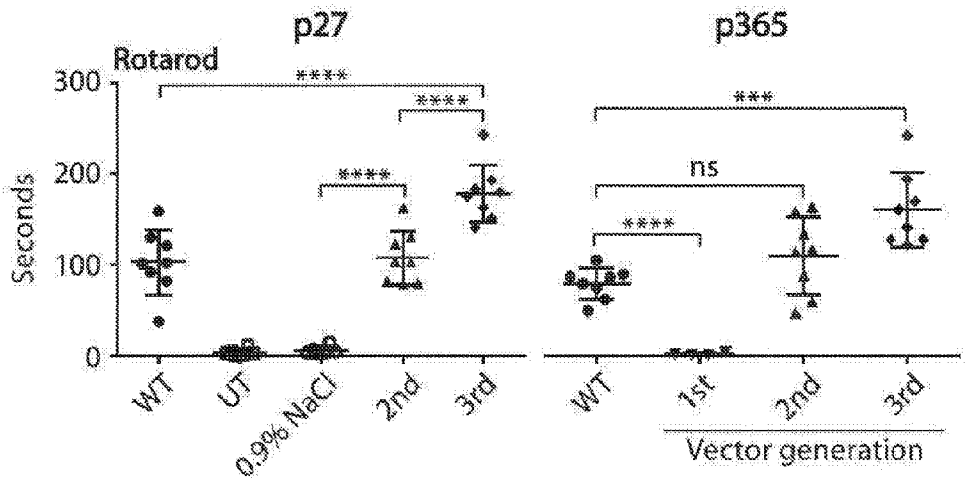

FIG. 30A

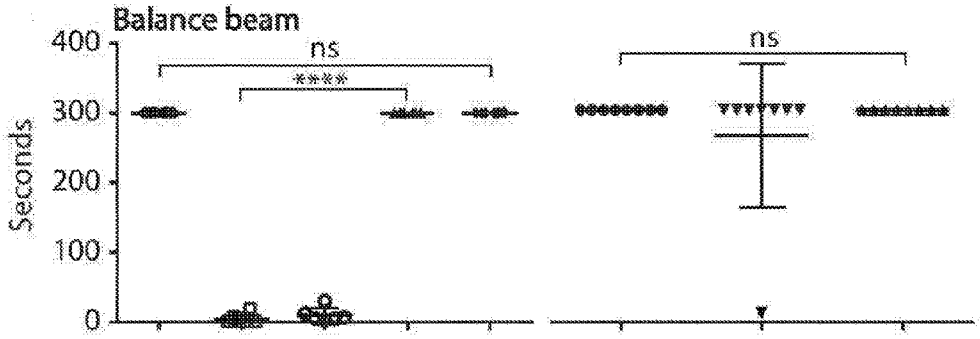

FIG. 30B

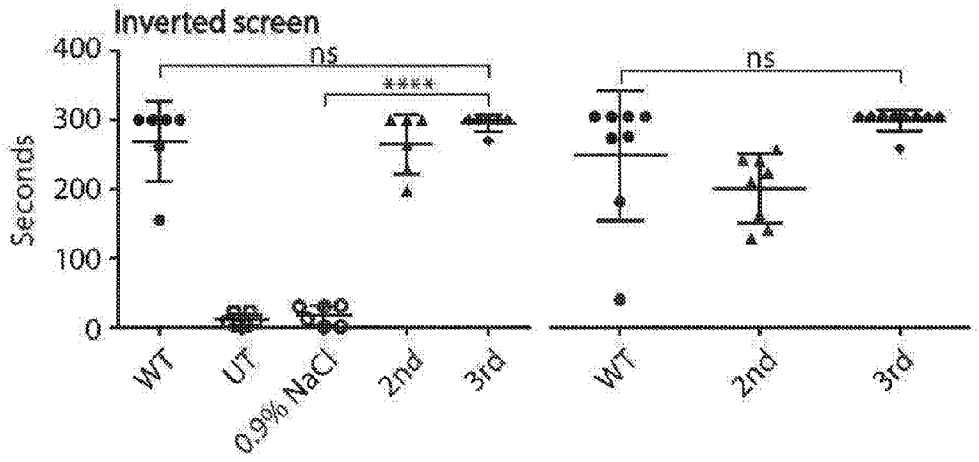

FIG. 30C

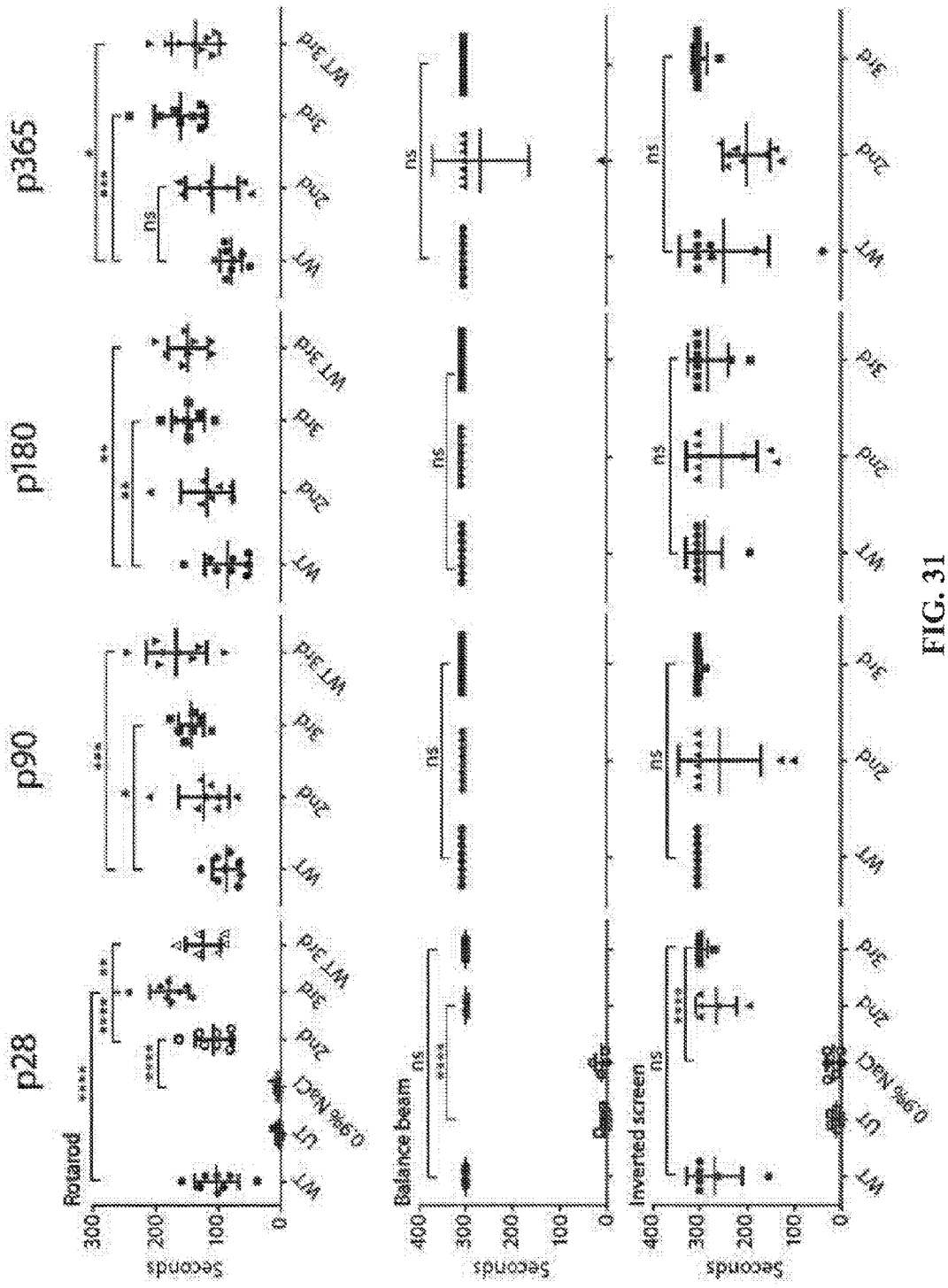
p28
p90
p180
p365
Rotarod
Balance beam
Inverted screen
Seconds
WT
UT
0.9% NaCl
2nd
3rd
ns

FIG. 31

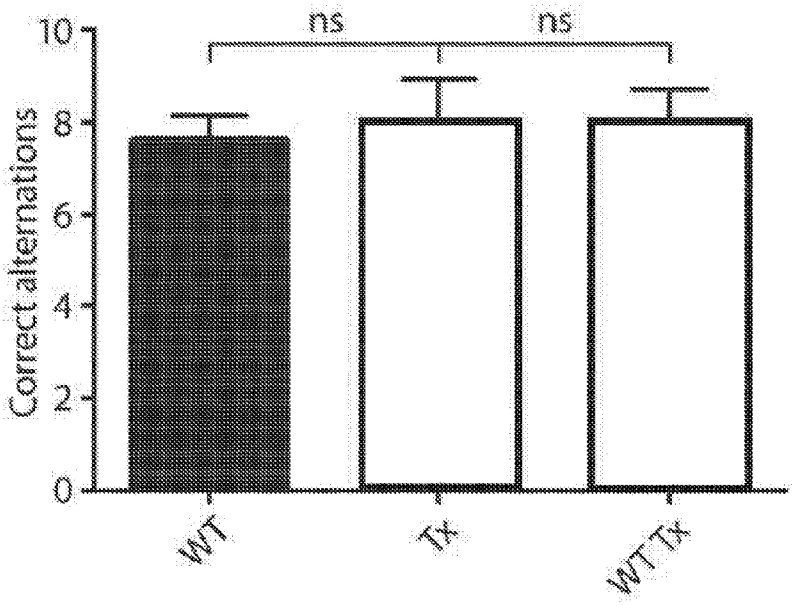

FIG. 32

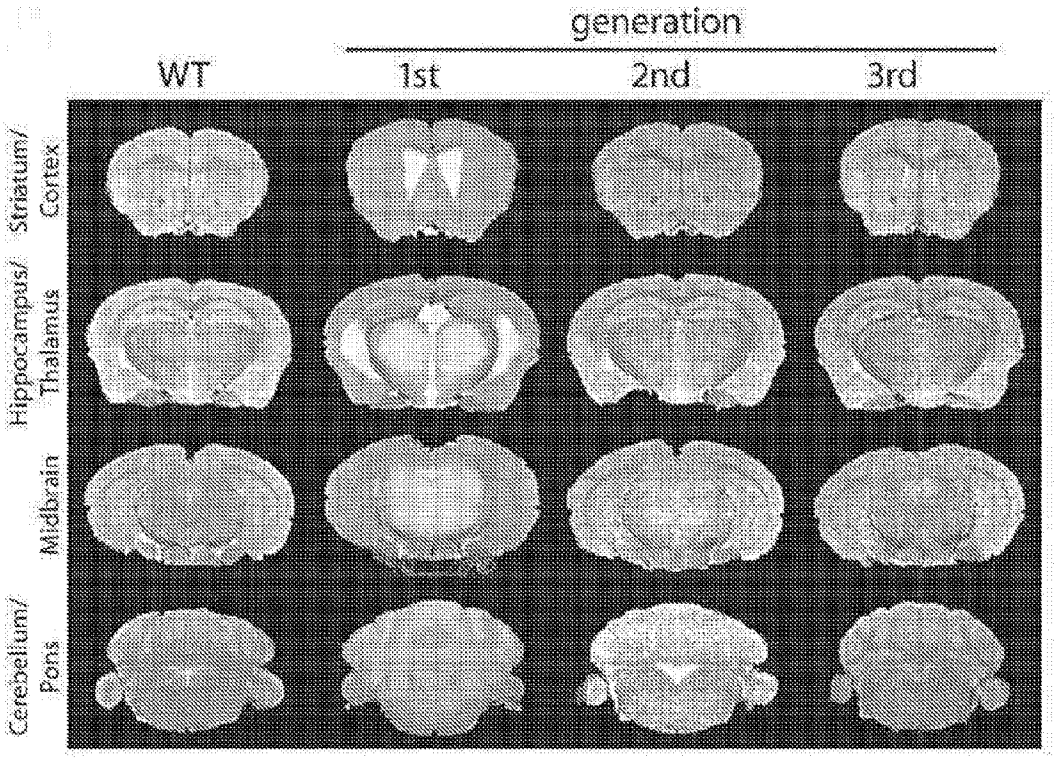

FIG. 33A

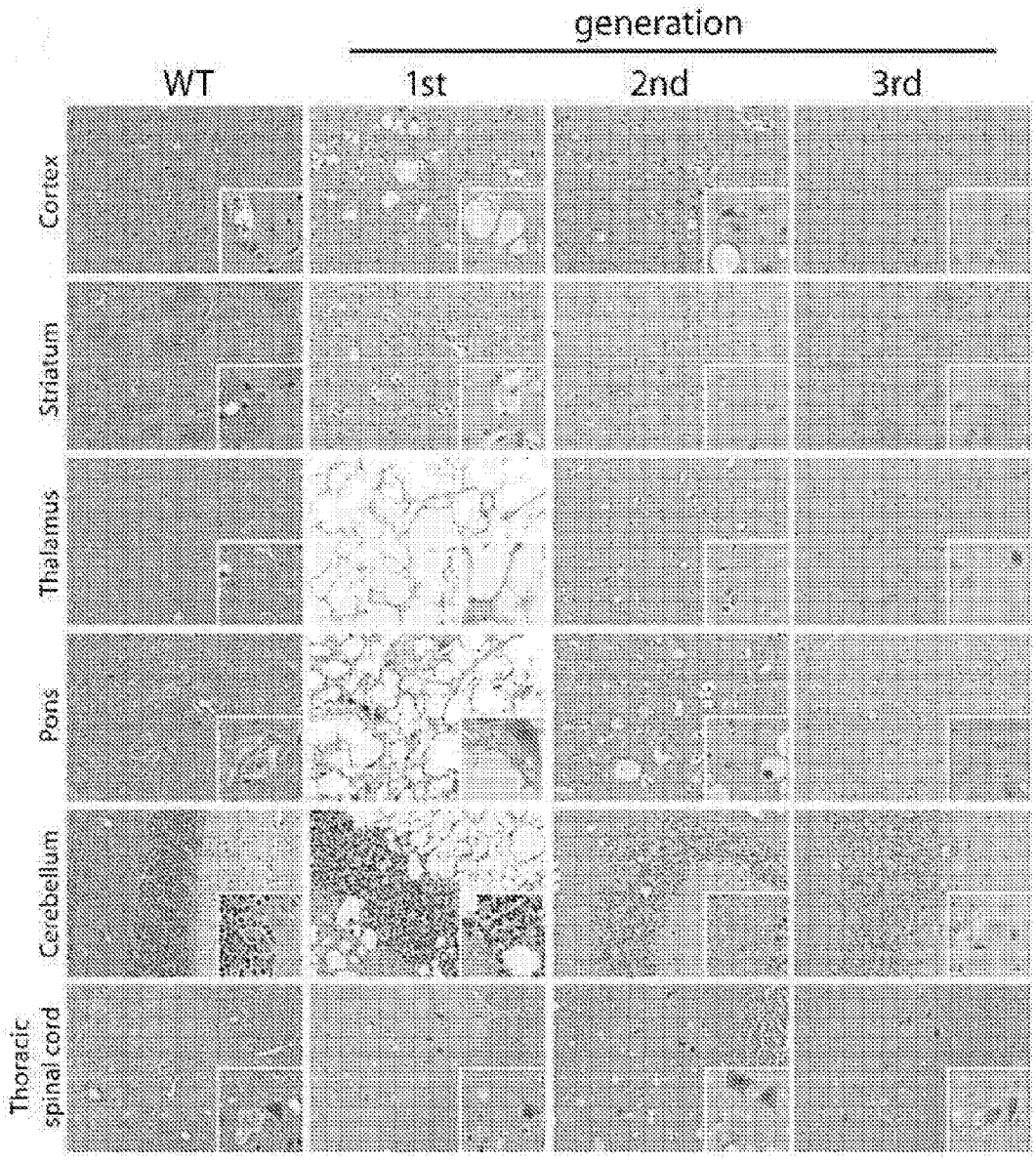
generation
WT
1st
2nd
3rd
Cortex
Striatum
Thalamus
Pons
Cerebellum
Thoracic spinal cord

FIG. 33B

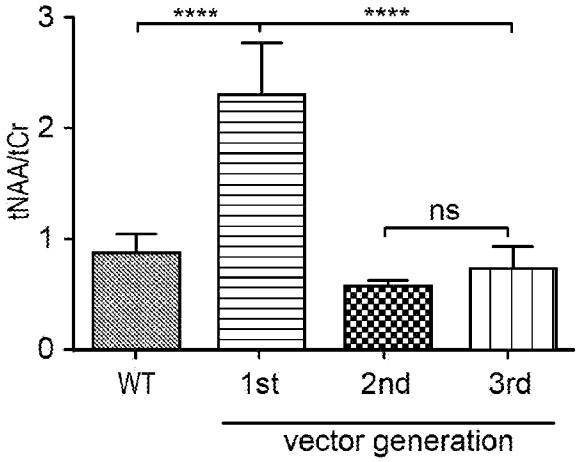

FIG. 33C

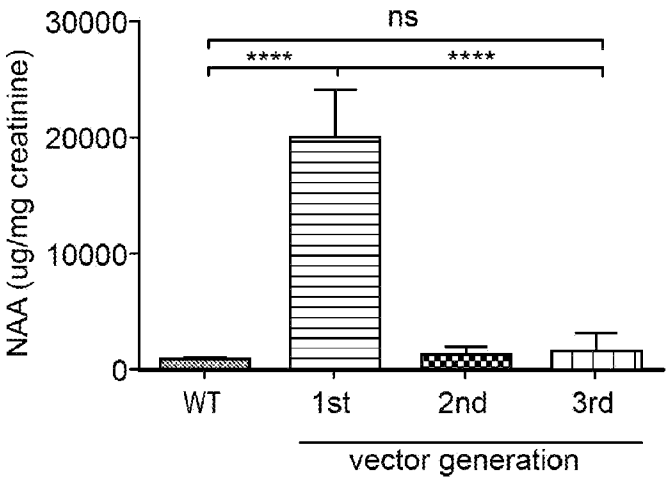

FIG. 33D

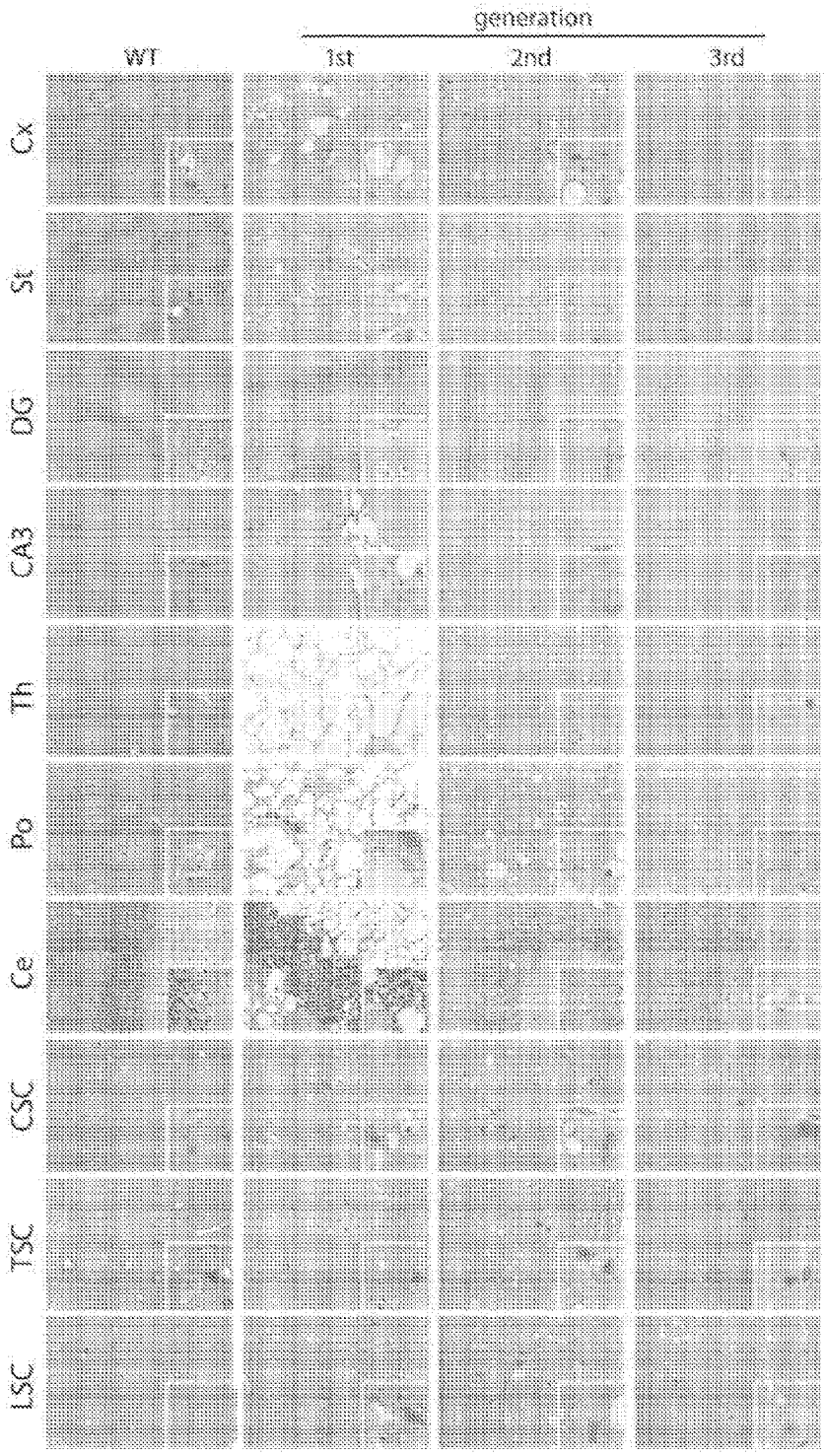

FIG. 34

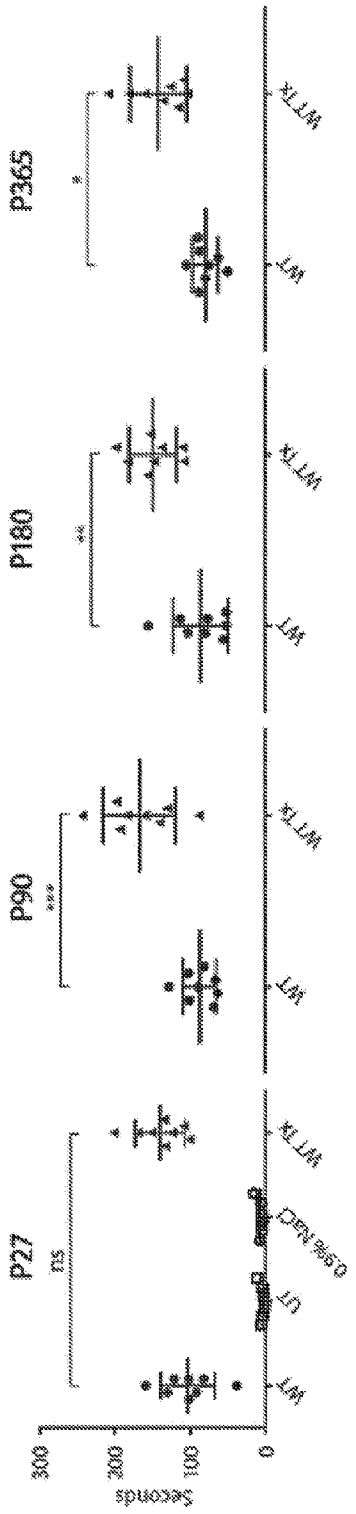
P365
P180
P90
P27
ns
Seconds
300
200
100
0
WT
UT
DEN 25kD
WT-X
XL-M

FIG. 35

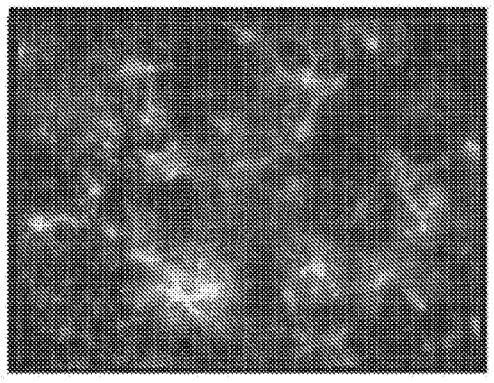

FIG. 36A

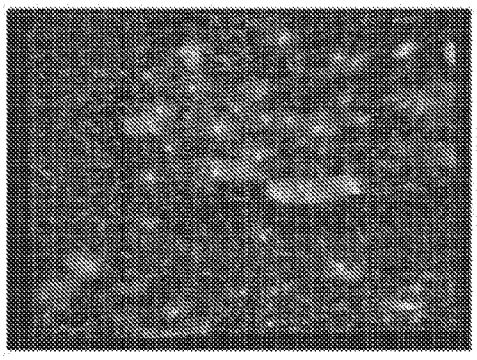

FIG. 36B

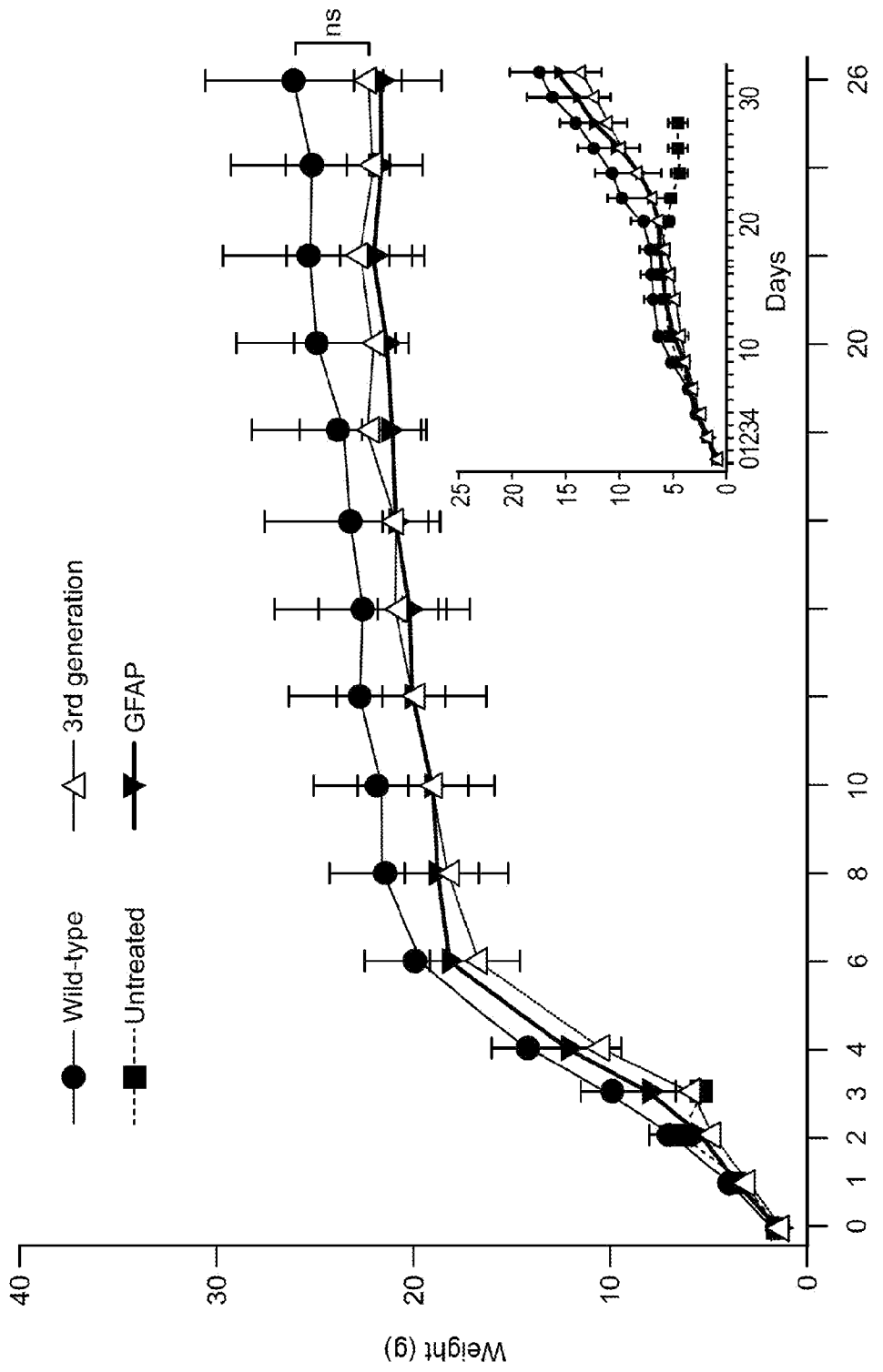
Wild-type
Untreated
3rd generation
GFAP
ns
Weight (g)
Weeks
Days
0
10
20
30
40
0 1 2 3 4 6 8 10 20 26
0 5 10 15 20 25
01234 10 20 30

FIG. 36C

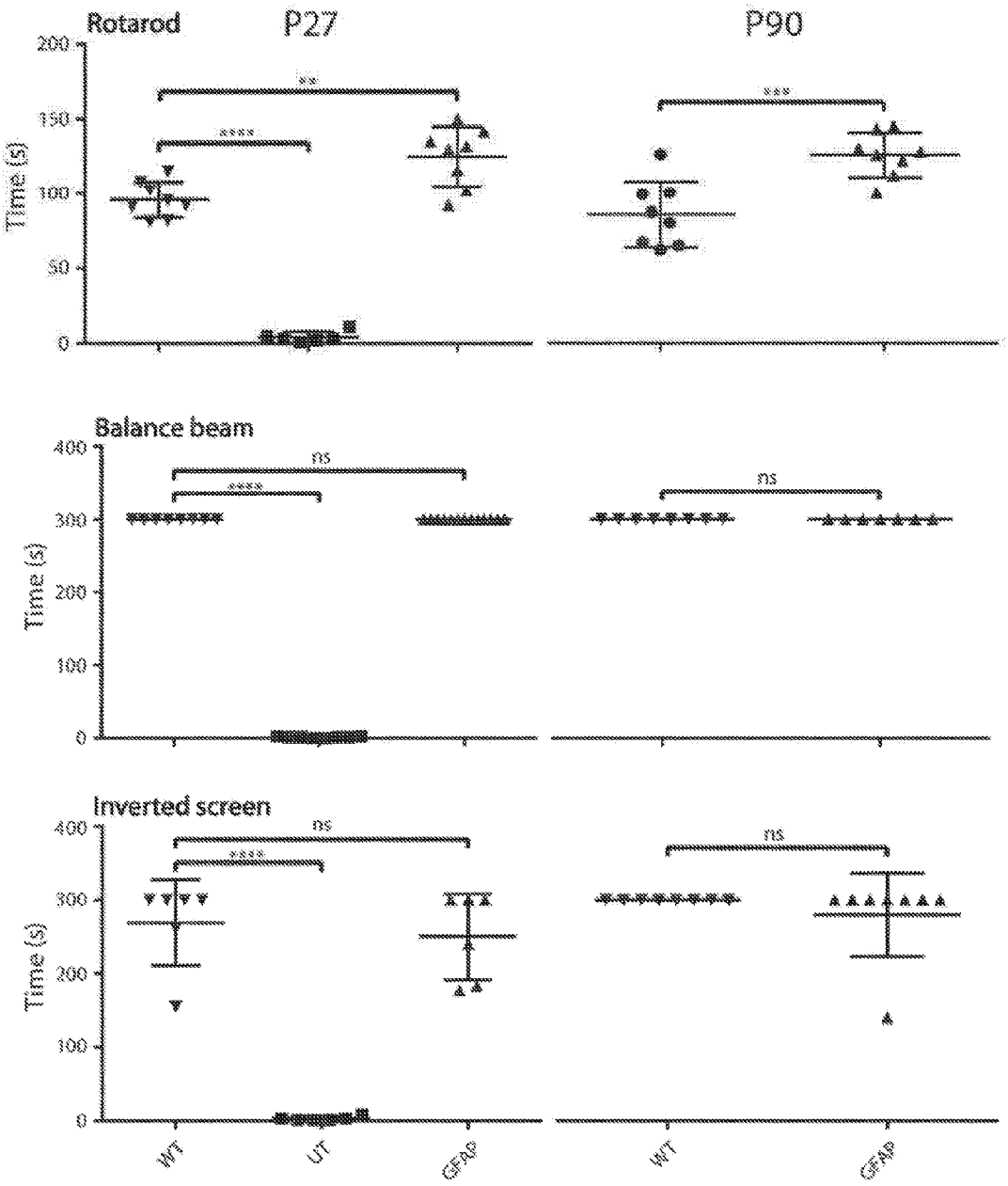
Rotarod
P27
P90
Time (s)
200
150
100
50
0
**
****
***
Balance beam
Time (s)
400
300
200
100
0
ns
****
ns
Inverted screen
Time (s)
400
300
200
100
0
ns
****
ns
WT
UT
GFAP
WT
GFAP

FIG. 36D

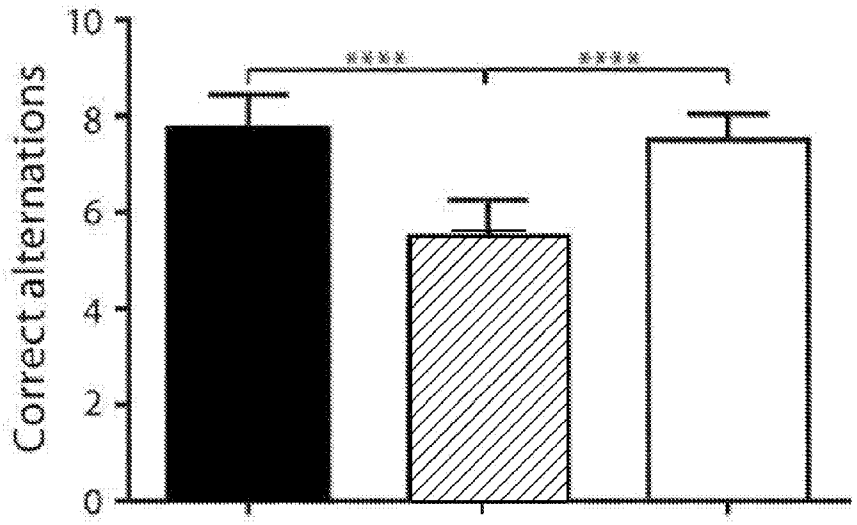

FIG. 36E

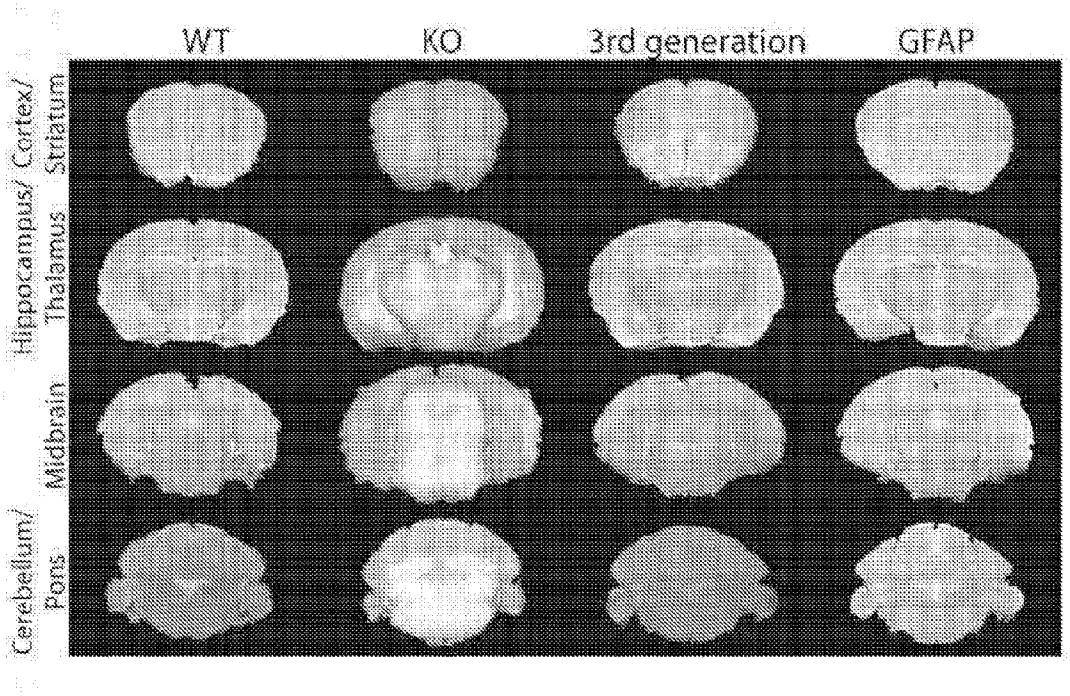

FIG. 36F

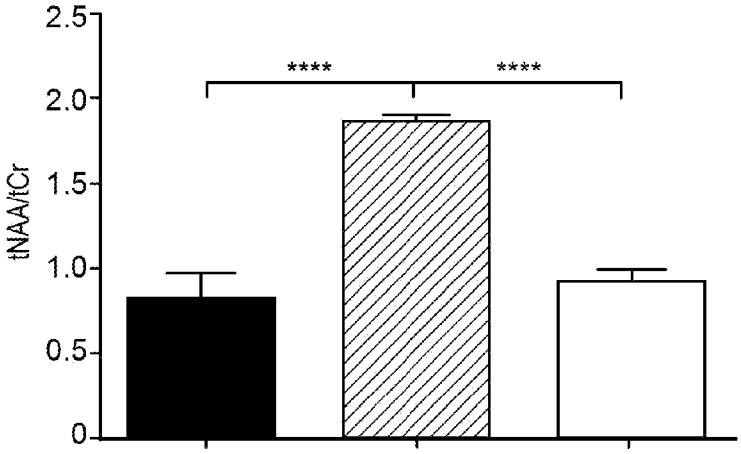

FIG. 36G

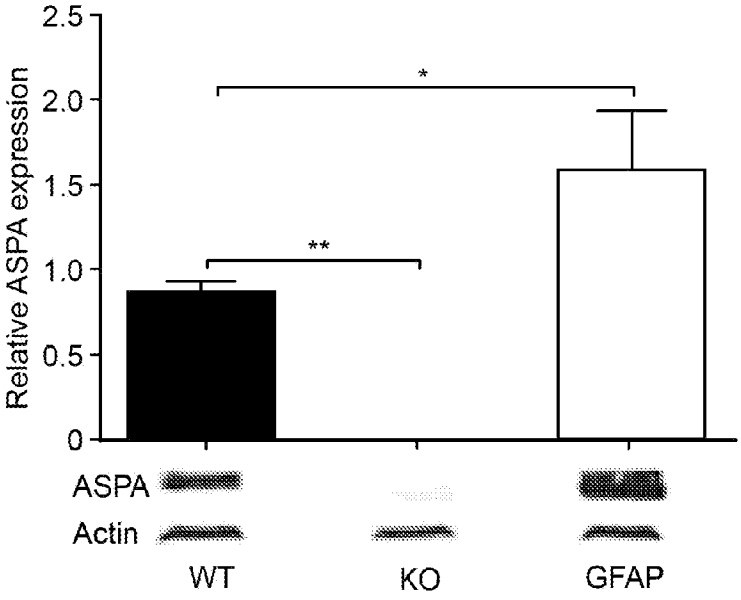

FIG. 36H

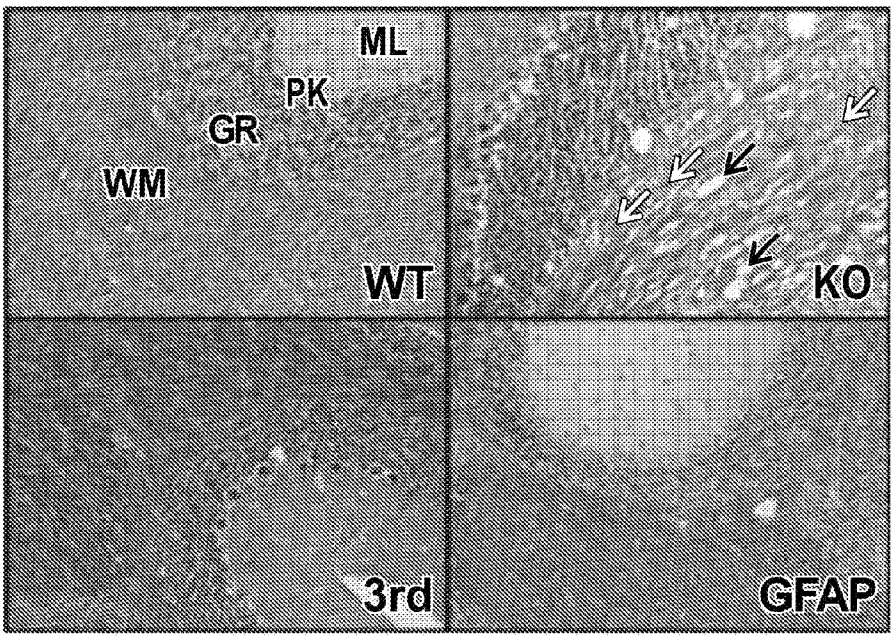

FIG. 36I

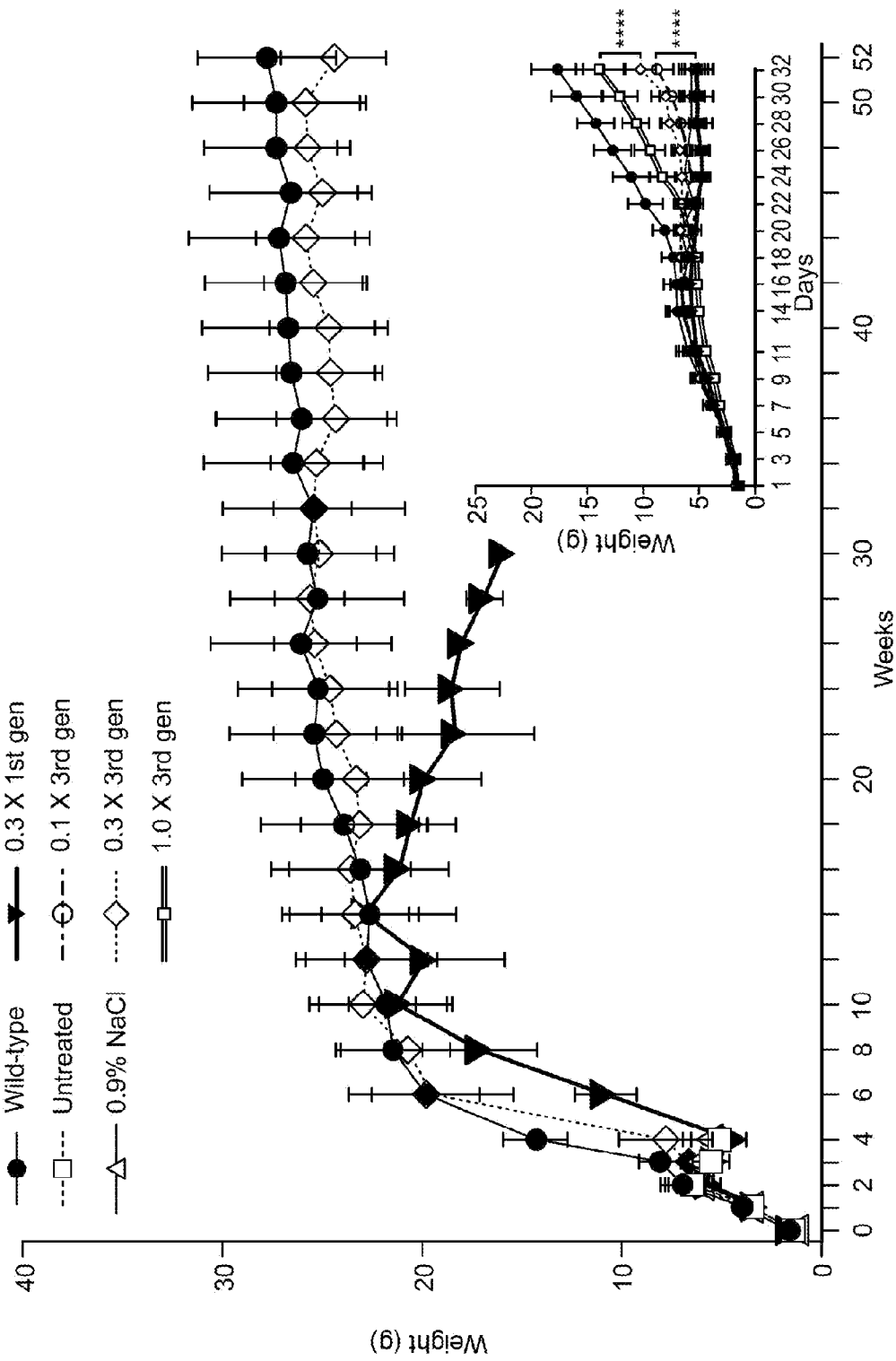
Wild-type
Untreated
0.9% NaCl
0.3 X 1st gen
0.1 X 3rd gen
0.3 X 3rd gen
1.0 X 3rd gen
Weight (g)
Weeks
Days
****
****

FIG. 37

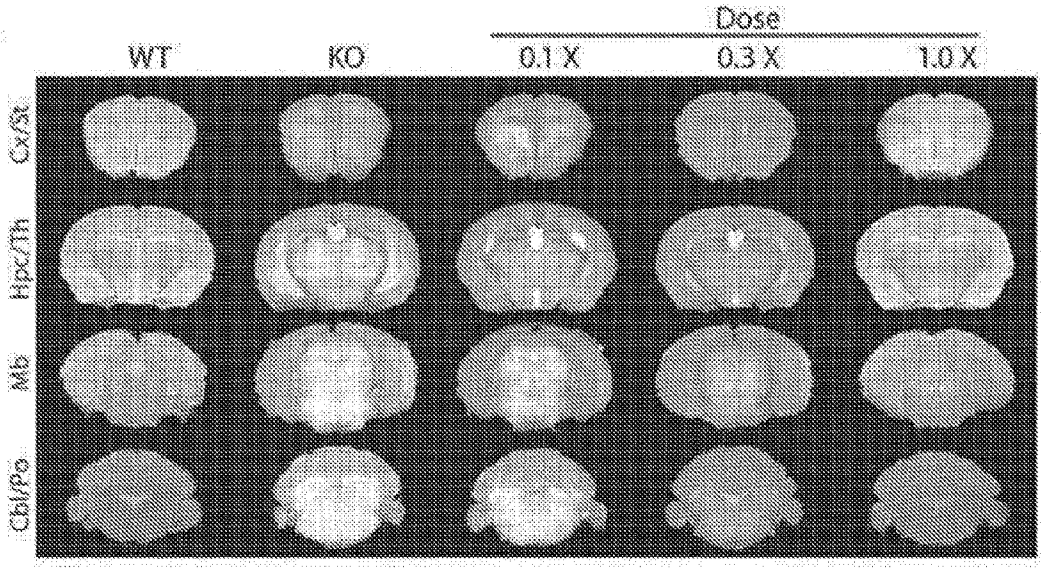

FIG. 38A

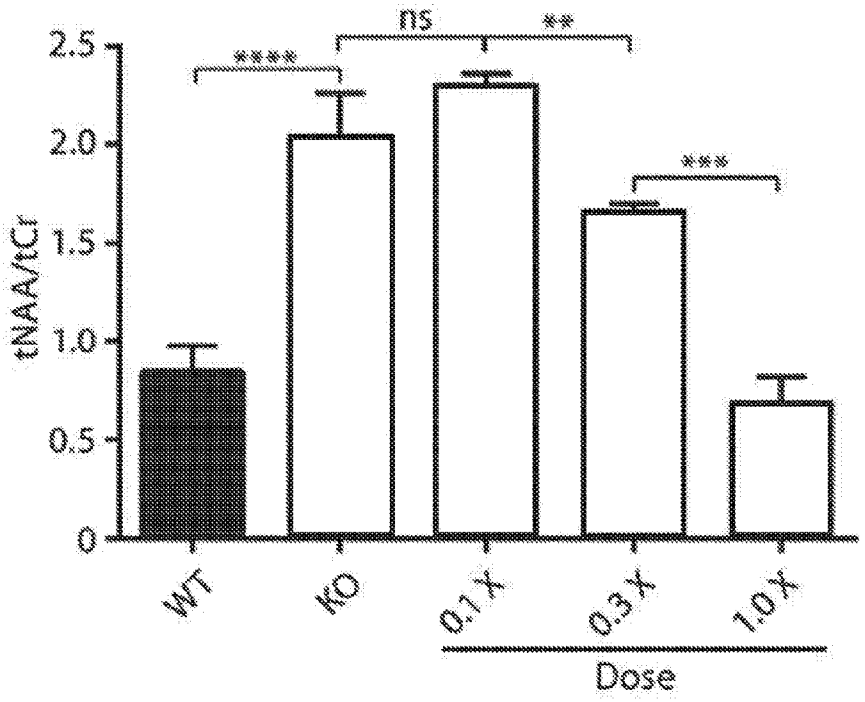

FIG. 38B

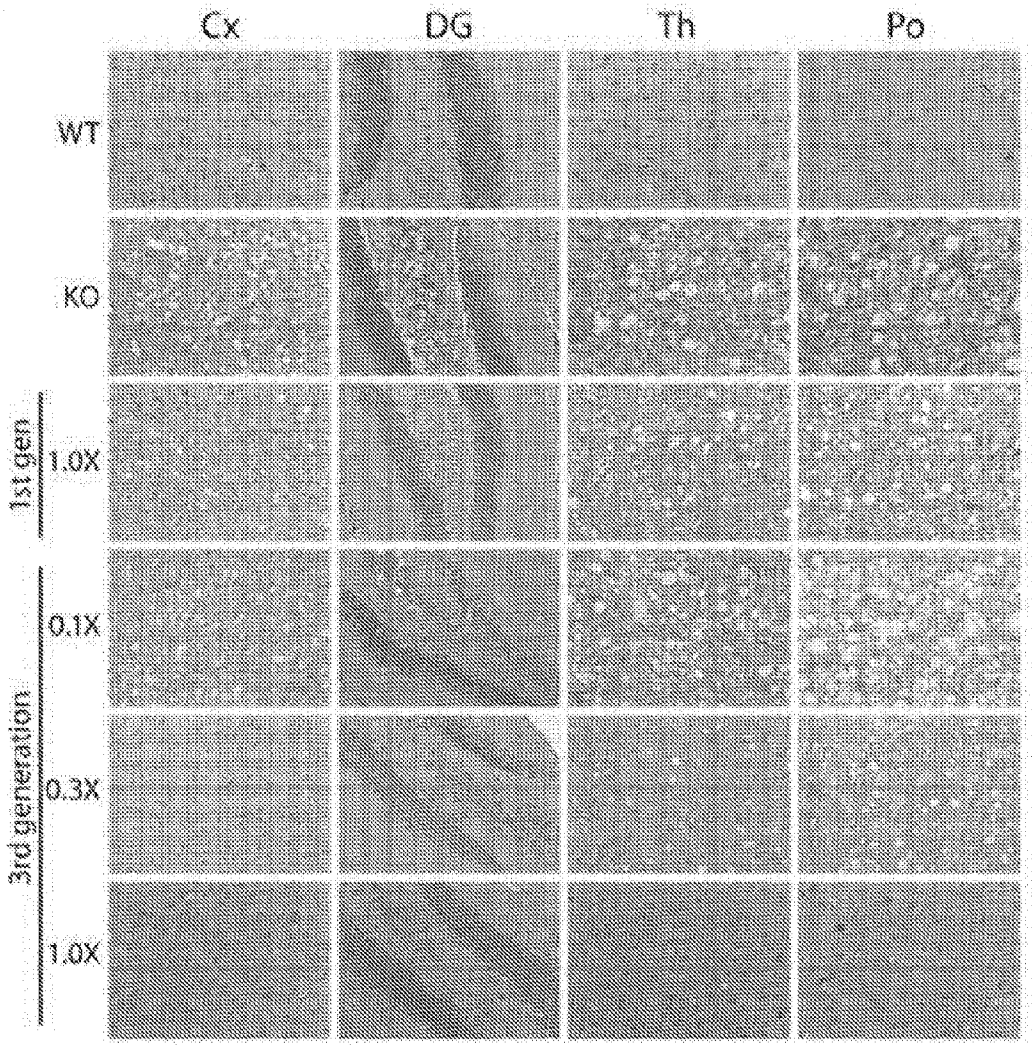

FIG. 38C

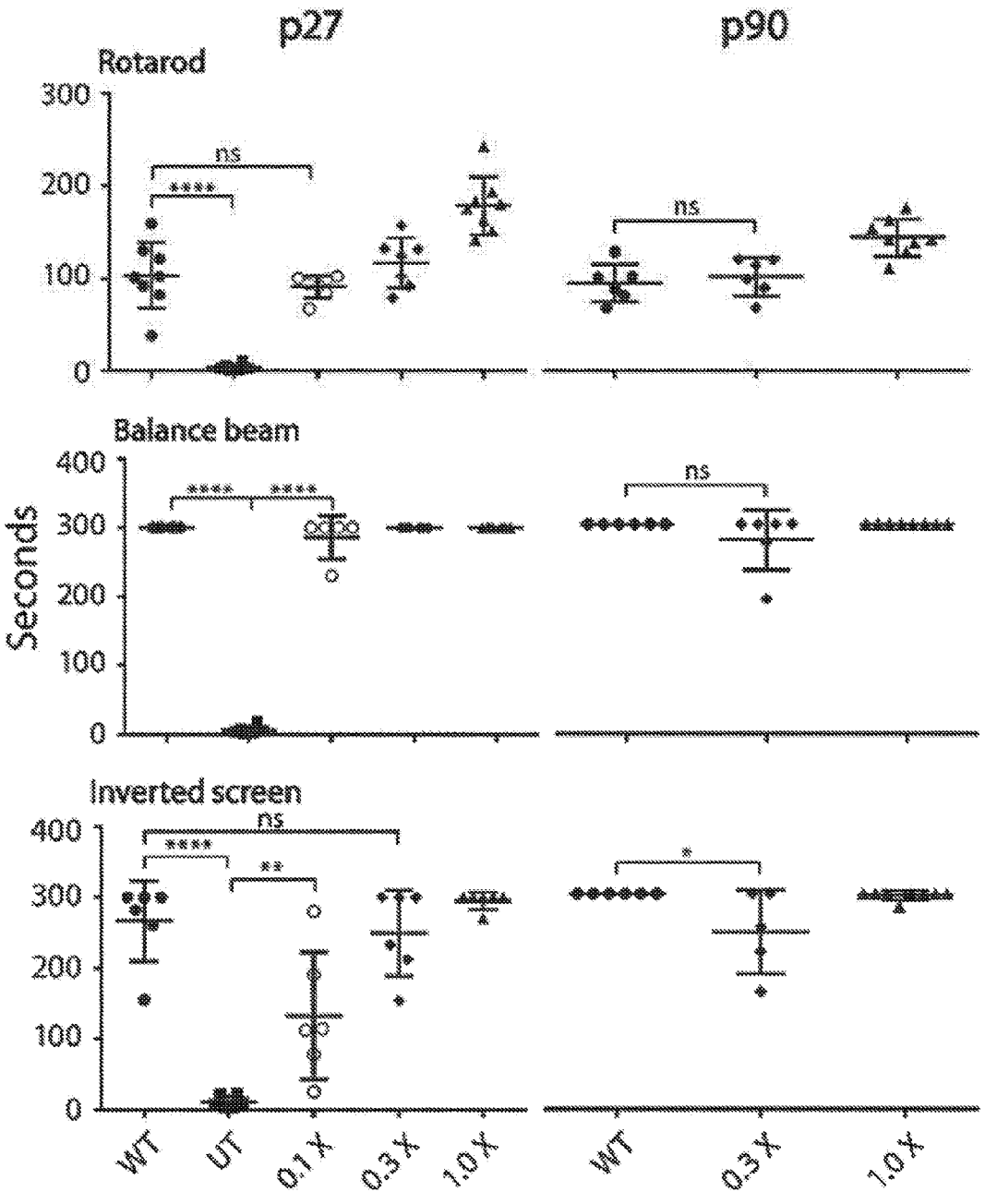
p27
p90
Rotarod
300
200
100
0
ns
****
ns
Balance beam
Seconds
400
300
200
100
0
****
****
ns
Inverted screen
400
300
200
100
0
ns
****
**
*
WT
UT
0.1 X
0.3 X
1.0 X
WT
0.3 X
1.0 X

FIG. 38D

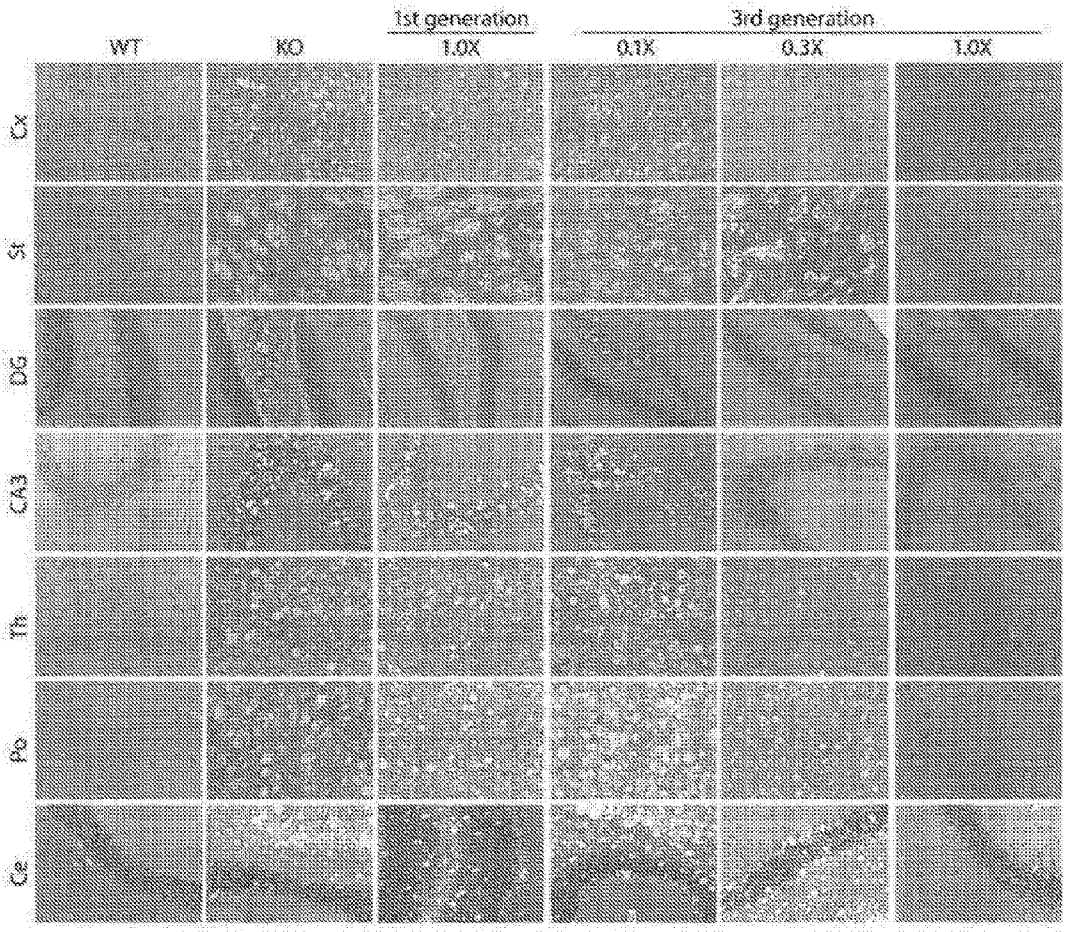
1st generation
3rd generation
WT
KO
1.0X
0.1X
0.3X
1.0X
Cx
St
DG
CA3
Th
Po
Ce

FIG. 39

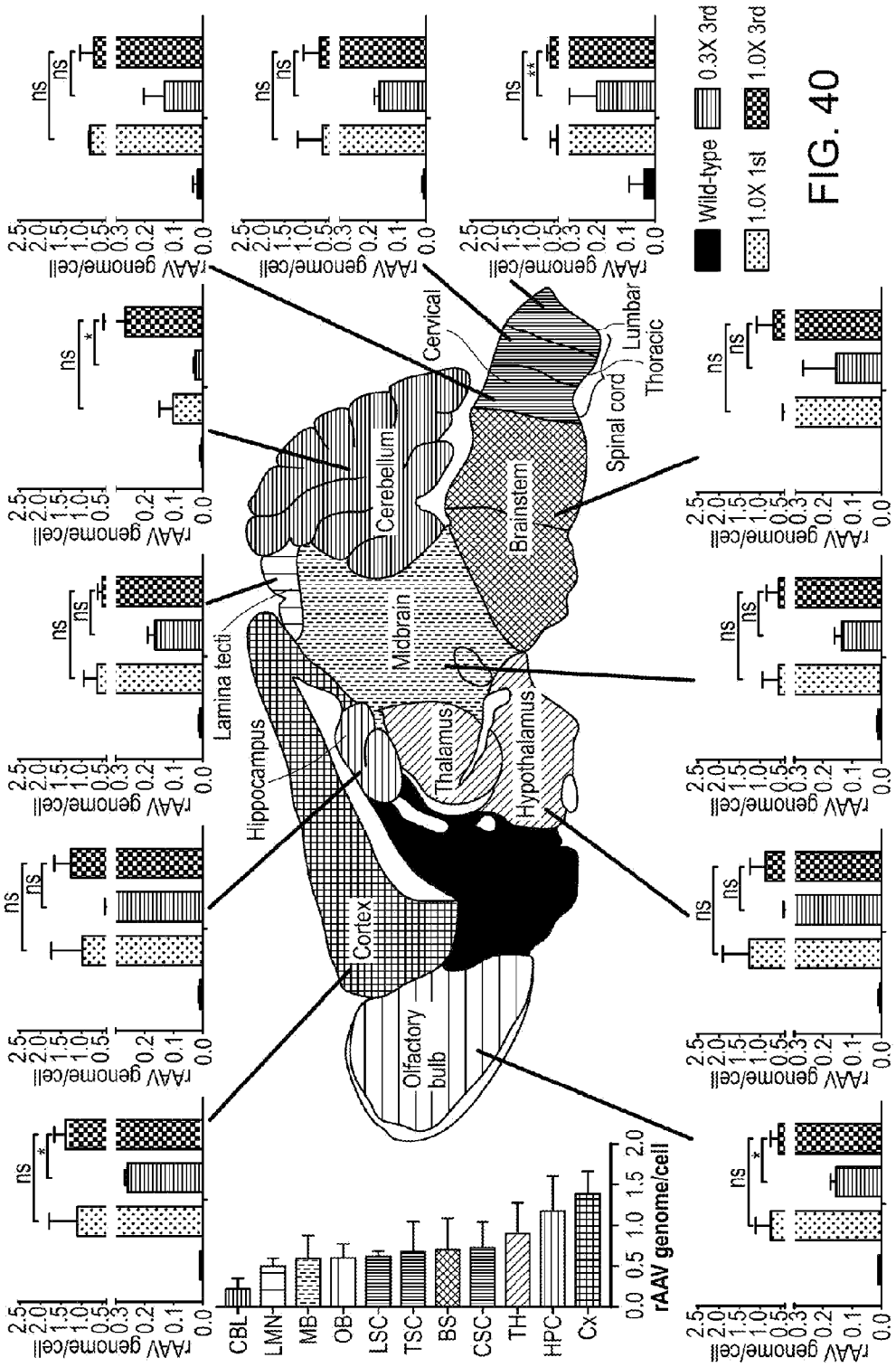
Wild-type
0.3X 3rd
1.0X 1st
1.0X 3rd
rAAV genome/cell
CBL
LMN
MB
OB
LSC
TSC
BS
CSC
TH
HPC
Cx
rAAV genome/cell
Cortex
Olfactory bulb
Hippocampus
Lamina tecti
Midbrain
Cerebellum
Thalamus
Hypothalamus
Brainstem
Cervical
Lumbar
Thoracic
Spinal cord

FIG. 40

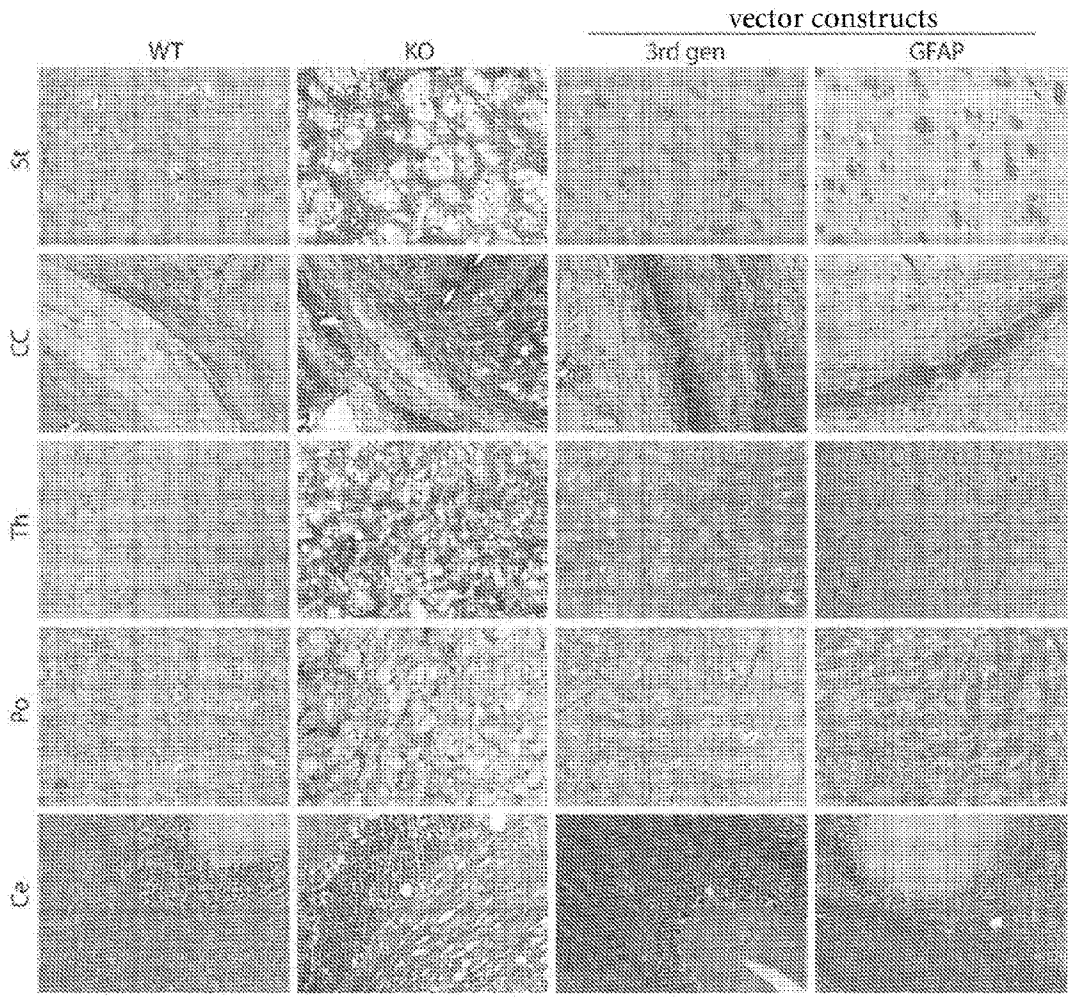

FIG. 41

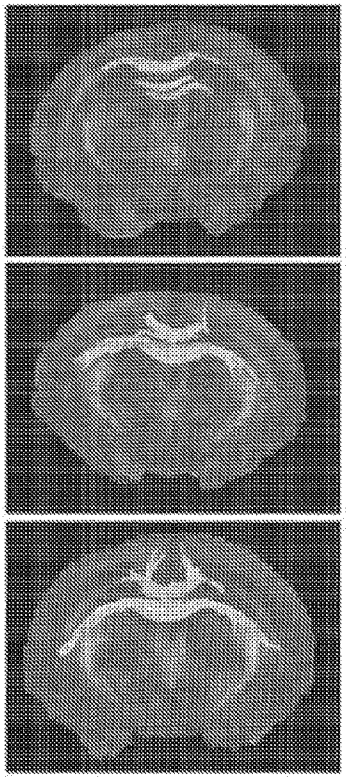

FIG. 42A

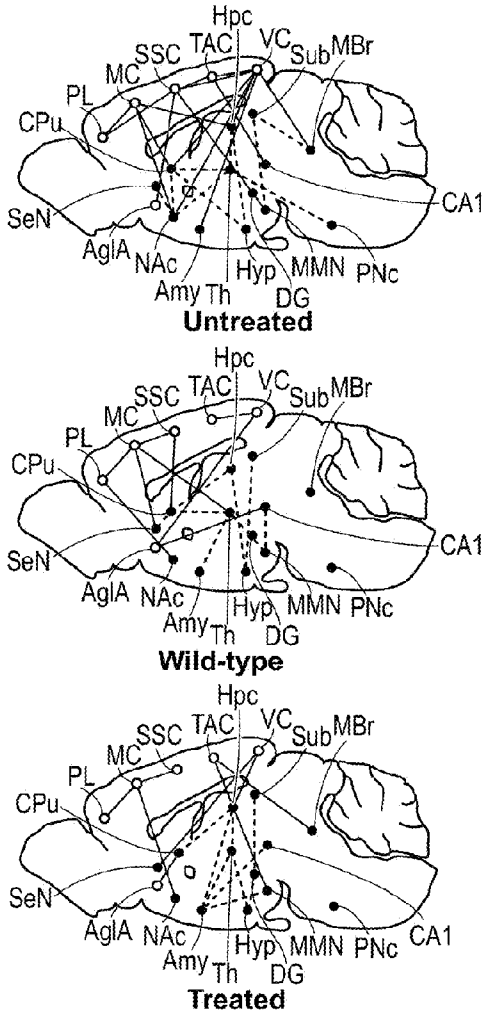

FIG. 42C

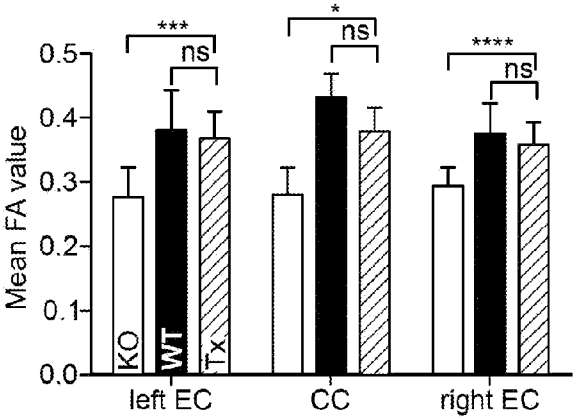

FIG. 42B

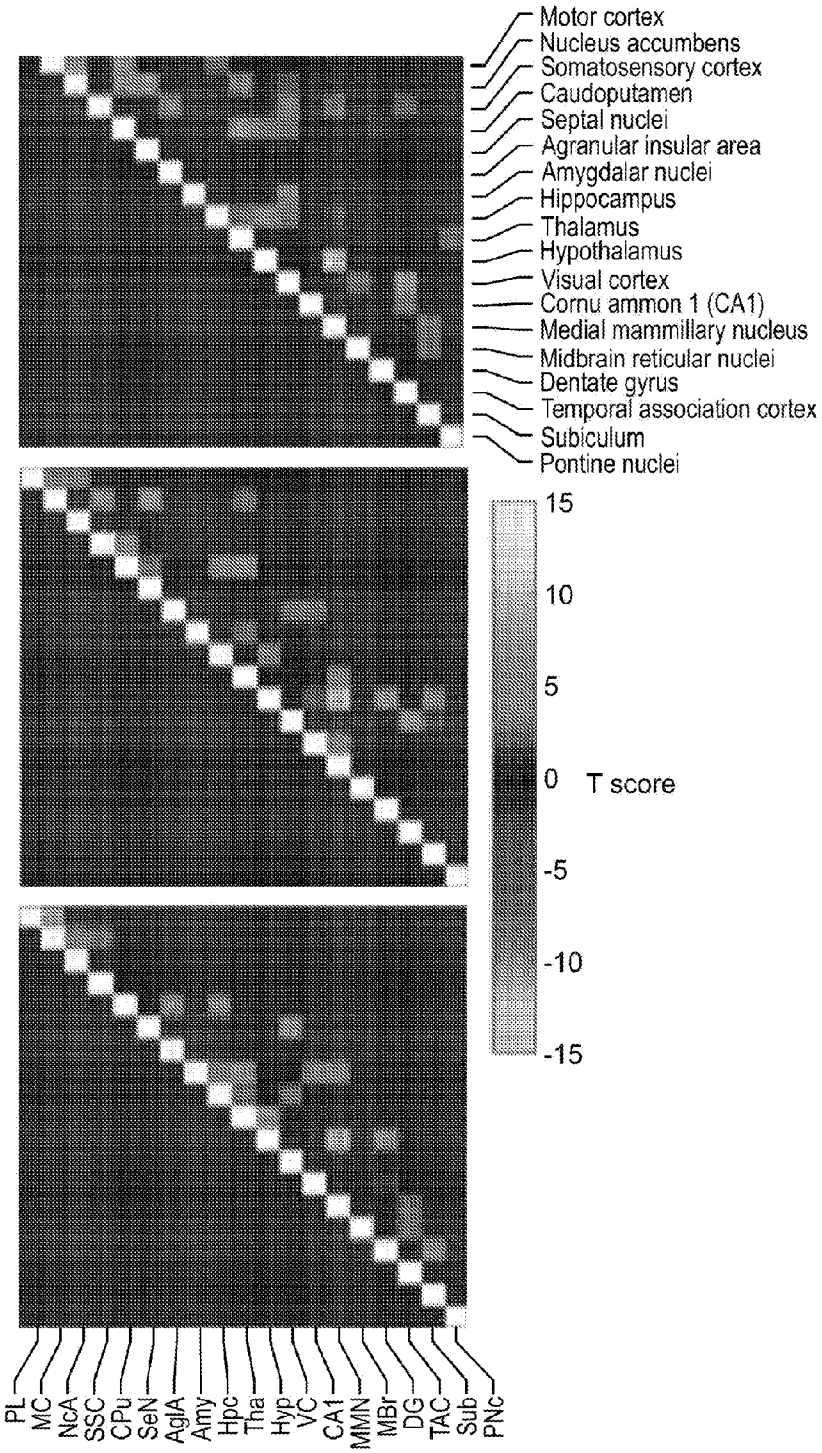
Motor cortex
Nucleus accumbens
Somatosensory cortex
Caudoputamen
Septal nuclei
Agranular insular area
Amygdalar nuclei
Hippocampus
Thalamus
Hypothalamus
Visual cortex
Cornu ammon 1 (CA1)
Medial mammillary nucleus
Midbrain reticular nuclei
Dentate gyrus
Temporal association cortex
Subiculum
Pontine nuclei
15
10
5
0
T score
-5
-10
-15
PL
MC
NcA
SSC
CPu
SeN
AgIA
Amy
Hpc
Tha
Hyp
VC
CA1
MMN
MBr
DG
TAC
Sub
PNc

FIG. 42D

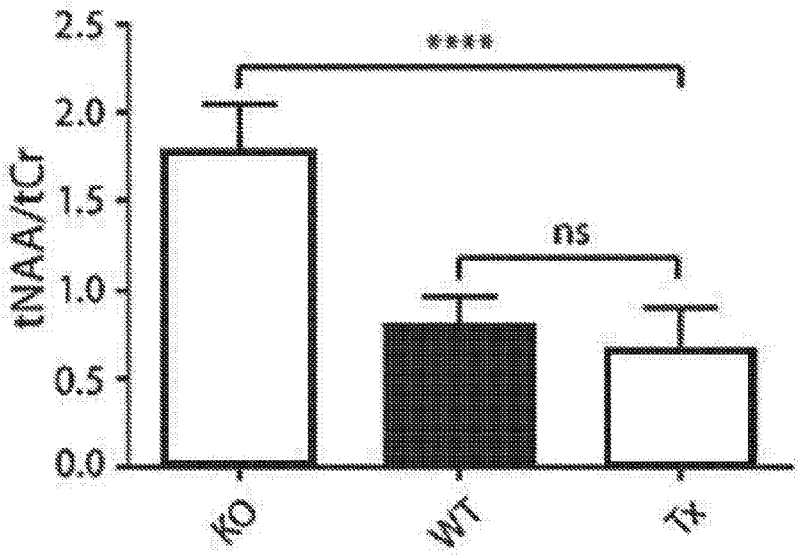

FIG. 42E

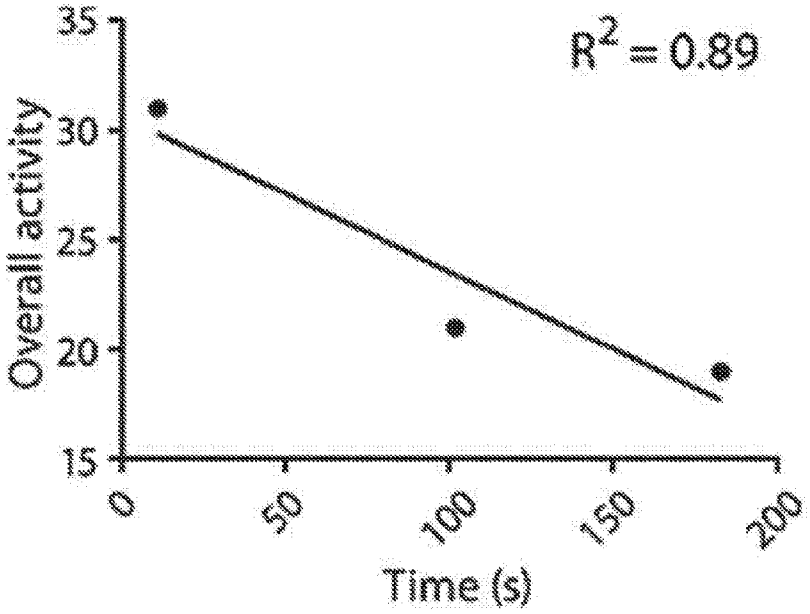

FIG. 42F

r01 = Prelimbic area
r02 = Motor cortex
r03 = Nucleus accumbens
r04 = Somatosensory cortex
r05 = Caudoputamen
r06 = Septal nuclei
r07 = Agranular insular area
r08 = Amygdalar nuclei
r09 = Hippocampus
r10 = Thalamus
r11 = Hypothalamus
r12 = Visual cortex

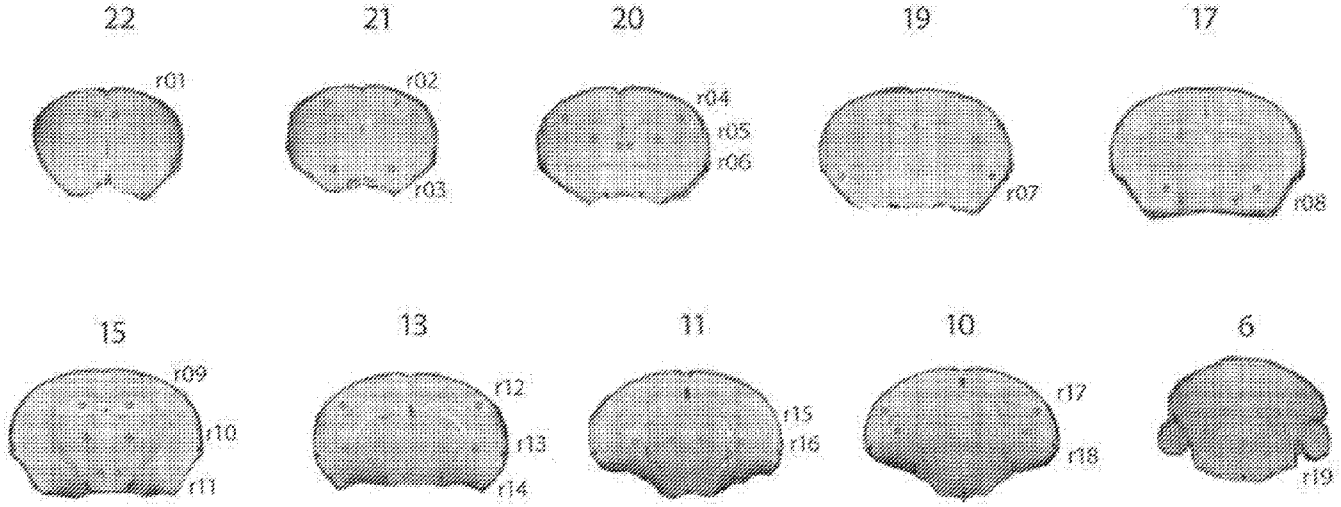

r13 = CA1
r14 = Medial mammillary nucleus
r15 = Midbrain reticular nuclei
r16 = Dentate gyrus
r17 = Temporal association cortex
r18 = Subiculum
r19 = Pontine nuclei

FIG. 43

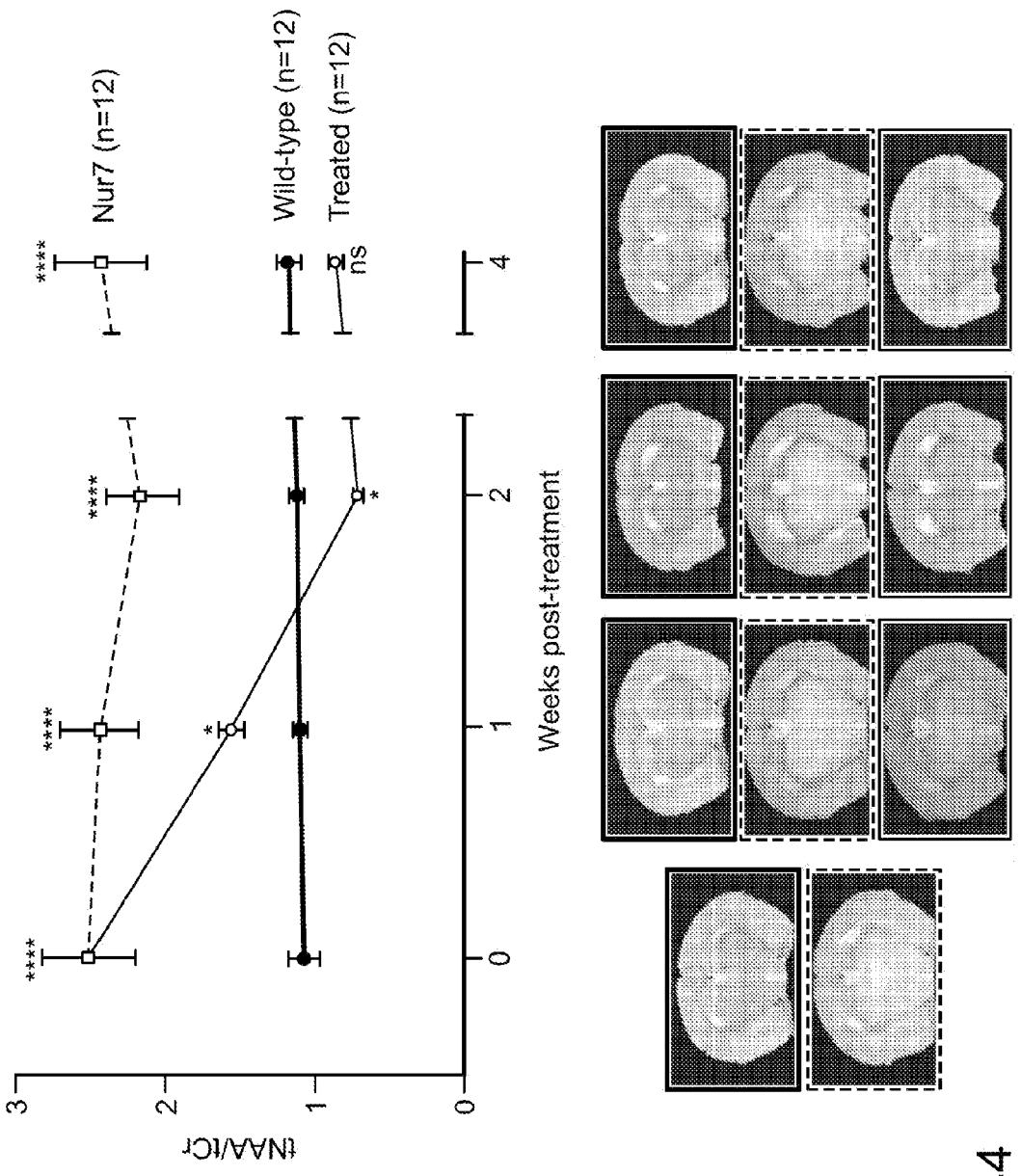
tNAA/tCr
3
2
1
0
0
1
2
Weeks post-treatment
4
Wild-type (n=12)
Treated (n=12)
Nur7 (n=12)
ns
*
**
****

FIG. 44

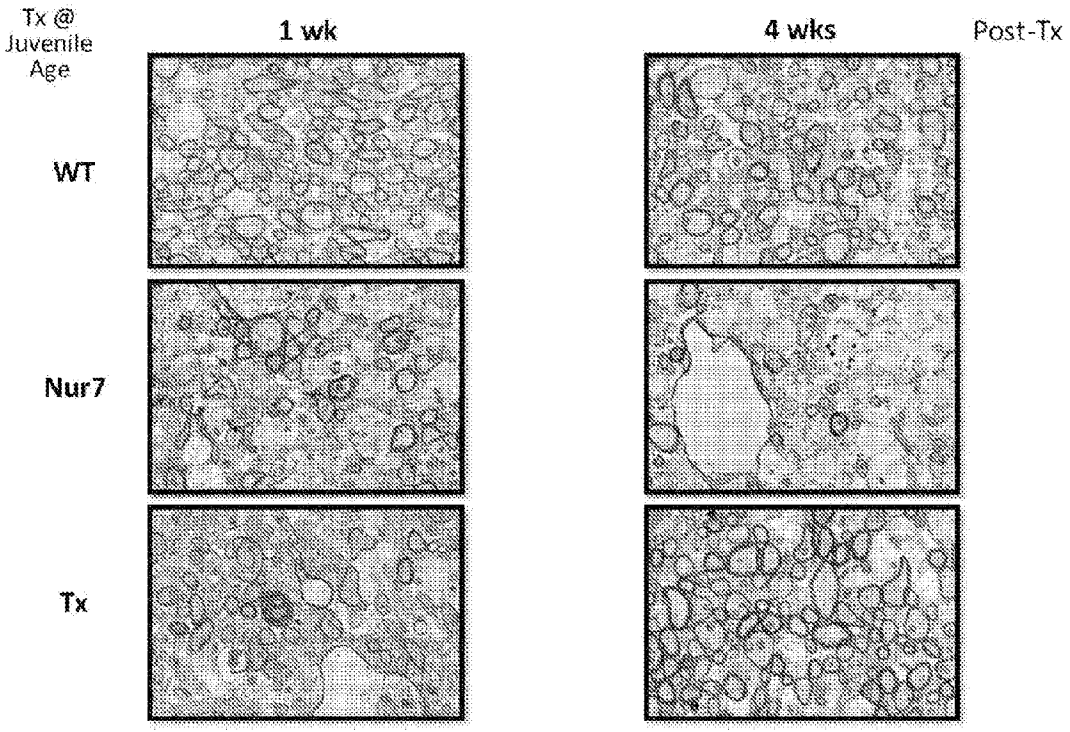

FIG. 45

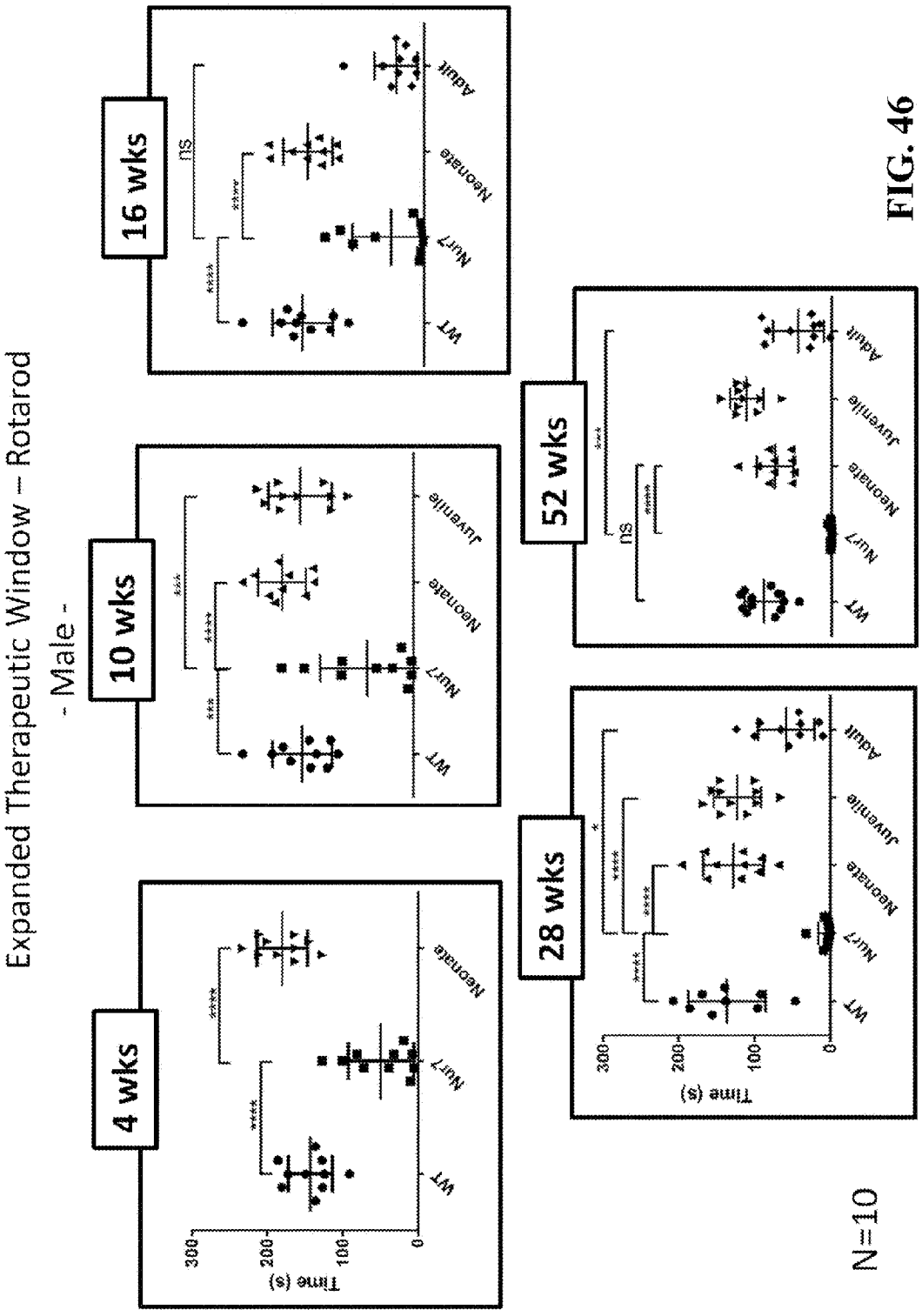
Expanded Therapeutic Window – Rotarod
- Male -
4 wks
10 wks
16 wks
28 wks
52 wks
Time (s)
300
200
100
0
WT
Nur7
Neonate
Juvenile
Adult
ns
N=10

FIG. 46

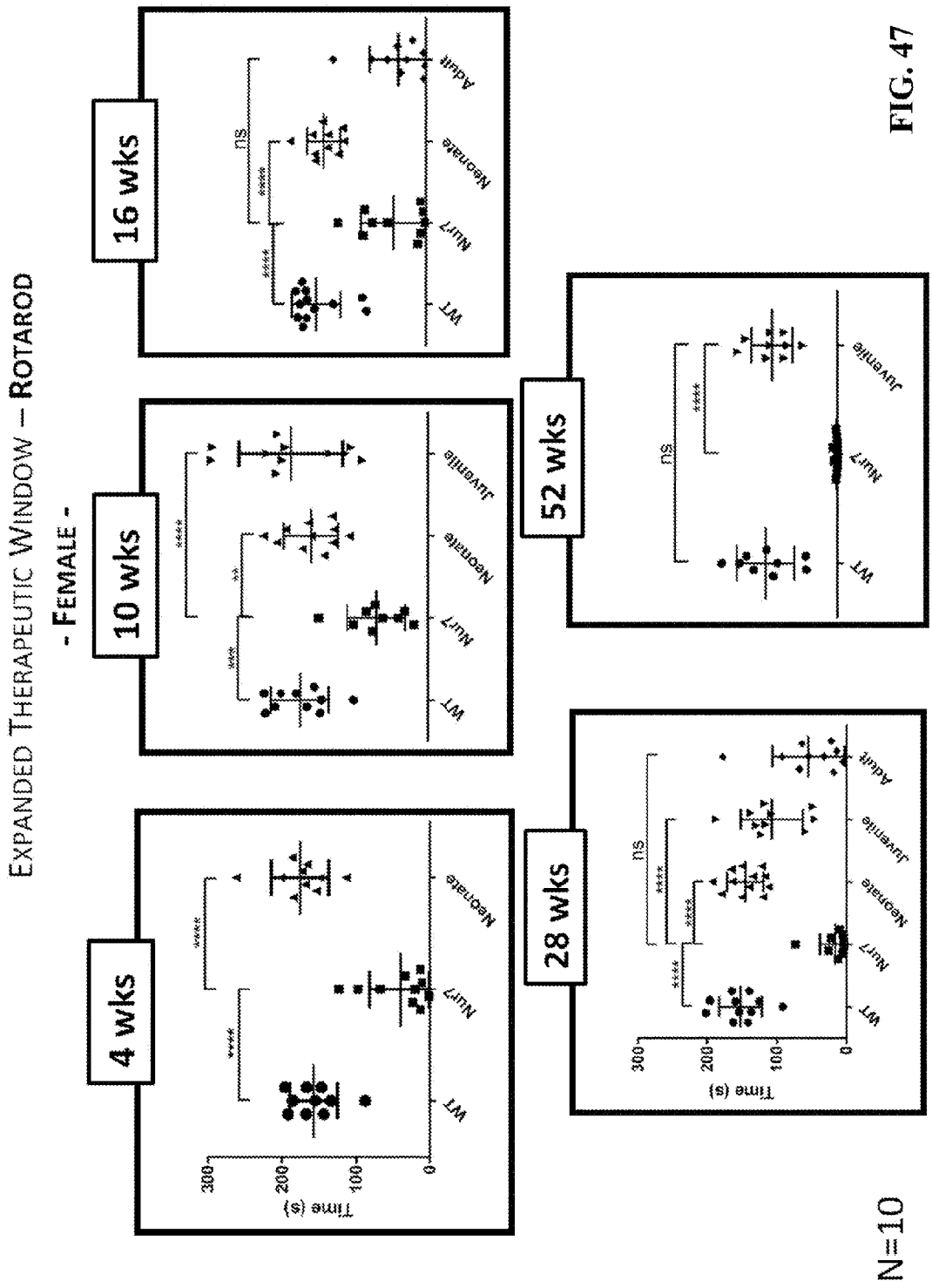
EXPANDED THERAPEUTIC WINDOW – ROTAROD
- FEMALE -
4 wks
10 wks
16 wks
28 wks
52 wks
Time (s)
WT
NLrr7
Neonate
Juvenile
Adult
ns
N=10

FIG. 47

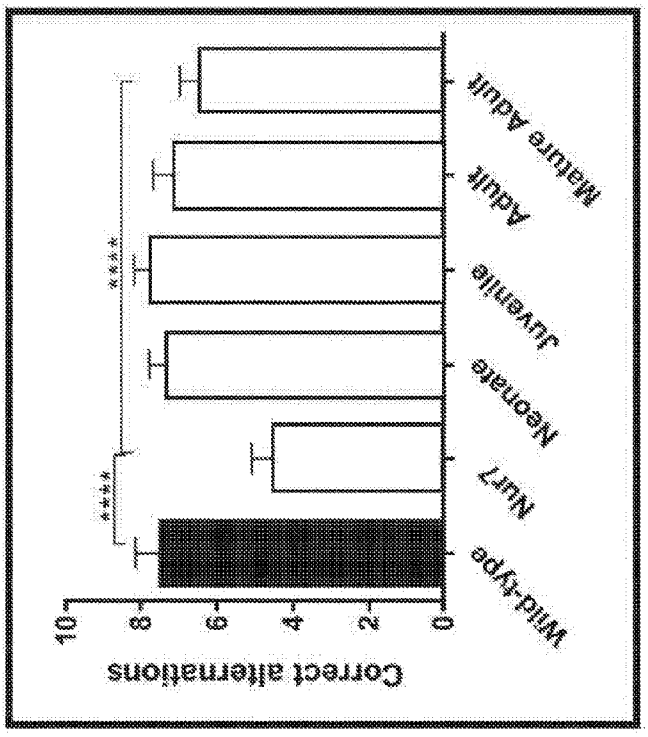
Correct alternations
0
2
4
6
8
10
****
****
Wild-type
Nurr1
Neonate
Juvenile
Adult
Mature Adult
N=8

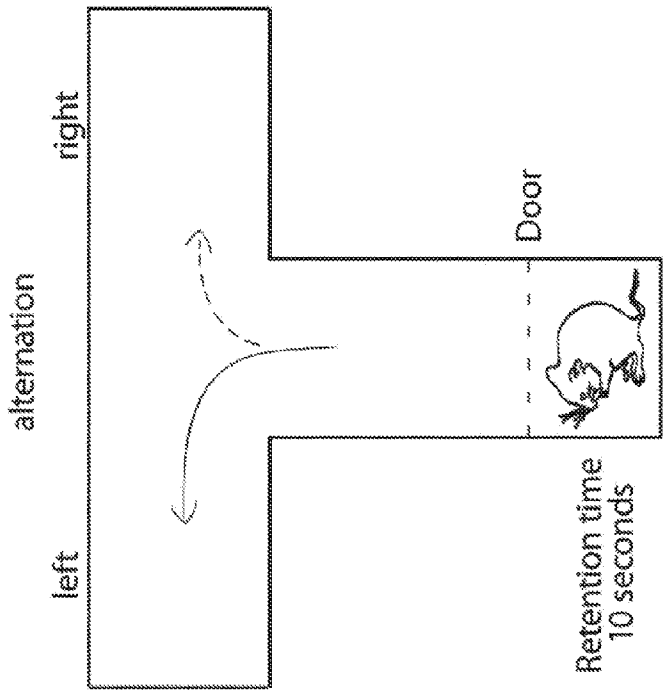
alternation
right
left
Door
Retention time
10 seconds

FIG. 48

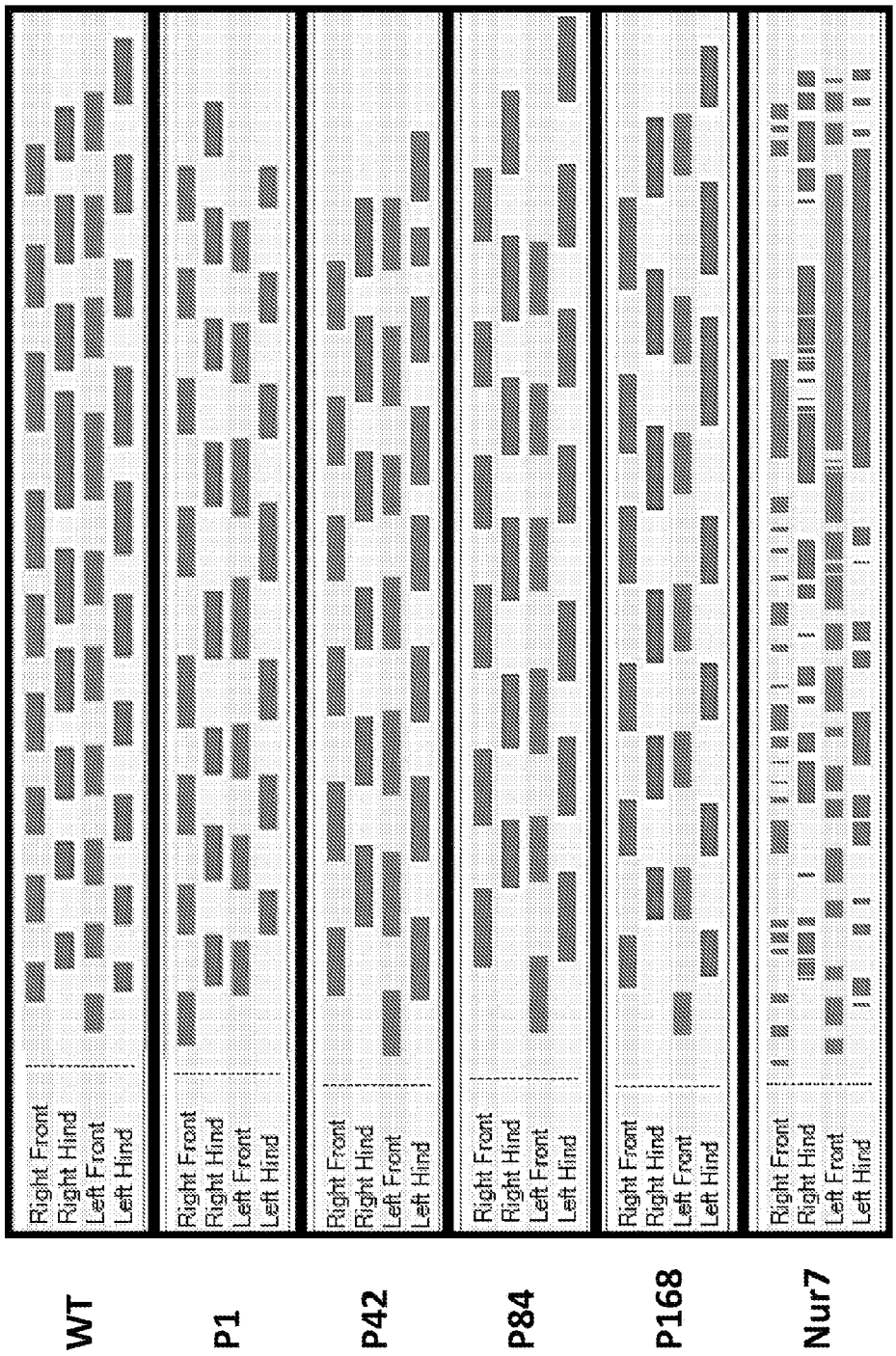
WT
P1
P42
P84
P168
Nur7
Right Front
Right Hind
Left Front
Left Hind

FIG. 49

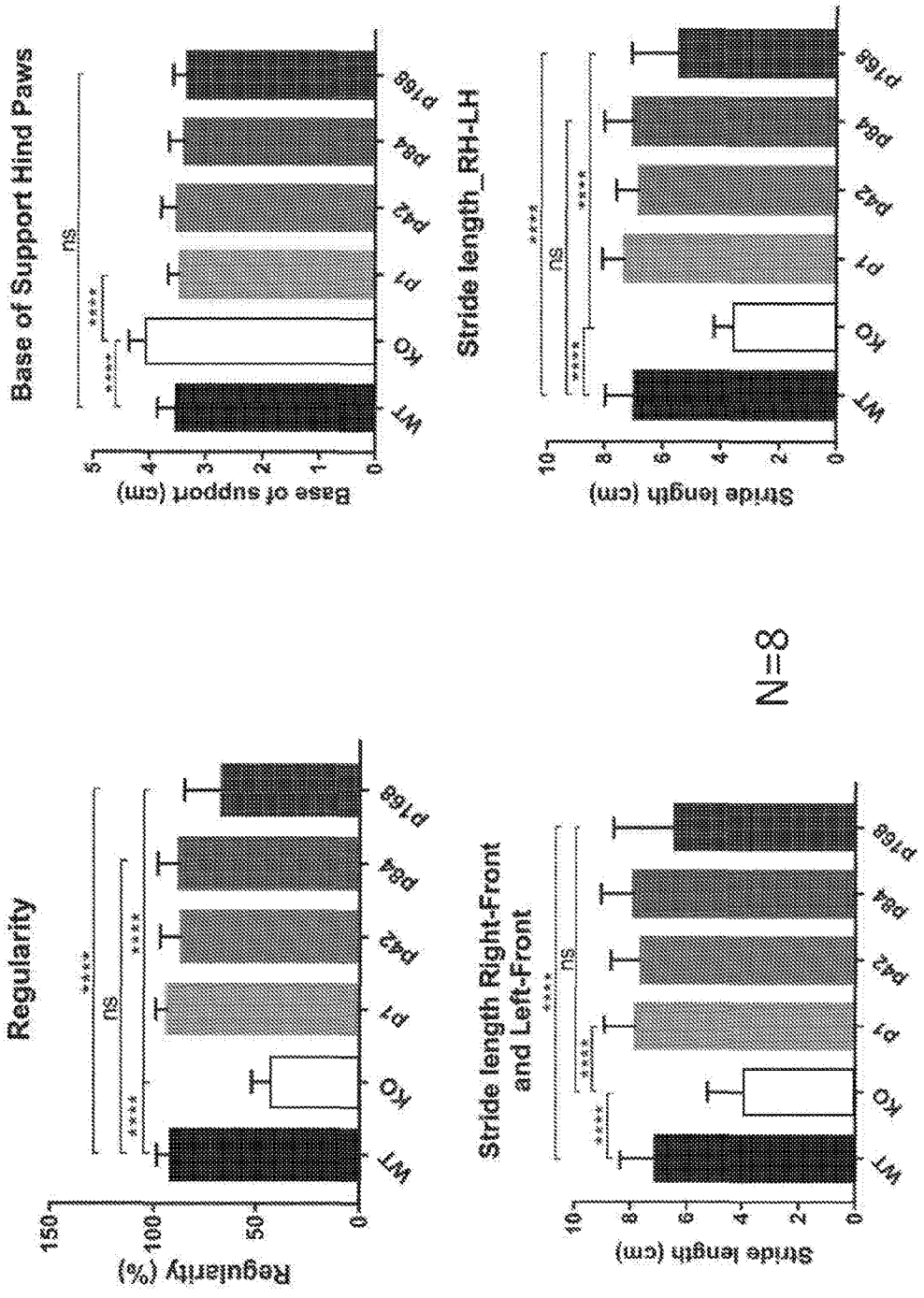
Base of Support Hind Paws
Base of support (cm)
Stride length_RH-LH
Stride length (cm)
Regularity
Regularity (%)
Stride length Right-Front and Left-Front
Stride length (cm)
WT
KO
P1
P42
P84
P168
ns
****
N=8

FIG. 50

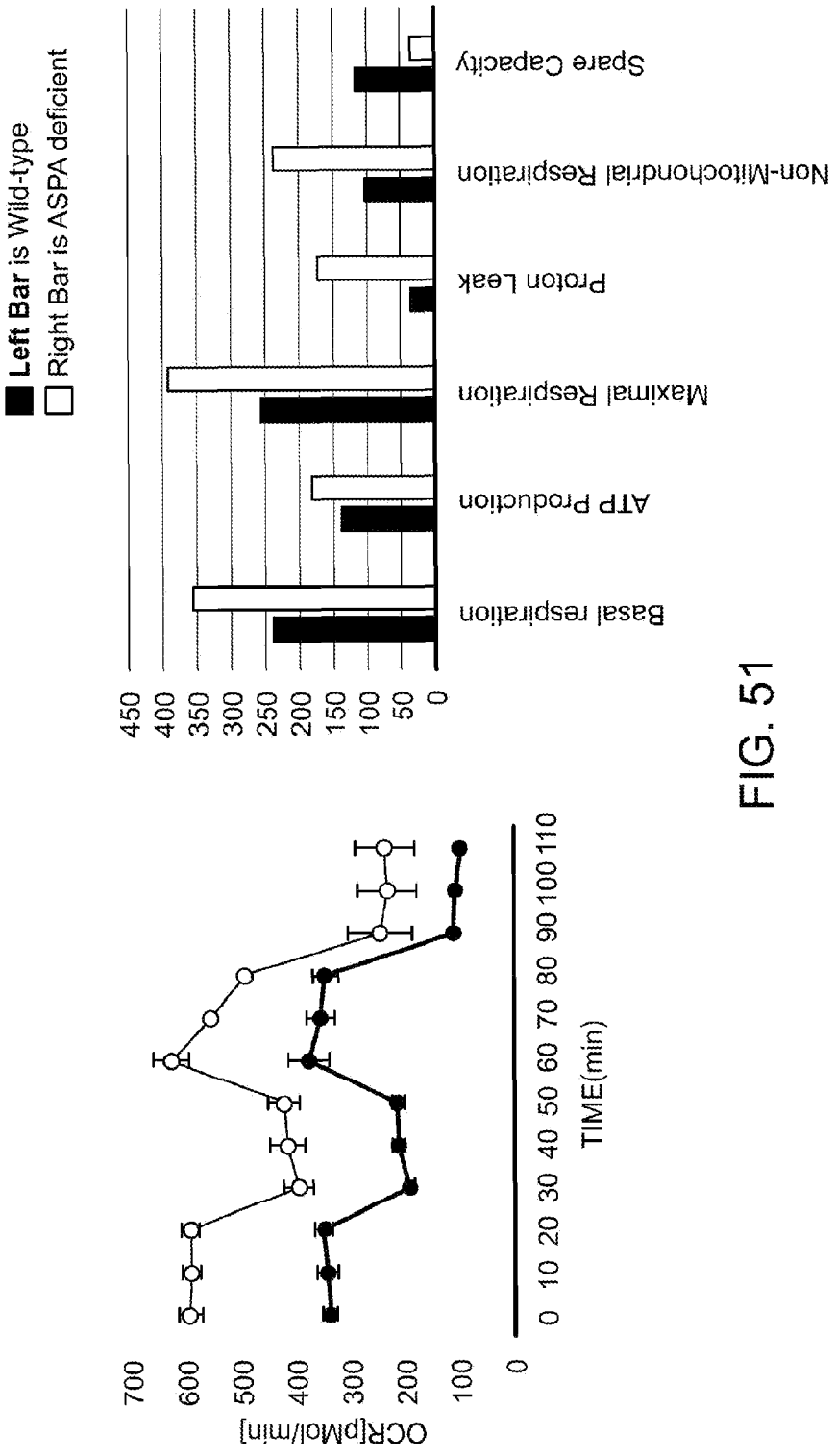
Left Bar is Wild-type
Right Bar is ASPA deficient
Basal respiration
ATP Production
Maximal Respiration
Proton Leak
Non-Mitochondrial Respiration
Spare Capacity
0
50
100
150
200
250
300
350
400
450
OCR[pMol/min]
100
200
300
400
500
600
700
0
0 10 20 30 40 50 60 70 80 90 100 110
TIME(min)

FIG. 51

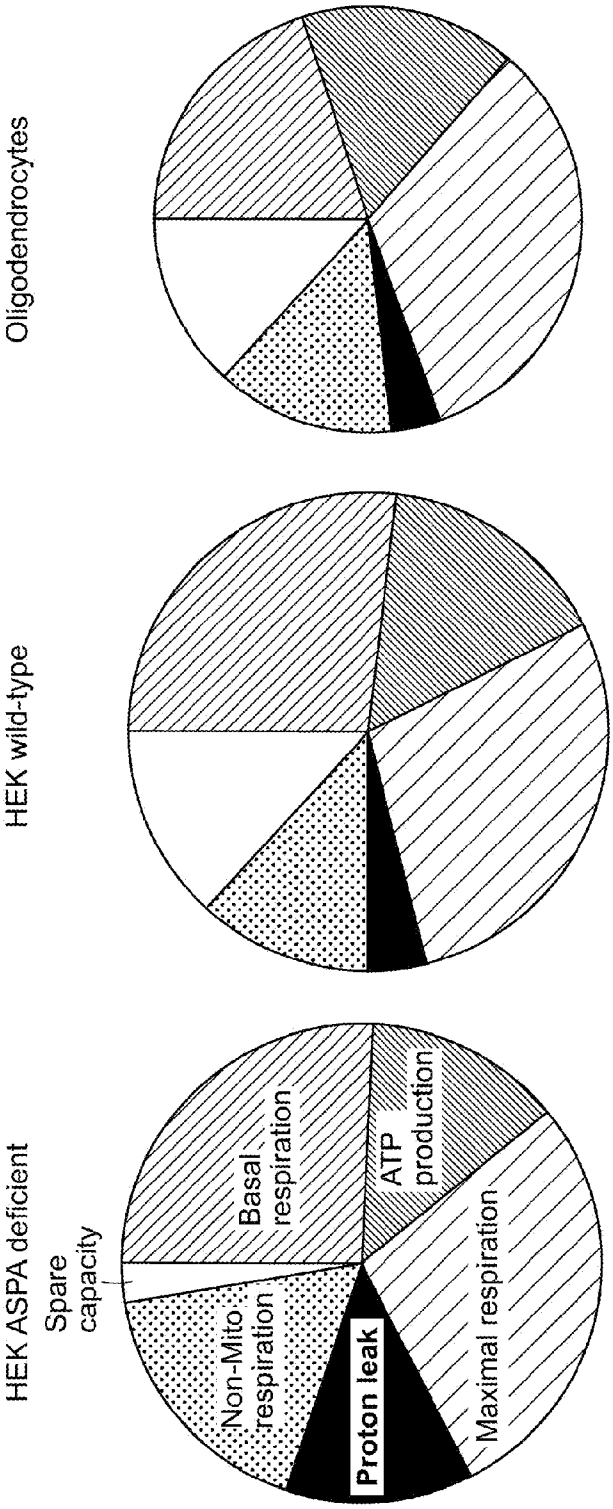
Oligodendrocytes
HEK wild-type
HEK ASPA deficient
Spare capacity
Basal respiration
ATP production
Non-Mito respiration
Proton leak
Maximal respiration

FIG. 52

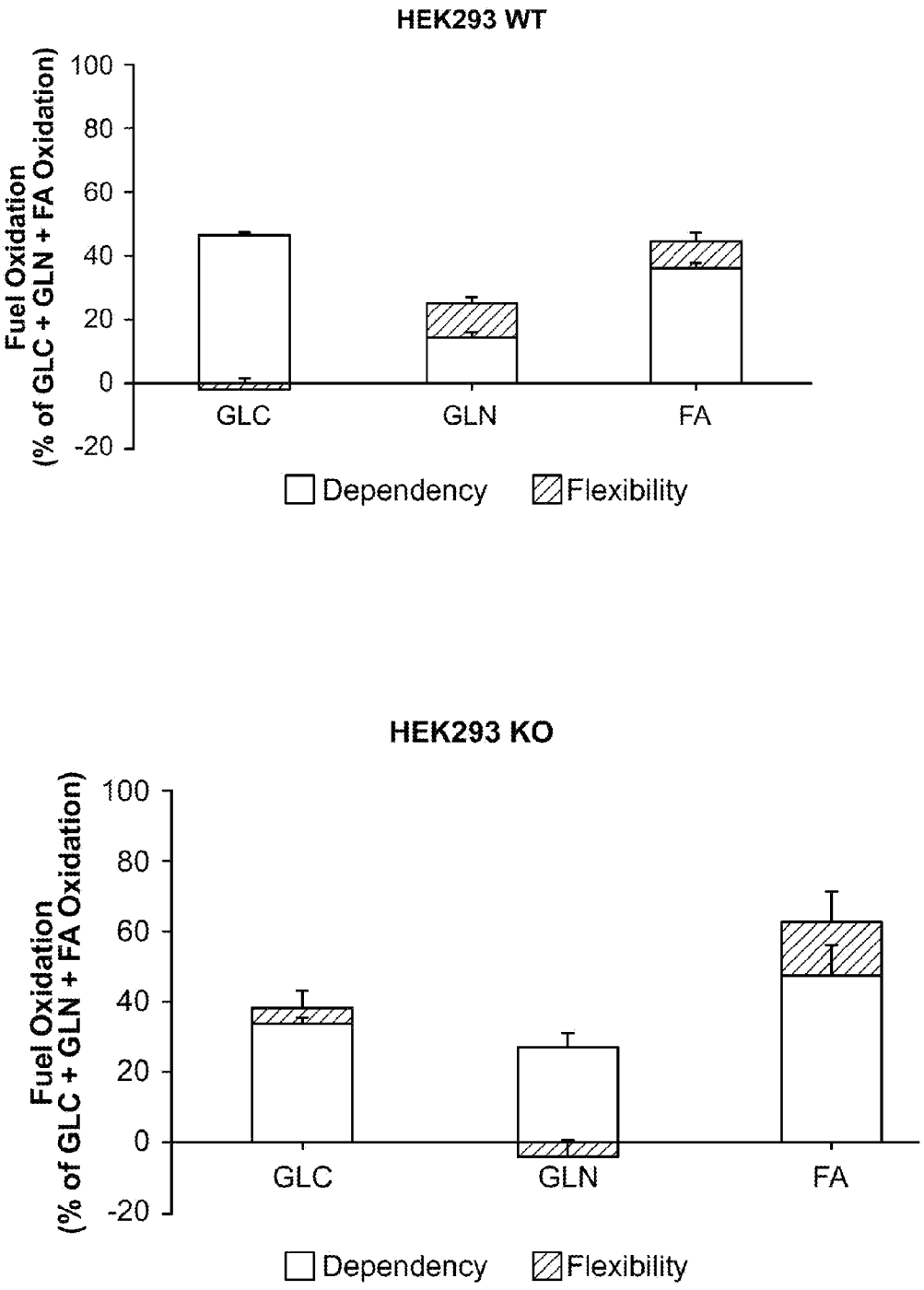
HEK293 WT
Fuel Oxidation
(% of GLC + GLN + FA Oxidation)
100
80
60
40
20
0
-20
GLC
GLN
FA
Dependency
Flexibility
HEK293 KO
Fuel Oxidation
(% of GLC + GLN + FA Oxidation)
100
80
60
40
20
0
-20
GLC
GLN
FA
Dependency
Flexibility

FIG. 53

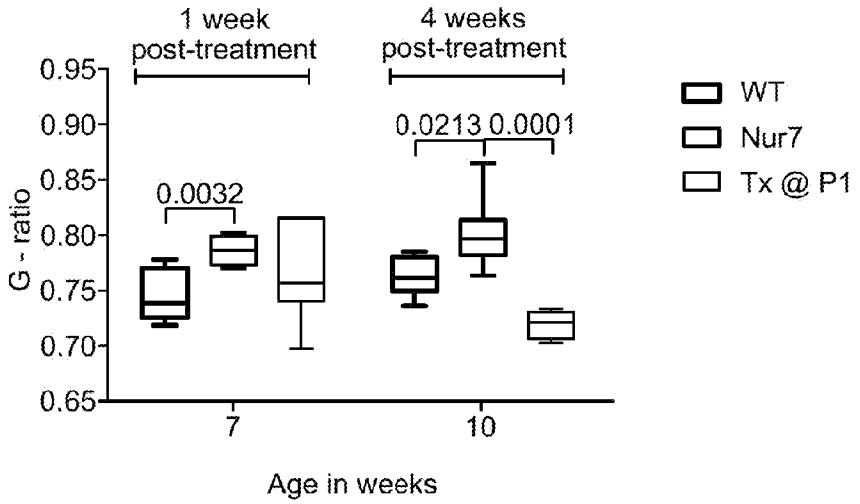
1 week
post-treatment
4 weeks
post-treatment
0.95
0.90
0.85
0.80
0.75
0.70
0.65
G - ratio
0.0032
0.0213
0.0001
WT
Nur7
Tx @ P1
7
10
Age in weeks

FIG. 54

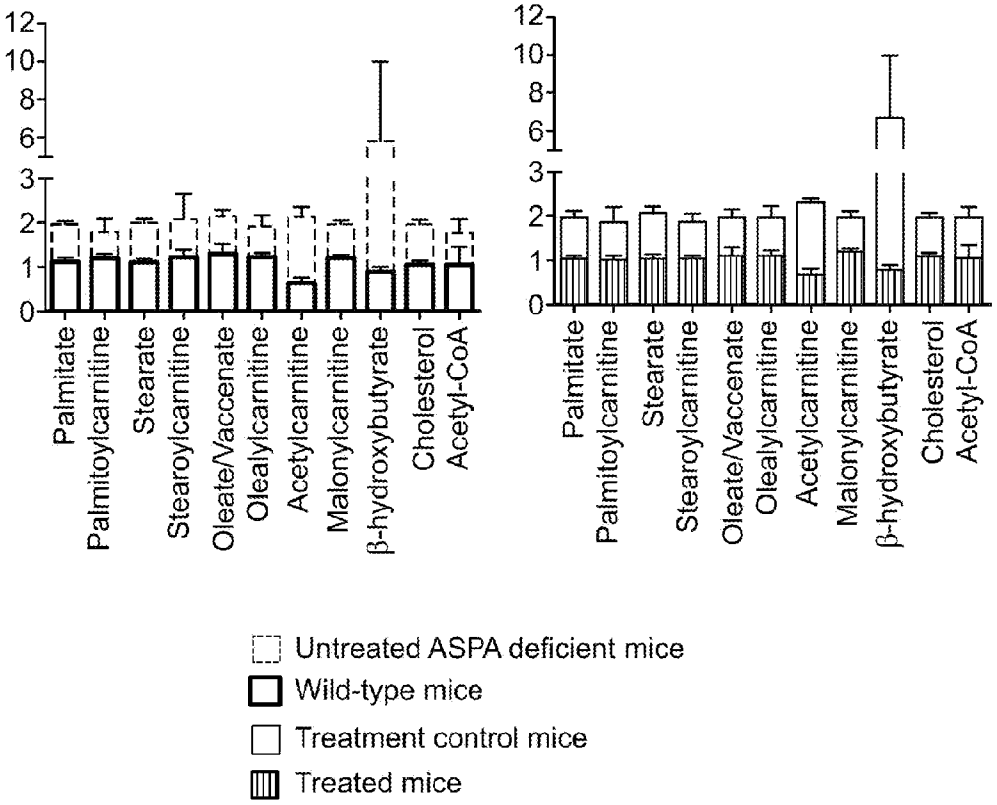
12
10
8
6
3
2
1
0
Palmitate
Palmitoylcarnitine
Stearate
Stearoylcarnitine
Oleate/Vaccenate
Olealylcarnitine
Acetylcarnitine
Malonylcarnitine
β-hydroxybutyrate
Cholesterol
Acetyl-CoA
Untreated ASPA deficient mice
Wild-type mice
Treatment control mice
Treated mice

FIG. 55

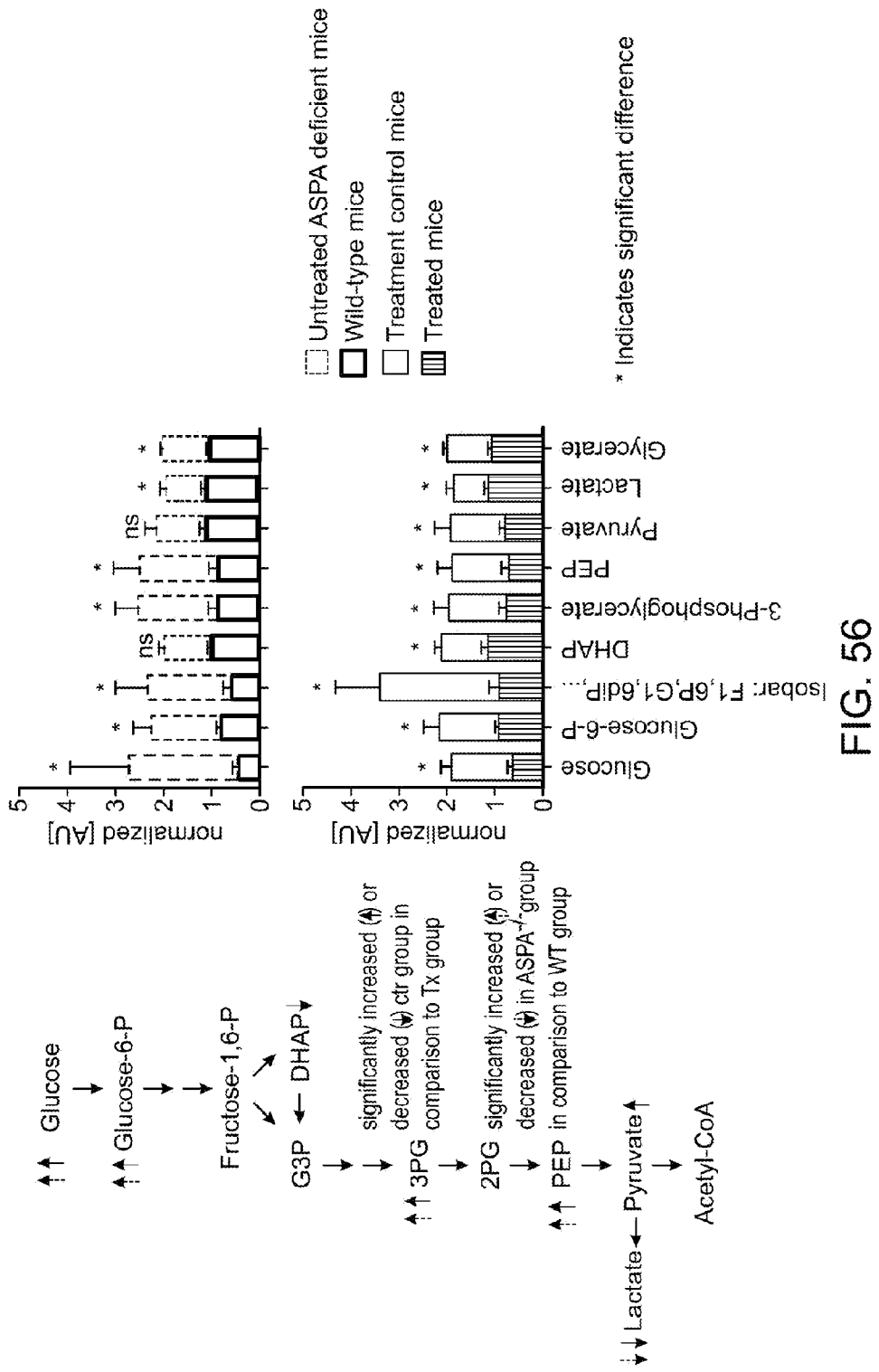
Glucose
Glucose-6-P
Fructose-1,6-P
G3P
DHAP
3PG
2PG
PEP
Lactate
Pyruvate
Acetyl-CoA
significantly increased (↑) or decreased (↓) ctr group in comparison to Tx group
2PG significantly increased (↑) or decreased (↓) in ASPA-/- group in comparison to WT group
normalized [AU]
Glucose
Glucose-6-P
Isobar: F1,6P,G1,6dlP,...
DHAP
3-Phosphoglycerate
PEP
Pyruvate
Lactate
Glycerate
ns
Untreated ASPA deficient mice
Wild-type mice
Treatment control mice
Treated mice
* Indicates significant difference

FIG. 56

Pathway Sort Order	Super Pathway	Sub Pathway	Biochemical Name	Platform	Comp ID	KEGG	HMDB	PubChem
1		Glycine, Serine and Threonine Metabolism	glycine	LC/MS pos early	58	C00037	HMDB00123	750
2			N-acetylglycine	LC/MS pos early	27710		HMDB00532	10972
5			dimethylglycine	LC/MS pos early	5086	C01026	HMDB00092	673
6			betaine	LC/MS pos early	3141	C00719	HMDB00043	247
7			betaine aldehyde	LC/MS pos early	15499	C00576	HMDB01252	249
9			serine	LC/MS pos early	1648	C00065	HMDB00187	5951
10			N-acetylserine	LC/MS pos early	37076		HMDB02931	65249
14			threonine	LC/MS pos early	1284	C00188	HMDB00167	6288
15			N-acetylthreonine	LC/MS neg	33939			152204
16			allo-threonine	LC/MS polar	15142	C05519	HMDB04041	99289
18			homoserine	LC/MS polar	18351	C00263	HMDB00719	12647
25		Alanine and Aspartate Metabolism	alanine	LC/MS pos early	1126	C00041	HMDB00161	5950
26			N-acetylalanine	LC/MS polar	1585	C02847	HMDB00766	88064
28			aspartate	LC/MS pos early	443	C00049	HMDB00191	5960

FIG. 57

30		asparagine	LC/MS pos early	512	C00152	HMDB00168	6267
32		N-acetylaspartate (NAA)	LC/MS neg	22185	C01042	HMDB00812	65065
39	Glutamate Metabolism	glutamate	LC/MS pos early	57	C00025	HMDB00148	611
40		glutamine	LC/MS pos early	53	C00064	HMDB00641	5961
41		N-acetylglutamate	LC/MS pos early	15720	C00624	HMDB01138	70914
42		N-acetylglutamine	LC/MS pos early	33943	C02716	HMDB06029	182230
43		N-acetyl-aspartyl-glutamate (NAAG)	LC/MS pos early	35665	C12270	HMDB01067	5255
44		gamma-aminobutyrate (GABA)	LC/MS pos early	1416	C00334	HMDB00112	119
51		pyroglutamine*	LC/MS pos early	46225			134508
56	Histidine Metabolism	histidine	LC/MS neg	59	C00135	HMDB00177	6274
57		N-acetylhistidine	LC/MS pos early	33946	C02997	HMDB32055	75619
58		1-methylhistidine	LC/MS pos early	30460	C01152	HMDB00001	92105
59		3-methylhistidine	LC/MS pos early	15677	C01152	HMDB00479	64969
67		imidazole propionate	LC/MS pos early	40730		HMDB02271	70630
68		imidazole lactate	LC/MS pos early	15716	C05568	HMDB02320	440129
70		1-methylhistamine	LC/MS pos early	43831	C05127	HMDB00898	3614
74		1-methylimidazoleacetate	LC/MS pos early	32350	C05828	HMDB02820	75810

FIG. 57 cont.

75		4-imidazoleacetate	LC/MS pos early	32349	C02835	HMDB02024	96215
78	Lysine Metabolism	lysine	LC/MS pos early	1301	C00047	HMDB00182	5962
80		N6-acetyllysine	LC/MS neg	36752	C02727	HMDB00206	92832
82		N6,N6,N6-trimethyllysine	LC/MS pos early	1498	C03793	HMDB01325	440120
84		saccharopine	LC/MS polar	1495	C00449	HMDB00279	160556
85		2-aminoadipate	LC/MS polar	6146	C00956	HMDB00510	469
88		glutarate (pentanedioate)	LC/MS polar	396	C00489	HMDB00661	743
89		glutarylcarnitine (C5)	LC/MS pos early	44664		HMDB13130	71464488
96		pipecolate	LC/MS pos early	1444	C00408	HMDB00070	849
106	Phenylalanine and Tyrosine Metabolism	phenylalanine	LC/MS pos early	64	C00079	HMDB00159	6140
107		N-acetylphenylalanine	LC/MS neg	33950	C03519	HMDB00512	74839
111		phenyllactate (PLA)	LC/MS polar	22130	C05607	HMDB00779	3848
119		tyrosine	LC/MS pos early	1299	C00082	HMDB00158	6057
120		N-acetyltyrosine	LC/MS neg	32390		HMDB00866	68310
130		3-(4-hydroxyphenyl)lactate	LC/MS neg	32197	C03672	HMDB00755	9378
135		phenol sulfate	LC/MS neg	32553	C02180	HMDB60015	74426
138		p-cresol sulfate	LC/MS neg	36103	C01468	HMDB11635	4615423

FIG. 57 cont.

158			homovanillate (HVA)	LC/MS neg	1101	C05582	HMDB00118	1738
172			O-methyltyrosine	LC/MS pos early	37451			76957
209		Tryptophan Metabolism	tryptophan	LC/MS pos early	54	C00078	HMDB00929	6305
213			indolelactate	LC/MS neg	18349	C02043	HMDB00671	92904
218			3-indoxyl sulfate	LC/MS neg	27672		HMDB00682	10258
219			kynurenine	LC/MS pos early	15140	C00328	HMDB00684	161166
234			5-hydroxyindoleacetate	LC/MS pos early	437	C05635	HMDB00763	1826
235			serotonin	LC/MS pos early	2342	C00780	HMDB00259	5202
250			C-glycosyltryptophan	LC/MS pos early	48782			10981970
255		Leucine, Isoleucine and Valine	leucine	LC/MS pos early	60	C00123	HMDB00687	6106
256			N-acetylleucine	LC/MS neg	1587	C02710	HMDB11756	70912
263			isovalerylcarnitine	LC/MS pos early	34407		HMDB00688	6426851
266	Amino Acid		beta-hydroxyisovalerate	LC/MS polar	12129		HMDB00754	69362
274			alpha-hydroxyisovalerate	LC/MS polar	46537		HMDB00407	99823
276			methylsuccinate	LC/MS polar	15745		HMDB01844	10349
284			isoleucine	LC/MS pos early	1125	C00407	HMDB00172	6306
286			N-acetylisoleucine	LC/MS neg	33967			2802421

FIG. 57 cont.

288	Metabolism	2-methylbutyrylcarnitine (C5)	LC/MS pos early	45095		HMDB00378	6426901
290		tiglylcarnitine	LC/MS pos early	35428		HMDB02366	22833596
293		2-hydroxy-3-methylvalerate	LC/MS neg	36746		HMDB00317	164623
295		ethylmalonate	LC/MS polar	15765		HMDB00622	11756
296		valine	LC/MS pos early	1649	C00183	HMDB00883	6287
297		N-acetylvaline	LC/MS neg	1591		HMDB11757	66789
300		isobutyrylcarnitine	LC/MS pos early	33441		HMDB00736	168379
302		3-hydroxyisobutyrate	LC/MS polar	1549	C06001	HMDB00336	87
312	Methionine, Cysteine, SAM and Taurine Metabolism	methionine	LC/MS pos early	1302	C00073	HMDB00696	6137
313		N-acetylmethionine	LC/MS neg	1589	C02712	HMDB11745	448580
314		N-formylmethionine	LC/MS neg	2829	C03145	HMDB01015	439750
317		methionine sulfoxide	LC/MS pos early	18374	C02989	HMDB02005	158980
318		N-acetylmethionine sulfoxide	LC/MS pos early	45428			193368
319		S-adenosylmethionine (SAM)	LC/MS pos early	15915	C00019	HMDB01185	34755
320		S-adenosylhomocysteine (SAH)	LC/MS neg	42382	C00021	HMDB00939	439155
324		cystathionine	LC/MS pos early	15705	C02291	HMDB00099	439258
329		cysteine	LC/MS pos early	1868	C00097	HMDB00574	5862

FIG. 57 cont.

337		cysteine sulfinic acid	LC/MS pos early	37443	C00606	HMDB00996	109
339		hypotaurine	LC/MS polar	590	C00519	HMDB00965	107812
340		taurine	LC/MS neg	2125	C00245	HMDB00251	1123
341		N-acetyltaurine	LC/MS polar	48187			159864
346		taurocyamine	LC/MS pos early	35117	C01959	HMDB03584	68340
347		2-hydroxybutyrate/2-hydroxyisobutyrate	LC/MS polar	52281			
348	Urea cycle; Arginine and Proline Metabolism	arginine	LC/MS pos early	1638	C00062	HMDB00517	232
349		urea	LC/MS pos early	1670	C00086	HMDB00294	1176
351		ornithine	LC/MS pos early	1493	C00077	HMDB03374	6262
352		proline	LC/MS pos early	1898	C00148	HMDB00162	145742
353		citrulline	LC/MS pos early	2132	C00327	HMDB00904	9750
354		argininosuccinate	LC/MS pos early	15497	C03406	HMDB00052	16950;828
355		homoarginine	LC/MS pos early	22137	C01924	HMDB00670	9085
356		homocitrulline	LC/MS pos early	22138	C02427	HMDB00679	65072
360		dimethylarginine (SDMA + ADMA)	LC/MS pos early	36808	C03626	HMDB01539	123831
361		N-acetylarginine	LC/MS pos early	33953	C02562	HMDB04620	67427
364		N-delta-acetylornithine	LC/MS pos early	43249			9920500

FIG. 57 cont.

370		trans-4-hydroxyproline	LC/MS pos early	32306	C01157	HMDB00725	5810
372		pro-hydroxy-pro	LC/MS pos early	35127		HMDB06695	11673055
373		N-monomethylarginine	LC/MS pos early	43586	C03884	HMDB29416	132862
377	Creatine Metabolism	creatine	LC/MS pos early	27718	C00300	HMDB00064	586
378		creatinine	LC/MS pos early	513	C00791	HMDB00562	588
380		creatine phosphate	LC/MS polar	33951	C02305	HMDB01511	587
383		guanidinoacetate	LC/MS pos early	43802	C00581	HMDB00128	763
387	Polyamine Metabolism	putrescine	LC/MS pos early	1408	C00134	HMDB01414	1045
388		spermine	LC/MS pos late	603	C00750	HMDB01256	1103
390		spermidine	LC/MS pos early	485	C00315	HMDB01257	1102
391		5-methylthioadenosine (MTA)	LC/MS pos early	1419	C00170	HMDB01173	439176
398	Guanidino and Acetamido Metabolism	1-methylguanidine	LC/MS pos early	48114	C02294	HMDB01522	10111
400		4-guanidinobutanoate	LC/MS pos early	15681	C01035	HMDB03464	500
402		glutathione, reduced (GSH)	LC/MS pos early	2127	C00051	HMDB00125	124886
403		glutathione, oxidized (GSSG)	LC/MS pos early	36783	C00127	HMDB03337	65359
405		cysteine-glutathione disulfide	LC/MS pos early	35159		HMDB00656	4247235
406		S-methylglutathione	LC/MS pos early	33944	C11347		3605667

FIG. 57 cont.

407		Glutathione Metabolism	S-lactoylglutathione	LC/MS pos early	15731	C03451	HMDB01066	440018
408			cysteinylglycine	LC/MS pos early	35637	C01419	HMDB00078	439498
410			5-oxoproline	LC/MS neg	1494	C01879	HMDB00267	7405
411			ophthalmate	LC/MS pos early	34592		HMDB05765	7018721
414			4-hydroxy-nonenal-glutathione	LC/MS neg	48487			
418		Gamma-glutamyl Amino Acid	gamma-glutamylalanine	LC/MS pos early	37063		HMDB29142	440103
420			gamma-glutamylglutamate	LC/MS pos early	36738	C05282	HMDB11737	92865
421			gamma-glutamylglutamine	LC/MS pos early	2730	C05283	HMDB11738	150914
422			gamma-glutamylglycine	LC/MS pos early	33949		HMDB11667	165527
423			gamma-glutamylhistidine	LC/MS pos early	18245			7017195
424			gamma-glutamylisoleucine*	LC/MS pos early	34456		HMDB11170	14253342
425			gamma-glutamylleucine	LC/MS pos early	18369		HMDB11171	151023
426			gamma-glutamyl-epsilon-lysine	LC/MS pos early	33934		HMDB03869	65254;14284565
427			gamma-glutamylmethionine	LC/MS neg	44872		HMDB29155	7009567
428			gamma-glutamylphenylalanine	LC/MS pos early	33422		HMDB00594	111299
431			gamma-glutamyltyrosine	LC/MS neg	2734		HMDB11741	94340

FIG. 57 cont.

432	Peptide		gamma-glutamylvaline	LC/MS pos early	43829		HMDB11172	7015683
434		Dipeptide Derivative	carnosine	LC/MS pos early	1768	C00386	HMDB00033	439224
436			homocarnosine	LC/MS polar	1633	C00884	HMDB00745	10243361
437			anserine	LC/MS pos early	15747	C01262	HMDB00194	112072
560		Dipeptide	glycylleucine	LC/MS pos early	34398	C02155	HMDB00759	92843
570			glycylvaline	LC/MS pos early	18357		HMDB28854	97417
594			isoleucylglycine	LC/MS pos early	40008			342532
612			leucylglycine	LC/MS pos early	40045			79070
660			phenylalanylalanine	LC/MS pos early	41374			6993123;5488196
664			phenylalanylglycine	LC/MS pos early	41370			98207
681			prolylglycine	LC/MS pos early	40703			7408076;6426709
760			valylglycine	LC/MS pos early	40475			136487
820			1,5-anhydroglucitol (1,5-AG)	LC/MS neg	20675	C07326	HMDB02712	64960
823			glucose	LC/MS polar	20488	C00031	HMDB00122	79025
824			glucose 6-phosphate	LC/MS polar	31260	C00668	HMDB01401	5958
830			isobar: fructose 1,6-diphosphate, glucose 1,6-diphosphate, myo-inositol 1,4 or 1,3-diphosphate	LC/MS neg	46896			

FIG. 57 cont.

832	Carbohydrate	Glycolysis, Gluconeogenesis, and Pyruvate Metabolism	dihydroxyacetone phosphate (DHAP)	LC/MS neg	15522	C00111	HMDB01473	668
837			3-phosphoglycerate	LC/MS neg	1414	C00597	HMDB00807	724
838			phosphoenolpyruvate (PEP)	LC/MS neg	597	C00074	HMDB00263	1005
839			pyruvate	LC/MS polar	22250	C00022	HMDB00243	1060
840			lactate	LC/MS polar	527	C00186	HMDB00190	612
843			glycerate	LC/MS polar	1572	C00258	HMDB00139	752
846		Pentose Phosphate Pathway	6-phosphogluconate	LC/MS neg	15442	C00345	HMDB01316	91493
849			ribose 1-phosphate	LC/MS polar	1763	C00620	HMDB01489	439236
851			sedoheptulose-7-phosphate	LC/MS neg	35649	C05382	HMDB01068	616
857		Pentose Metabolism	ribose	LC/MS polar	1471	C00121	HMDB00283	5779
858			ribitol	LC/MS polar	15772	C00474	HMDB00508	6912
859			ribonate	LC/MS polar	27731	C01685	HMDB00867	5460677
880			arabitol/xylitol	LC/MS polar	48885			
882			arabonate/xylonate	LC/MS polar	48255			
886		Glycogen Metabolism	maltotetraose	LC/MS neg	15910	C02052	HMDB01296	446495
888			maltotriose	LC/MS neg	44688	C01835	HMDB01262	439586

FIG. 57 cont.

891		maltose	LC/MS polar	15586	C00208	HMDB00163	10991469
927	Fructose, Mannose and Galactose Metabolism	fructose	LC/MS polar	577	C00095	HMDB00660	5984
932		mannitol/sorbitol	LC/MS polar	46142	C01507	HMDB00247	5780
933		mannose	LC/MS polar	584	C00159	HMDB00169	18950
951		galactonate	LC/MS polar	27719	C00880	HMDB00565	128869
955	Nucleotide Sugar	UDP-glucose	LC/MS polar	32344	C00029	HMDB00286	8629
959		UDP-galactose	LC/MS polar	15860	C00052	HMDB00302	18068
960		UDP-glucuronate	LC/MS neg	2763	C00167	HMDB00935	17473
962		guanosine 5'-diphospho-fucose	LC/MS neg	15903			
964		UDP-N-acetylglucosamine	LC/MS polar	35162	C00043	HMDB00290	445675
965		UDP-N-acetylgalactosamine	LC/MS polar	18396	C00203	HMDB00304	439185
967		cytidine 5'-monophospho-N-acetylneuraminic acid	LC/MS polar	36831	C00128	HMDB01176	448209
973	Aminosugar Metabolism	glucosamine-6-phosphate	LC/MS polar	580	C00352	HMDB01254	439217
981		N-acetylglucosamine 6-phosphate	LC/MS polar	15107	C00357	HMDB02817	439219
988		N-acetylneuraminate	LC/MS polar	32377	C00270	HMDB00230	439197
1000		erythronate*	LC/MS polar	42420		HMDB00613	2781043

FIG. 57 cont.

1003		Advanced Glycation End-product	N6-carboxymethyllysine	LC/MS pos early	36713			
1007	Energy	TCA Cycle	citrate	LC/MS neg	1564	C00158	HMDB00094	311
1009			aconitate [cis or trans]	LC/MS neg	46173	C00417	HMDB00072	
1011			isocitrate	LC/MS pos early	12110	C00311	HMDB00193	1198
1012			alpha-ketoglutarate	LC/MS polar	528	C00026	HMDB00208	51
1014			succinylcarnitine	LC/MS pos early	37058			
1016			fumarate	LC/MS polar	1643	C00122	HMDB00134	444972
1017			malate	LC/MS polar	1303	C00149	HMDB00156	525
1027			2-methylcitrate/homocitrate	LC/MS neg	52282			
1028		Oxidative Phosphorylation	acetylphosphate	LC/MS polar	15488	C00227	HMDB01494	186
1030			phosphate	LC/MS neg	42109	C00009	HMDB01429	1061
1032		Medium Chain Fatty Acid	caproate (6:0)	LC/MS neg	32489	C01585	HMDB00535	8892
1033			heptanoate (7:0)	LC/MS neg	1644	C17714	HMDB00666	8094
1045			palmitate (16:0)	LC/MS neg	1336	C00249	HMDB00220	985
1046			palmitoleate (16:1n7)	LC/MS neg	33447	C08362	HMDB03229	445638
1048			margarate (17:0)	LC/MS neg	1121		HMDB02259	10465
1049			10-heptadecenoate (17:1n7)	LC/MS neg	33971		HMDB60038	5312435

FIG. 57 cont.

1050	Long Chain Fatty Acid	stearate (18:0)	LC/MS neg	1358	C01530	HMDB00827	5281
1058		nonadecanoate (19:0)	LC/MS neg	1356	C16535	HMDB00772	12591
1059		10-nonadecenoate (19:1n9)	LC/MS neg	33972		HMDB13622	5312513
1064		eicosenoate (20:1)	LC/MS neg	33587		HMDB02231	5282768
1068		erucate (22:1n9)	LC/MS neg	1552	C08316	HMDB02068	5281116
1075		oleate/vaccenate (18:1)	LC/MS neg	52285			
1079	Polyunsaturated Fatty Acid (n3 and n6)	eicosapentaenoate (EPA; 20:5n3)	LC/MS neg	16467	C06428	HMDB01999	446284
1080		docosapentaenoate (n3 DPA; 22:5n3)	LC/MS neg	32504	C16513	HMDB01976	6441454
1081		docosahexaenoate (DHA; 22:6n3)	LC/MS neg	44675	C06429	HMDB02183	445580
1082		docosatrienoate (22:3n3)	LC/MS neg	32417	C16534	HMDB02823	5312556
1085		linoleate (18:2n6)	LC/MS neg	1105	C01595	HMDB00673	5280450
1087		linolenate [alpha or gamma; (18:3n3 or 6)]	LC/MS neg	34035	C06426	HMDB03073	5280934
1089		dihomo-linolenate (20:3n3 or n6)	LC/MS neg	35718	C03242	HMDB02925	5280581
1090		arachidonate (20:4n6)	LC/MS neg	1110	C00219	HMDB01043	444899
1091		adrenate (22:4n6)	LC/MS neg	32980	C16527	HMDB02226	5497181

FIG. 57 cont.

1092		docosapentaenoate (n6 DPA; 22:5n6)	LC/MS neg	37478	C16513	HMDB01976	6441454
1093		docosadienoate (22:2n6)	LC/MS neg	32415	C16533	HMDB61714	5282807
1094		dihomo-linoleate (20:2n6)	LC/MS neg	17805	C16525	HMDB05060	6439848
1096		mead acid (20:3n9)	LC/MS neg	35174		HMDB10378	5312531
1161	Fatty Acid, Dicarboxylate	2-hydroxyglutarate	LC/MS polar	37253	C02630	HMDB00606	43
1164		2-hydroxyadipate	LC/MS polar	31934	C02360	HMDB00321	193530
1214	Fatty Acid, Amino	2-aminoheptanoate	LC/MS pos early	43761			227939
1227	Fatty Acid Synthesis	malonylcarnitine	LC/MS pos early	37059		HMDB02095	22833583
1228		malonate	LC/MS polar	15872	C00383	HMDB00691	867
1230	Fatty Acid Metabolism	acetyl CoA	LC/MS neg	43840	C00024	HMDB01206	444493
1241	Fatty Acid Metabolism (also BCAA Metabolism)	butyrylcarnitine	LC/MS pos early	32412	C02862	HMDB02013	439829
1244		propionylcarnitine	LC/MS pos early	32452	C03017	HMDB00824	107738
1247		methylmalonate (MMA)	LC/MS polar	1496	C02170	HMDB00202	487
1258		acetylcarnitine	LC/MS pos early	32198	C02571	HMDB00201	1
1259		3-hydroxybutyrylcarnitine (1)	LC/MS pos early	43264		HMDB13127	53481617
1260		3-hydroxybutyrylcarnitine (2)	LC/MS pos early	52984			
1262		hexanoylcarnitine	LC/MS pos early	32328		HMDB00705	6426853

FIG. 57 cont.

1268	Fatty Acid Metabolism(Acyl Carnitine)	laurylcarnitine	LC/MS pos late	34534		HMDB02250	10427569
1269		myristoylcarnitine	LC/MS pos late	33952		HMDB05066	53477791
1271		palmitoylcarnitine	LC/MS pos late	44681	C02990	HMDB00222	461
1272		stearoylcarnitine	LC/MS pos late	34409		HMDB00848	6426855
1273		linoleoylcarnitine*	LC/MS pos late	46223		HMDB06469	6450015
1274		oleoylcarnitine	LC/MS pos late	35160		HMDB05065	6441392;53477789
1282	Carnitine Metabolism	deoxycarnitine	LC/MS pos early	36747	C01181	HMDB01161	134
1283		carnitine	LC/MS pos early	15500	C00318	HMDB00062	10917
1288	Ketone Bodies	3-hydroxybutyrate (BHBA)	LC/MS polar	542	C01089	HMDB00357	441
1289	Neurotransmitter	acetylcholine	LC/MS pos early	18790			
1293	Fatty Acid, Monohydroxy	2-hydroxydecanoate	LC/MS neg	42489			21488
1296		2-hydroxystearate	LC/MS neg	17945	C03045		69417
1318		13-HODE + 9-HODE	LC/MS neg	37752			43013
1369	Eicosanoid	prostaglandin F2alpha	LC/MS neg	19398	C00639	HMDB01139	5280363
1405		5-HETE	LC/MS neg	37372	C04805	HMDB11134	5280733
1410		12-HETE	LC/MS neg	37536		HMDB06111	5312983
1411		15-HETE	LC/MS neg	37538	C04742	HMDB02110	5280724

FIG. 57 cont.

1419	Endocannabinoid	oleoyl ethanolamide	LC/MS neg	38102		HMDB02088	5283454
1422		palmitoyl ethanolamide	LC/MS pos late	38165	C16512	HMDB02100	4671
1423		stearoyl ethanolamide	LC/MS pos late	38625		HMDB13078	27902
1429		N-oleoyltaurine	LC/MS neg	39732			6437033
1430		N-stearoyltaurine	LC/MS neg	39730			168274
1431		N-palmitoyltaurine	LC/MS neg	39835			
1435	Inositol Metabolism	myo-inositol	LC/MS polar	1124	C00137	HMDB00211	892
1443		inositol 1-phosphate (I1P)	LC/MS polar	43849	C04006	HMDB00213	440194
1463		choline	LC/MS pos early	15506	C00114	HMDB00097	305
1464		choline phosphate	LC/MS polar	34396	C00588	HMDB01565	1014
1465		cytidine 5'-diphosphocholine	LC/MS pos early	34418	C00307	HMDB01413	13804
1466		glycerophosphorylcholine (GPC)	LC/MS pos early	15990	C00670	HMDB00086	71920
1470		phosphoethanolamine	LC/MS neg	1600	C00346	HMDB00224	1015
1471		cytidine-5'-diphosphoethanolamine	LC/MS polar	34410	C00570	HMDB01564	123727
1472		glycerophosphoethanolamine	LC/MS polar	37455	C01233	HMDB00114	123874
1473		trimethylamine N-oxide	LC/MS pos early	40406	C01104	HMDB00925	1145
1474		glycerophosphoinositol*	LC/MS pos early	52307			

FIG. 57 cont.

1475		1,2-dipalmitoyl-GPC (16:0/16:0)	LC/MS pos late	19130		HMDB00564	452110
1476		1-palmitoyl-2-oleoyl-GPC (16:0/18:1)	LC/MS pos late	52461			6436017
1477		1-stearoyl-2-arachidonoyl-GPC (18:0/20:4)	LC/MS pos late	42450			16219824
1478		1-palmitoyl-2-linoleoyl-GPC (16:0/18:2)	LC/MS pos late	42446			5287971
1480		1-stearoyl-2-oleoyl-GPC (18:0/18:1)	LC/MS pos late	52438			
1482		1,2-dioleoyl-GPC (18:1/18:1)*	LC/MS pos late	52457			10350317
1483		1-palmitoyl-2-arachidonoyl-GPC (16:0/20:4)	LC/MS pos late	52462			10747814
1484		1-stearoyl-2-linoleoyl-GPC (18:0/18:2)*	LC/MS pos late	52452			
1488		1-palmitoyl-2-palmitoleoyl-GPC (16:0/16:1)*	LC/MS pos late	52470			
1491	Phospholipid Metabolism	1-stearoyl-2-arachidonoyl-GPI (18:0/20:4)	LC/MS polar	52449			
1492		1-oleoyl-2-linoleoyl-GPC (18:1/18:2)*	LC/MS pos late	52453			
1496		1-palmitoyl-2-arachidonoyl-GPI (16:0/20:4)*	LC/MS polar	52467			
1498		1-palmitoyl-2-oleoyl-GPG (16:0/18:1)	LC/MS polar	52448			5283509

FIG. 57 cont.

1500	Lipid	1-palmitoyl-2-oleoyl-GPE (16:0/18:1)	LC/MS pos late	19263		HMDB05320	5283496
1502		1-stearoyl-2-arachidonoyl-GPE (18:0/20:4)	LC/MS pos late	52447			5289133
1504		1-stearoyl-2-oleoyl-GPE (18:0/18:1)	LC/MS pos late	42448			
1505		1-palmitoyl-2-arachidonoyl-GPE (16:0/20:4)*	LC/MS pos late	52464		HMDB05323	9546800
1507		1-palmitoyl-2-linoleoyl-GPE (16:0/18:2)	LC/MS pos late	42449		HMDB05322	9546747
1524		1-palmitoyl-2-stearoyl-GPC (16:0/18:0)	LC/MS pos late	52616			
1525		1,2-dioleoyl-GPE (18:1/18:1)	LC/MS pos late	52609			9546757
1533		1-palmitoyl-2-linolenoyl-GPC (16:0/18:3)*	LC/MS pos late	52684			
1536		1-palmitoleoyl-2-linoleoyl-GPC (16:1/18:2)*	LC/MS pos late	52683			
1541		1,2-dilinoleoyl-GPC (18:2/18:2)	LC/MS pos late	52603			5288075
1544		1-oleoyl-2-linoleoyl-GPE (18:1/18:2)*	LC/MS pos late	52687		HMDB05349	9546753
1549		1-linoleoyl-2-arachidonoyl-GPC (18:2/20:4n6)*	LC/MS pos late	52710			
1557		1-palmitoyl-2-oleoyl-GPS (16:0/18:1)	LC/MS pos late	19261	C13880		5283499

FIG. 57 cont.

1593	Phosphatidylserine (PS)	1-stearoyl-2-arachidonoyl-GPS (18:0/20:4)	LC/MS pos late	52235			
1594		1-stearoyl-2-oleoyl-GPS (18:0/18:1)	LC/MS polar	48494			9547087
1600	Lysolipid	1-palmitoyl-GPC (16:0)	LC/MS pos late	33955		HMDB10382	86554
1601		2-palmitoyl-GPC (16:0)*	LC/MS pos late	35253		HMDB61702	15061532
1602		1-palmitoleoyl-GPC (16:1)*	LC/MS pos late	33230		HMDB10383	24779461
1606		1-stearoyl-GPC (18:0)	LC/MS pos late	33961		HMDB10384	497299
1608		1-oleoyl-GPC (18:1)	LC/MS pos late	48258		HMDB02815	16081932
1611		1-linoleoyl-GPC (18:2)	LC/MS pos late	34419	C04100	HMDB10386	11988421
1623		1-arachidonoyl-GPC (20:4n6)*	LC/MS neg	34061	C05208	HMDB10395	
1633		1-lignoceroyl-GPC (24:0)	LC/MS pos late	49617			
1636		1-palmitoyl-GPE (16:0)	LC/MS neg	35631		HMDB11503	9547069
1639		1-stearoyl-GPE (18:0)	LC/MS neg	42398		HMDB11130	9547068
1640		2-stearoyl-GPE (18:0)*	LC/MS neg	41220			
1641		1-oleoyl-GPE (18:1)	LC/MS neg	35628		HMDB11506	9547071
1645		1-linoleoyl-GPE (18:2)*	LC/MS neg	32635		HMDB11507	52925130
1649		1-arachidonoyl-GPE (20:4n6)*	LC/MS neg	35186		HMDB11517	42607465
1659		1-palmitoyl-GPI (16:0)*	LC/MS neg	35305		HMDB61695	

FIG. 57 cont.

1662		1-stearoyl-GPI (18:0)	LC/MS neg	19324		HMDB61696	
1664		1-oleoyl-GPI (18:1)*	LC/MS neg	36602			
1670		1-arachidonoyl-GPI (20:4)*	LC/MS neg	34214		HMDB61690	
1672		1-stearoyl-GPS (18:0)*	LC/MS pos late	45966			9547101
1673		1-oleoyl-GPS (18:1)	LC/MS neg	19260			9547099
1683		1-palmitoyl-GPG (16:0)*	LC/MS neg	45970			3300276
1685		1-palmitoyl-GPS (16:0)*	LC/MS neg	46130			9547100
1688		1-oleoyl-GPG (18:1)*	LC/MS neg	45968			
1701	Plasmalogen	1-(1-enyl-palmitoyl)-2-oleoyl-GPE (P-16:0/18:1)*	LC/MS pos late	52477			
1703		1-(1-enyl-palmitoyl)-2-palmitoyl-GPC (P-16:0/16:0)*	LC/MS pos late	52716			11146967
1705		1-(1-enyl-palmitoyl)-2-arachidonoyl-GPE (P-16:0/20:4)*	LC/MS pos late	52673			
1707		1-(1-enyl-palmitoyl)-2-oleoyl-GPC (P-16:0/18:1)*	LC/MS pos late	52478			
1709		1-(1-enyl-stearoyl)-2-oleoyl-GPE (P-18:0/18:1)	LC/MS pos late	52614			
1711		1-(1-enyl-palmitoyl)-2-arachidonoyl-GPC (P-16:0/20:4)*	LC/MS pos late	52689			

FIG. 57 cont.

1715		1-(1-enyl-stearoyl)-2-arachidonoyl-GPE (P-18:0/20:4)*	LC/MS polar	52475		HMDB05779	9547058
1721	Lysoplasmalogen	1-(1-enyl-palmitoyl)-GPE (P-16:0)*	LC/MS neg	39270			
1723		1-(1-enyl-oleoyl)-GPE (P-18:1)*	LC/MS neg	44621			
1725		1-(1-enyl-stearoyl)-GPE (P-18:0)*	LC/MS neg	39271			
1726	Glycerolipid Metabolism	glycerol	LC/MS pos early	15122	C00116	HMDB00131	753
1727		glycerol 3-phosphate	LC/MS polar	43847	C00093	HMDB00126	754
1732		glycerophosphoglycerol	LC/MS polar	46857	C03274		439964
1738	Monoacylglycerol	2-palmitoylglycerol (16:0)	LC/MS neg	33419		HMDB11533	123409
1743		2-oleoylglycerol (18:1)	LC/MS neg	21232			5319879
1745		2-linoleoylglycerol (18:2)	LC/MS neg	32506		HMDB11538	5365676
1747		1-arachidonylglycerol (20:4)	LC/MS neg	34397	C13857	HMDB11572	5282281
1748		2-arachidonoylglycerol (20:4)	LC/MS neg	19266	C13856	HMDB04666	5282280
1752		1-docosahexaenoylglycerol (22:6)	LC/MS neg	35153		HMDB11587	
1755		2-docosahexaenoylglycerol (22:6)*	LC/MS neg	48675		HMDB11557	
1767	Diacylglycerol	1-oleoyl-3-linoleoyl-glycerol (18:1/18:2)	LC/MS pos late	46799			
1770		1-palmitoyl-3-linoleoyl-glycerol (16:0/18:2)*	LC/MS pos late	52634			

FIG. 57 cont.

1773		N-palmitoyl-sphinganine (d18:0/16:0)	LC/MS pos late	52604		HMDB11760	5283572
1774		sphinganine	LC/MS pos late	17769	C00836	HMDB00269	3126
1777		palmitoyl sphingomyelin (d18:1/16:0)	LC/MS pos late	37506			9939941
1778		stearoyl sphingomyelin (d18:1/18:0)	LC/MS pos late	19503	C00550	HMDB01348	6453725
1779		sphingomyelin (d18:1/18:1, d18:2/18:0)	LC/MS pos late	37529			6443882
1783		sphingosine	LC/MS pos late	17747	C00319	HMDB00252	5353955
1791		N-palmitoyl-sphingosine (d18:1/16:0)	LC/MS pos late	44877		HMDB04949	5283564
1793		sphingomyelin (d18:1/14:0, d16:1/16:0)*	LC/MS pos late	42463			11433862
1795		sphingomyelin (d18:1/24:1, d18:2/24:0)*	LC/MS pos late	47153			
1796		sphingomyelin (d18:2/16:0, d18:1/16:1)*	LC/MS pos late	42459			
1797		sphingomyelin (d18:1/20:1, d18:2/20:0)*	LC/MS pos late	48491			
1798		behenoyl sphingomyelin (d18:1/22:0)*	LC/MS pos late	48492			
1799	Sphingolipid Metabolism	sphingomyelin (d18:1/22:1, d18:2/22:0, d16:1/24:1)*	LC/MS pos late	48493			

FIG. 57 cont.

1800		sphingomyelin (d18:1/20:0, d16:1/22:0)*	LC/MS pos late	48490			
1801		palmitoyl dihydrosphingomyelin (d18:0/16:0)*	LC/MS pos late	52434			9939965
1802		sphingomyelin (d18:1/15:0, d16:1/17:0)*	LC/MS pos late	52433			
1803		sphingomyelin (d18:1/21:0, d17:1/22:0, d16:1/23:0)*	LC/MS pos late	52495			
1804		sphingomyelin (d18:2/23:0, d18:1/23:1, d17:1/24:1)*	LC/MS pos late	52435			
1805		sphingomyelin (d18:2/24:1, d18:1/24:2)*	LC/MS pos late	52437			
1806		tricosanoyl sphingomyelin (d18:1/23:0)*	LC/MS pos late	52436			
1807		sphingomyelin (d18:1/17:0, d17:1/18:0, d19:1/16:0)	LC/MS pos late	52615			
1809		3-sulfo-nervonoyl-galactosylceramide (d18:1/24:1)	LC/MS polar	52621			
1810		glycosyl-N-stearoyl-sphingosine	LC/MS pos late	52234			
1811		glycosyl-N-palmitoyl-sphingosine	LC/MS pos late	53013			
1815	Mevalonate Metabolism	3-hydroxy-3-methylglutarate	LC/MS polar	531	C03761	HMDB00355	1662
1826		desmosterol	LC/MS pos late	6065	C01802	HMDB02719	439577

FIG. 57 cont.

1827	Sterol	cholesterol	LC/MS pos late	63	C00187	HMDB00067	11025495
1847		4-cholesten-3-one	LC/MS pos late	38125	C00599	HMDB00921	91477
1868		7-hydroxycholesterol (alpha or beta)	LC/MS pos late	47890			
1910	Steroid	corticosterone	LC/MS neg	5983	C02140	HMDB01547	5753
1995	Primary Bile Acid Metabolism	taurocholate	LC/MS neg	18497	C05122	HMDB00036	6675
2002		tauro-beta-muricholate	LC/MS neg	33983		HMDB00932	168408
2087	Fatty Acid Metabolism (Acyl Choline)	palmitoylcholine	LC/MS pos late	52944			151731
2598	Purine Metabolism, (Hypo)Xanthine/Inosine containing	inosine 5'-monophosphate (IMP)	LC/MS pos early	2133	C00130	HMDB00175	8582
2599		inosine	LC/MS neg	1123	C00294	HMDB00195	6021
2600		hypoxanthine	LC/MS neg	3127	C00262	HMDB00157	790
2601		xanthine	LC/MS pos early	3147	C00385	HMDB00292	1188
2603		xanthosine	LC/MS neg	15136	C01762	HMDB00299	64959
2606		2'-deoxyinosine	LC/MS neg	15076	C05512	HMDB00071	65058
2608		urate	LC/MS neg	1604	C00366	HMDB00289	1175
2609		allantoin	LC/MS polar	1107	C02350	HMDB00462	204
2613		adenosine 5'-diphosphate (ADP)	LC/MS neg	3108	C00008	HMDB01341	6022

FIG. 57 cont.

2614	Nucleotide	Purine Metabolism, Adenine containing	adenosine 5'-monophosphate (AMP)	LC/MS pos early	32342	C00020	HMDB00045	6083
2615			adenosine 3'-monophosphate (3'-AMP)	LC/MS neg	35142	C01367	HMDB03540	41211
2616			adenosine 2'-monophosphate (2'-AMP)	LC/MS neg	36815	C00946	HMDB11617	94136
2617			adenosine 3',5'-cyclic monophosphate (cAMP)	LC/MS neg	2831	C00575	HMDB00058	6076
2621			adenosine	LC/MS pos early	555	C00212	HMDB00050	60961
2622			adenine	LC/MS pos early	554	C00147	HMDB00034	190
2627			N1-methyladenosine	LC/MS pos early	15650	C02494	HMDB03331	27476
2637			N6-carbamoylthreonyladenosine	LC/MS neg	35157		HMDB41623	161466
2646			N6-succinyladenosine	LC/MS pos early	48130		HMDB00912	
2648		Purine Metabolism, Guanine containing	guanosine 5'- diphosphate (GDP)	LC/MS neg	2848	C00035	HMDB01201	8977
2649			guanosine 5'- monophosphate (5'-GMP)	LC/MS pos early	2849	C00144	HMDB01397	6804
2654			guanosine	LC/MS neg	1573	C00387	HMDB00133	6802
2655			guanine	LC/MS pos early	32352	C00242	HMDB00132	764
2657			7-methylguanine	LC/MS neg	35114	C02242	HMDB00897	11361
2663			N2,N2-dimethylguanosine	LC/MS pos early	35137		HMDB04824	92919

FIG. 57 cont.

2671			2'-deoxyguanosine	LC/MS neg	1411	C00330	HMDB00085	187790
2675		Pyrimidine Metabolism, Orotate containing	orotate	LC/MS polar	1505	C00295	HMDB00226	967
2677			orotidine	LC/MS polar	35172	C01103	HMDB00788	92751
2682		Pyrimidine Metabolism, Uracil containing	uridine 5'-monophosphate (UMP)	LC/MS polar	2856	C00105	HMDB00288	6030
2687			uridine	LC/MS neg	606	C00299	HMDB00296	6029
2688			uracil	LC/MS polar	605	C00106	HMDB00300	1174
2689			pseudouridine	LC/MS pos early	33442	C02067	HMDB00767	15047
2701			2'-deoxyuridine	LC/MS neg	1412	C00526	HMDB00012	13712
2704			beta-alanine	LC/MS pos early	55	C00099	HMDB00056	239
2710		Pyrimidine Metabolism, Cytidine containing	cytidine 5'-monophosphate (5'-CMP)	LC/MS pos early	2372	C00055	HMDB00095	6131
2713			cytidine	LC/MS pos early	514	C00475	HMDB00089	6175
2715			3-methylcytidine	LC/MS pos early	35132			159649
2721			2'-deoxycytidine 5'-monophosphate	LC/MS pos early	533	C00239	HMDB01202	13945
2723			2'-deoxycytidine	LC/MS pos early	15949	C00881	HMDB00014	13711
2729		Pyrimidine Metabolism, Thymine containing	thymidine	LC/MS neg	2183	C00214	HMDB00273	5789
2734		Purine and Pyrimidine Metabolism	methylphosphate	LC/MS pos early	37070		HMDB61711	13130

FIG. 57 cont.

2740	Cofactors and Vitamins	Nicotinate and Nicotinamide Metabolism	nicotinamide	LC/MS pos early	594	C00153	HMDB01406	936
2743			nicotinamide riboside	LC/MS pos early	33013	C03150	HMDB00855	439924
2744			nicotinamide adenine dinucleotide (NAD+)	LC/MS pos early	5278	C00003	HMDB00902	5893
2752			1-methylnicotinamide	LC/MS pos early	27665	C02918	HMDB00699	10129985
2757			trigonelline (N'-methylnicotinate)	LC/MS pos early	32401	C01004	HMDB00875	5570
2759			N1-Methyl-2-pyridone-5-carboxamide	LC/MS pos early	40469	C05842	HMDB04193	69698
2760			adenosine 5'-diphosphoribose (ADP-ribose)	LC/MS neg	558	C00301	HMDB01178	192
2762		Riboflavin Metabolism	riboflavin (Vitamin B2)	LC/MS pos early	1827	C00255	HMDB00244	493570
2763			flavin adenine dinucleotide (FAD)	LC/MS neg	2134	C00016	HMDB01248	643975
2764			flavin mononucleotide (FMN)	LC/MS neg	15797	C00061	HMDB01520	710
2765		Pantothenate and CoA Metabolism	pantothenate	LC/MS pos early	1508	C00864	HMDB00210	6613
2767			phosphopantetheine	LC/MS neg	15504	C01134	HMDB01416	987
2768			3'-dephosphocoenzyme A	LC/MS neg	18289	C00882	HMDB01373	444485
2769			coenzyme A	LC/MS neg	46322	C00010	HMDB01423	317
2773			ascorbate (Vitamin C)	LC/MS neg	32354	C00072	HMDB00044	

FIG. 57 cont.

2774	Ascorbate and Aldarate Metabolism	dehydroascorbate	LC/MS neg	34302	C05422	HMDB01264	835
2775		threonate	LC/MS polar	27738	C01620	HMDB00943	151152
2777		oxalate (ethanedioate)	LC/MS polar	20694	C00209	HMDB02329	971
2778		gulonic acid*	LC/MS polar	46957			9794176
2779	Tocopherol Metabolism	alpha-tocopherol	LC/MS pos late	1561	C02477	HMDB01893	14985
2801	Tetrahydrobiopterin Metabolism	dihydrobiopterin	LC/MS pos early	35129	C00268	HMDB00038	1879
2814	Hemoglobin and Porphyrin Metabolism	heme	LC/MS pos late	41754	C00032	HMDB03178	26945
2818		biliverdin	LC/MS pos late	2137	C00500	HMDB01008	5353439
2826	Thiamine Metabolism	thiamin (Vitamin B1)	LC/MS pos early	5341	C00378	HMDB00235	1130
2827		thiamin monophosphate	LC/MS pos early	15798	C01081	HMDB02666	3382778
2828		thiamin diphosphate	LC/MS neg	35670	C00068	HMDB01372	1132
2833	Vitamin A Metabolism	retinol (Vitamin A)	LC/MS pos late	1806	C00473	HMDB00305	445354
2839	Vitamin B6 Metabolism	pyridoxamine	LC/MS pos early	2150	C00534	HMDB01431	1052
2840		pyridoxamine phosphate	LC/MS pos early	3138	C00647	HMDB01555	1053
2842		pyridoxal	LC/MS pos early	1651	C00250	HMDB01545	1050
2843		pyridoxate	LC/MS neg	31555	C00847	HMDB00017	6723
2845	Benzoate Metabolism	hippurate	LC/MS neg	15753	C01586	HMDB00714	464

FIG. 57 cont.

2874	Xenobiotics	Benzoate Metabolism	catechol sulfate	LC/MS neg	35320	C00090	HMDB59724	3083879
3049		Food Component/Plant	gluconate	LC/MS polar	587	C00257	HMDB00625	10690
3116			ergothioneine	LC/MS pos early	37459	C05570	HMDB03045	3032311
3118			erythritol	LC/MS polar	20699	C00503	HMDB02994	222285
3172			N-glycolylneuraminate	LC/MS pos early	37123	C03410	HMDB00833	123802
3224			stachydrine	LC/MS pos early	34384	C10172	HMDB04827	115244
3246			methyl glucopyranoside (alpha + beta)	LC/MS neg	46144			
3310		Bacterial/Fungal	tartronate (hydroxymalonate)	LC/MS neg	20693	C02287	HMDB35227	45
3522		Drug	salicylate	LC/MS polar	1515	C00805	HMDB01895	338
3634		Chemical	O-sulfo-L-tyrosine	LC/MS neg	45413			514186
3680			S-(3-hydroxypropyl)mercapturic acid (HPMA)	LC/MS neg	44552			3371179

FIG. 57 cont.

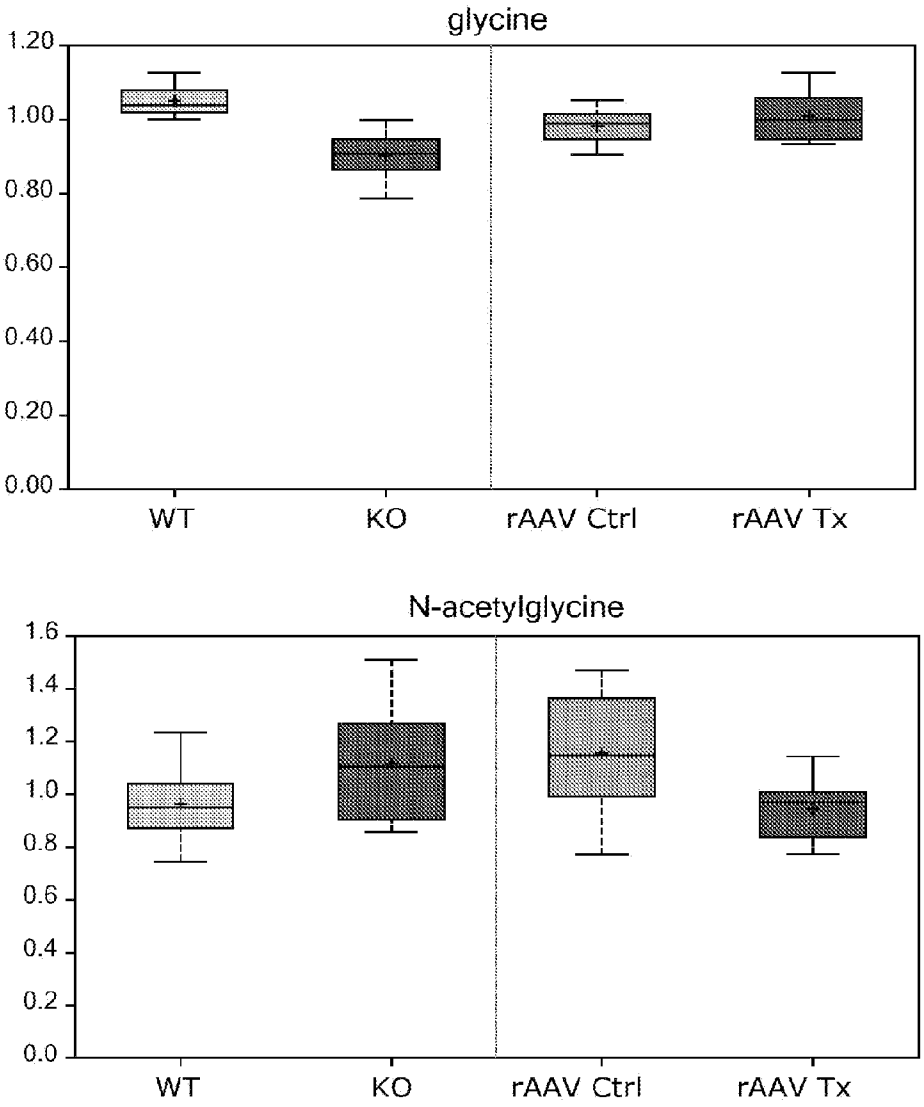
glycine
1.20
1.00
0.80
0.60
0.40
0.20
0.00
WT
KO
rAAV Ctrl
rAAV Tx
N-acetylglycine
1.6
1.4
1.2
1.0
0.8
0.6
0.4
0.2
0.0
WT
KO
rAAV Ctrl
rAAV Tx

FIG. 57 cont.

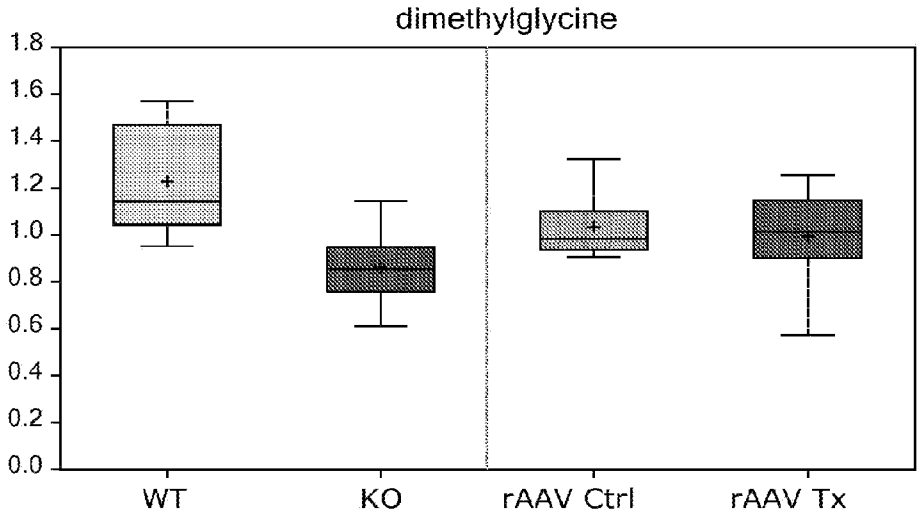
dimethylglycine
1.8
1.6
1.4
1.2
1.0
0.8
0.6
0.4
0.2
0.0
WT
KO
rAAV Ctrl
rAAV Tx

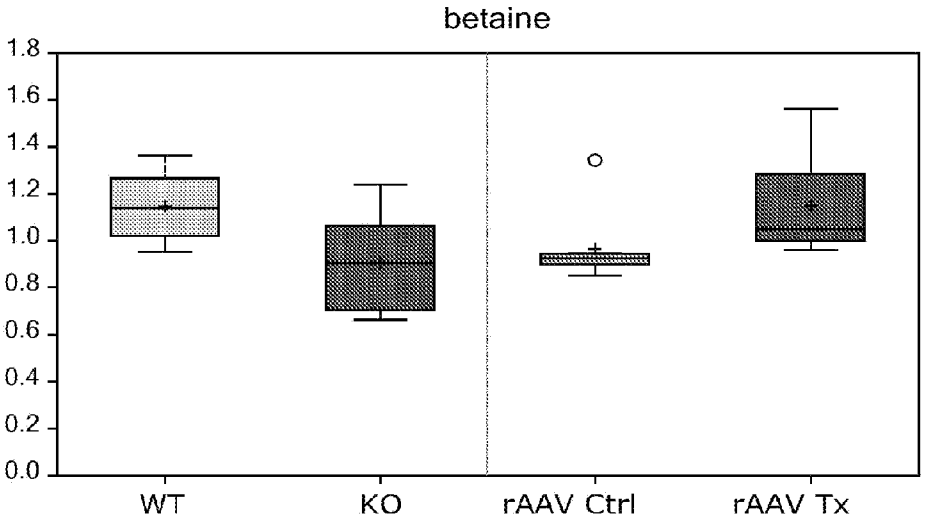
betaine
1.8
1.6
1.4
1.2
1.0
0.8
0.6
0.4
0.2
0.0
WT
KO
rAAV Ctrl
rAAV Tx

FIG. 57 cont.

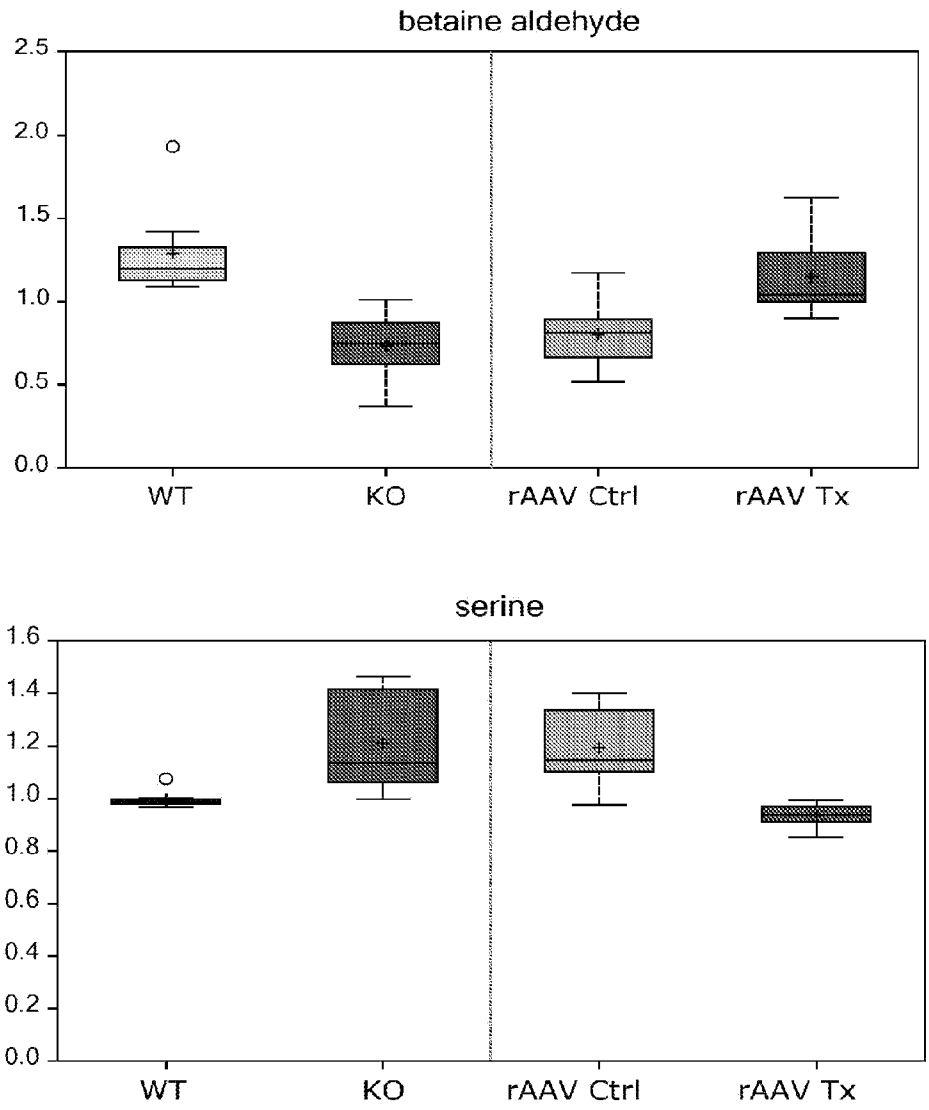
betaine aldehyde
2.5
2.0
1.5
1.0
0.5
0.0
WT
KO
rAAV Ctrl
rAAV Tx
serine
1.6
1.4
1.2
1.0
0.8
0.6
0.4
0.2
0.0
WT
KO
rAAV Ctrl
rAAV Tx

FIG. 57 cont.

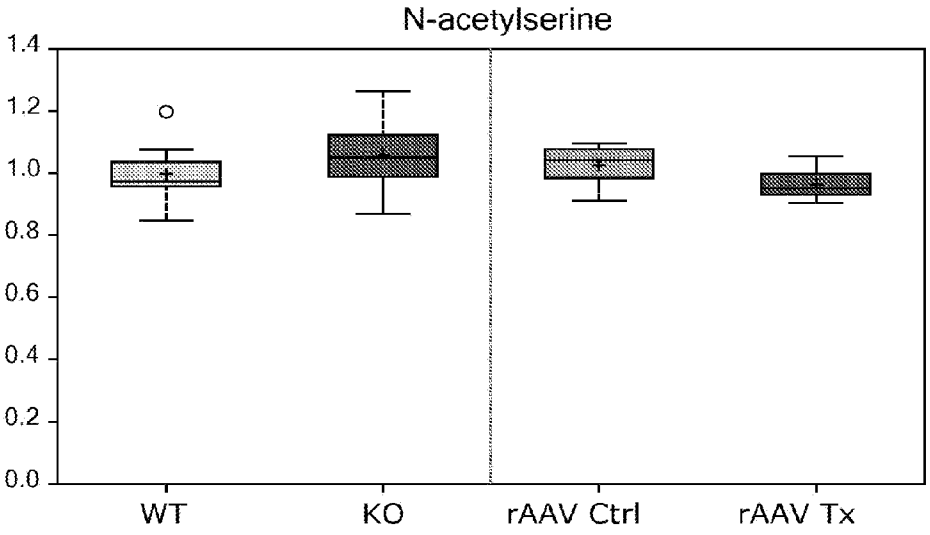
N-acetylserine
1.4
1.2
1.0
0.8
0.6
0.4
0.2
0.0
WT
KO
rAAV Ctrl
rAAV Tx

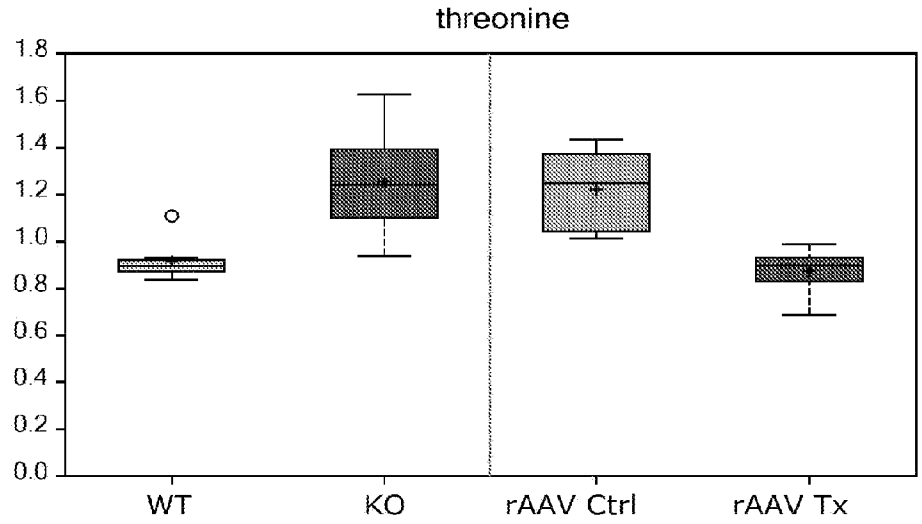
threonine
1.8
1.6
1.4
1.2
1.0
0.8
0.6
0.4
0.2
0.0
WT
KO
rAAV Ctrl
rAAV Tx

FIG. 57 cont.

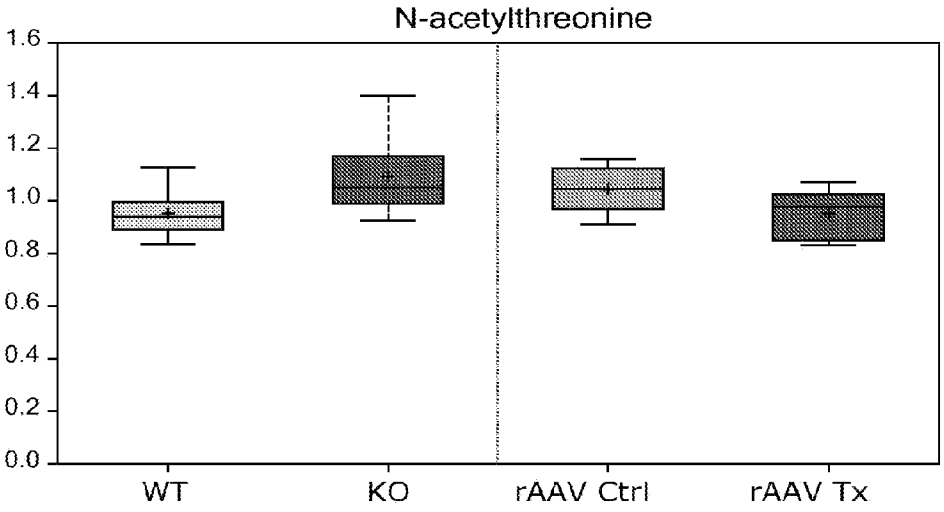
N-acetylthreonine
1.6
1.4
1.2
1.0
0.8
0.6
0.4
0.2
0.0
WT
KO
rAAV Ctrl
rAAV Tx

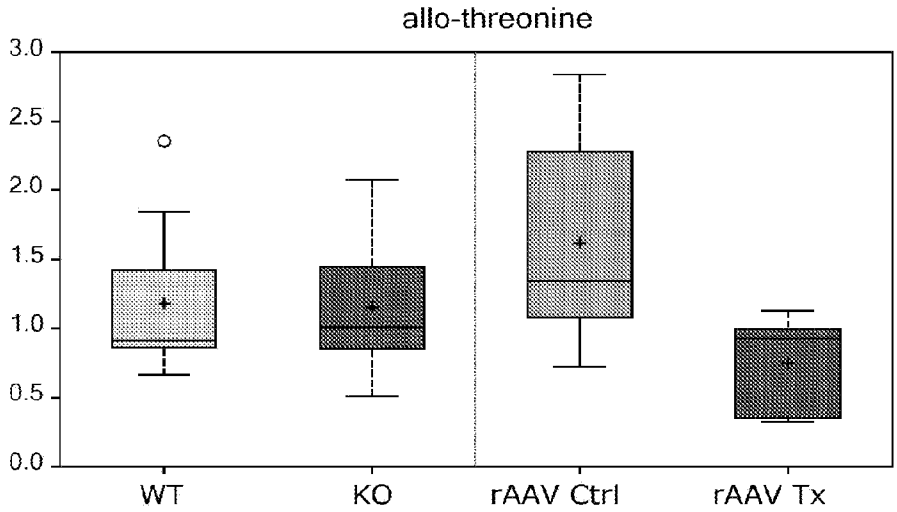
allo-threonine
3.0
2.5
2.0
1.5
1.0
0.5
0.0
WT
KO
rAAV Ctrl
rAAV Tx

FIG. 57 cont.

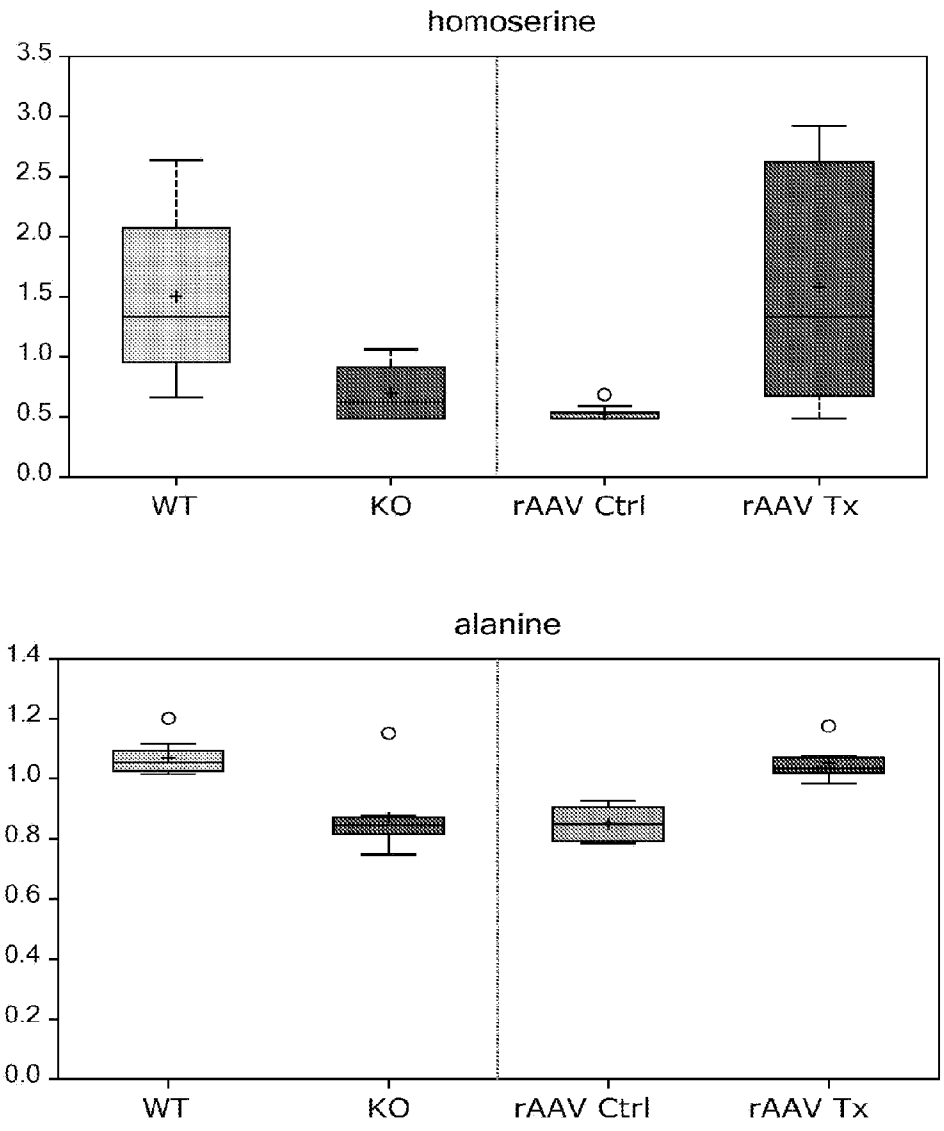
homoserine
3.5
3.0
2.5
2.0
1.5
1.0
0.5
0.0
WT
KO
rAAV Ctrl
rAAV Tx
alanine
1.4
1.2
1.0
0.8
0.6
0.4
0.2
0.0
WT
KO
rAAV Ctrl
rAAV Tx

FIG. 57 cont.

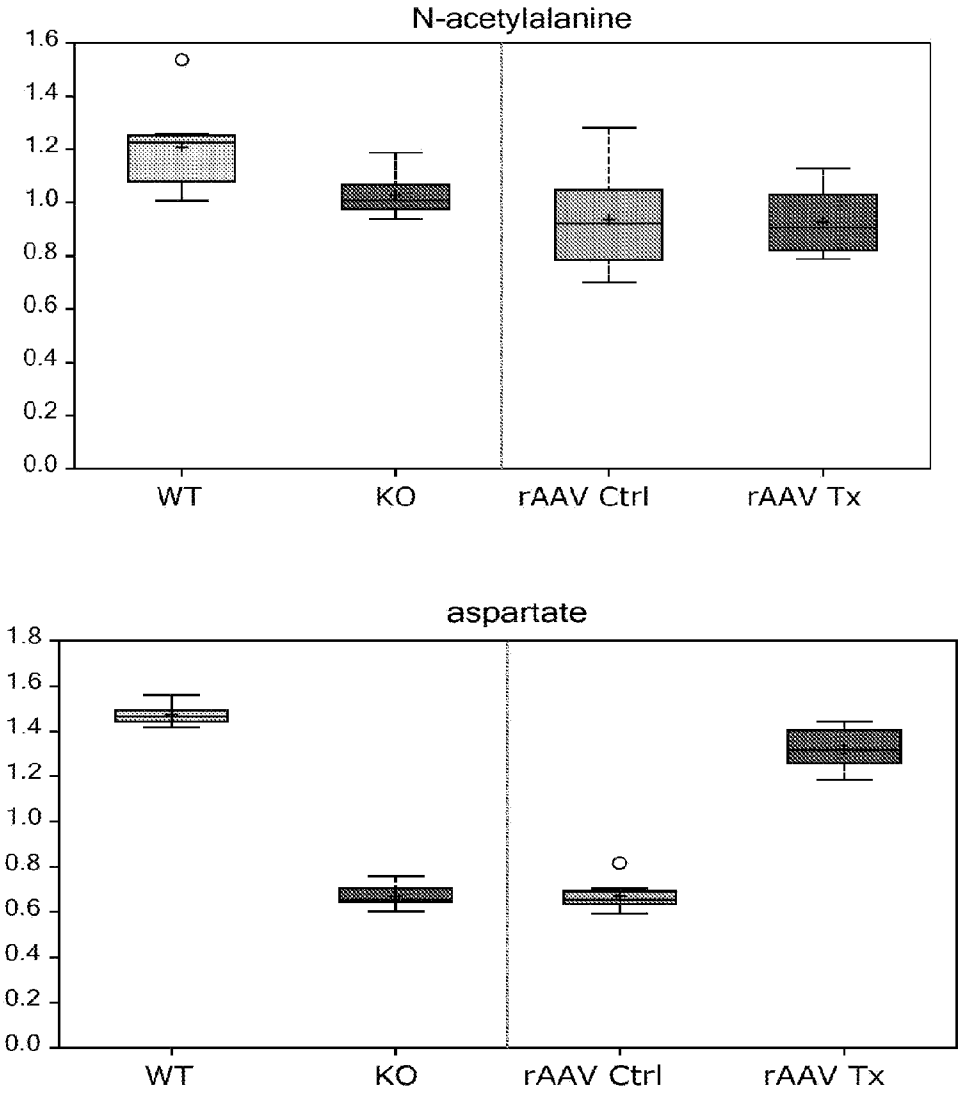
N-acetylalanine
1.6
1.4
1.2
1.0
0.8
0.6
0.4
0.2
0.0
WT
KO
rAAV Ctrl
rAAV Tx
aspartate
1.8
1.6
1.4
1.2
1.0
0.8
0.6
0.4
0.2
0.0
WT
KO
rAAV Ctrl
rAAV Tx

FIG. 57 cont.

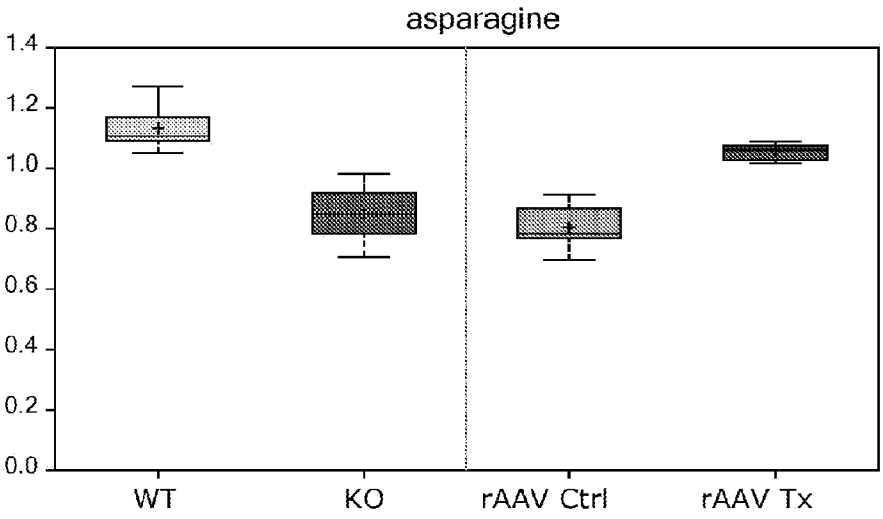
asparagine
1.4
1.2
1.0
0.8
0.6
0.4
0.2
0.0
WT
KO
rAAV Ctrl
rAAV Tx

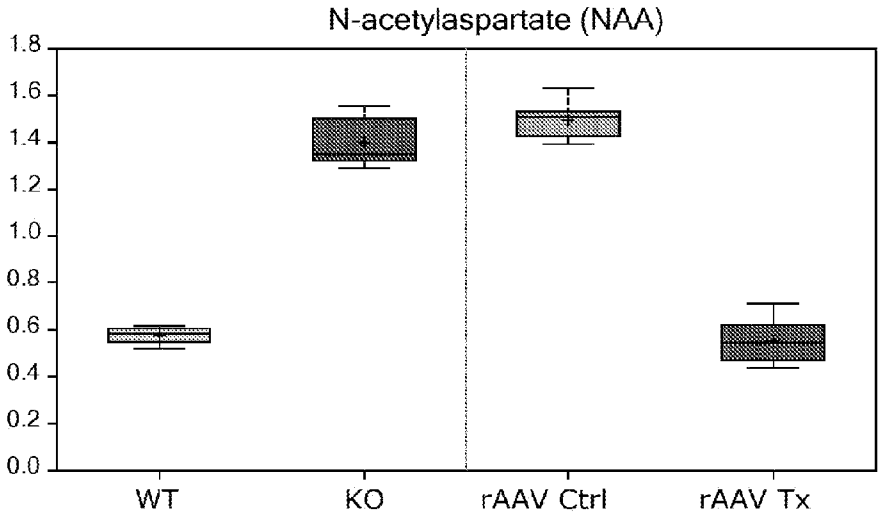
N-acetylaspartate (NAA)
1.8
1.6
1.4
1.2
1.0
0.8
0.6
0.4
0.2
0.0
WT
KO
rAAV Ctrl
rAAV Tx

FIG. 57 cont.

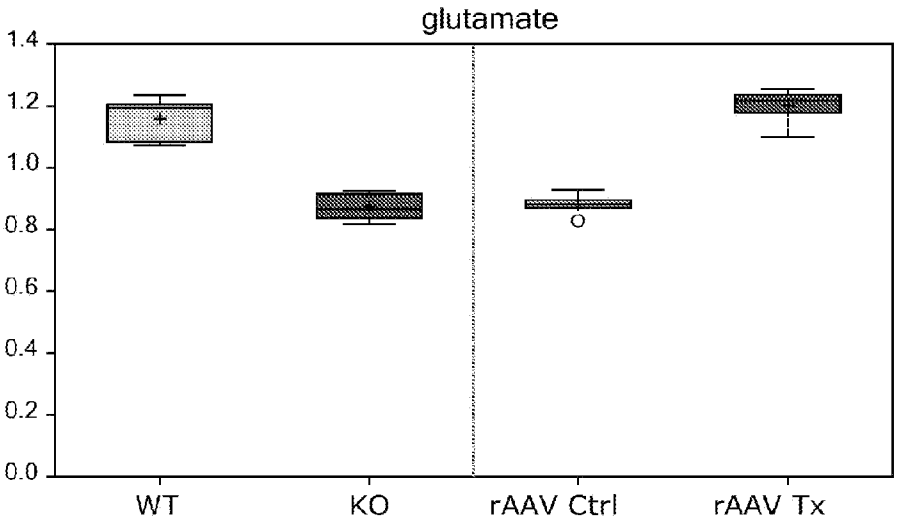
glutamate
1.4
1.2
1.0
0.8
0.6
0.4
0.2
0.0
WT
KO
rAAV Ctrl
rAAV Tx

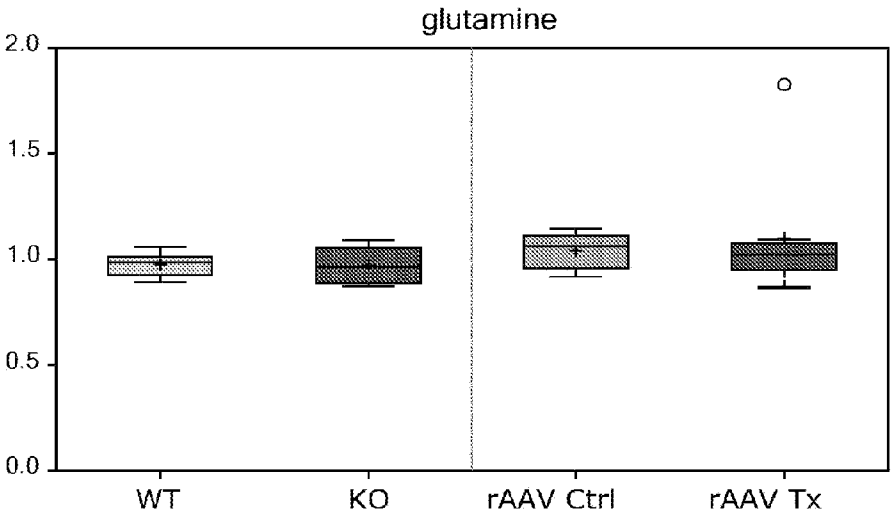
glutamine
2.0
1.5
1.0
0.5
0.0
WT
KO
rAAV Ctrl
rAAV Tx

FIG. 57 cont.

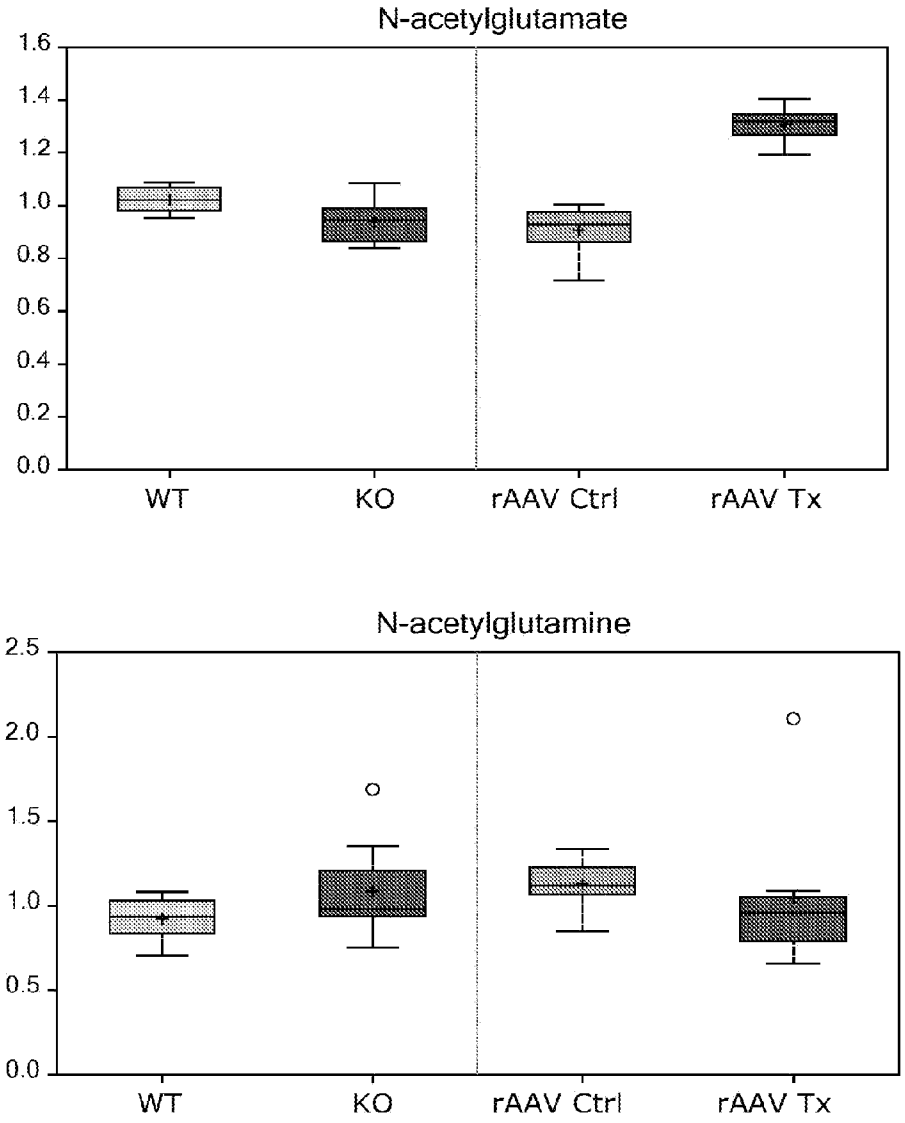
N-acetylglutamate
1.6
1.4
1.2
1.0
0.8
0.6
0.4
0.2
0.0
WT
KO
rAAV Ctrl
rAAV Tx
N-acetylglutamine
2.5
2.0
1.5
1.0
0.5
0.0
WT
KO
rAAV Ctrl
rAAV Tx

FIG. 57 cont.

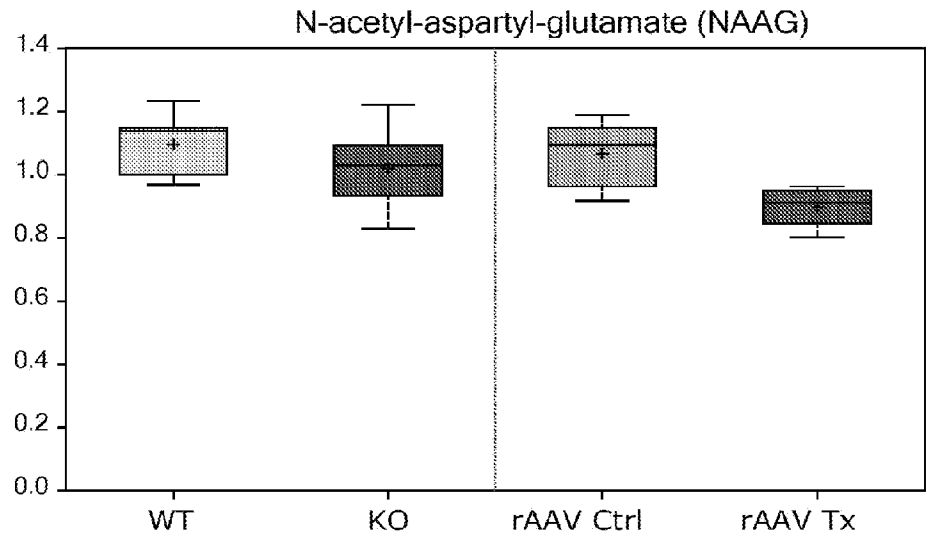
N-acetyl-aspartyl-glutamate (NAAG)
1.4
1.2
1.0
0.8
0.6
0.4
0.2
0.0
WT
KO
rAAV Ctrl
rAAV Tx

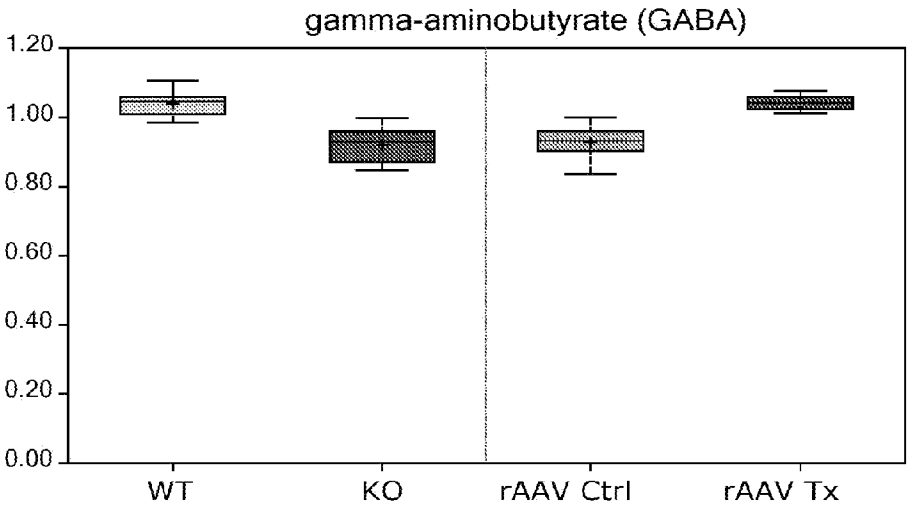
gamma-aminobutyrate (GABA)
1.20
1.00
0.80
0.60
0.40
0.20
0.00
WT
KO
rAAV Ctrl
rAAV Tx

FIG. 57 cont.

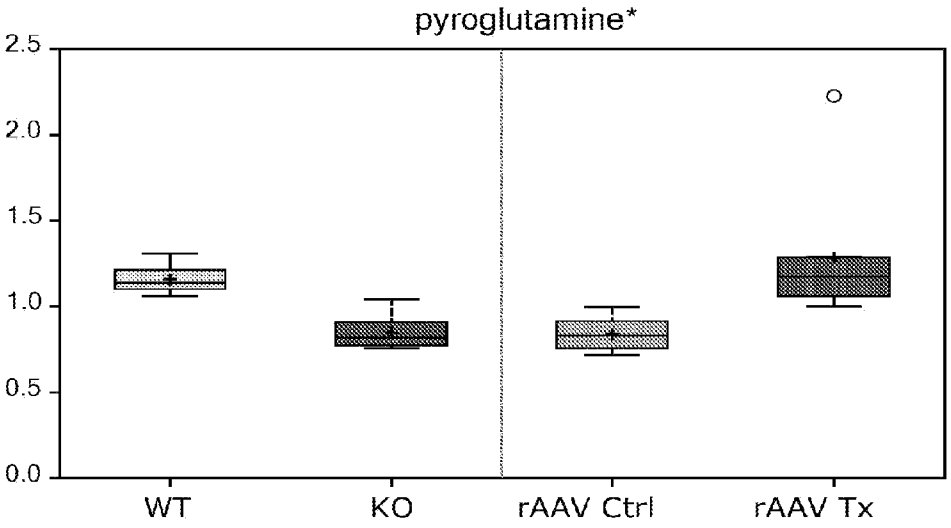
pyroglutamine*
2.5
2.0
1.5
1.0
0.5
0.0
WT
KO
rAAV Ctrl
rAAV Tx

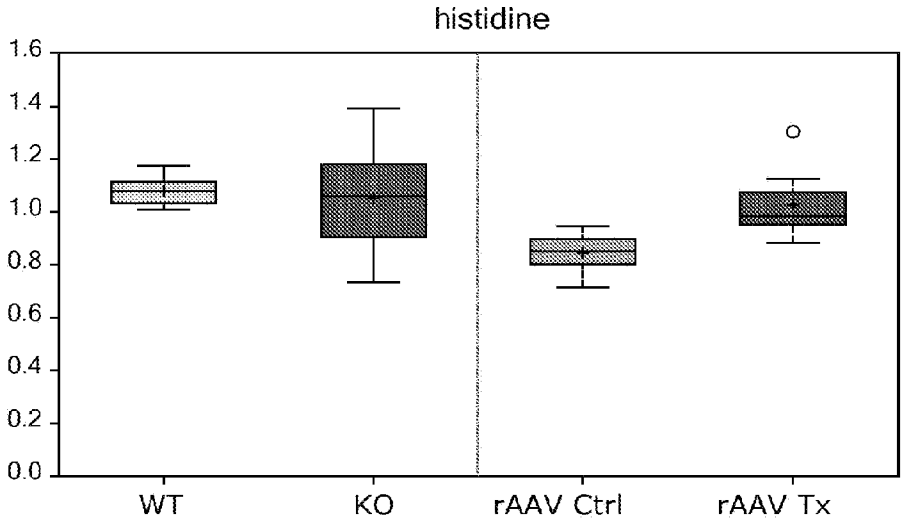
histidine
1.6
1.4
1.2
1.0
0.8
0.6
0.4
0.2
0.0
WT
KO
rAAV Ctrl
rAAV Tx

FIG. 57 cont.

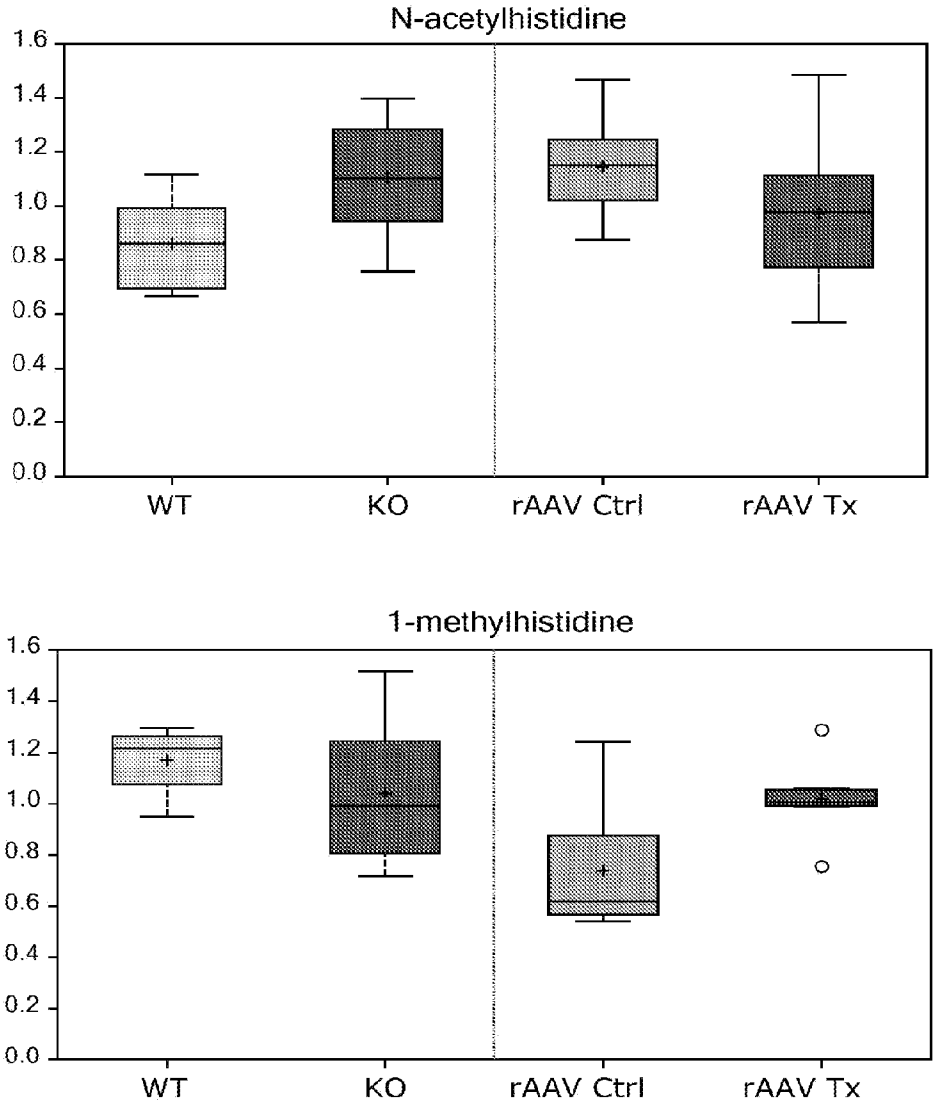
N-acetylhistidine
1.6
1.4
1.2
1.0
0.8
0.6
0.4
0.2
0.0
WT
KO
rAAV Ctrl
rAAV Tx
1-methylhistidine
1.6
1.4
1.2
1.0
0.8
0.6
0.4
0.2
0.0
WT
KO
rAAV Ctrl
rAAV Tx

FIG. 57 cont.

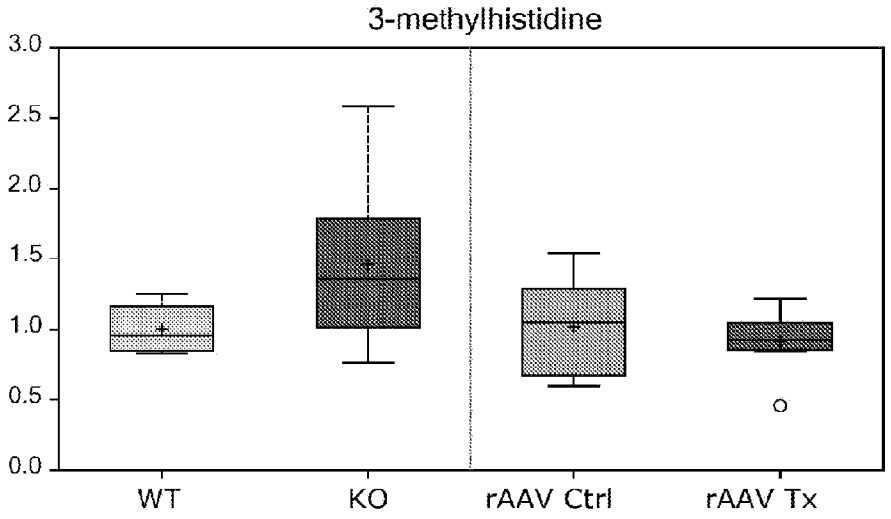
3-methylhistidine
3.0
2.5
2.0
1.5
1.0
0.5
0.0
WT
KO
rAAV Ctrl
rAAV Tx

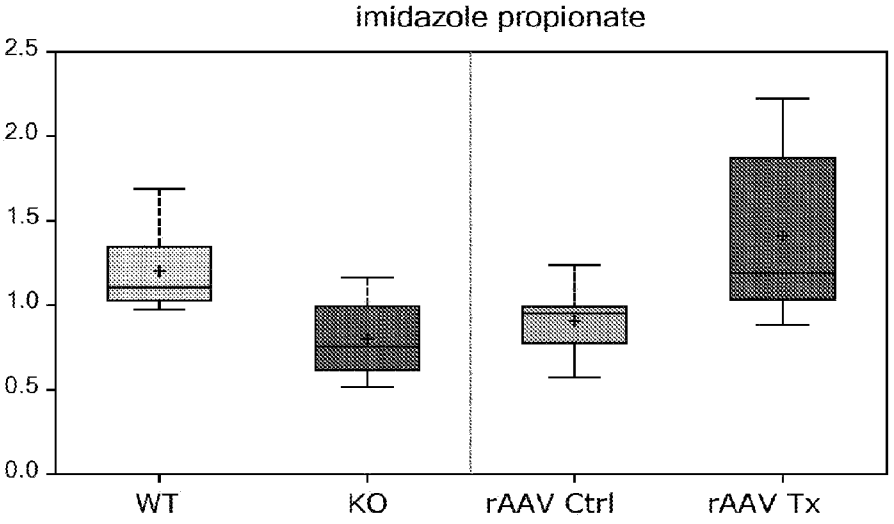
imidazole propionate
2.5
2.0
1.5
1.0
0.5
0.0
WT
KO
rAAV Ctrl
rAAV Tx

FIG. 57 cont.

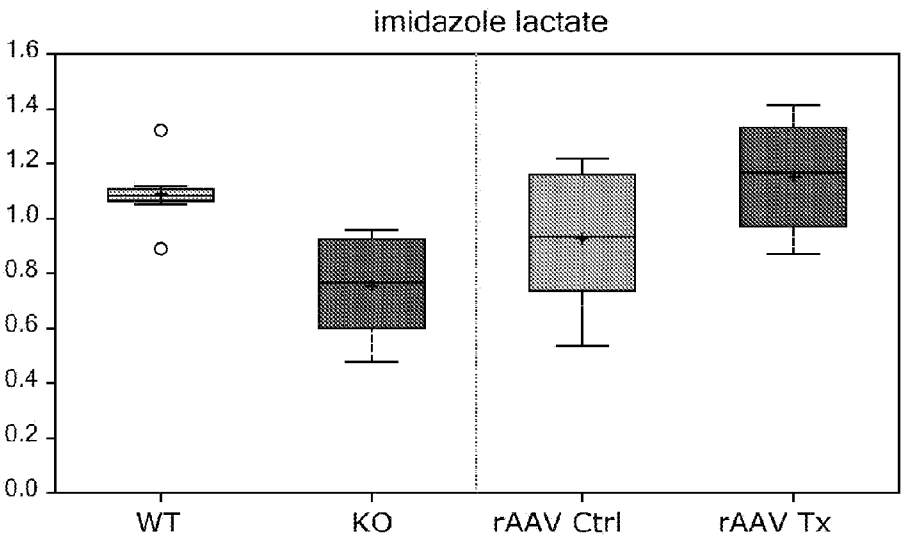
imidazole lactate
1.6
1.4
1.2
1.0
0.8
0.6
0.4
0.2
0.0
WT
KO
rAAV Ctrl
rAAV Tx

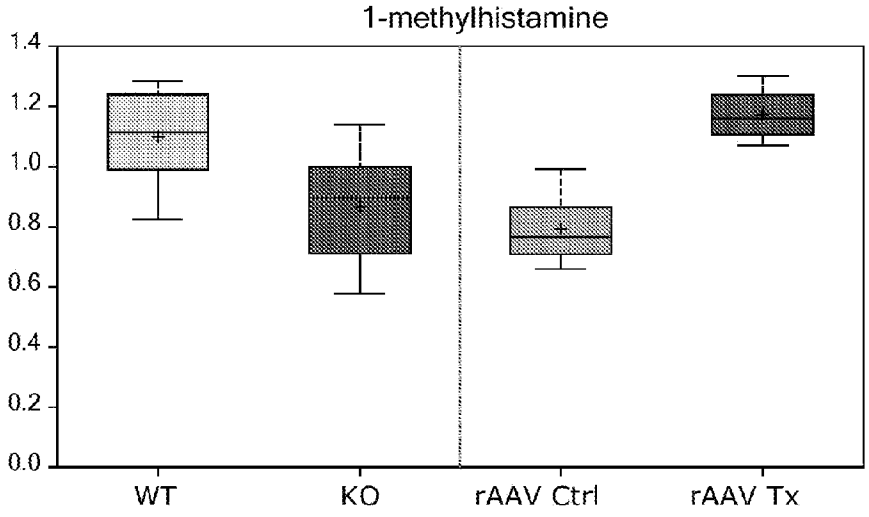
1-methylhistamine
1.4
1.2
1.0
0.8
0.6
0.4
0.2
0.0
WT
KO
rAAV Ctrl
rAAV Tx

FIG. 57 cont.

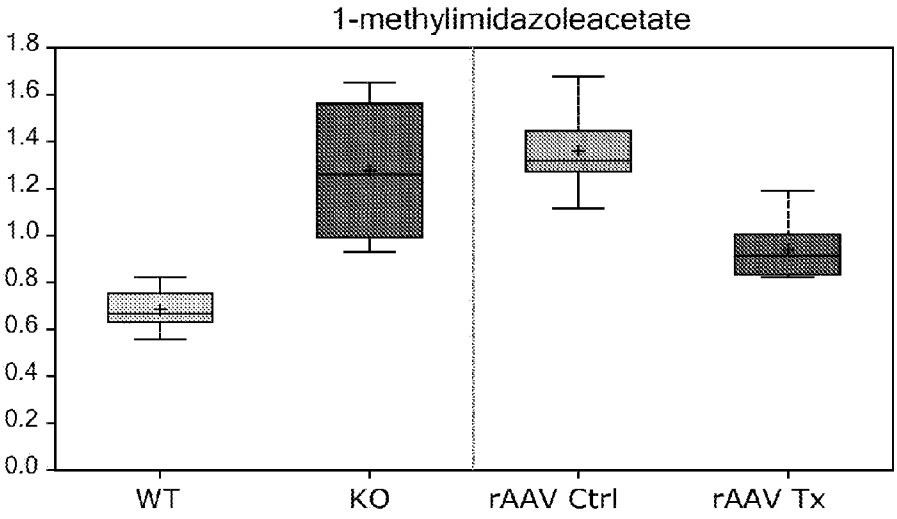
1-methylimidazoleacetate
1.8
1.6
1.4
1.2
1.0
0.8
0.6
0.4
0.2
0.0
WT
KO
rAAV Ctrl
rAAV Tx

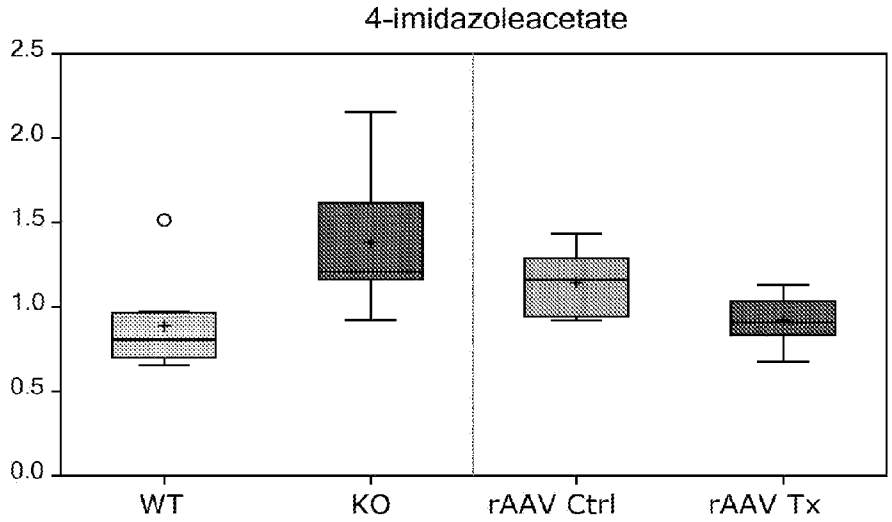
4-imidazoleacetate
2.5
2.0
1.5
1.0
0.5
0.0
WT
KO
rAAV Ctrl
rAAV Tx

FIG. 57 cont.

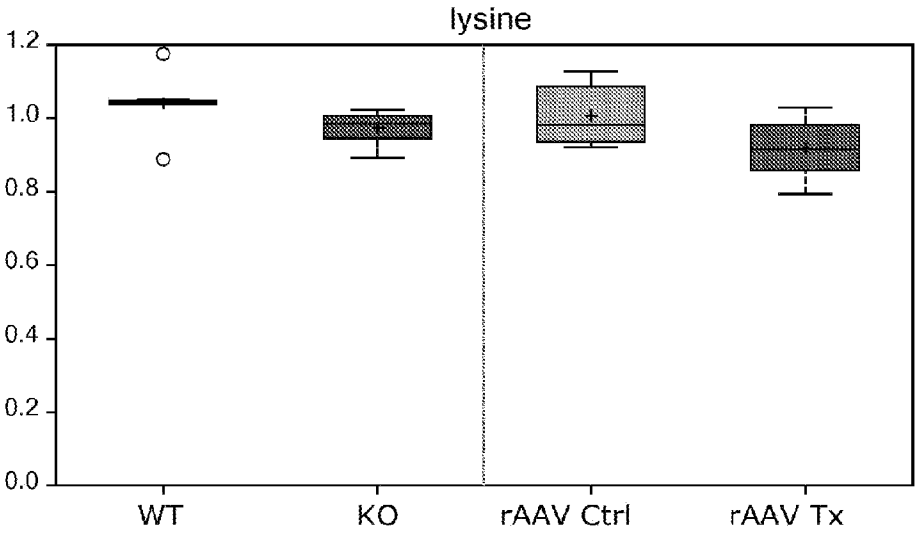
lysine
1.2
1.0
0.8
0.6
0.4
0.2
0.0
WT
KO
rAAV Ctrl
rAAV Tx

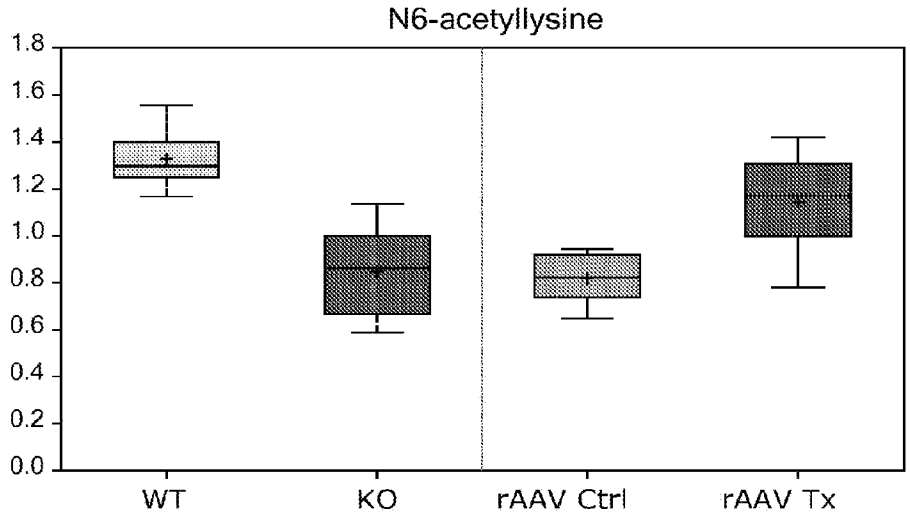
N6-acetyllysine
1.8
1.6
1.4
1.2
1.0
0.8
0.6
0.4
0.2
0.0
WT
KO
rAAV Ctrl
rAAV Tx

FIG. 57 cont.

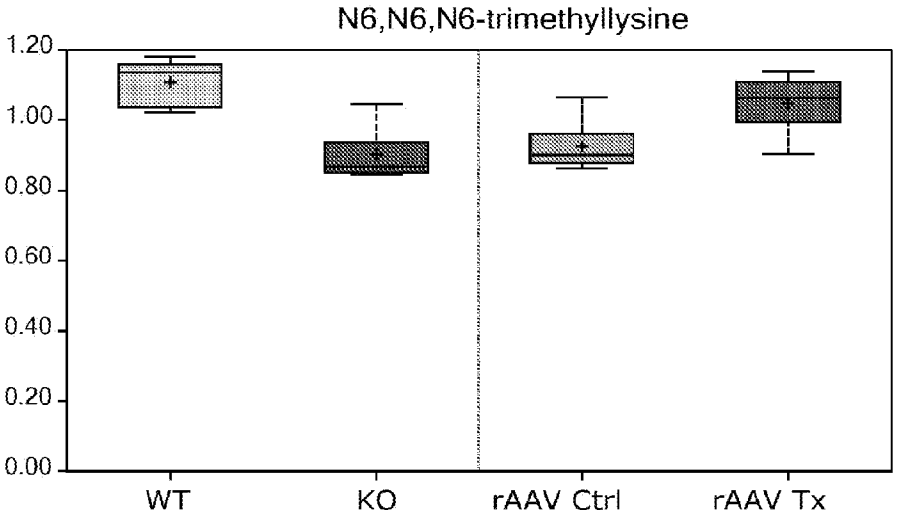
N6,N6,N6-trimethyllysine
1.20
1.00
0.80
0.60
0.40
0.20
0.00
WT
KO
rAAV Ctrl
rAAV Tx

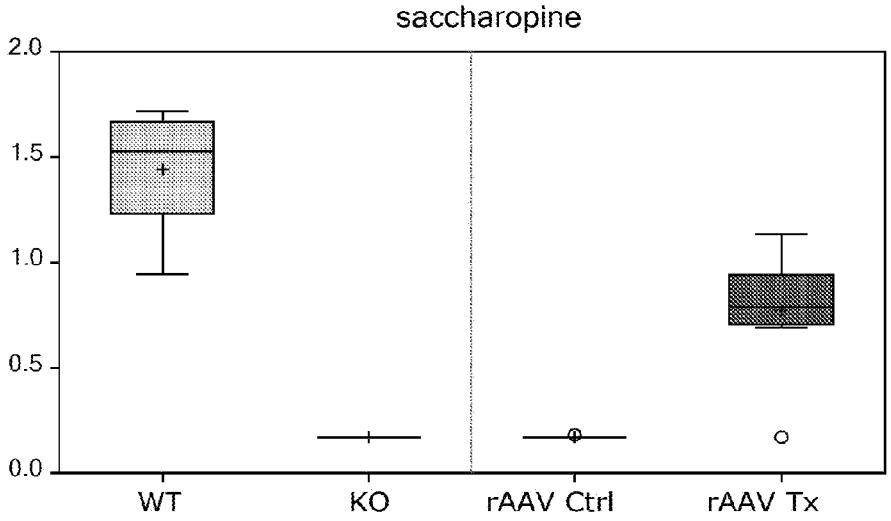
saccharopine
2.0
1.5
1.0
0.5
0.0
WT
KO
rAAV Ctrl
rAAV Tx

FIG. 57 cont.

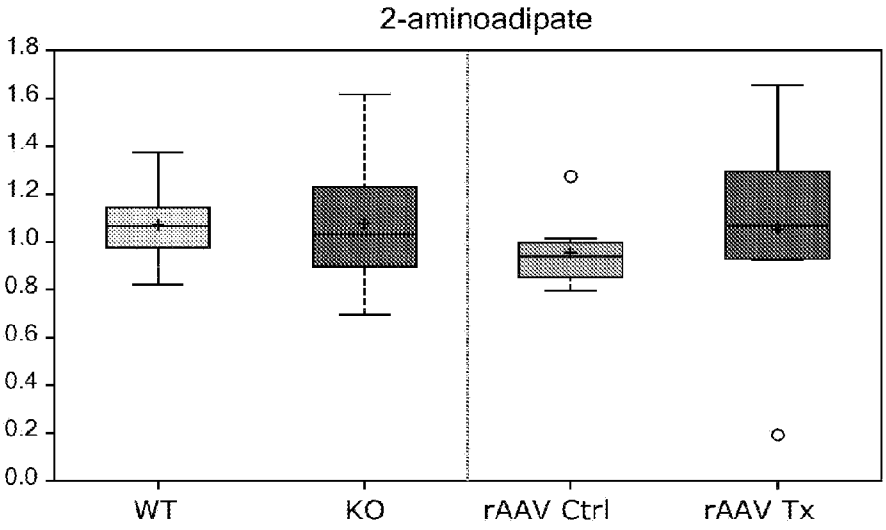
2-aminoadipate
1.8
1.6
1.4
1.2
1.0
0.8
0.6
0.4
0.2
0.0
WT
KO
rAAV Ctrl
rAAV Tx

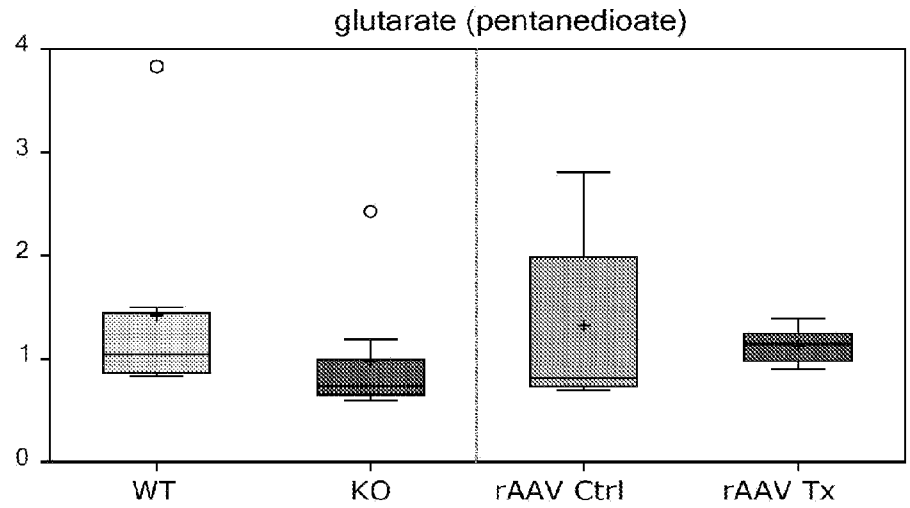
glutarate (pentanedioate)
4
3
2
1
0
WT
KO
rAAV Ctrl
rAAV Tx

FIG. 57 cont.

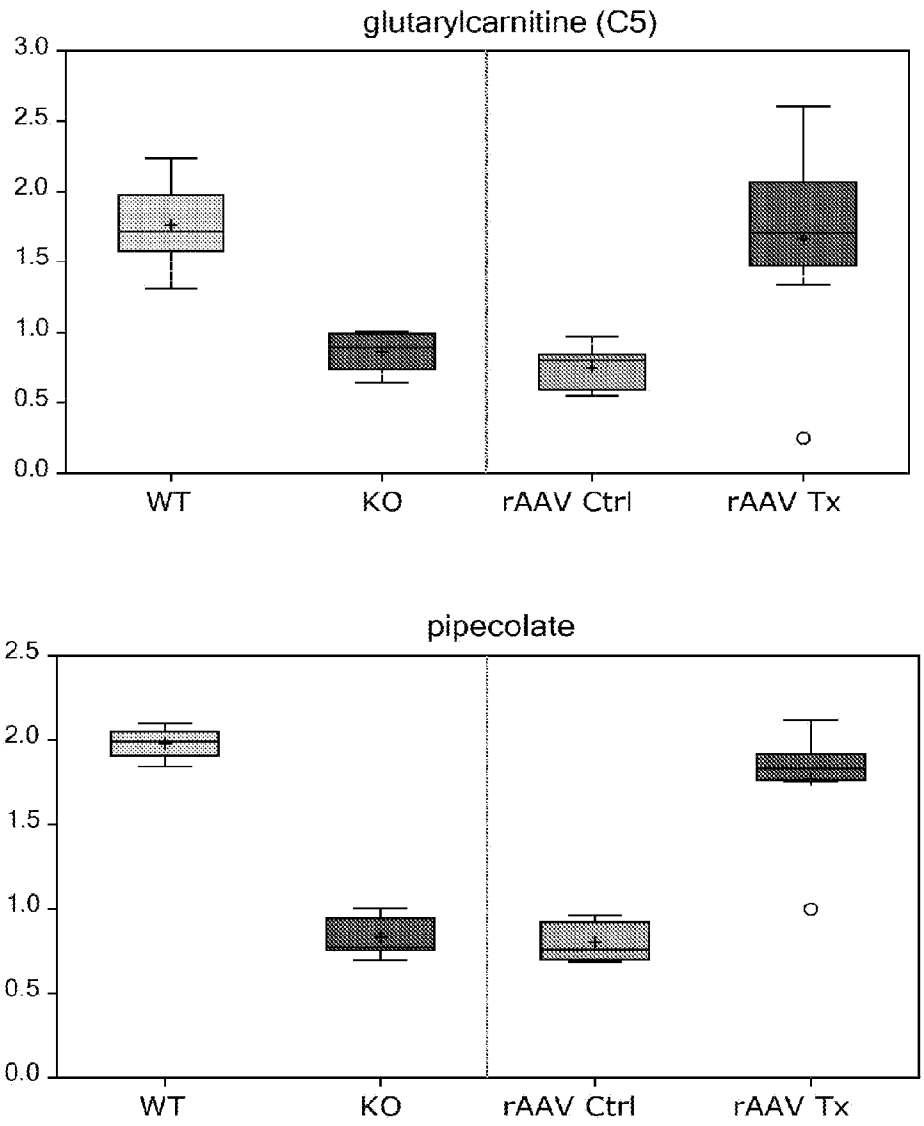
glutarylcarnitine (C5)
3.0
2.5
2.0
1.5
1.0
0.5
0.0
WT
KO
rAAV Ctrl
rAAV Tx
pipecolate
2.5
2.0
1.5
1.0
0.5
0.0
WT
KO
rAAV Ctrl
rAAV Tx

FIG. 57 cont.

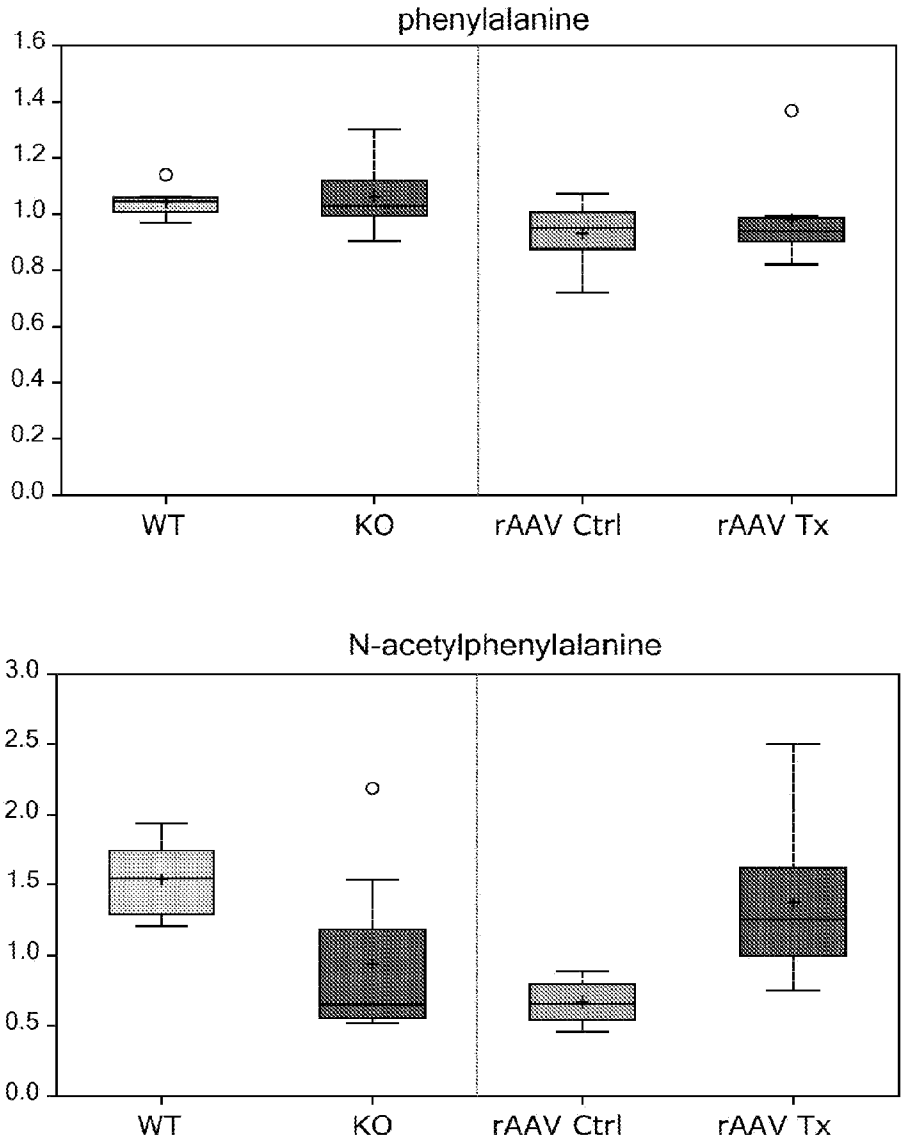
phenylalanine
1.6
1.4
1.2
1.0
0.8
0.6
0.4
0.2
0.0
WT
KO
rAAV Ctrl
rAAV Tx
N-acetylphenylalanine
3.0
2.5
2.0
1.5
1.0
0.5
0.0
WT
KO
rAAV Ctrl
rAAV Tx

FIG. 57 cont.

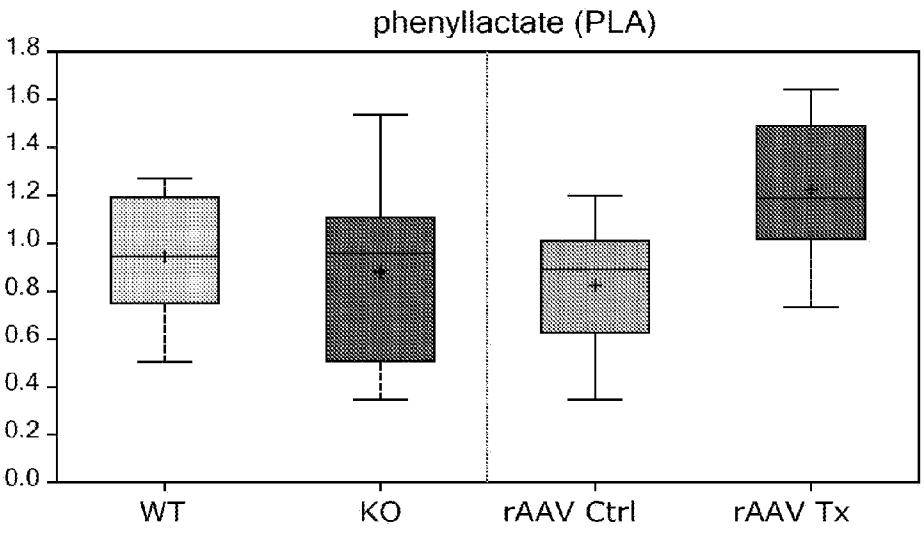
phenyllactate (PLA)
1.8
1.6
1.4
1.2
1.0
0.8
0.6
0.4
0.2
0.0
WT
KO
rAAV Ctrl
rAAV Tx

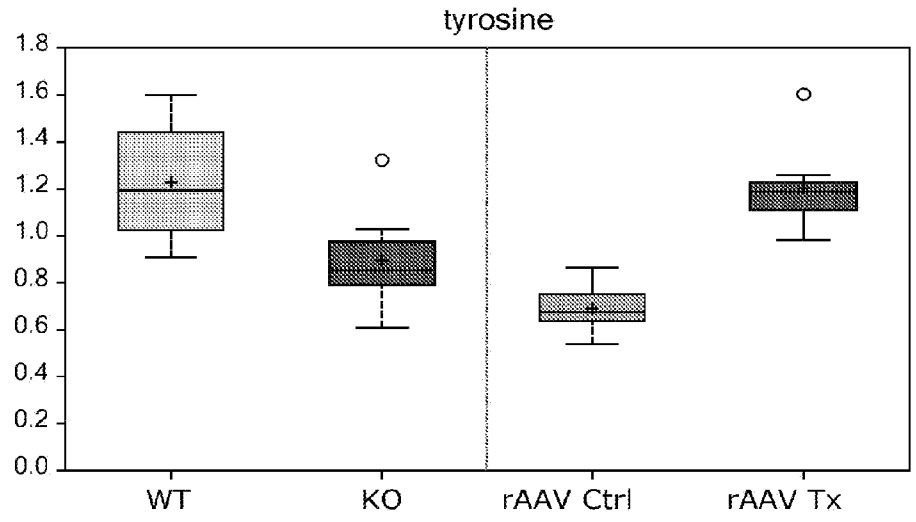
tyrosine
1.8
1.6
1.4
1.2
1.0
0.8
0.6
0.4
0.2
0.0
WT
KO
rAAV Ctrl
rAAV Tx

FIG. 57 cont.

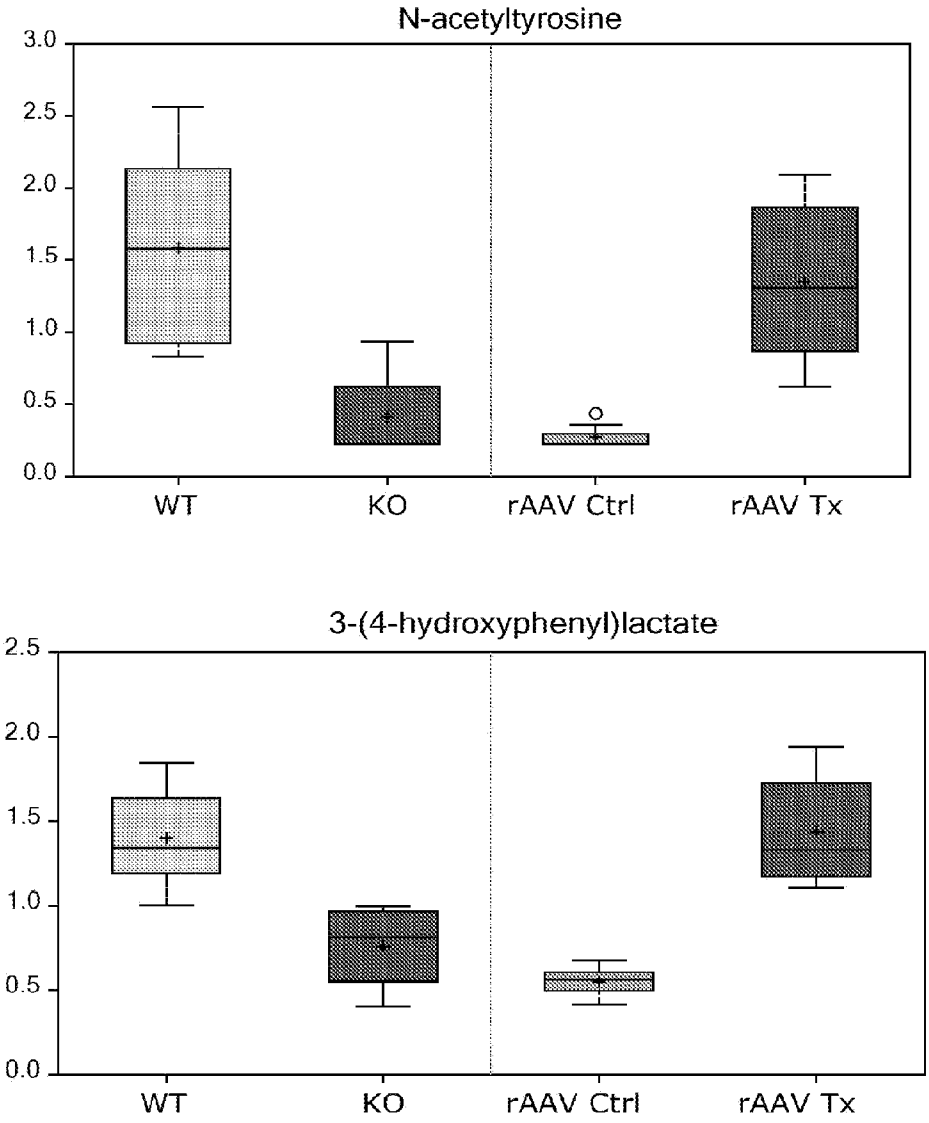
N-acetyltyrosine
3.0
2.5
2.0
1.5
1.0
0.5
0.0
WT
KO
rAAV Ctrl
rAAV Tx
3-(4-hydroxyphenyl)lactate
2.5
2.0
1.5
1.0
0.5
0.0
WT
KO
rAAV Ctrl
rAAV Tx

FIG. 57 cont.

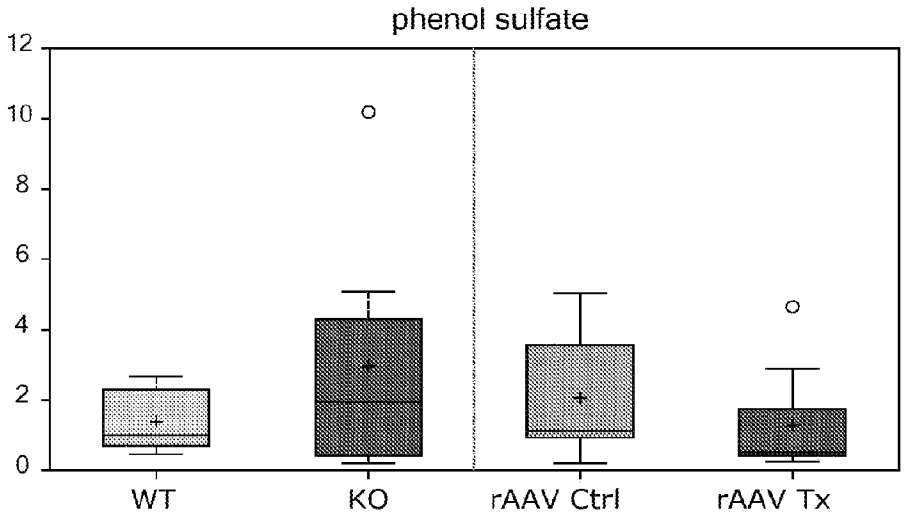
phenol sulfate
12
10
8
6
4
2
0
WT
KO
rAAV Ctrl
rAAV Tx

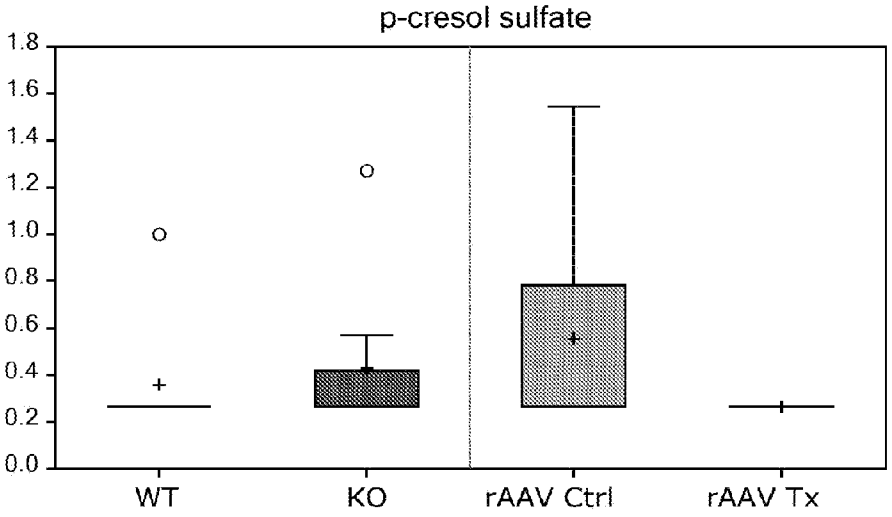
p-cresol sulfate
1.8
1.6
1.4
1.2
1.0
0.8
0.6
0.4
0.2
0.0
WT
KO
rAAV Ctrl
rAAV Tx

FIG. 57 cont.

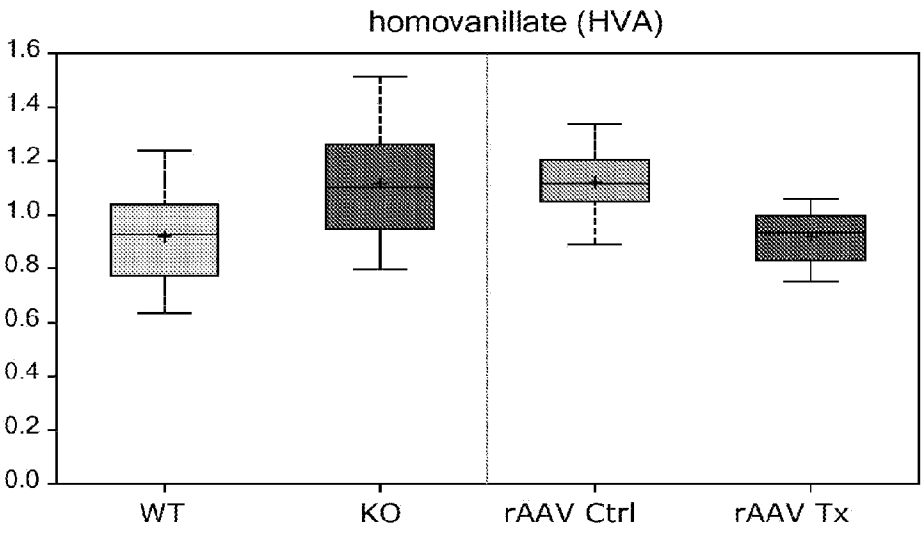
homovanillate (HVA)
1.6
1.4
1.2
1.0
0.8
0.6
0.4
0.2
0.0
WT
KO
rAAV Ctrl
rAAV Tx

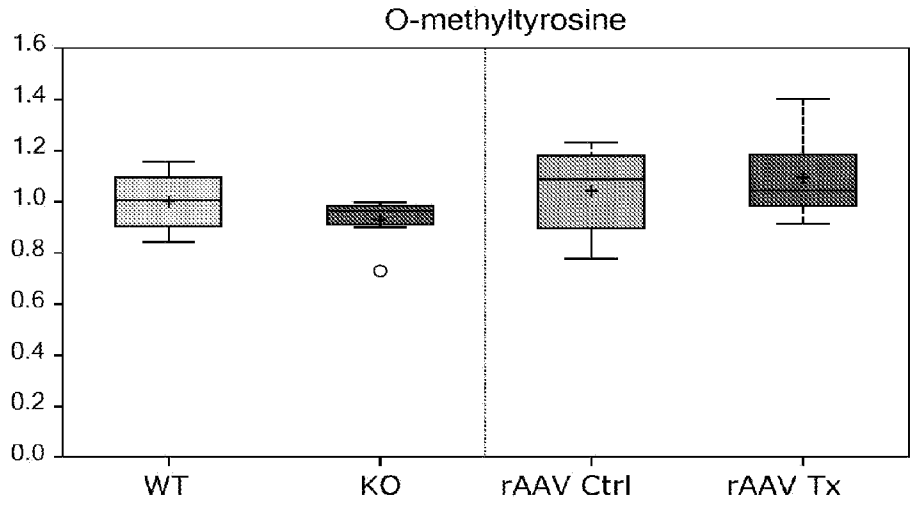
O-methyltyrosine
1.6
1.4
1.2
1.0
0.8
0.6
0.4
0.2
0.0
WT
KO
rAAV Ctrl
rAAV Tx

FIG. 57 cont.

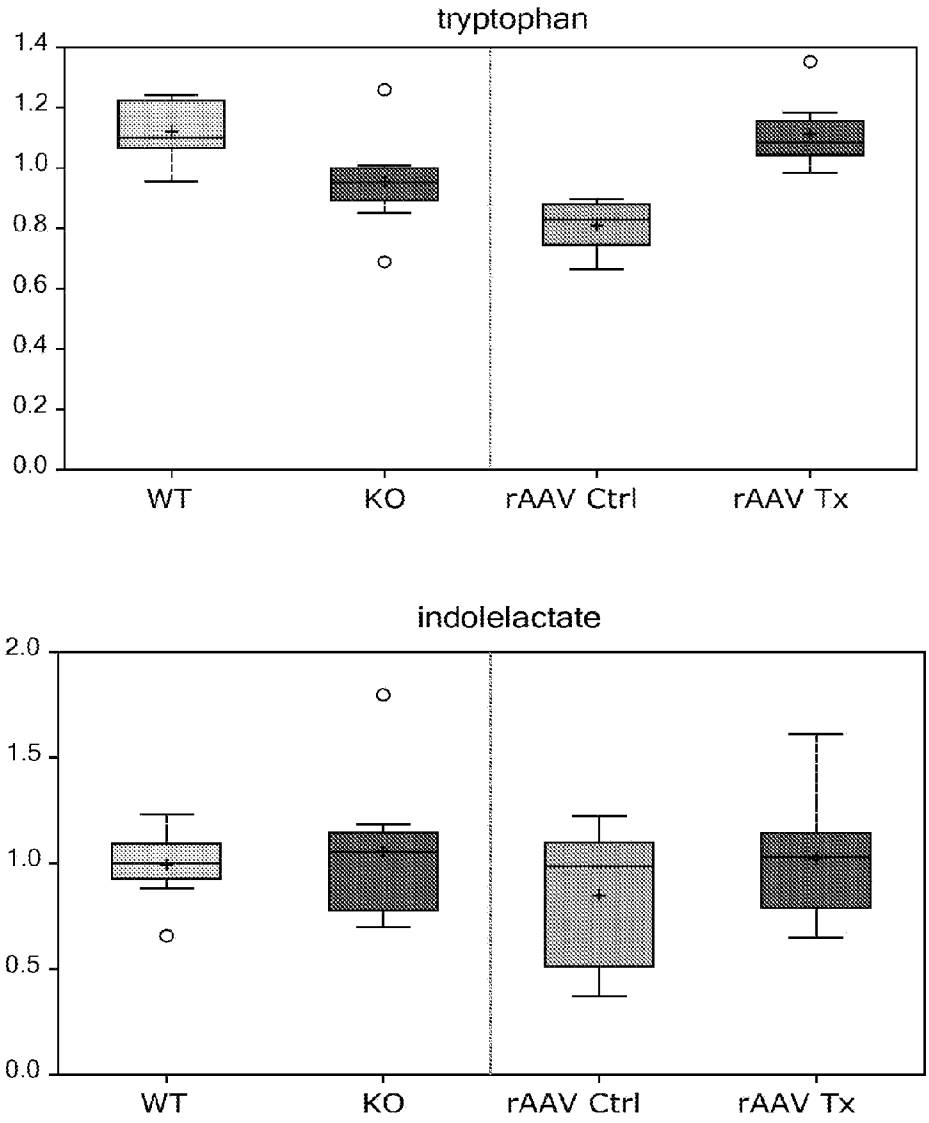
tryptophan
1.4
1.2
1.0
0.8
0.6
0.4
0.2
0.0
WT
KO
rAAV Ctrl
rAAV Tx
indolelactate
2.0
1.5
1.0
0.5
0.0
WT
KO
rAAV Ctrl
rAAV Tx

FIG. 57 cont.

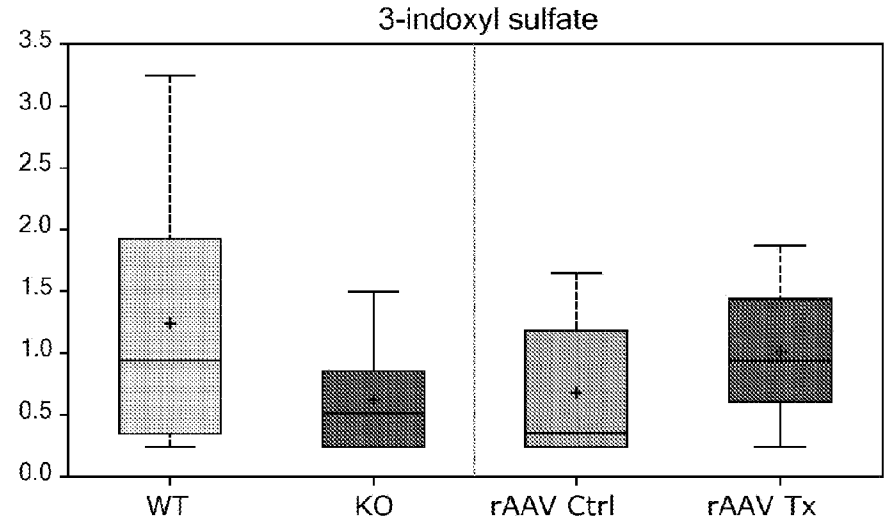
3-indoxyl sulfate
3.5
3.0
2.5
2.0
1.5
1.0
0.5
0.0
WT
KO
rAAV Ctrl
rAAV Tx

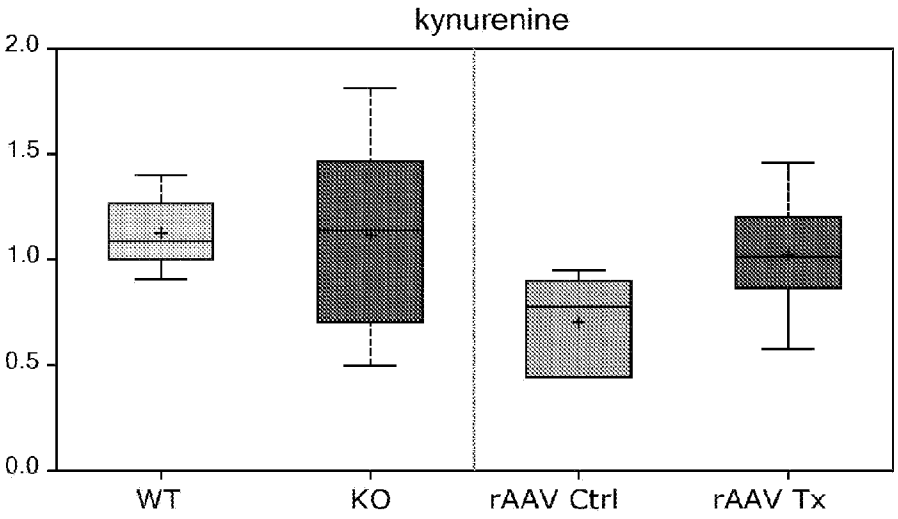
kynurenine
2.0
1.5
1.0
0.5
0.0
WT
KO
rAAV Ctrl
rAAV Tx

FIG. 57 cont.

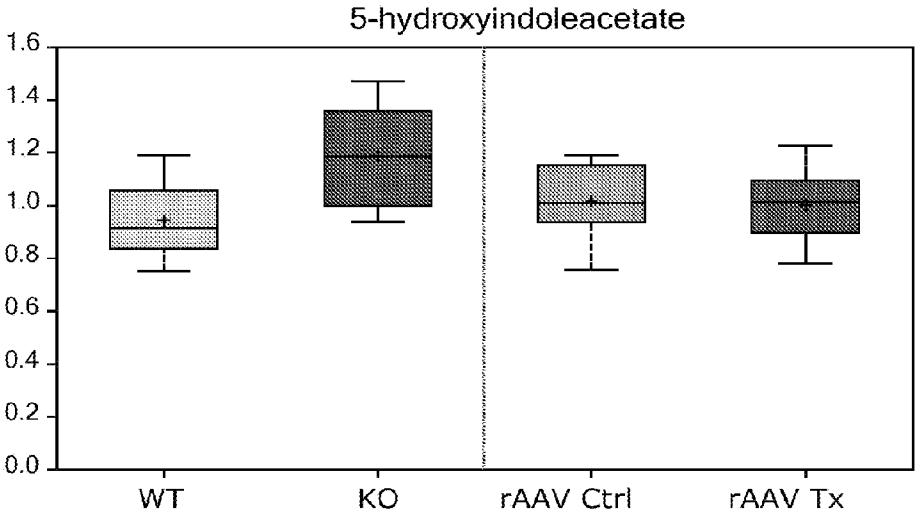
5-hydroxyindoleacetate
1.6
1.4
1.2
1.0
0.8
0.6
0.4
0.2
0.0
WT
KO
rAAV Ctrl
rAAV Tx

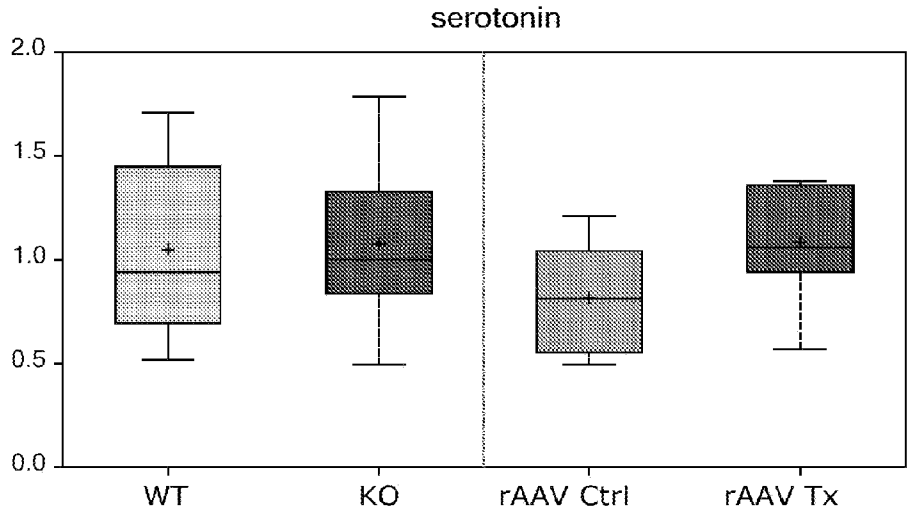
serotonin
2.0
1.5
1.0
0.5
0.0
WT
KO
rAAV Ctrl
rAAV Tx

FIG. 57 cont.

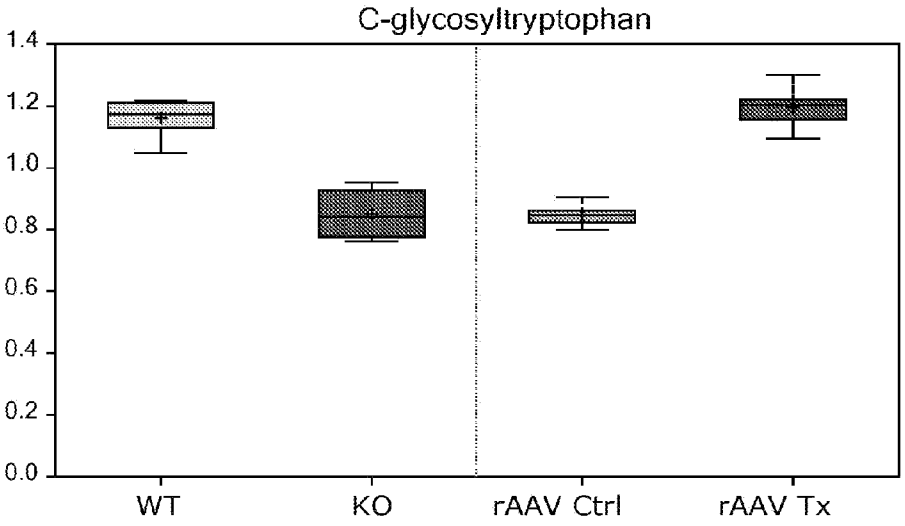
C-glycosyltryptophan
1.4
1.2
1.0
0.8
0.6
0.4
0.2
0.0
WT
KO
rAAV Ctrl
rAAV Tx

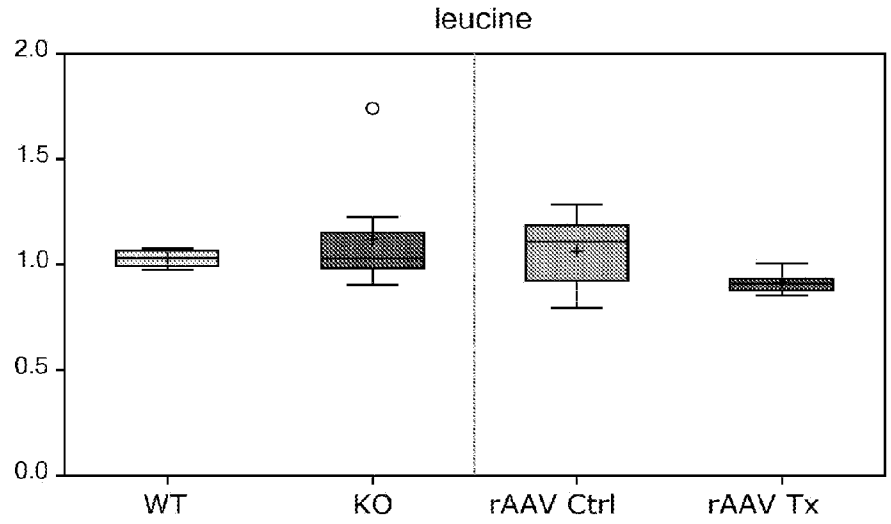
leucine
2.0
1.5
1.0
0.5
0.0
WT
KO
rAAV Ctrl
rAAV Tx

FIG. 57 cont.

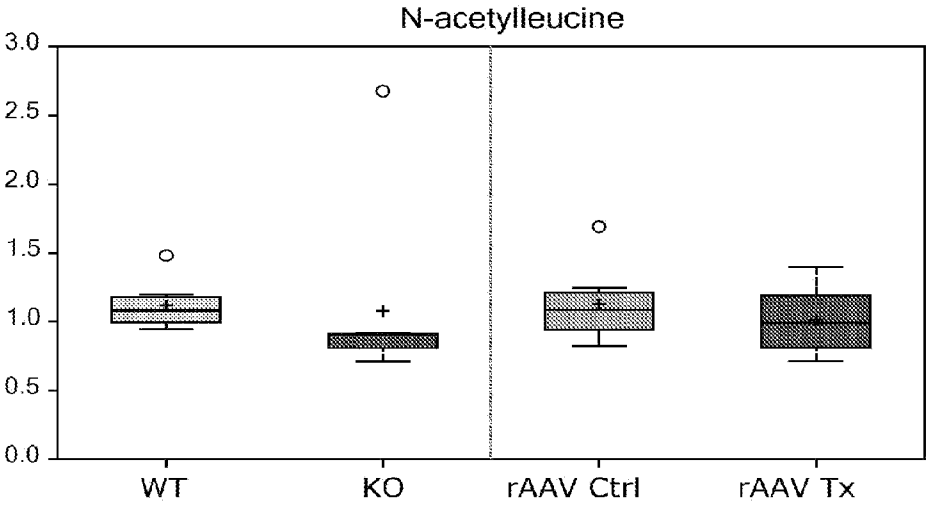
N-acetylleucine
3.0
2.5
2.0
1.5
1.0
0.5
0.0
WT
KO
rAAV Ctrl
rAAV Tx

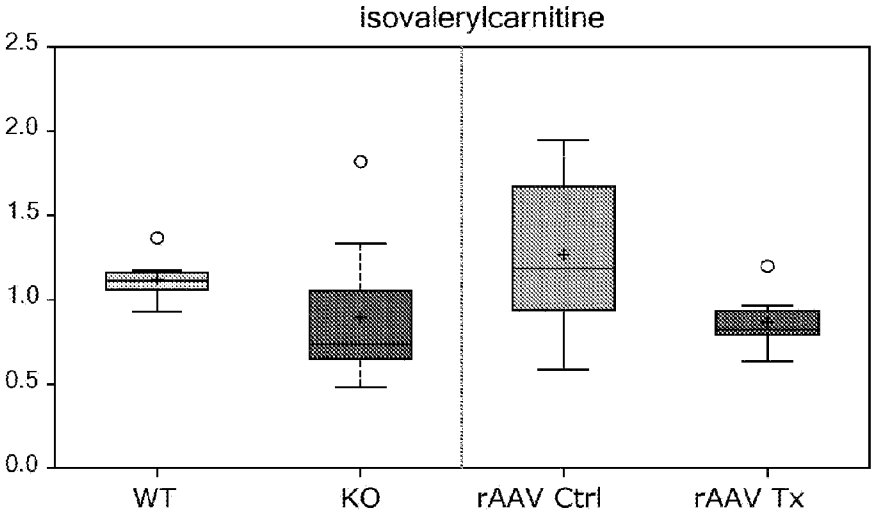
isovalerylcarnitine
2.5
2.0
1.5
1.0
0.5
0.0
WT
KO
rAAV Ctrl
rAAV Tx

FIG. 57 cont.

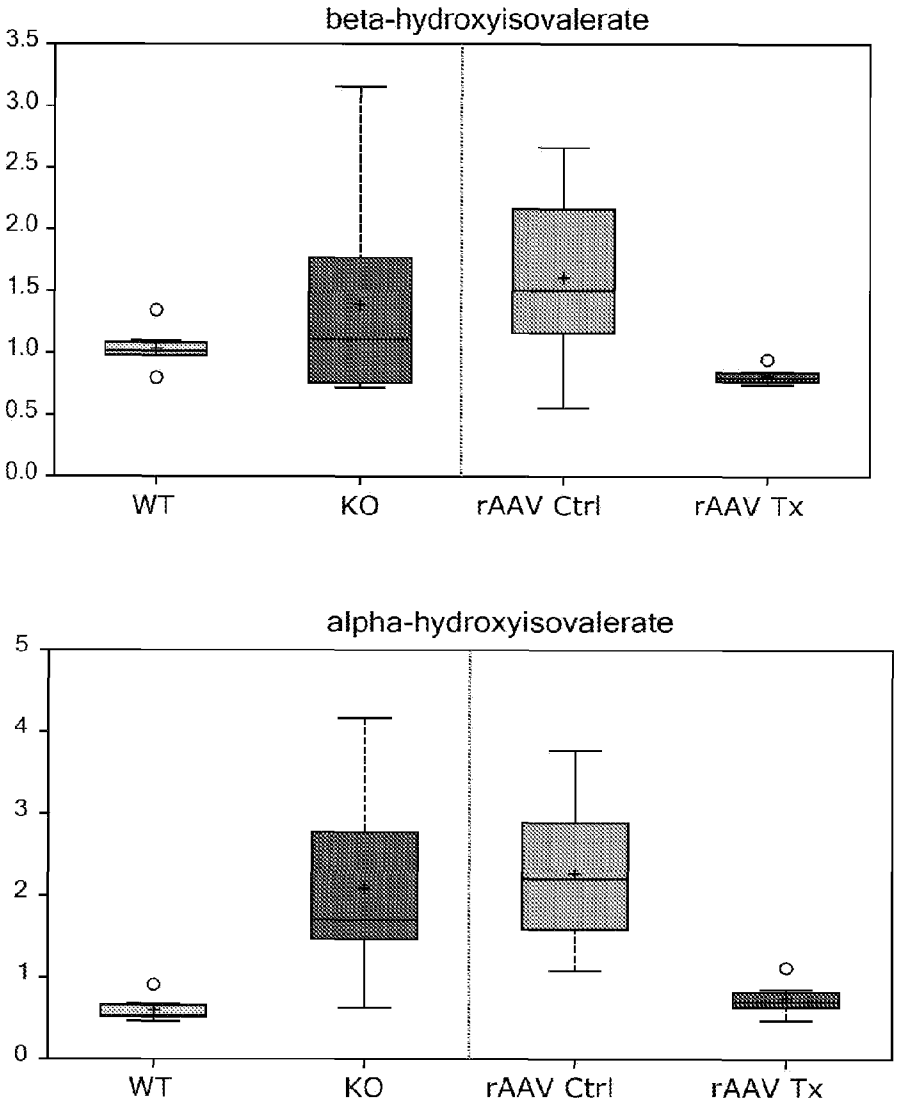
beta-hydroxyisovalerate
3.5
3.0
2.5
2.0
1.5
1.0
0.5
0.0
WT
KO
rAAV Ctrl
rAAV Tx
alpha-hydroxyisovalerate
5
4
3
2
1
0
WT
KO
rAAV Ctrl
rAAV Tx

FIG. 57 cont.

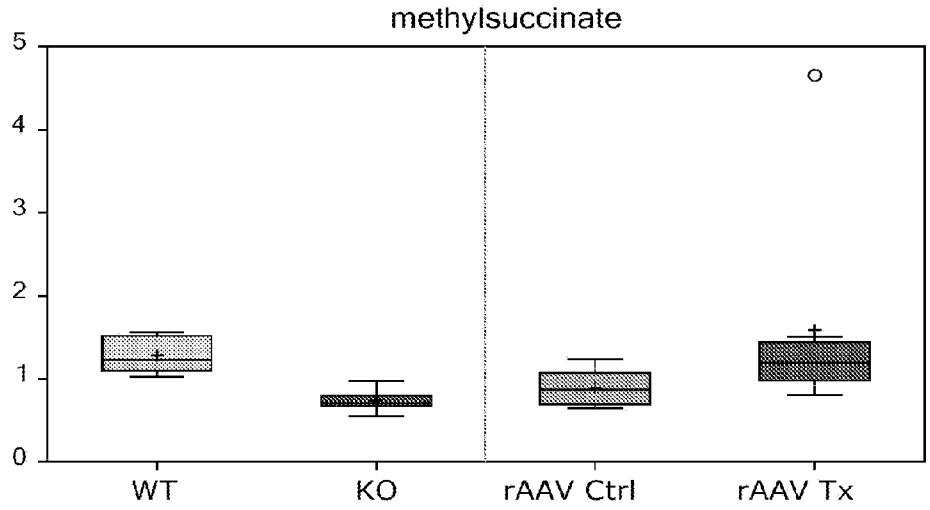
methylsuccinate
5
4
3
2
1
0
WT
KO
rAAV Ctrl
rAAV Tx

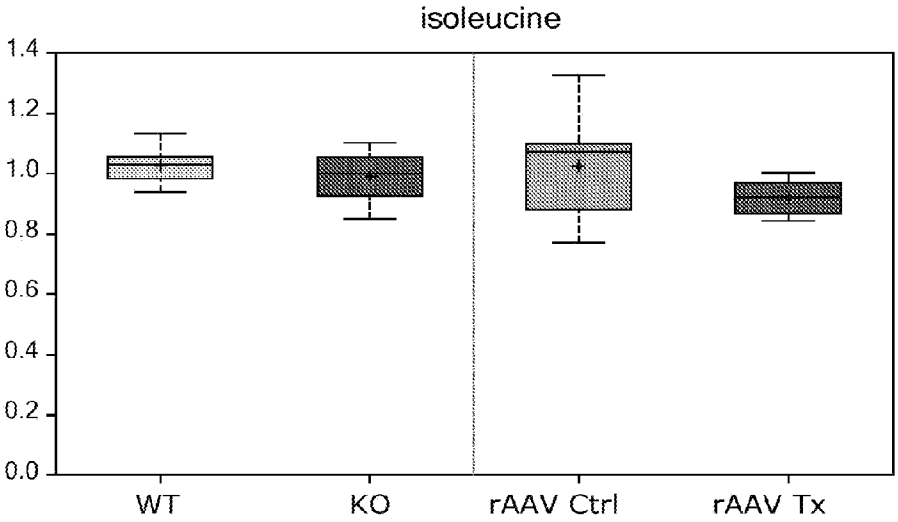
isoleucine
1.4
1.2
1.0
0.8
0.6
0.4
0.2
0.0
WT
KO
rAAV Ctrl
rAAV Tx

FIG. 57 cont.

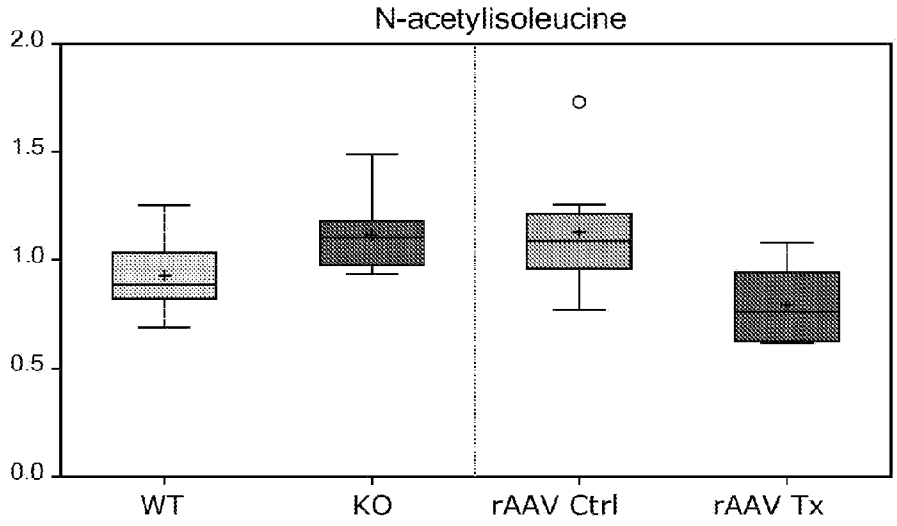
N-acetylisoleucine
2.0
1.5
1.0
0.5
0.0
WT
KO
rAAV Ctrl
rAAV Tx

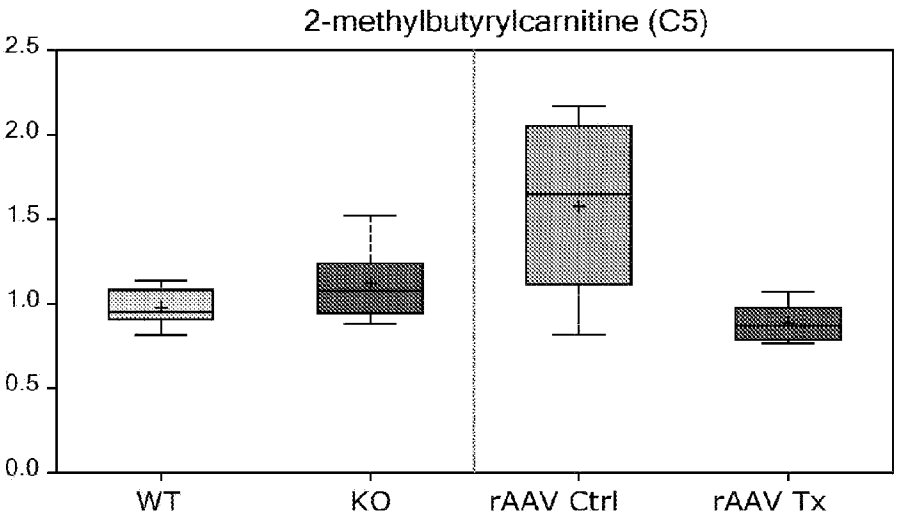
2-methylbutyrylcarnitine (C5)
2.5
2.0
1.5
1.0
0.5
0.0
WT
KO
rAAV Ctrl
rAAV Tx

FIG. 57 cont.

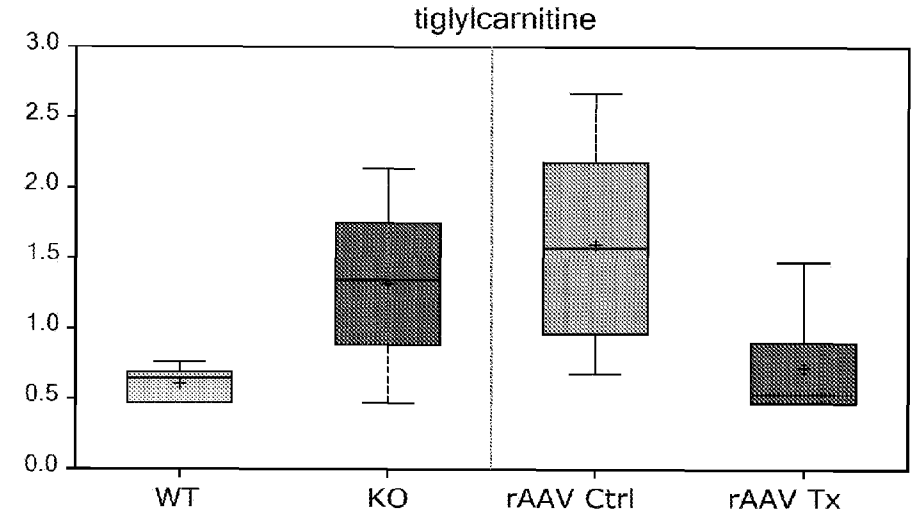
tiglylcarnitine
3.0
2.5
2.0
1.5
1.0
0.5
0.0
WT
KO
rAAV Ctrl
rAAV Tx

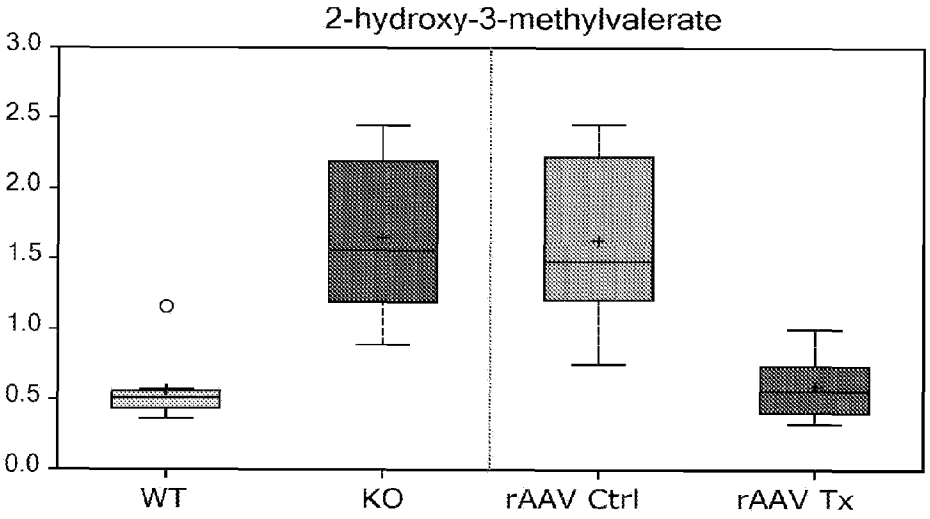
2-hydroxy-3-methylvalerate
3.0
2.5
2.0
1.5
1.0
0.5
0.0
WT
KO
rAAV Ctrl
rAAV Tx

FIG. 57 cont.

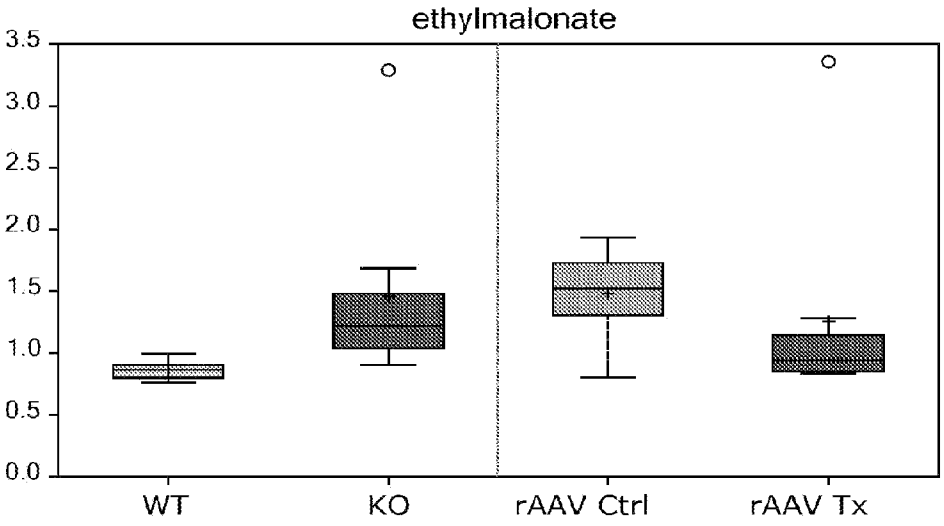
ethylmalonate
3.5
3.0
2.5
2.0
1.5
1.0
0.5
0.0
WT
KO
rAAV Ctrl
rAAV Tx

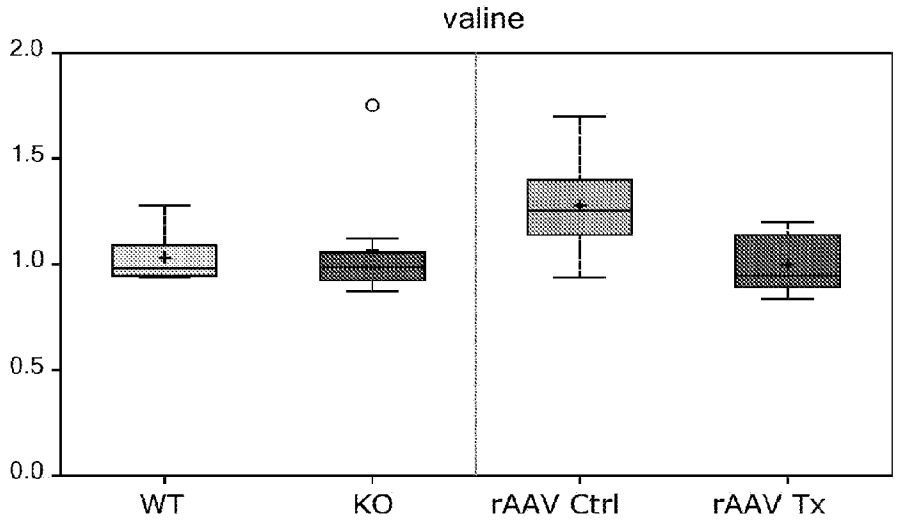
valine
2.0
1.5
1.0
0.5
0.0
WT
KO
rAAV Ctrl
rAAV Tx

FIG. 57 cont.

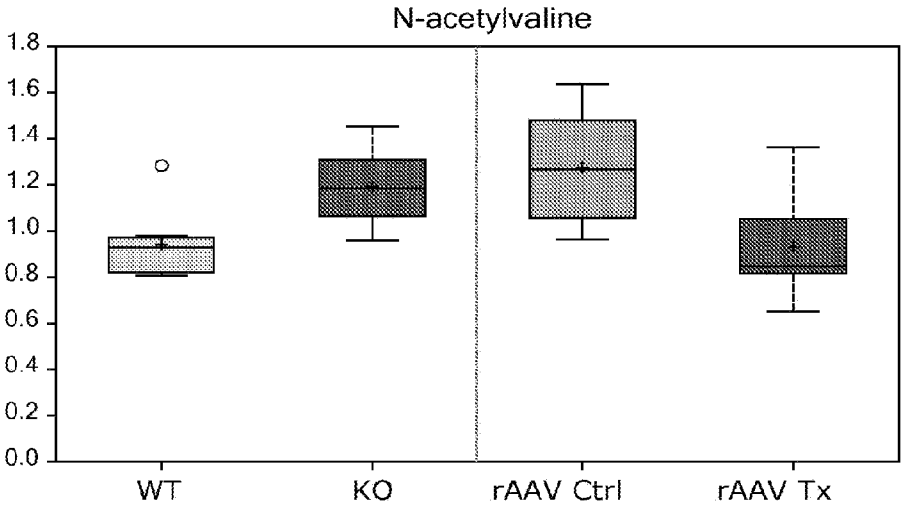
N-acetylvaline
1.8
1.6
1.4
1.2
1.0
0.8
0.6
0.4
0.2
0.0
WT
KO
rAAV Ctrl
rAAV Tx

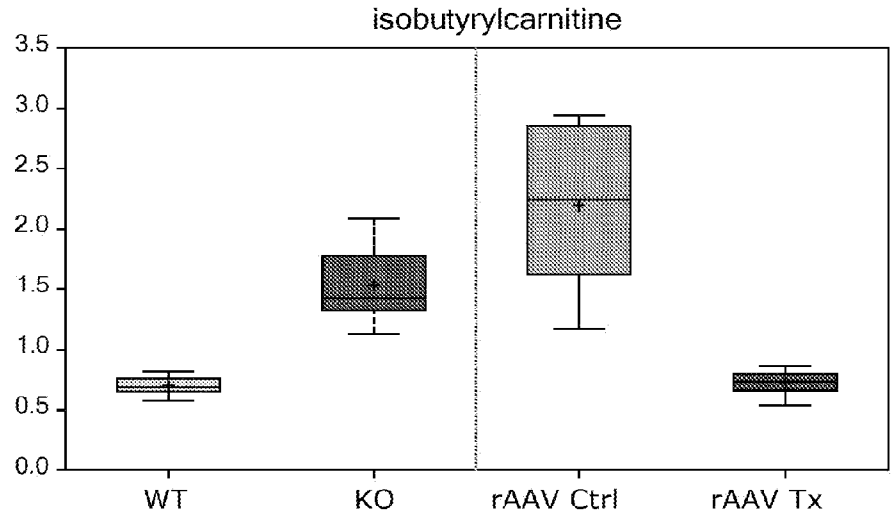
isobutyrylcarnitine
3.5
3.0
2.5
2.0
1.5
1.0
0.5
0.0
WT
KO
rAAV Ctrl
rAAV Tx

FIG. 57 cont.

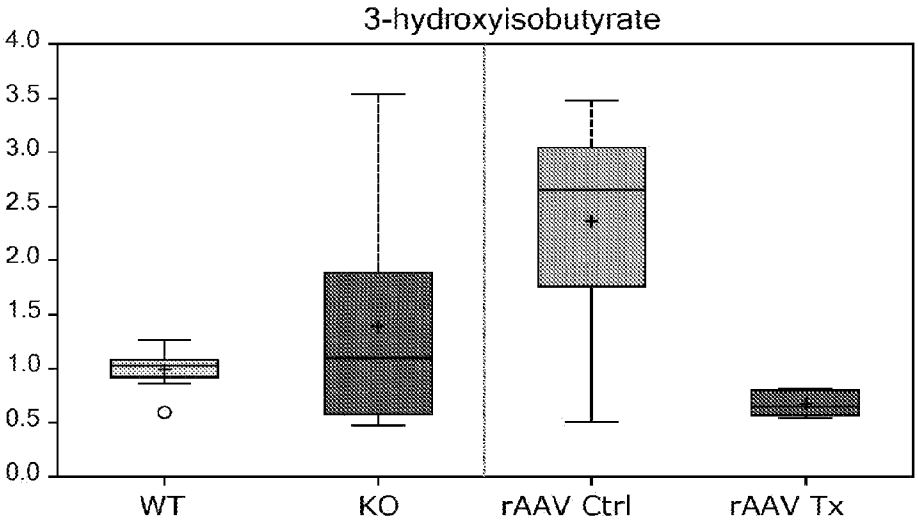
3-hydroxyisobutyrate
4.0
3.5
3.0
2.5
2.0
1.5
1.0
0.5
0.0
WT
KO
rAAV Ctrl
rAAV Tx

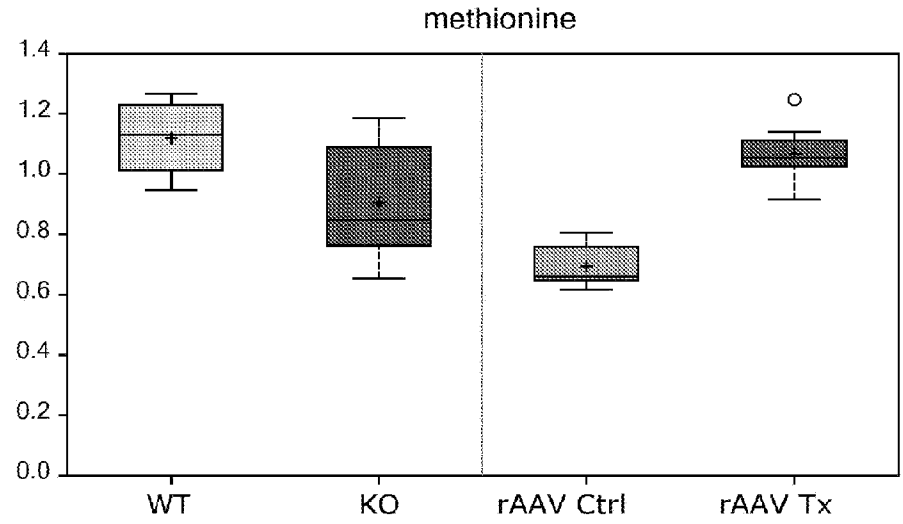
methionine
1.4
1.2
1.0
0.8
0.6
0.4
0.2
0.0
WT
KO
rAAV Ctrl
rAAV Tx

FIG. 57 cont.

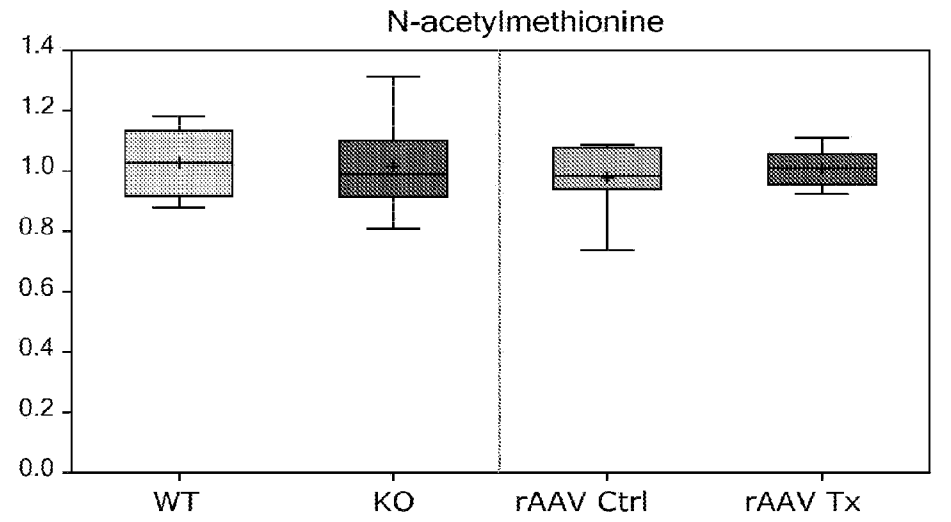
N-acetylmethionine
1.4
1.2
1.0
0.8
0.6
0.4
0.2
0.0
WT
KO
rAAV Ctrl
rAAV Tx

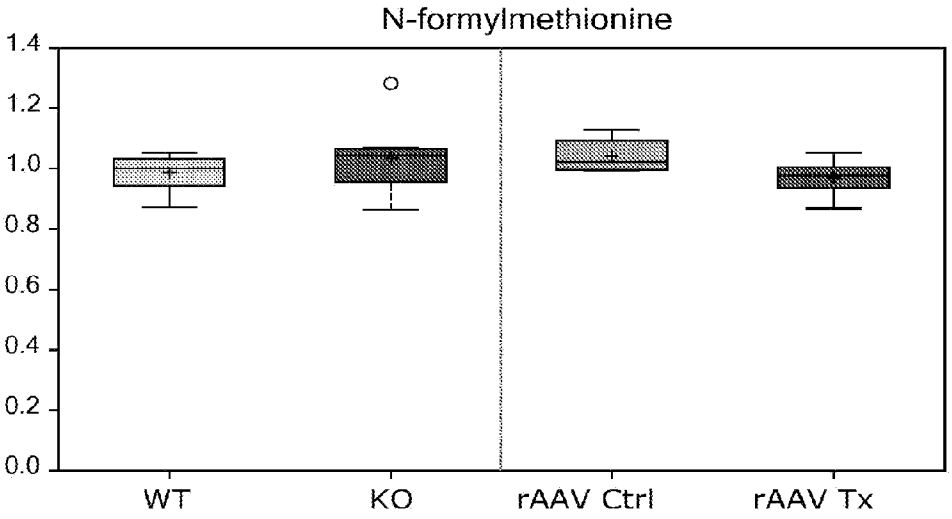
N-formylmethionine
1.4
1.2
1.0
0.8
0.6
0.4
0.2
0.0
WT
KO
rAAV Ctrl
rAAV Tx

FIG. 57 cont.

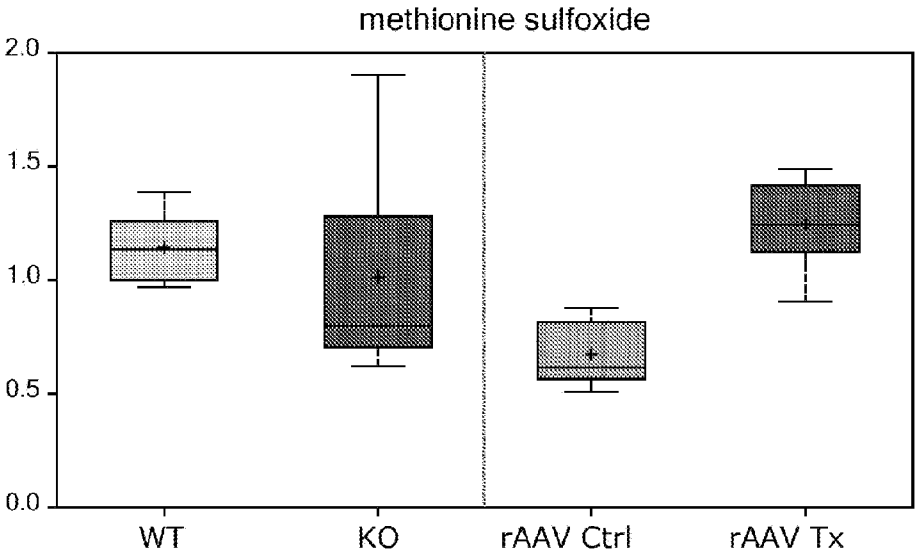
methionine sulfoxide
2.0
1.5
1.0
0.5
0.0
WT
KO
rAAV Ctrl
rAAV Tx

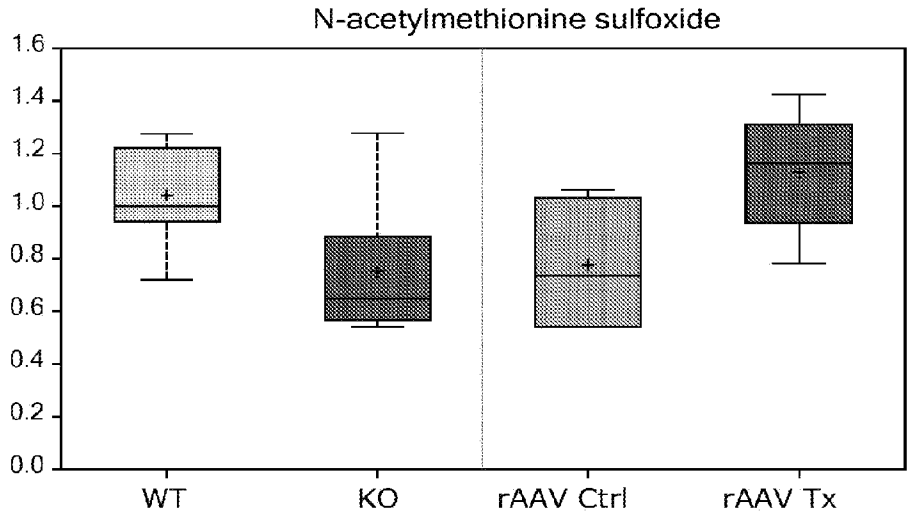
N-acetylmethionine sulfoxide
1.6
1.4
1.2
1.0
0.8
0.6
0.4
0.2
0.0
WT
KO
rAAV Ctrl
rAAV Tx

FIG. 57 cont.

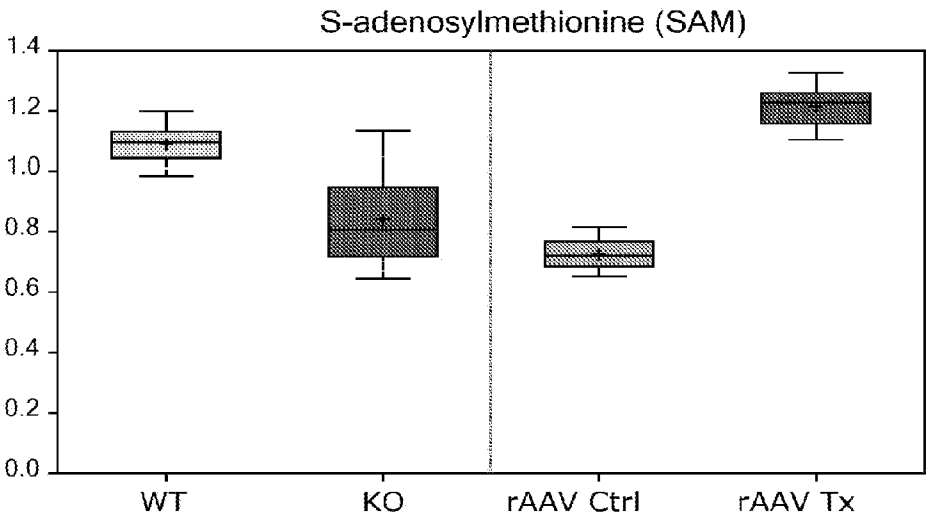
S-adenosylmethionine (SAM)
1.4
1.2
1.0
0.8
0.6
0.4
0.2
0.0
WT
KO
rAAV Ctrl
rAAV Tx

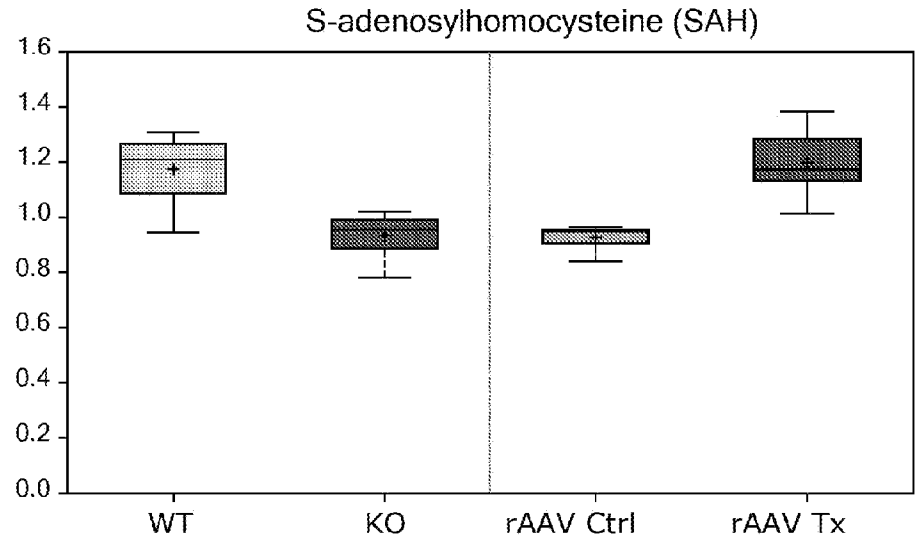
S-adenosylhomocysteine (SAH)
1.6
1.4
1.2
1.0
0.8
0.6
0.4
0.2
0.0
WT
KO
rAAV Ctrl
rAAV Tx

FIG. 57 cont.

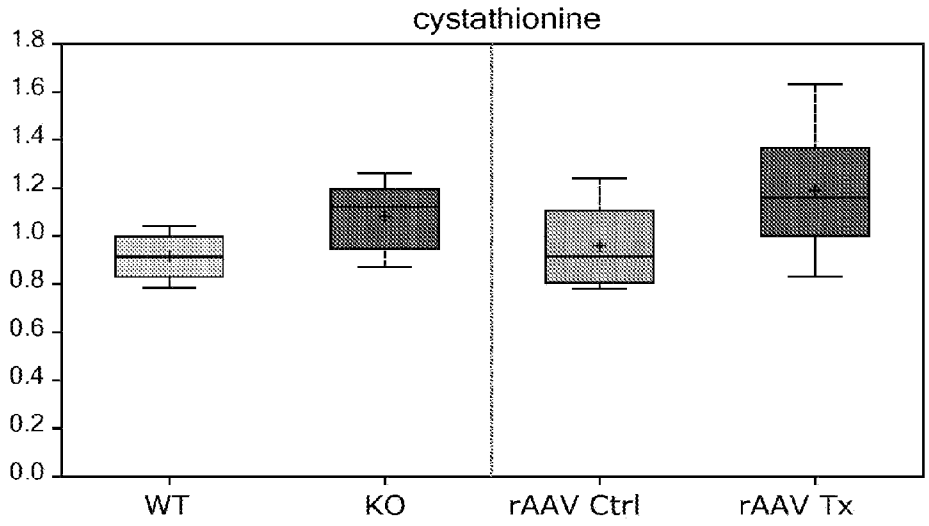
cystathionine
1.8
1.6
1.4
1.2
1.0
0.8
0.6
0.4
0.2
0.0
WT
KO
rAAV Ctrl
rAAV Tx

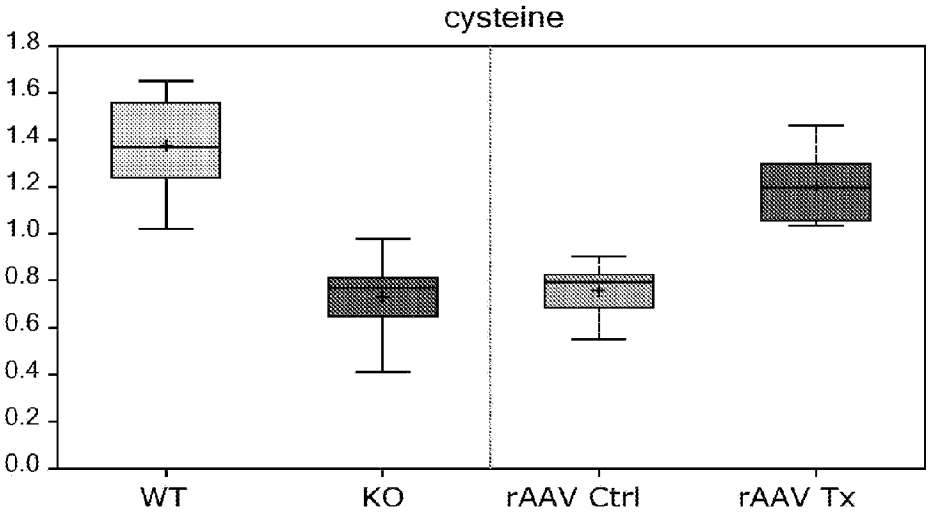
cysteine
1.8
1.6
1.4
1.2
1.0
0.8
0.6
0.4
0.2
0.0
WT
KO
rAAV Ctrl
rAAV Tx

FIG. 57 cont.

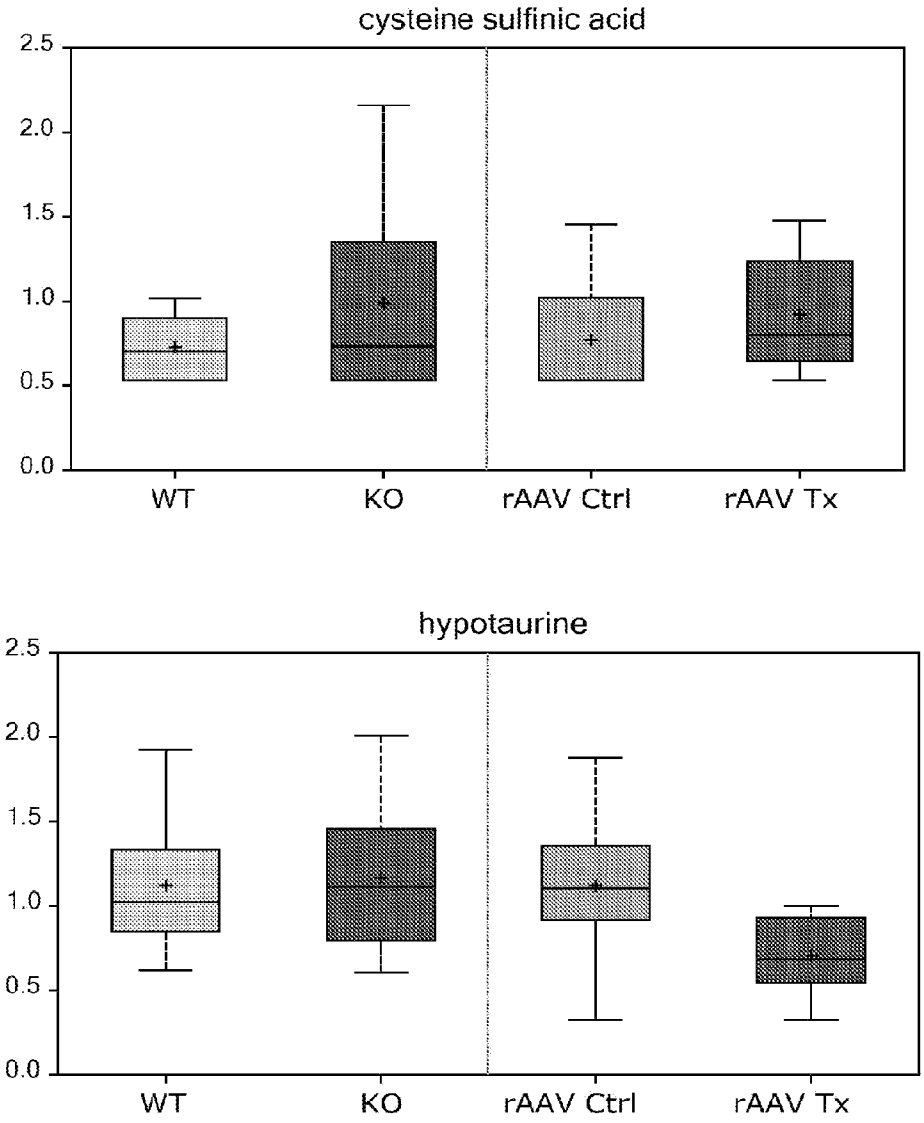
cysteine sulfinic acid
2.5
2.0
1.5
1.0
0.5
0.0
WT
KO
rAAV Ctrl
rAAV Tx
hypotaurine
2.5
2.0
1.5
1.0
0.5
0.0
WT
KO
rAAV Ctrl
rAAV Tx

FIG. 57 cont.

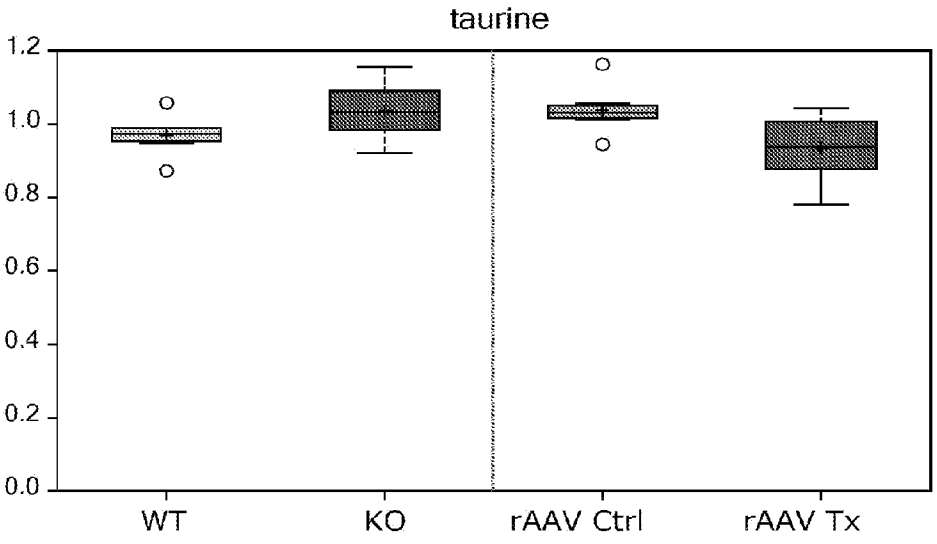
taurine
1.2
1.0
0.8
0.6
0.4
0.2
0.0
WT
KO
rAAV Ctrl
rAAV Tx

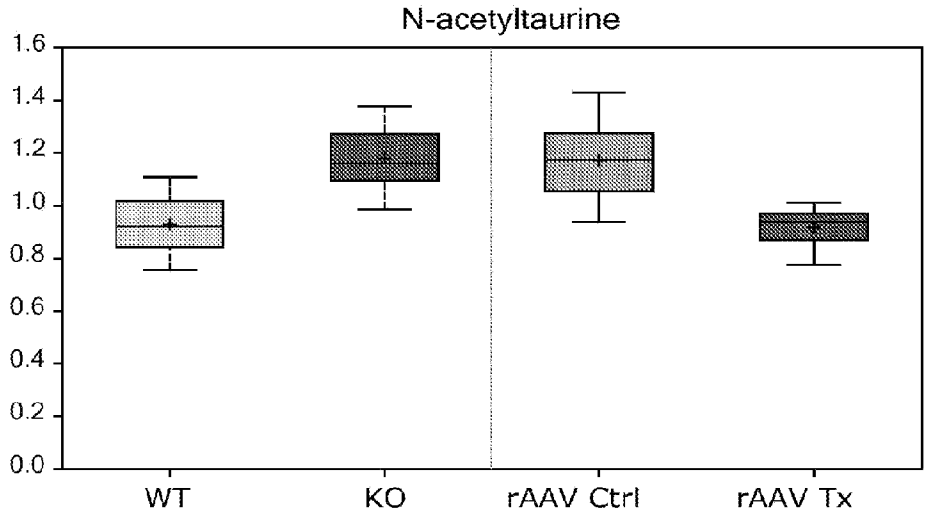
N-acetyltaurine
1.6
1.4
1.2
1.0
0.8
0.6
0.4
0.2
0.0
WT
KO
rAAV Ctrl
rAAV Tx

FIG. 57 cont.

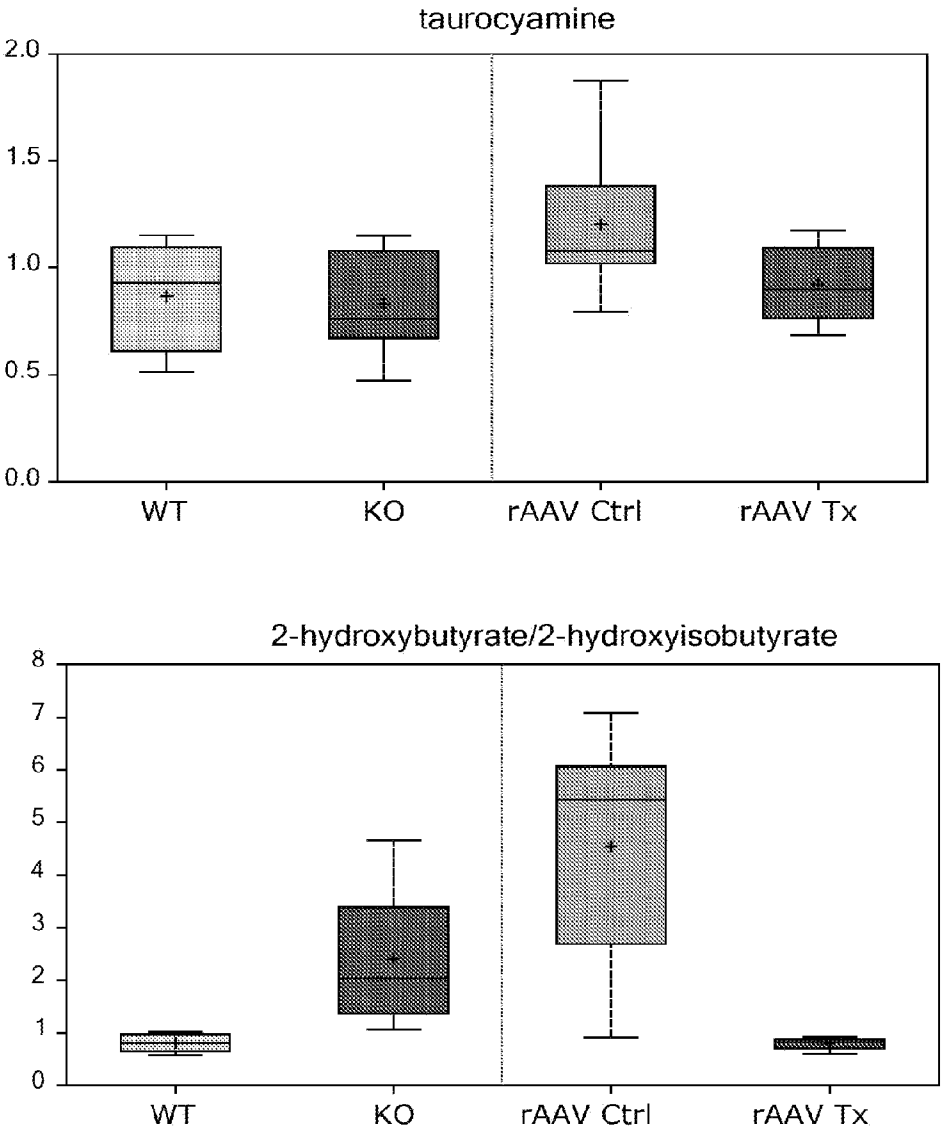
taurocyamine
2.0
1.5
1.0
0.5
0.0
WT
KO
rAAV Ctrl
rAAV Tx
2-hydroxybutyrate/2-hydroxyisobutyrate
8
7
6
5
4
3
2
1
0
WT
KO
rAAV Ctrl
rAAV Tx

FIG. 57 cont.

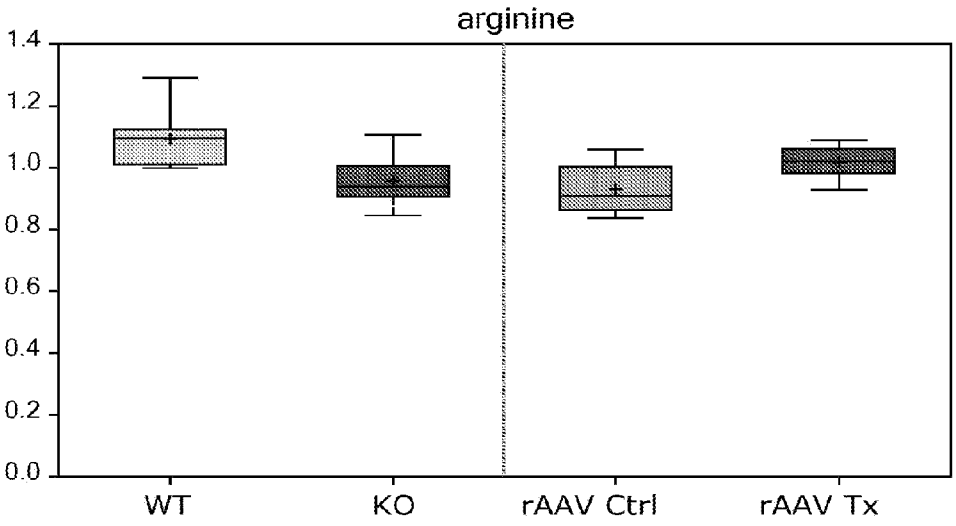
arginine
1.4
1.2
1.0
0.8
0.6
0.4
0.2
0.0
WT
KO
rAAV Ctrl
rAAV Tx

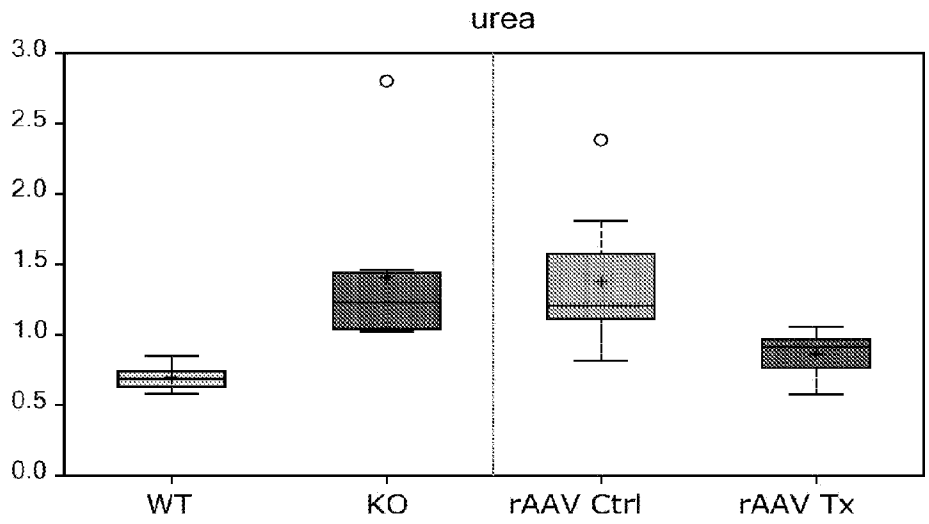
urea
3.0
2.5
2.0
1.5
1.0
0.5
0.0
WT
KO
rAAV Ctrl
rAAV Tx

FIG. 57 cont.

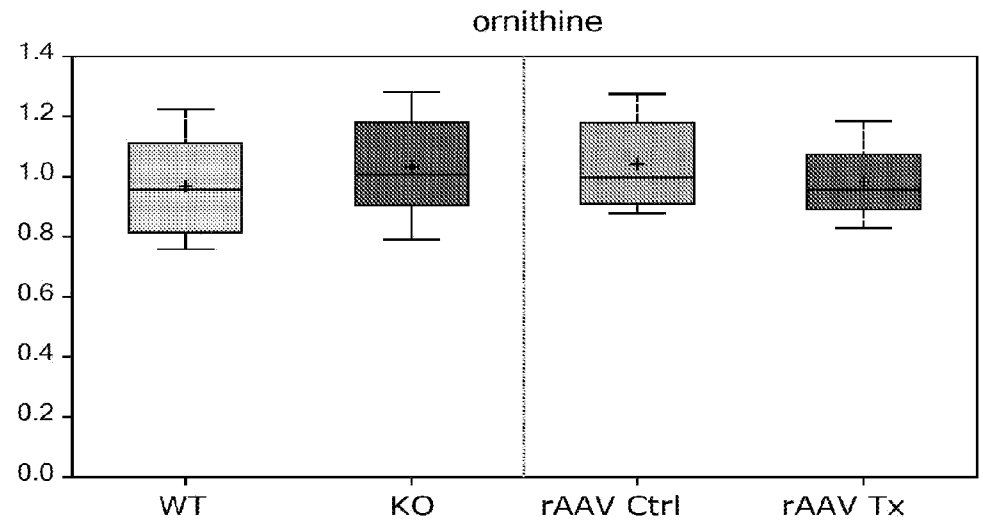
ornithine
1.4
1.2
1.0
0.8
0.6
0.4
0.2
0.0
WT
KO
rAAV Ctrl
rAAV Tx

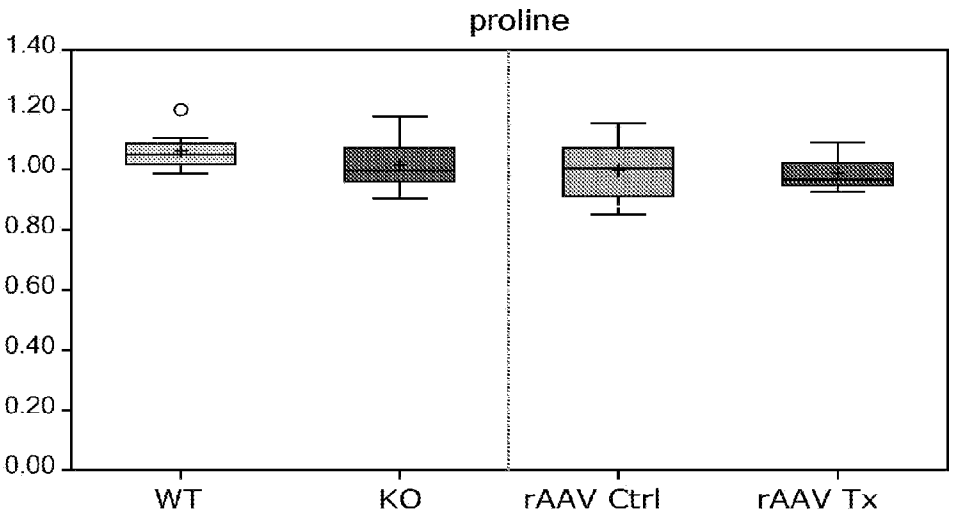
proline
1.40
1.20
1.00
0.80
0.60
0.40
0.20
0.00
WT
KO
rAAV Ctrl
rAAV Tx

FIG. 57 cont.

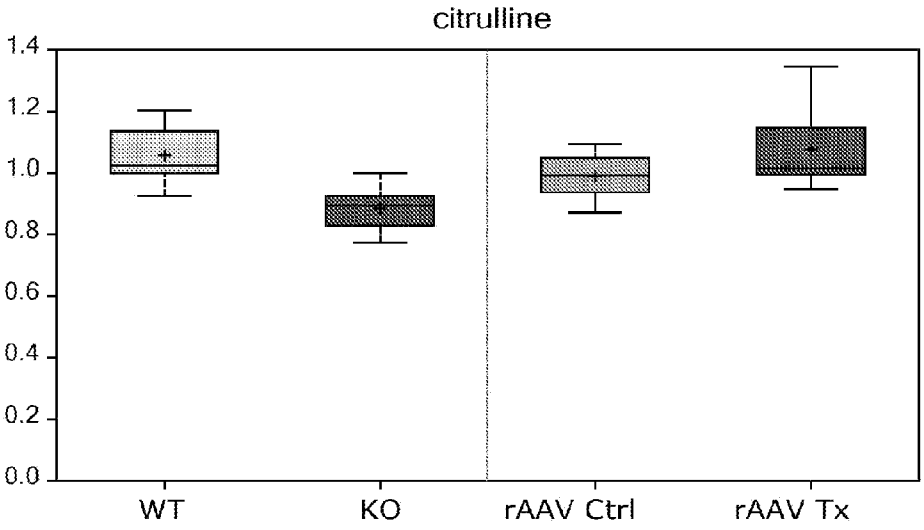
citrulline
1.4
1.2
1.0
0.8
0.6
0.4
0.2
0.0
WT
KO
rAAV Ctrl
rAAV Tx

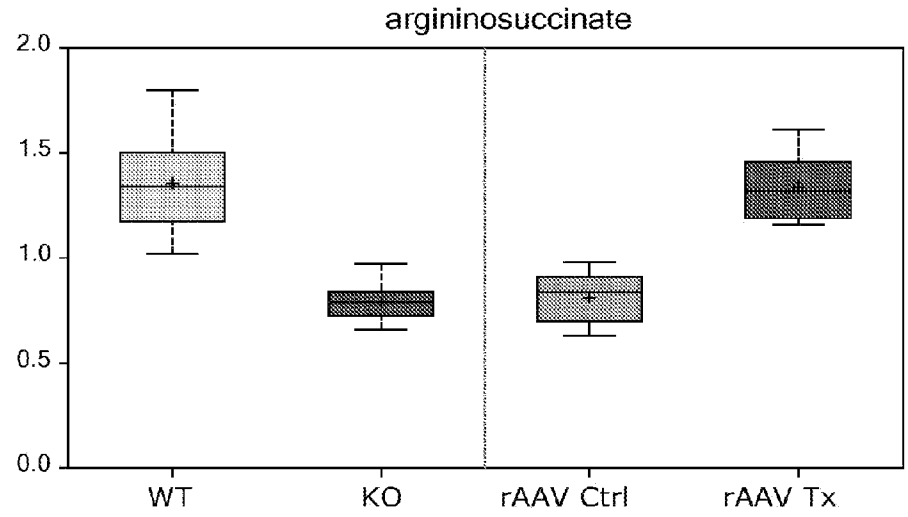
argininosuccinate
2.0
1.5
1.0
0.5
0.0
WT
KO
rAAV Ctrl
rAAV Tx

FIG. 57 cont.

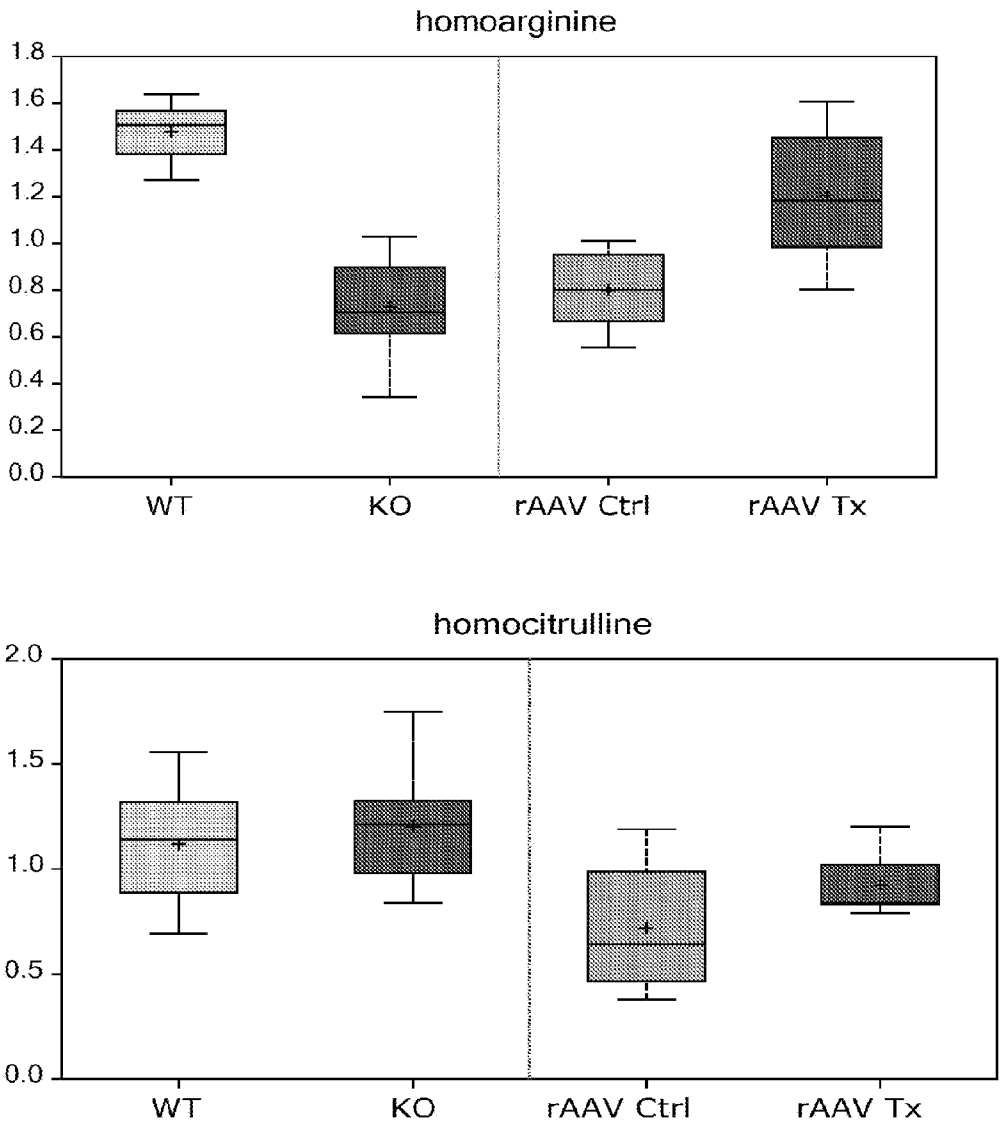
homoarginine
1.8
1.6
1.4
1.2
1.0
0.8
0.6
0.4
0.2
0.0
WT
KO
rAAV Ctrl
rAAV Tx
homocitrulline
2.0
1.5
1.0
0.5
0.0
WT
KO
rAAV Ctrl
rAAV Tx

FIG. 57 cont.

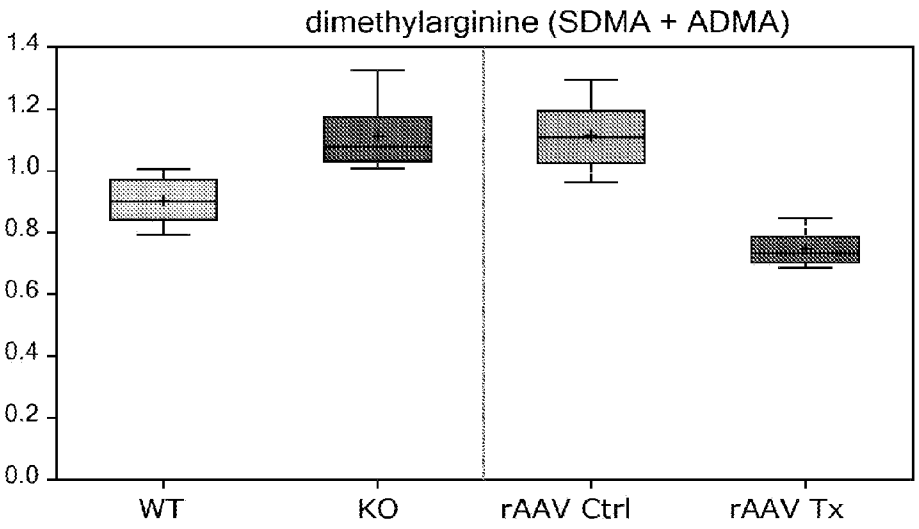
dimethylarginine (SDMA + ADMA)
1.4
1.2
1.0
0.8
0.6
0.4
0.2
0.0
WT
KO
rAAV Ctrl
rAAV Tx

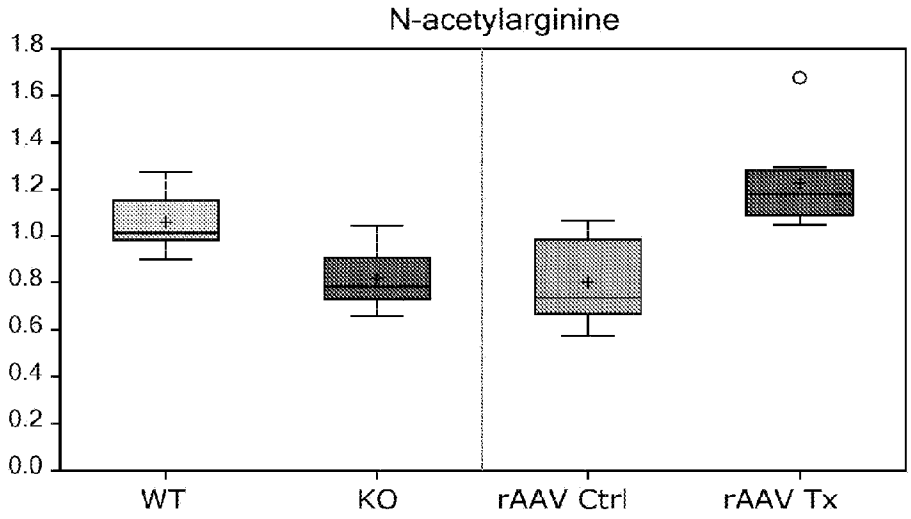
N-acetylarginine
1.8
1.6
1.4
1.2
1.0
0.8
0.6
0.4
0.2
0.0
WT
KO
rAAV Ctrl
rAAV Tx

FIG. 57 cont.

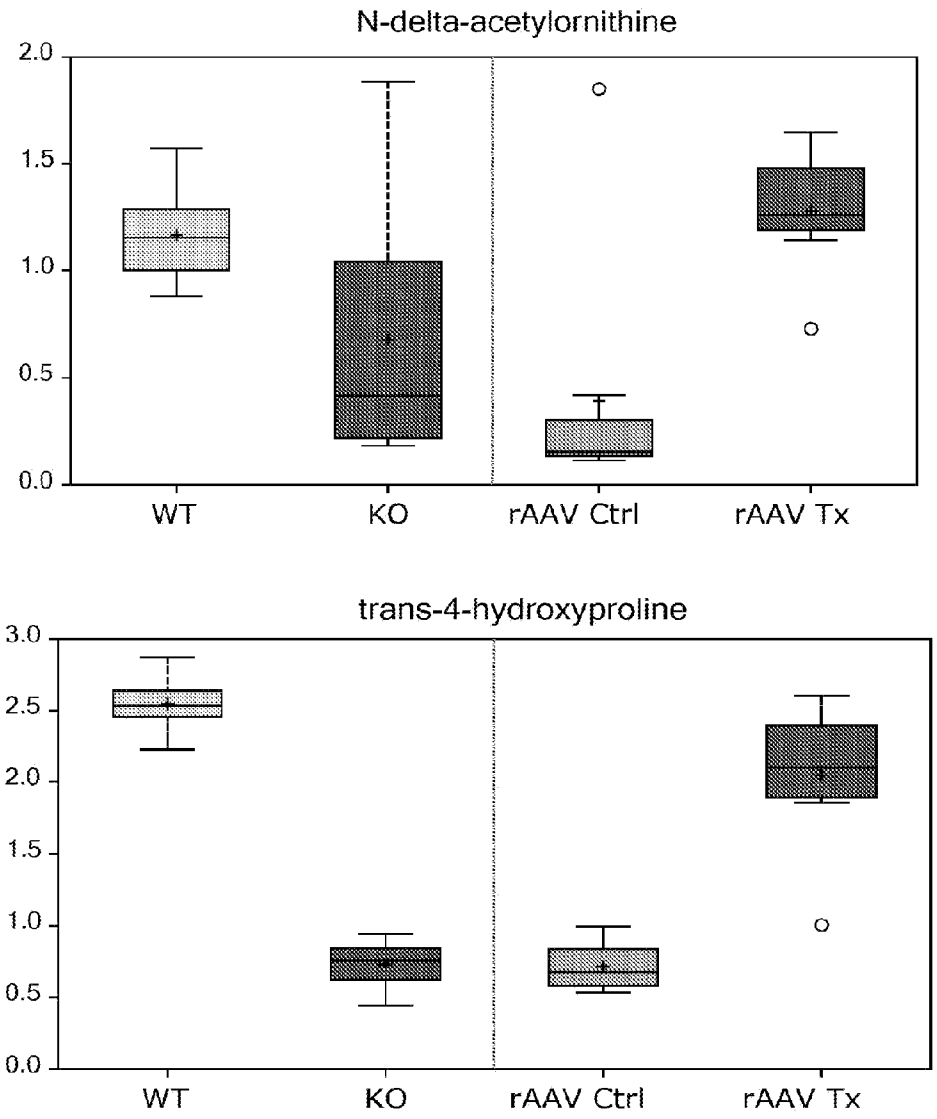
N-delta-acetylornithine
2.0
1.5
1.0
0.5
0.0
WT
KO
rAAV Ctrl
rAAV Tx
trans-4-hydroxyproline
3.0
2.5
2.0
1.5
1.0
0.5
0.0
WT
KO
rAAV Ctrl
rAAV Tx

FIG. 57 cont.

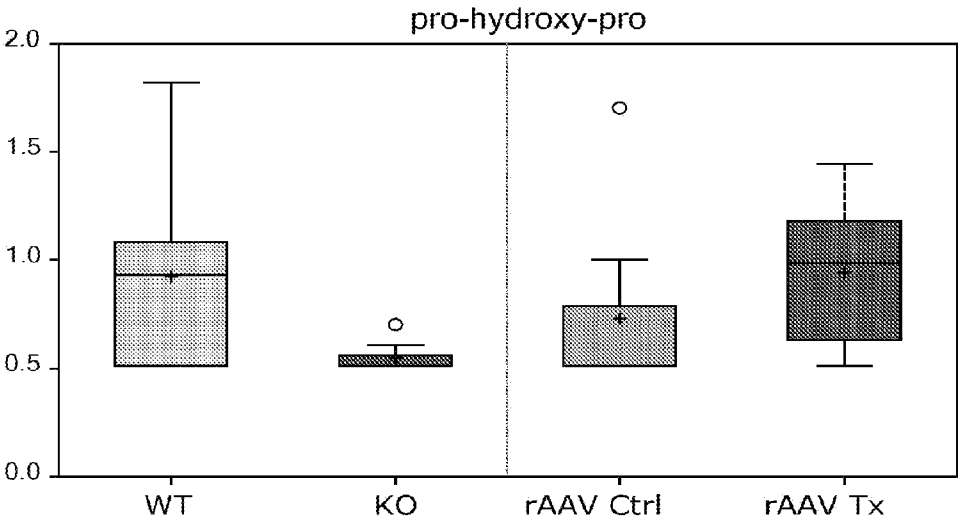
pro-hydroxy-pro
2.0
1.5
1.0
0.5
0.0
WT
KO
rAAV Ctrl
rAAV Tx

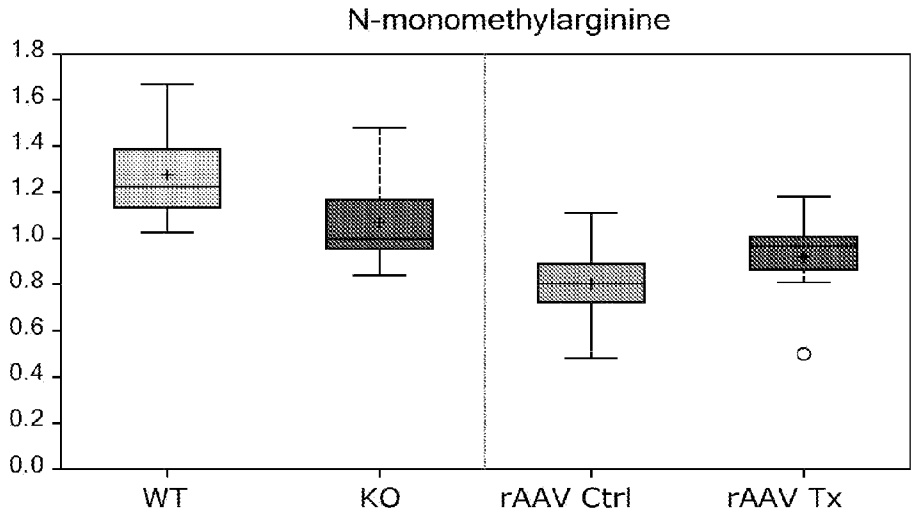
N-monomethylarginine
1.8
1.6
1.4
1.2
1.0
0.8
0.6
0.4
0.2
0.0
WT
KO
rAAV Ctrl
rAAV Tx

FIG. 57 cont.

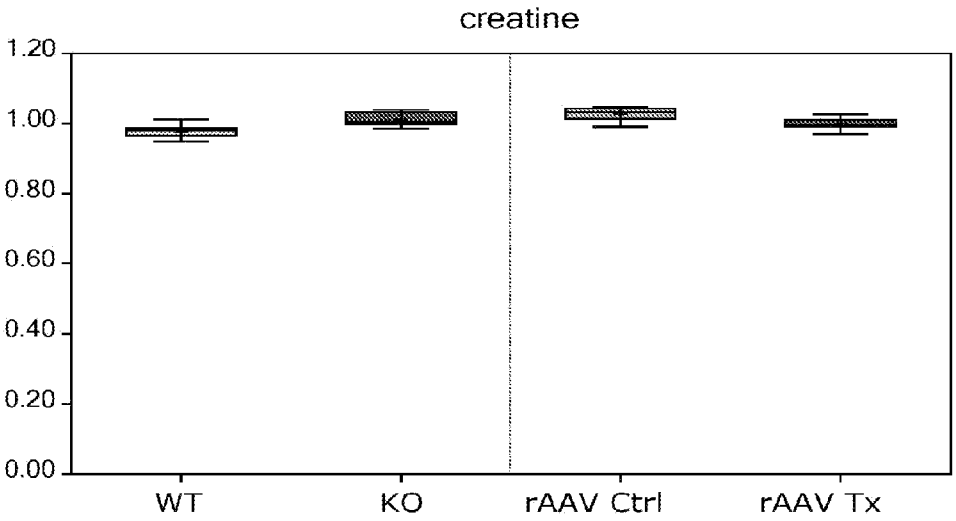
creatine
1.20
1.00
0.80
0.60
0.40
0.20
0.00
WT
KO
rAAV Ctrl
rAAV Tx

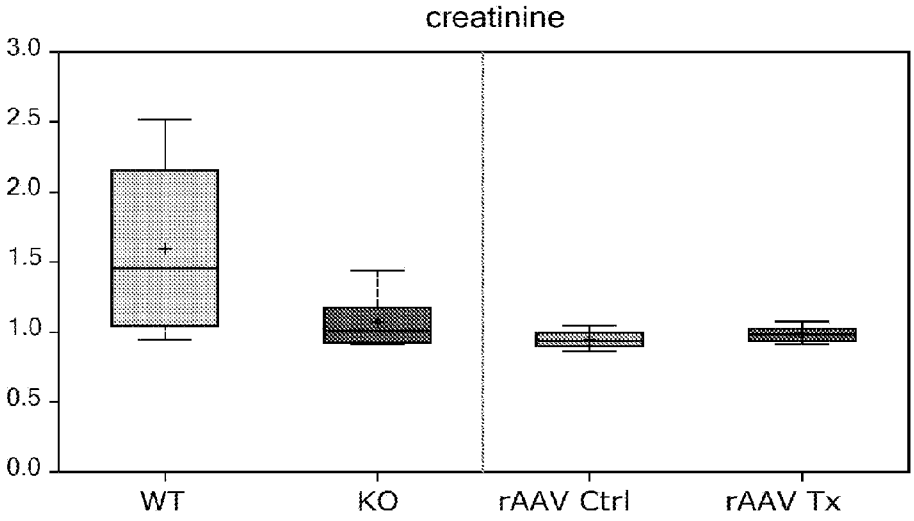
creatinine
3.0
2.5
2.0
1.5
1.0
0.5
0.0
WT
KO
rAAV Ctrl
rAAV Tx

FIG. 57 cont.

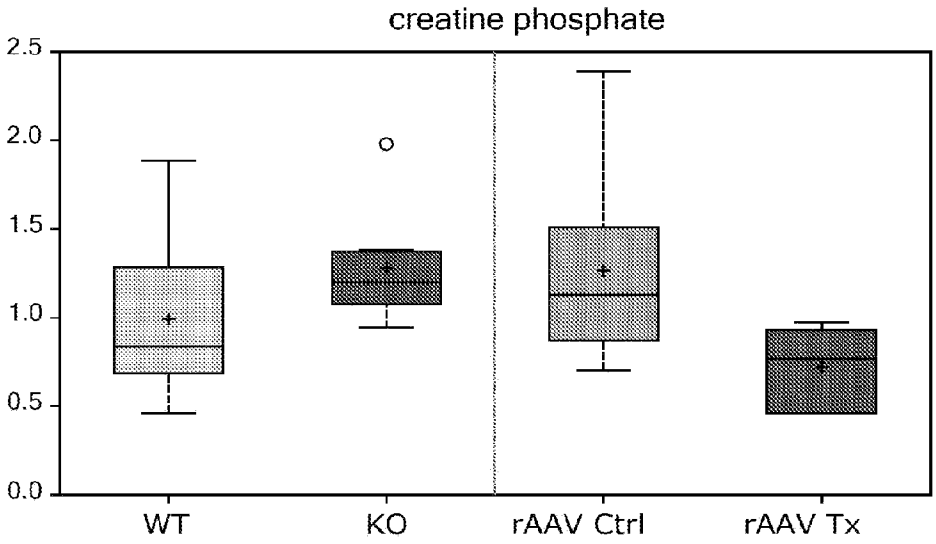
creatine phosphate
2.5
2.0
1.5
1.0
0.5
0.0
WT
KO
rAAV Ctrl
rAAV Tx

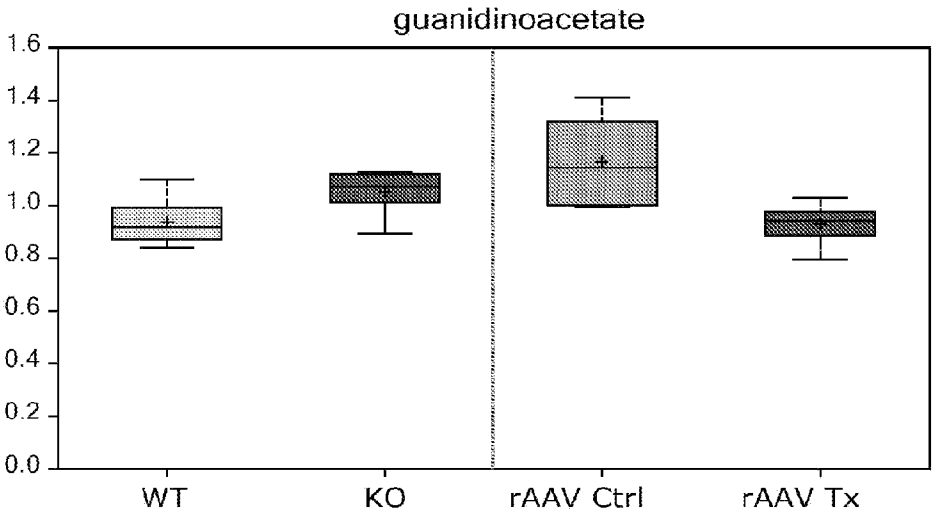
guanidinoacetate
1.6
1.4
1.2
1.0
0.8
0.6
0.4
0.2
0.0
WT
KO
rAAV Ctrl
rAAV Tx

FIG. 57 cont.

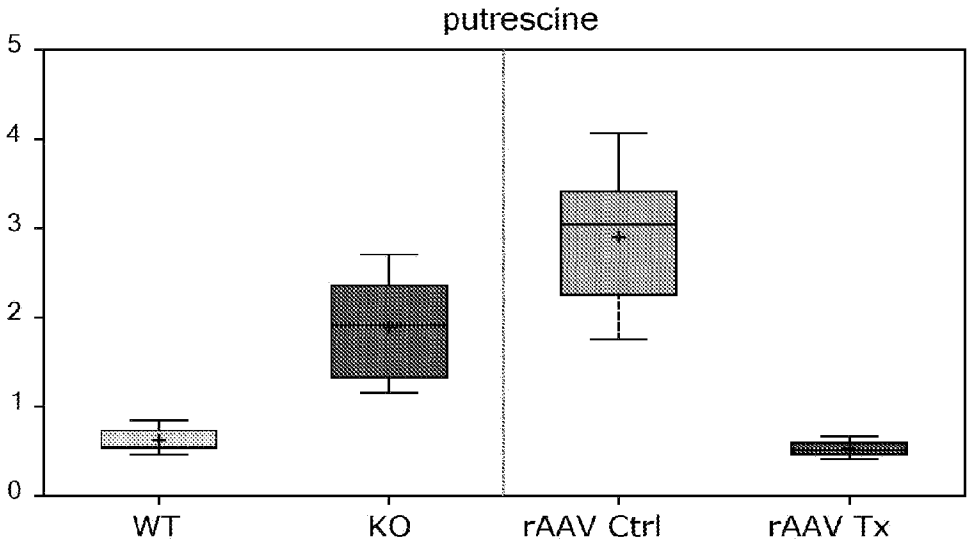
putrescine
5
4
3
2
1
0
WT
KO
rAAV Ctrl
rAAV Tx

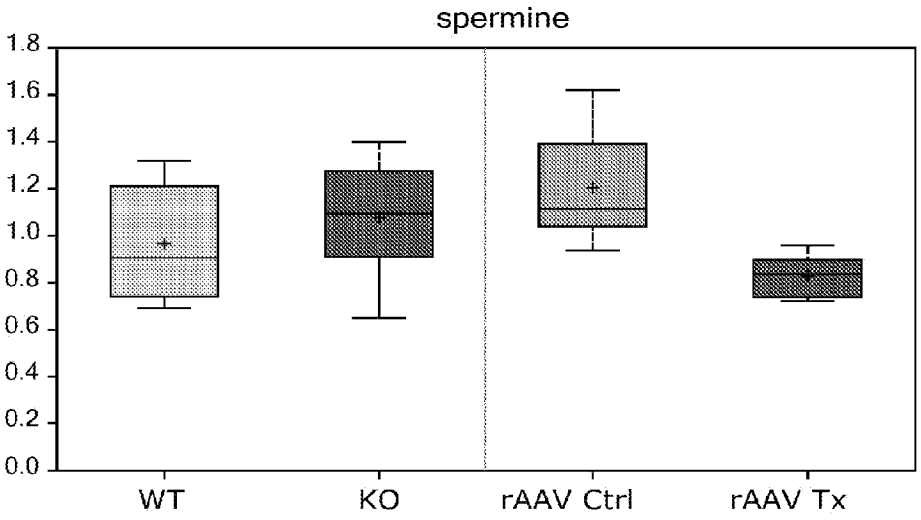
spermine
1.8
1.6
1.4
1.2
1.0
0.8
0.6
0.4
0.2
0.0
WT
KO
rAAV Ctrl
rAAV Tx

FIG. 57 cont.

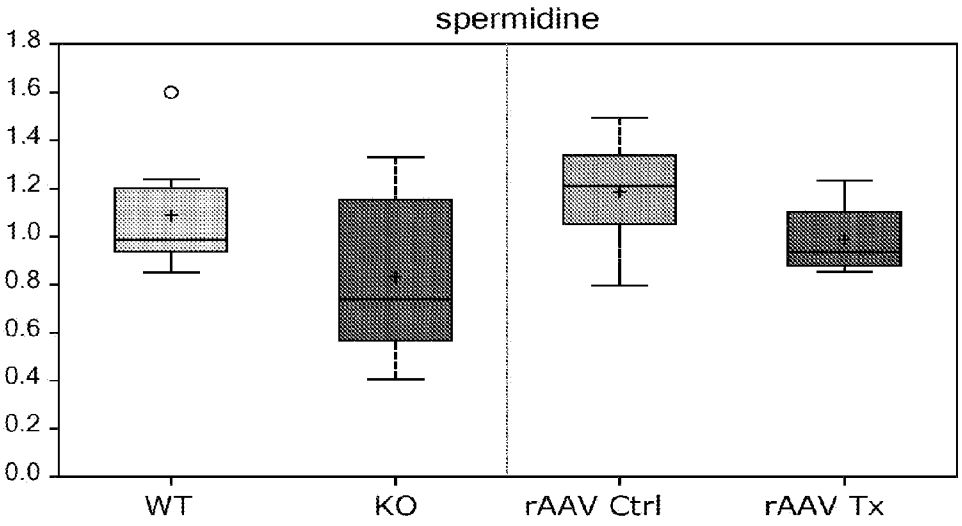
spermidine
1.8
1.6
1.4
1.2
1.0
0.8
0.6
0.4
0.2
0.0
WT
KO
rAAV Ctrl
rAAV Tx

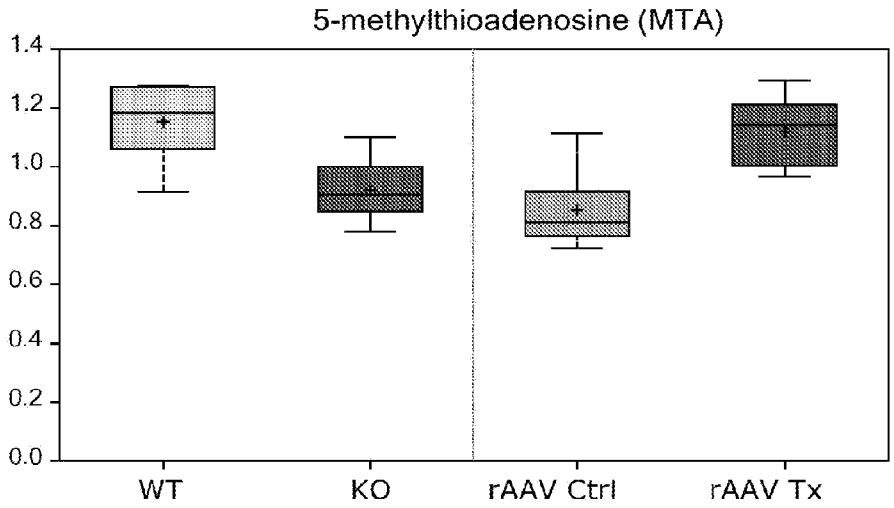
5-methylthioadenosine (MTA)
1.4
1.2
1.0
0.8
0.6
0.4
0.2
0.0
WT
KO
rAAV Ctrl
rAAV Tx

FIG. 57 cont.

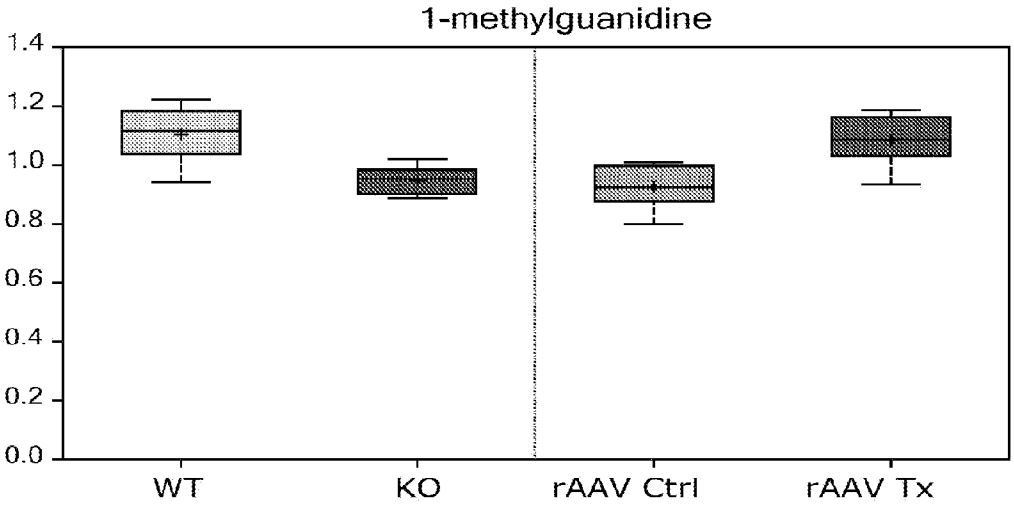
1-methylguanidine
1.4
1.2
1.0
0.8
0.6
0.4
0.2
0.0
WT
KO
rAAV Ctrl
rAAV Tx

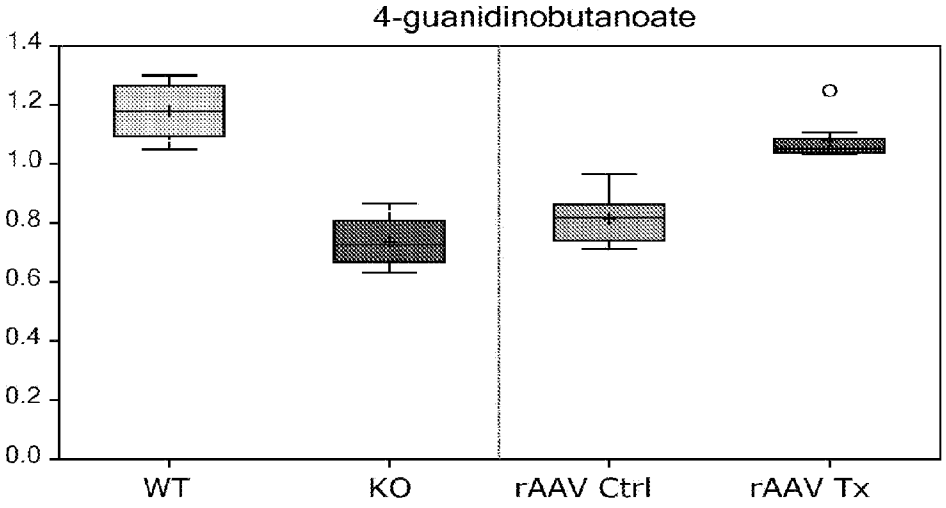
4-guanidinobutanoate
1.4
1.2
1.0
0.8
0.6
0.4
0.2
0.0
WT
KO
rAAV Ctrl
rAAV Tx

FIG. 57 cont.

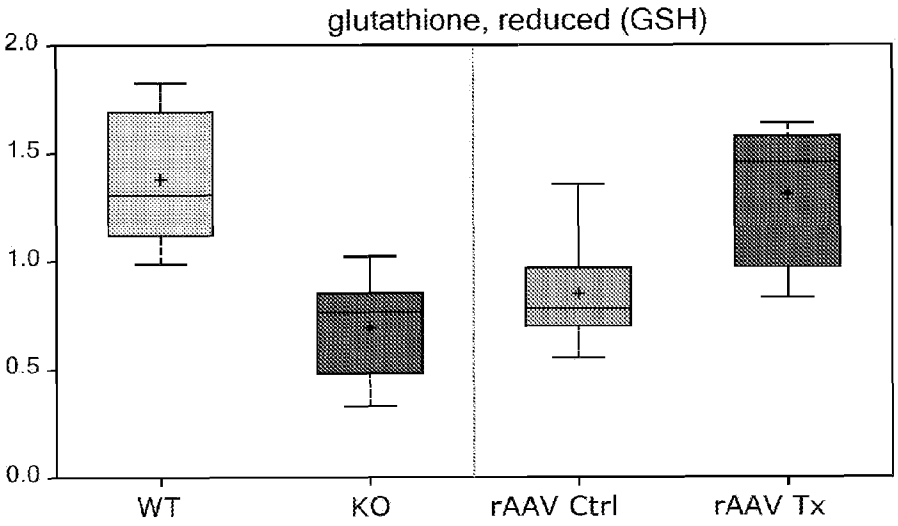
glutathione, reduced (GSH)
2.0
1.5
1.0
0.5
0.0
WT
KO
rAAV Ctrl
rAAV Tx

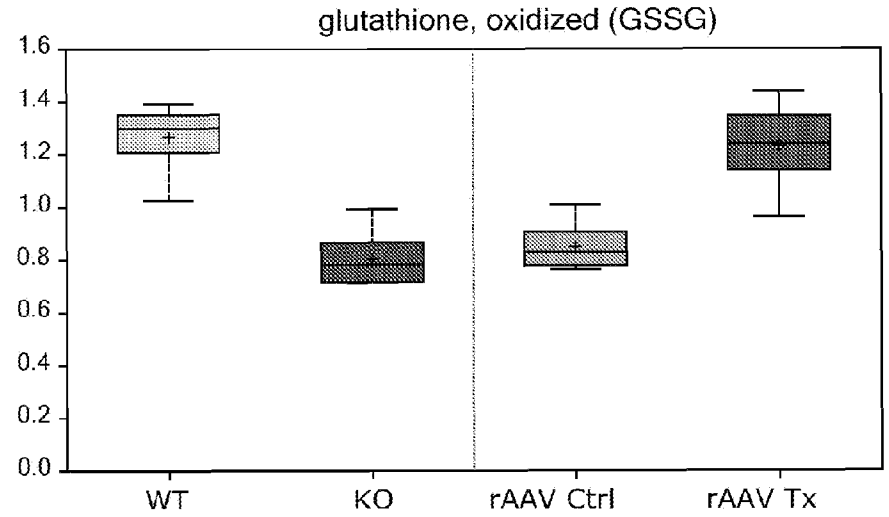
glutathione, oxidized (GSSG)
1.6
1.4
1.2
1.0
0.8
0.6
0.4
0.2
0.0
WT
KO
rAAV Ctrl
rAAV Tx

FIG. 57 cont.

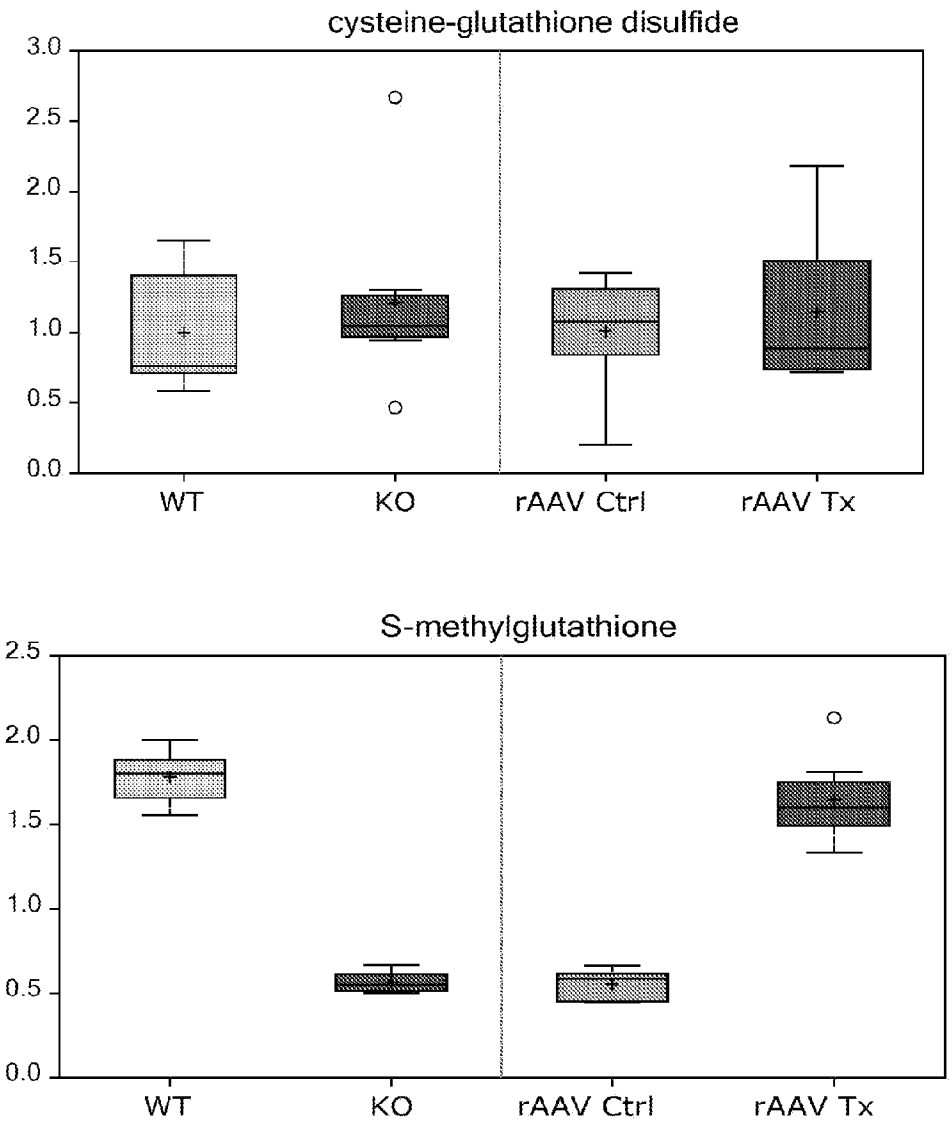
cysteine-glutathione disulfide
3.0
2.5
2.0
1.5
1.0
0.5
0.0
WT
KO
rAAV Ctrl
rAAV Tx
S-methylglutathione
2.5
2.0
1.5
1.0
0.5
0.0
WT
KO
rAAV Ctrl
rAAV Tx

FIG. 57 cont.

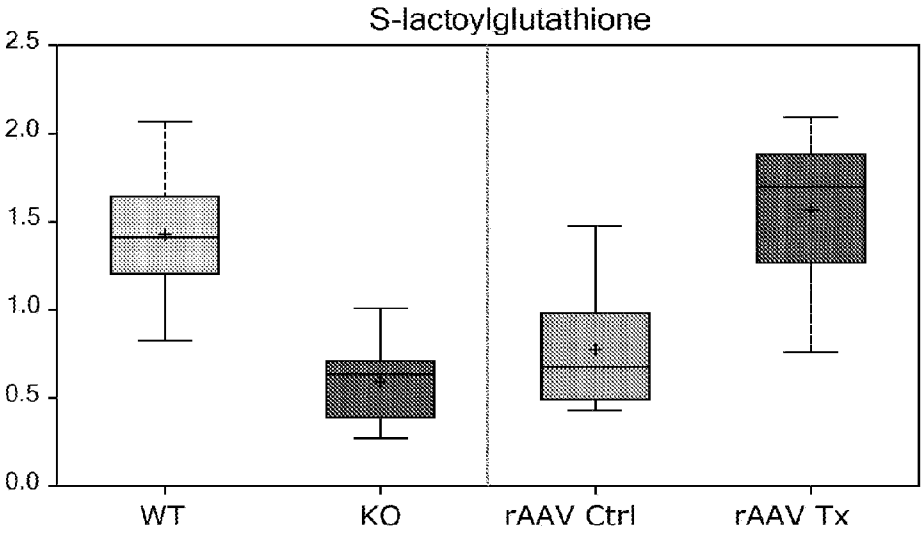
S-lactoylglutathione
2.5
2.0
1.5
1.0
0.5
0.0
WT
KO
rAAV Ctrl
rAAV Tx

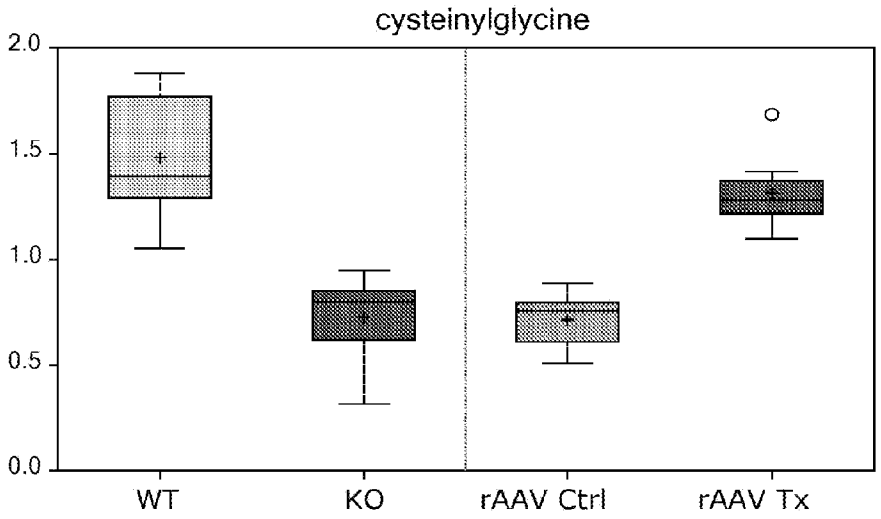
cysteinylglycine
2.0
1.5
1.0
0.5
0.0
WT
KO
rAAV Ctrl
rAAV Tx

FIG. 57 cont.

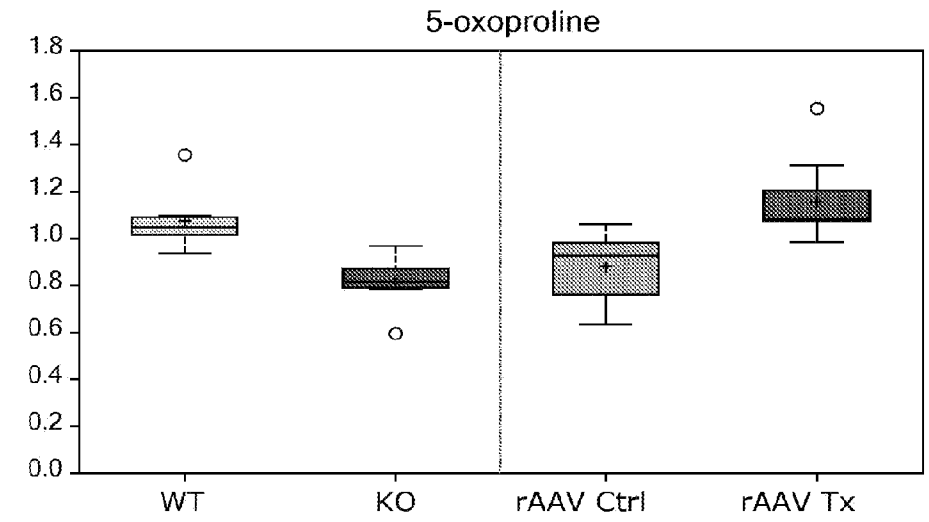
5-oxoproline
1.8
1.6
1.4
1.2
1.0
0.8
0.6
0.4
0.2
0.0
WT
KO
rAAV Ctrl
rAAV Tx

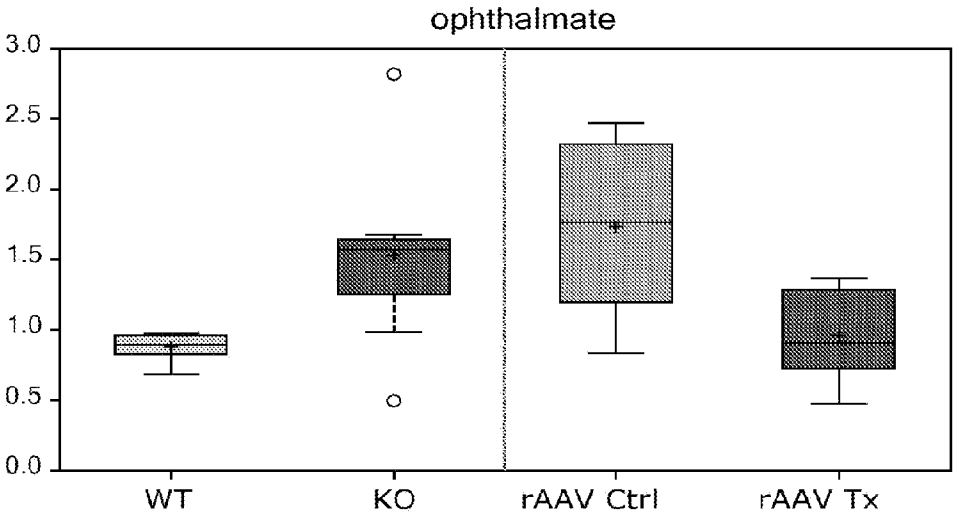
ophthalmate
3.0
2.5
2.0
1.5
1.0
0.5
0.0
WT
KO
rAAV Ctrl
rAAV Tx

FIG. 57 cont.

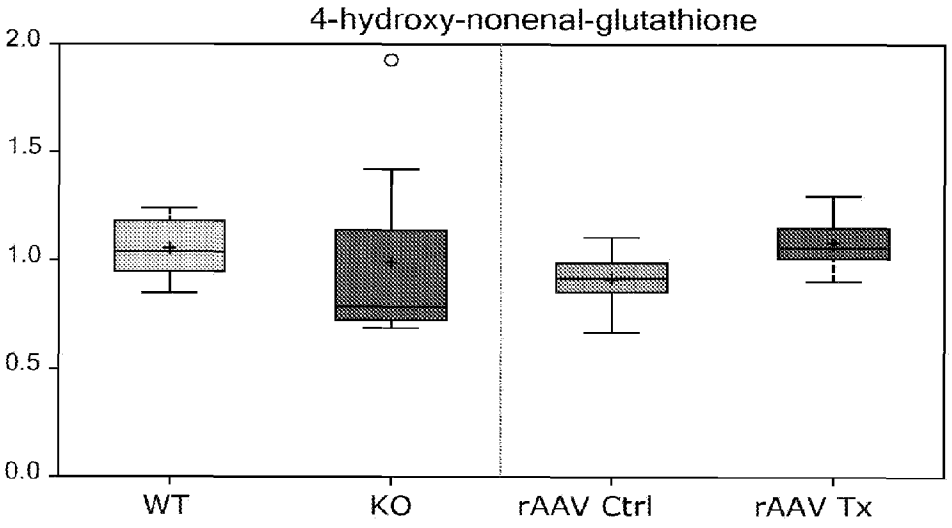
4-hydroxy-nonenal-glutathione
2.0
1.5
1.0
0.5
0.0
WT
KO
rAAV Ctrl
rAAV Tx

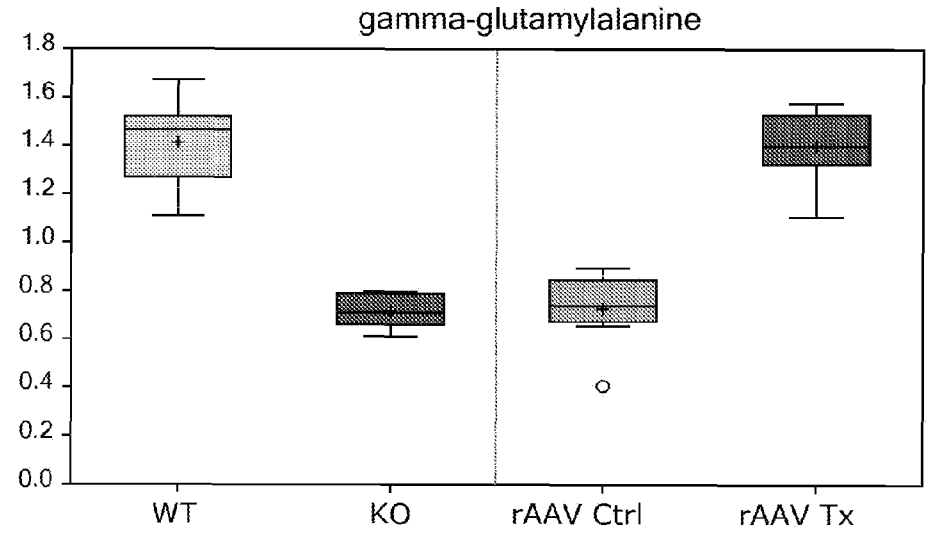
gamma-glutamylalanine
1.8
1.6
1.4
1.2
1.0
0.8
0.6
0.4
0.2
0.0
WT
KO
rAAV Ctrl
rAAV Tx

FIG. 57 cont.

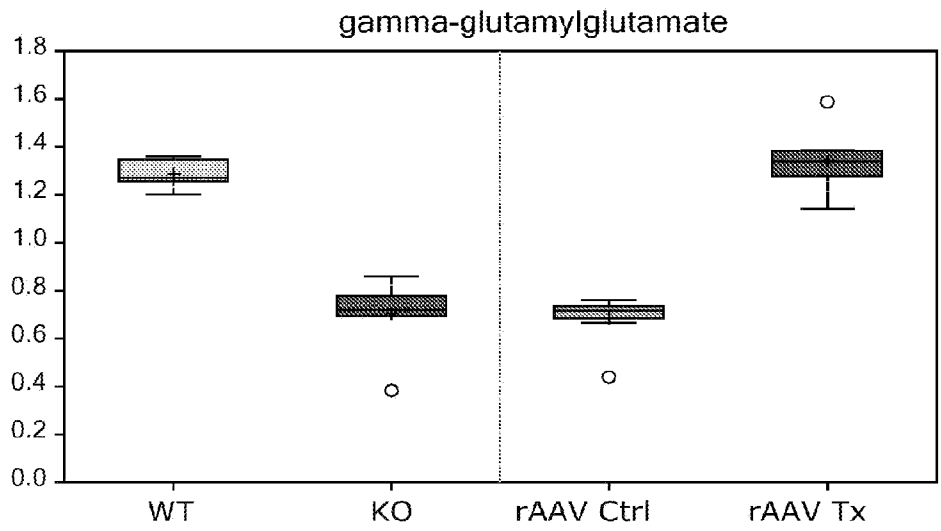
gamma-glutamylglutamate
1.8
1.6
1.4
1.2
1.0
0.8
0.6
0.4
0.2
0.0
WT
KO
rAAV Ctrl
rAAV Tx

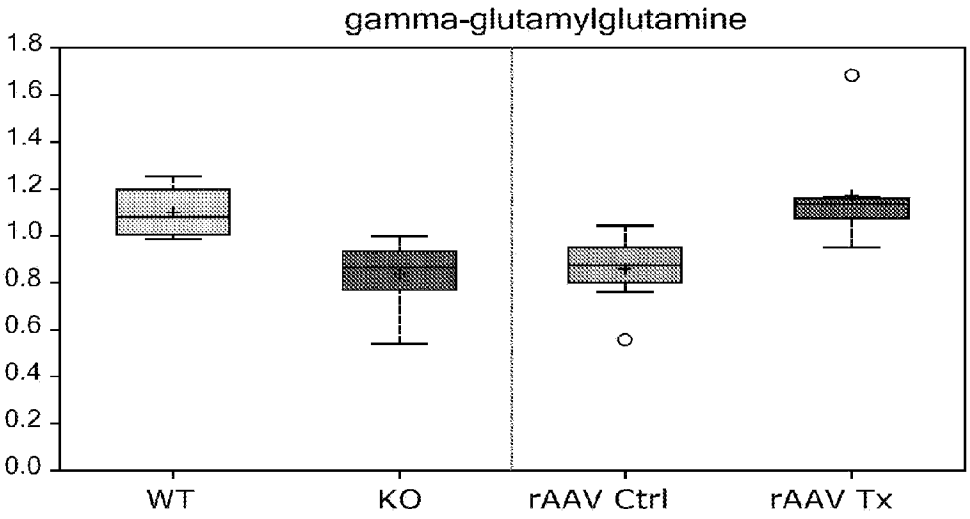
gamma-glutamylglutamine
1.8
1.6
1.4
1.2
1.0
0.8
0.6
0.4
0.2
0.0
WT
KO
rAAV Ctrl
rAAV Tx

FIG. 57 cont.

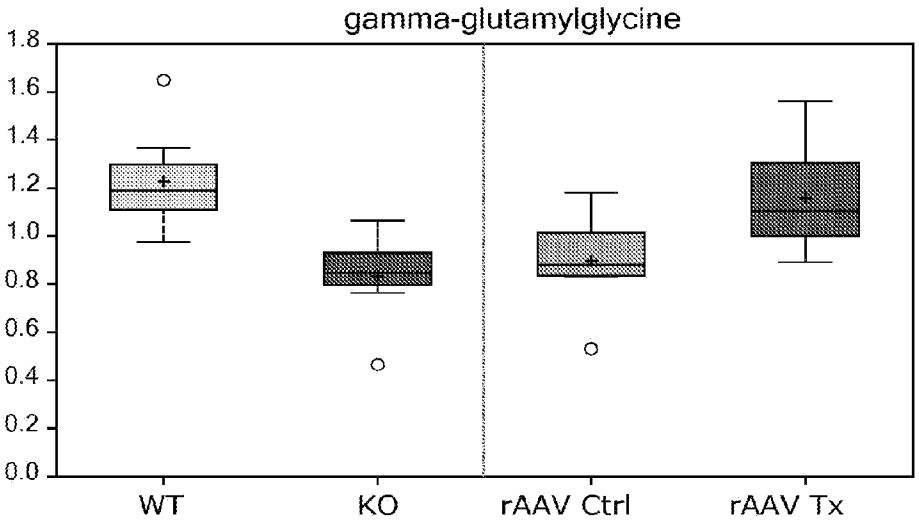
gamma-glutamylglycine
1.8
1.6
1.4
1.2
1.0
0.8
0.6
0.4
0.2
0.0
WT
KO
rAAV Ctrl
rAAV Tx

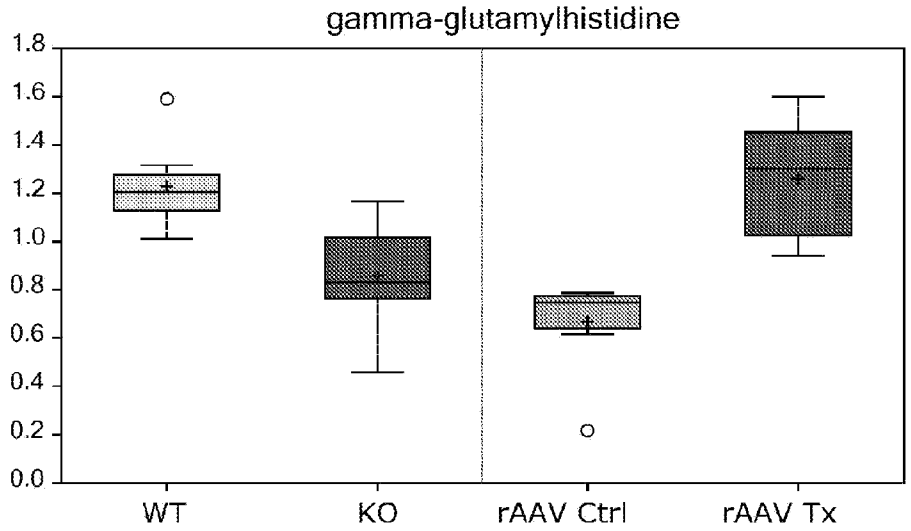
gamma-glutamylhistidine
1.8
1.6
1.4
1.2
1.0
0.8
0.6
0.4
0.2
0.0
WT
KO
rAAV Ctrl
rAAV Tx

FIG. 57 cont.

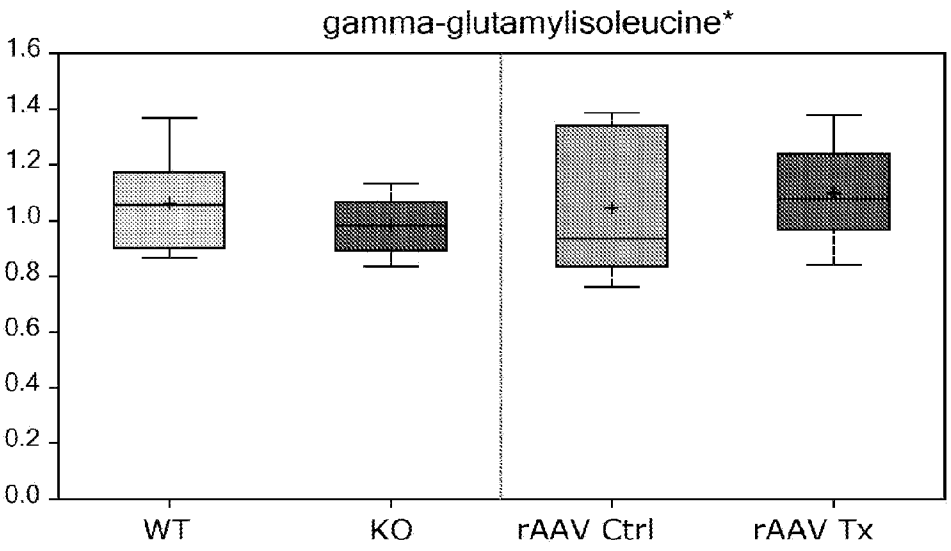
gamma-glutamylisoleucine*
1.6
1.4
1.2
1.0
0.8
0.6
0.4
0.2
0.0
WT
KO
rAAV Ctrl
rAAV Tx

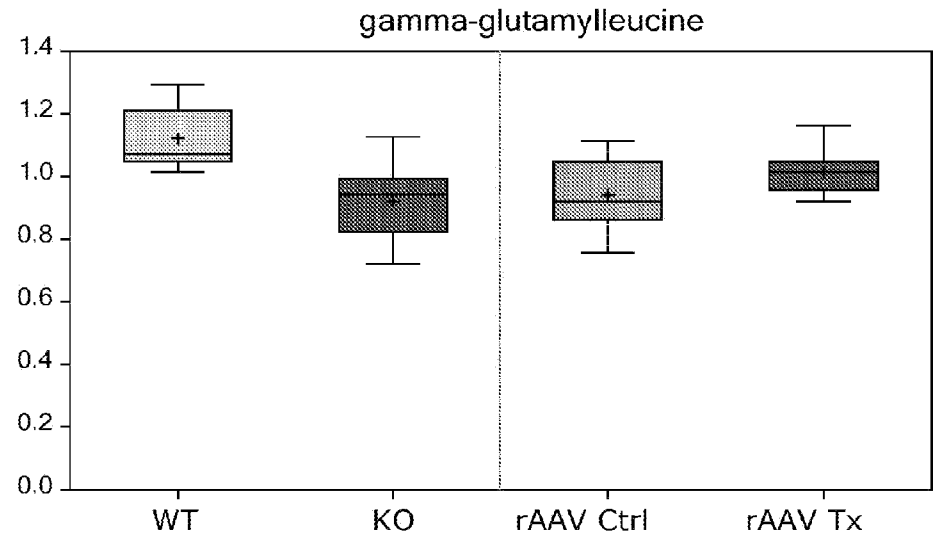
gamma-glutamylleucine
1.4
1.2
1.0
0.8
0.6
0.4
0.2
0.0
WT
KO
rAAV Ctrl
rAAV Tx

FIG. 57 cont.

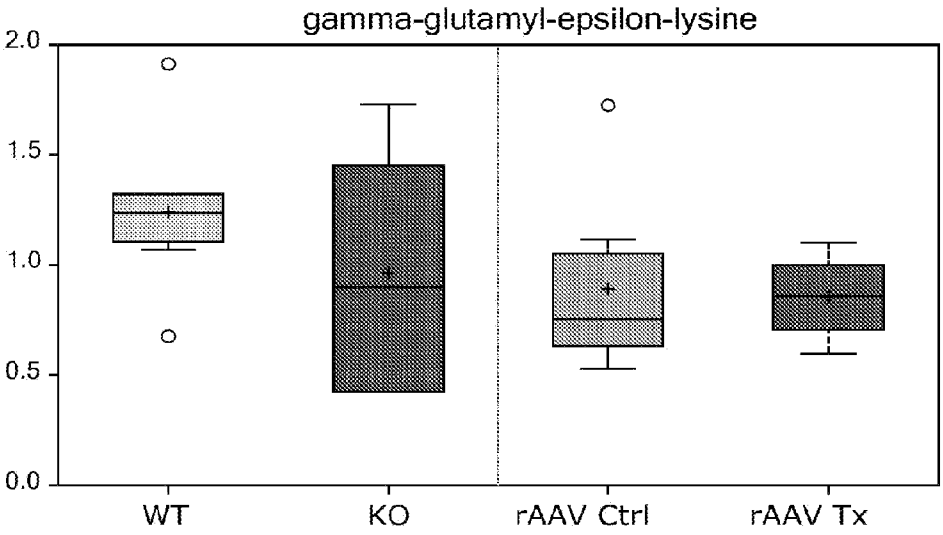
gamma-glutamyl-epsilon-lysine
2.0
1.5
1.0
0.5
0.0
WT
KO
rAAV Ctrl
rAAV Tx

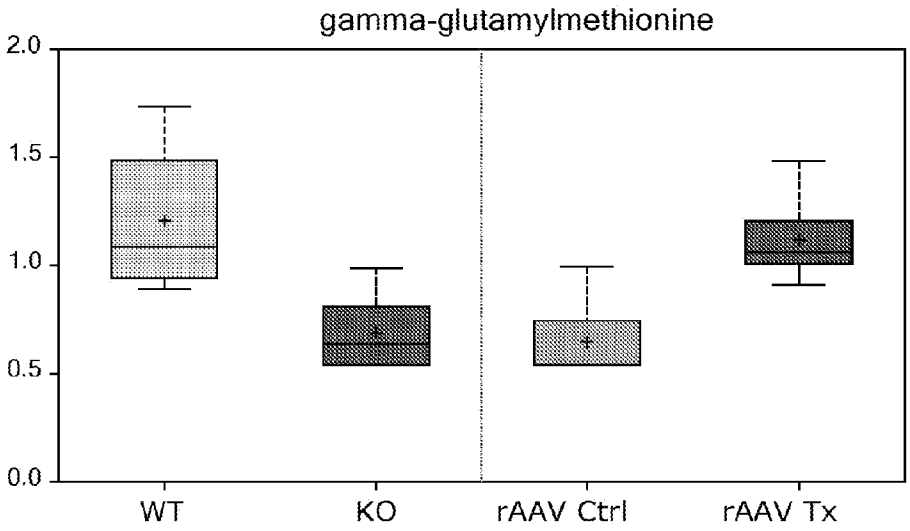
gamma-glutamylmethionine
2.0
1.5
1.0
0.5
0.0
WT
KO
rAAV Ctrl
rAAV Tx

FIG. 57 cont.

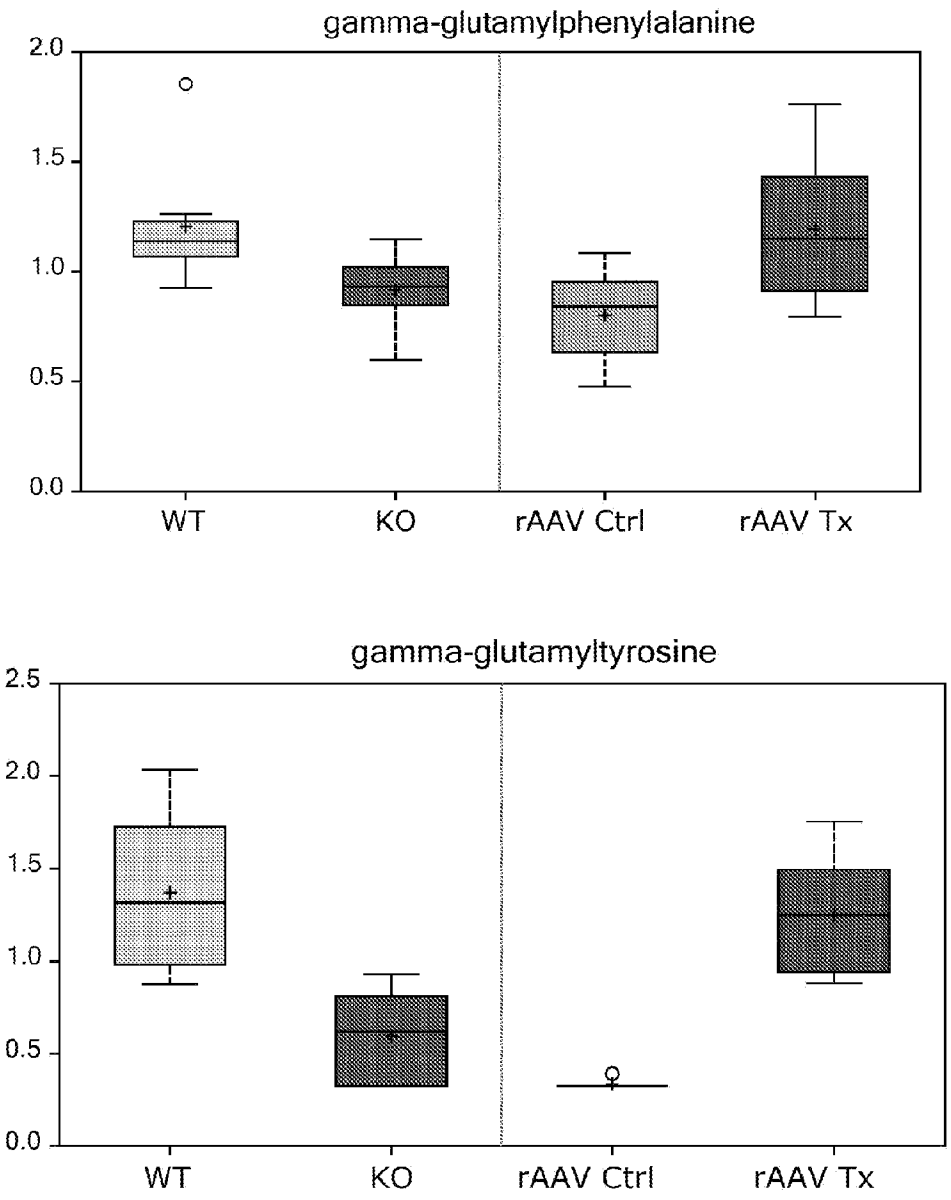
gamma-glutamylphenylalanine
2.0
1.5
1.0
0.5
0.0
WT
KO
rAAV Ctrl
rAAV Tx
gamma-glutamyltyrosine
2.5
2.0
1.5
1.0
0.5
0.0
WT
KO
rAAV Ctrl
rAAV Tx

FIG. 57 cont.

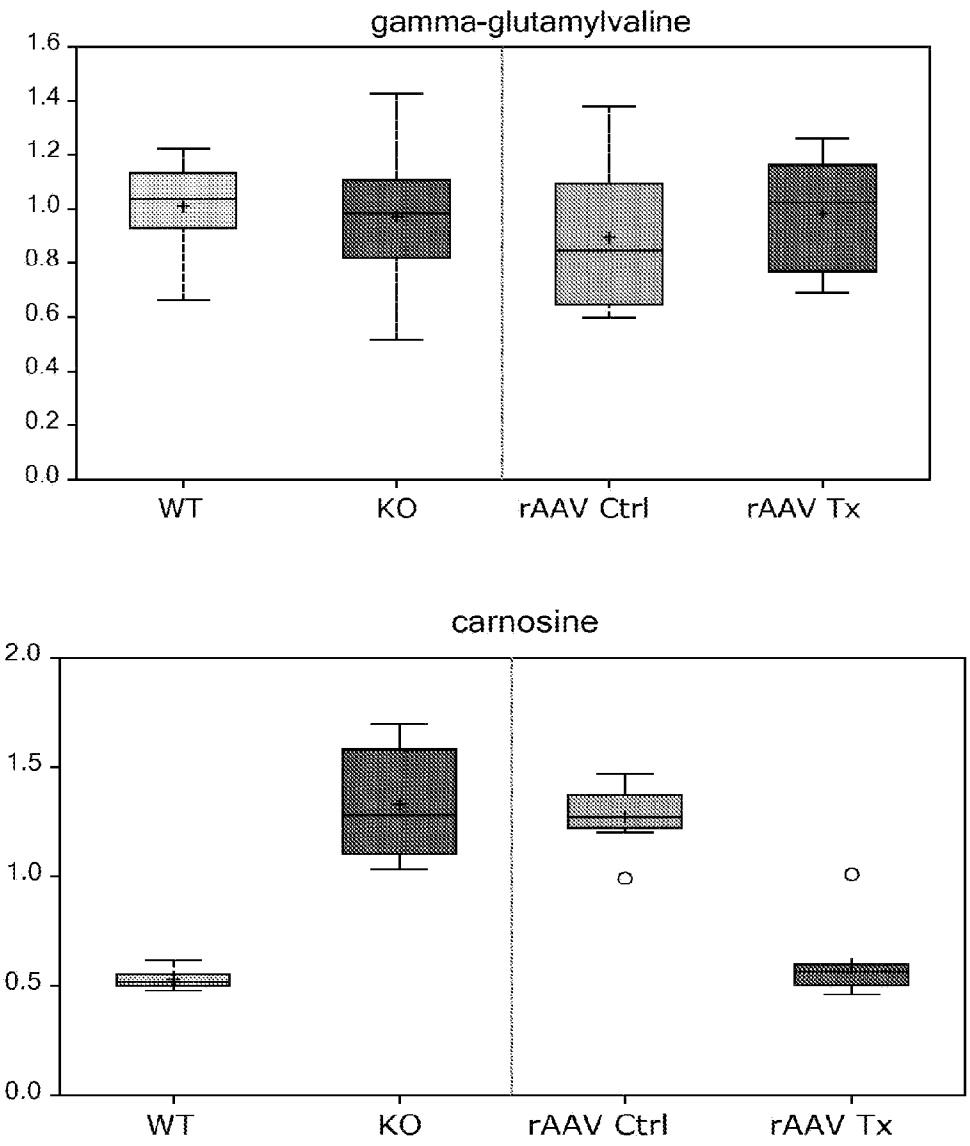
gamma-glutamylvaline
1.6
1.4
1.2
1.0
0.8
0.6
0.4
0.2
0.0
WT
KO
rAAV Ctrl
rAAV Tx
carnosine
2.0
1.5
1.0
0.5
0.0
WT
KO
rAAV Ctrl
rAAV Tx

FIG. 57 cont.

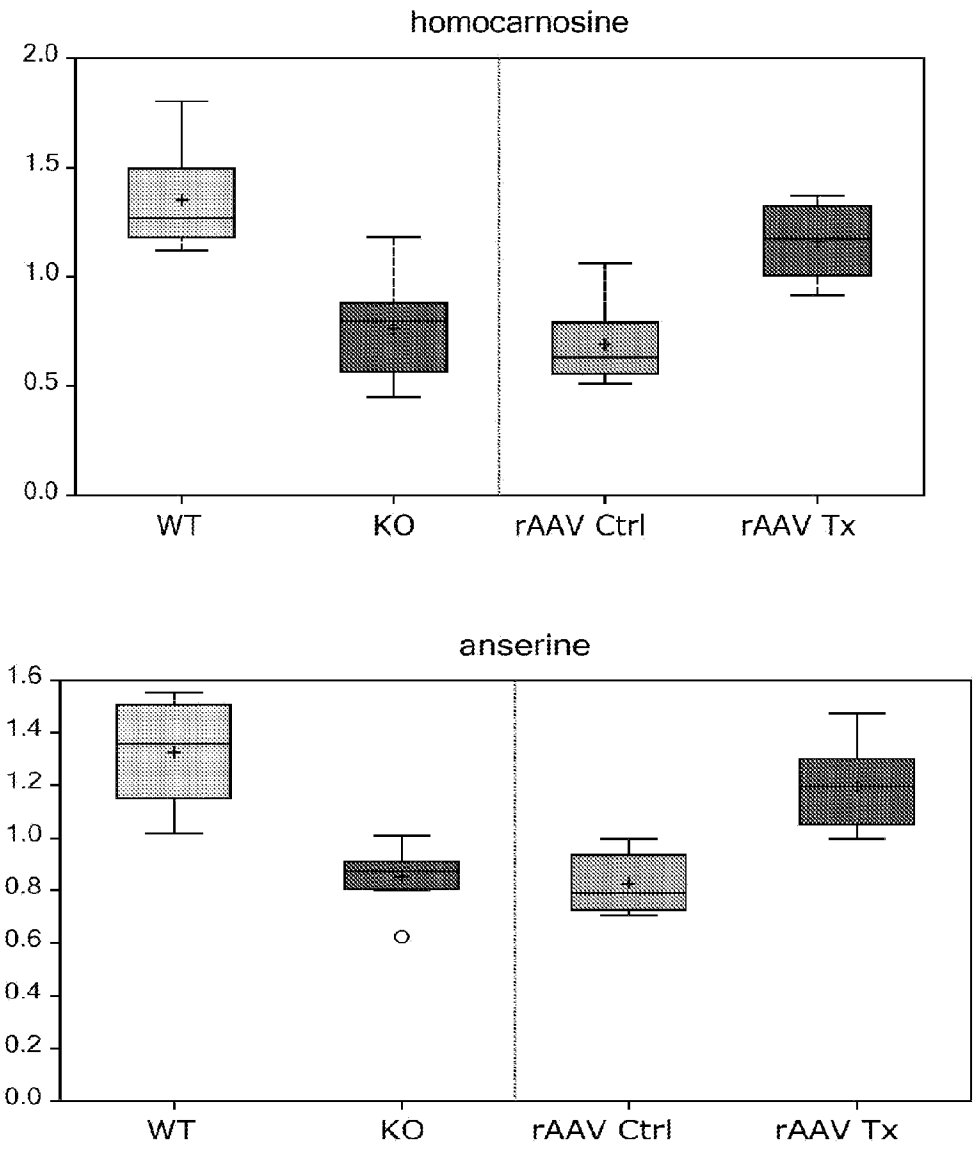
homocarnosine
2.0
1.5
1.0
0.5
0.0
WT
KO
rAAV Ctrl
rAAV Tx
anserine
1.6
1.4
1.2
1.0
0.8
0.6
0.4
0.2
0.0
WT
KO
rAAV Ctrl
rAAV Tx

FIG. 57 cont.

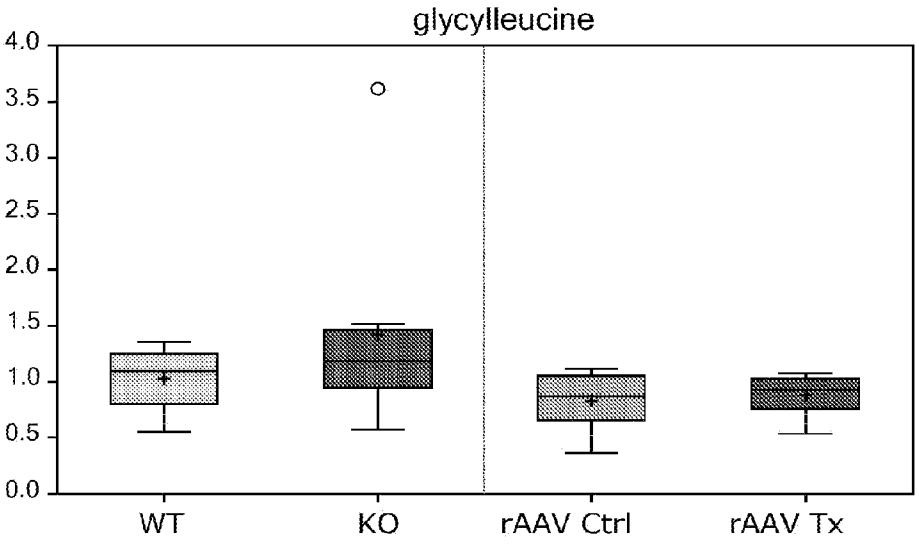
glycylleucine
4.0
3.5
3.0
2.5
2.0
1.5
1.0
0.5
0.0
WT
KO
rAAV Ctrl
rAAV Tx

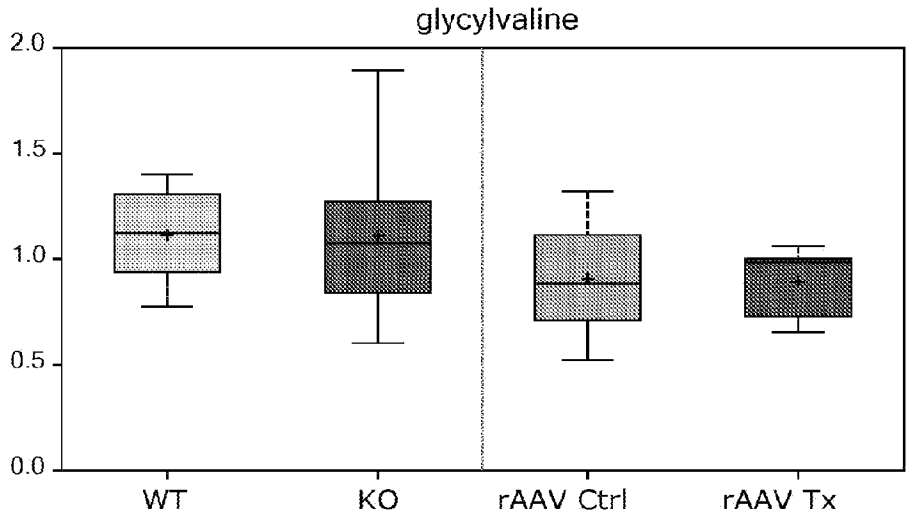
glycylvaline
2.0
1.5
1.0
0.5
0.0
WT
KO
rAAV Ctrl
rAAV Tx

FIG. 57 cont.

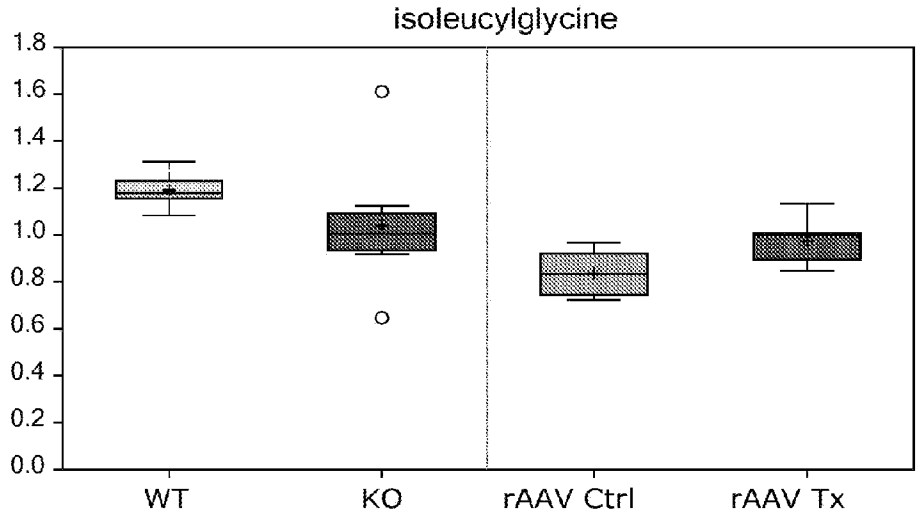
isoleucylglycine
1.8
1.6
1.4
1.2
1.0
0.8
0.6
0.4
0.2
0.0
WT
KO
rAAV Ctrl
rAAV Tx

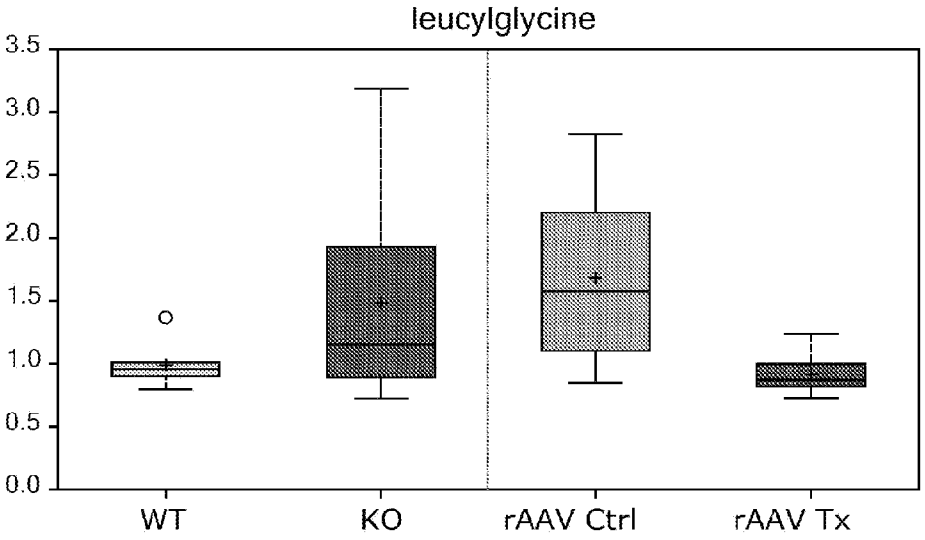
leucylglycine
3.5
3.0
2.5
2.0
1.5
1.0
0.5
0.0
WT
KO
rAAV Ctrl
rAAV Tx

FIG. 57 cont.

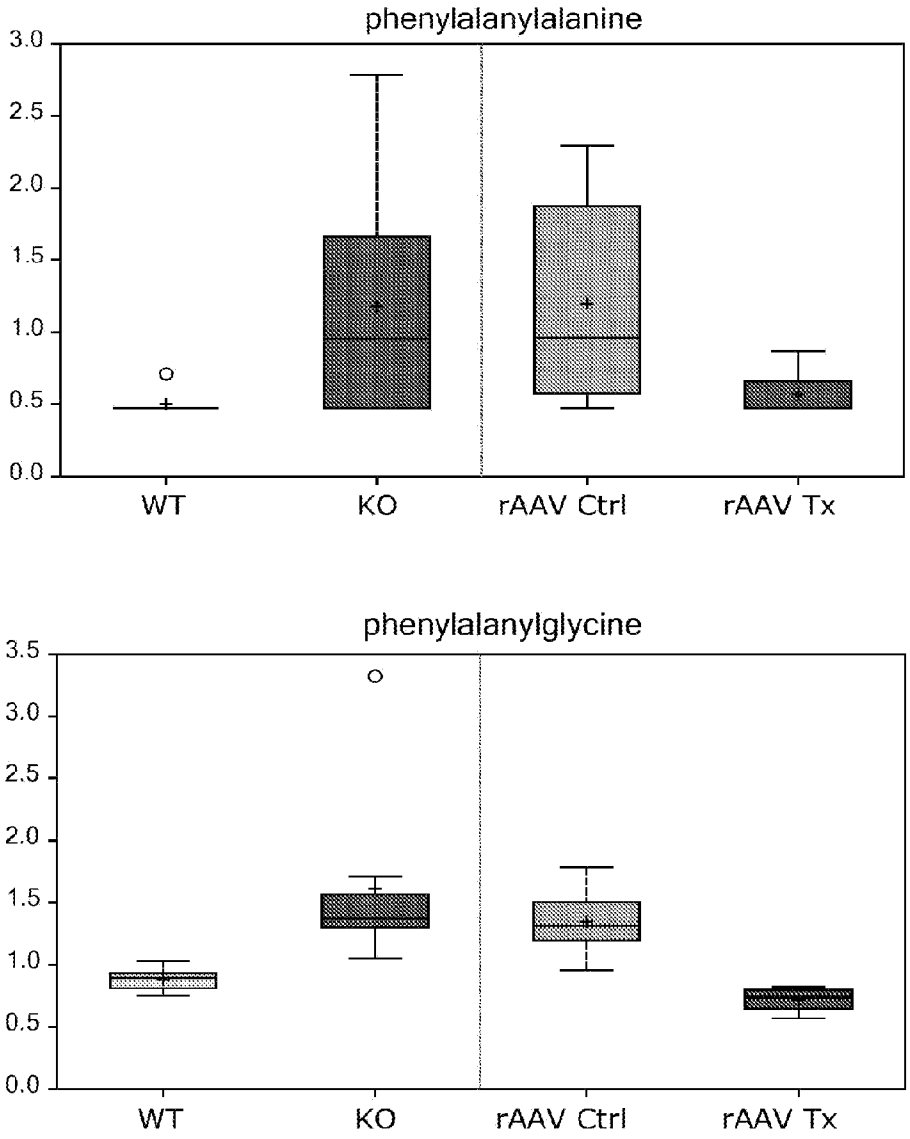
phenylalanylalanine
3.0
2.5
2.0
1.5
1.0
0.5
0.0
WT
KO
rAAV Ctrl
rAAV Tx
phenylalanylglycine
3.5
3.0
2.5
2.0
1.5
1.0
0.5
0.0
WT
KO
rAAV Ctrl
rAAV Tx

FIG. 57 cont.

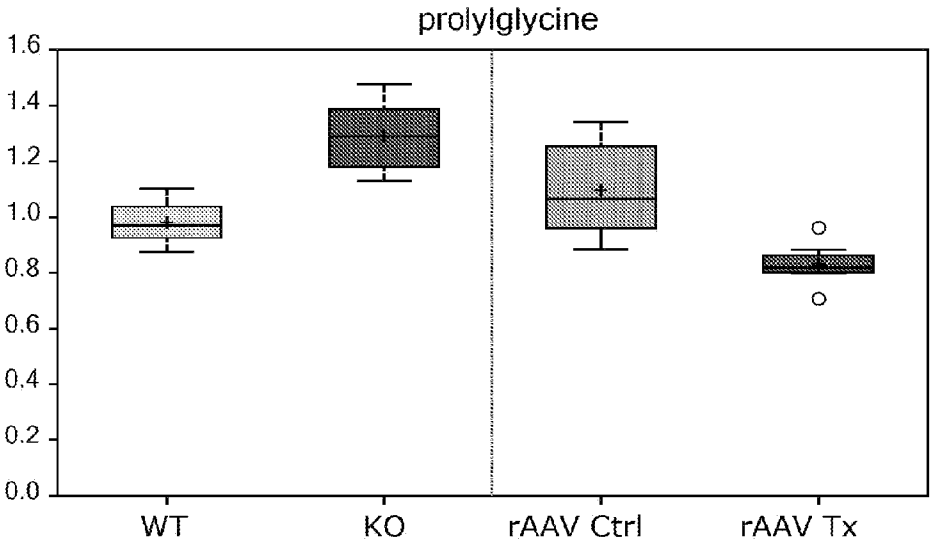
prolylglycine
1.6
1.4
1.2
1.0
0.8
0.6
0.4
0.2
0.0
WT
KO
rAAV Ctrl
rAAV Tx

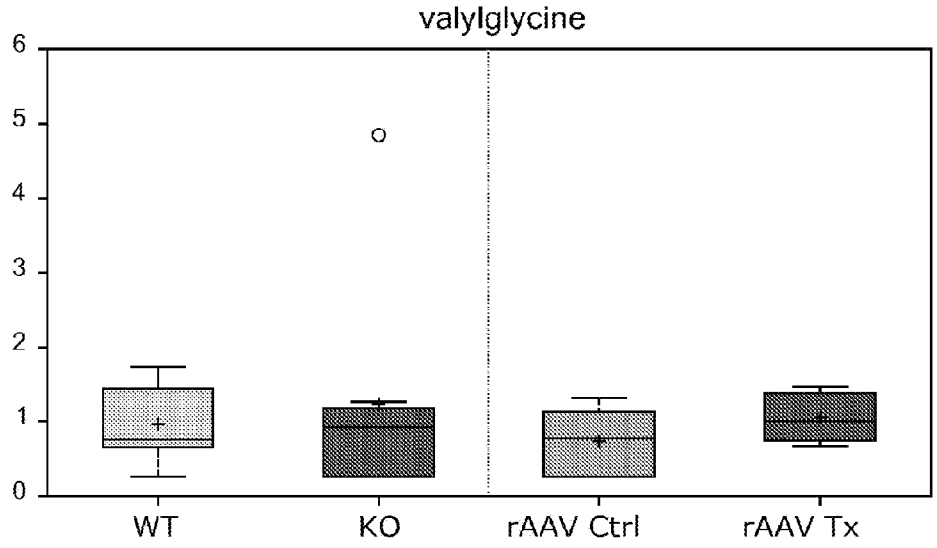
valylglycine
6
5
4
3
2
1
0
WT
KO
rAAV Ctrl
rAAV Tx

FIG. 57 cont.

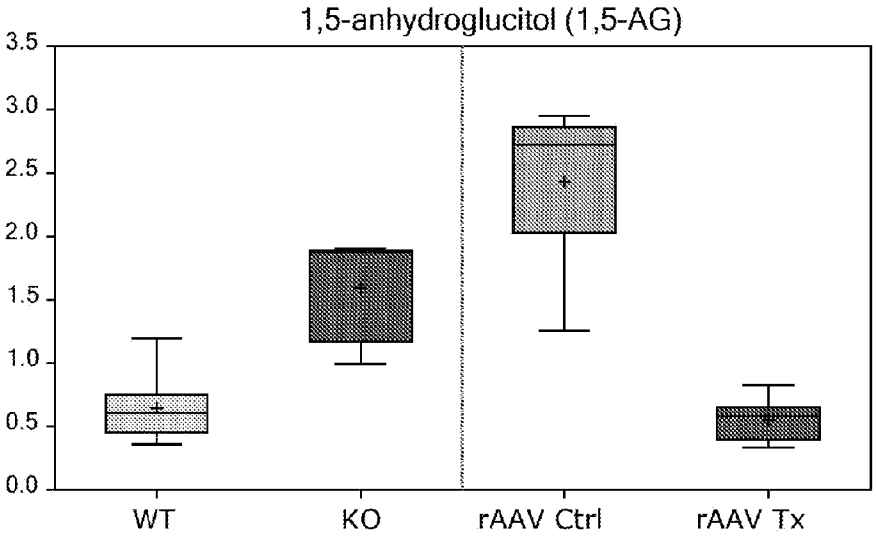
1,5-anhydroglucitol (1,5-AG)
3.5
3.0
2.5
2.0
1.5
1.0
0.5
0.0
WT
KO
rAAV Ctrl
rAAV Tx

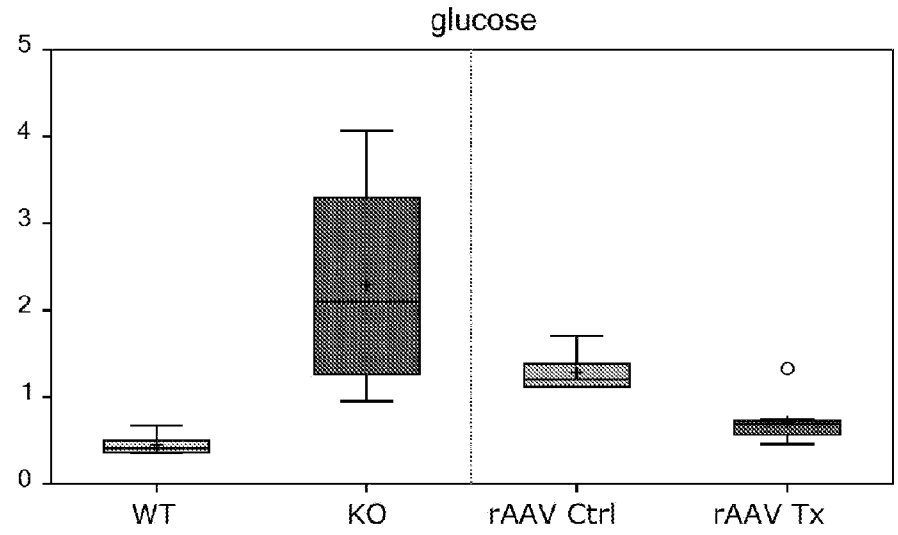
glucose
5
4
3
2
1
0
WT
KO
rAAV Ctrl
rAAV Tx

FIG. 57 cont.

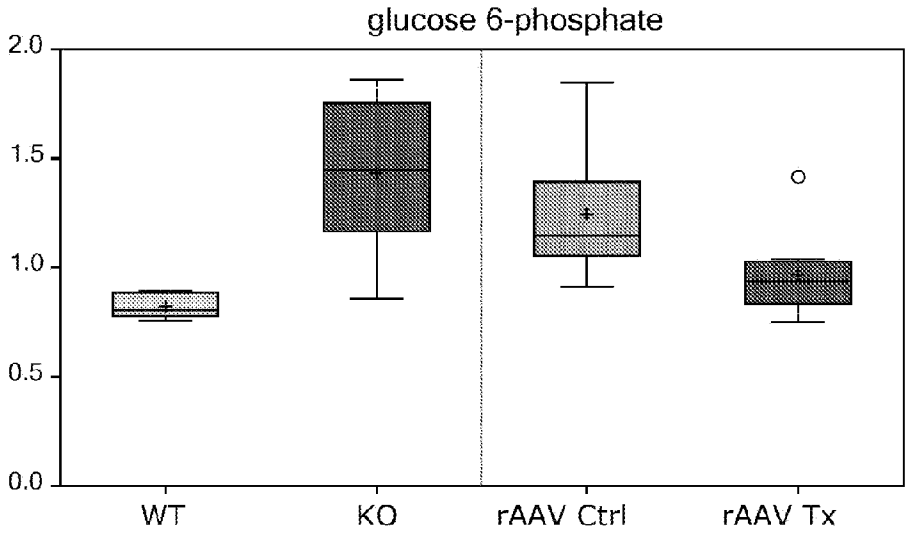
glucose 6-phosphate
2.0
1.5
1.0
0.5
0.0
WT
KO
rAAV Ctrl
rAAV Tx

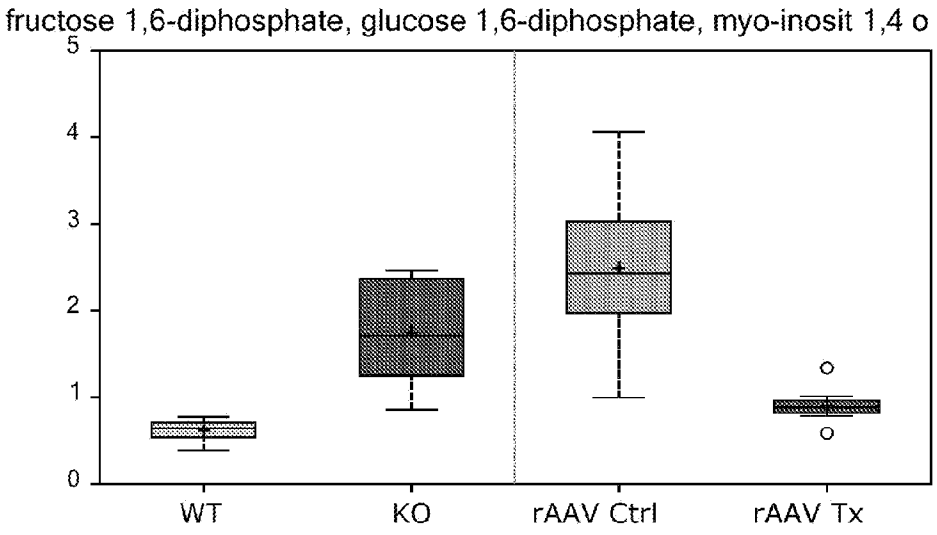
fructose 1,6-diphosphate, glucose 1,6-diphosphate, myo-inosit 1,4 o
5
4
3
2
1
0
WT
KO
rAAV Ctrl
rAAV Tx

FIG. 57 cont.

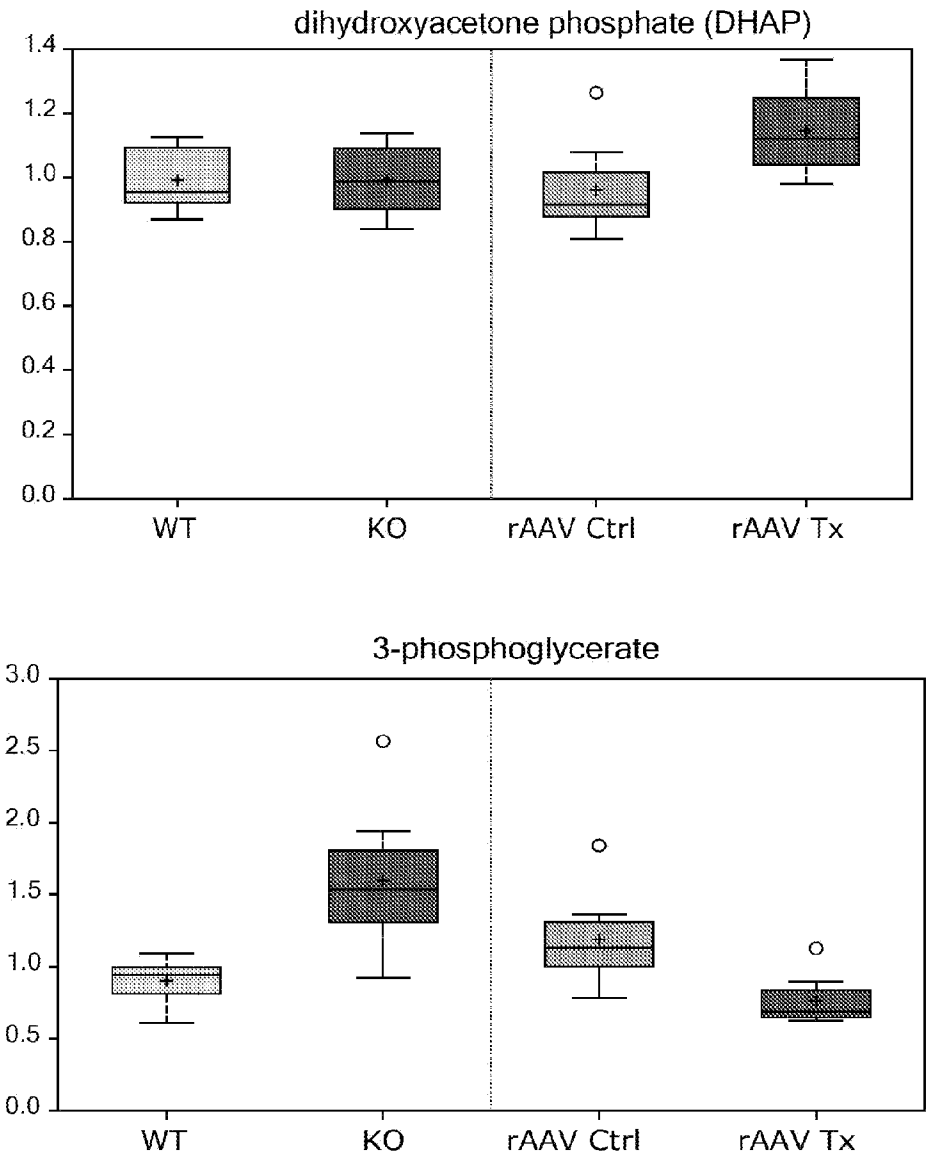
dihydroxyacetone phosphate (DHAP)
1.4
1.2
1.0
0.8
0.6
0.4
0.2
0.0
WT
KO
rAAV Ctrl
rAAV Tx
3-phosphoglycerate
3.0
2.5
2.0
1.5
1.0
0.5
0.0
WT
KO
rAAV Ctrl
rAAV Tx

FIG. 57 cont.

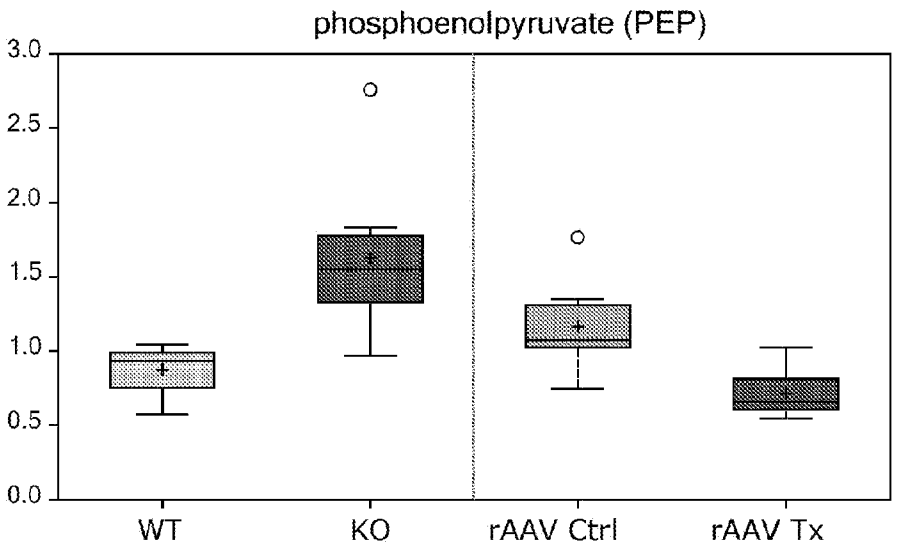
phosphoenolpyruvate (PEP)
3.0
2.5
2.0
1.5
1.0
0.5
0.0
WT
KO
rAAV Ctrl
rAAV Tx

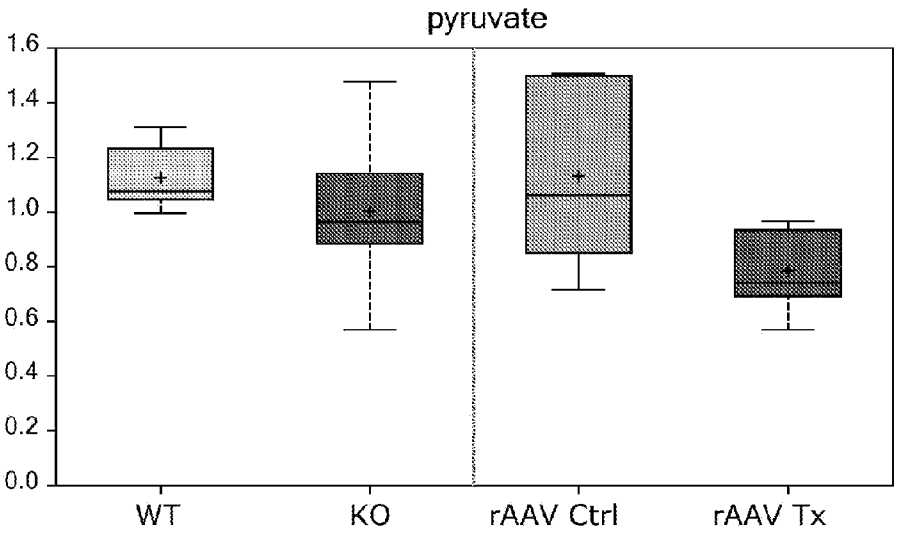
pyruvate
1.6
1.4
1.2
1.0
0.8
0.6
0.4
0.2
0.0
WT
KO
rAAV Ctrl
rAAV Tx

FIG. 57 cont.

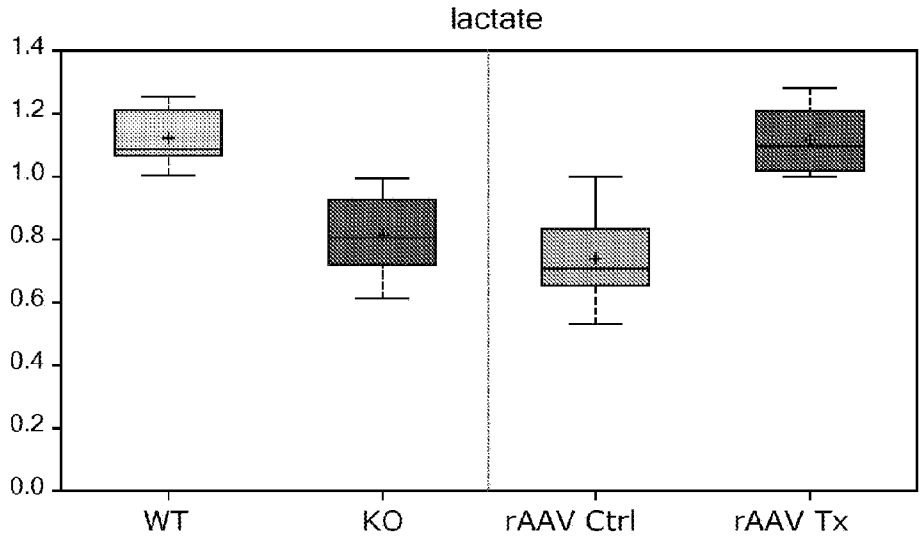
lactate
1.4
1.2
1.0
0.8
0.6
0.4
0.2
0.0
WT
KO
rAAV Ctrl
rAAV Tx

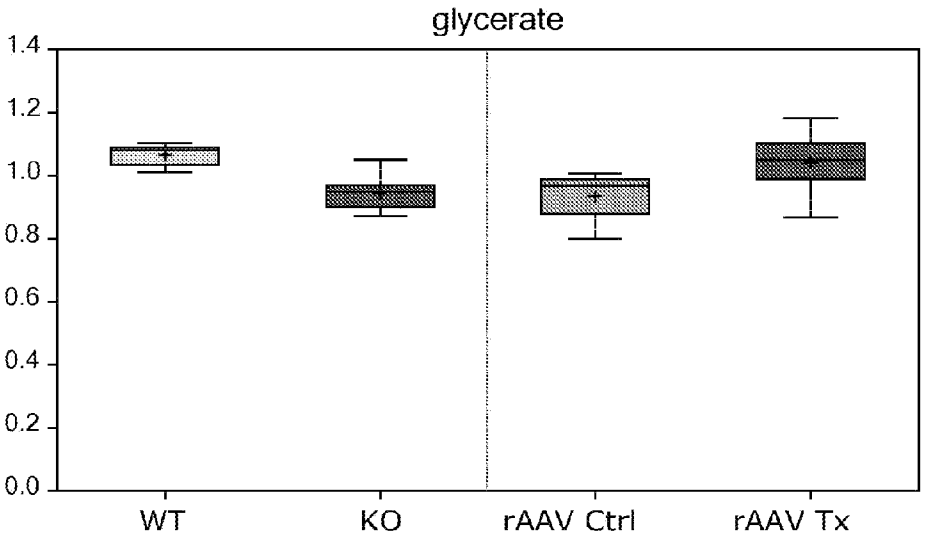
glycerate
1.4
1.2
1.0
0.8
0.6
0.4
0.2
0.0
WT
KO
rAAV Ctrl
rAAV Tx

FIG. 57 cont.

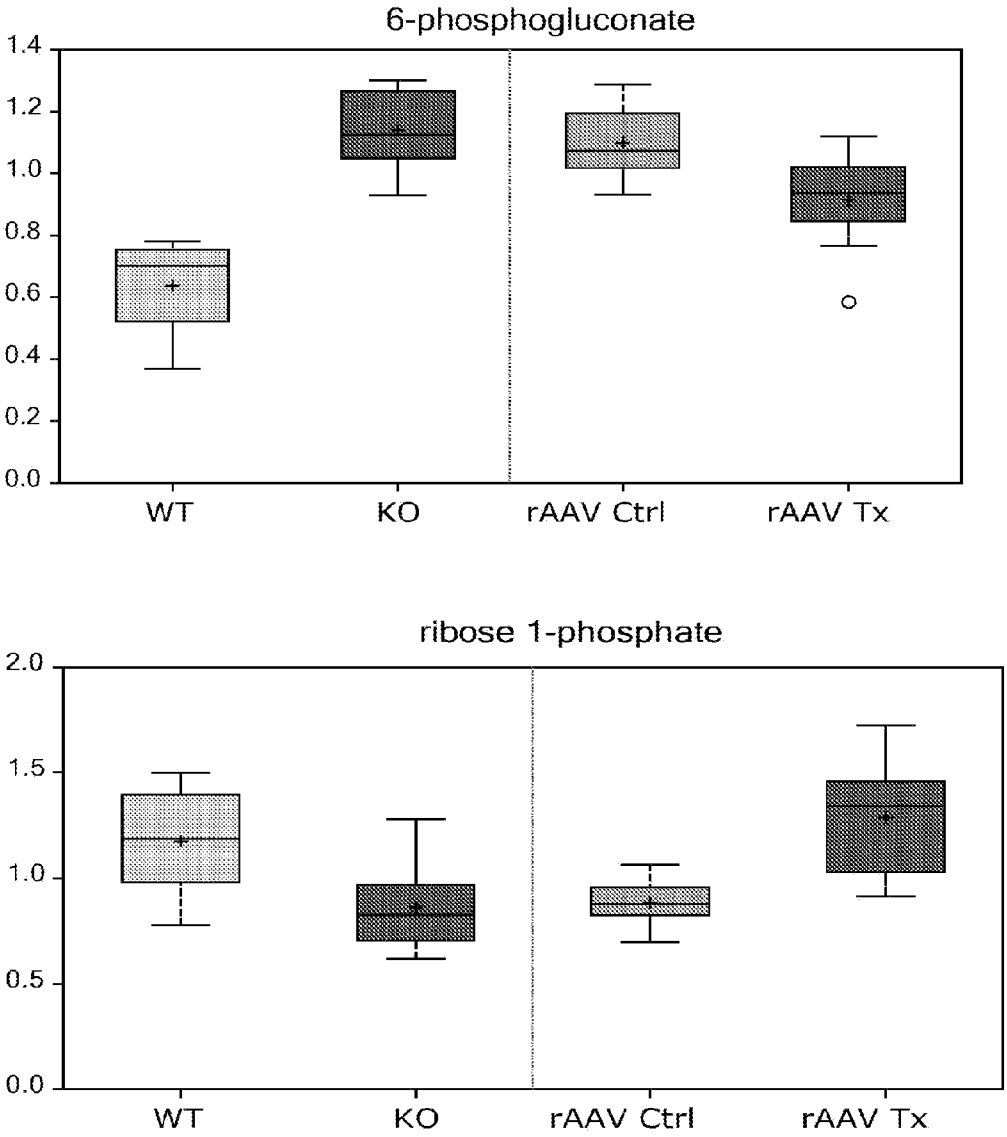
6-phosphogluconate
1.4
1.2
1.0
0.8
0.6
0.4
0.2
0.0
WT
KO
rAAV Ctrl
rAAV Tx
ribose 1-phosphate
2.0
1.5
1.0
0.5
0.0
WT
KO
rAAV Ctrl
rAAV Tx

FIG. 57 cont.

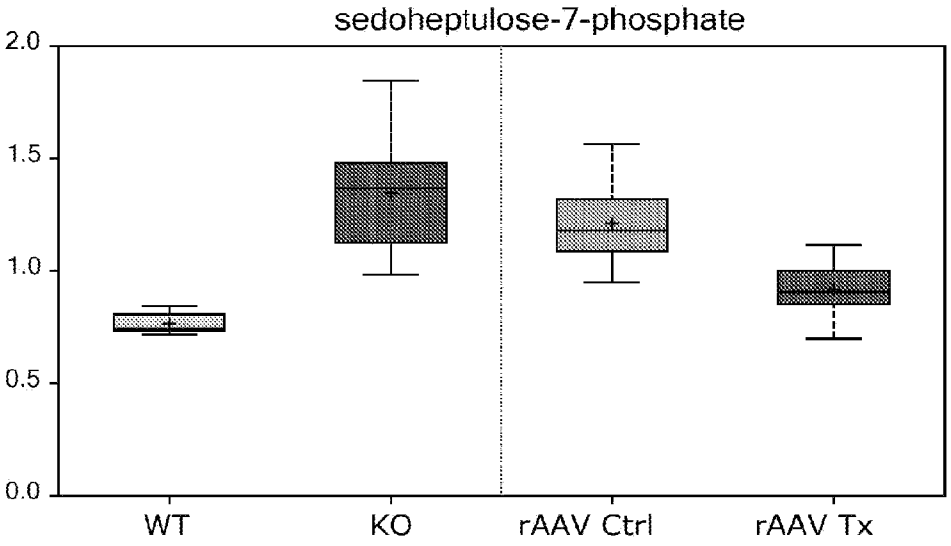
sedoheptulose-7-phosphate
2.0
1.5
1.0
0.5
0.0
WT
KO
rAAV Ctrl
rAAV Tx

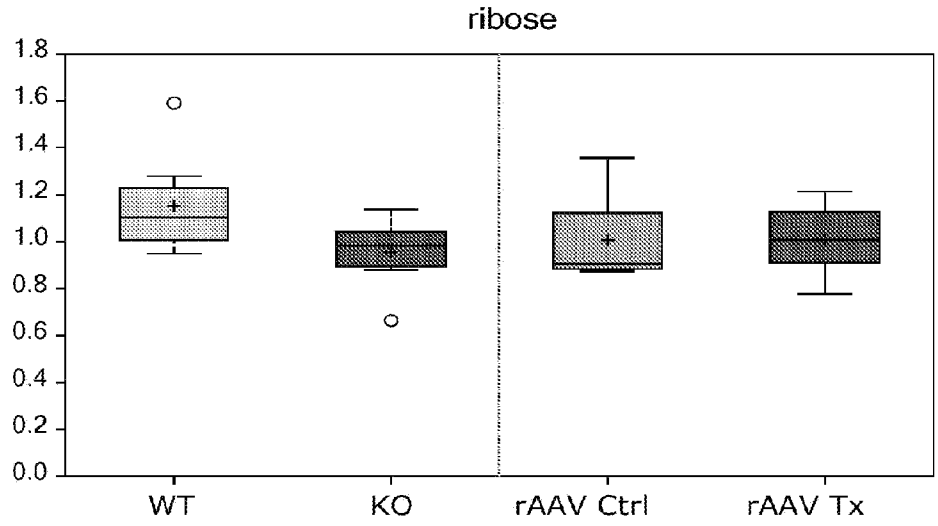
ribose
1.8
1.6
1.4
1.2
1.0
0.8
0.6
0.4
0.2
0.0
WT
KO
rAAV Ctrl
rAAV Tx

FIG. 57 cont.

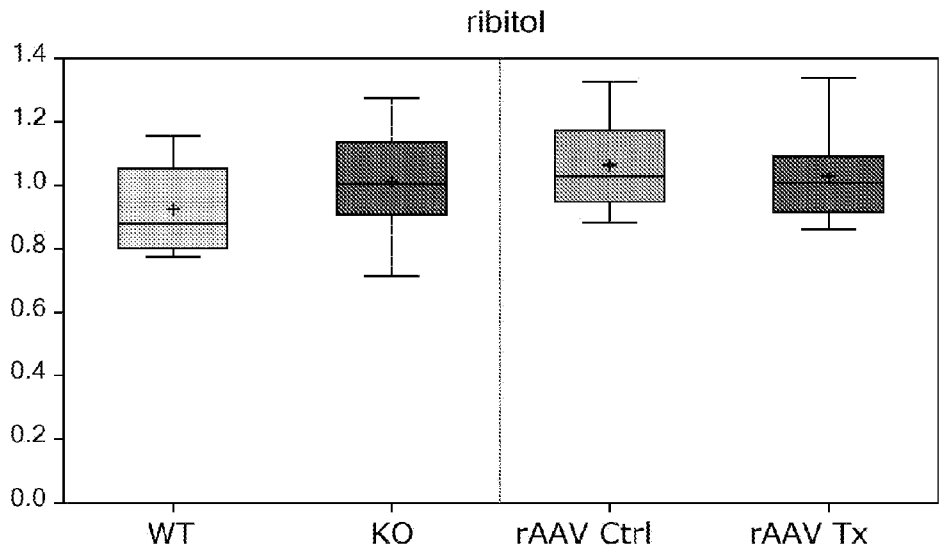
ribitol
1.4
1.2
1.0
0.8
0.6
0.4
0.2
0.0
WT
KO
rAAV Ctrl
rAAV Tx

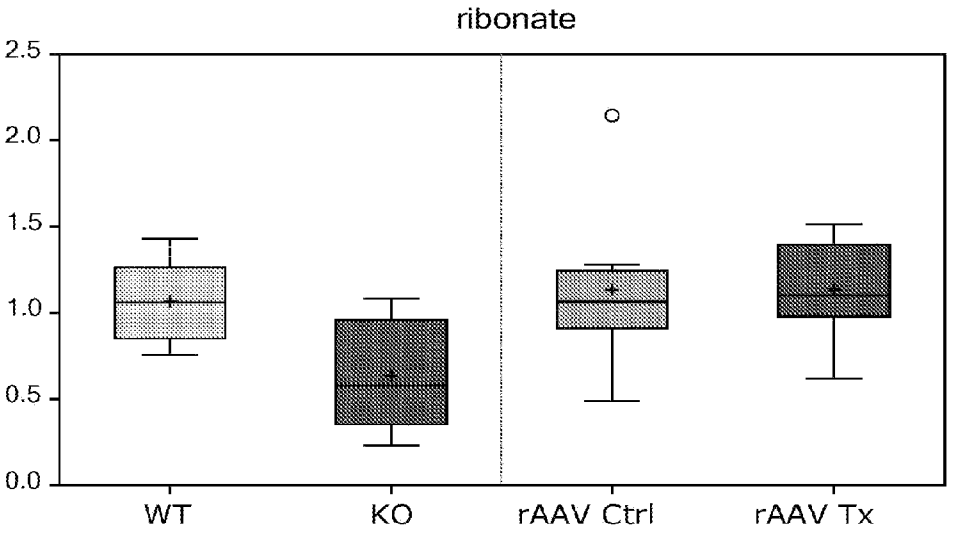
ribonate
2.5
2.0
1.5
1.0
0.5
0.0
WT
KO
rAAV Ctrl
rAAV Tx

FIG. 57 cont.

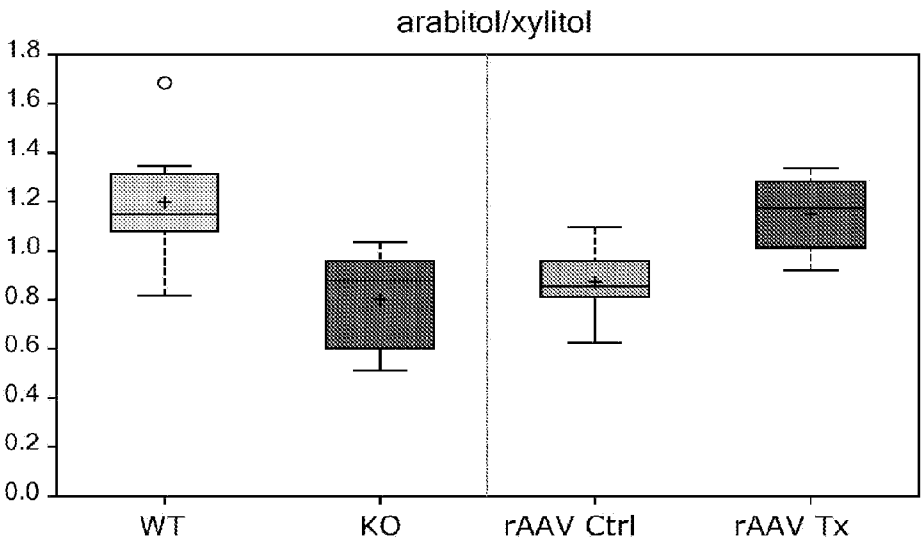
arabitol/xylitol
1.8
1.6
1.4
1.2
1.0
0.8
0.6
0.4
0.2
0.0
WT
KO
rAAV Ctrl
rAAV Tx

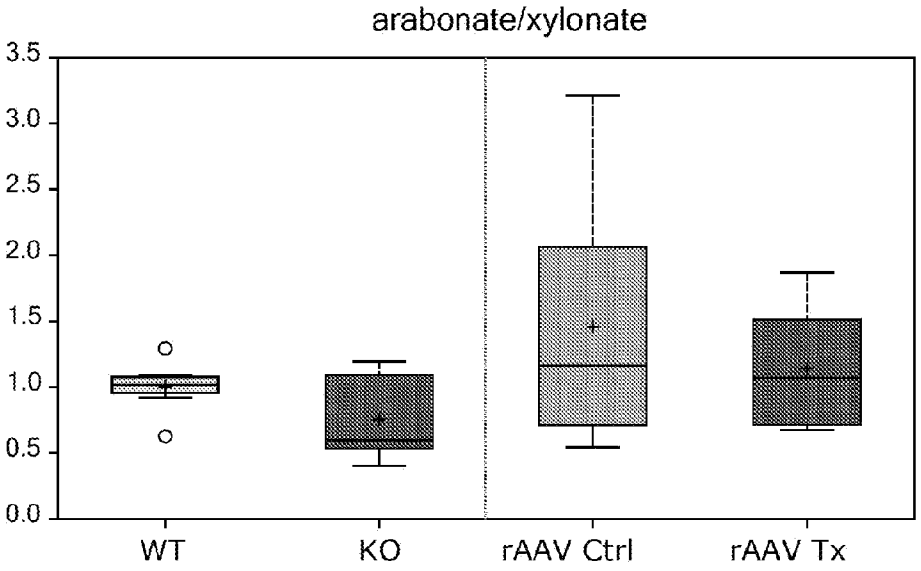
arabonate/xylonate
3.5
3.0
2.5
2.0
1.5
1.0
0.5
0.0
WT
KO
rAAV Ctrl
rAAV Tx

FIG. 57 cont.

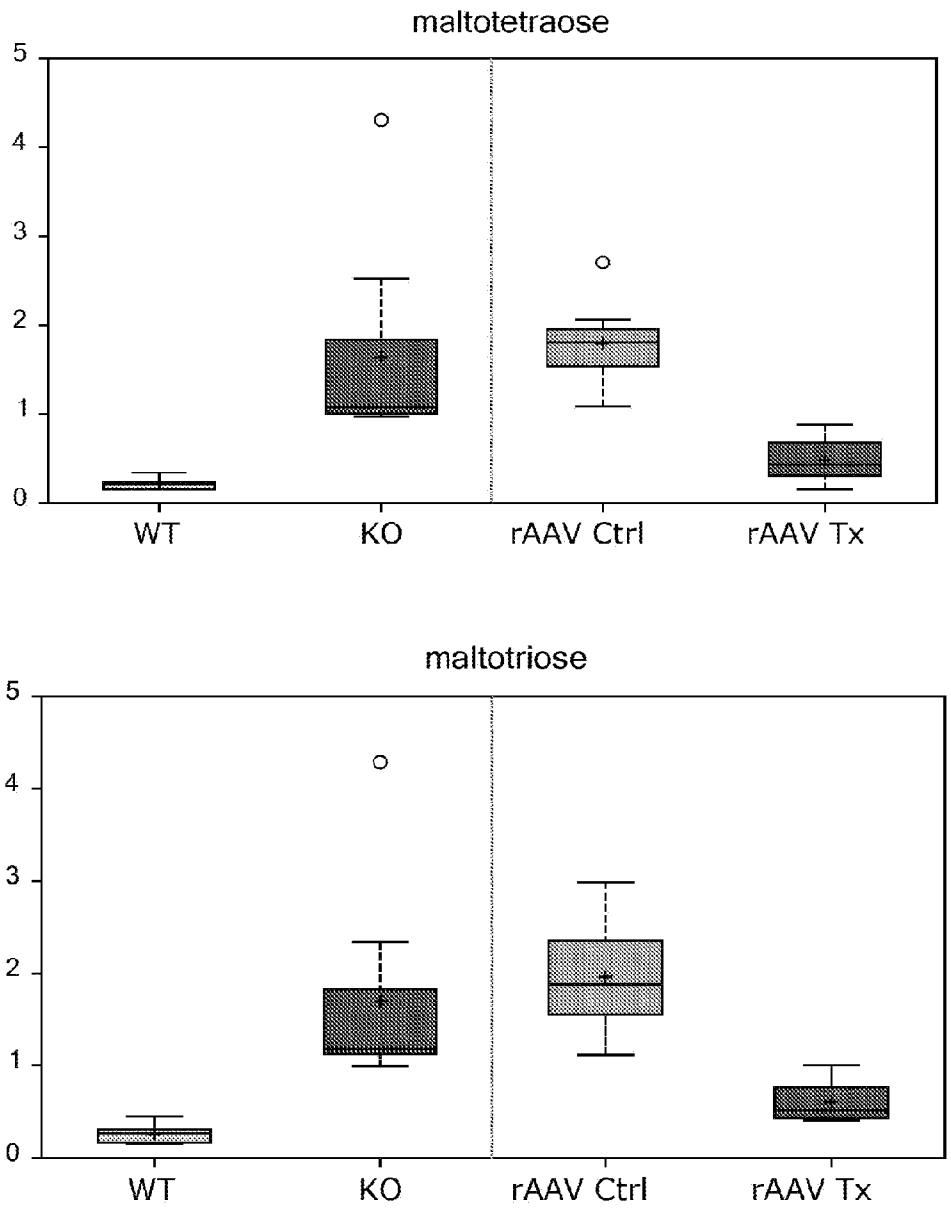
maltotetraose
5
4
3
2
1
0
WT
KO
rAAV Ctrl
rAAV Tx
maltotriose
5
4
3
2
1
0
WT
KO
rAAV Ctrl
rAAV Tx

FIG. 57 cont.

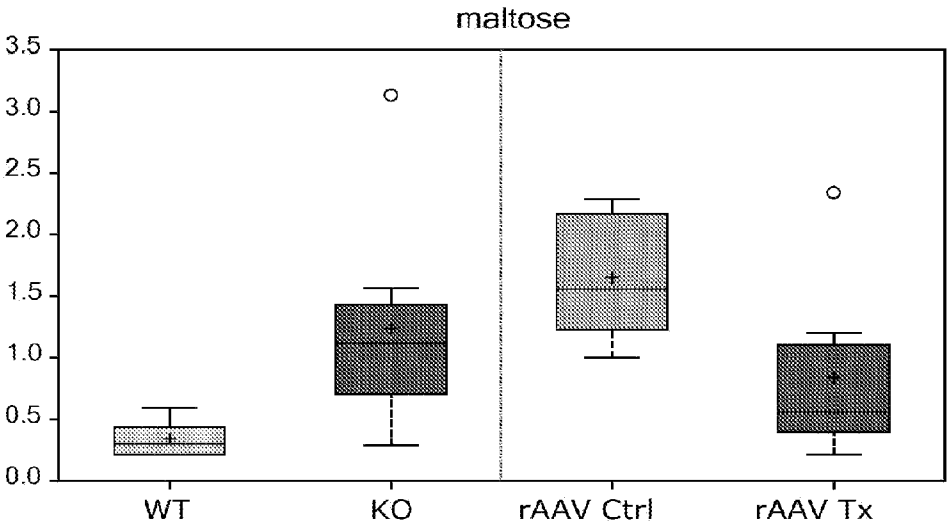
maltose
3.5
3.0
2.5
2.0
1.5
1.0
0.5
0.0
WT
KO
rAAV Ctrl
rAAV Tx

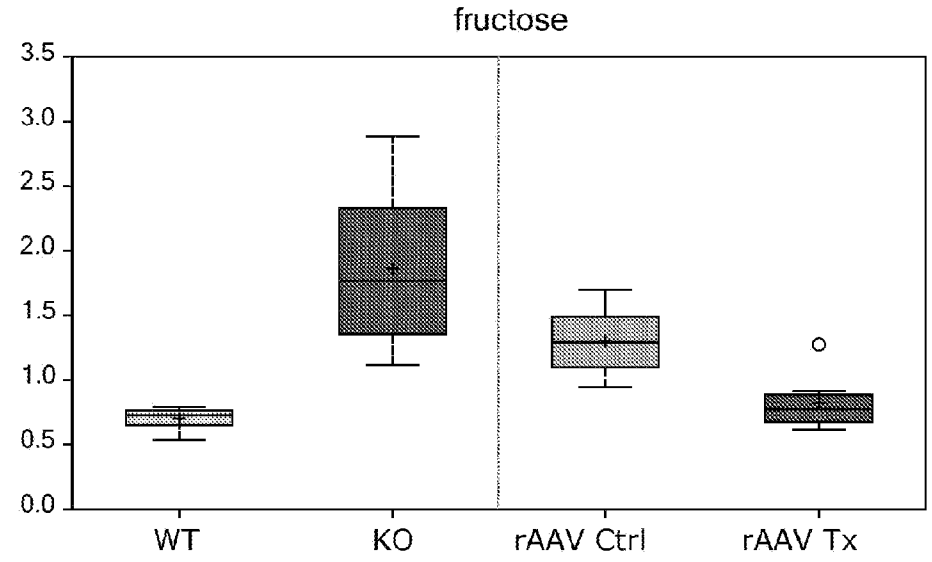
fructose
3.5
3.0
2.5
2.0
1.5
1.0
0.5
0.0
WT
KO
rAAV Ctrl
rAAV Tx

FIG. 57 cont.

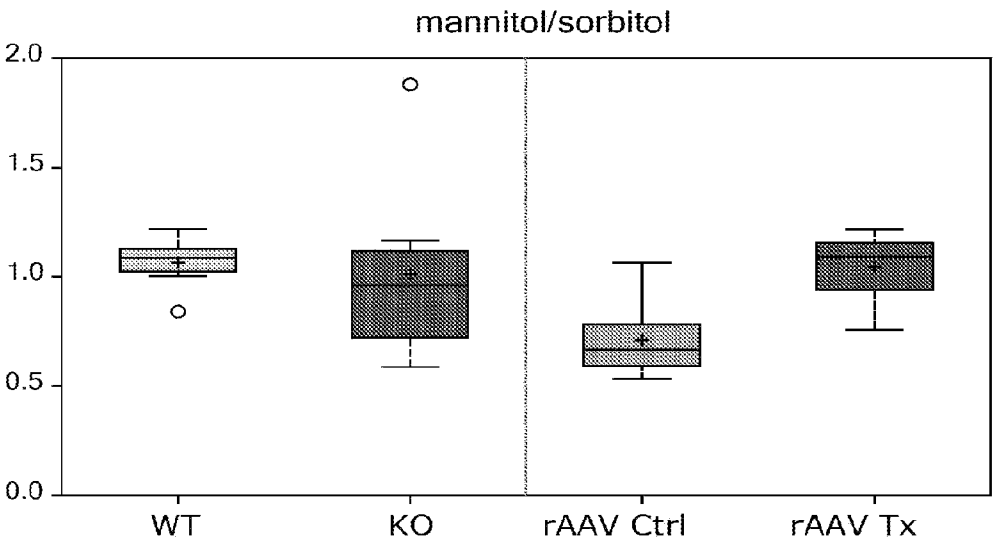
mannitol/sorbitol
2.0
1.5
1.0
0.5
0.0
WT
KO
rAAV Ctrl
rAAV Tx

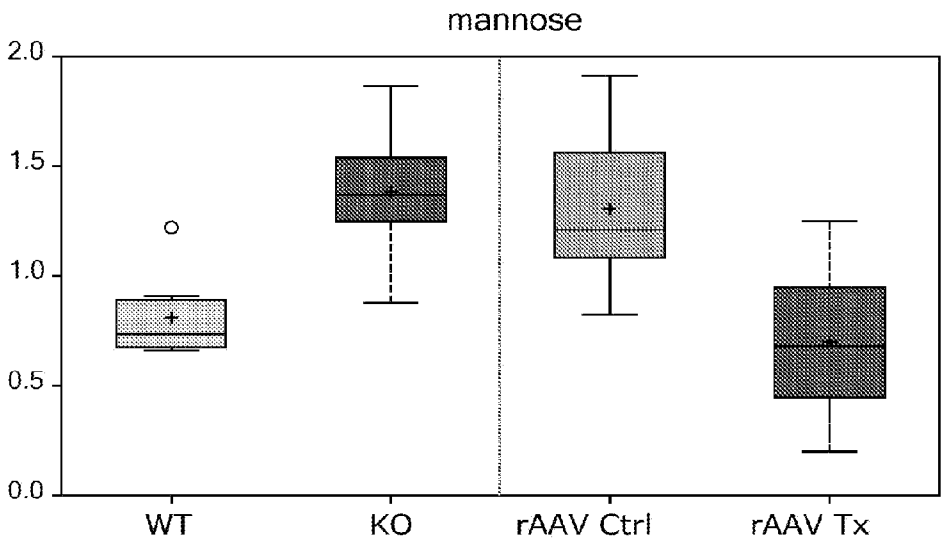
mannose
2.0
1.5
1.0
0.5
0.0
WT
KO
rAAV Ctrl
rAAV Tx

FIG. 57 cont.

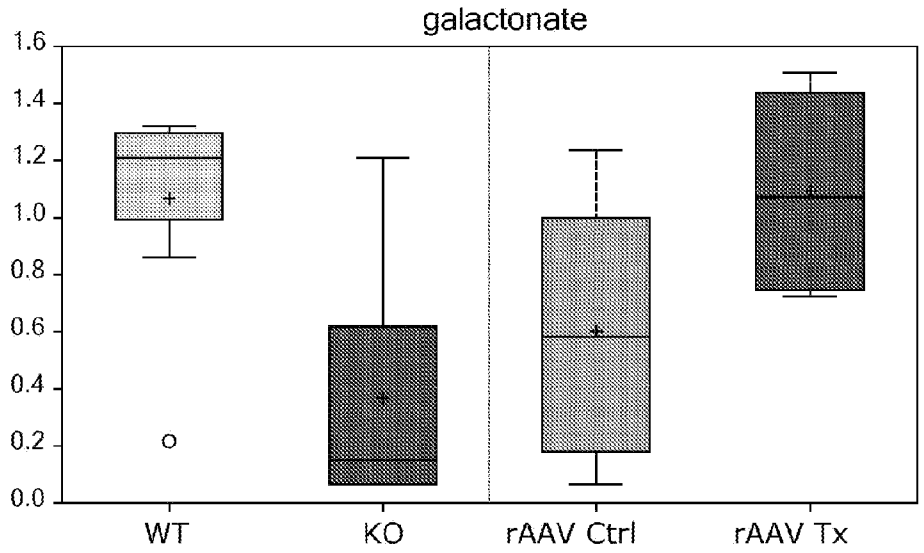
galactonate
1.6
1.4
1.2
1.0
0.8
0.6
0.4
0.2
0.0
WT
KO
rAAV Ctrl
rAAV Tx

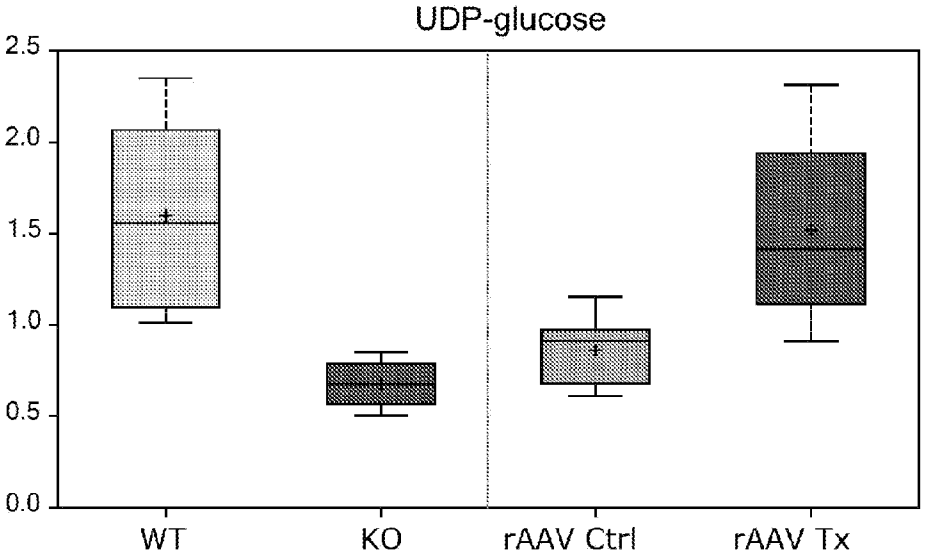
UDP-glucose
2.5
2.0
1.5
1.0
0.5
0.0
WT
KO
rAAV Ctrl
rAAV Tx

FIG. 57 cont.

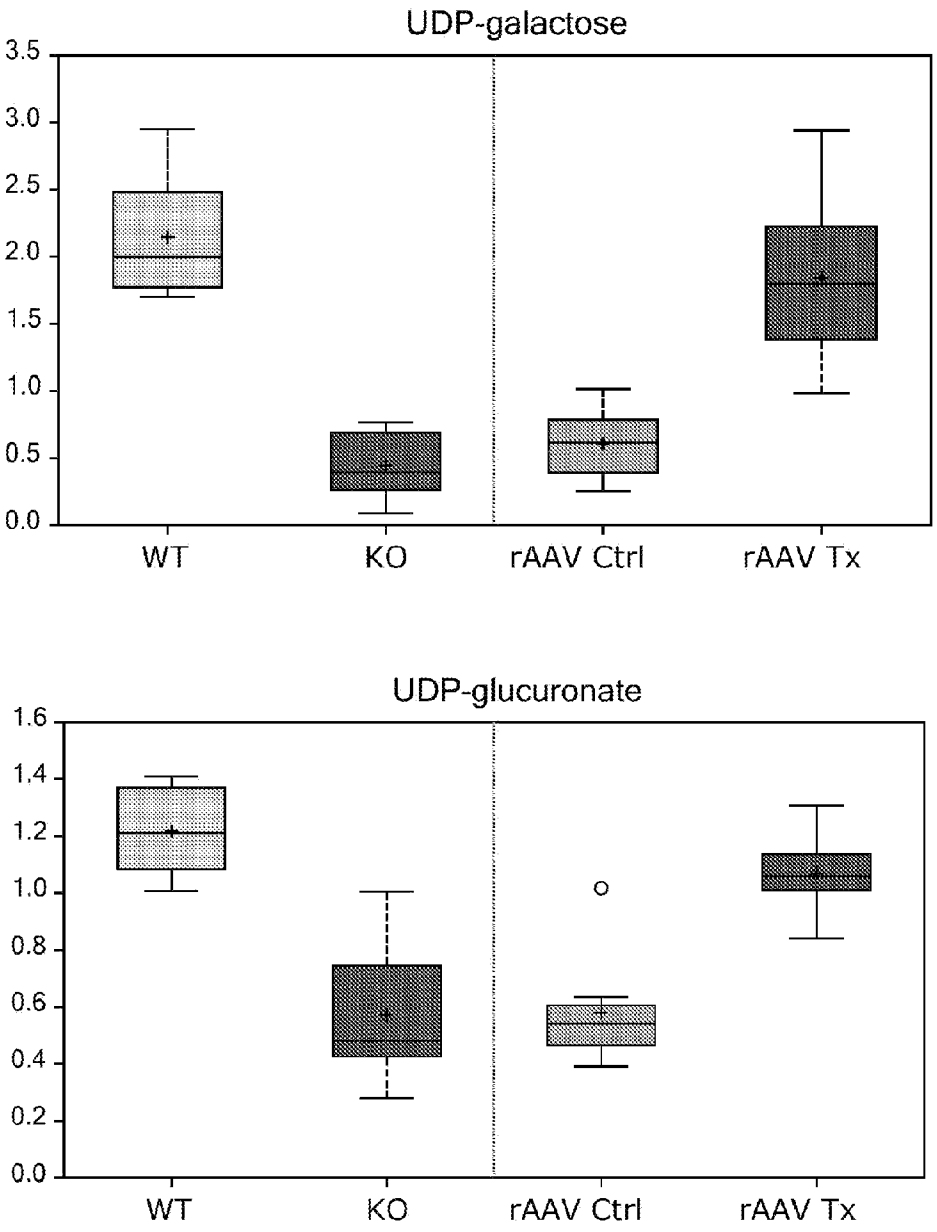
UDP-galactose
3.5
3.0
2.5
2.0
1.5
1.0
0.5
0.0
WT
KO
rAAV Ctrl
rAAV Tx
UDP-glucuronate
1.6
1.4
1.2
1.0
0.8
0.6
0.4
0.2
0.0
WT
KO
rAAV Ctrl
rAAV Tx

FIG. 57 cont.

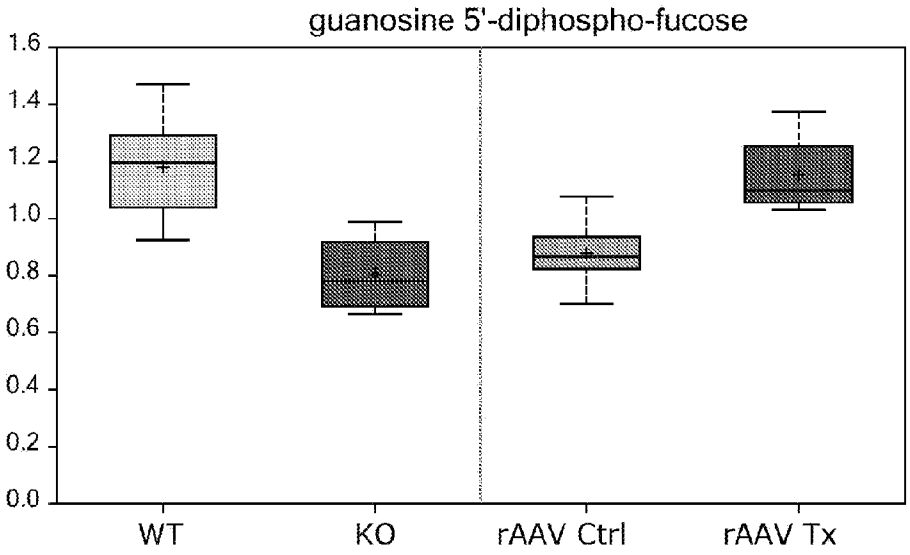
guanosine 5'-diphospho-fucose
1.6
1.4
1.2
1.0
0.8
0.6
0.4
0.2
0.0
WT
KO
rAAV Ctrl
rAAV Tx

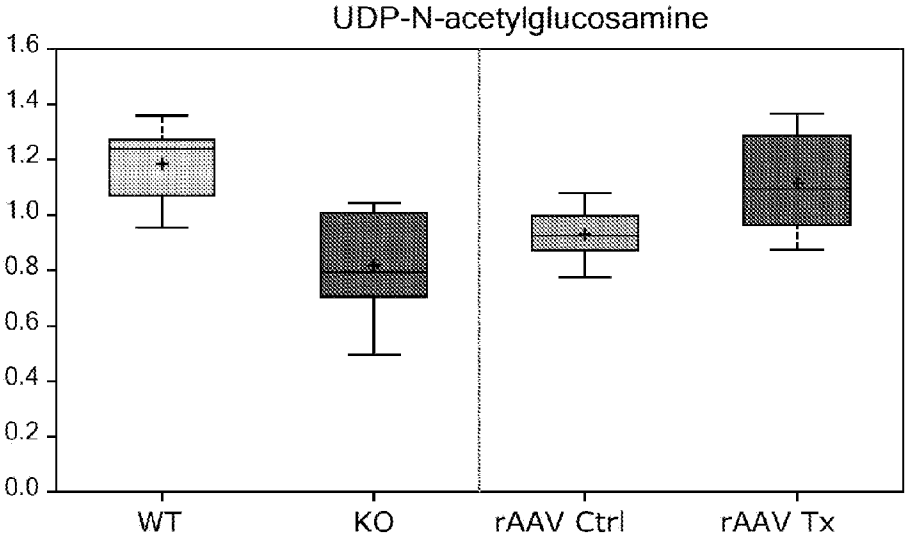
UDP-N-acetylglucosamine
1.6
1.4
1.2
1.0
0.8
0.6
0.4
0.2
0.0
WT
KO
rAAV Ctrl
rAAV Tx

FIG. 57 cont.

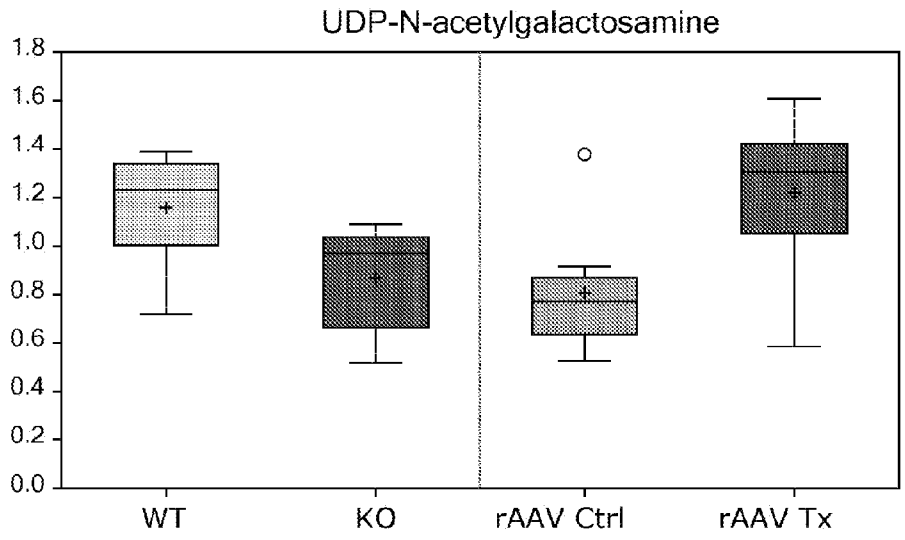
UDP-N-acetylgalactosamine
1.8
1.6
1.4
1.2
1.0
0.8
0.6
0.4
0.2
0.0
WT
KO
rAAV Ctrl
rAAV Tx

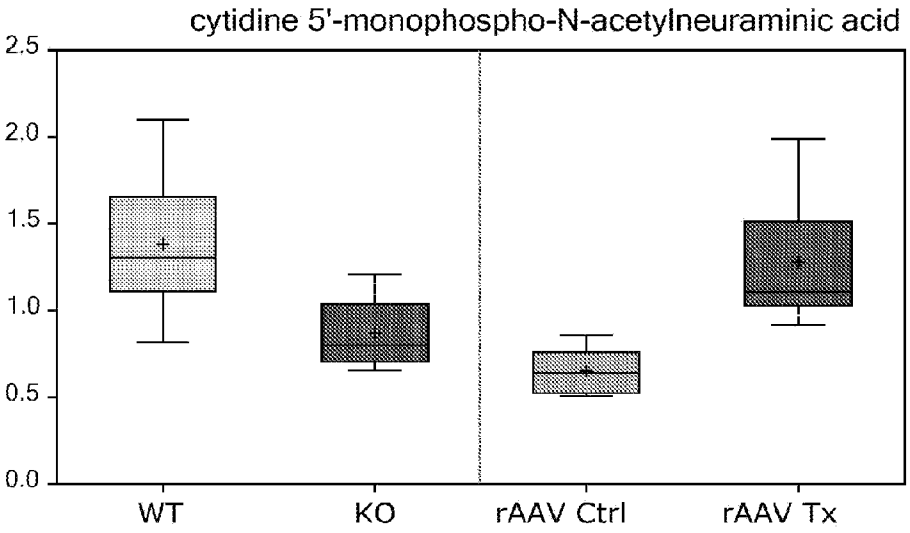
cytidine 5'-monophospho-N-acetylneuraminic acid
2.5
2.0
1.5
1.0
0.5
0.0
WT
KO
rAAV Ctrl
rAAV Tx

FIG. 57 cont.

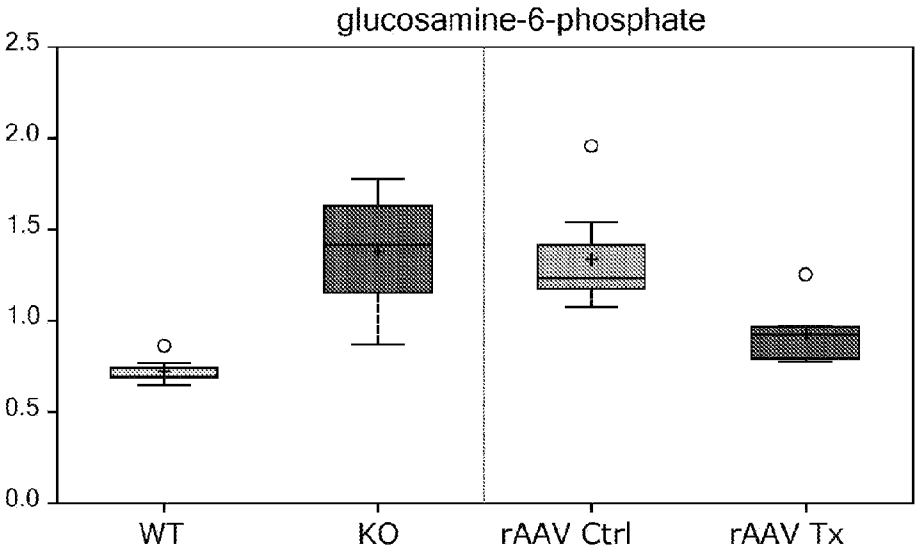
glucosamine-6-phosphate
2.5
2.0
1.5
1.0
0.5
0.0
WT
KO
rAAV Ctrl
rAAV Tx

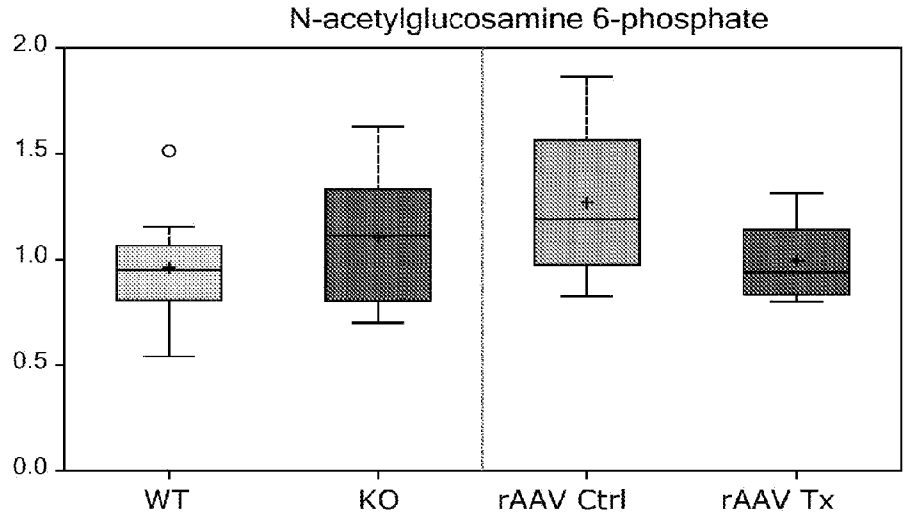
N-acetylglucosamine 6-phosphate
2.0
1.5
1.0
0.5
0.0
WT
KO
rAAV Ctrl
rAAV Tx

FIG. 57 cont.

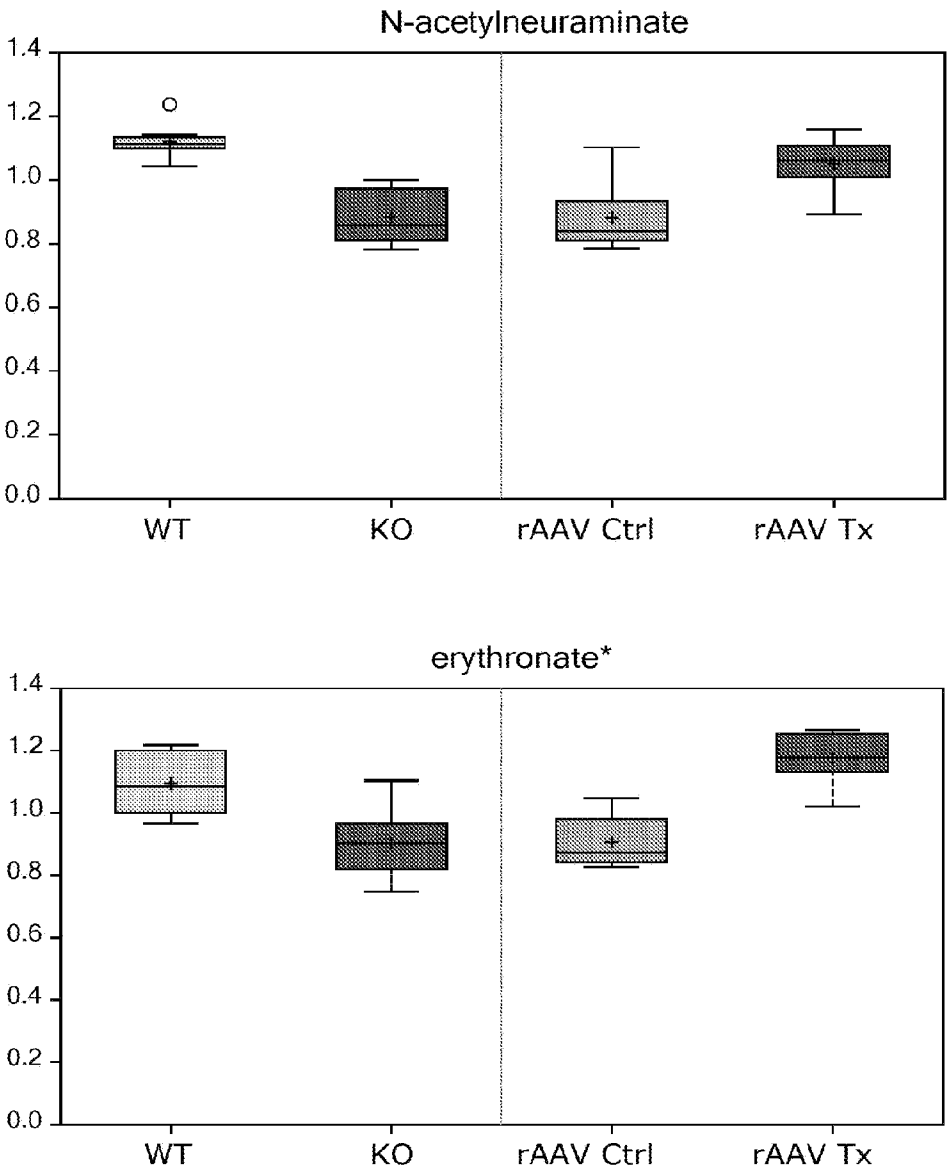
N-acetylneuraminate
1.4
1.2
1.0
0.8
0.6
0.4
0.2
0.0
WT
KO
rAAV Ctrl
rAAV Tx
erythronate*
1.4
1.2
1.0
0.8
0.6
0.4
0.2
0.0
WT
KO
rAAV Ctrl
rAAV Tx

FIG. 57 cont.

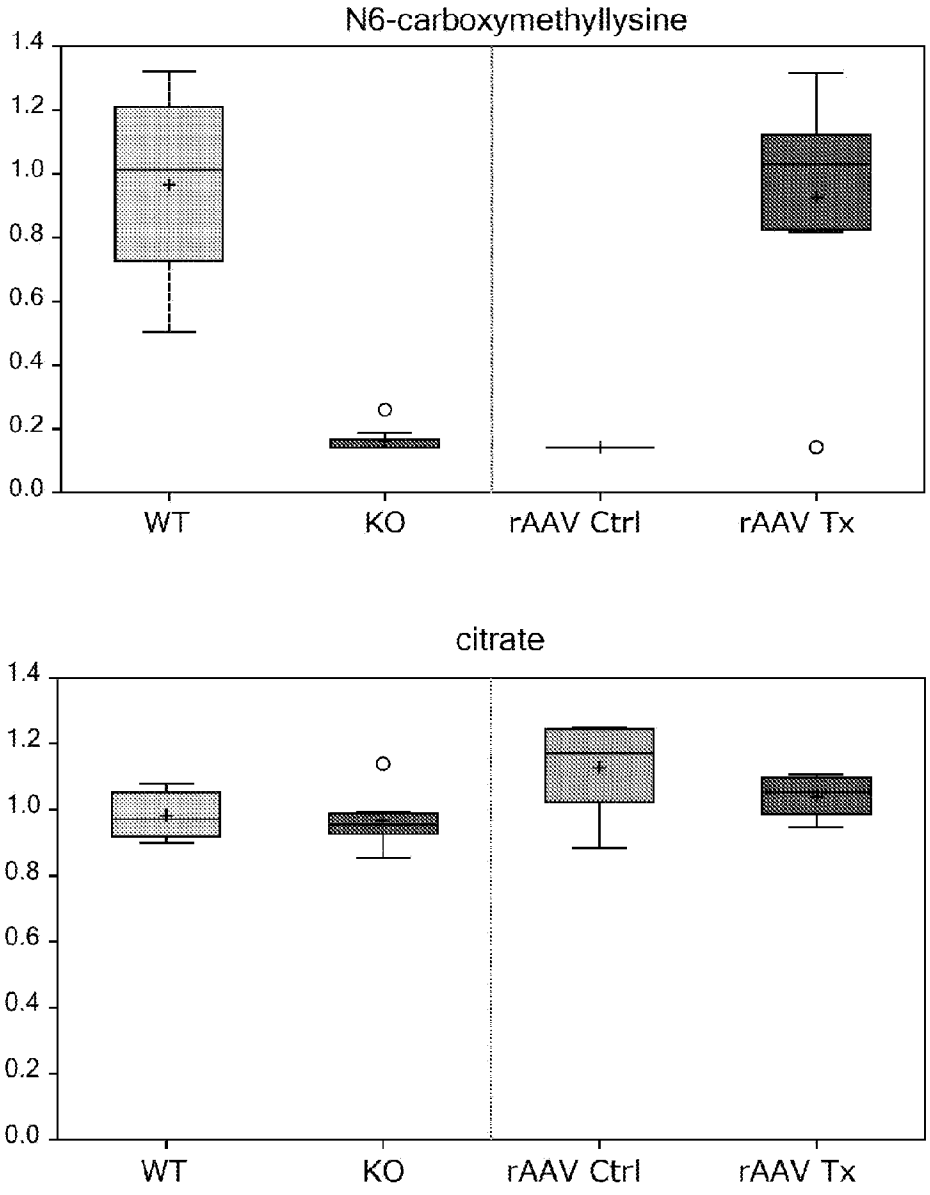
N6-carboxymethyllysine
1.4
1.2
1.0
0.8
0.6
0.4
0.2
0.0
WT
KO
rAAV Ctrl
rAAV Tx
citrate
1.4
1.2
1.0
0.8
0.6
0.4
0.2
0.0
WT
KO
rAAV Ctrl
rAAV Tx

FIG. 57 cont.

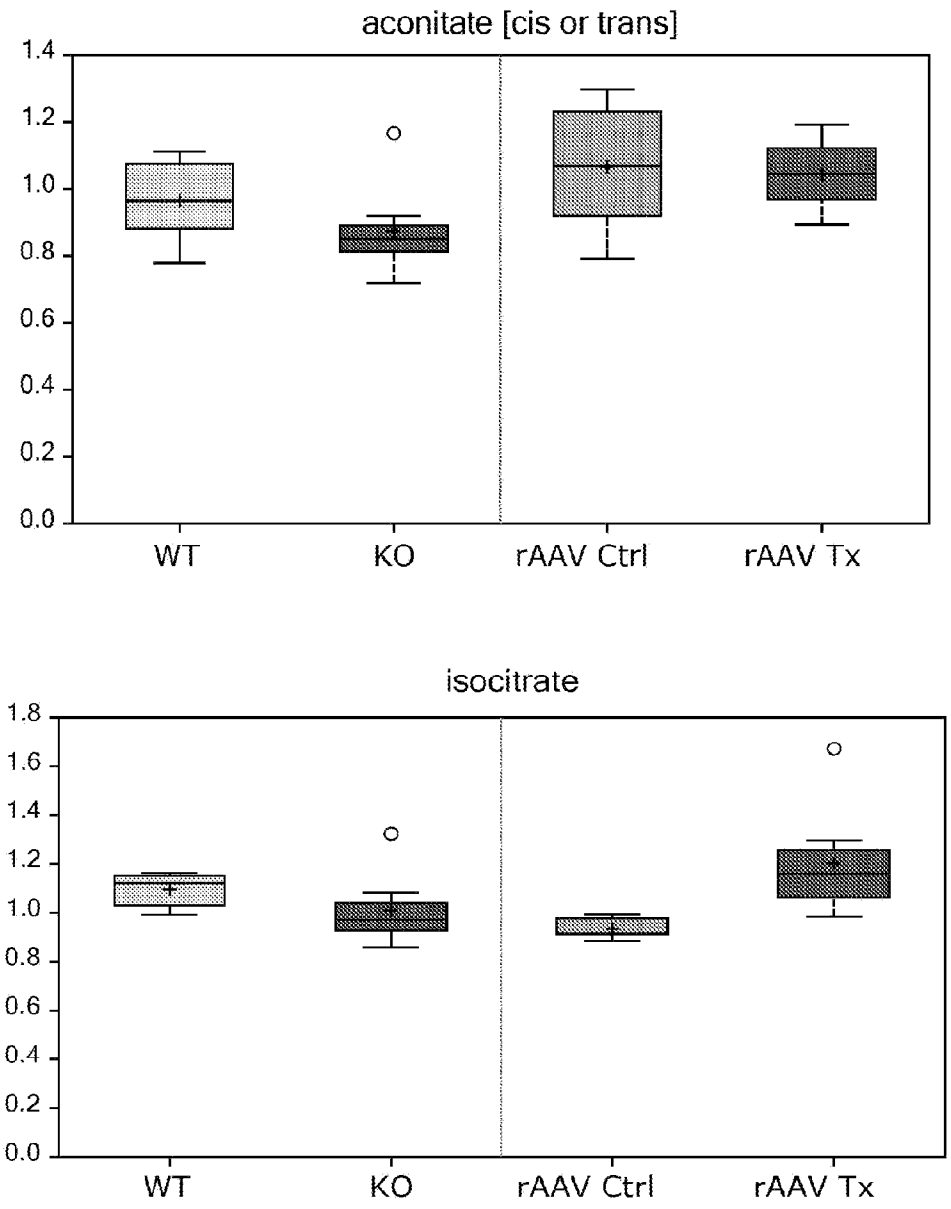
aconitate [cis or trans]
1.4
1.2
1.0
0.8
0.6
0.4
0.2
0.0
WT
KO
rAAV Ctrl
rAAV Tx
isocitrate
1.8
1.6
1.4
1.2
1.0
0.8
0.6
0.4
0.2
0.0
WT
KO
rAAV Ctrl
rAAV Tx

FIG. 57 cont.

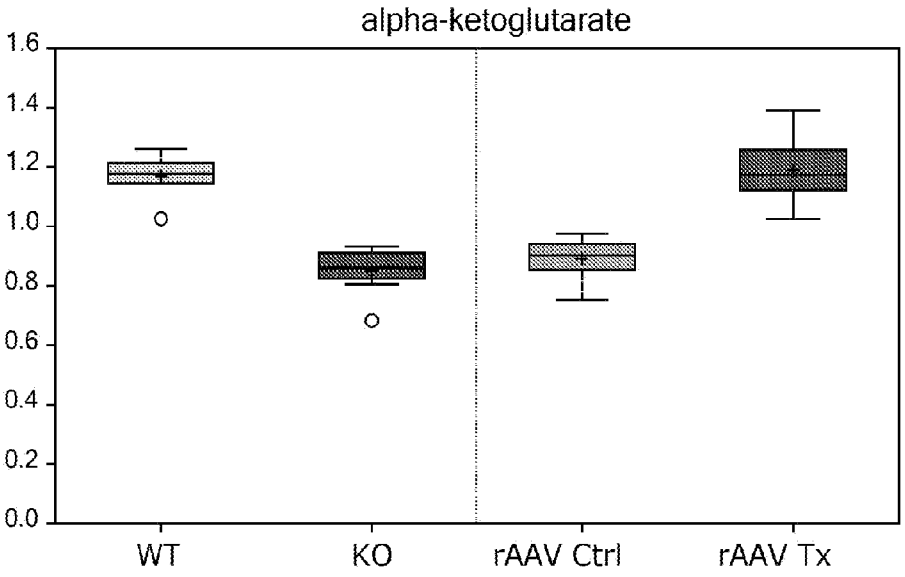
alpha-ketoglutarate
1.6
1.4
1.2
1.0
0.8
0.6
0.4
0.2
0.0
WT
KO
rAAV Ctrl
rAAV Tx

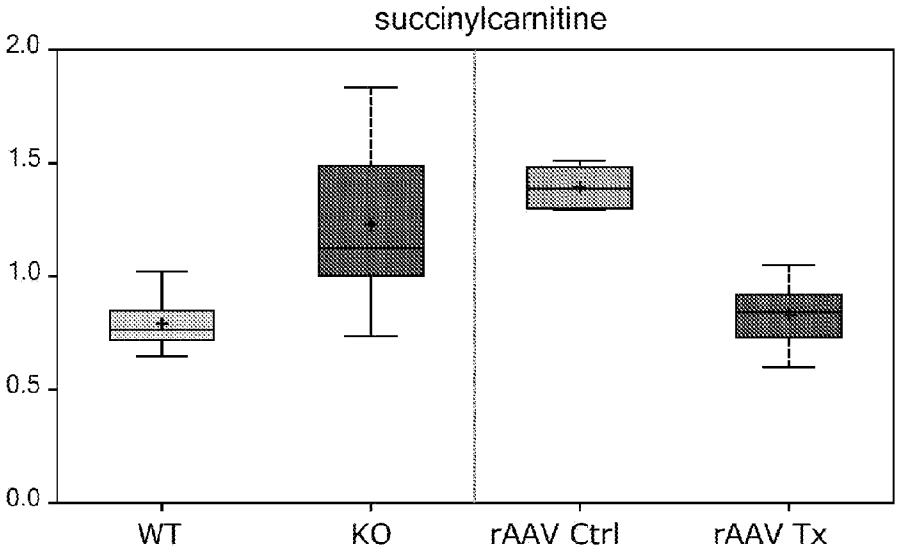
succinylcarnitine
2.0
1.5
1.0
0.5
0.0
WT
KO
rAAV Ctrl
rAAV Tx

FIG. 57 cont.

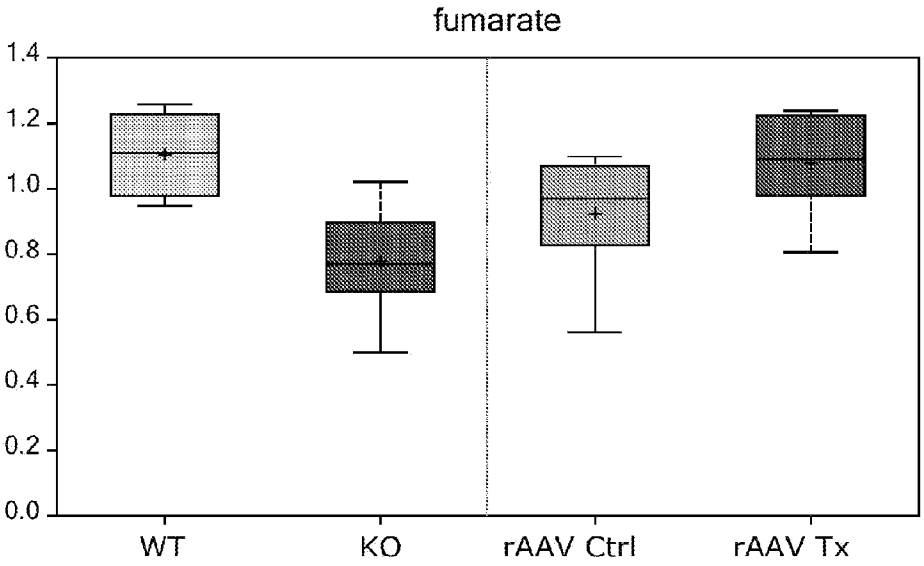
fumarate
1.4
1.2
1.0
0.8
0.6
0.4
0.2
0.0
WT
KO
rAAV Ctrl
rAAV Tx

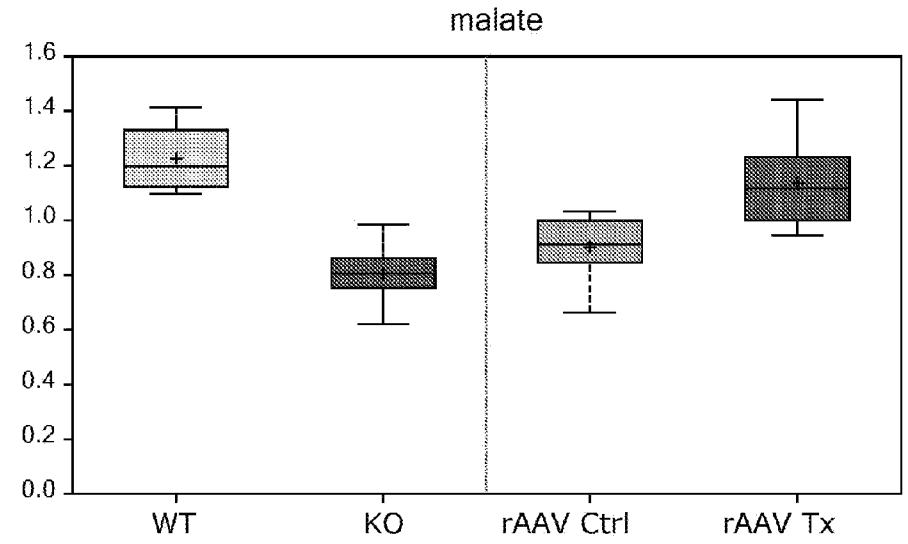
malate
1.6
1.4
1.2
1.0
0.8
0.6
0.4
0.2
0.0
WT
KO
rAAV Ctrl
rAAV Tx

FIG. 57 cont.

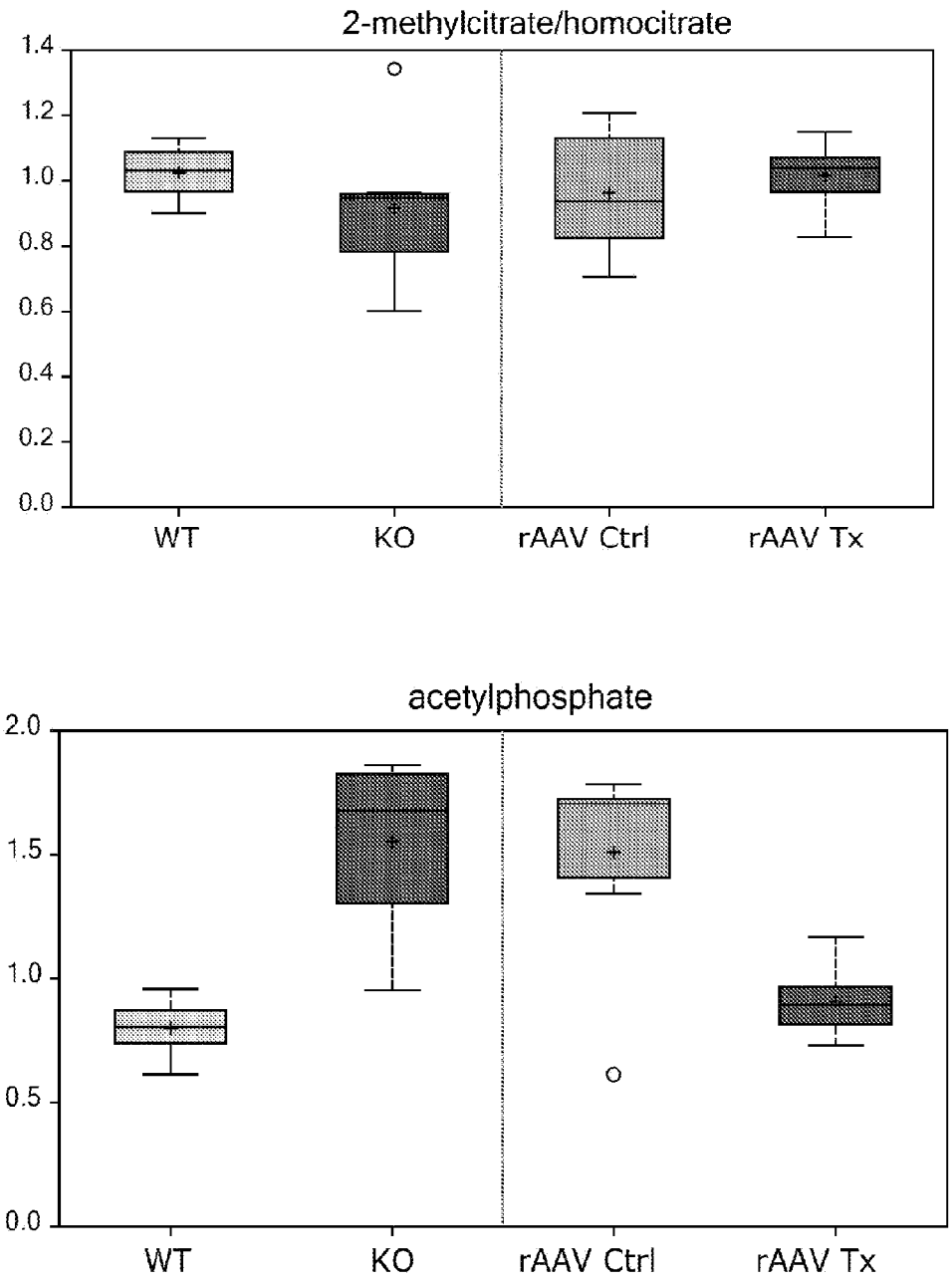
2-methylcitrate/homocitrate
1.4
1.2
1.0
0.8
0.6
0.4
0.2
0.0
WT
KO
rAAV Ctrl
rAAV Tx
acetylphosphate
2.0
1.5
1.0
0.5
0.0
WT
KO
rAAV Ctrl
rAAV Tx

FIG. 57 cont.

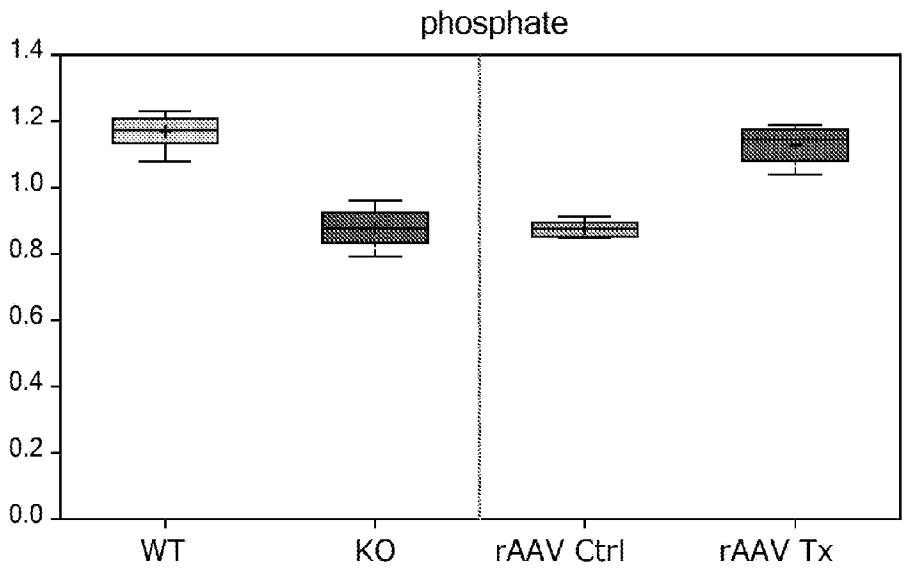
phosphate
1.4
1.2
1.0
0.8
0.6
0.4
0.2
0.0
WT
KO
rAAV Ctrl
rAAV Tx

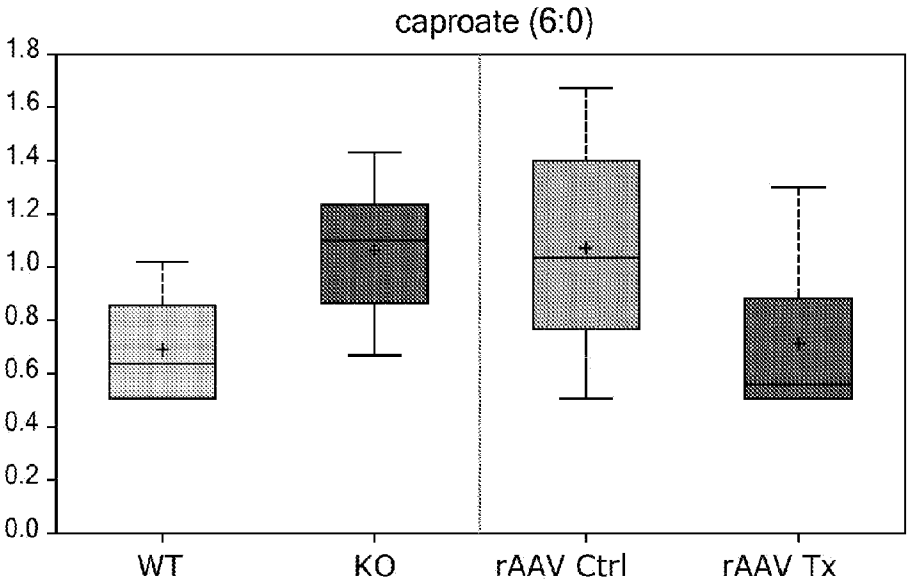
caproate (6:0)
1.8
1.6
1.4
1.2
1.0
0.8
0.6
0.4
0.2
0.0
WT
KO
rAAV Ctrl
rAAV Tx

FIG. 57 cont.

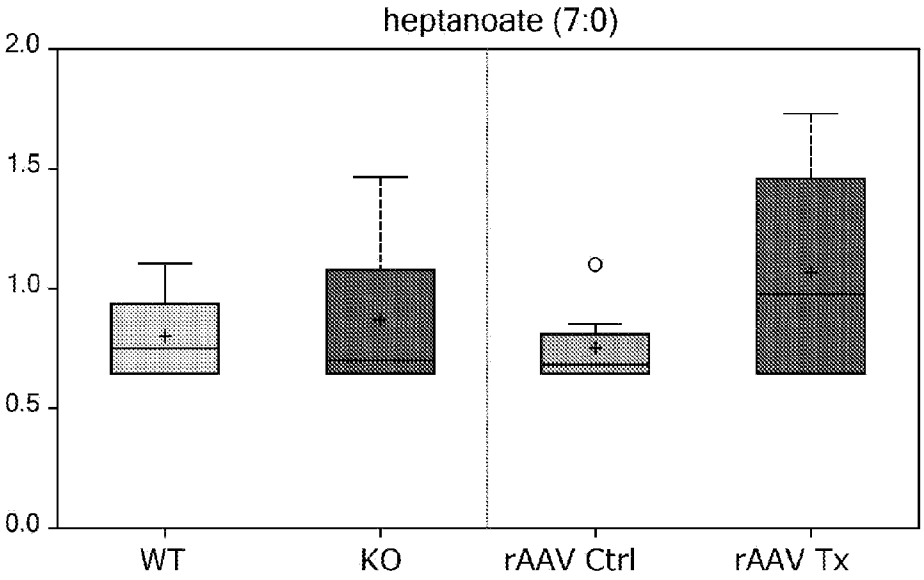
heptanoate (7:0)
2.0
1.5
1.0
0.5
0.0
WT
KO
rAAV Ctrl
rAAV Tx

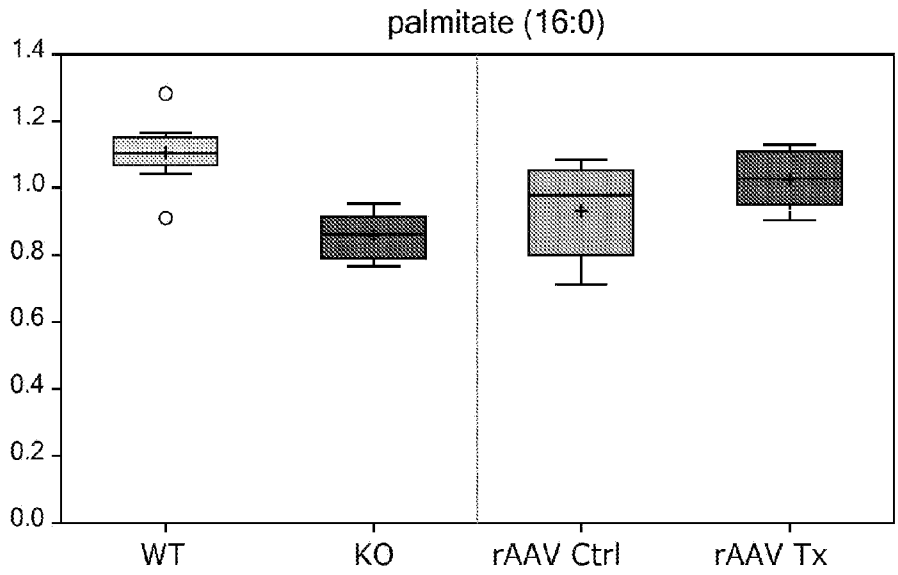
palmitate (16:0)
1.4
1.2
1.0
0.8
0.6
0.4
0.2
0.0
WT
KO
rAAV Ctrl
rAAV Tx

FIG. 57 cont.

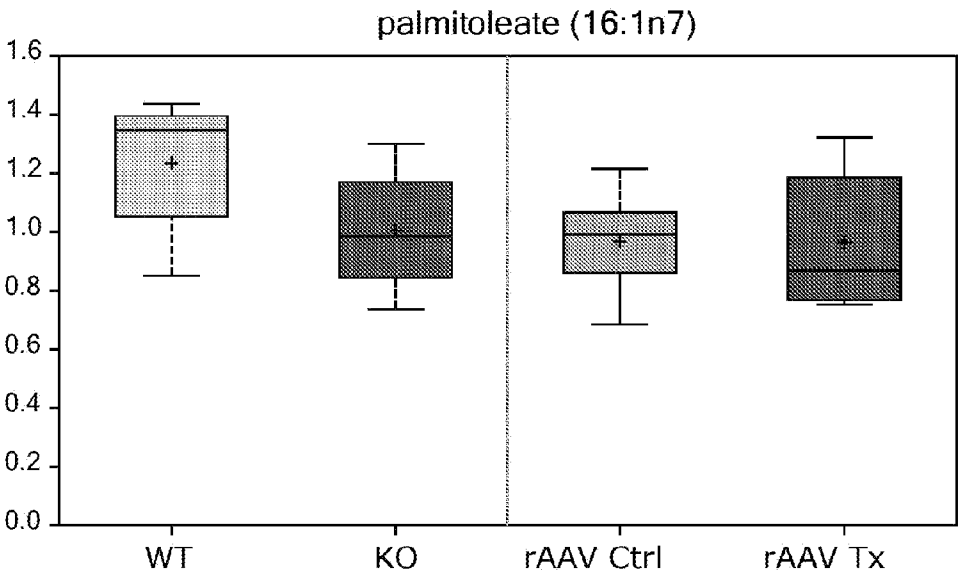
palmitoleate (16:1n7)
1.6
1.4
1.2
1.0
0.8
0.6
0.4
0.2
0.0
WT
KO
rAAV Ctrl
rAAV Tx

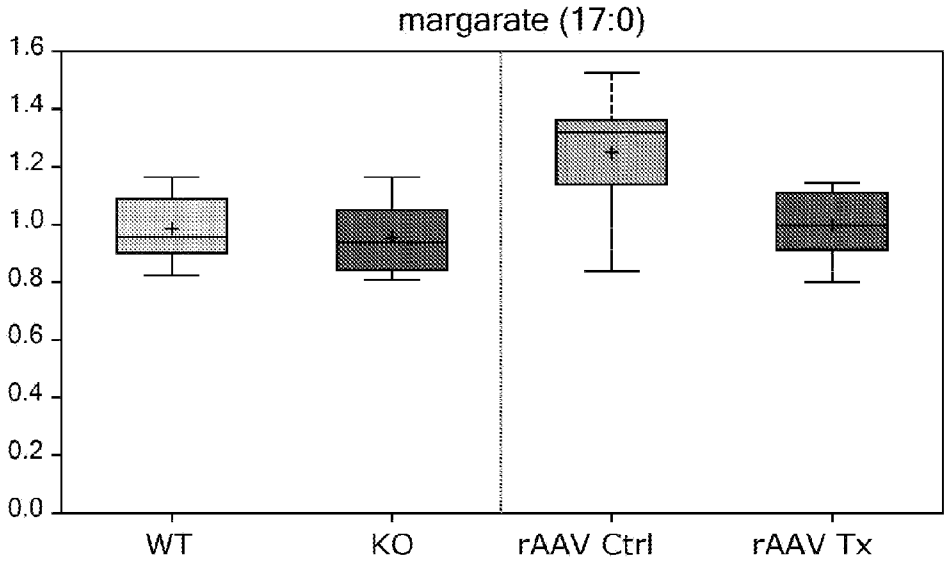
margarate (17:0)
1.6
1.4
1.2
1.0
0.8
0.6
0.4
0.2
0.0
WT
KO
rAAV Ctrl
rAAV Tx

FIG. 57 cont.

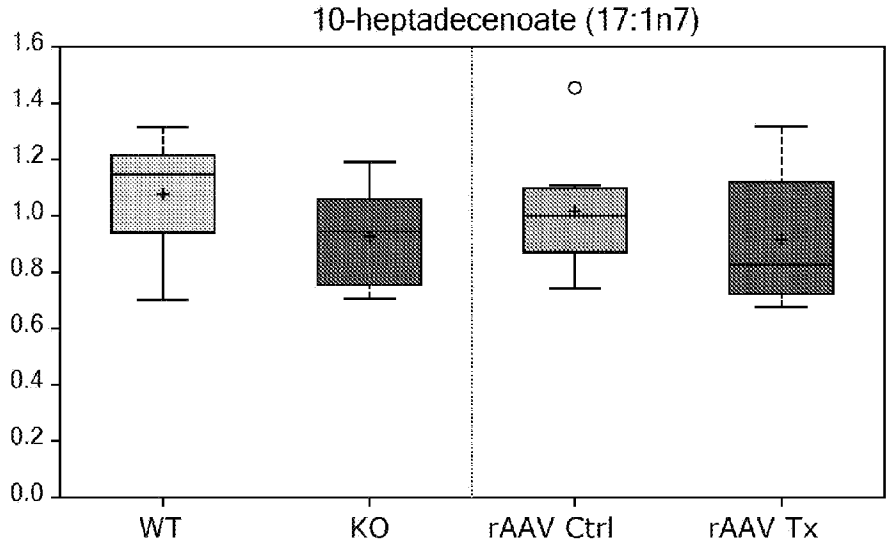
10-heptadecenoate (17:1n7)
1.6
1.4
1.2
1.0
0.8
0.6
0.4
0.2
0.0
WT
KO
rAAV Ctrl
rAAV Tx

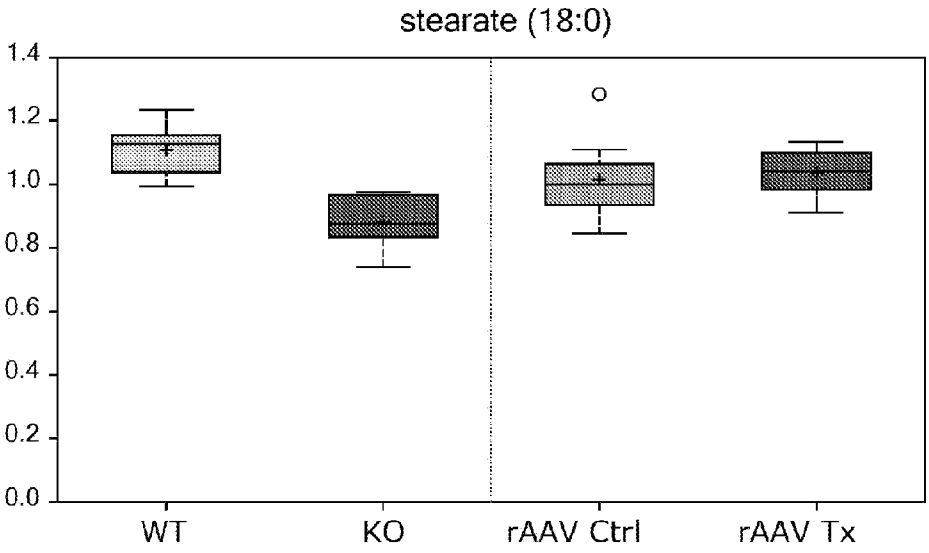
stearate (18:0)
1.4
1.2
1.0
0.8
0.6
0.4
0.2
0.0
WT
KO
rAAV Ctrl
rAAV Tx

FIG. 57 cont.

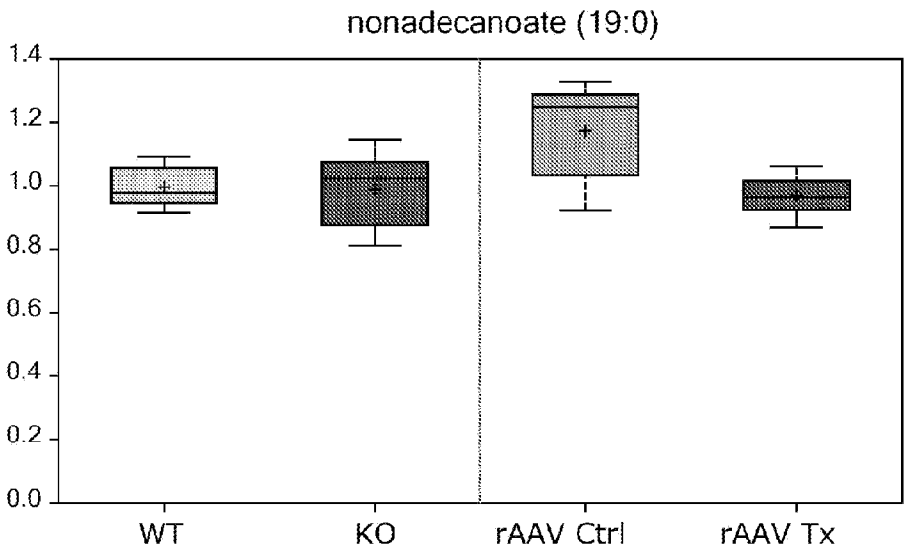
nonadecanoate (19:0)
1.4
1.2
1.0
0.8
0.6
0.4
0.2
0.0
WT
KO
rAAV Ctrl
rAAV Tx

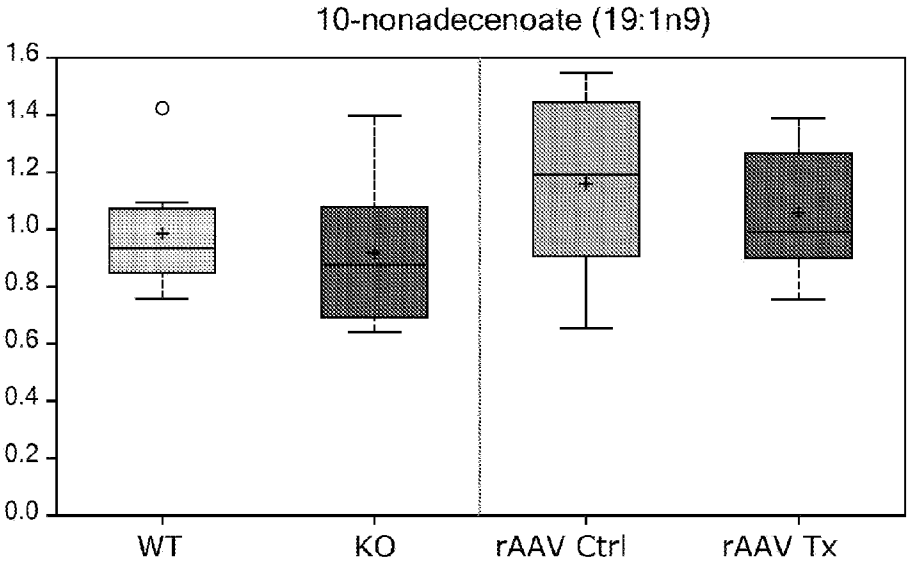
10-nonadecenoate (19:1n9)
1.6
1.4
1.2
1.0
0.8
0.6
0.4
0.2
0.0
WT
KO
rAAV Ctrl
rAAV Tx

FIG. 57 cont.

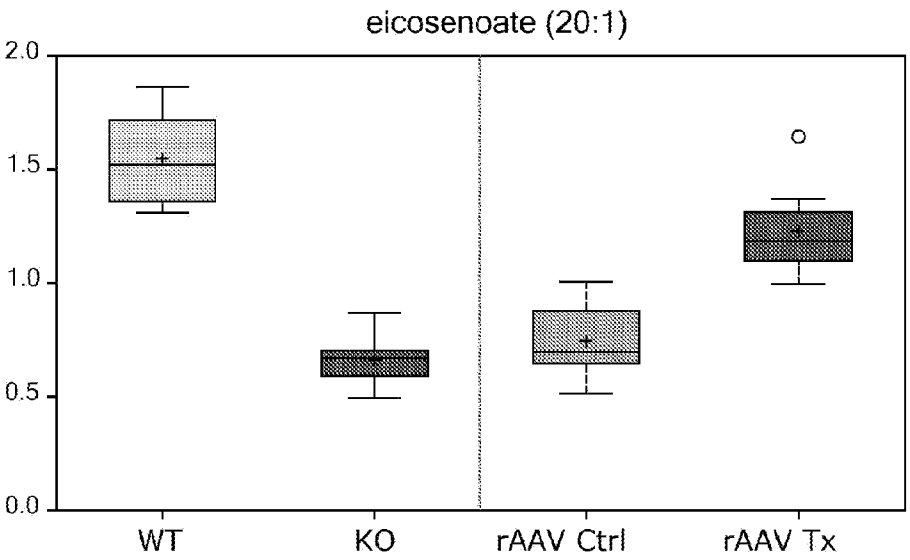
eicosenoate (20:1)
2.0
1.5
1.0
0.5
0.0
WT
KO
rAAV Ctrl
rAAV Tx

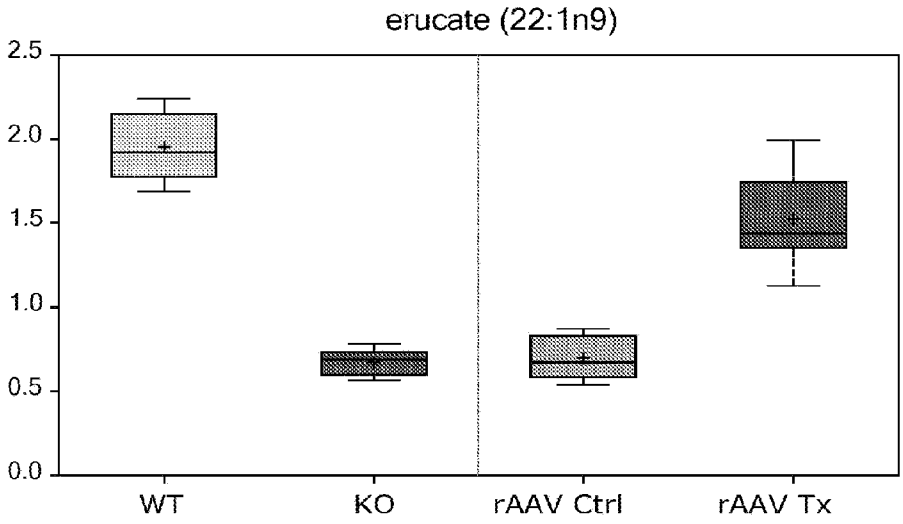
erucate (22:1n9)
2.5
2.0
1.5
1.0
0.5
0.0
WT
KO
rAAV Ctrl
rAAV Tx

FIG. 57 cont.

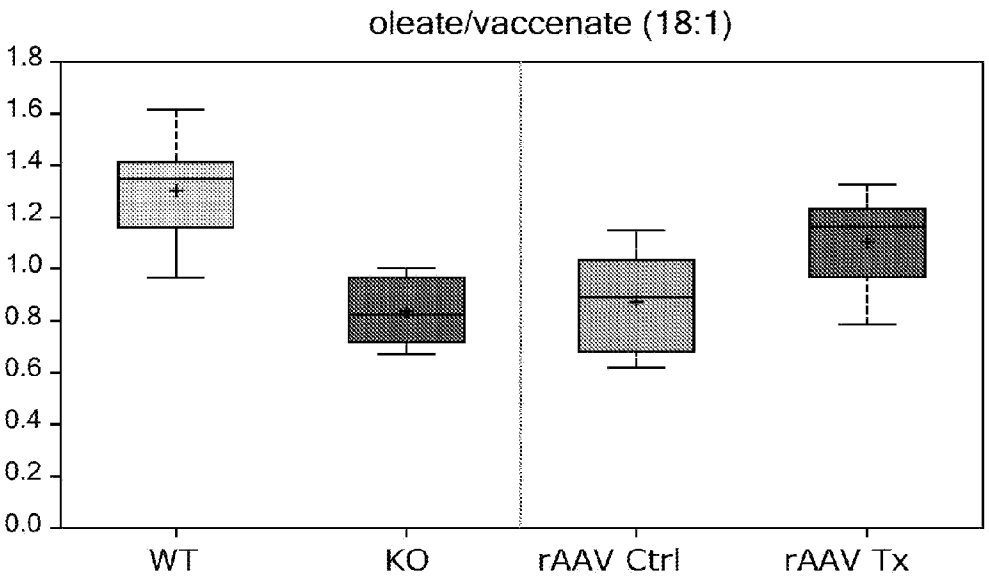
oleate/vaccenate (18:1)
1.8
1.6
1.4
1.2
1.0
0.8
0.6
0.4
0.2
0.0
WT
KO
rAAV Ctrl
rAAV Tx

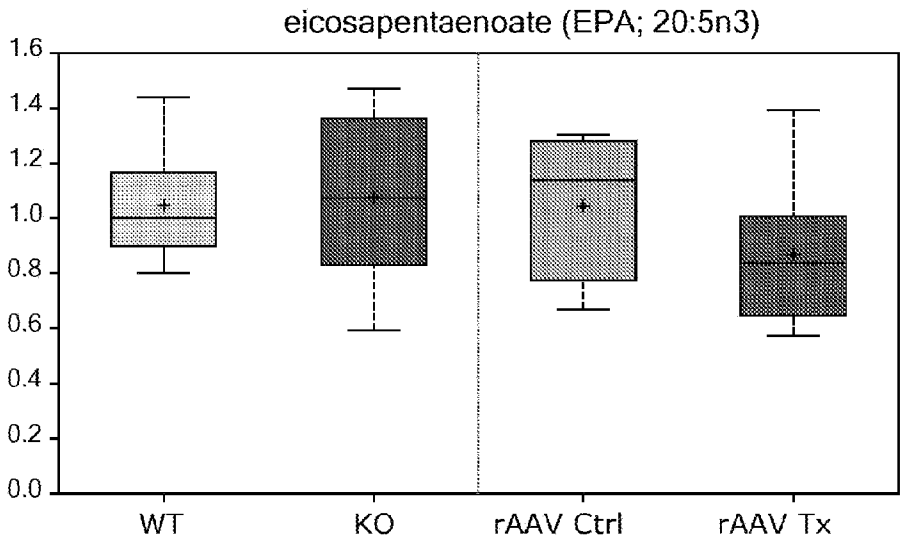
eicosapentaenoate (EPA; 20:5n3)
1.6
1.4
1.2
1.0
0.8
0.6
0.4
0.2
0.0
WT
KO
rAAV Ctrl
rAAV Tx

FIG. 57 cont.

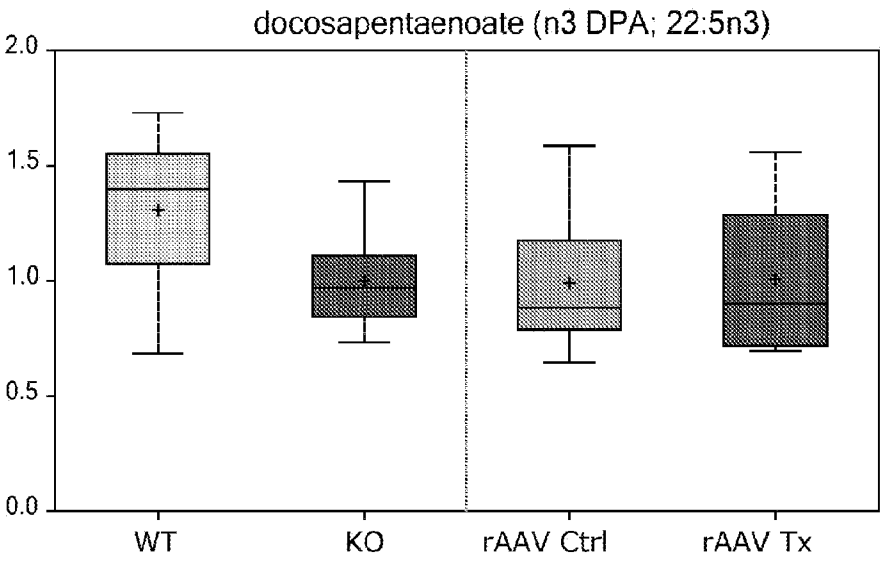
docosapentaenoate (n3 DPA; 22:5n3)
2.0
1.5
1.0
0.5
0.0
WT
KO
rAAV Ctrl
rAAV Tx

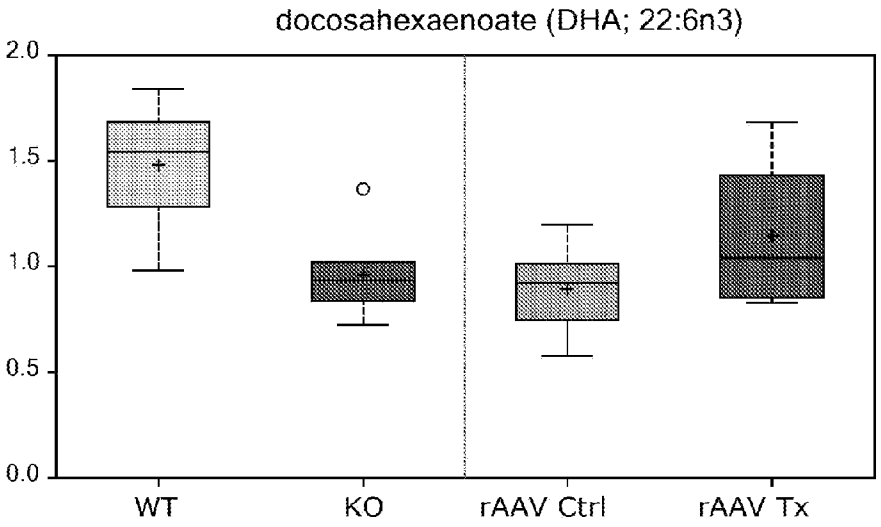
docosahexaenoate (DHA; 22:6n3)
2.0
1.5
1.0
0.5
0.0
WT
KO
rAAV Ctrl
rAAV Tx

FIG. 57 cont.

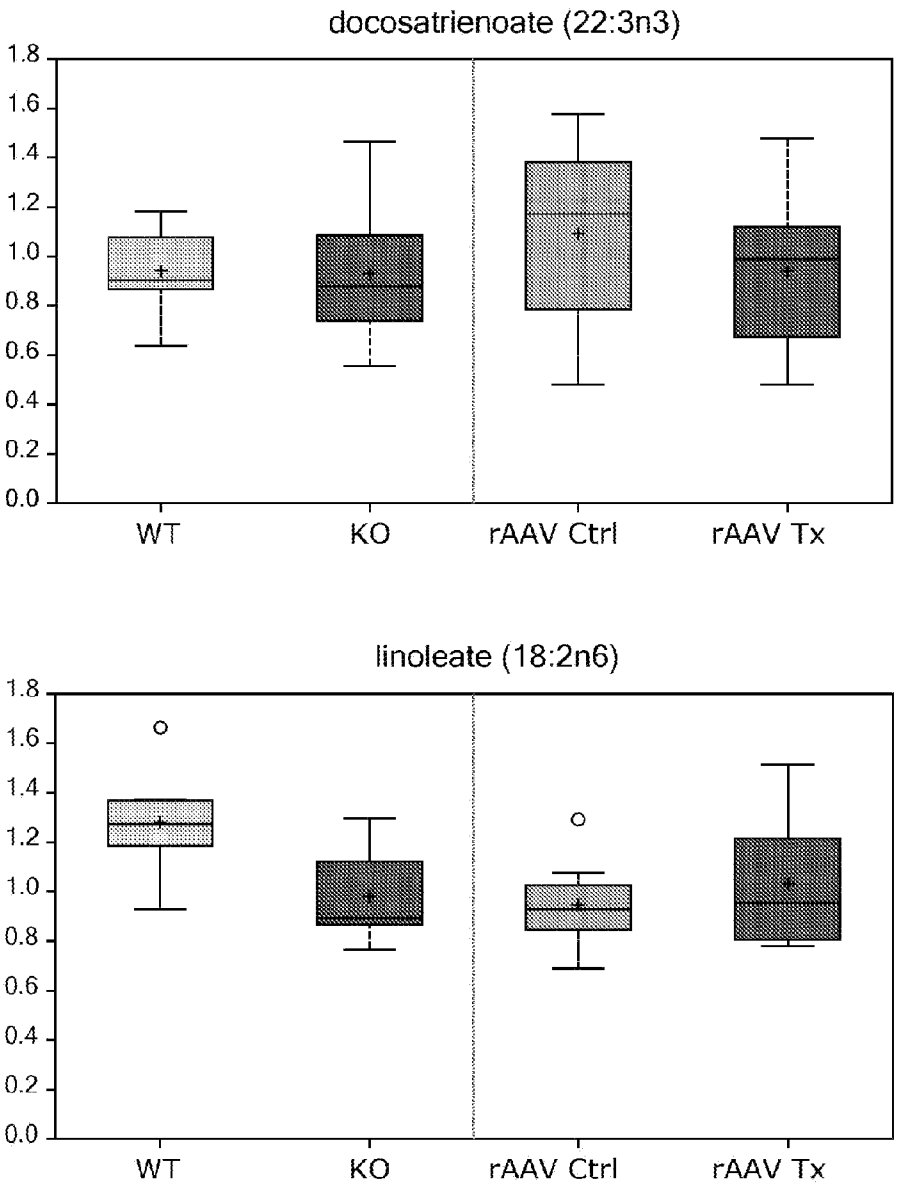
docosatrienoate (22:3n3)
1.8
1.6
1.4
1.2
1.0
0.8
0.6
0.4
0.2
0.0
WT
KO
rAAV Ctrl
rAAV Tx
linoleate (18:2n6)
1.8
1.6
1.4
1.2
1.0
0.8
0.6
0.4
0.2
0.0
WT
KO
rAAV Ctrl
rAAV Tx

FIG. 57 cont.

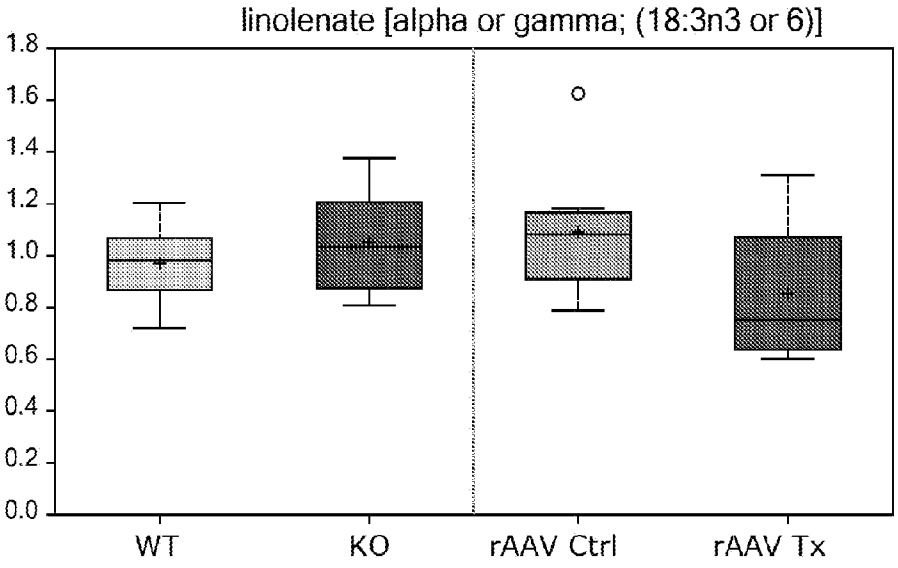
linolenate [alpha or gamma; (18:3n3 or 6)]
1.8
1.6
1.4
1.2
1.0
0.8
0.6
0.4
0.2
0.0
WT
KO
rAAV Ctrl
rAAV Tx

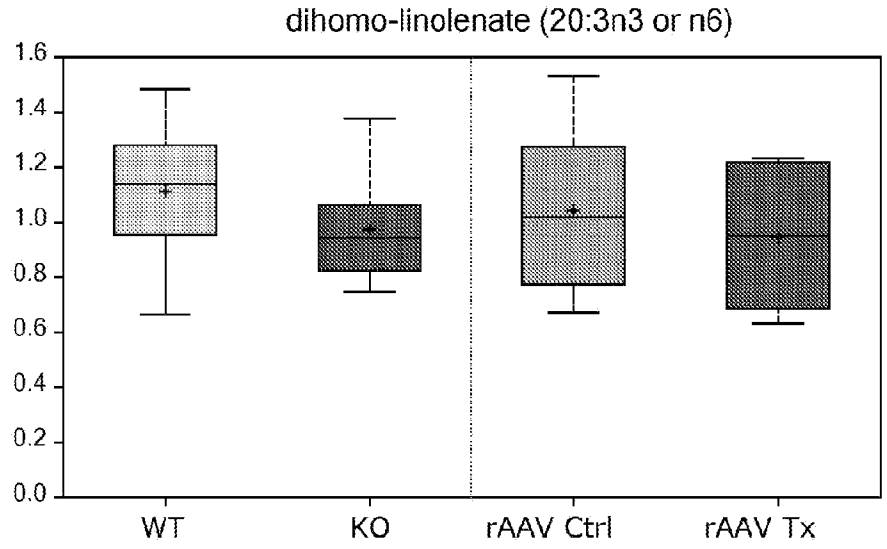
dihomo-linolenate (20:3n3 or n6)
1.6
1.4
1.2
1.0
0.8
0.6
0.4
0.2
0.0
WT
KO
rAAV Ctrl
rAAV Tx

FIG. 57 cont.

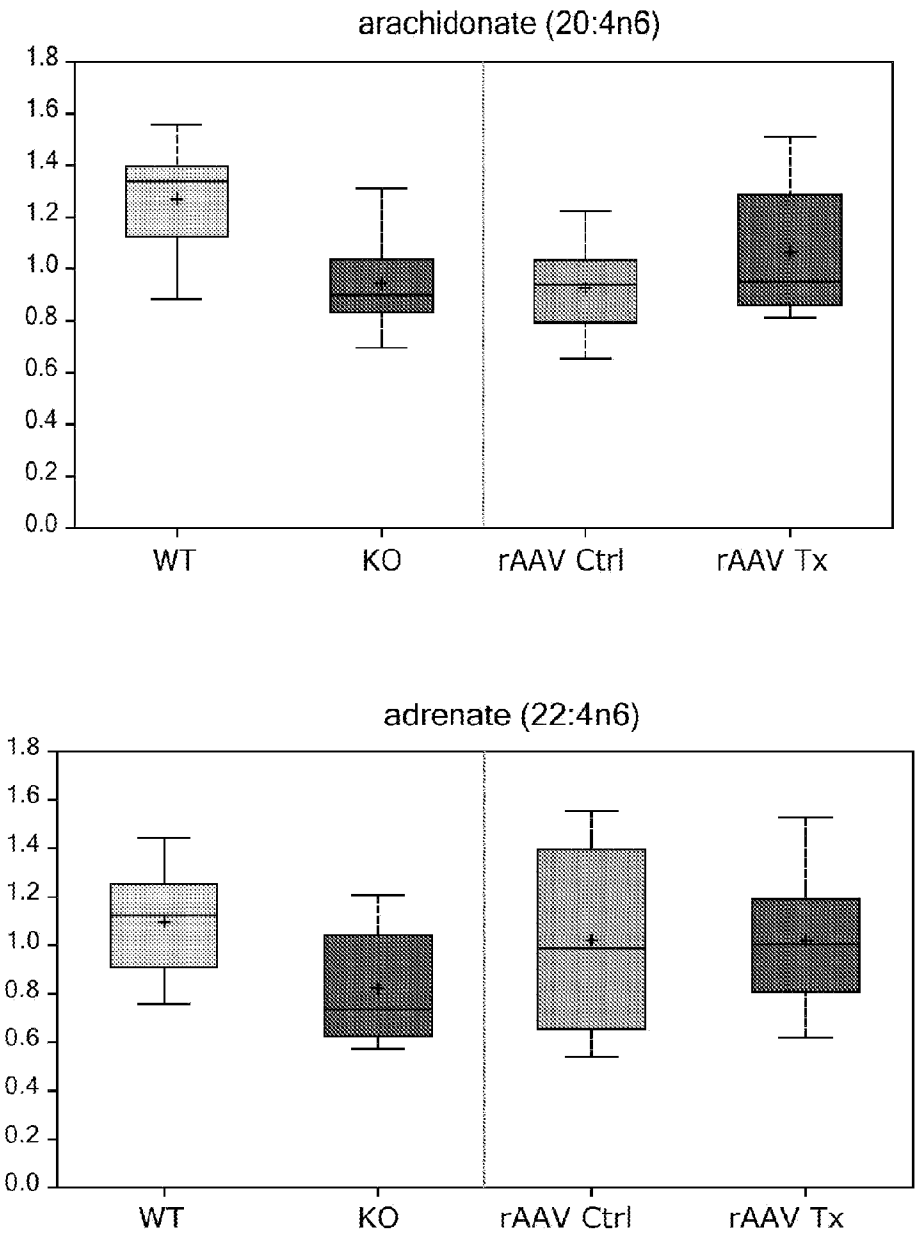
arachidonate (20:4n6)
1.8
1.6
1.4
1.2
1.0
0.8
0.6
0.4
0.2
0.0
WT
KO
rAAV Ctrl
rAAV Tx
adrenate (22:4n6)
1.8
1.6
1.4
1.2
1.0
0.8
0.6
0.4
0.2
0.0
WT
KO
rAAV Ctrl
rAAV Tx

FIG. 57 cont.

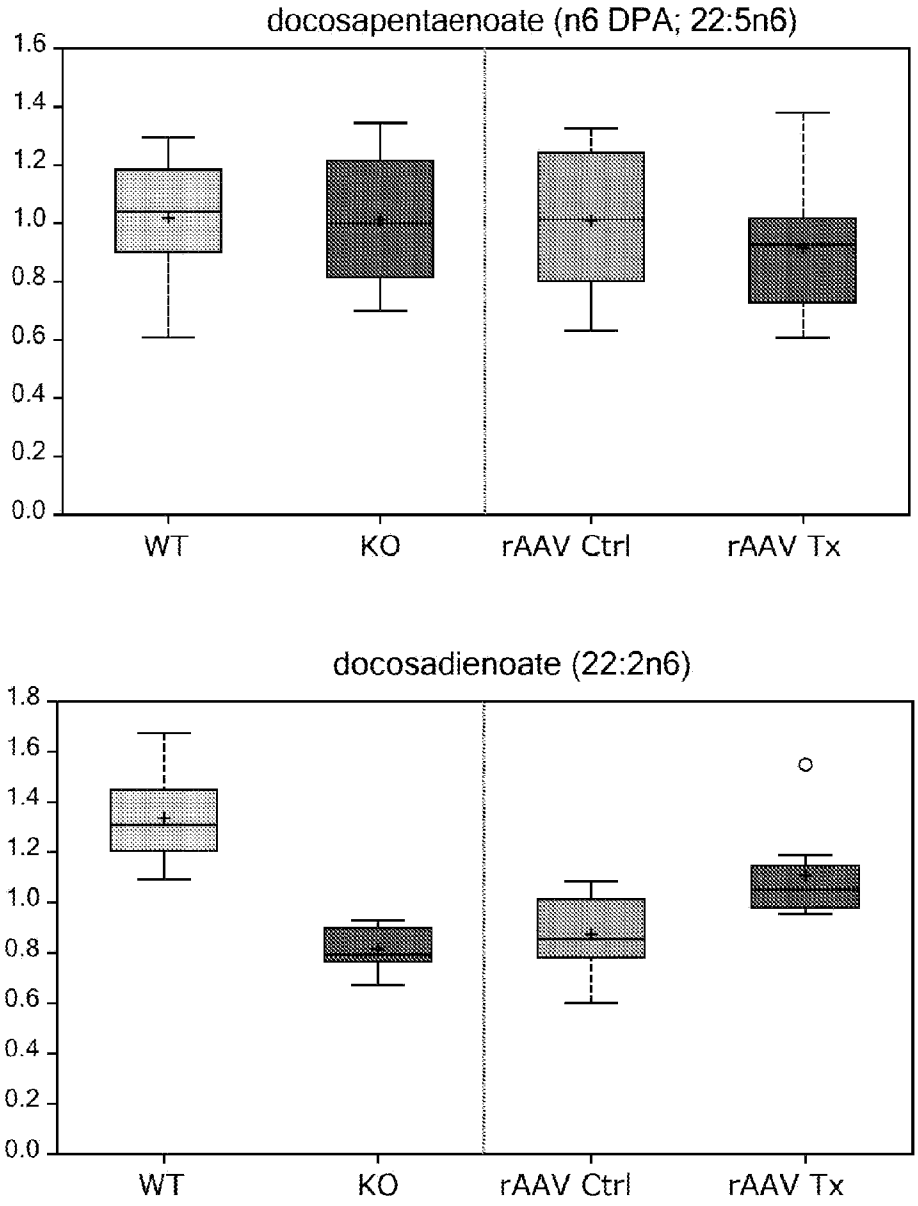
docosapentaenoate (n6 DPA; 22:5n6)
1.6
1.4
1.2
1.0
0.8
0.6
0.4
0.2
0.0
WT
KO
rAAV Ctrl
rAAV Tx
docosadienoate (22:2n6)
1.8
1.6
1.4
1.2
1.0
0.8
0.6
0.4
0.2
0.0
WT
KO
rAAV Ctrl
rAAV Tx

FIG. 57 cont.

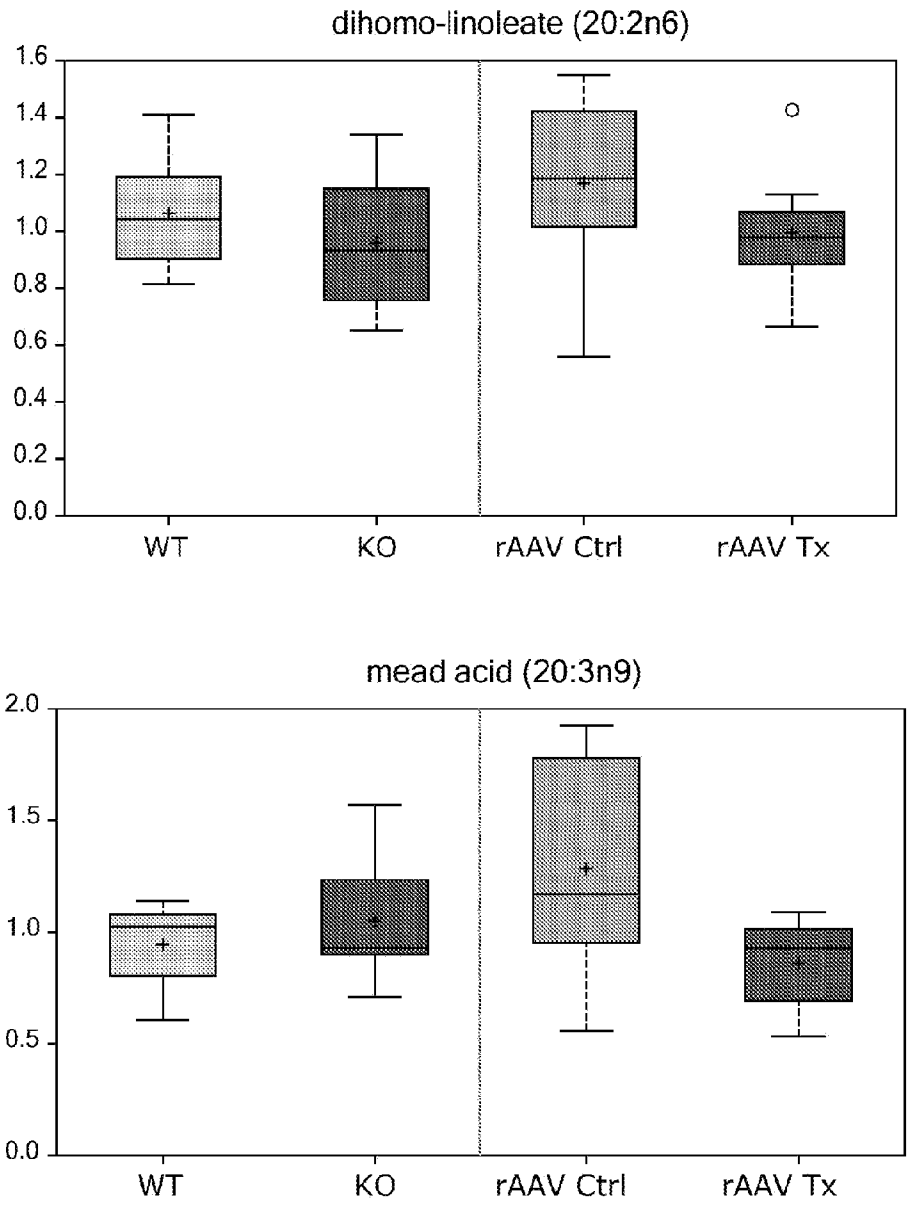
dihomo-linoleate (20:2n6)
1.6
1.4
1.2
1.0
0.8
0.6
0.4
0.2
0.0
WT
KO
rAAV Ctrl
rAAV Tx
mead acid (20:3n9)
2.0
1.5
1.0
0.5
0.0
WT
KO
rAAV Ctrl
rAAV Tx

FIG. 57 cont.

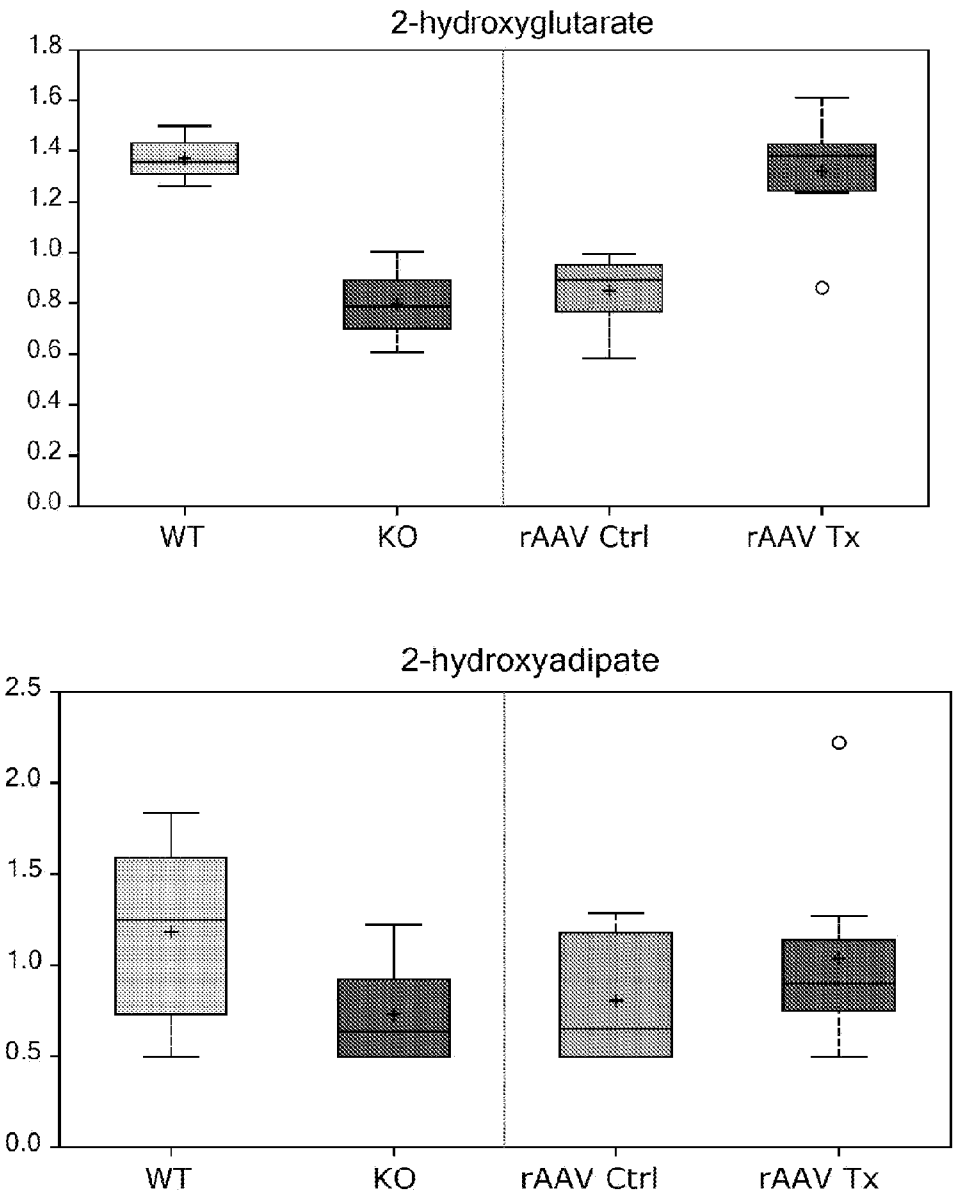
2-hydroxyglutarate
1.8
1.6
1.4
1.2
1.0
0.8
0.6
0.4
0.2
0.0
WT
KO
rAAV Ctrl
rAAV Tx
2-hydroxyadipate
2.5
2.0
1.5
1.0
0.5
0.0
WT
KO
rAAV Ctrl
rAAV Tx

FIG. 57 cont.

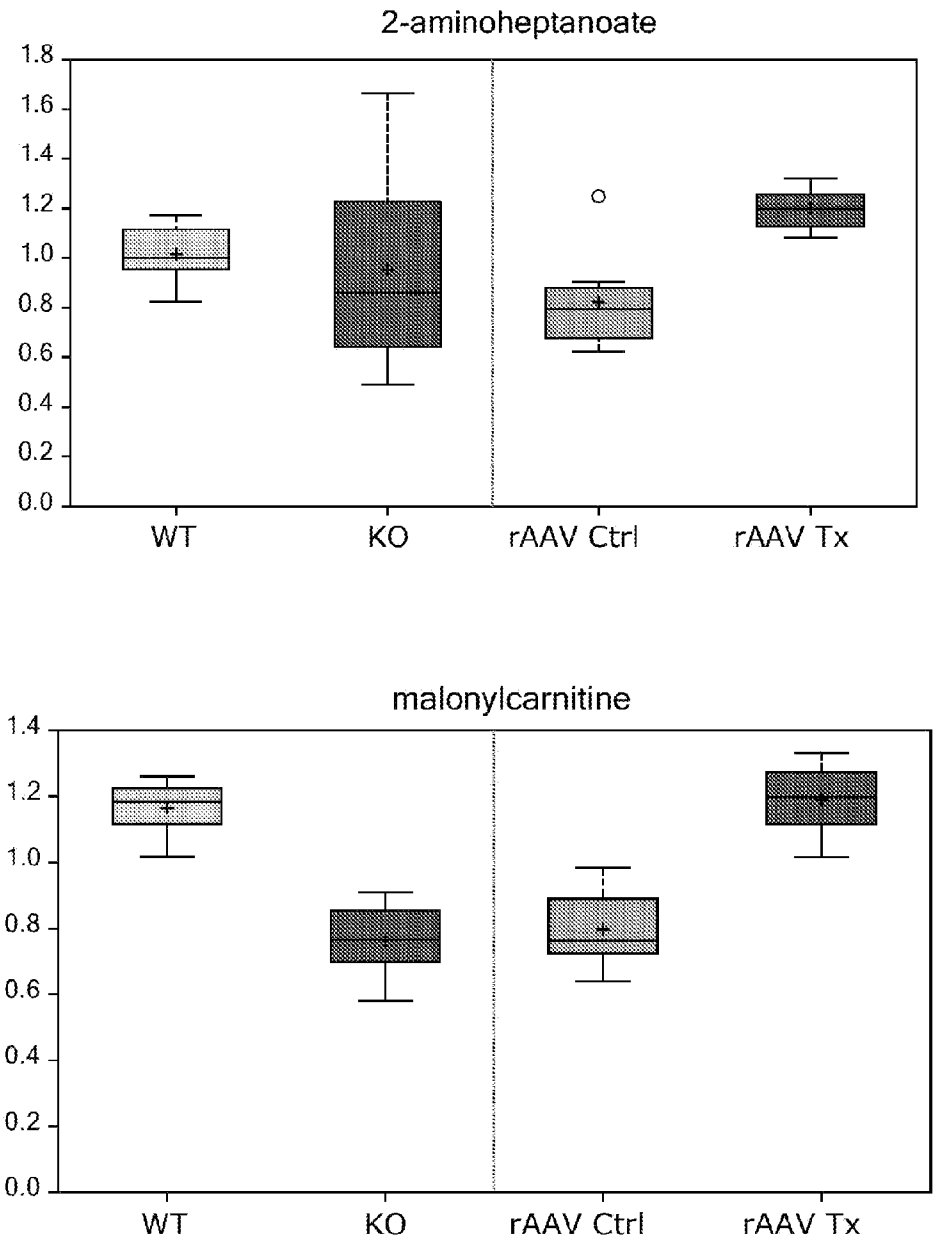
2-aminoheptanoate
1.8
1.6
1.4
1.2
1.0
0.8
0.6
0.4
0.2
0.0
WT
KO
rAAV Ctrl
rAAV Tx
malonylcarnitine
1.4
1.2
1.0
0.8
0.6
0.4
0.2
0.0
WT
KO
rAAV Ctrl
rAAV Tx

FIG. 57 cont.

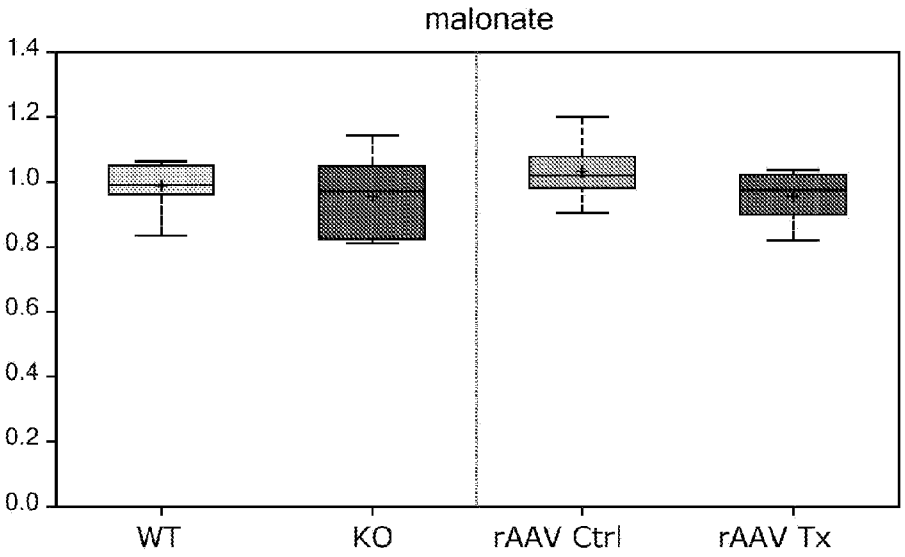
malonate
1.4
1.2
1.0
0.8
0.6
0.4
0.2
0.0
WT
KO
rAAV Ctrl
rAAV Tx

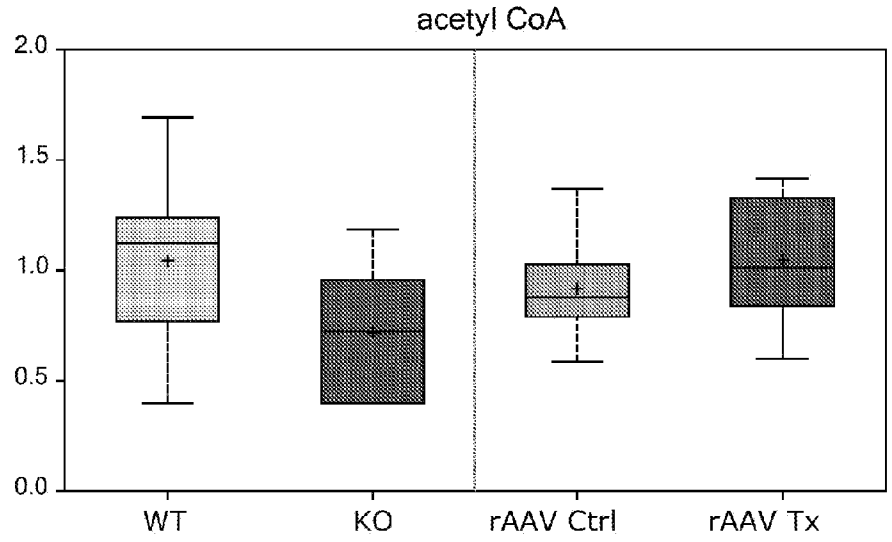
acetyl CoA
2.0
1.5
1.0
0.5
0.0
WT
KO
rAAV Ctrl
rAAV Tx

FIG. 57 cont.

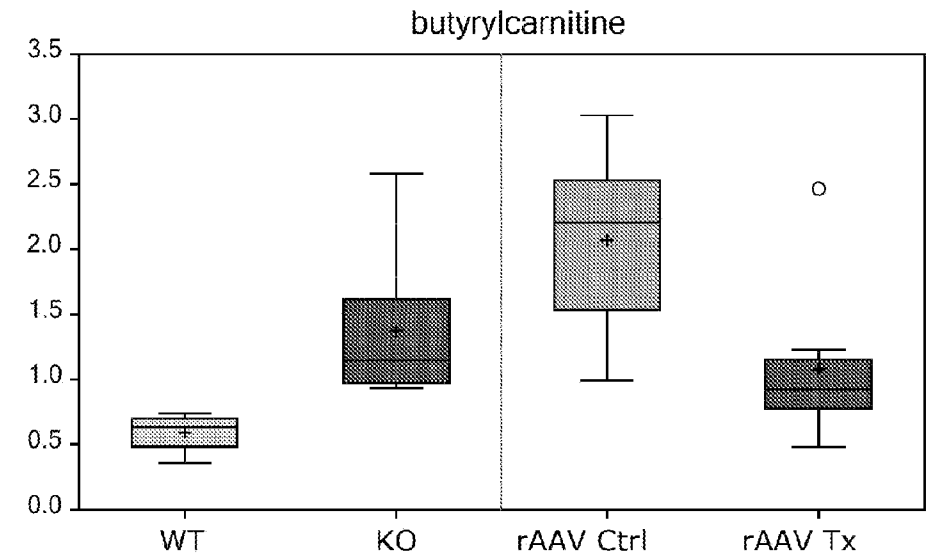
butyrylcarnitine
3.5
3.0
2.5
2.0
1.5
1.0
0.5
0.0
WT
KO
rAAV Ctrl
rAAV Tx

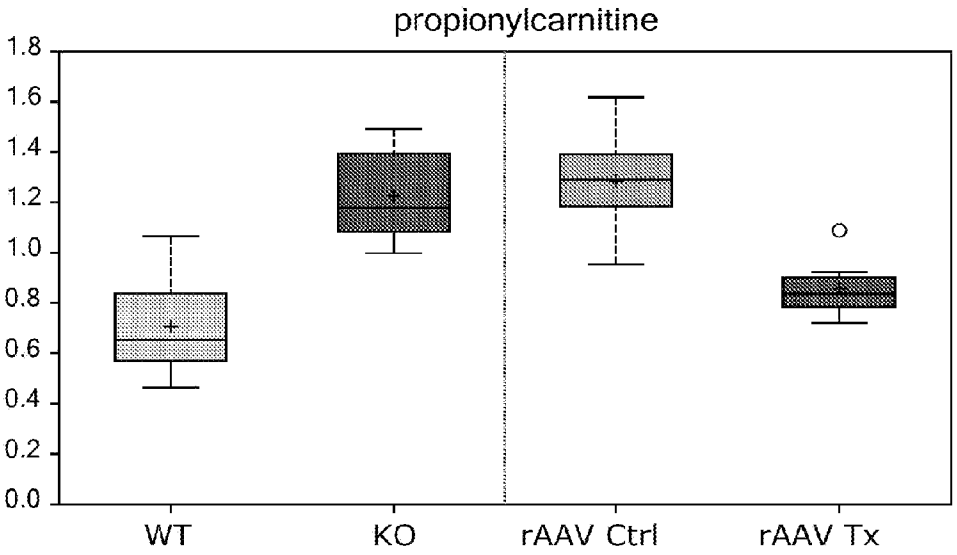
propionylcarnitine
1.8
1.6
1.4
1.2
1.0
0.8
0.6
0.4
0.2
0.0
WT
KO
rAAV Ctrl
rAAV Tx

FIG. 57 cont.

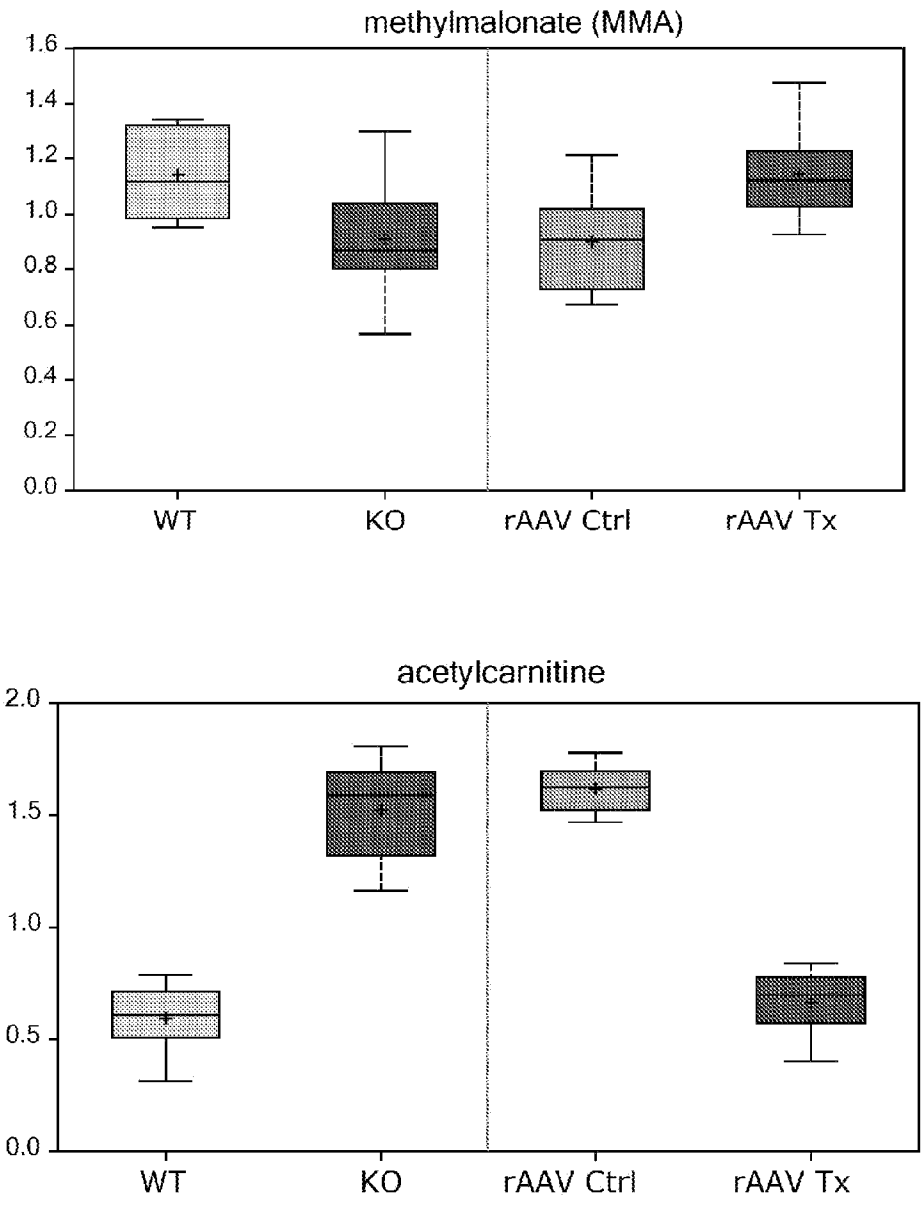
methylmalonate (MMA)
1.6
1.4
1.2
1.0
0.8
0.6
0.4
0.2
0.0
WT
KO
rAAV Ctrl
rAAV Tx
acetylcarnitine
2.0
1.5
1.0
0.5
0.0
WT
KO
rAAV Ctrl
rAAV Tx

FIG. 57 cont.

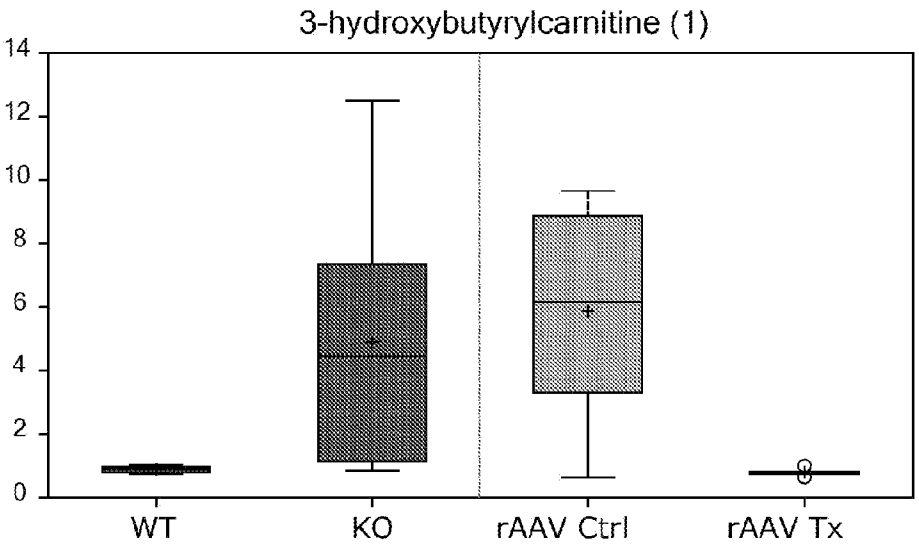
3-hydroxybutyrylcarnitine (1)
14
12
10
8
6
4
2
0
WT
KO
rAAV Ctrl
rAAV Tx

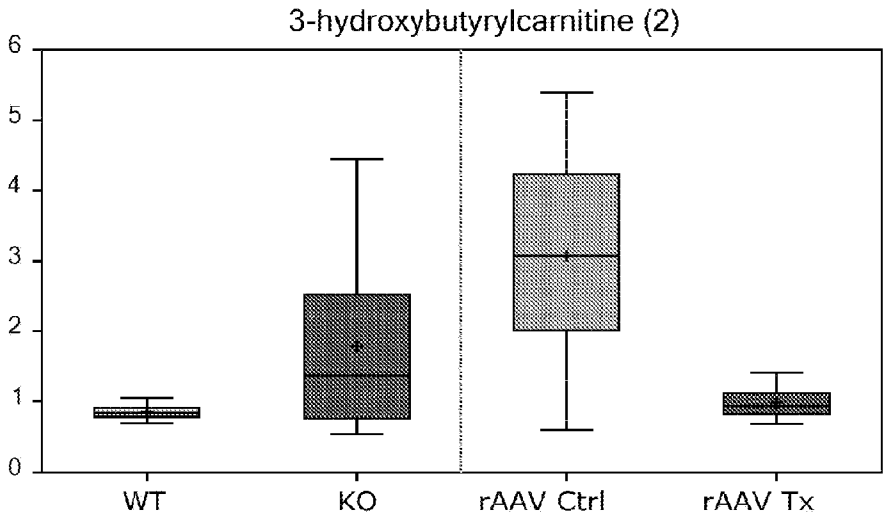
3-hydroxybutyrylcarnitine (2)
6
5
4
3
2
1
0
WT
KO
rAAV Ctrl
rAAV Tx

FIG. 57 cont.

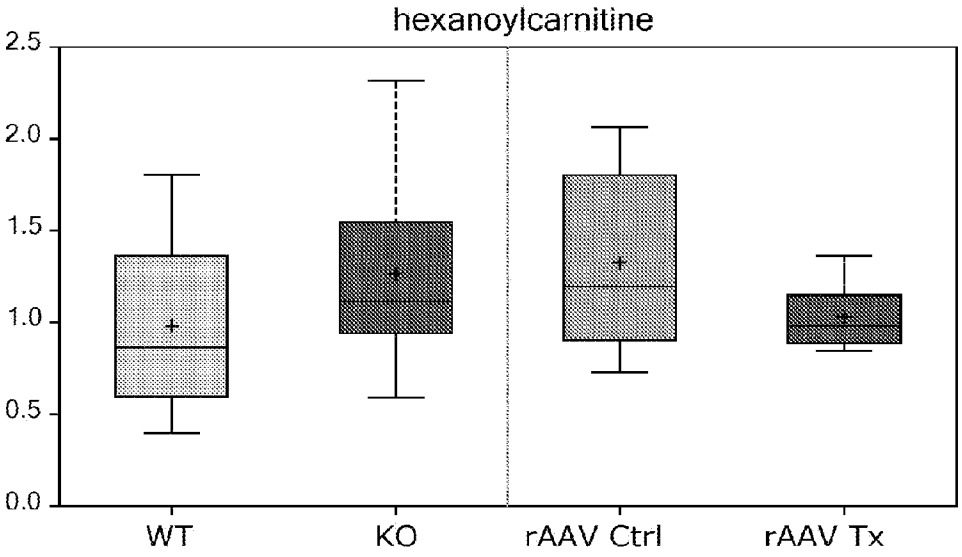
hexanoylcarnitine
2.5
2.0
1.5
1.0
0.5
0.0
WT
KO
rAAV Ctrl
rAAV Tx

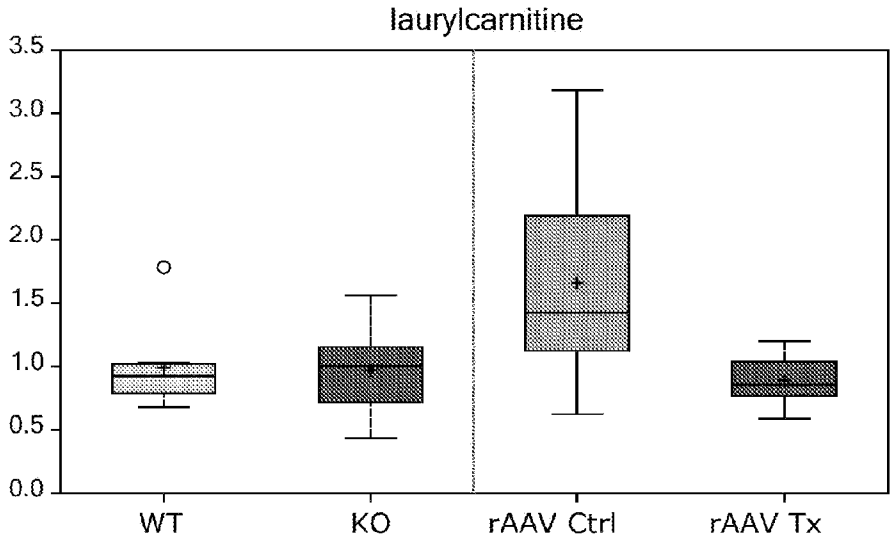
laurylcarnitine
3.5
3.0
2.5
2.0
1.5
1.0
0.5
0.0
WT
KO
rAAV Ctrl
rAAV Tx

FIG. 57 cont.

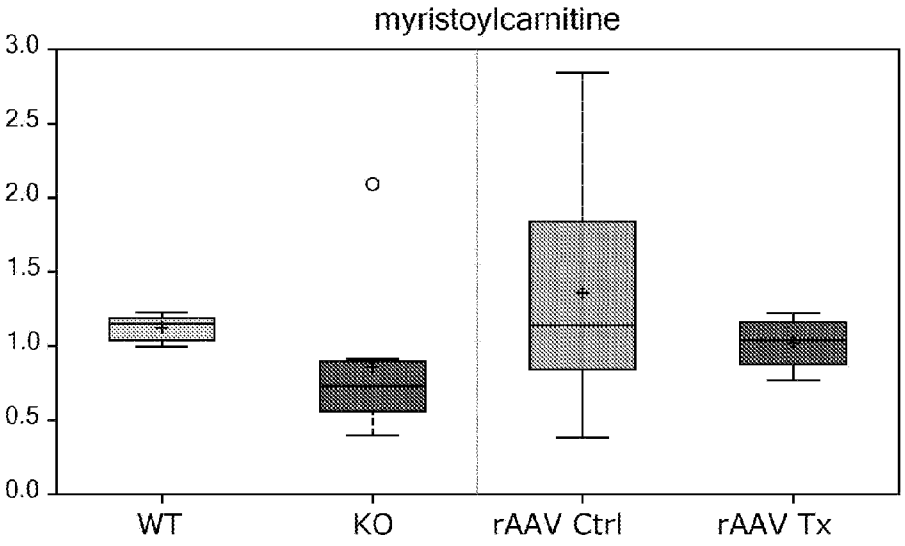
myristoylcarnitine
3.0
2.5
2.0
1.5
1.0
0.5
0.0
WT
KO
rAAV Ctrl
rAAV Tx

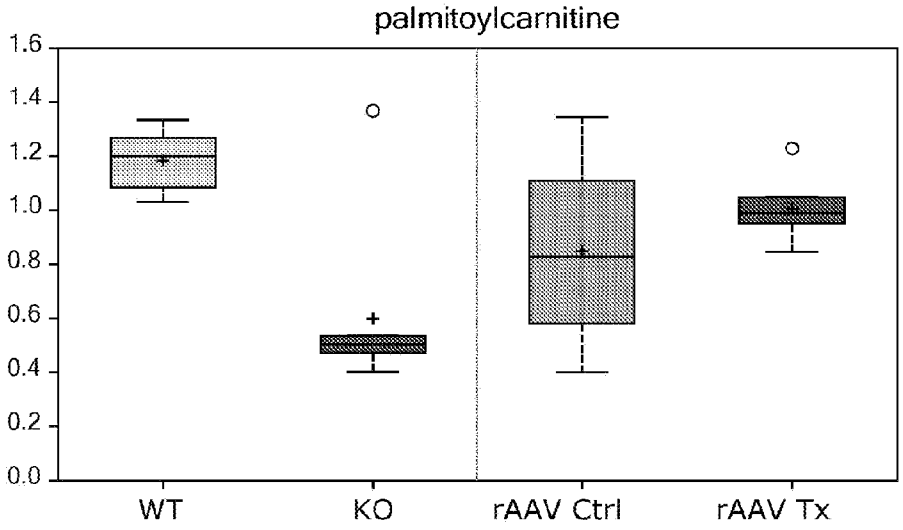
palmitoylcarnitine
1.6
1.4
1.2
1.0
0.8
0.6
0.4
0.2
0.0
WT
KO
rAAV Ctrl
rAAV Tx

FIG. 57 cont.

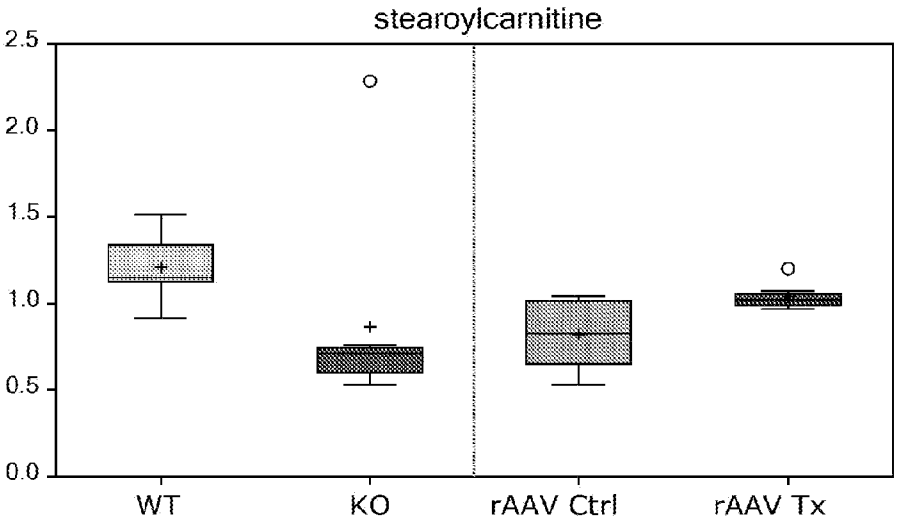
stearoylcarnitine
2.5
2.0
1.5
1.0
0.5
0.0
WT
KO
rAAV Ctrl
rAAV Tx

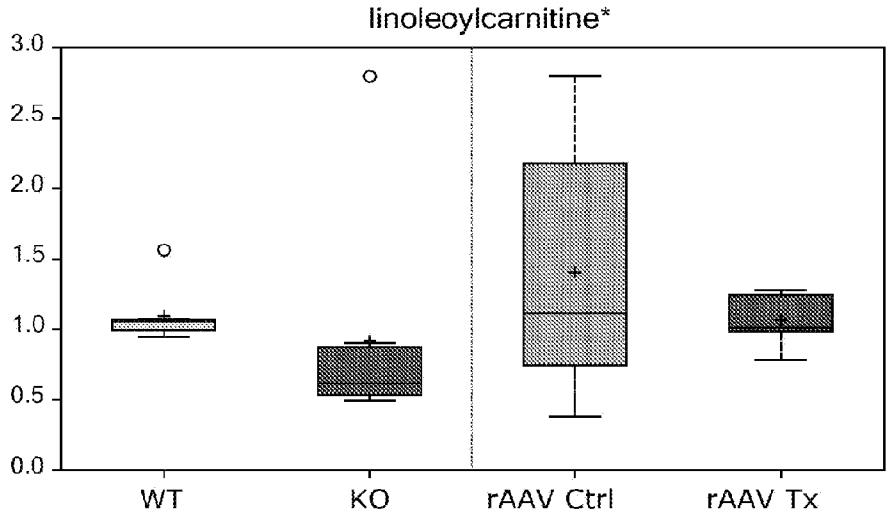
linoleoylcarnitine*
3.0
2.5
2.0
1.5
1.0
0.5
0.0
WT
KO
rAAV Ctrl
rAAV Tx

FIG. 57 cont.

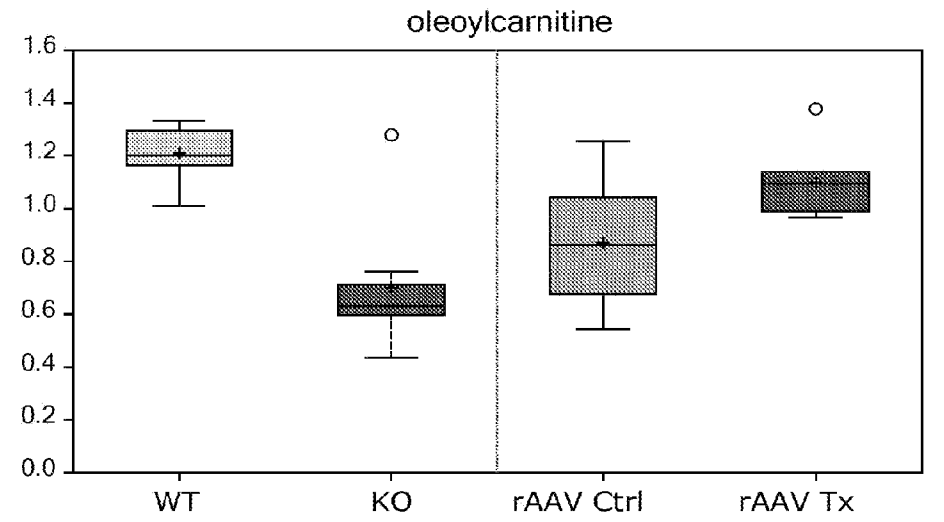
oleoylcarnitine
1.6
1.4
1.2
1.0
0.8
0.6
0.4
0.2
0.0
WT
KO
rAAV Ctrl
rAAV Tx

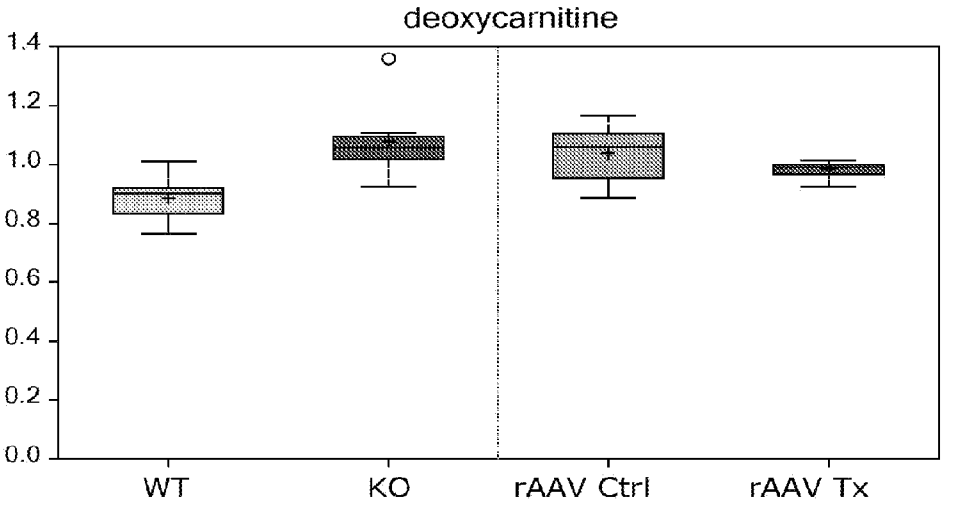
deoxycarnitine
1.4
1.2
1.0
0.8
0.6
0.4
0.2
0.0
WT
KO
rAAV Ctrl
rAAV Tx

FIG. 57 cont.

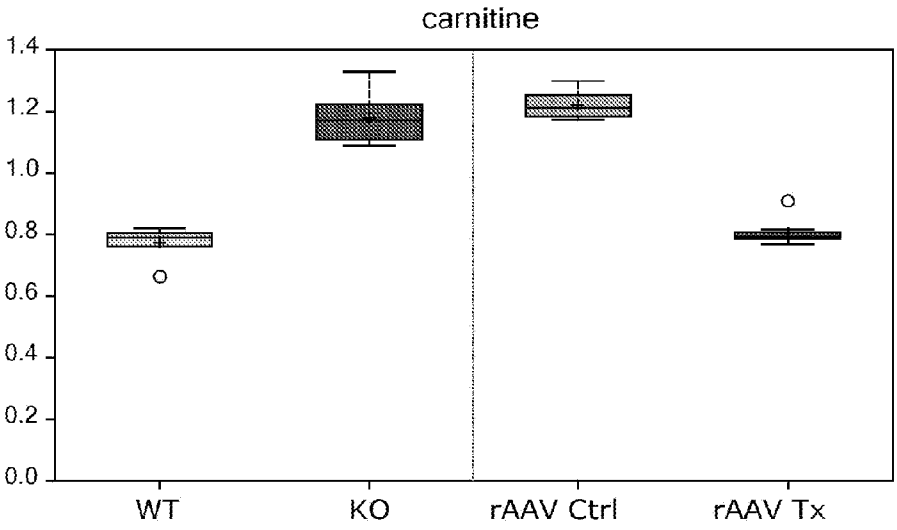
carnitine
1.4
1.2
1.0
0.8
0.6
0.4
0.2
0.0
WT
KO
rAAV Ctrl
rAAV Tx

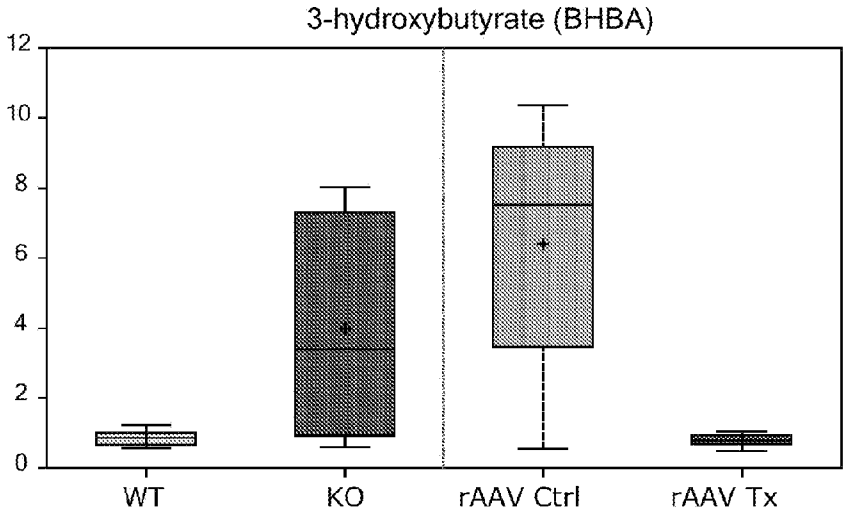
3-hydroxybutyrate (BHBA)
12
10
8
6
4
2
0
WT
KO
rAAV Ctrl
rAAV Tx

FIG. 57 cont.

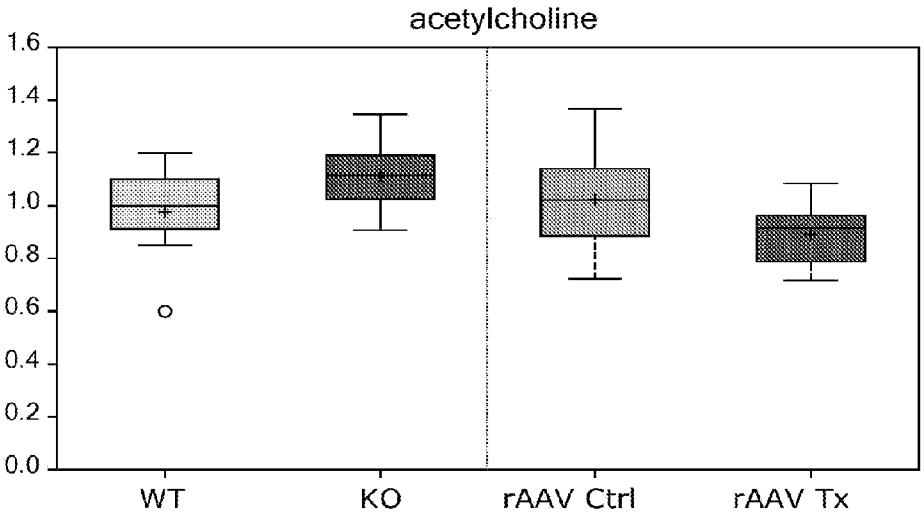
acetylcholine
1.6
1.4
1.2
1.0
0.8
0.6
0.4
0.2
0.0
WT
KO
rAAV Ctrl
rAAV Tx

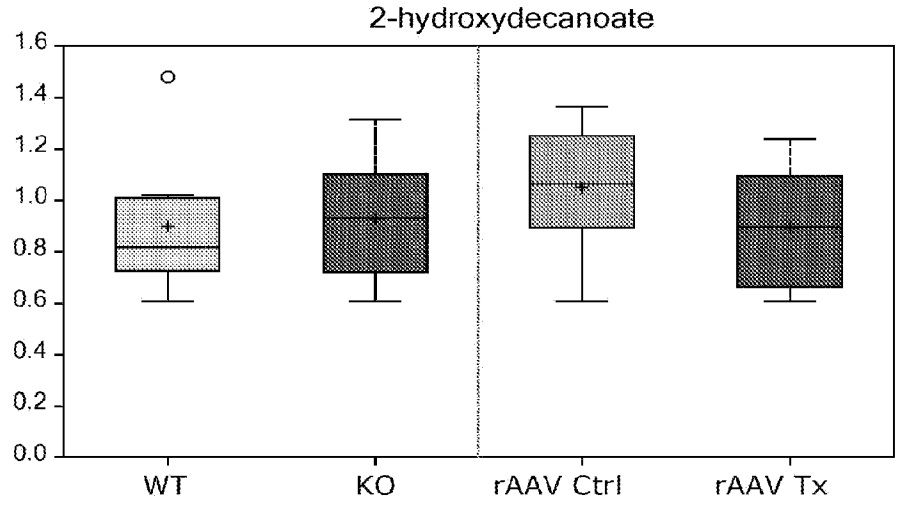
2-hydroxydecanoate
1.6
1.4
1.2
1.0
0.8
0.6
0.4
0.2
0.0
WT
KO
rAAV Ctrl
rAAV Tx

FIG. 57 cont.

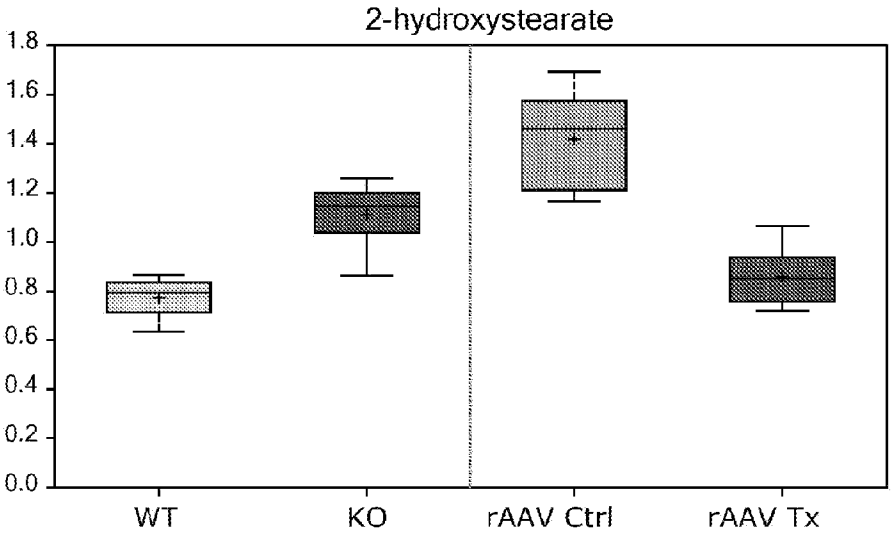
2-hydroxystearate
1.8
1.6
1.4
1.2
1.0
0.8
0.6
0.4
0.2
0.0
WT
KO
rAAV Ctrl
rAAV Tx

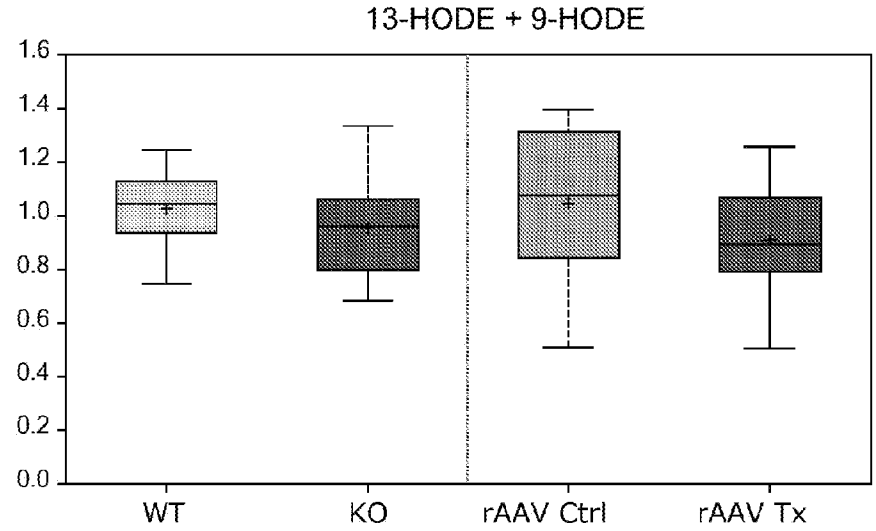
13-HODE + 9-HODE
1.6
1.4
1.2
1.0
0.8
0.6
0.4
0.2
0.0
WT
KO
rAAV Ctrl
rAAV Tx

FIG. 57 cont.

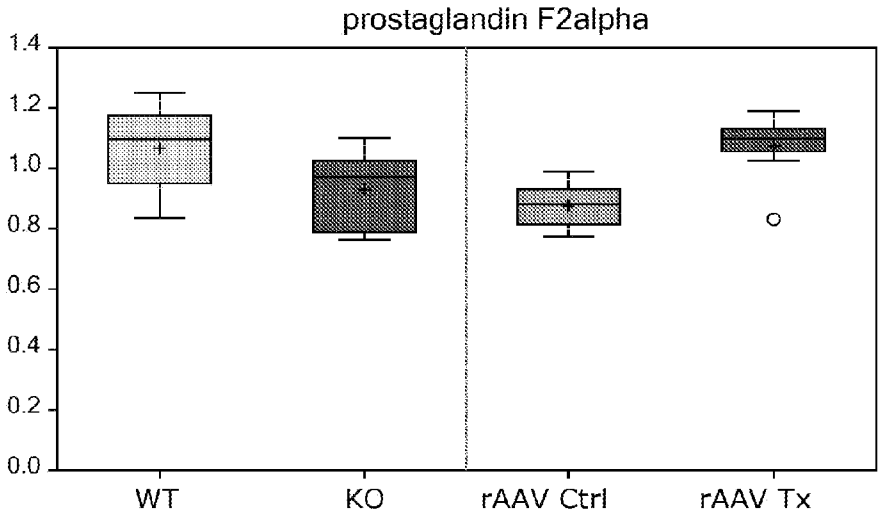
prostaglandin F2alpha
1.4
1.2
1.0
0.8
0.6
0.4
0.2
0.0
WT
KO
rAAV Ctrl
rAAV Tx

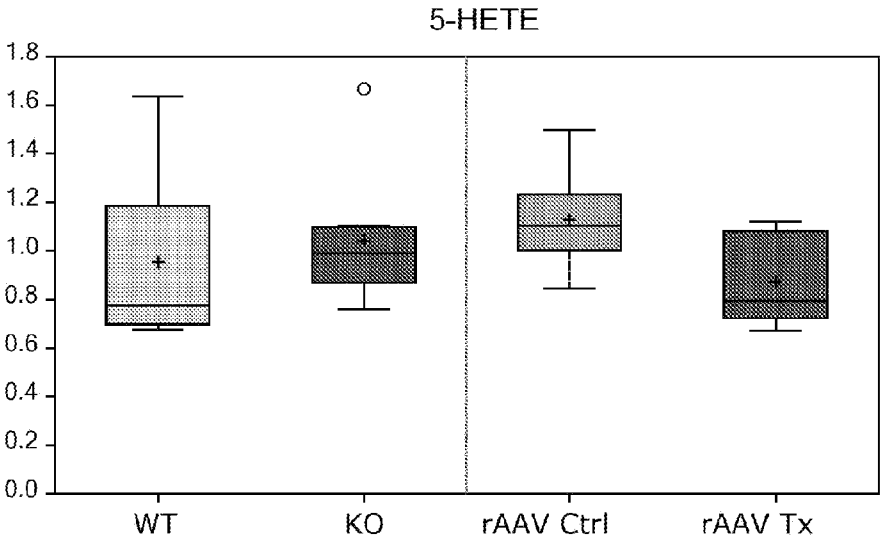
5-HETE
1.8
1.6
1.4
1.2
1.0
0.8
0.6
0.4
0.2
0.0
WT
KO
rAAV Ctrl
rAAV Tx

FIG. 57 cont.

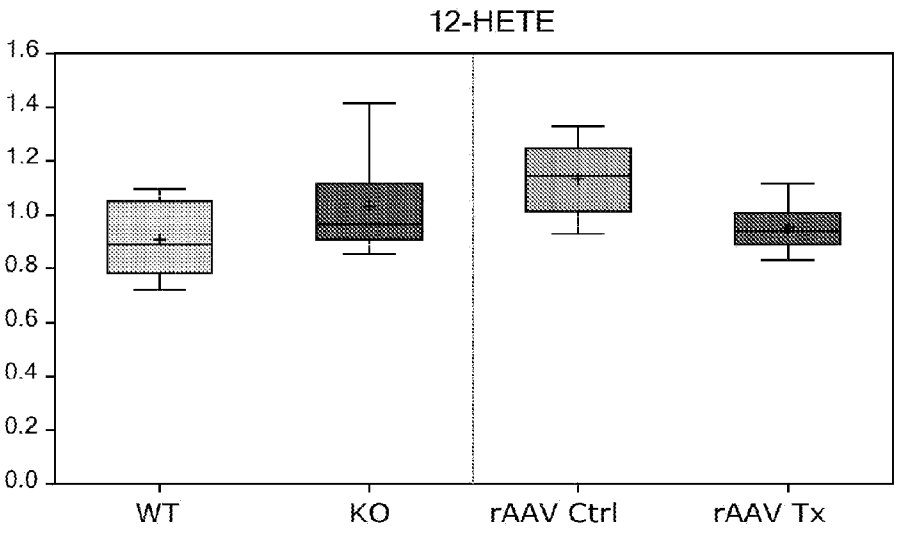
12-HETE
1.6
1.4
1.2
1.0
0.8
0.6
0.4
0.2
0.0
WT
KO
rAAV Ctrl
rAAV Tx

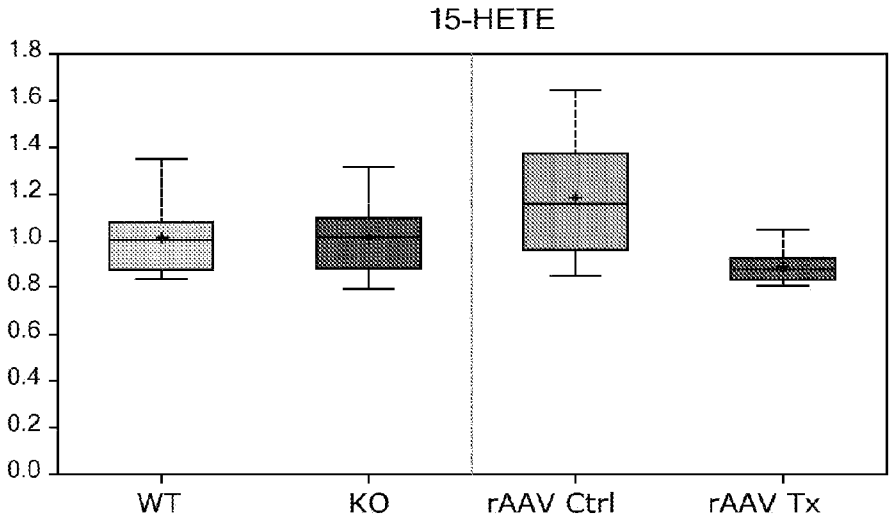
15-HETE
1.8
1.6
1.4
1.2
1.0
0.8
0.6
0.4
0.2
0.0
WT
KO
rAAV Ctrl
rAAV Tx

FIG. 57 cont.

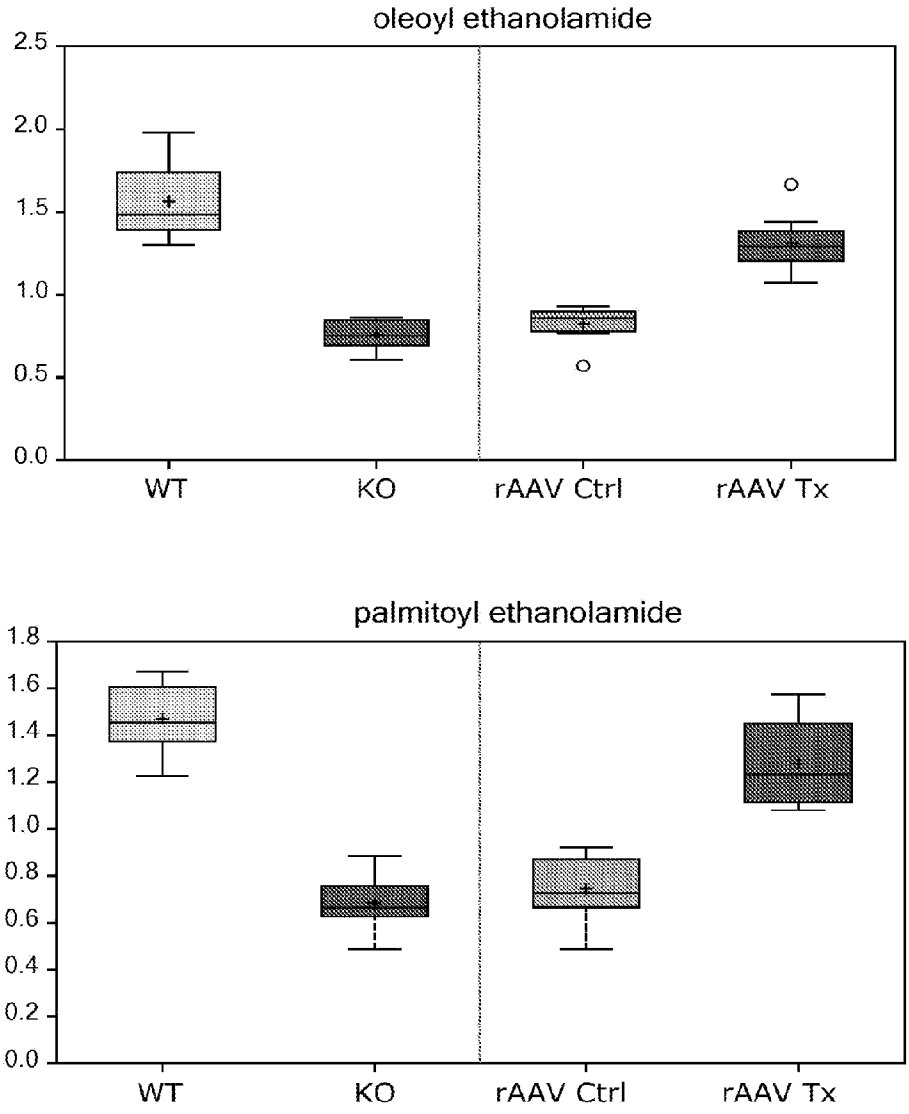
oleoyl ethanolamide
2.5
2.0
1.5
1.0
0.5
0.0
WT
KO
rAAV Ctrl
rAAV Tx
palmitoyl ethanolamide
1.8
1.6
1.4
1.2
1.0
0.8
0.6
0.4
0.2
0.0
WT
KO
rAAV Ctrl
rAAV Tx

FIG. 57 cont.

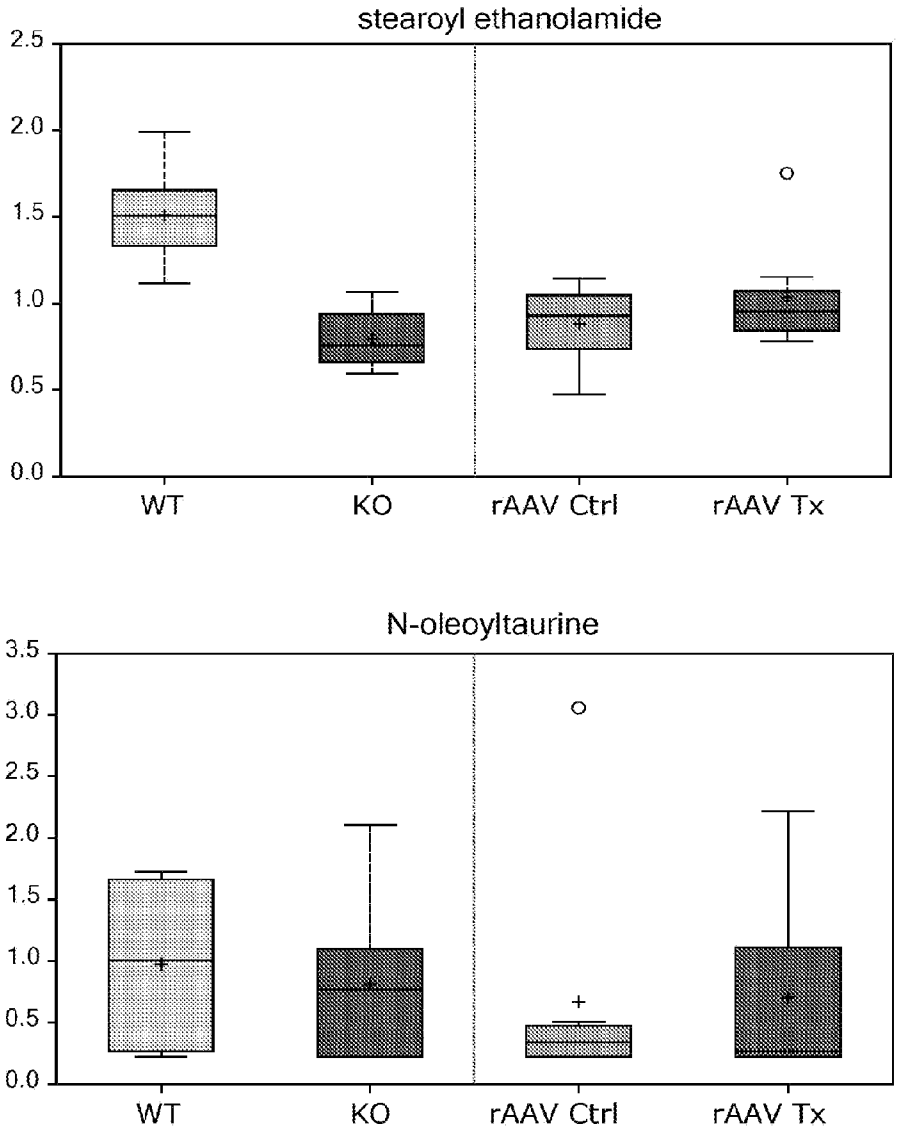
stearoyl ethanolamide
2.5
2.0
1.5
1.0
0.5
0.0
WT
KO
rAAV Ctrl
rAAV Tx
N-oleoyltaurine
3.5
3.0
2.5
2.0
1.5
1.0
0.5
0.0
WT
KO
rAAV Ctrl
rAAV Tx

FIG. 57 cont.

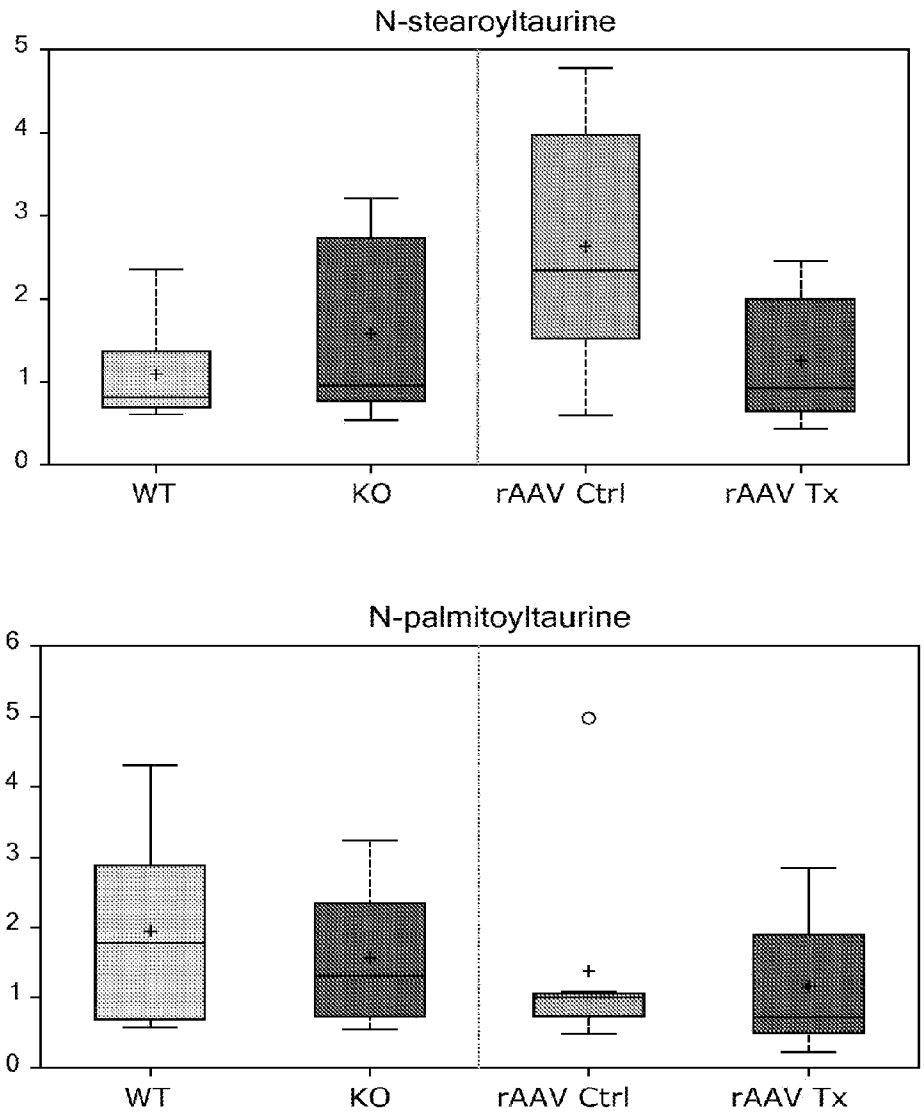
N-stearoyltaurine
5
4
3
2
1
0
WT
KO
rAAV Ctrl
rAAV Tx
N-palmitoyltaurine
6
5
4
3
2
1
0
WT
KO
rAAV Ctrl
rAAV Tx

FIG. 57 cont.

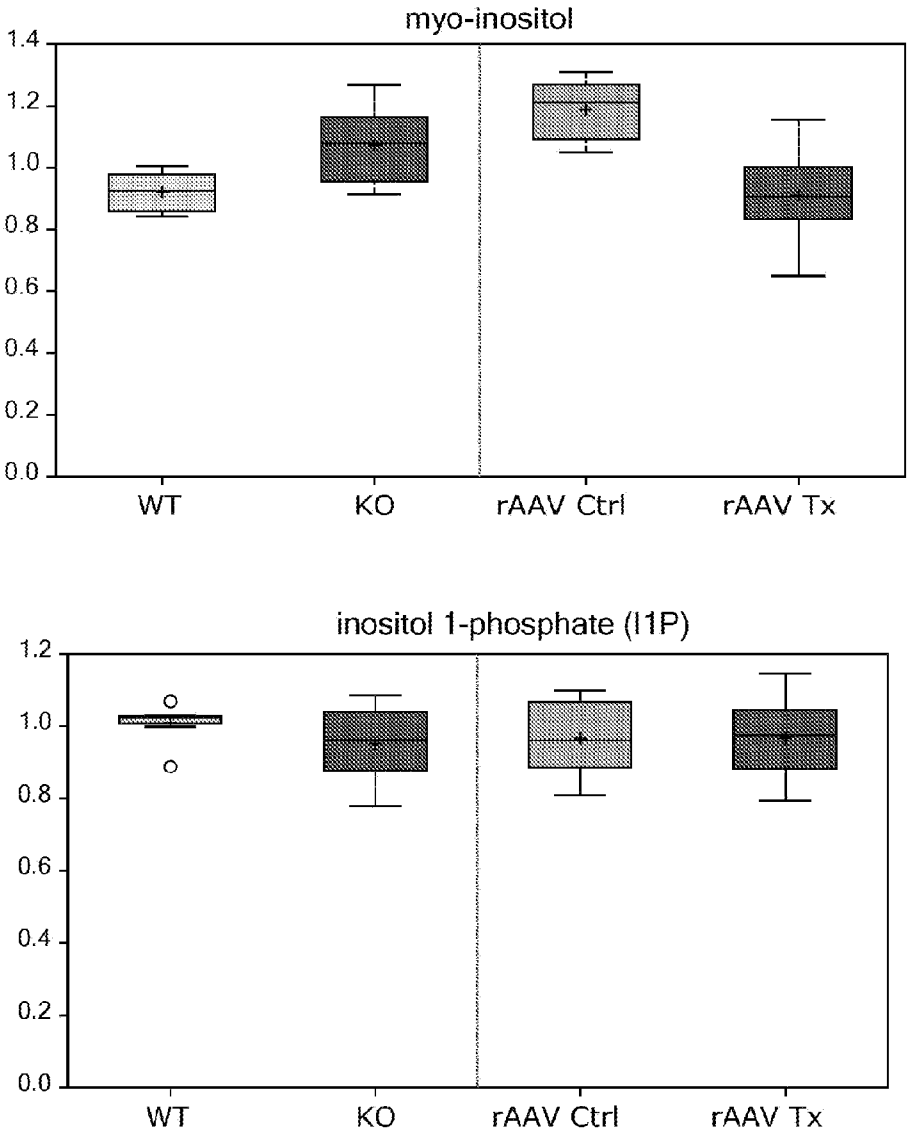
myo-inositol
1.4
1.2
1.0
0.8
0.6
0.4
0.2
0.0
WT
KO
rAAV Ctrl
rAAV Tx
inositol 1-phosphate (I1P)
1.2
1.0
0.8
0.6
0.4
0.2
0.0
WT
KO
rAAV Ctrl
rAAV Tx

FIG. 57 cont.

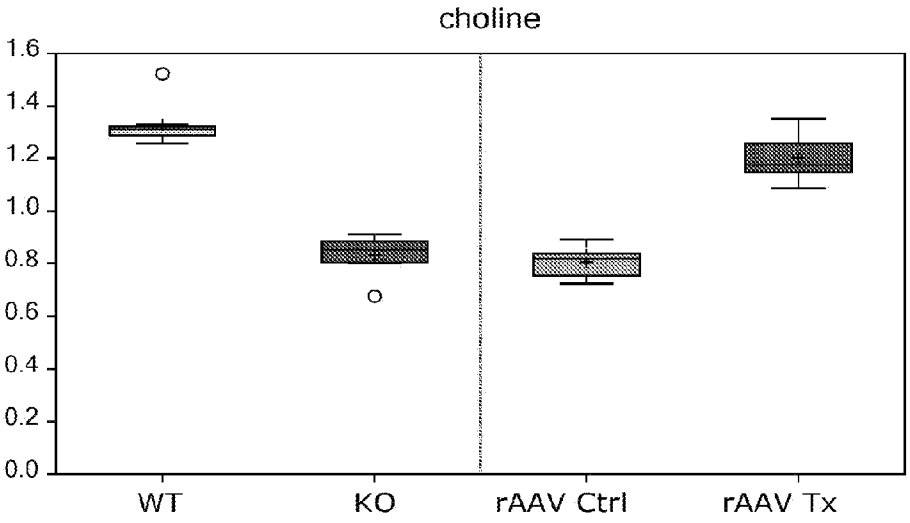
choline
1.6
1.4
1.2
1.0
0.8
0.6
0.4
0.2
0.0
WT
KO
rAAV Ctrl
rAAV Tx

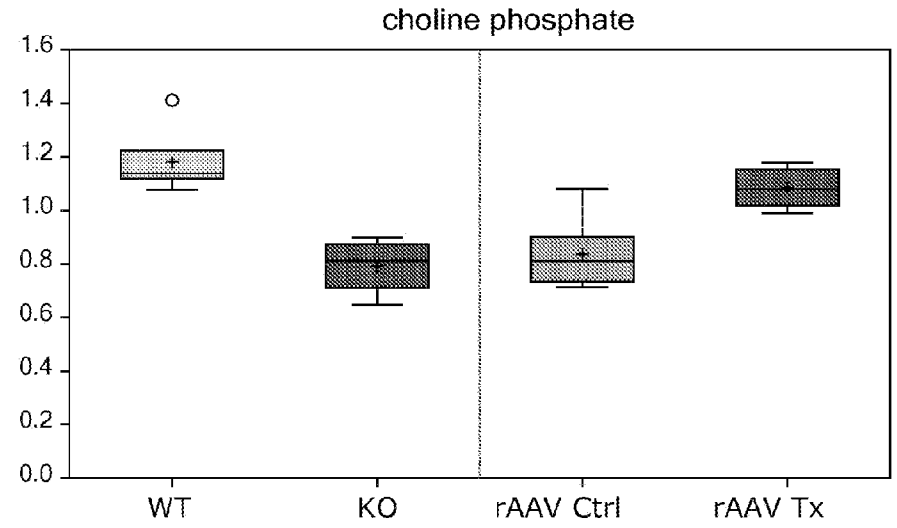
choline phosphate
1.6
1.4
1.2
1.0
0.8
0.6
0.4
0.2
0.0
WT
KO
rAAV Ctrl
rAAV Tx

FIG. 57 cont.

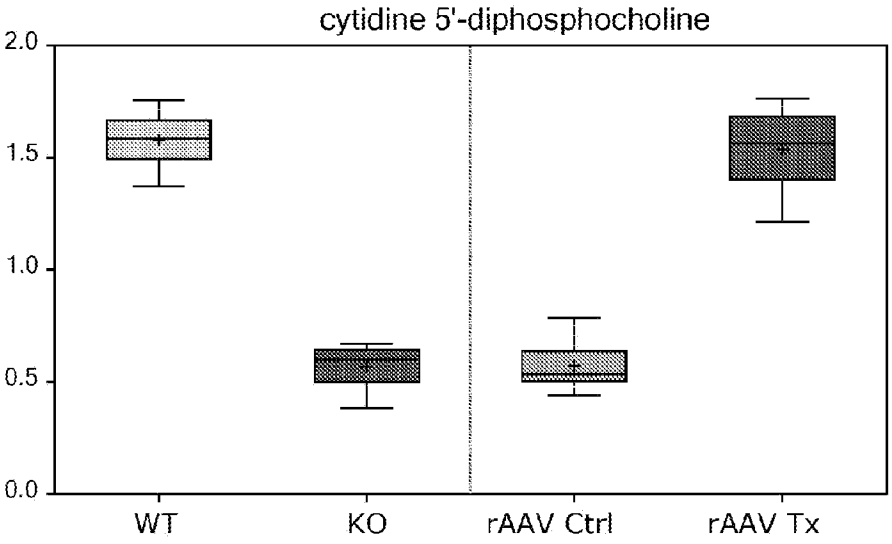
cytidine 5'-diphosphocholine
2.0
1.5
1.0
0.5
0.0
WT
KO
rAAV Ctrl
rAAV Tx

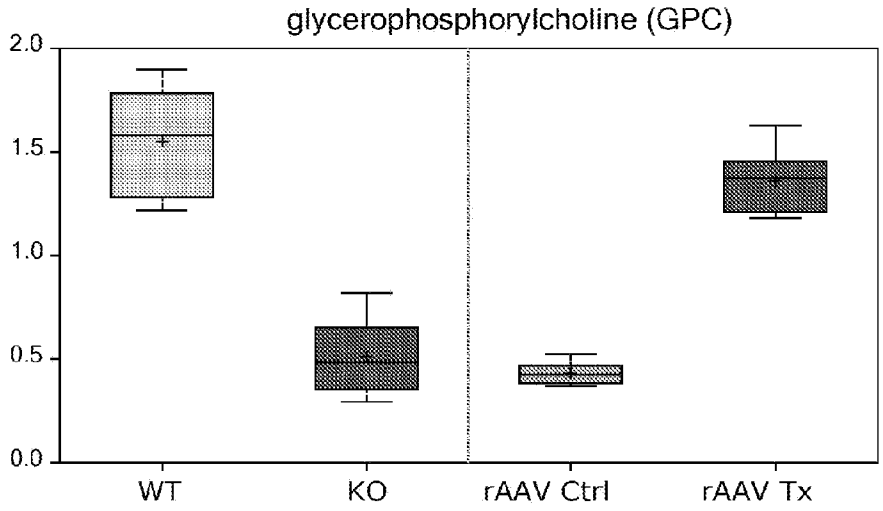
glycerophosphorylcholine (GPC)
2.0
1.5
1.0
0.5
0.0
WT
KO
rAAV Ctrl
rAAV Tx

FIG. 57 cont.

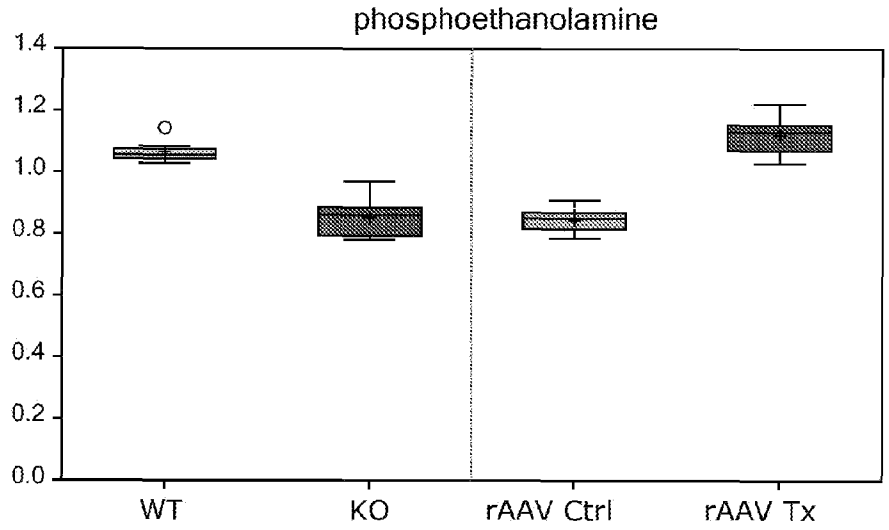
phosphoethanolamine
1.4
1.2
1.0
0.8
0.6
0.4
0.2
0.0
WT
KO
rAAV Ctrl
rAAV Tx

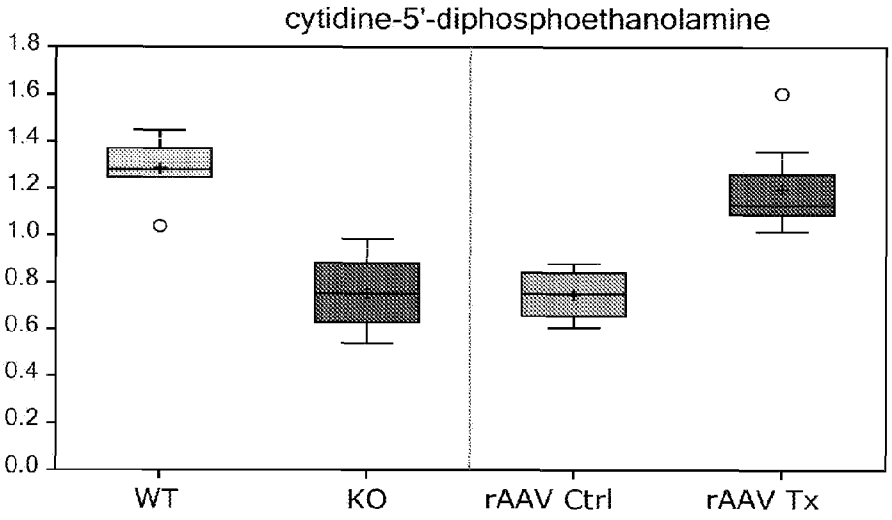
cytidine-5'-diphosphoethanolamine
1.8
1.6
1.4
1.2
1.0
0.8
0.6
0.4
0.2
0.0
WT
KO
rAAV Ctrl
rAAV Tx

FIG. 57 cont.

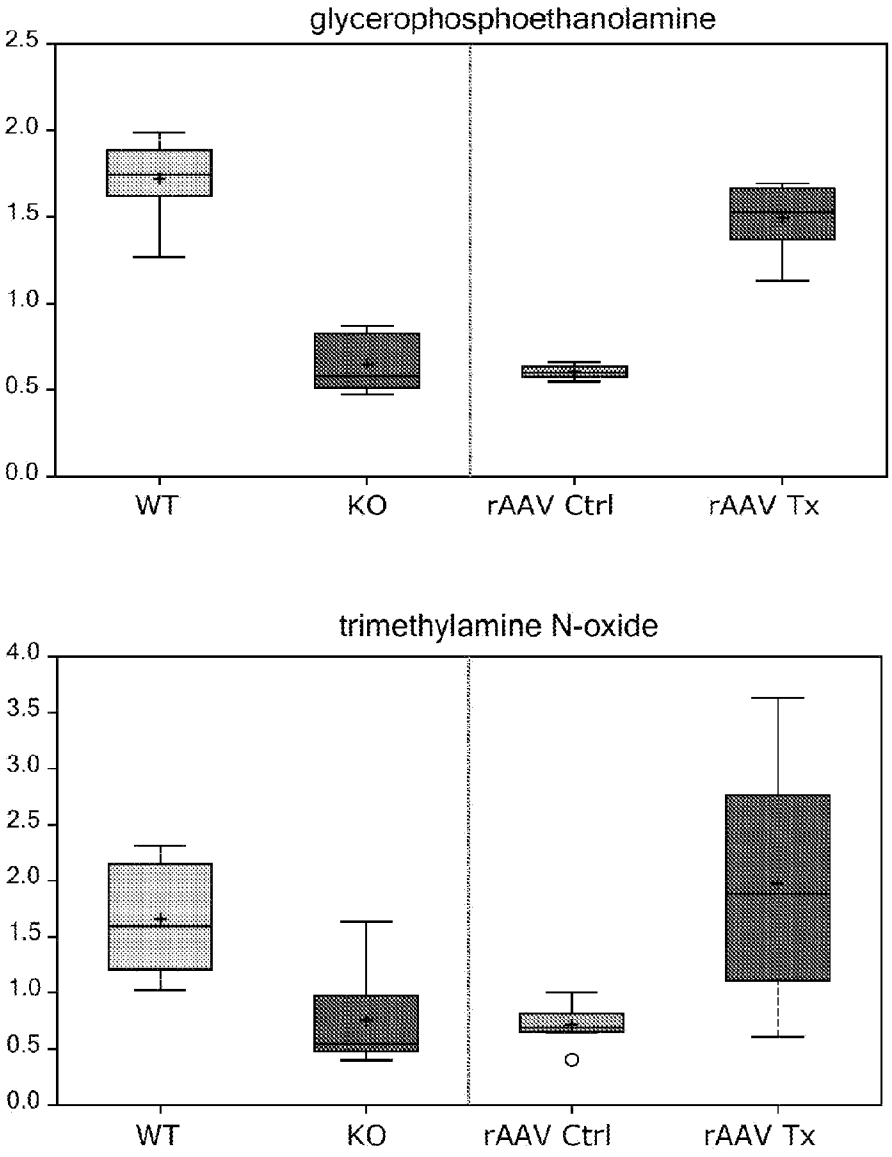
glycerophosphoethanolamine
2.5
2.0
1.5
1.0
0.5
0.0
WT
KO
rAAV Ctrl
rAAV Tx
trimethylamine N-oxide
4.0
3.5
3.0
2.5
2.0
1.5
1.0
0.5
0.0
WT
KO
rAAV Ctrl
rAAV Tx

FIG. 57 cont.

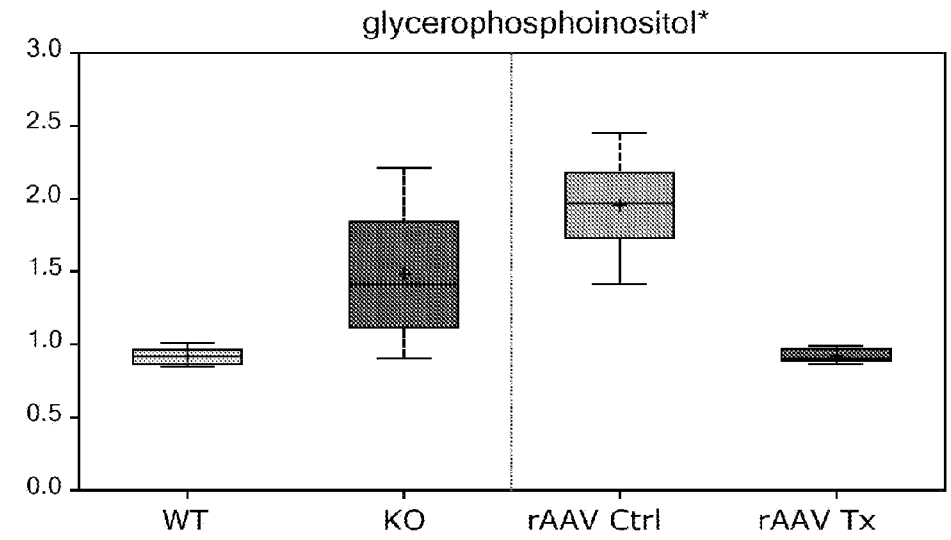
glycerophosphoinositol*
3.0
2.5
2.0
1.5
1.0
0.5
0.0
WT
KO
rAAV Ctrl
rAAV Tx

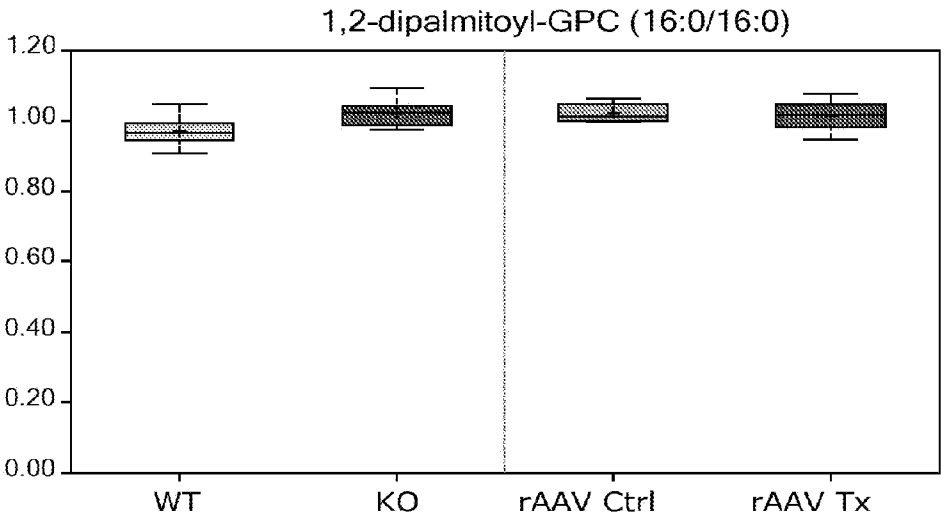
1,2-dipalmitoyl-GPC (16:0/16:0)
1.20
1.00
0.80
0.60
0.40
0.20
0.00
WT
KO
rAAV Ctrl
rAAV Tx

FIG. 57 cont.

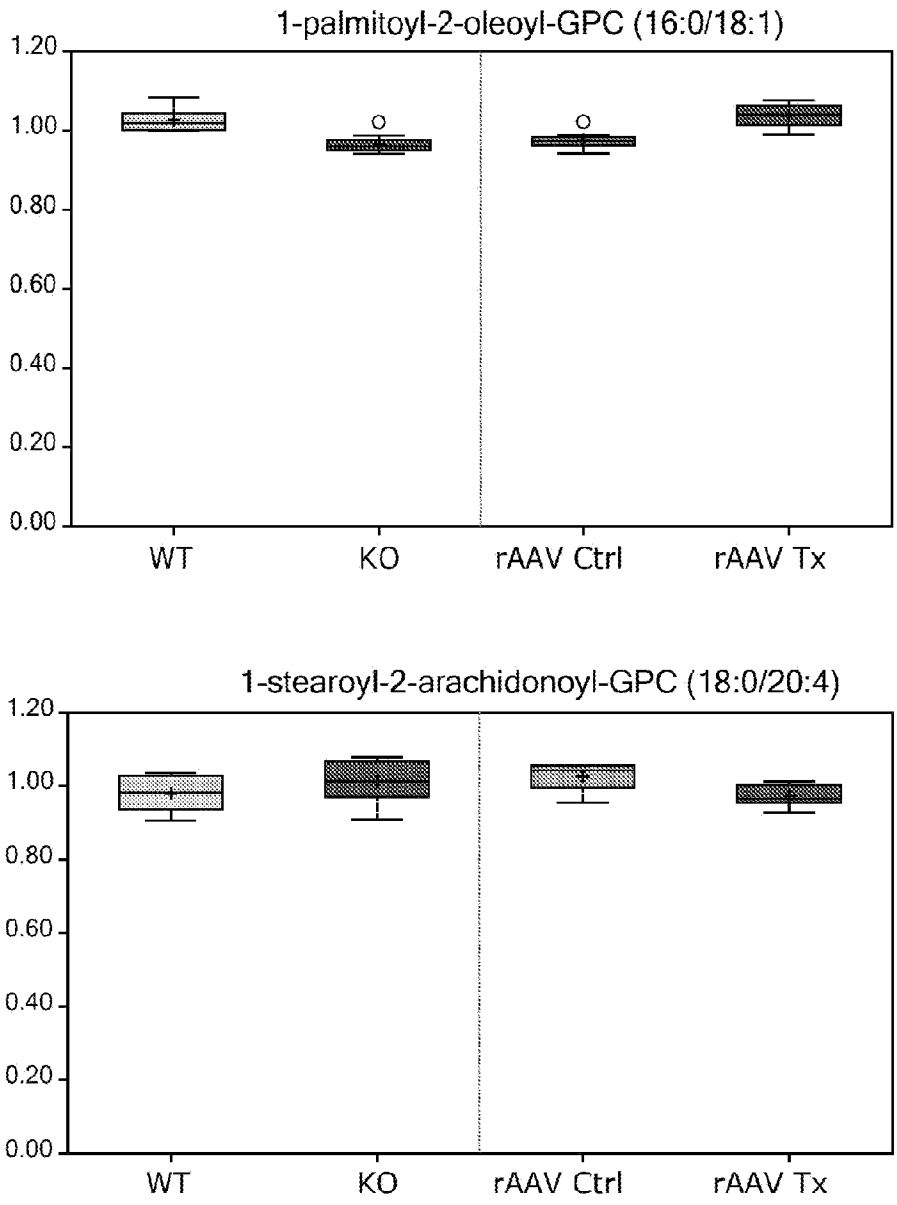
1-palmitoyl-2-oleoyl-GPC (16:0/18:1)
1.20
1.00
0.80
0.60
0.40
0.20
0.00
WT
KO
rAAV Ctrl
rAAV Tx
1-stearoyl-2-arachidonoyl-GPC (18:0/20:4)
1.20
1.00
0.80
0.60
0.40
0.20
0.00
WT
KO
rAAV Ctrl
rAAV Tx

FIG. 57 cont.

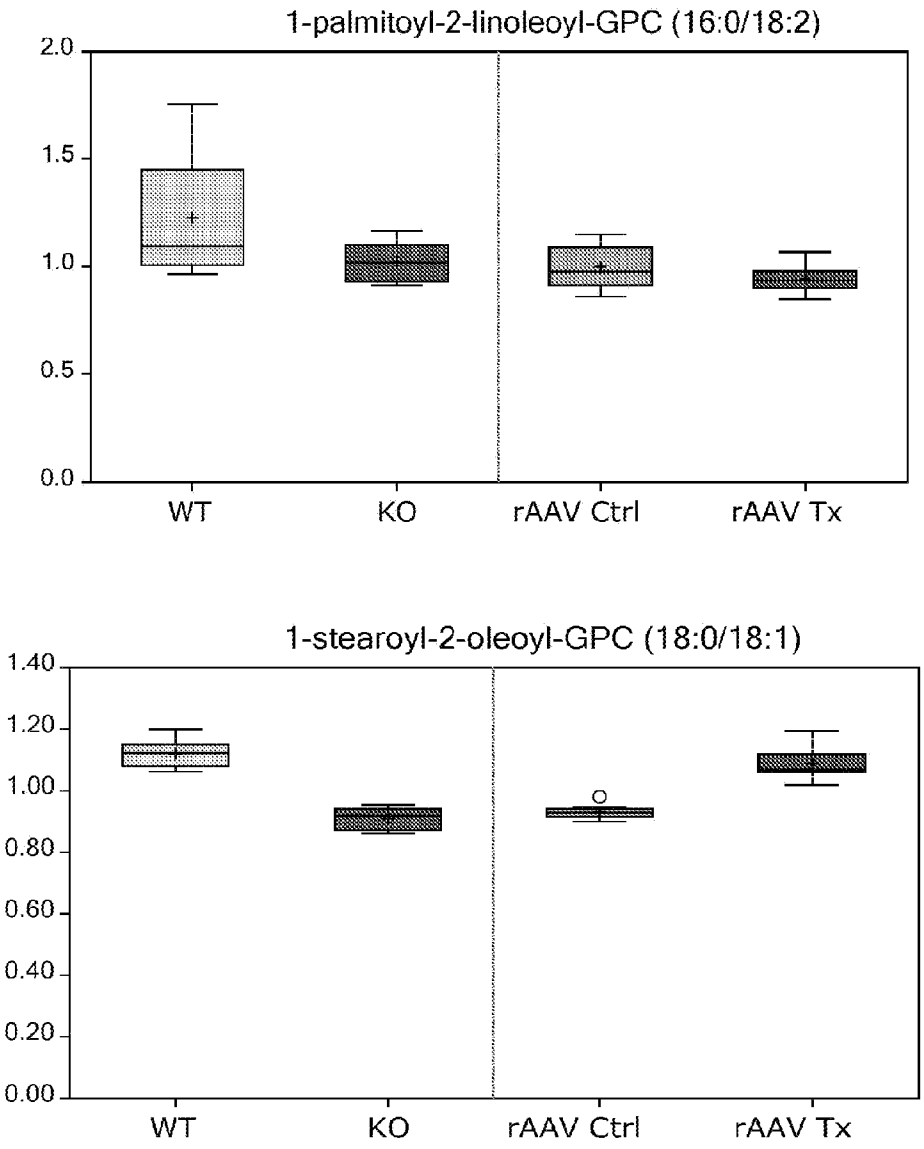
1-palmitoyl-2-linoleoyl-GPC (16:0/18:2)
2.0
1.5
1.0
0.5
0.0
WT
KO
rAAV Ctrl
rAAV Tx
1-stearoyl-2-oleoyl-GPC (18:0/18:1)
1.40
1.20
1.00
0.80
0.60
0.40
0.20
0.00
WT
KO
rAAV Ctrl
rAAV Tx

FIG. 57 cont.

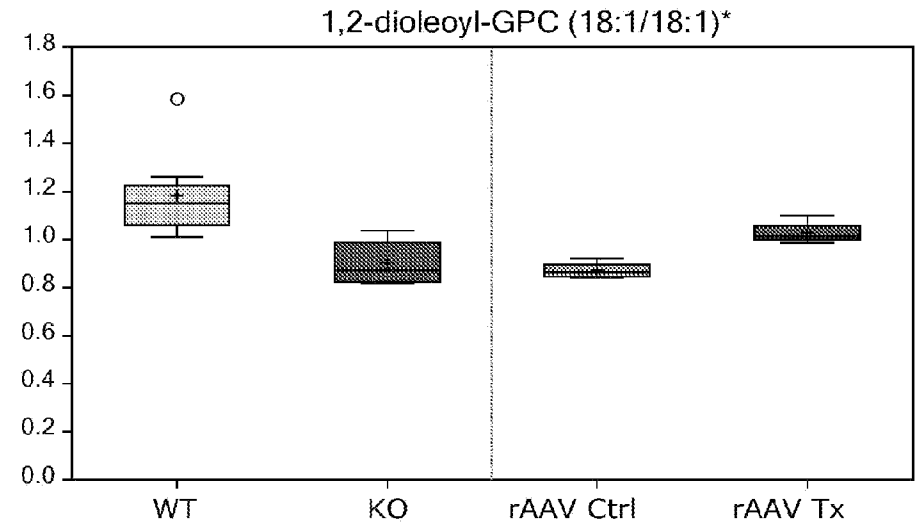
1,2-dioleoyl-GPC (18:1/18:1)*
1.8
1.6
1.4
1.2
1.0
0.8
0.6
0.4
0.2
0.0
WT
KO
rAAV Ctrl
rAAV Tx

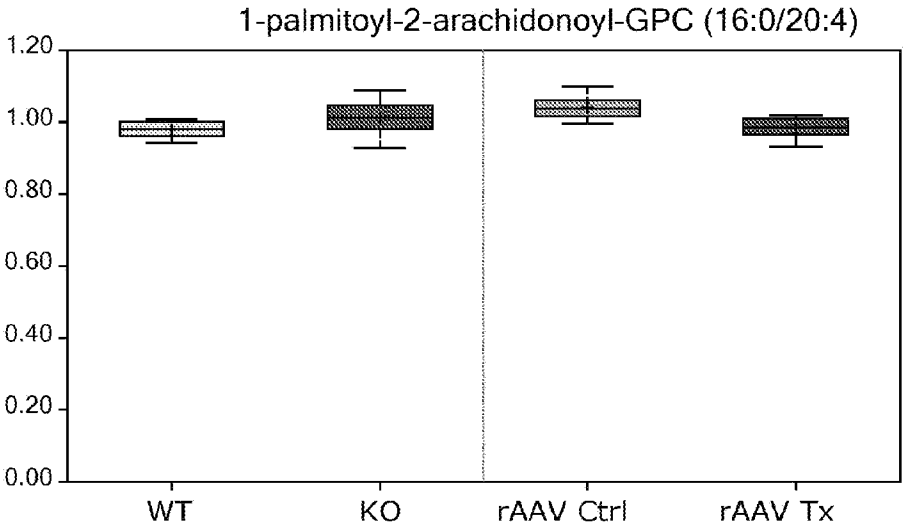
1-palmitoyl-2-arachidonoyl-GPC (16:0/20:4)
1.20
1.00
0.80
0.60
0.40
0.20
0.00
WT
KO
rAAV Ctrl
rAAV Tx

FIG. 57 cont.

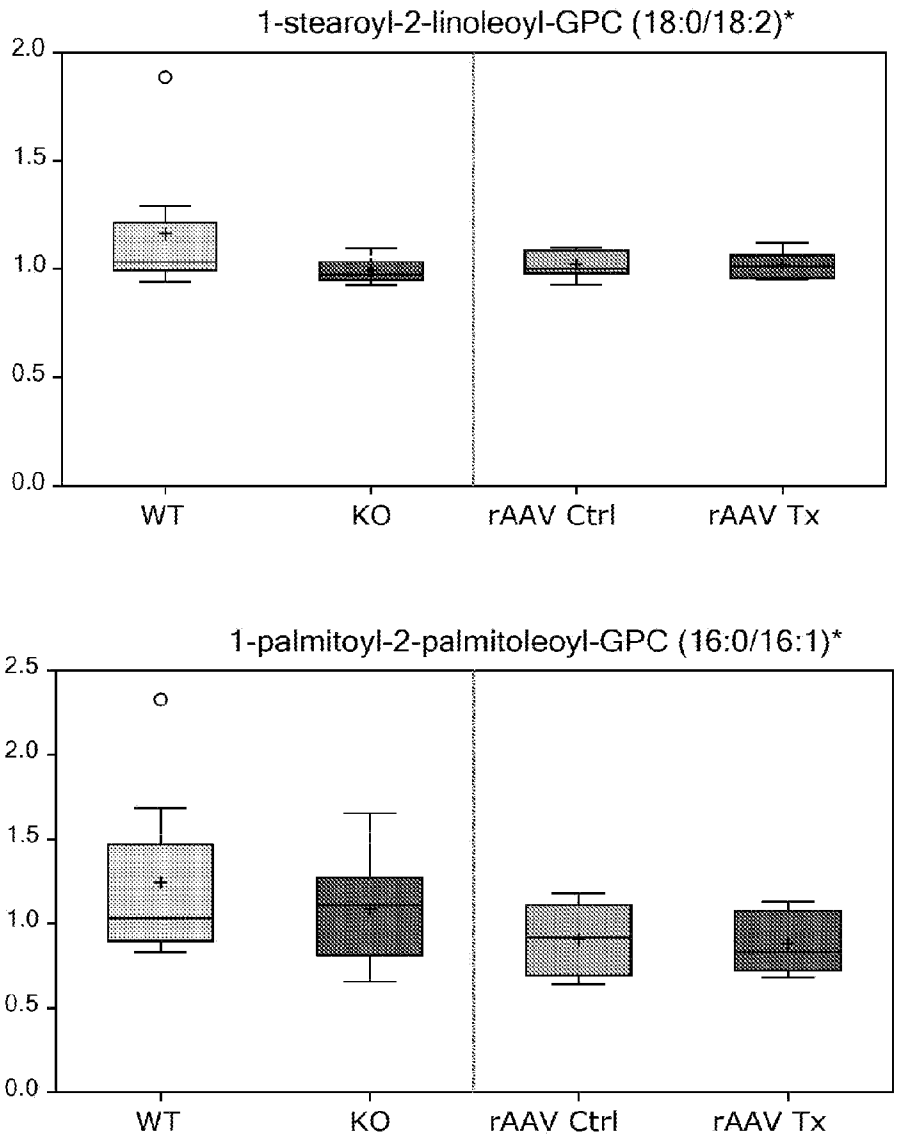
1-stearoyl-2-linoleoyl-GPC (18:0/18:2)*
2.0
1.5
1.0
0.5
0.0
WT
KO
rAAV Ctrl
rAAV Tx
1-palmitoyl-2-palmitoleoyl-GPC (16:0/16:1)*
2.5
2.0
1.5
1.0
0.5
0.0
WT
KO
rAAV Ctrl
rAAV Tx

FIG. 57 cont.

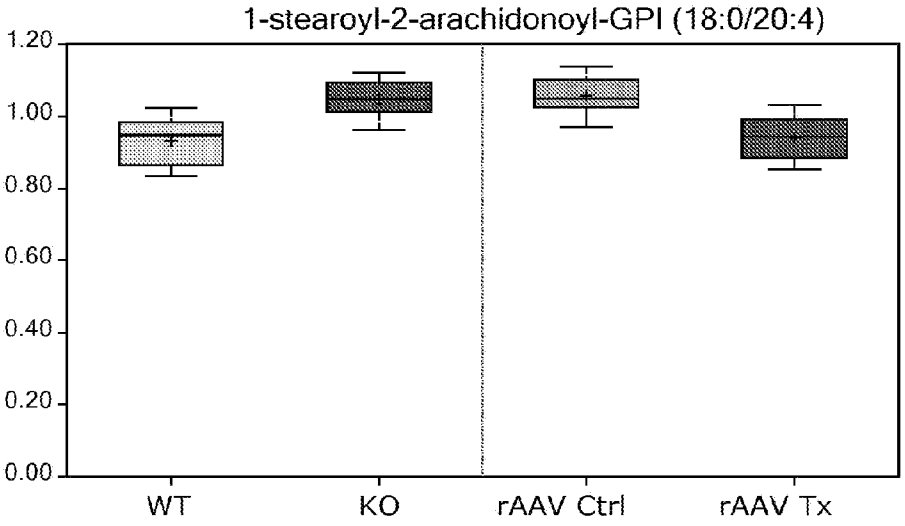
1-stearoyl-2-arachidonoyl-GPI (18:0/20:4)
1.20
1.00
0.80
0.60
0.40
0.20
0.00
WT
KO
rAAV Ctrl
rAAV Tx

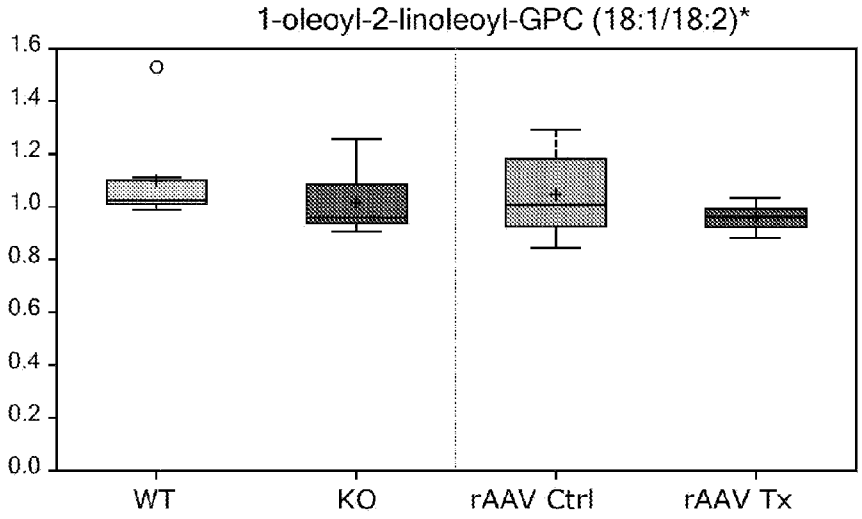
1-oleoyl-2-linoleoyl-GPC (18:1/18:2)*
1.6
1.4
1.2
1.0
0.8
0.6
0.4
0.2
0.0
WT
KO
rAAV Ctrl
rAAV Tx

FIG. 57 cont.

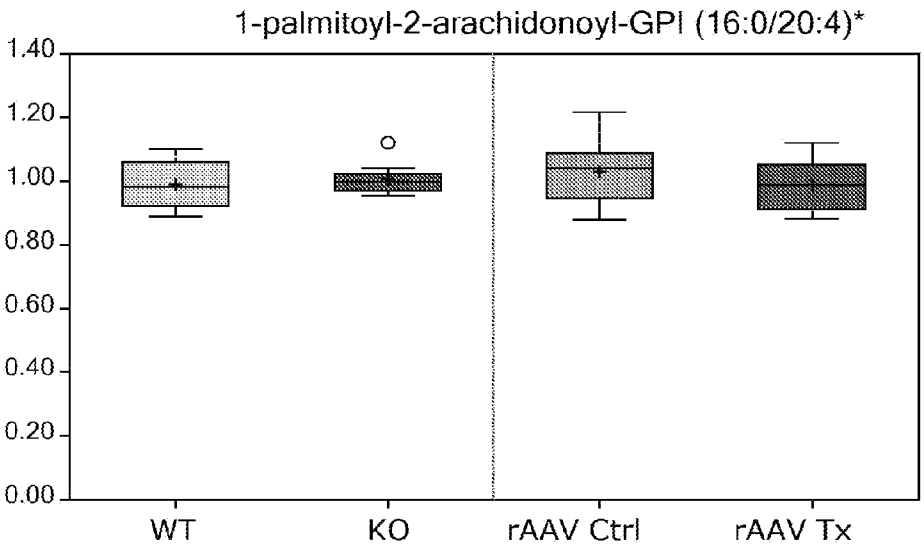
1-palmitoyl-2-arachidonoyl-GPI (16:0/20:4)*
1.40
1.20
1.00
0.80
0.60
0.40
0.20
0.00
WT
KO
rAAV Ctrl
rAAV Tx

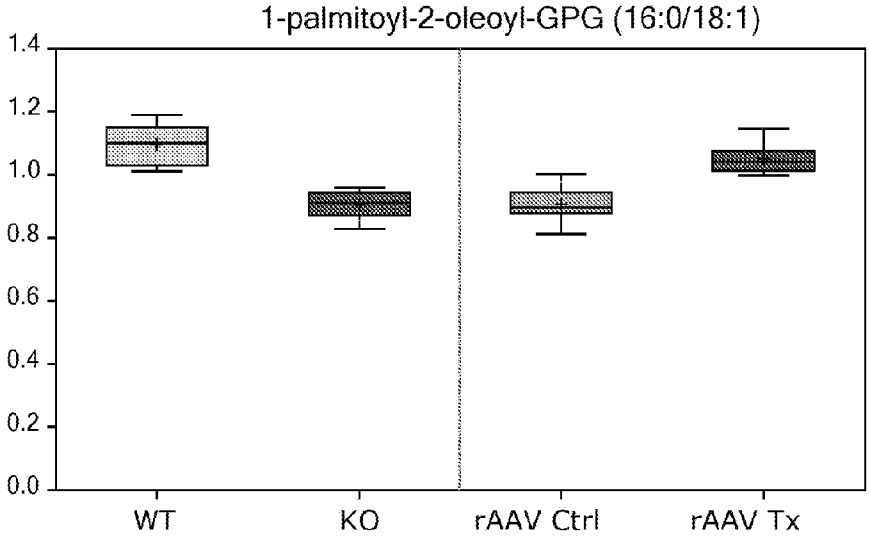
1-palmitoyl-2-oleoyl-GPG (16:0/18:1)
1.4
1.2
1.0
0.8
0.6
0.4
0.2
0.0
WT
KO
rAAV Ctrl
rAAV Tx

FIG. 57 cont.

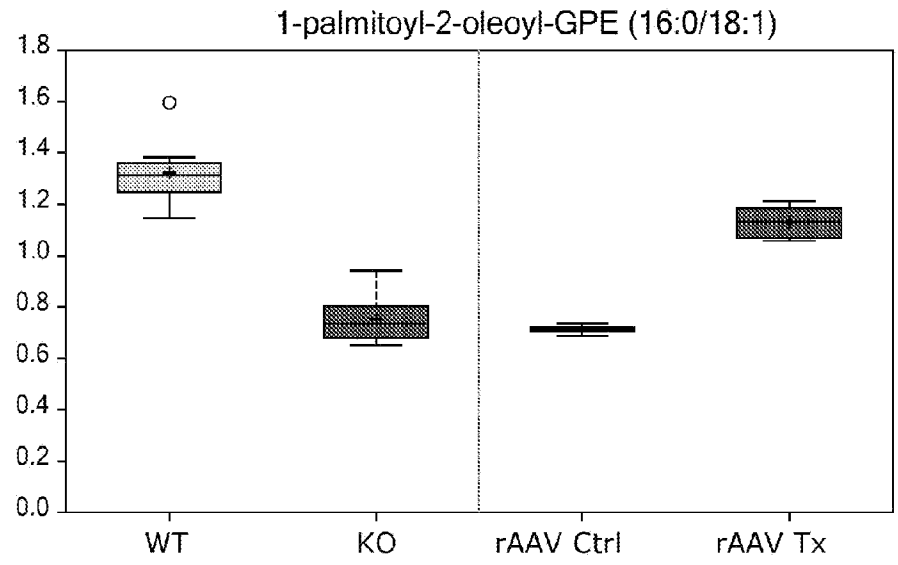
1-palmitoyl-2-oleoyl-GPE (16:0/18:1)
1.8
1.6
1.4
1.2
1.0
0.8
0.6
0.4
0.2
0.0
WT
KO
rAAV Ctrl
rAAV Tx

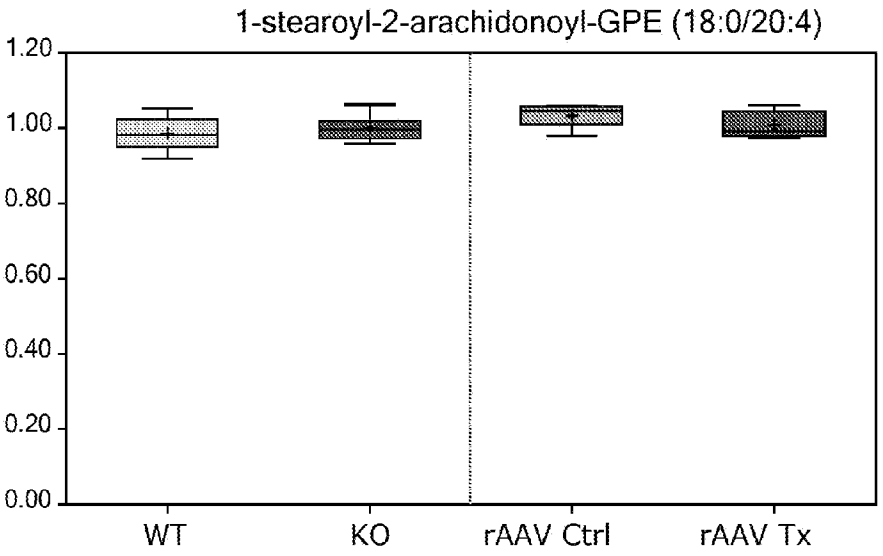
1-stearoyl-2-arachidonoyl-GPE (18:0/20:4)
1.20
1.00
0.80
0.60
0.40
0.20
0.00
WT
KO
rAAV Ctrl
rAAV Tx

FIG. 57 cont.

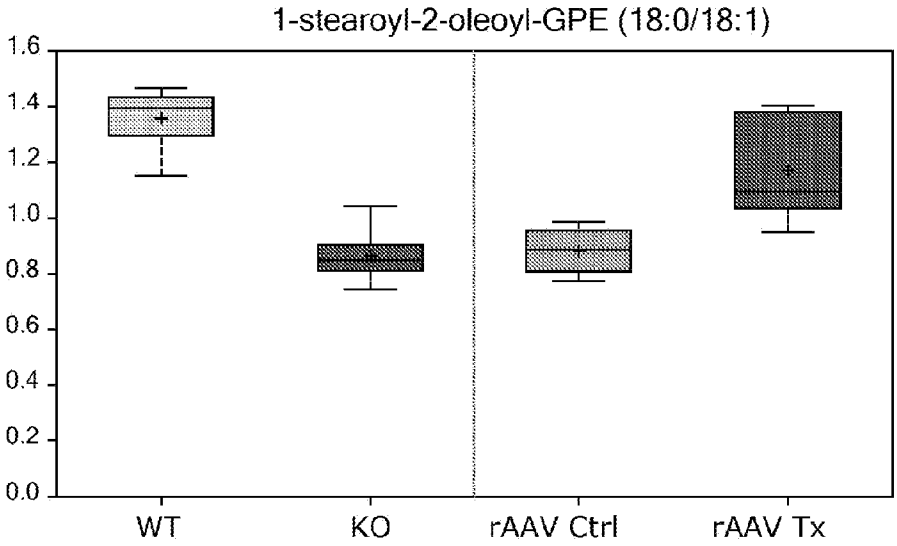
1-stearoyl-2-oleoyl-GPE (18:0/18:1)
1.6
1.4
1.2
1.0
0.8
0.6
0.4
0.2
0.0
WT
KO
rAAV Ctrl
rAAV Tx

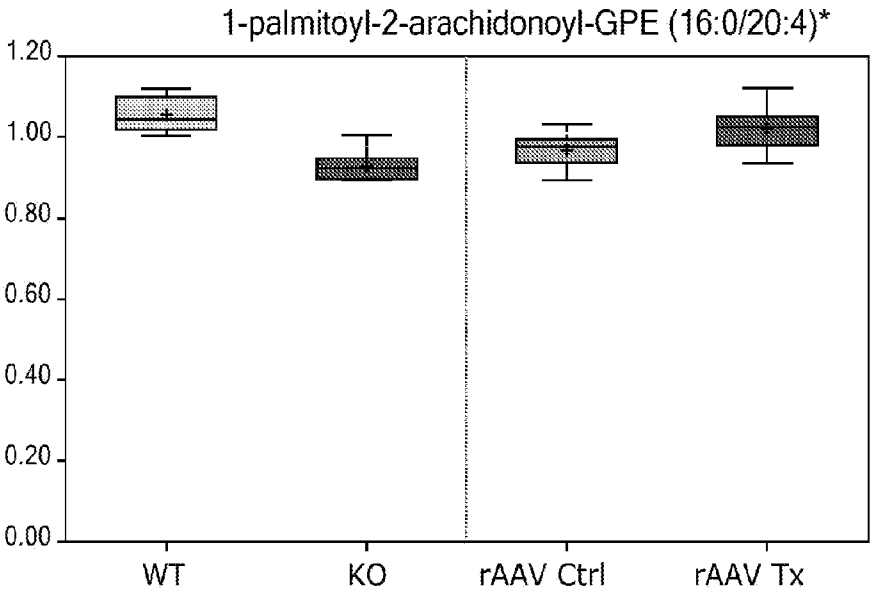
1-palmitoyl-2-arachidonoyl-GPE (16:0/20:4)*
1.20
1.00
0.80
0.60
0.40
0.20
0.00
WT
KO
rAAV Ctrl
rAAV Tx

FIG. 57 cont.

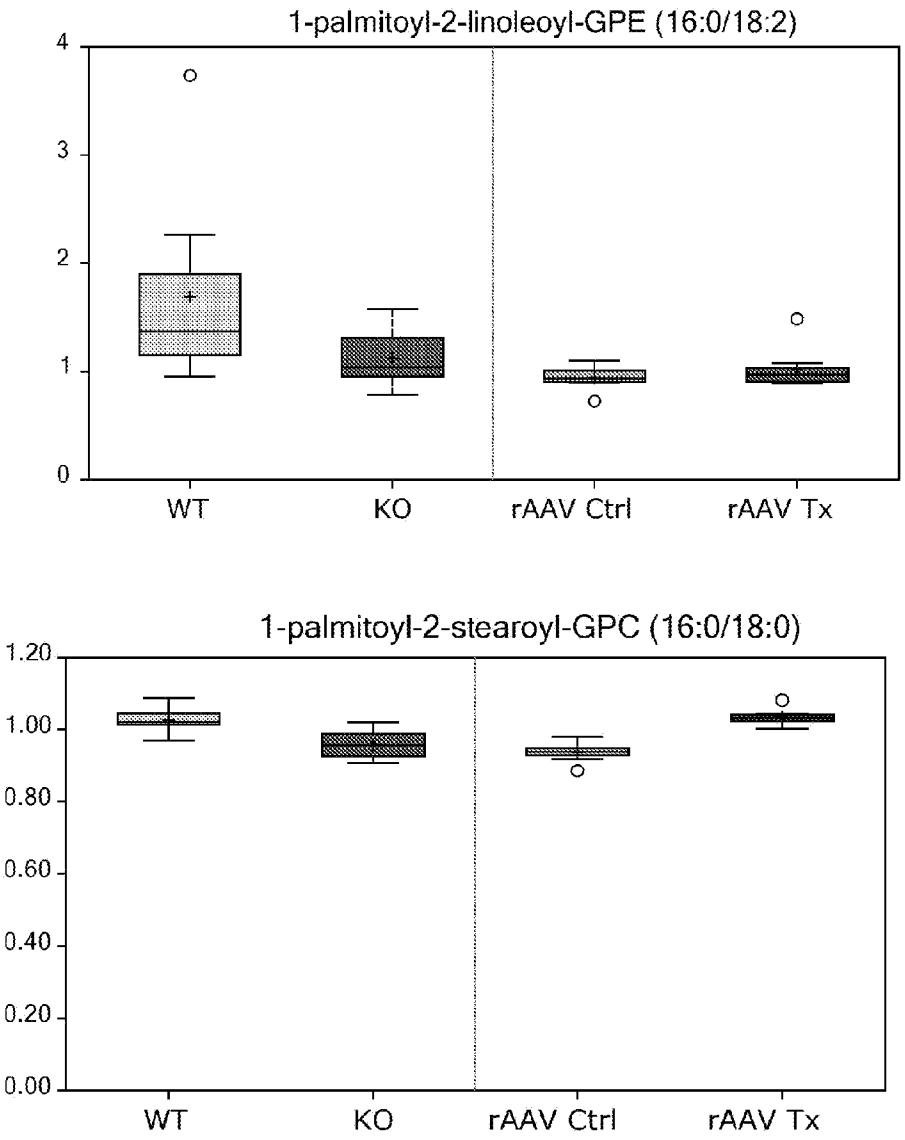
1-palmitoyl-2-linoleoyl-GPE (16:0/18:2)
4
3
2
1
0
WT
KO
rAAV Ctrl
rAAV Tx
1-palmitoyl-2-stearoyl-GPC (16:0/18:0)
1.20
1.00
0.80
0.60
0.40
0.20
0.00
WT
KO
rAAV Ctrl
rAAV Tx

FIG. 57 cont.

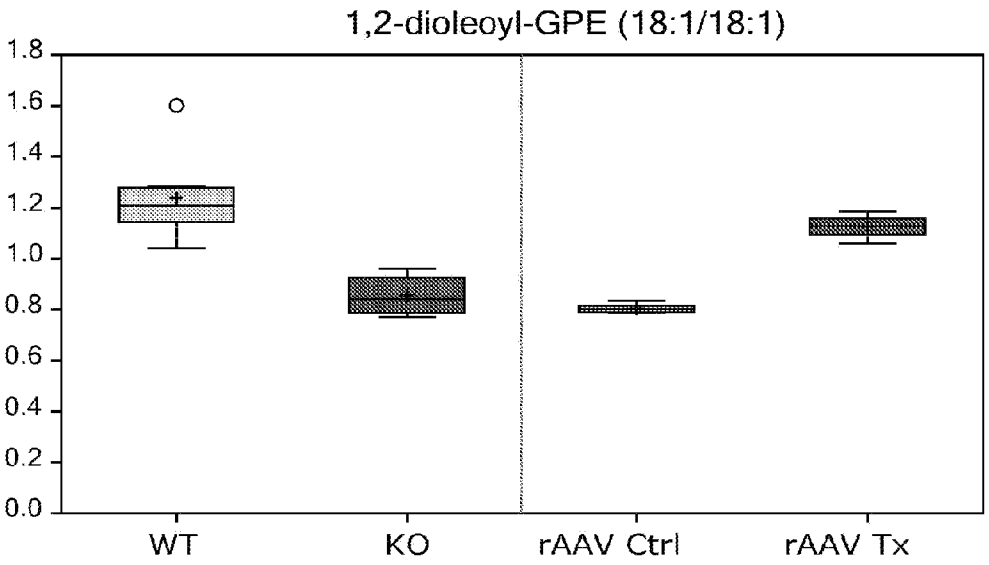
1,2-dioleoyl-GPE (18:1/18:1)
1.8
1.6
1.4
1.2
1.0
0.8
0.6
0.4
0.2
0.0
WT
KO
rAAV Ctrl
rAAV Tx

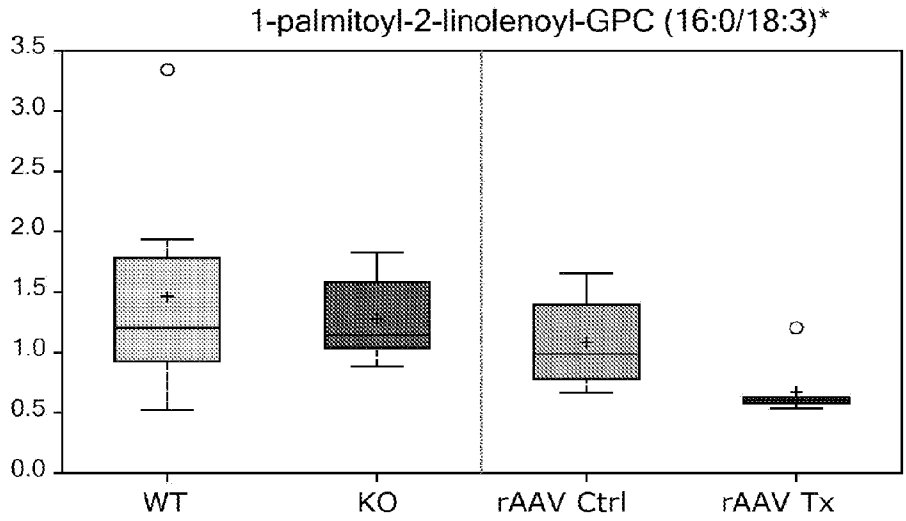
1-palmitoyl-2-linolenoyl-GPC (16:0/18:3)*
3.5
3.0
2.5
2.0
1.5
1.0
0.5
0.0
WT
KO
rAAV Ctrl
rAAV Tx

FIG. 57 cont.

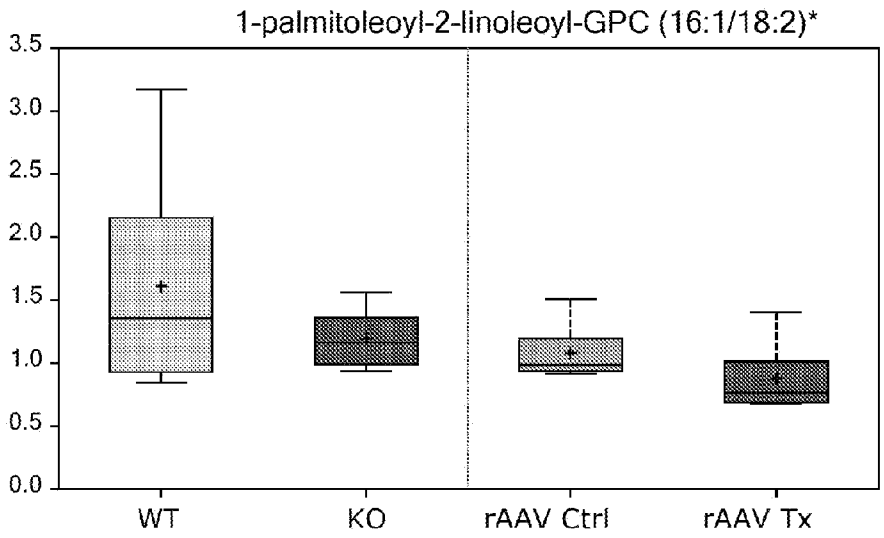
1-palmitoleoyl-2-linoleoyl-GPC (16:1/18:2)*
3.5
3.0
2.5
2.0
1.5
1.0
0.5
0.0
WT
KO
rAAV Ctrl
rAAV Tx

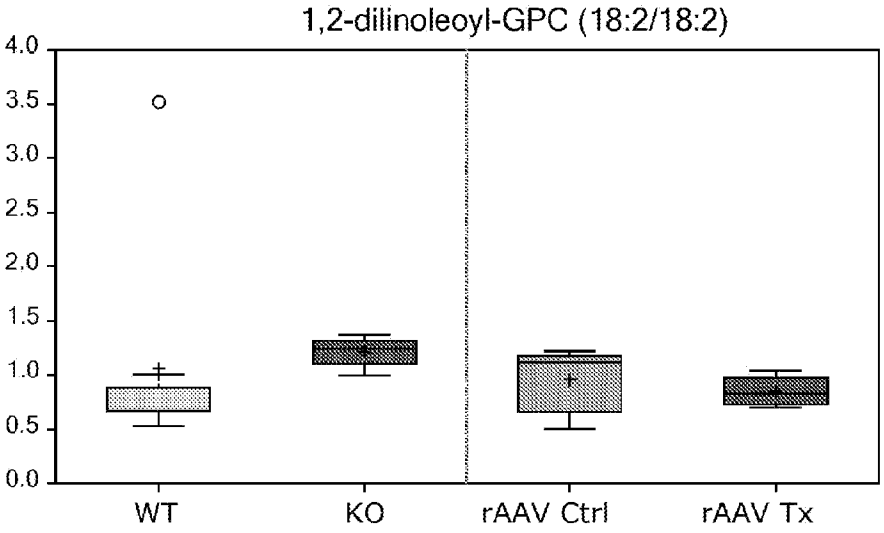
1,2-dilinoleoyl-GPC (18:2/18:2)
4.0
3.5
3.0
2.5
2.0
1.5
1.0
0.5
0.0
WT
KO
rAAV Ctrl
rAAV Tx

FIG. 57 cont.

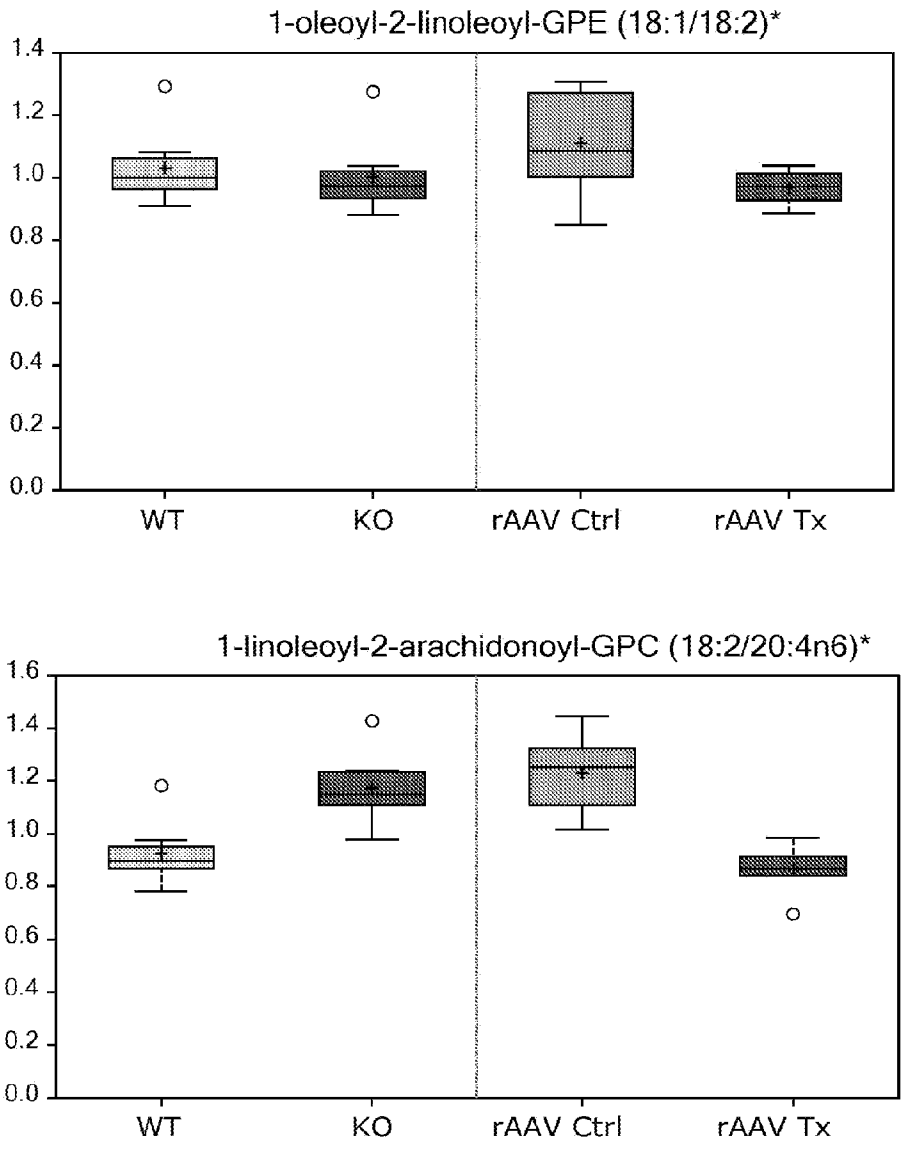
1-oleoyl-2-linoleoyl-GPE (18:1/18:2)*
1.4
1.2
1.0
0.8
0.6
0.4
0.2
0.0
WT
KO
rAAV Ctrl
rAAV Tx
1-linoleoyl-2-arachidonoyl-GPC (18:2/20:4n6)*
1.6
1.4
1.2
1.0
0.8
0.6
0.4
0.2
0.0
WT
KO
rAAV Ctrl
rAAV Tx

FIG. 57 cont.

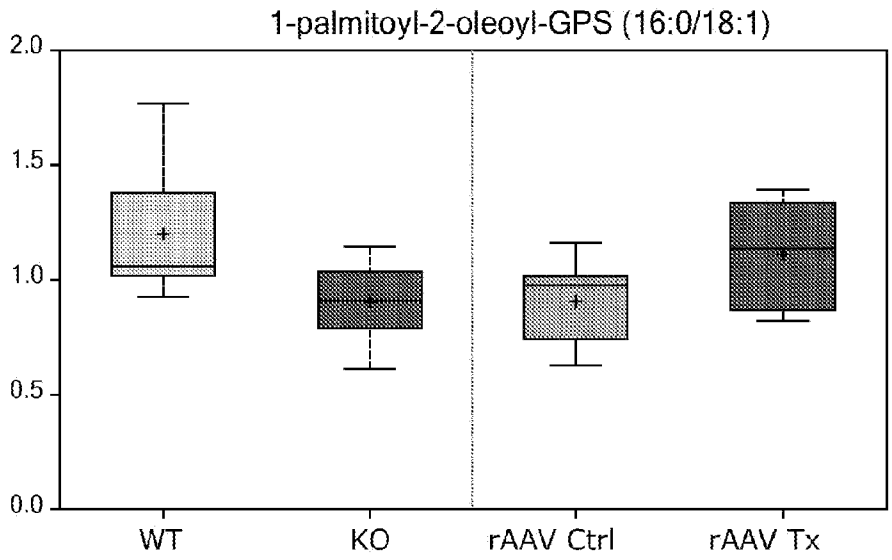
1-palmitoyl-2-oleoyl-GPS (16:0/18:1)
2.0
1.5
1.0
0.5
0.0
WT
KO
rAAV Ctrl
rAAV Tx

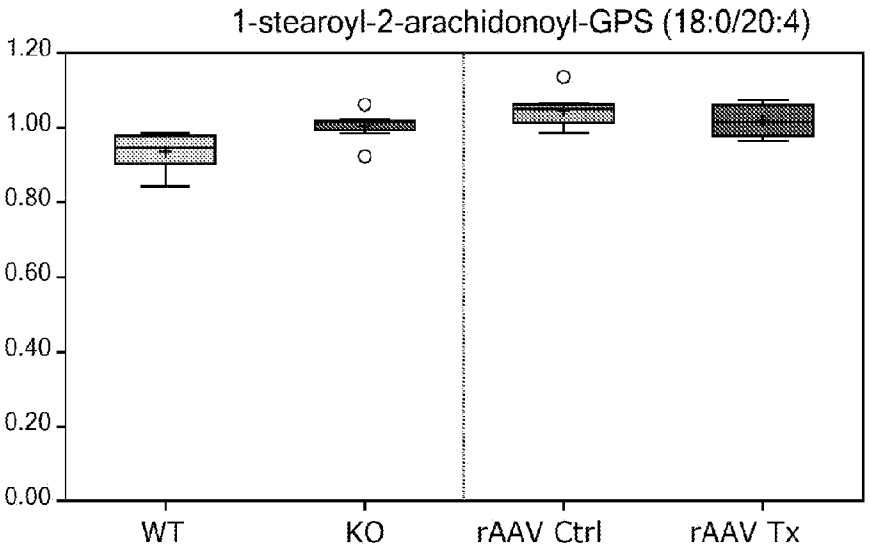
1-stearoyl-2-arachidonoyl-GPS (18:0/20:4)
1.20
1.00
0.80
0.60
0.40
0.20
0.00
WT
KO
rAAV Ctrl
rAAV Tx

FIG. 57 cont.

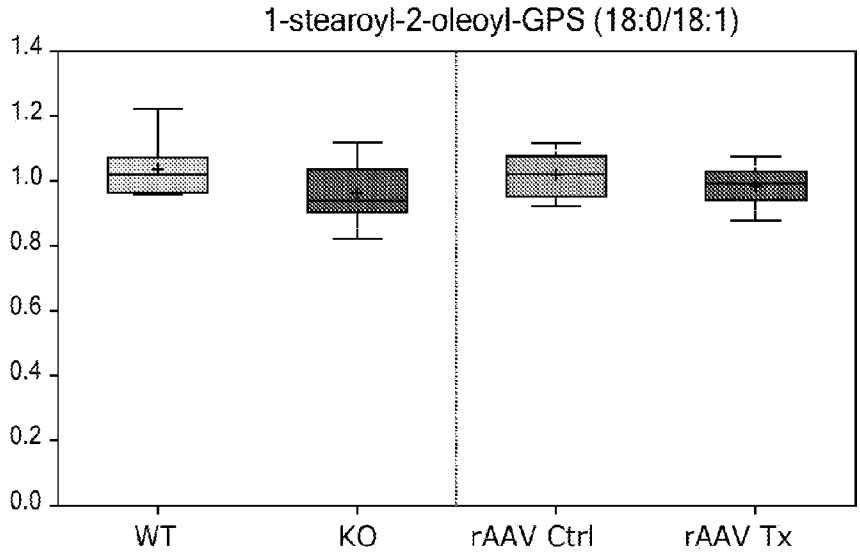
1-stearoyl-2-oleoyl-GPS (18:0/18:1)
1.4
1.2
1.0
0.8
0.6
0.4
0.2
0.0
WT
KO
rAAV Ctrl
rAAV Tx

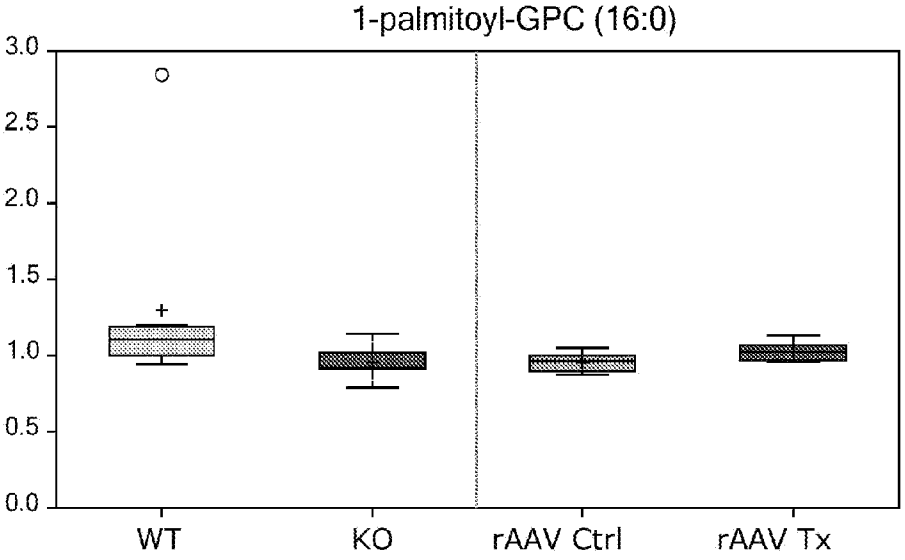
1-palmitoyl-GPC (16:0)
3.0
2.5
2.0
1.5
1.0
0.5
0.0
WT
KO
rAAV Ctrl
rAAV Tx

FIG. 57 cont.

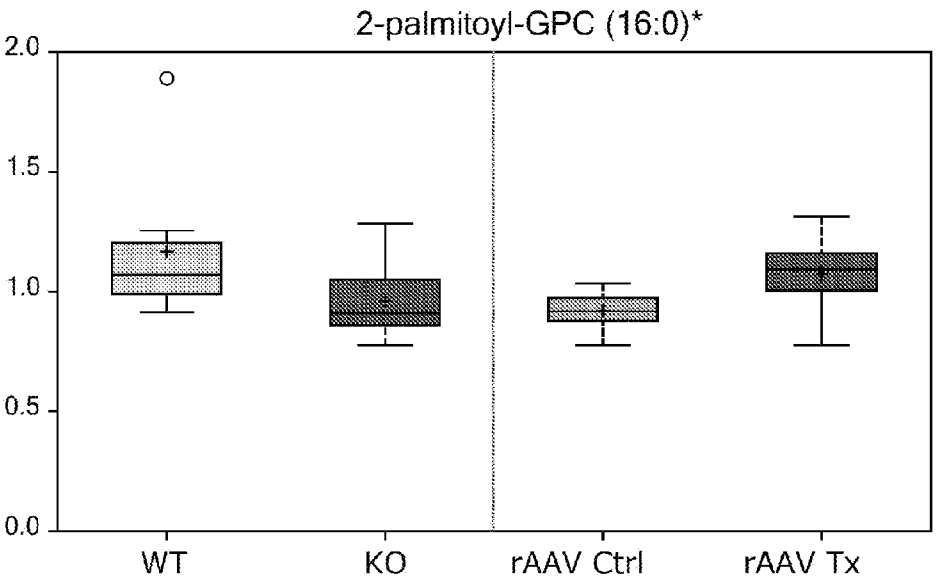
2-palmitoyl-GPC (16:0)*
2.0
1.5
1.0
0.5
0.0
WT
KO
rAAV Ctrl
rAAV Tx

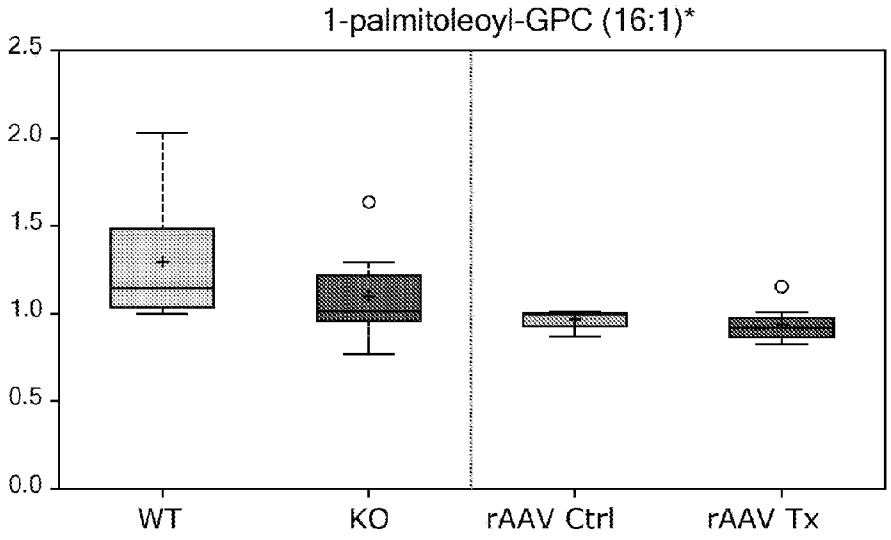
1-palmitoleoyl-GPC (16:1)*
2.5
2.0
1.5
1.0
0.5
0.0
WT
KO
rAAV Ctrl
rAAV Tx

FIG. 57 cont.

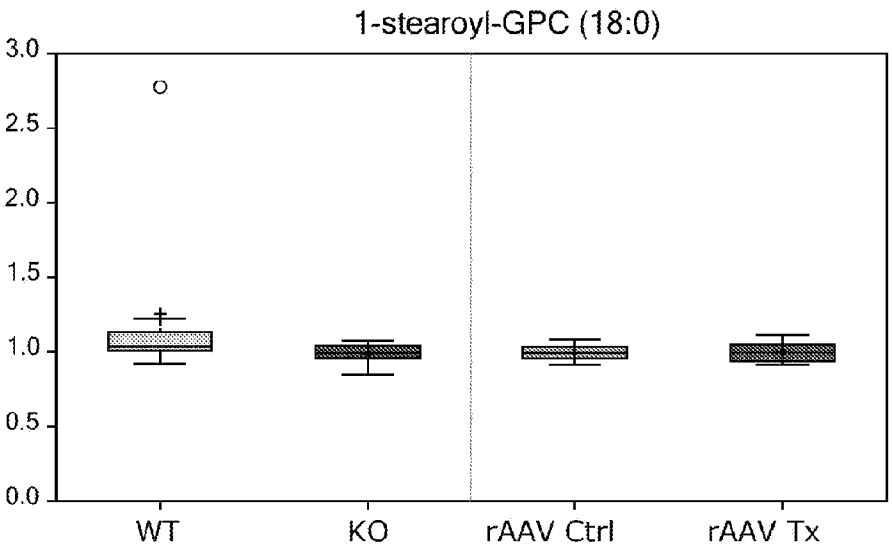
1-stearoyl-GPC (18:0)
3.0
2.5
2.0
1.5
1.0
0.5
0.0
WT
KO
rAAV Ctrl
rAAV Tx

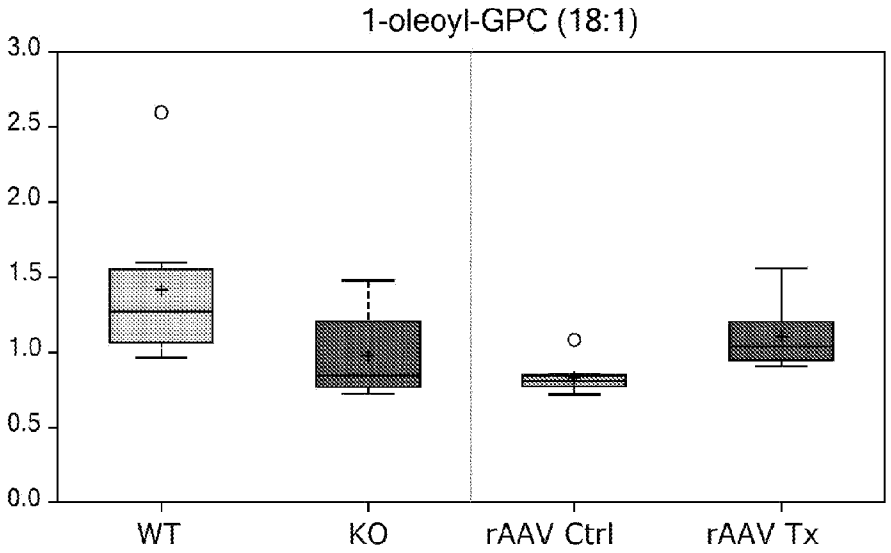
1-oleoyl-GPC (18:1)
3.0
2.5
2.0
1.5
1.0
0.5
0.0
WT
KO
rAAV Ctrl
rAAV Tx

FIG. 57 cont.

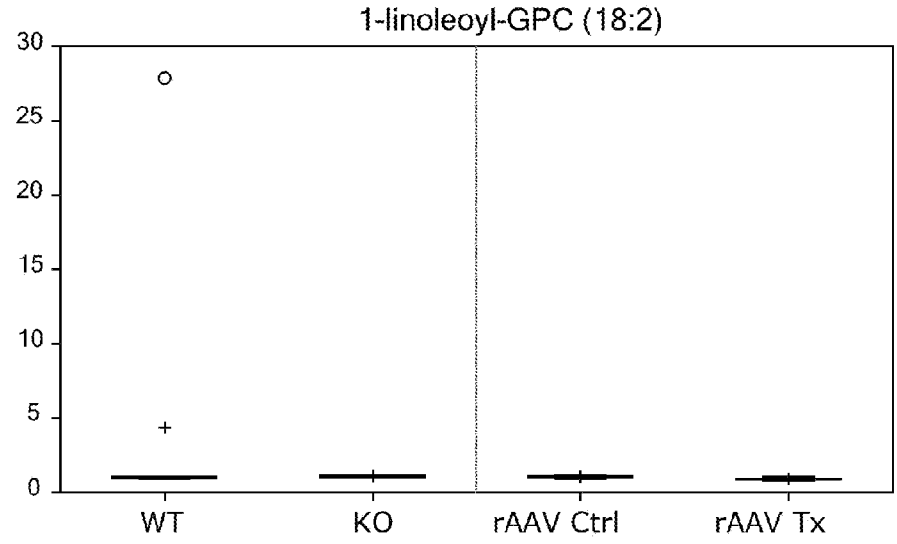
1-linoleoyl-GPC (18:2)
30
25
20
15
10
5
0
WT
KO
rAAV Ctrl
rAAV Tx

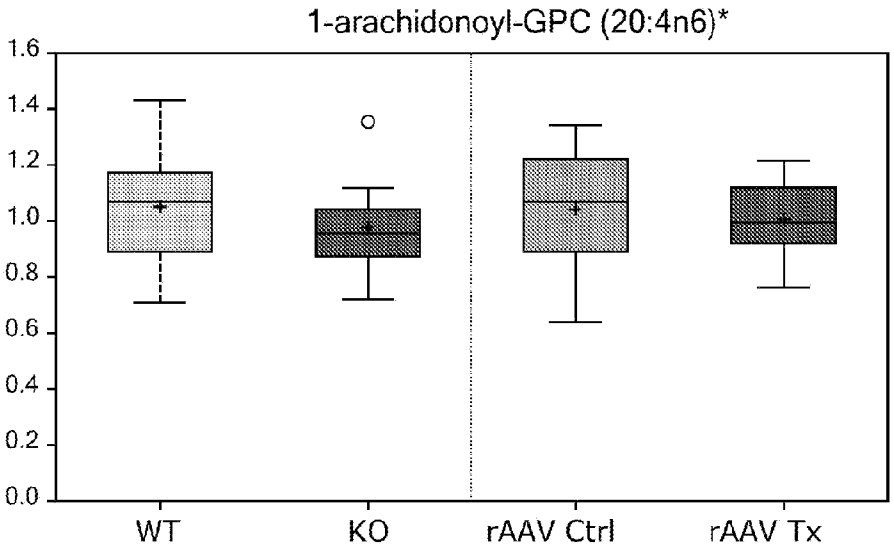
1-arachidonoyl-GPC (20:4n6)*
1.6
1.4
1.2
1.0
0.8
0.6
0.4
0.2
0.0
WT
KO
rAAV Ctrl
rAAV Tx

FIG. 57 cont.

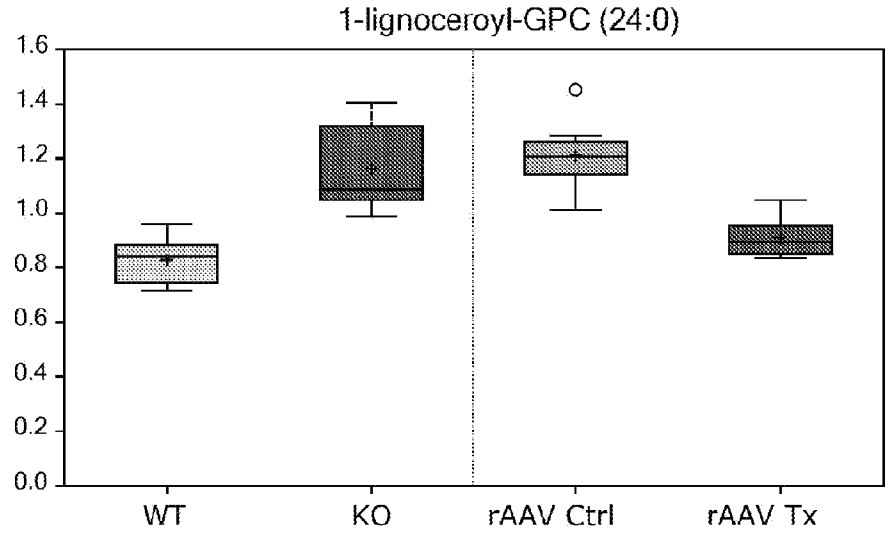
1-lignoceroyl-GPC (24:0)
1.6
1.4
1.2
1.0
0.8
0.6
0.4
0.2
0.0
WT
KO
rAAV Ctrl
rAAV Tx

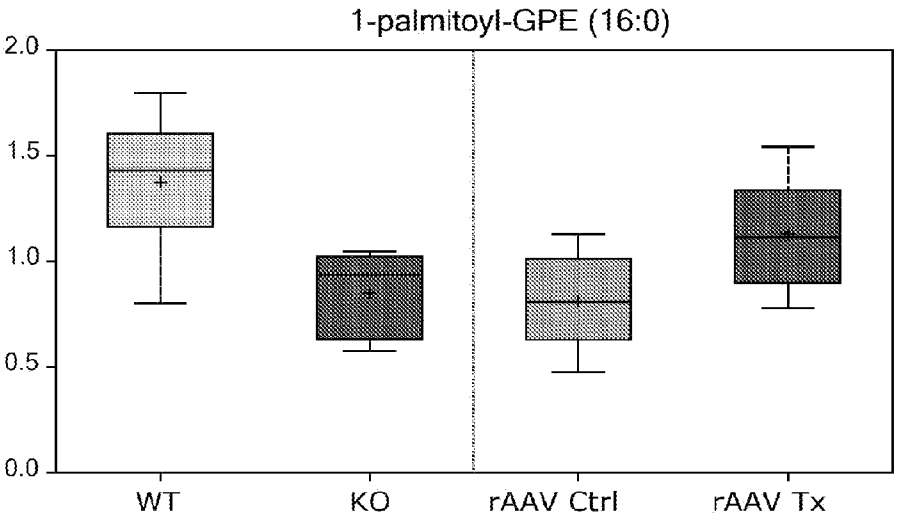
1-palmitoyl-GPE (16:0)
2.0
1.5
1.0
0.5
0.0
WT
KO
rAAV Ctrl
rAAV Tx

FIG. 57 cont.

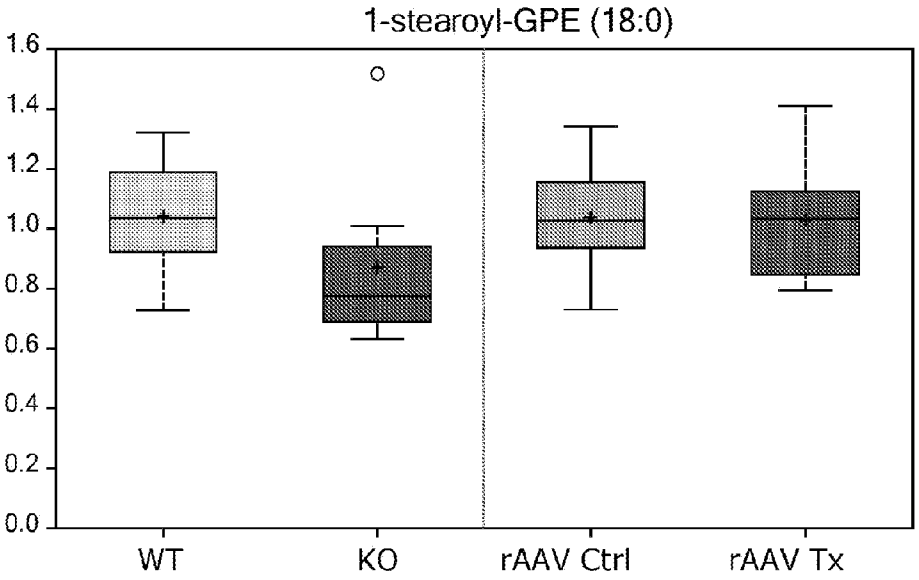
1-stearoyl-GPE (18:0)
1.6
1.4
1.2
1.0
0.8
0.6
0.4
0.2
0.0
WT
KO
rAAV Ctrl
rAAV Tx

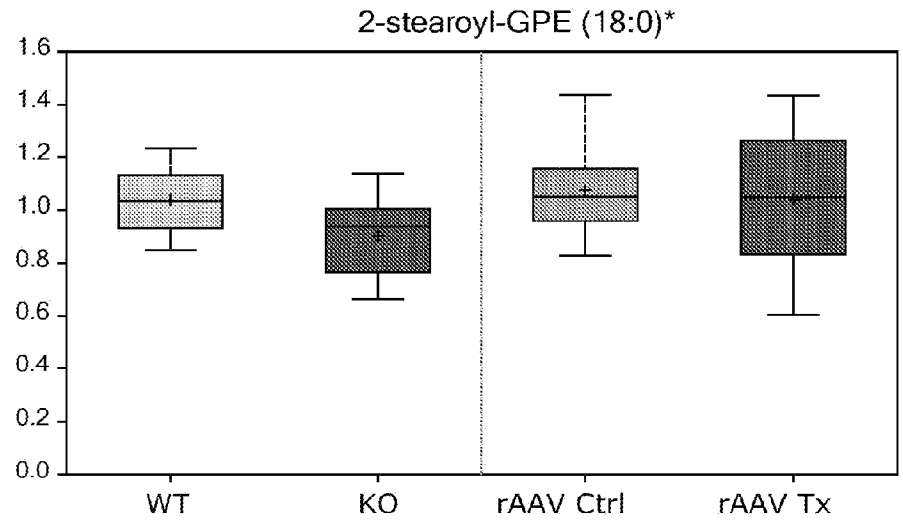
2-stearoyl-GPE (18:0)*
1.6
1.4
1.2
1.0
0.8
0.6
0.4
0.2
0.0
WT
KO
rAAV Ctrl
rAAV Tx

FIG. 57 cont.

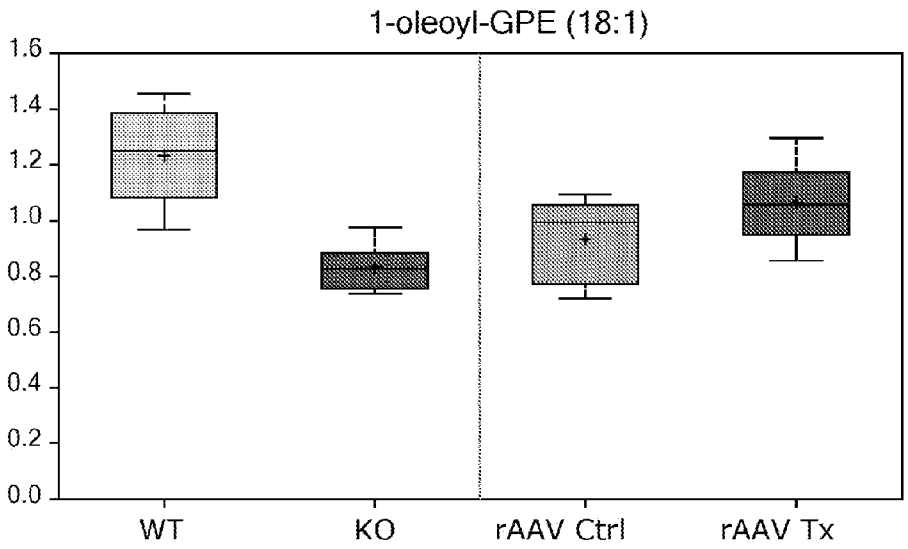
1-oleoyl-GPE (18:1)
1.6
1.4
1.2
1.0
0.8
0.6
0.4
0.2
0.0
WT
KO
rAAV Ctrl
rAAV Tx

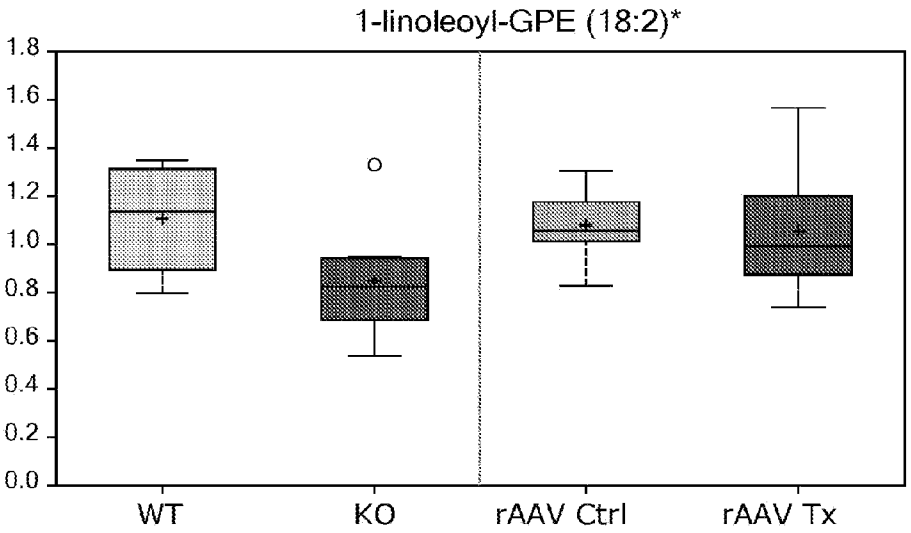
1-linoleoyl-GPE (18:2)*
1.8
1.6
1.4
1.2
1.0
0.8
0.6
0.4
0.2
0.0
WT
KO
rAAV Ctrl
rAAV Tx

FIG. 57 cont.

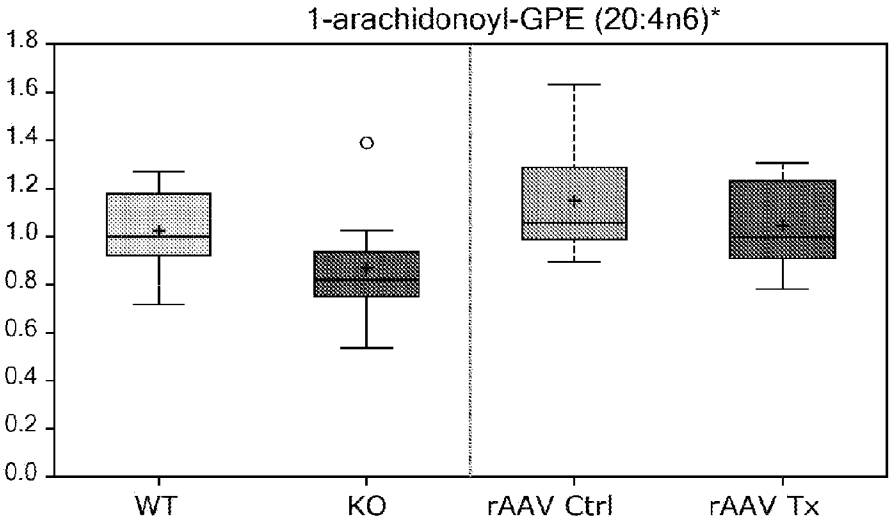
1-arachidonoyl-GPE (20:4n6)*
1.8
1.6
1.4
1.2
1.0
0.8
0.6
0.4
0.2
0.0
WT
KO
rAAV Ctrl
rAAV Tx

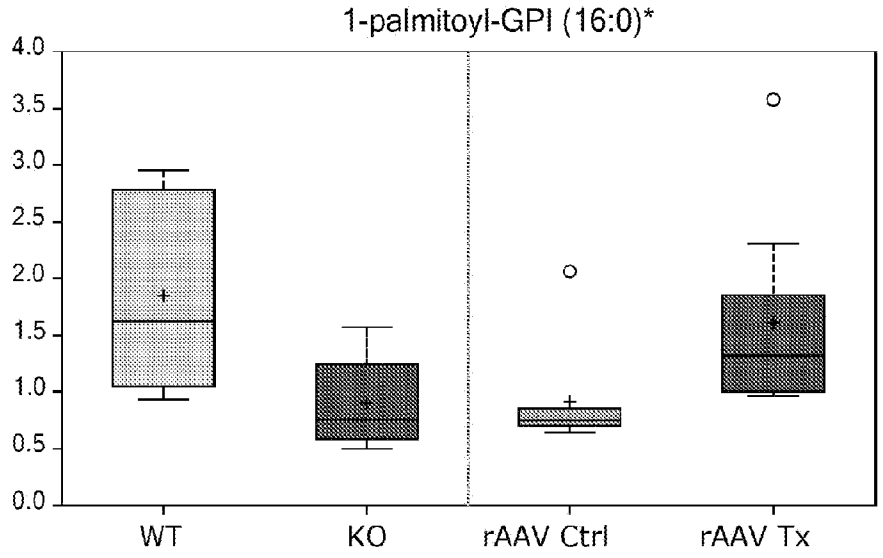
1-palmitoyl-GPI (16:0)*
4.0
3.5
3.0
2.5
2.0
1.5
1.0
0.5
0.0
WT
KO
rAAV Ctrl
rAAV Tx

FIG. 57 cont.

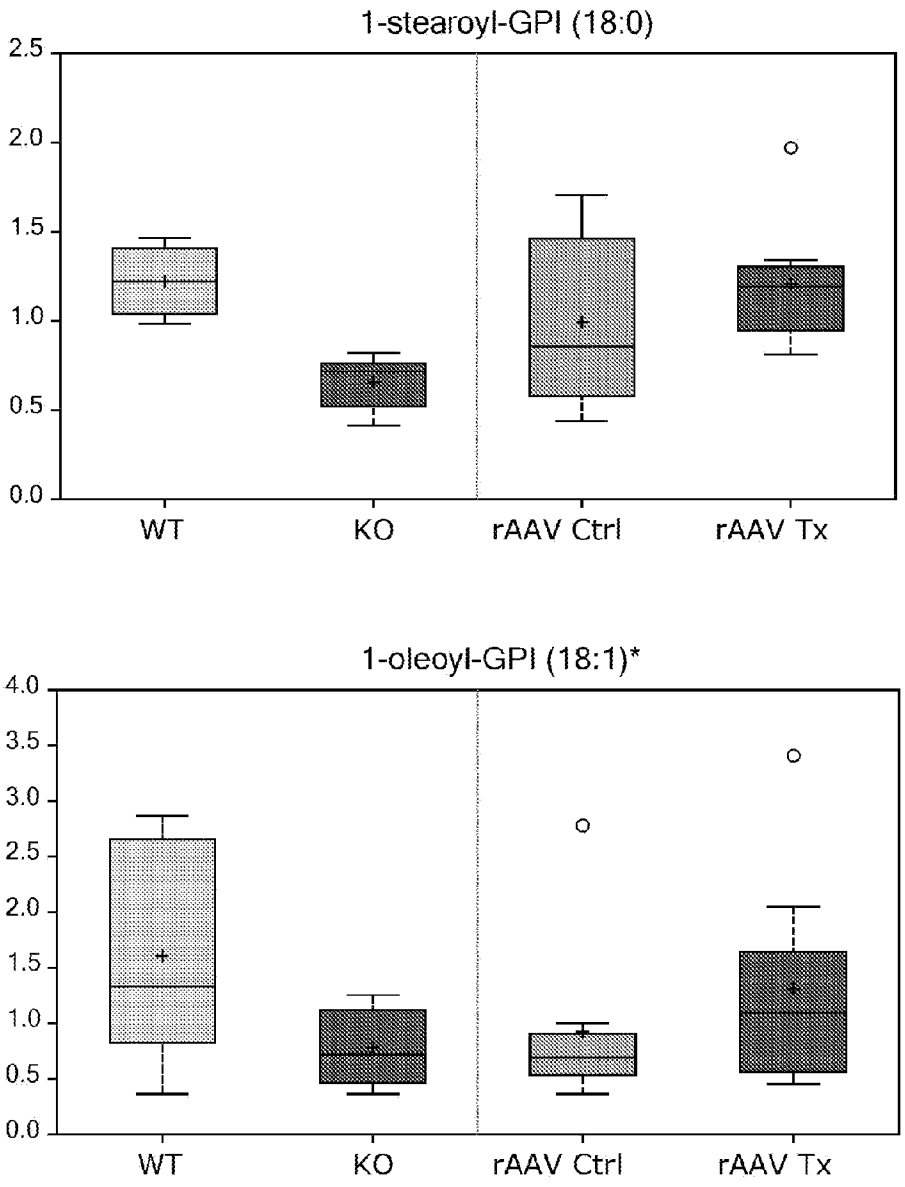
1-stearoyl-GPI (18:0)
2.5
2.0
1.5
1.0
0.5
0.0
WT
KO
rAAV Ctrl
rAAV Tx
1-oleoyl-GPI (18:1)*
4.0
3.5
3.0
2.5
2.0
1.5
1.0
0.5
0.0
WT
KO
rAAV Ctrl
rAAV Tx

FIG. 57 cont.

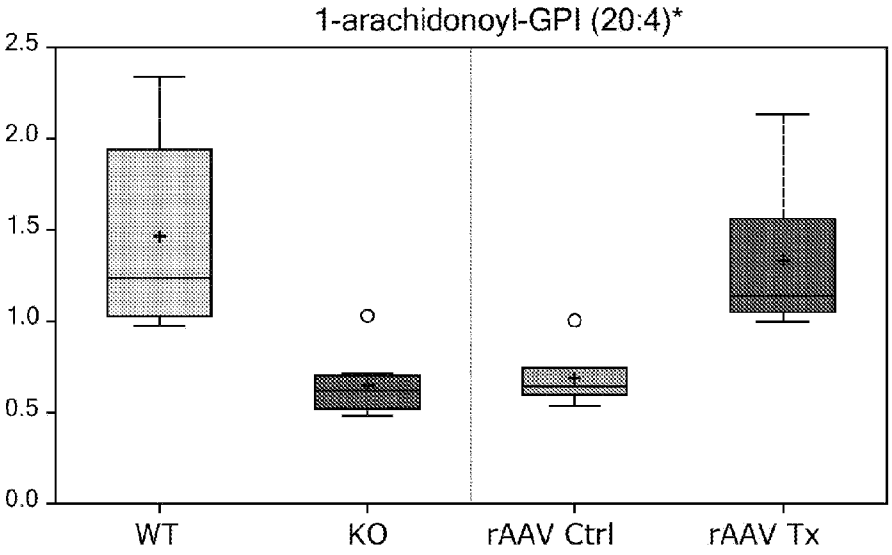
1-arachidonoyl-GPI (20:4)*
2.5
2.0
1.5
1.0
0.5
0.0
WT
KO
rAAV Ctrl
rAAV Tx

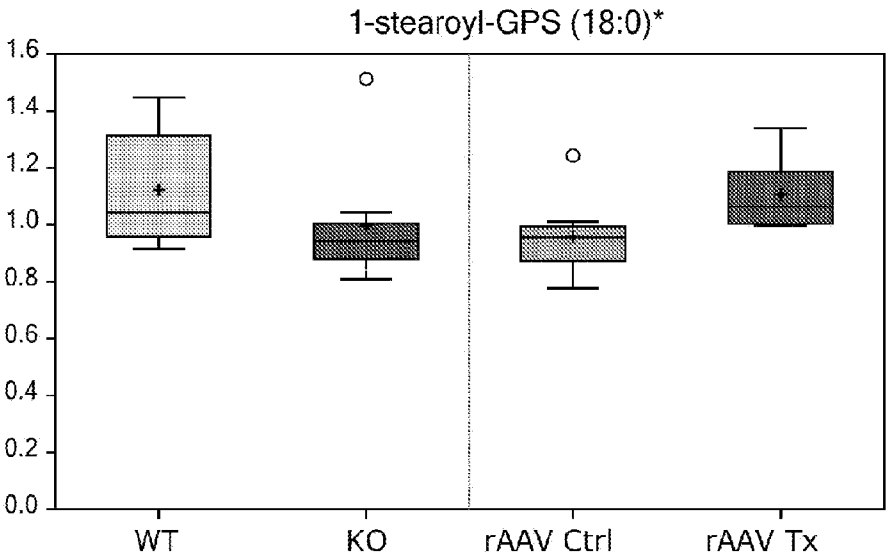
1-stearoyl-GPS (18:0)*
1.6
1.4
1.2
1.0
0.8
0.6
0.4
0.2
0.0
WT
KO
rAAV Ctrl
rAAV Tx

FIG. 57 cont.

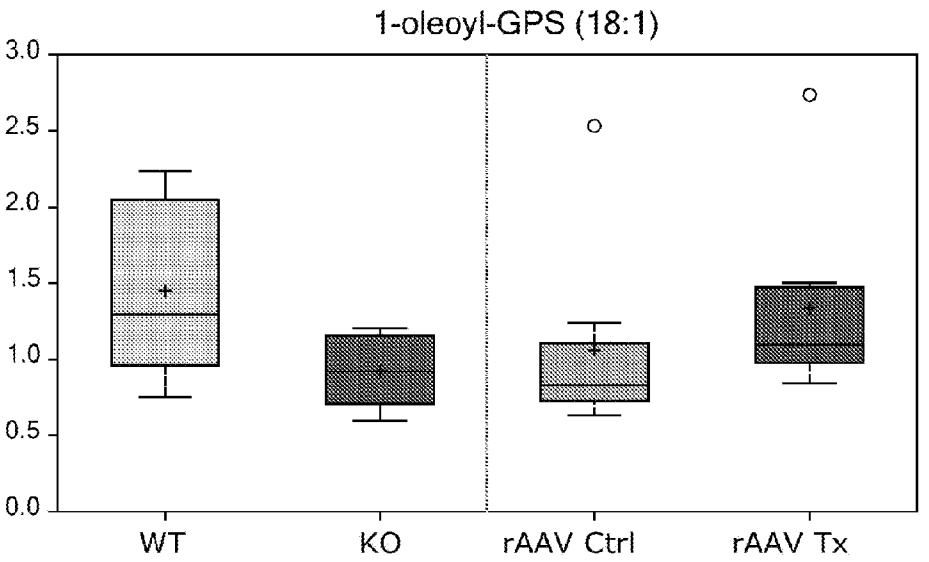
1-oleoyl-GPS (18:1)
3.0
2.5
2.0
1.5
1.0
0.5
0.0
WT
KO
rAAV Ctrl
rAAV Tx

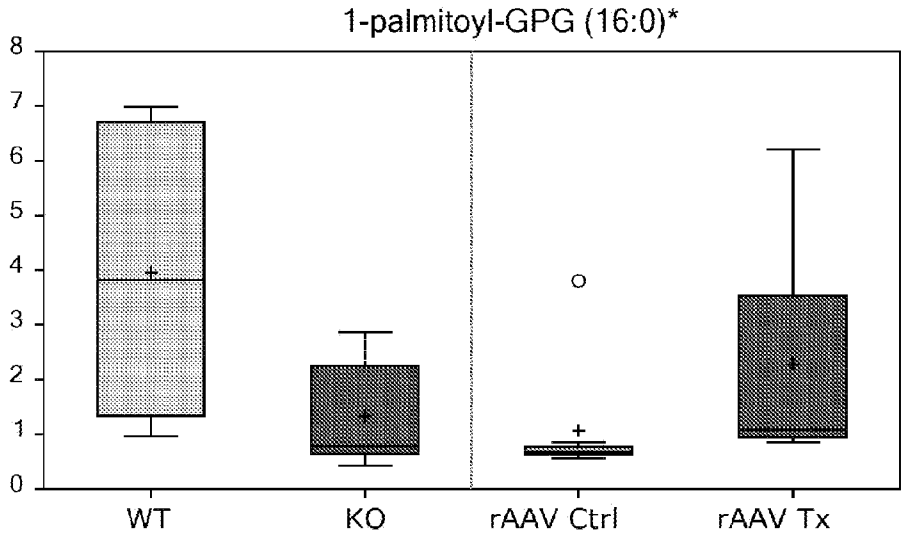
1-palmitoyl-GPG (16:0)*
8
7
6
5
4
3
2
1
0
WT
KO
rAAV Ctrl
rAAV Tx

FIG. 57 cont.

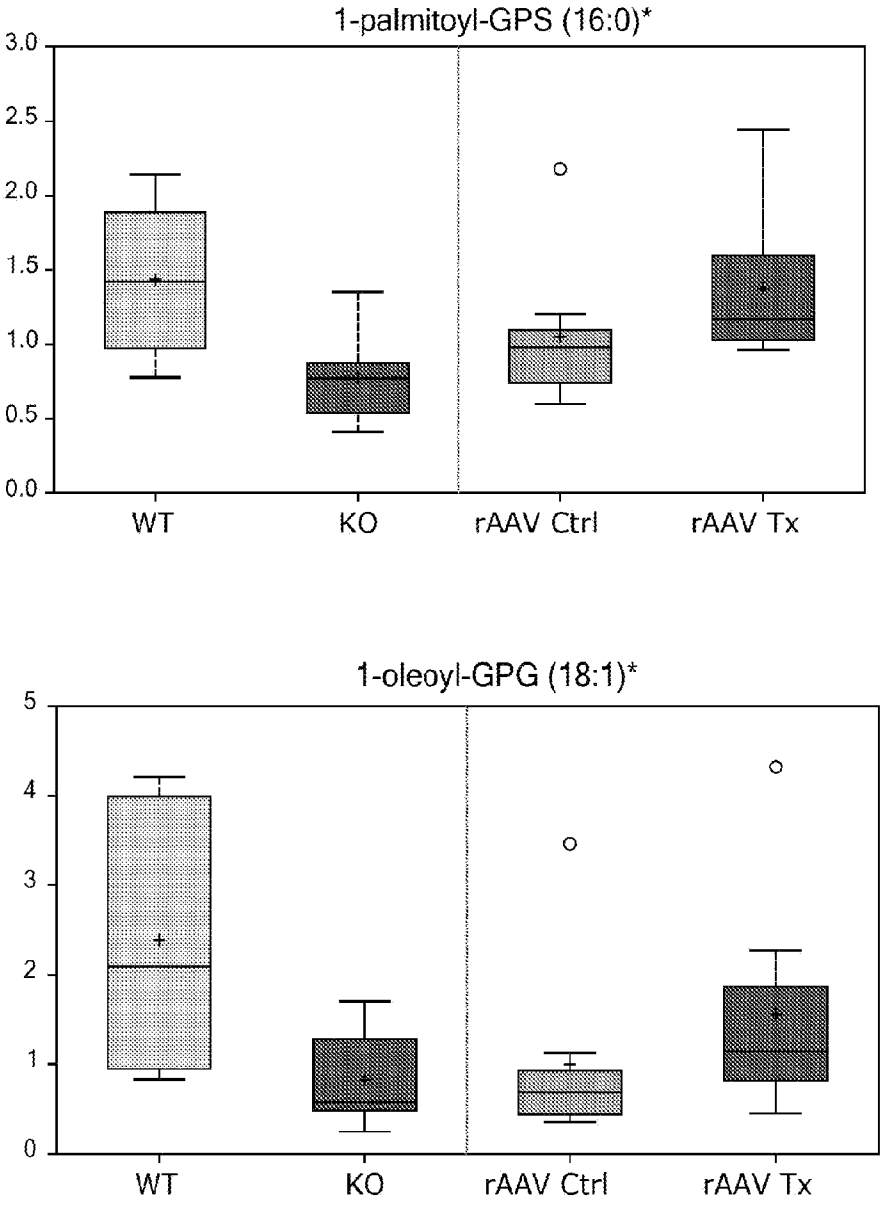
1-palmitoyl-GPS (16:0)*
3.0
2.5
2.0
1.5
1.0
0.5
0.0
WT
KO
rAAV Ctrl
rAAV Tx
1-oleoyl-GPG (18:1)*
5
4
3
2
1
0
WT
KO
rAAV Ctrl
rAAV Tx

FIG. 57 cont.

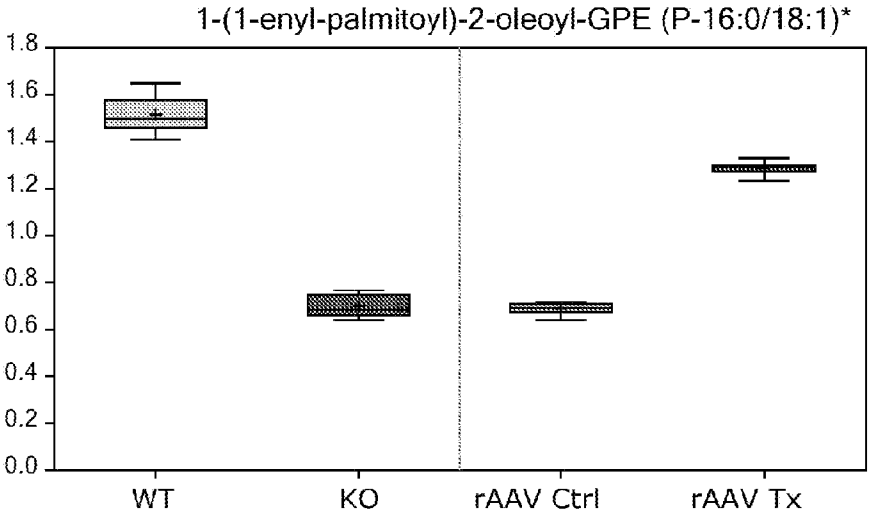
1-(1-enyl-palmitoyl)-2-oleoyl-GPE (P-16:0/18:1)*
1.8
1.6
1.4
1.2
1.0
0.8
0.6
0.4
0.2
0.0
WT
KO
rAAV Ctrl
rAAV Tx

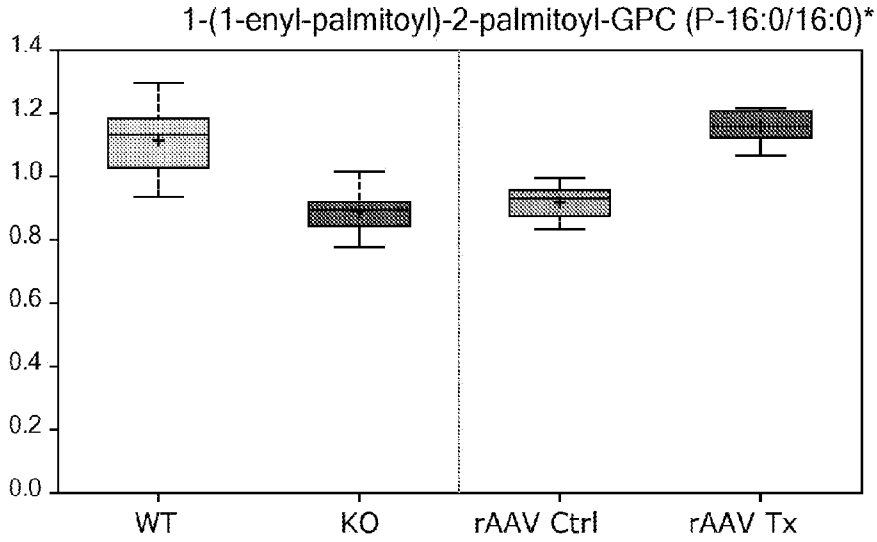
1-(1-enyl-palmitoyl)-2-palmitoyl-GPC (P-16:0/16:0)*
1.4
1.2
1.0
0.8
0.6
0.4
0.2
0.0
WT
KO
rAAV Ctrl
rAAV Tx

FIG. 57 cont.

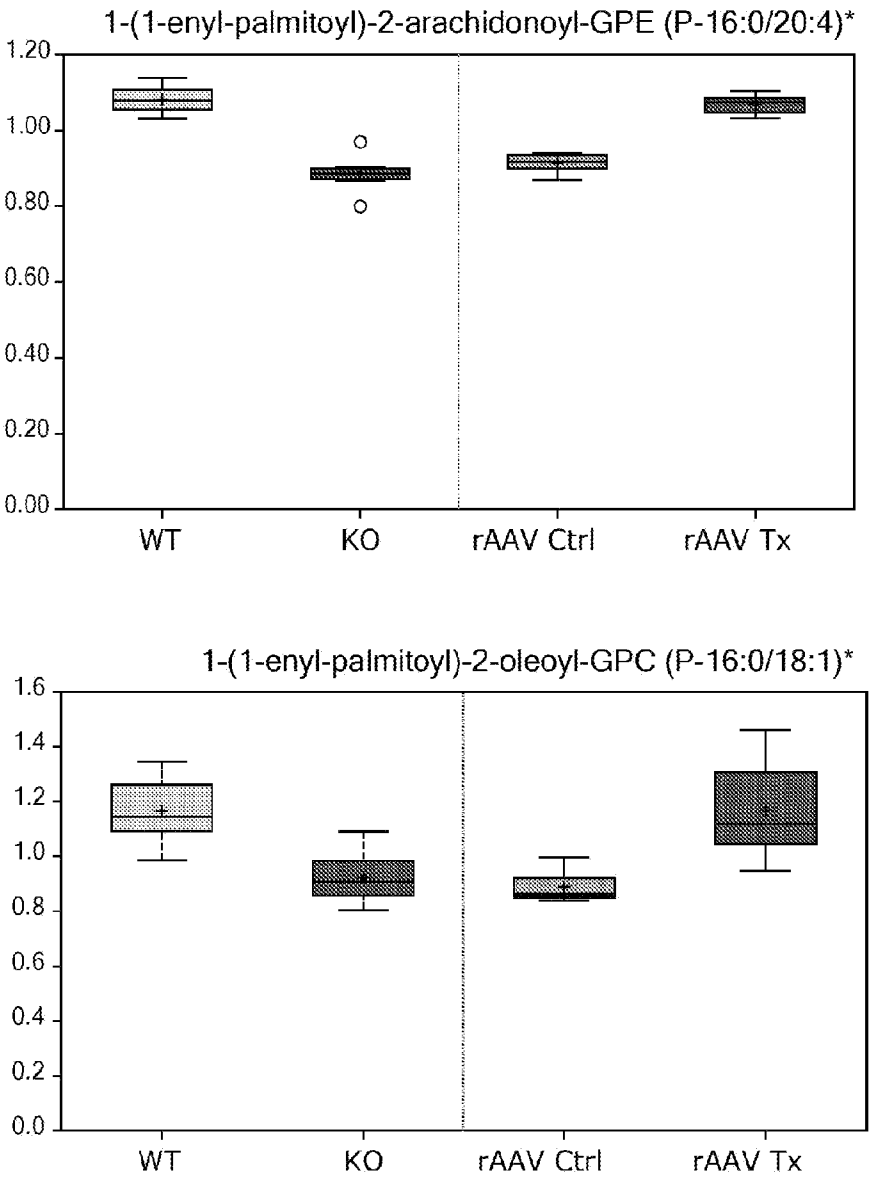
1-(1-enyl-palmitoyl)-2-arachidonoyl-GPE (P-16:0/20:4)*
1.20
1.00
0.80
0.60
0.40
0.20
0.00
WT
KO
rAAV Ctrl
rAAV Tx
1-(1-enyl-palmitoyl)-2-oleoyl-GPC (P-16:0/18:1)*
1.6
1.4
1.2
1.0
0.8
0.6
0.4
0.2
0.0
WT
KO
rAAV Ctrl
rAAV Tx

FIG. 57 cont.

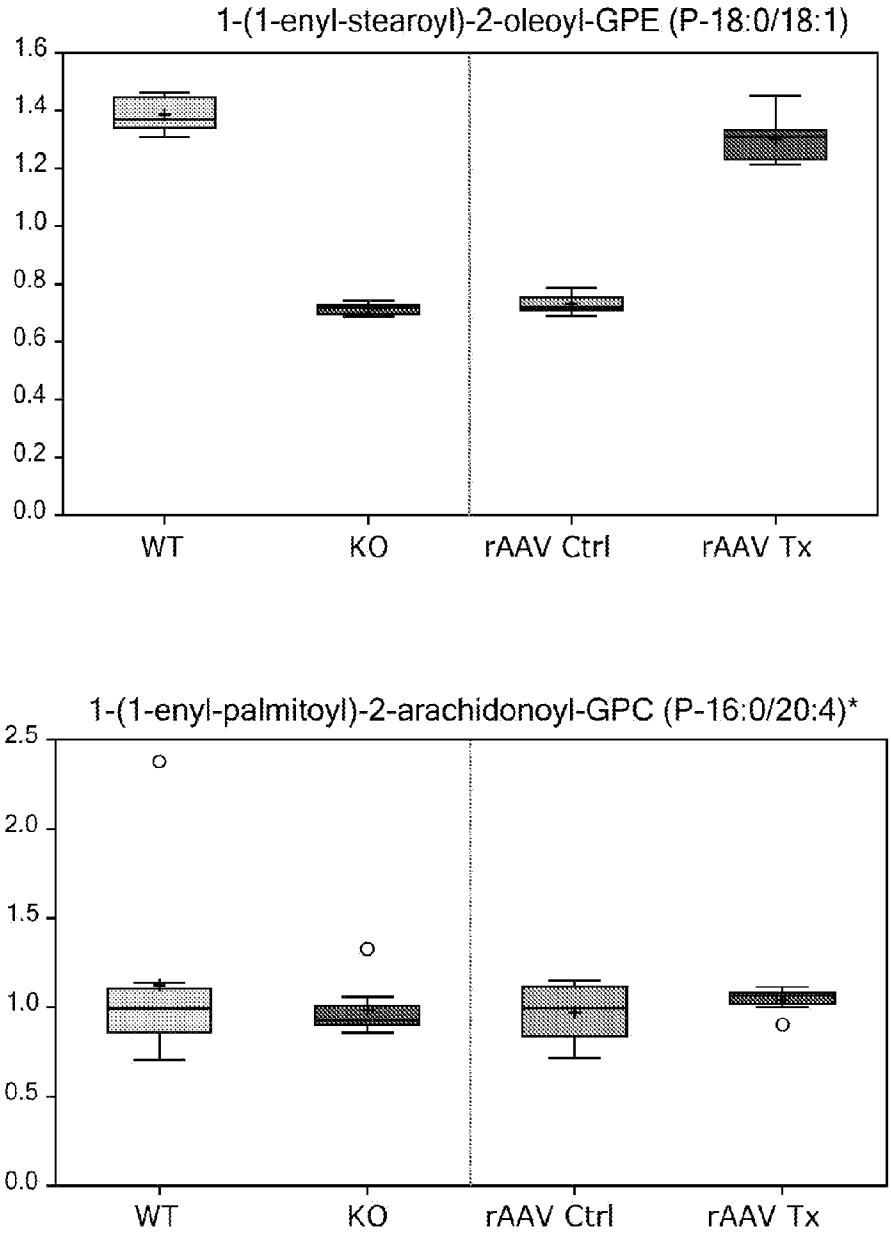
1-(1-enyl-stearoyl)-2-oleoyl-GPE (P-18:0/18:1)
1.6
1.4
1.2
1.0
0.8
0.6
0.4
0.2
0.0
WT
KO
rAAV Ctrl
rAAV Tx
1-(1-enyl-palmitoyl)-2-arachidonoyl-GPC (P-16:0/20:4)*
2.5
2.0
1.5
1.0
0.5
0.0
WT
KO
rAAV Ctrl
rAAV Tx

FIG. 57 cont.

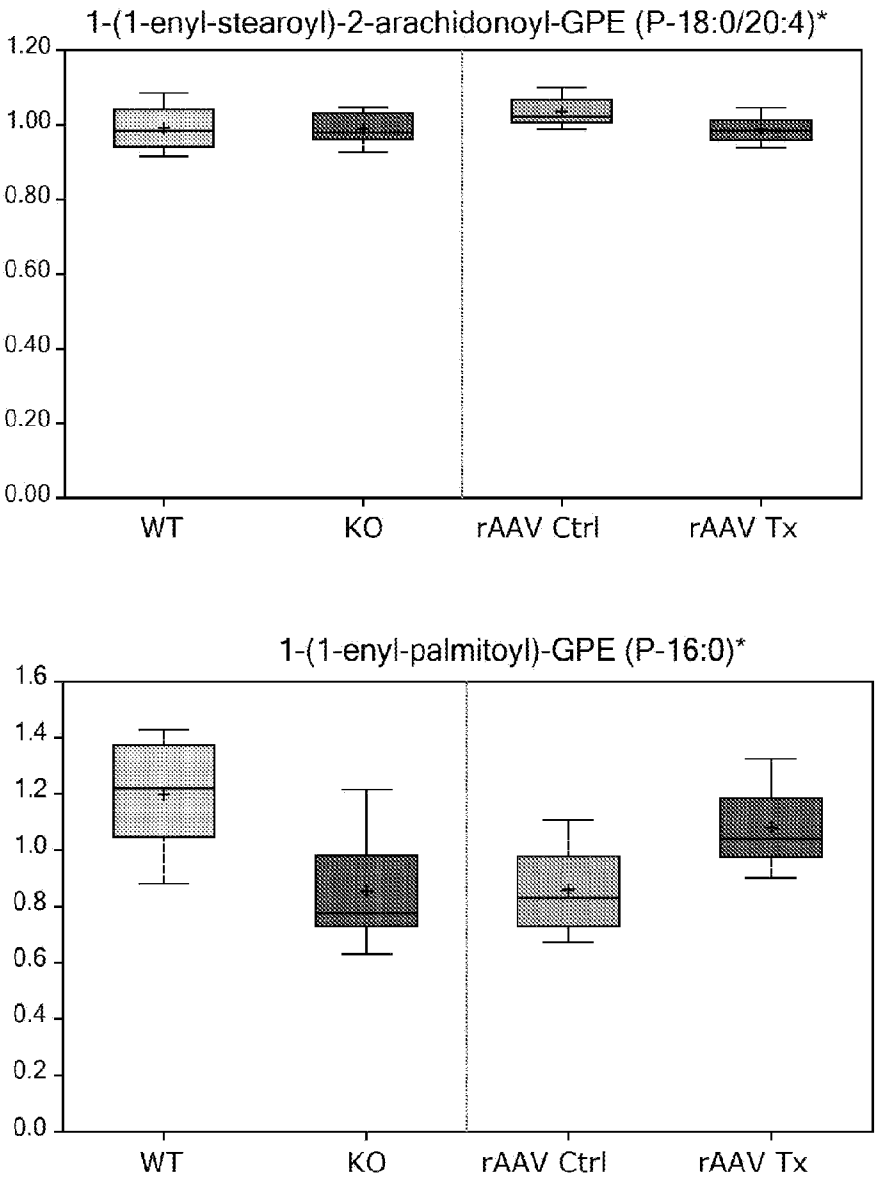
1-(1-enyl-stearoyl)-2-arachidonoyl-GPE (P-18:0/20:4)*
1.20
1.00
0.80
0.60
0.40
0.20
0.00
WT
KO
rAAV Ctrl
rAAV Tx
1-(1-enyl-palmitoyl)-GPE (P-16:0)*
1.6
1.4
1.2
1.0
0.8
0.6
0.4
0.2
0.0
WT
KO
rAAV Ctrl
rAAV Tx

FIG. 57 cont.

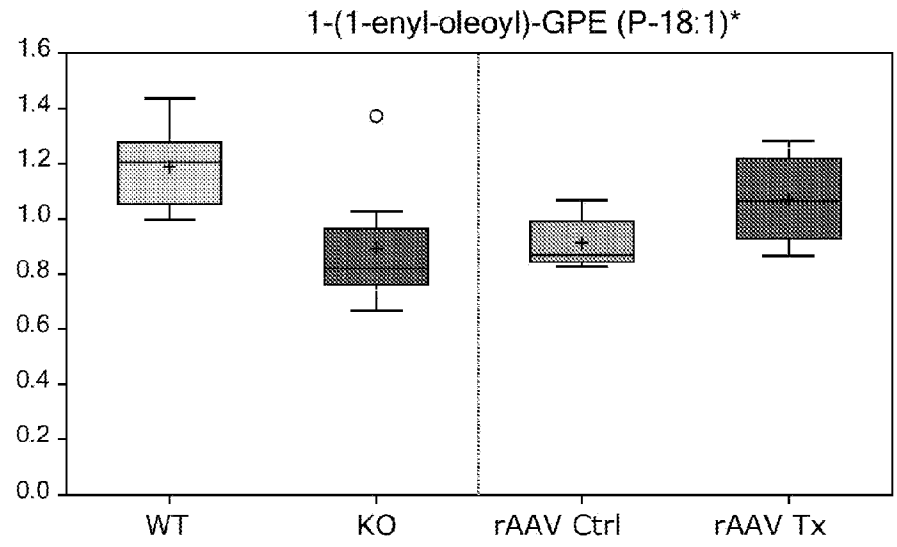
1-(1-enyl-oleoyl)-GPE (P-18:1)*
1.6
1.4
1.2
1.0
0.8
0.6
0.4
0.2
0.0
WT
KO
rAAV Ctrl
rAAV Tx

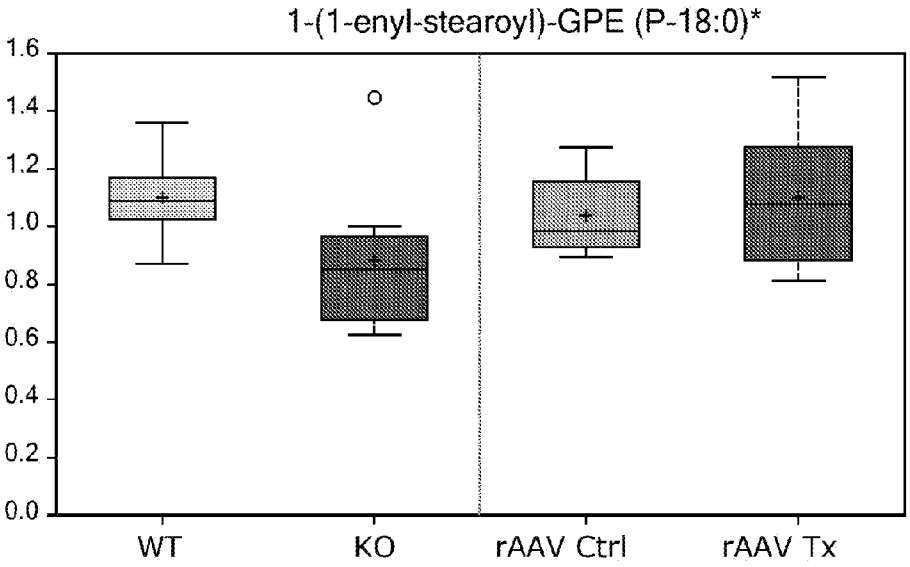
1-(1-enyl-stearoyl)-GPE (P-18:0)*
1.6
1.4
1.2
1.0
0.8
0.6
0.4
0.2
0.0
WT
KO
rAAV Ctrl
rAAV Tx

FIG. 57 cont.

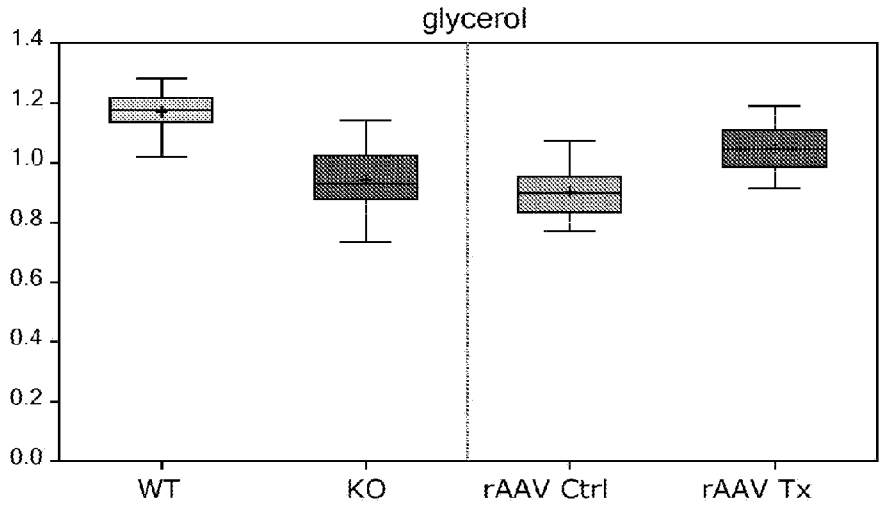
glycerol
1.4
1.2
1.0
0.8
0.6
0.4
0.2
0.0
WT
KO
rAAV Ctrl
rAAV Tx

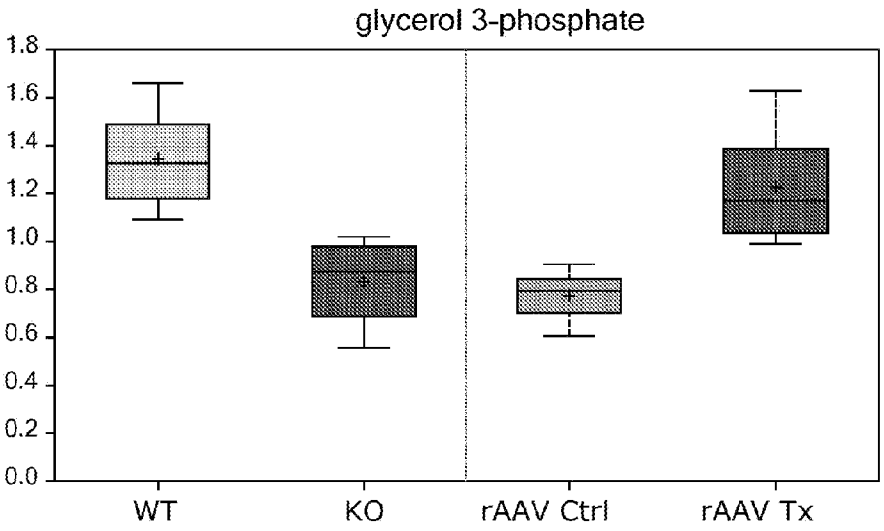
glycerol 3-phosphate
1.8
1.6
1.4
1.2
1.0
0.8
0.6
0.4
0.2
0.0
WT
KO
rAAV Ctrl
rAAV Tx

FIG. 57 cont.

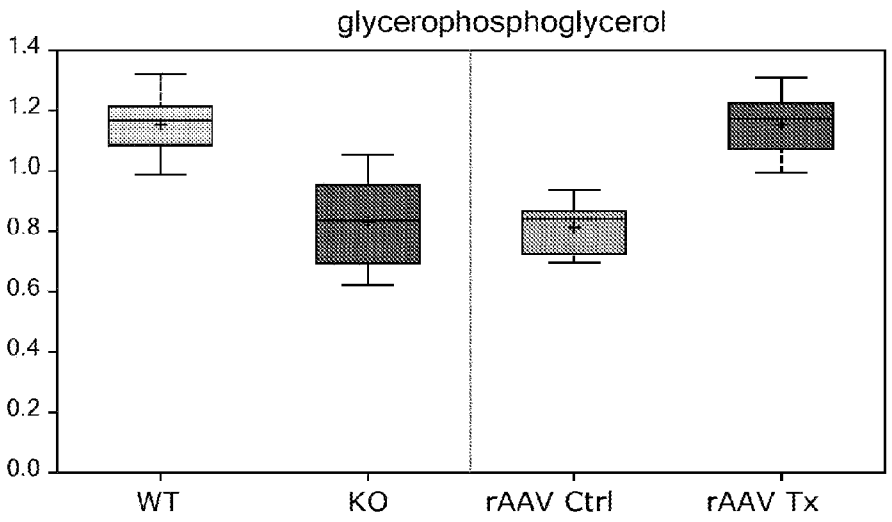
glycerophosphoglycerol
1.4
1.2
1.0
0.8
0.6
0.4
0.2
0.0
WT
KO
rAAV Ctrl
rAAV Tx

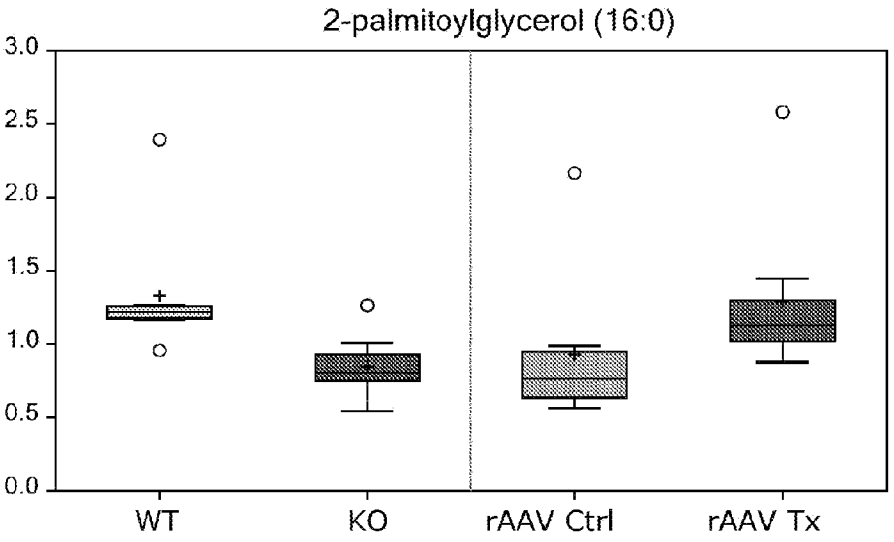
2-palmitoylglycerol (16:0)
3.0
2.5
2.0
1.5
1.0
0.5
0.0
WT
KO
rAAV Ctrl
rAAV Tx

FIG. 57 cont.

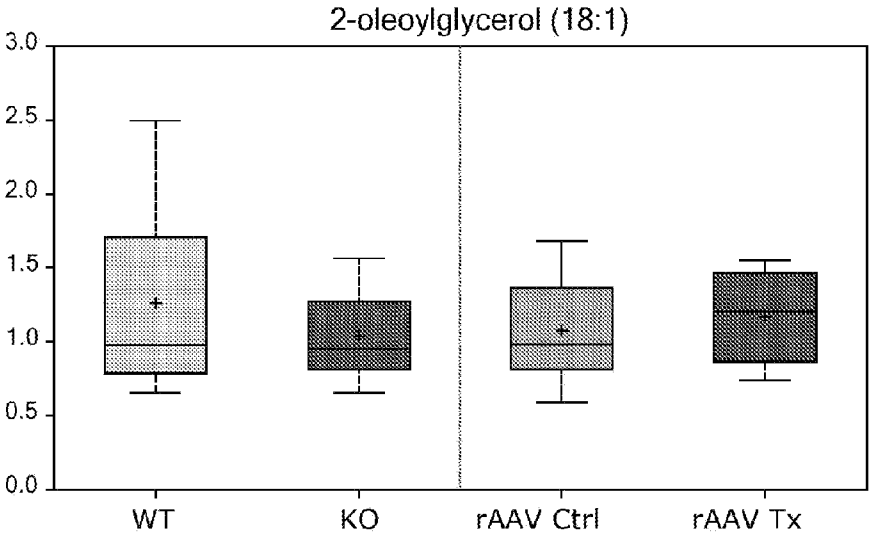
2-oleoylglycerol (18:1)
3.0
2.5
2.0
1.5
1.0
0.5
0.0
WT
KO
rAAV Ctrl
rAAV Tx

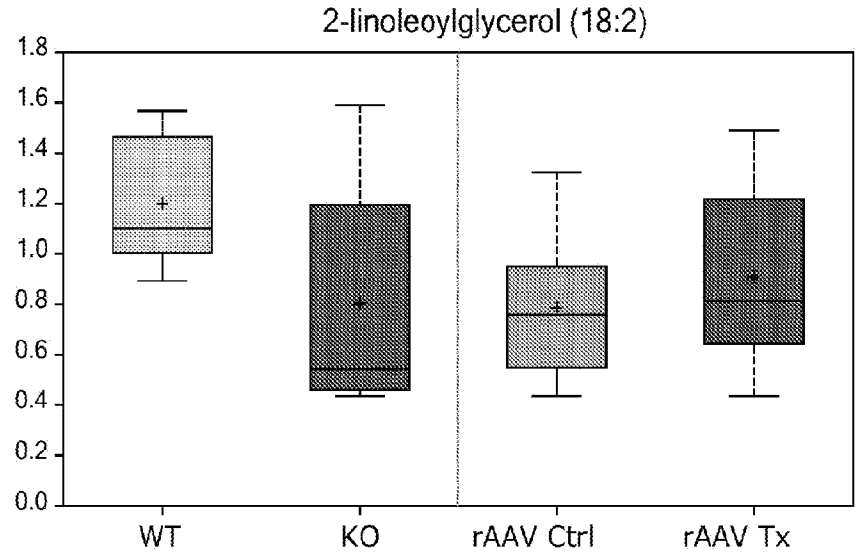
2-linoleoylglycerol (18:2)
1.8
1.6
1.4
1.2
1.0
0.8
0.6
0.4
0.2
0.0
WT
KO
rAAV Ctrl
rAAV Tx

FIG. 57 cont.

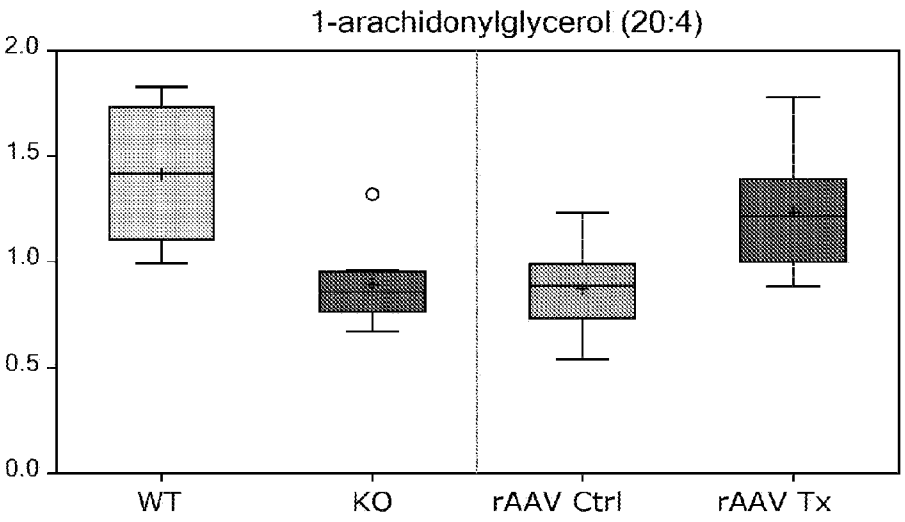
1-arachidonylglycerol (20:4)
2.0
1.5
1.0
0.5
0.0
WT
KO
rAAV Ctrl
rAAV Tx

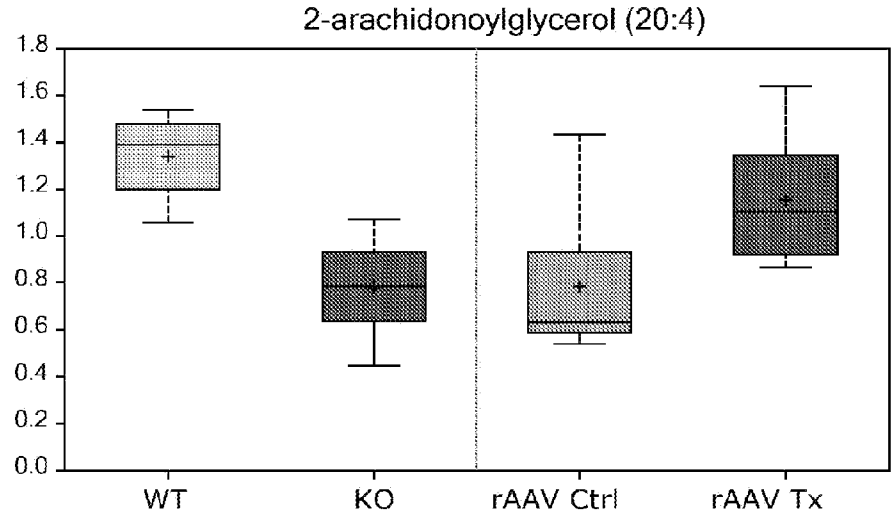
2-arachidonoylglycerol (20:4)
1.8
1.6
1.4
1.2
1.0
0.8
0.6
0.4
0.2
0.0
WT
KO
rAAV Ctrl
rAAV Tx

FIG. 57 cont.

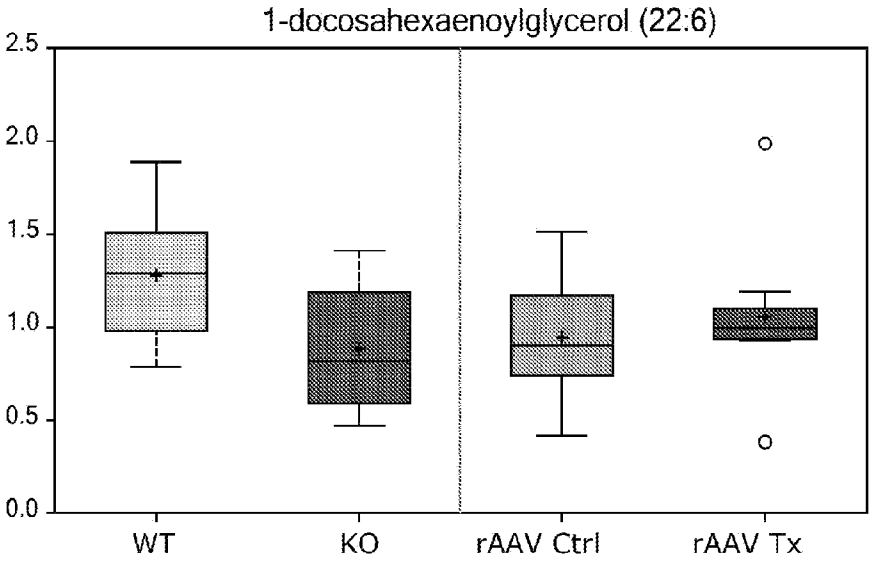
1-docosahexaenoylglycerol (22:6)
2.5
2.0
1.5
1.0
0.5
0.0
WT
KO
rAAV Ctrl
rAAV Tx

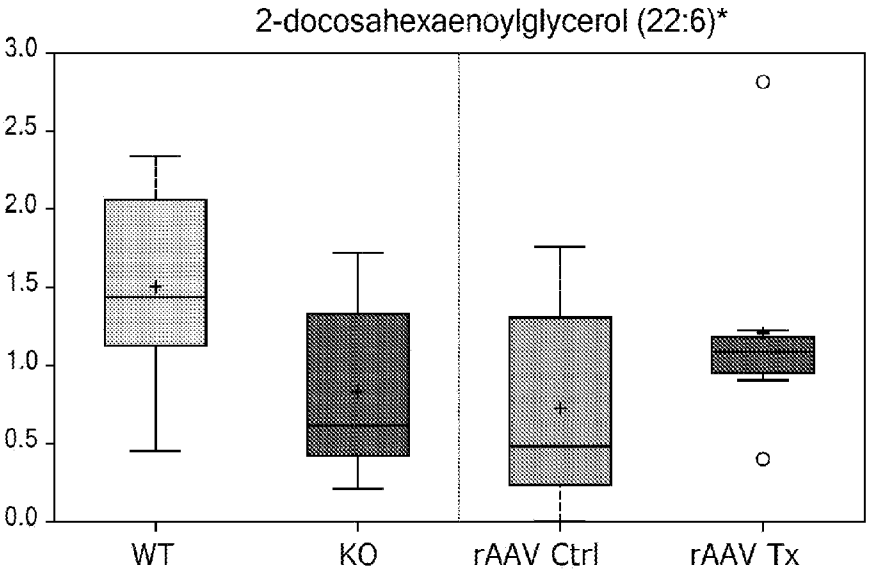
2-docosahexaenoylglycerol (22:6)*
3.0
2.5
2.0
1.5
1.0
0.5
0.0
WT
KO
rAAV Ctrl
rAAV Tx

FIG. 57 cont.

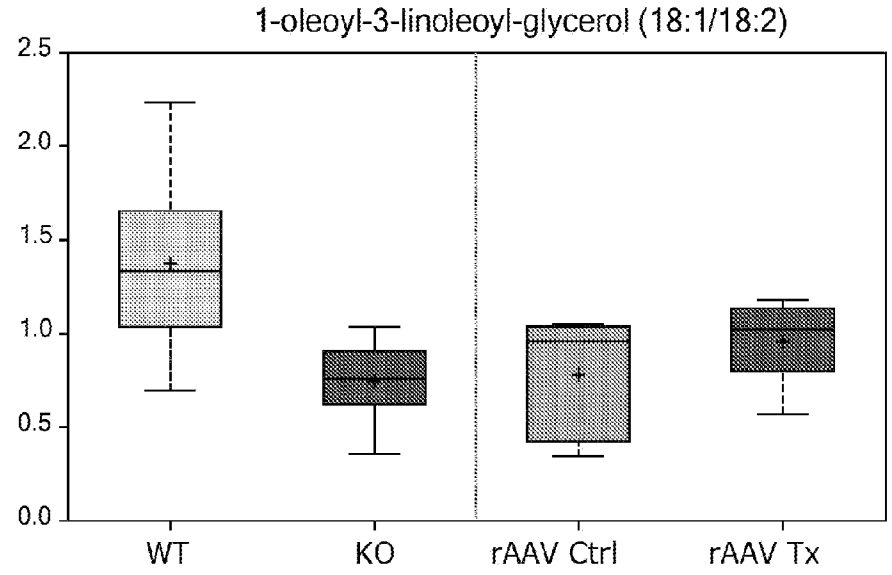
1-oleoyl-3-linoleoyl-glycerol (18:1/18:2)
2.5
2.0
1.5
1.0
0.5
0.0
WT
KO
rAAV Ctrl
rAAV Tx

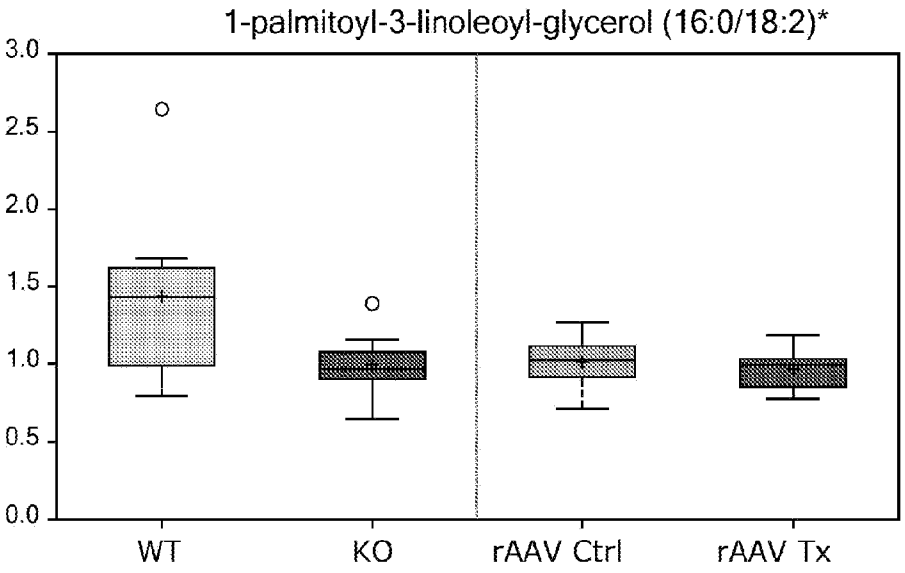
1-palmitoyl-3-linoleoyl-glycerol (16:0/18:2)*
3.0
2.5
2.0
1.5
1.0
0.5
0.0
WT
KO
rAAV Ctrl
rAAV Tx

FIG. 57 cont.

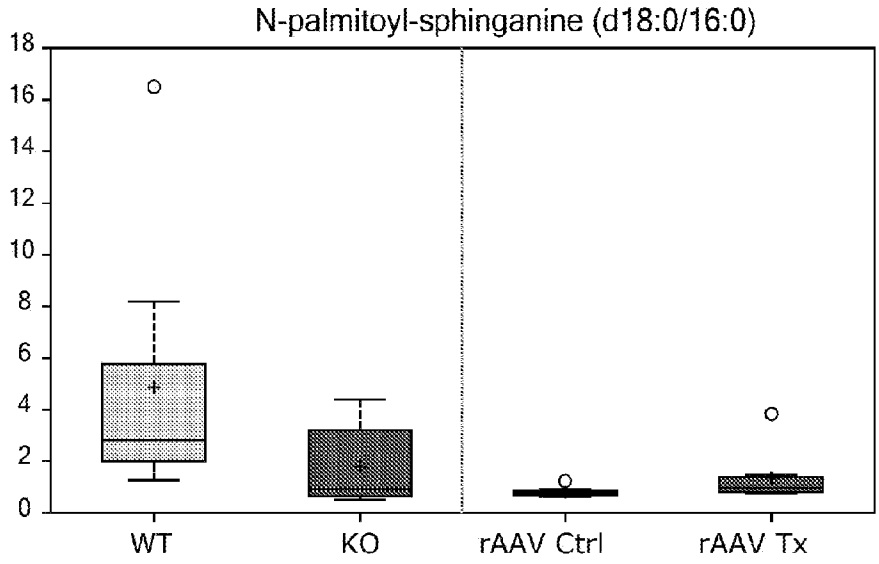
N-palmitoyl-sphinganine (d18:0/16:0)
18
16
14
12
10
8
6
4
2
0
WT
KO
rAAV Ctrl
rAAV Tx

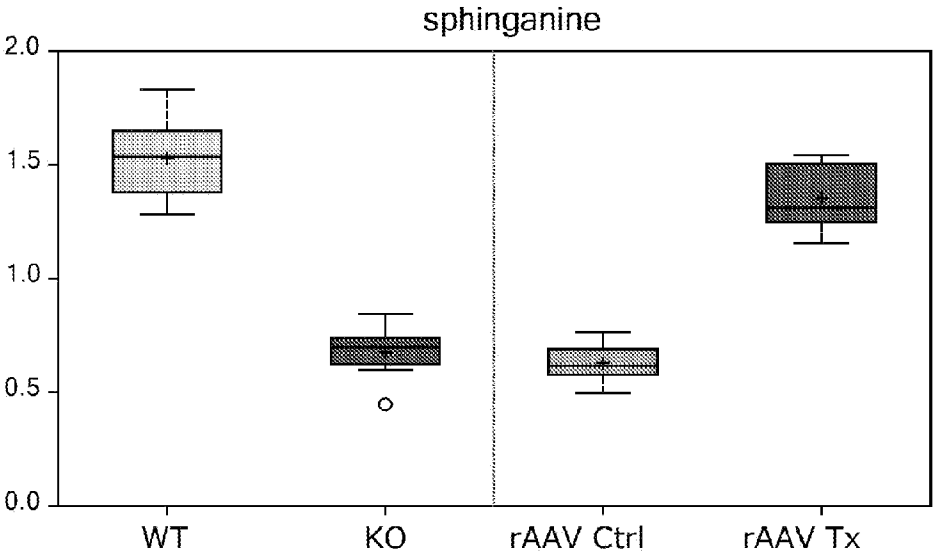
sphinganine
2.0
1.5
1.0
0.5
0.0
WT
KO
rAAV Ctrl
rAAV Tx

FIG. 57 cont.

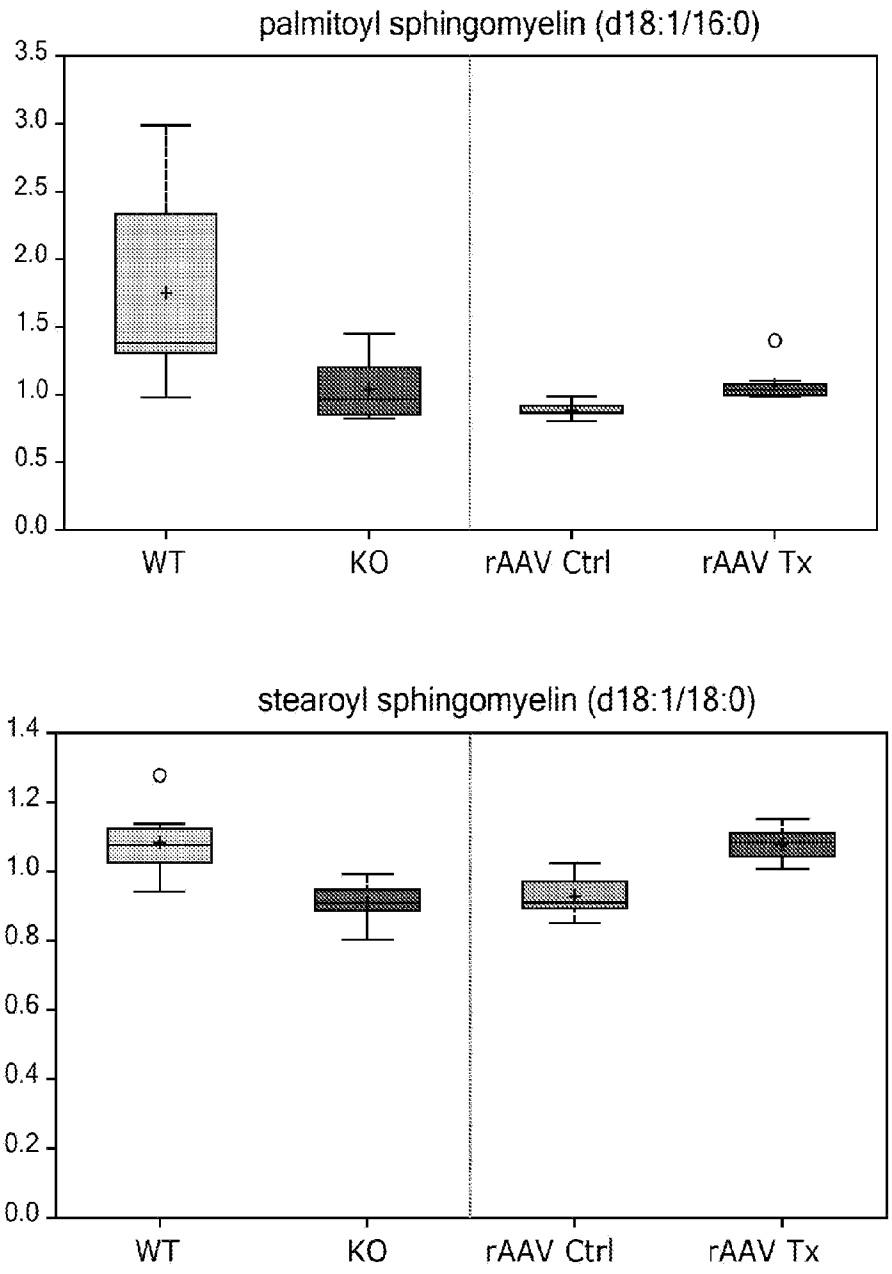
palmitoyl sphingomyelin (d18:1/16:0)
3.5
3.0
2.5
2.0
1.5
1.0
0.5
0.0
WT
KO
rAAV Ctrl
rAAV Tx
stearoyl sphingomyelin (d18:1/18:0)
1.4
1.2
1.0
0.8
0.6
0.4
0.2
0.0
WT
KO
rAAV Ctrl
rAAV Tx

FIG. 57 cont.

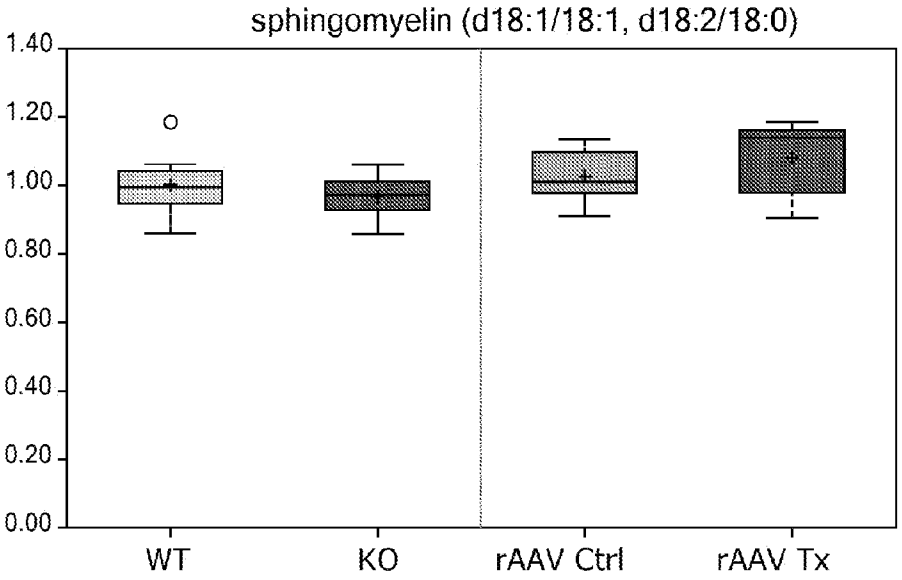
sphingomyelin (d18:1/18:1, d18:2/18:0)
1.40
1.20
1.00
0.80
0.60
0.40
0.20
0.00
WT
KO
rAAV Ctrl
rAAV Tx

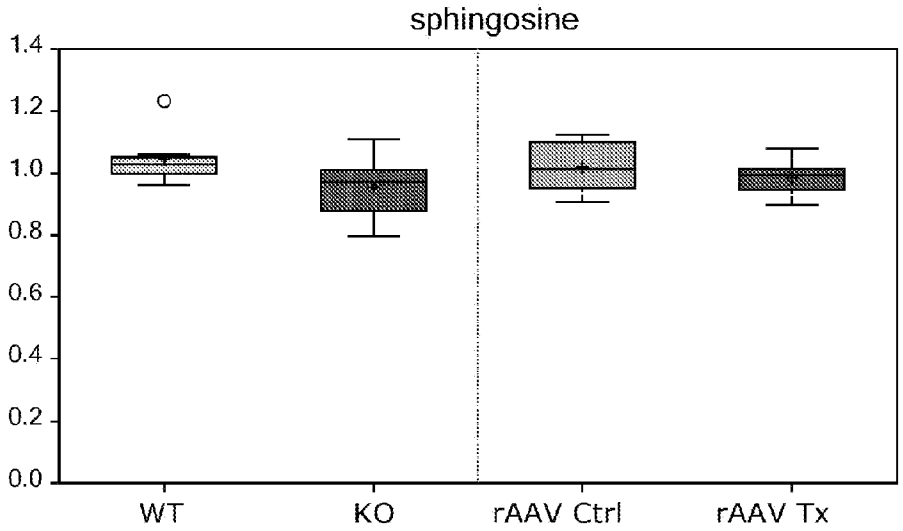
sphingosine
1.4
1.2
1.0
0.8
0.6
0.4
0.2
0.0
WT
KO
rAAV Ctrl
rAAV Tx

FIG. 57 cont.

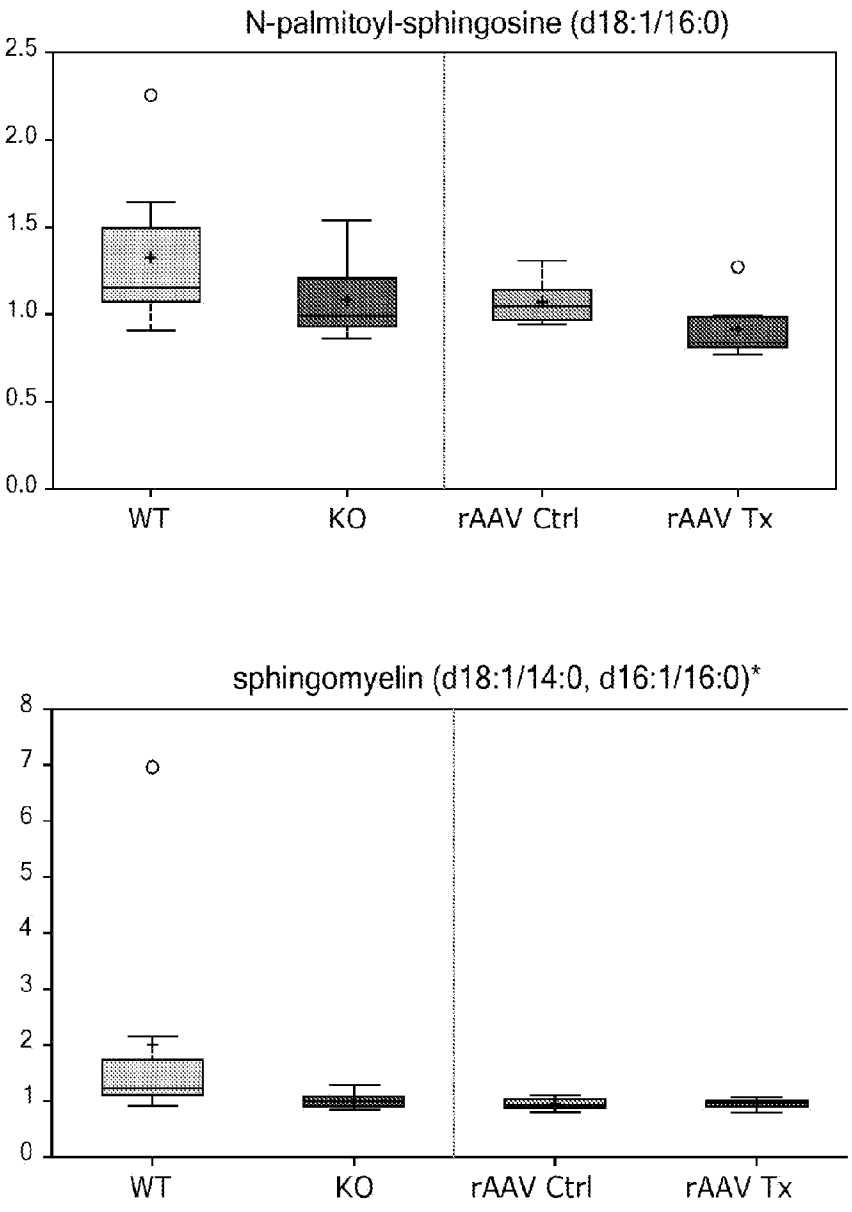
N-palmitoyl-sphingosine (d18:1/16:0)
2.5
2.0
1.5
1.0
0.5
0.0
WT
KO
rAAV Ctrl
rAAV Tx
sphingomyelin (d18:1/14:0, d16:1/16:0)*
8
7
6
5
4
3
2
1
0
WT
KO
rAAV Ctrl
rAAV Tx

FIG. 57 cont.

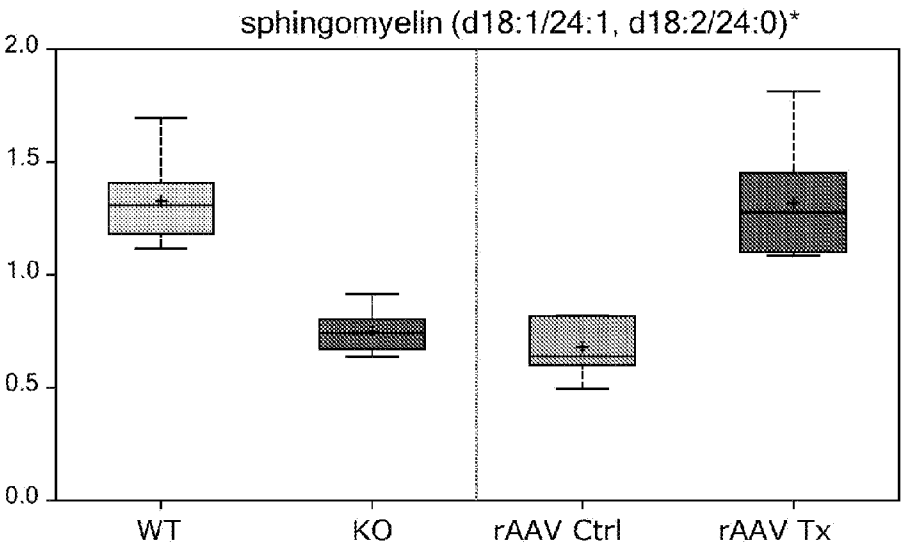
sphingomyelin (d18:1/24:1, d18:2/24:0)*
2.0
1.5
1.0
0.5
0.0
WT
KO
rAAV Ctrl
rAAV Tx

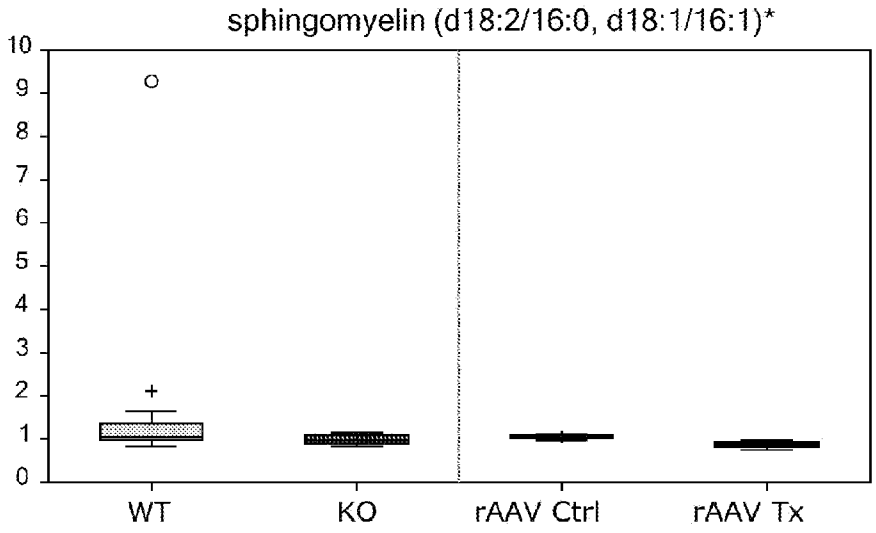
sphingomyelin (d18:2/16:0, d18:1/16:1)*
10
9
8
7
6
5
4
3
2
1
0
WT
KO
rAAV Ctrl
rAAV Tx

FIG. 57 cont.

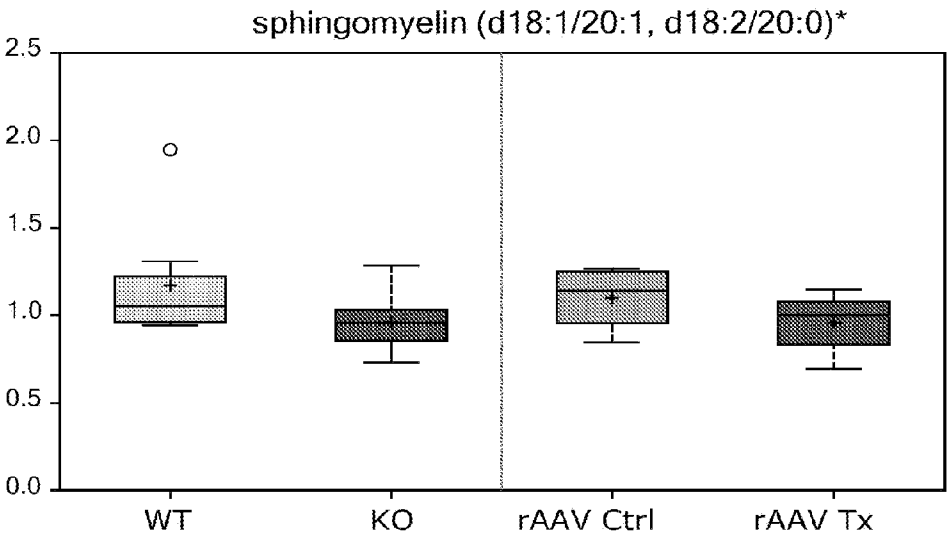
sphingomyelin (d18:1/20:1, d18:2/20:0)*
2.5
2.0
1.5
1.0
0.5
0.0
WT
KO
rAAV Ctrl
rAAV Tx

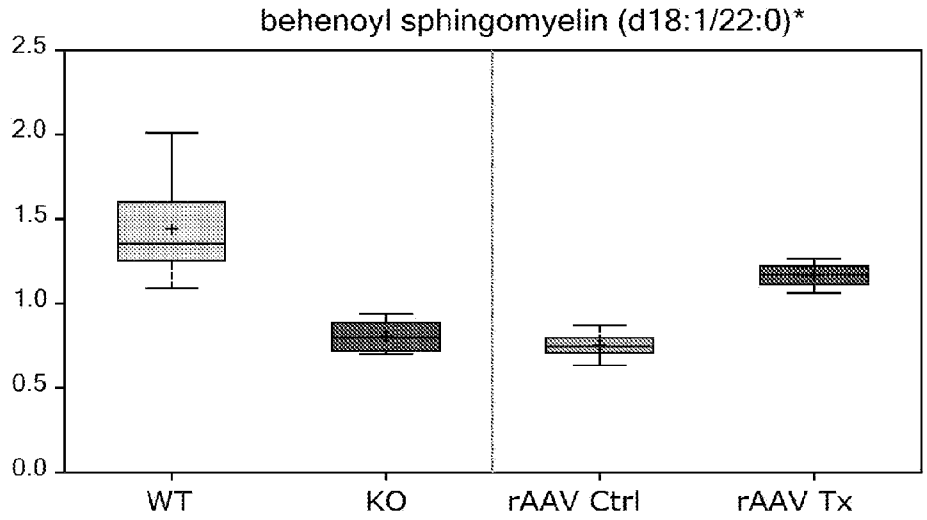
behenoyl sphingomyelin (d18:1/22:0)*
2.5
2.0
1.5
1.0
0.5
0.0
WT
KO
rAAV Ctrl
rAAV Tx

FIG. 57 cont.

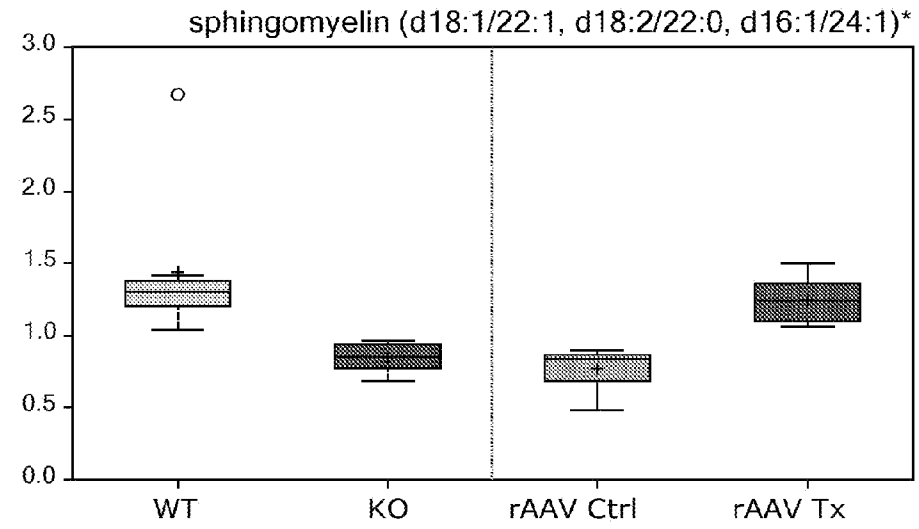
sphingomyelin (d18:1/22:1, d18:2/22:0, d16:1/24:1)*
3.0
2.5
2.0
1.5
1.0
0.5
0.0
WT
KO
rAAV Ctrl
rAAV Tx

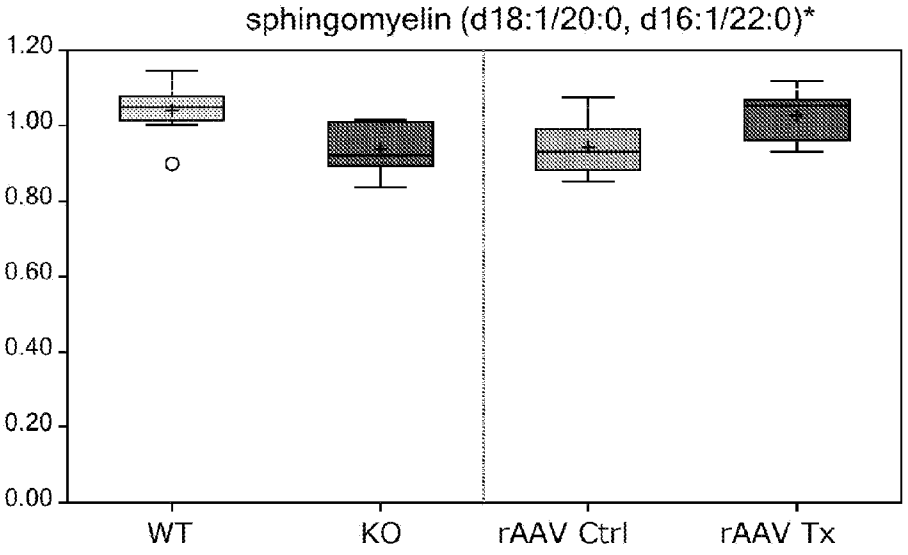
sphingomyelin (d18:1/20:0, d16:1/22:0)*
1.20
1.00
0.80
0.60
0.40
0.20
0.00
WT
KO
rAAV Ctrl
rAAV Tx

FIG. 57 cont.

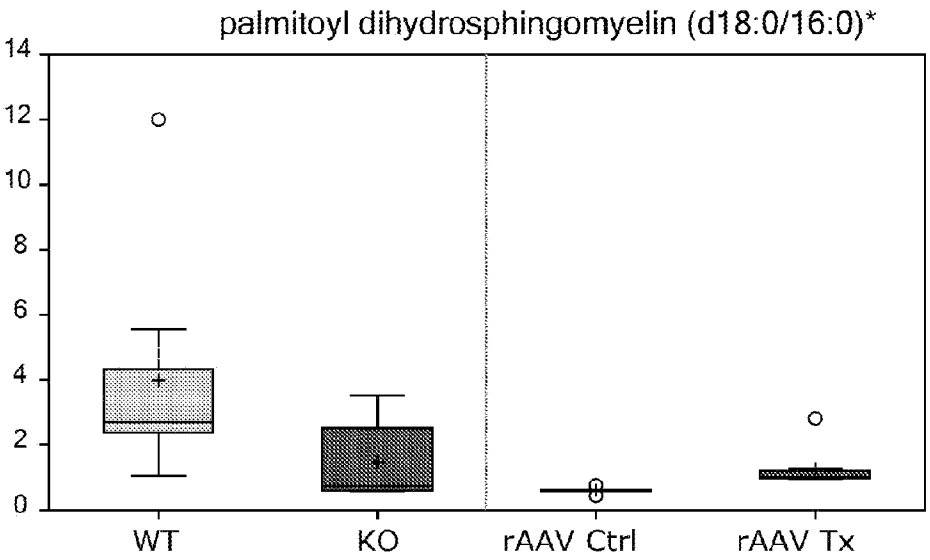
palmitoyl dihydrosphingomyelin (d18:0/16:0)*
14
12
10
8
6
4
2
0
WT
KO
rAAV Ctrl
rAAV Tx

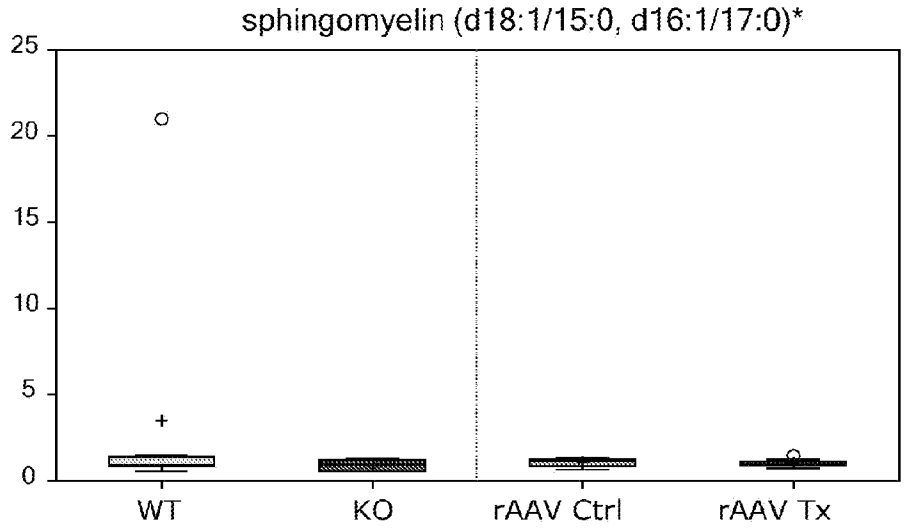
sphingomyelin (d18:1/15:0, d16:1/17:0)*
25
20
15
10
5
0
WT
KO
rAAV Ctrl
rAAV Tx

FIG. 57 cont.

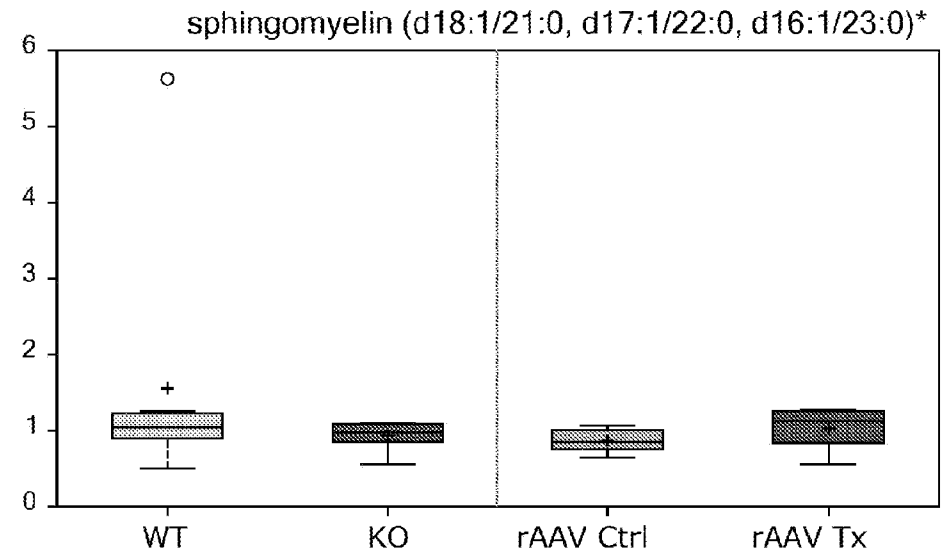
sphingomyelin (d18:1/21:0, d17:1/22:0, d16:1/23:0)*
6
5
4
3
2
1
0
WT
KO
rAAV Ctrl
rAAV Tx

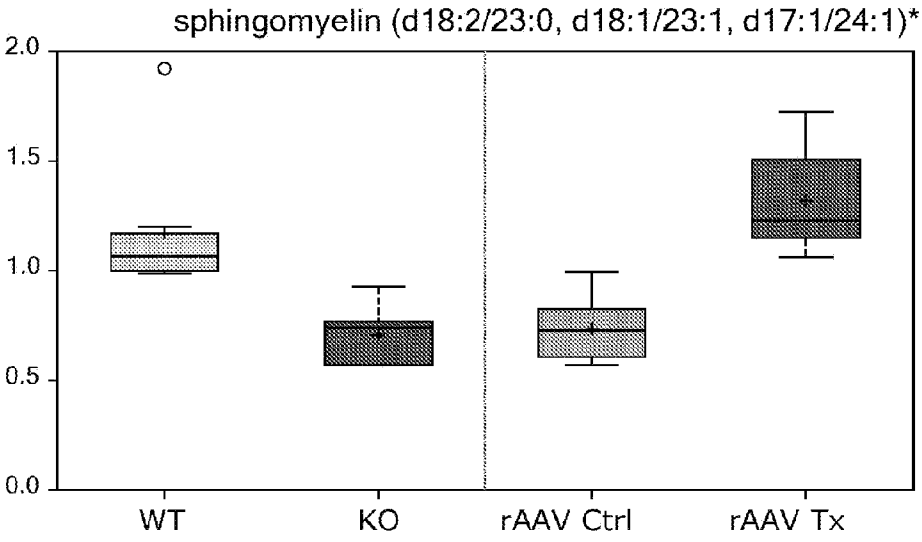
sphingomyelin (d18:2/23:0, d18:1/23:1, d17:1/24:1)*
2.0
1.5
1.0
0.5
0.0
WT
KO
rAAV Ctrl
rAAV Tx

FIG. 57 cont.

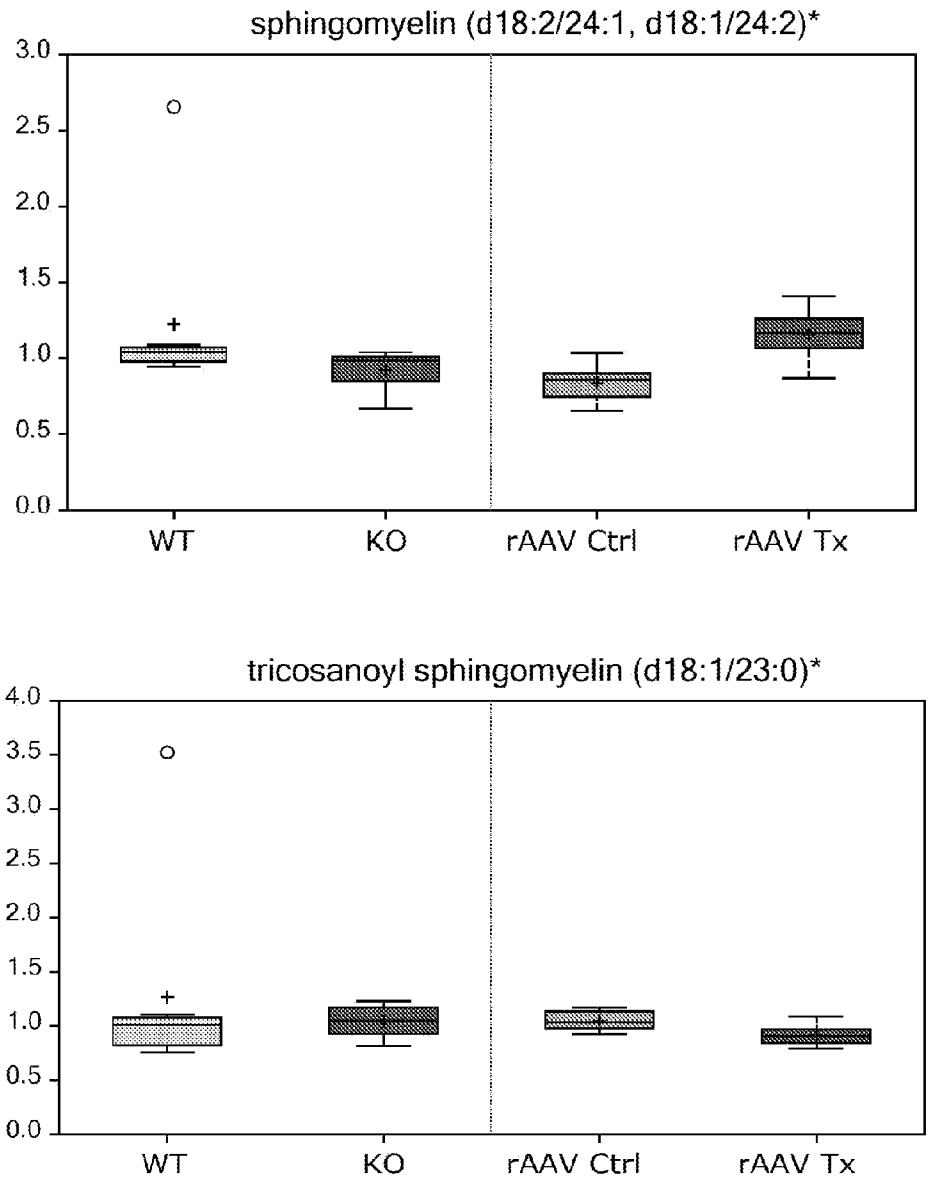
sphingomyelin (d18:2/24:1, d18:1/24:2)*
3.0
2.5
2.0
1.5
1.0
0.5
0.0
WT
KO
rAAV Ctrl
rAAV Tx
tricosanoyl sphingomyelin (d18:1/23:0)*
4.0
3.5
3.0
2.5
2.0
1.5
1.0
0.5
0.0
WT
KO
rAAV Ctrl
rAAV Tx

FIG. 57 cont.

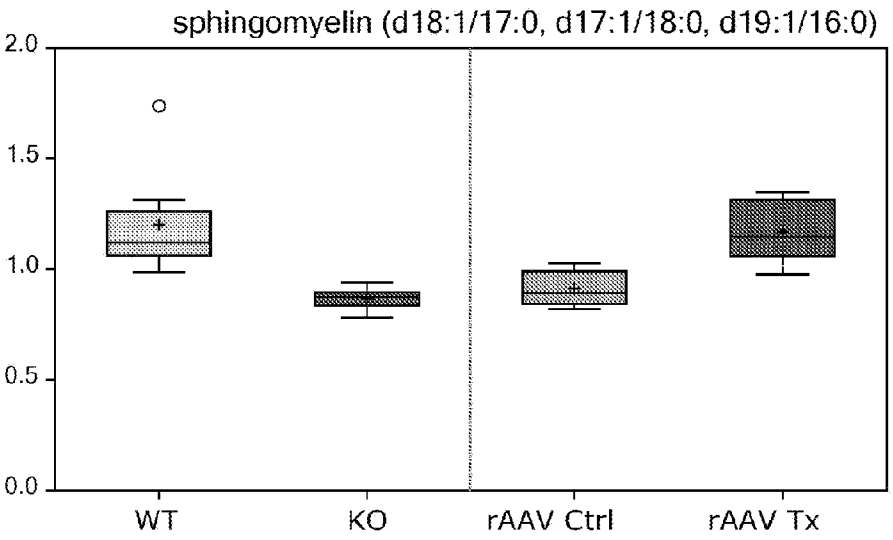
sphingomyelin (d18:1/17:0, d17:1/18:0, d19:1/16:0)
2.0
1.5
1.0
0.5
0.0
WT
KO
rAAV Ctrl
rAAV Tx

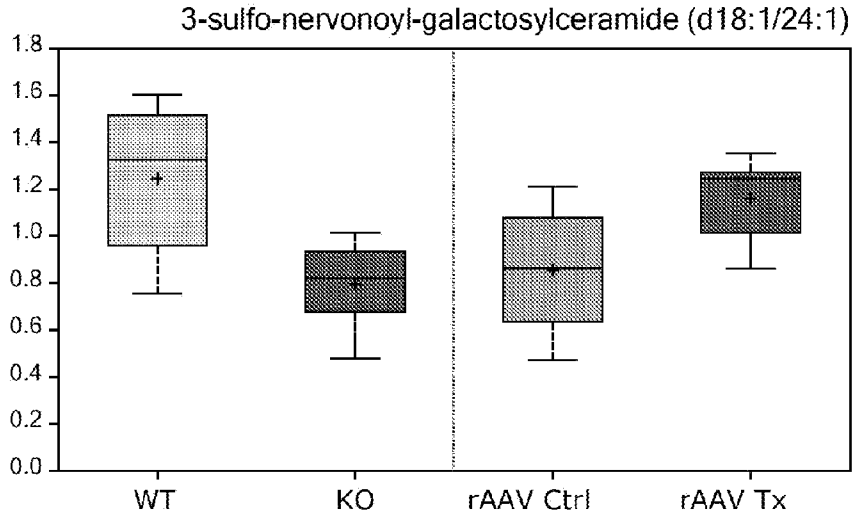
3-sulfo-nervonoyl-galactosylceramide (d18:1/24:1)
1.8
1.6
1.4
1.2
1.0
0.8
0.6
0.4
0.2
0.0
WT
KO
rAAV Ctrl
rAAV Tx

FIG. 57 cont.

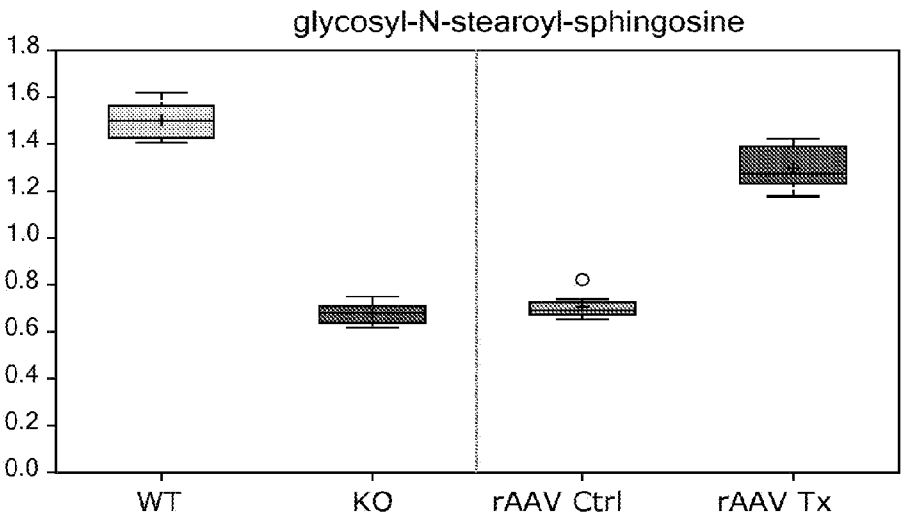
glycosyl-N-stearoyl-sphingosine
1.8
1.6
1.4
1.2
1.0
0.8
0.6
0.4
0.2
0.0
WT
KO
rAAV Ctrl
rAAV Tx

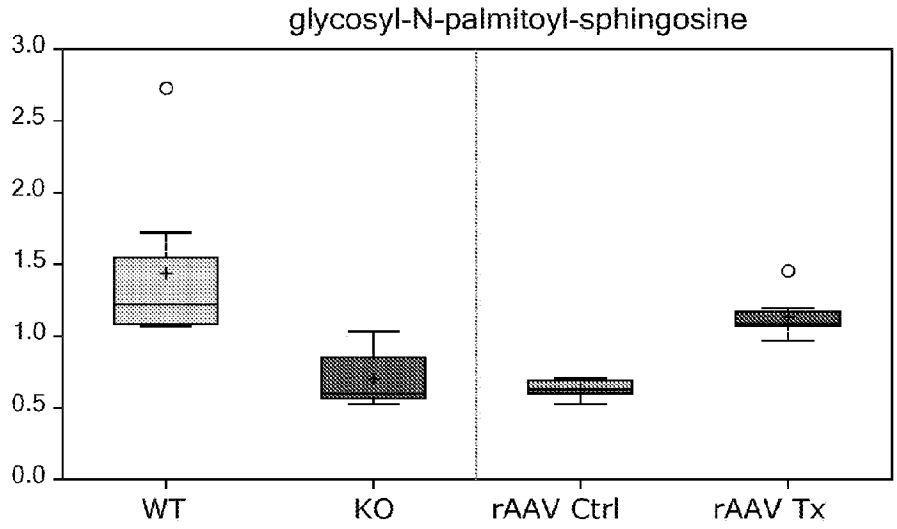
glycosyl-N-palmitoyl-sphingosine
3.0
2.5
2.0
1.5
1.0
0.5
0.0
WT
KO
rAAV Ctrl
rAAV Tx

FIG. 57 cont.

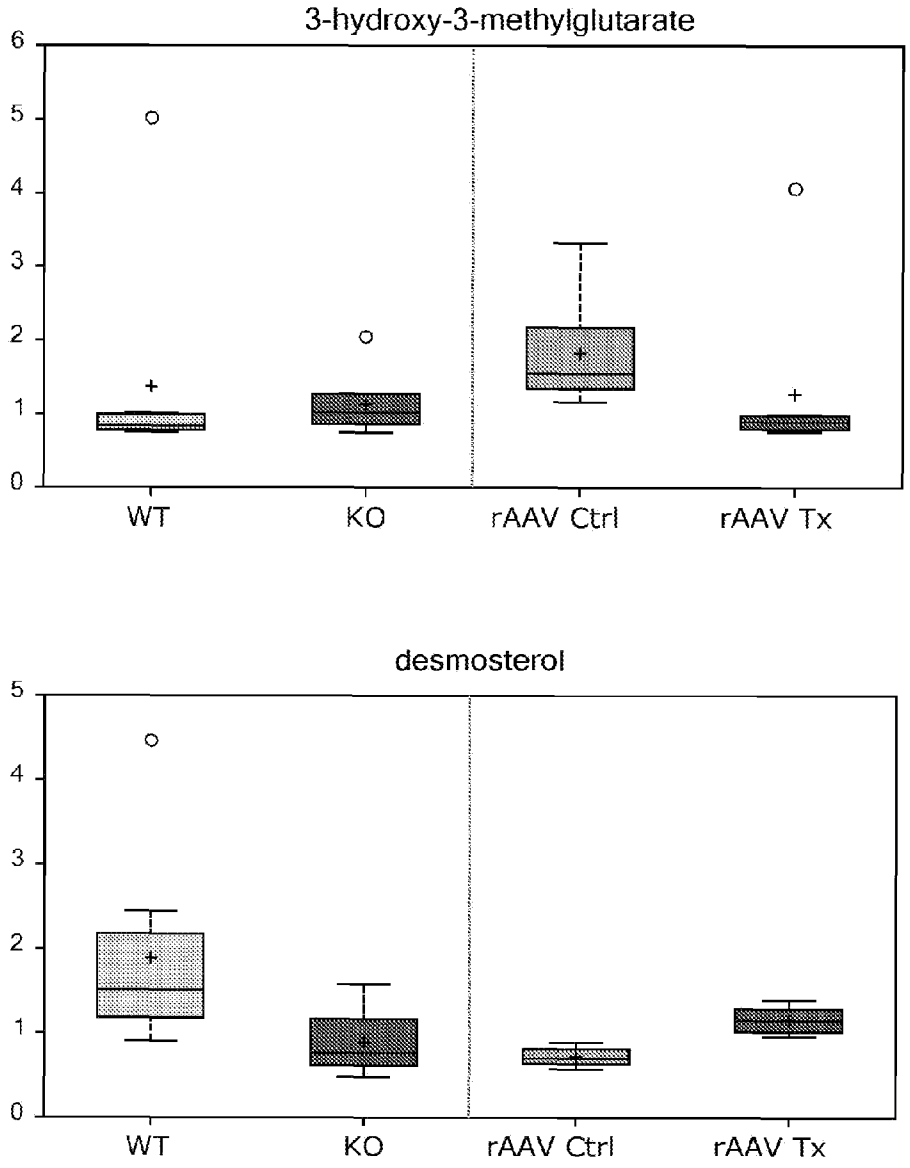
3-hydroxy-3-methylglutarate
6
5
4
3
2
1
0
WT
KO
rAAV Ctrl
rAAV Tx
desmosterol
5
4
3
2
1
0
WT
KO
rAAV Ctrl
rAAV Tx

FIG. 57 cont.

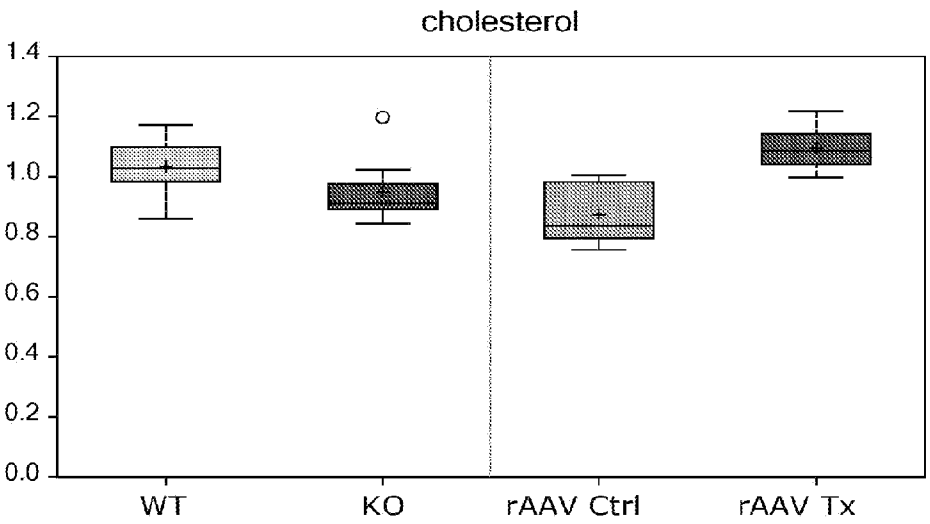
cholesterol
1.4
1.2
1.0
0.8
0.6
0.4
0.2
0.0
WT
KO
rAAV Ctrl
rAAV Tx

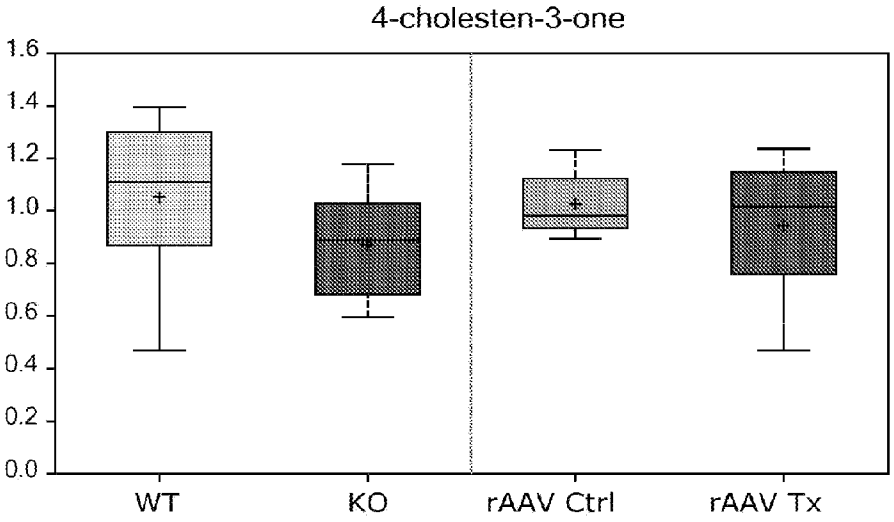
4-cholesten-3-one
1.6
1.4
1.2
1.0
0.8
0.6
0.4
0.2
0.0
WT
KO
rAAV Ctrl
rAAV Tx

FIG. 57 cont.

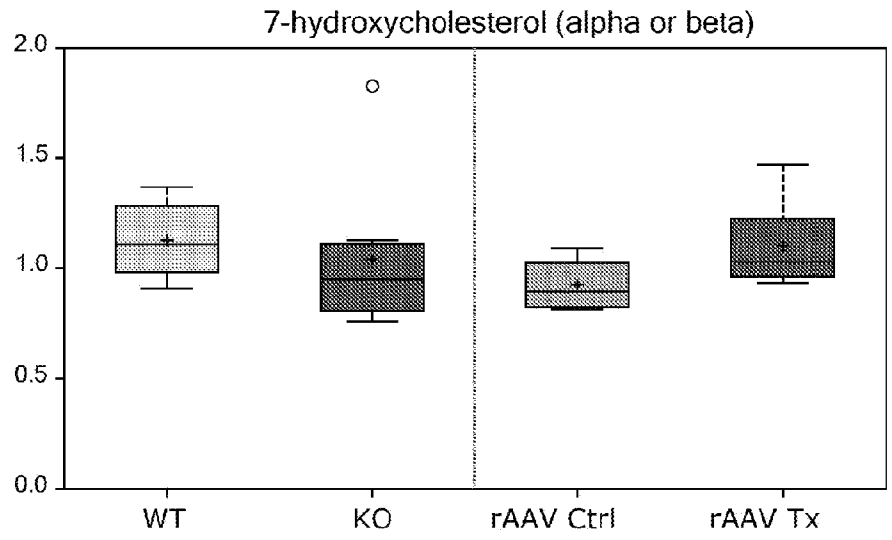
7-hydroxycholesterol (alpha or beta)
2.0
1.5
1.0
0.5
0.0
WT
KO
rAAV Ctrl
rAAV Tx

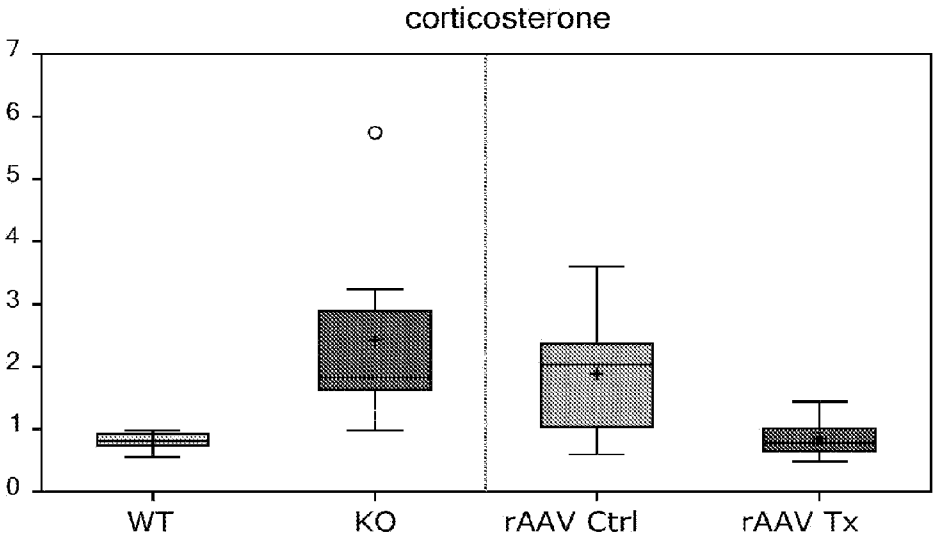
corticosterone
7
6
5
4
3
2
1
0
WT
KO
rAAV Ctrl
rAAV Tx

FIG. 57 cont.

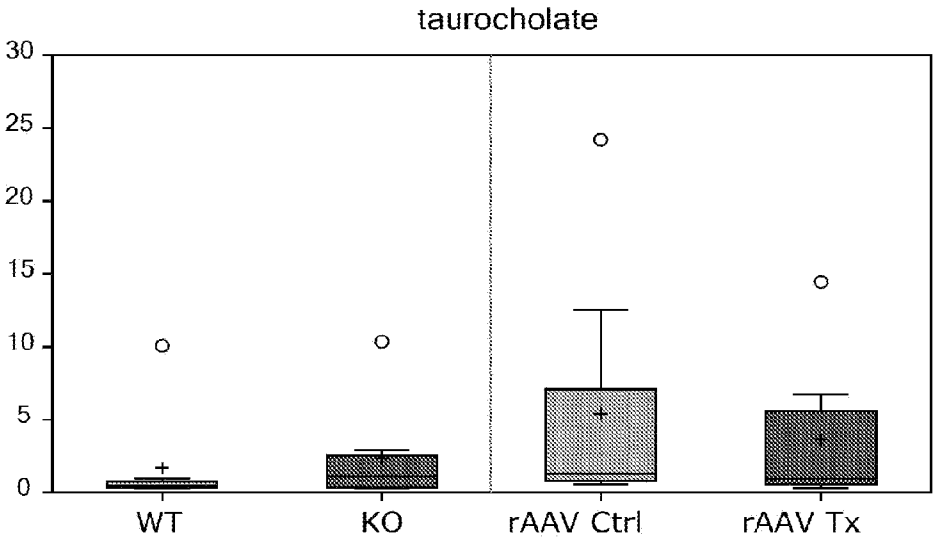
taurocholate
30
25
20
15
10
5
0
WT
KO
rAAV Ctrl
rAAV Tx

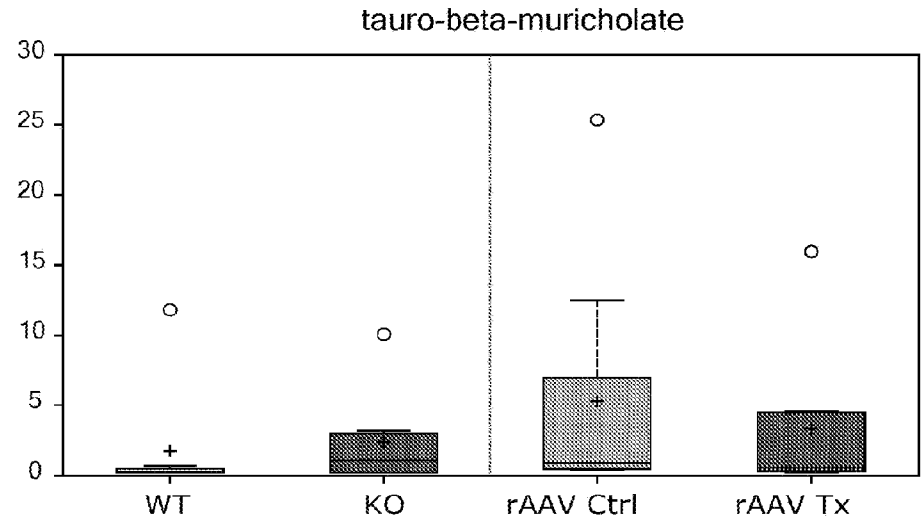
tauro-beta-muricholate
30
25
20
15
10
5
0
WT
KO
rAAV Ctrl
rAAV Tx

FIG. 57 cont.

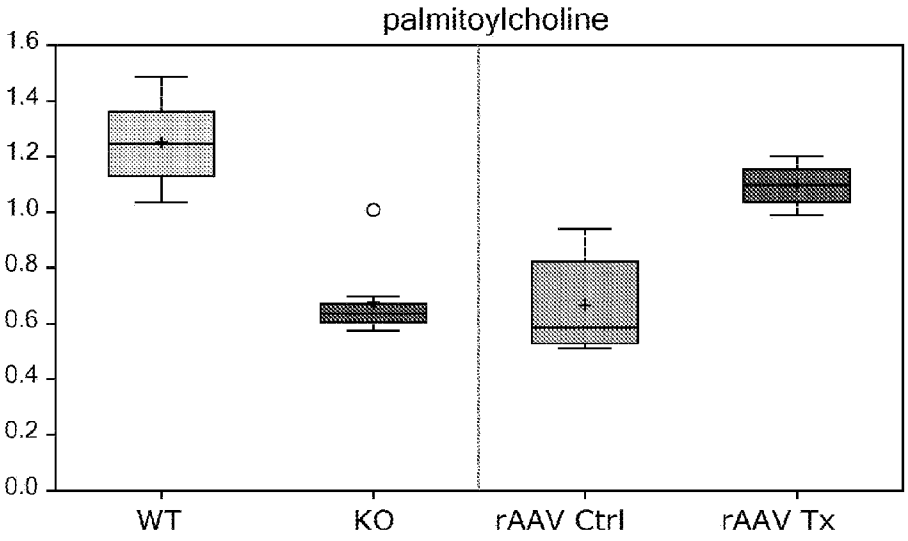
palmitoylcholine
1.6
1.4
1.2
1.0
0.8
0.6
0.4
0.2
0.0
WT
KO
rAAV Ctrl
rAAV Tx

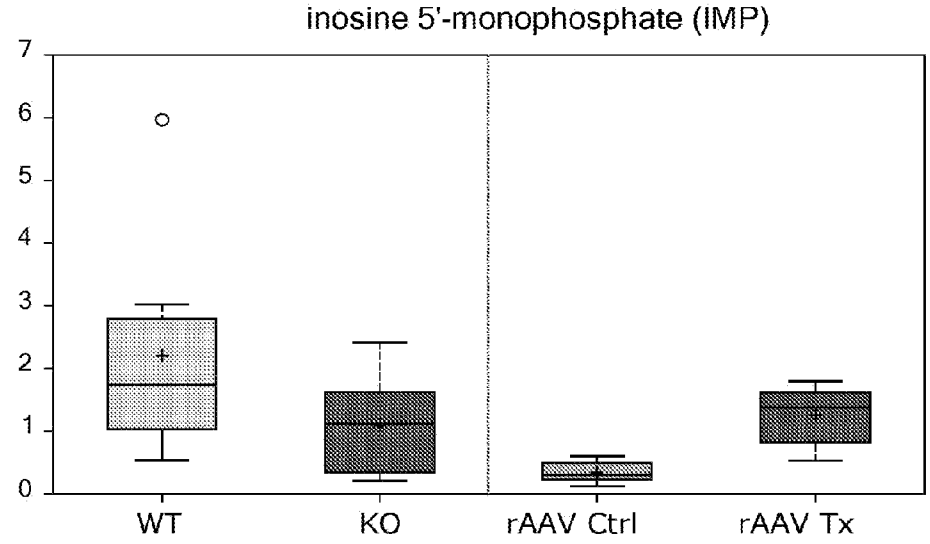
inosine 5'-monophosphate (IMP)
7
6
5
4
3
2
1
0
WT
KO
rAAV Ctrl
rAAV Tx

FIG. 57 cont.

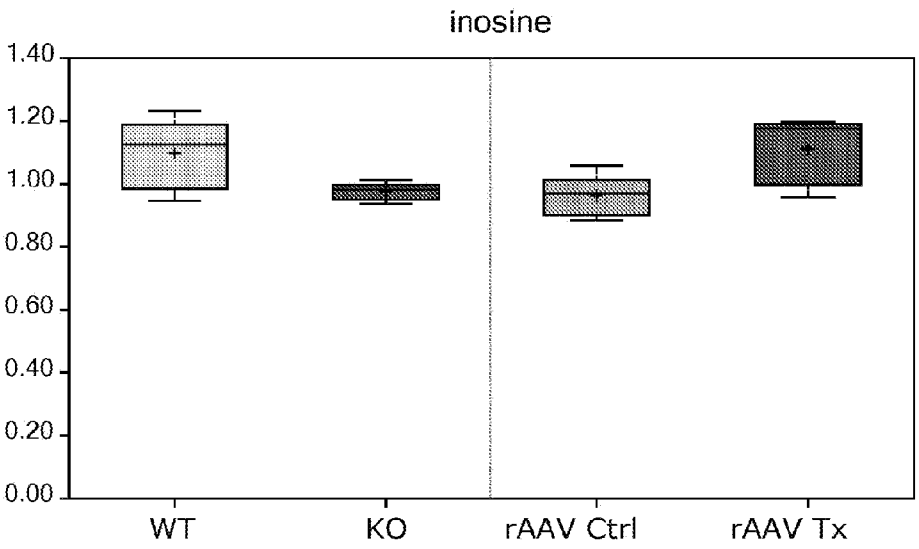
inosine
1.40
1.20
1.00
0.80
0.60
0.40
0.20
0.00
WT
KO
rAAV Ctrl
rAAV Tx

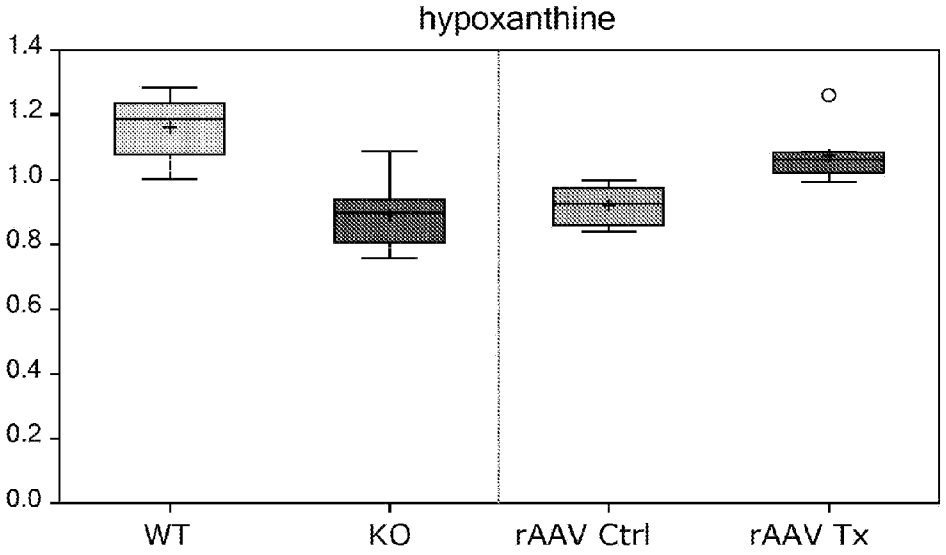
hypoxanthine
1.4
1.2
1.0
0.8
0.6
0.4
0.2
0.0
WT
KO
rAAV Ctrl
rAAV Tx

FIG. 57 cont.

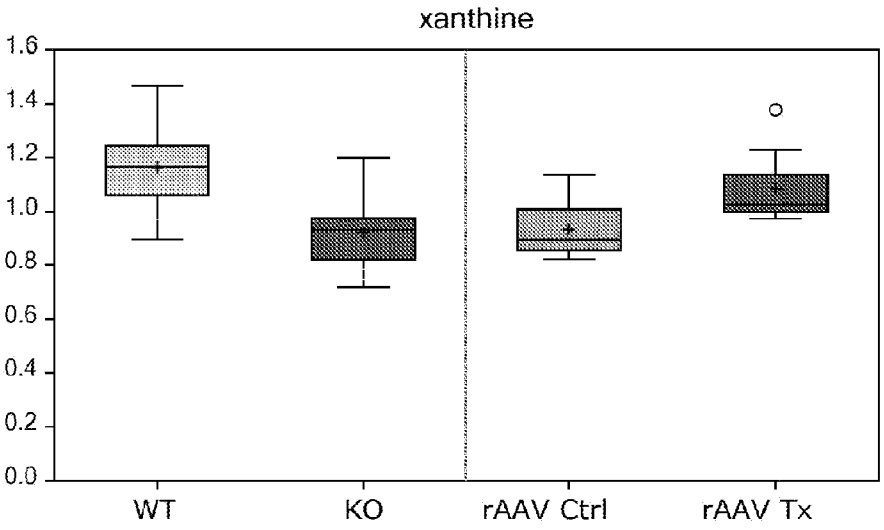
xanthine
1.6
1.4
1.2
1.0
0.8
0.6
0.4
0.2
0.0
WT
KO
rAAV Ctrl
rAAV Tx

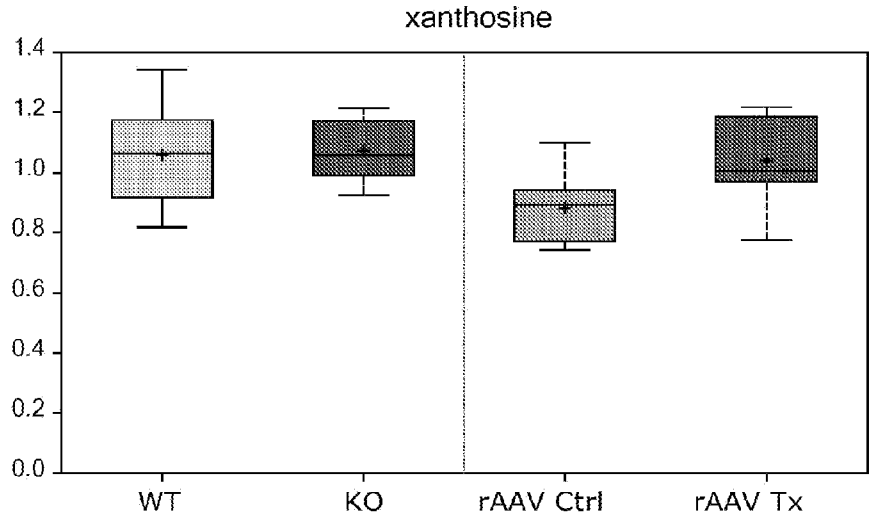
xanthosine
1.4
1.2
1.0
0.8
0.6
0.4
0.2
0.0
WT
KO
rAAV Ctrl
rAAV Tx

FIG. 57 cont.

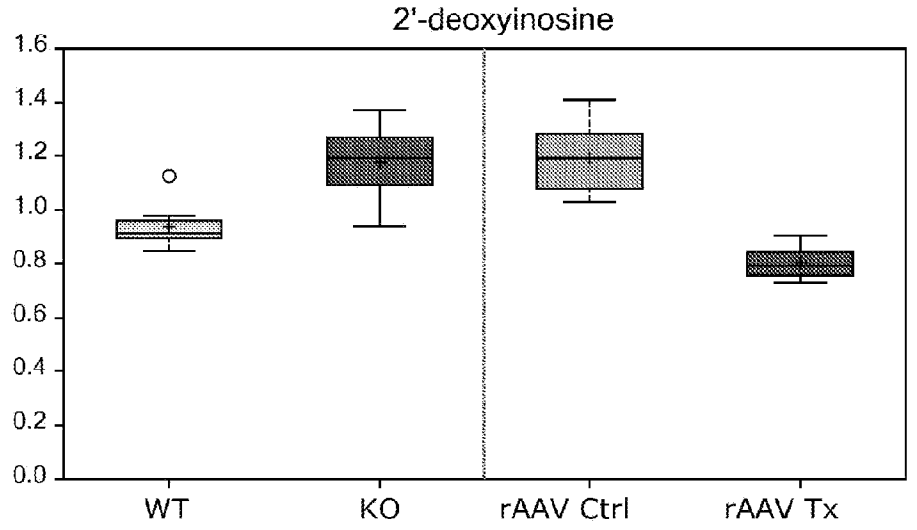
2'-deoxyinosine
1.6
1.4
1.2
1.0
0.8
0.6
0.4
0.2
0.0
WT
KO
rAAV Ctrl
rAAV Tx

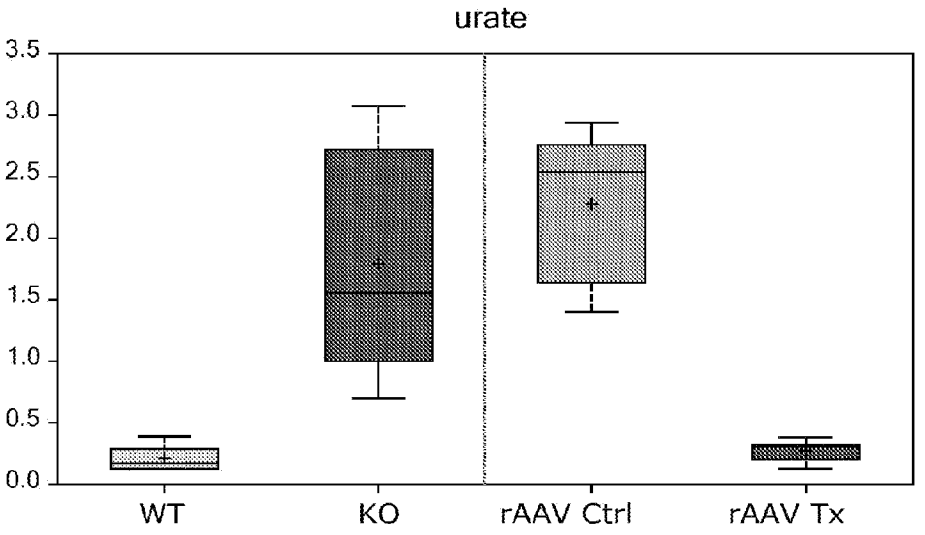
urate
3.5
3.0
2.5
2.0
1.5
1.0
0.5
0.0
WT
KO
rAAV Ctrl
rAAV Tx

FIG. 57 cont.

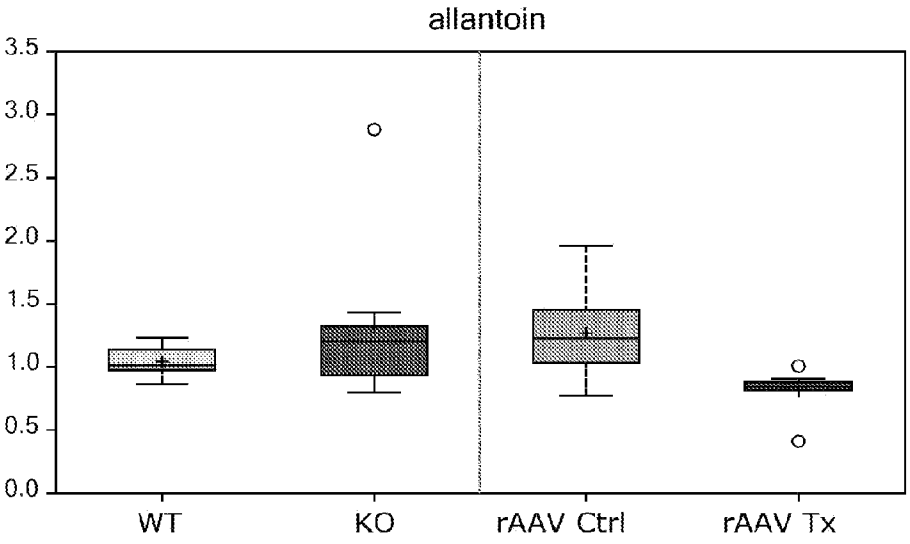
allantoin
3.5
3.0
2.5
2.0
1.5
1.0
0.5
0.0
WT
KO
rAAV Ctrl
rAAV Tx

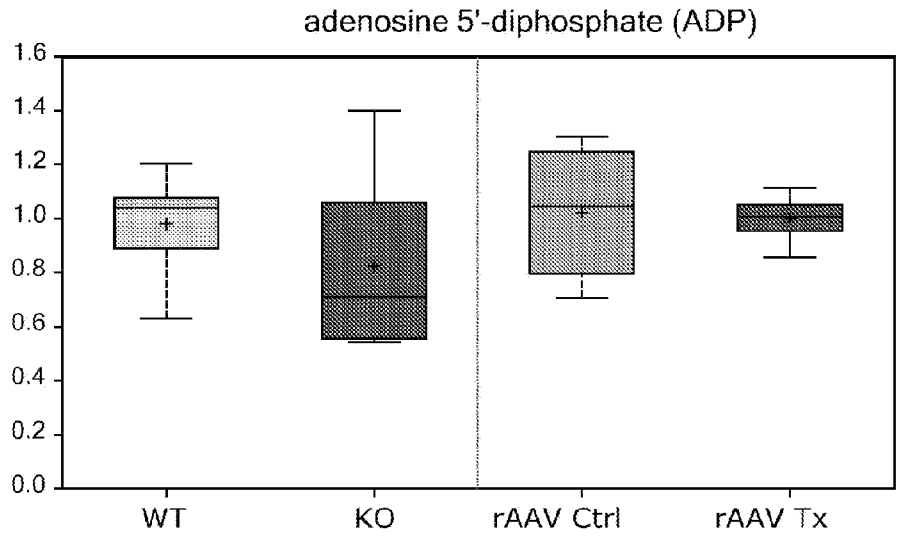
adenosine 5'-diphosphate (ADP)
1.6
1.4
1.2
1.0
0.8
0.6
0.4
0.2
0.0
WT
KO
rAAV Ctrl
rAAV Tx

FIG. 57 cont.

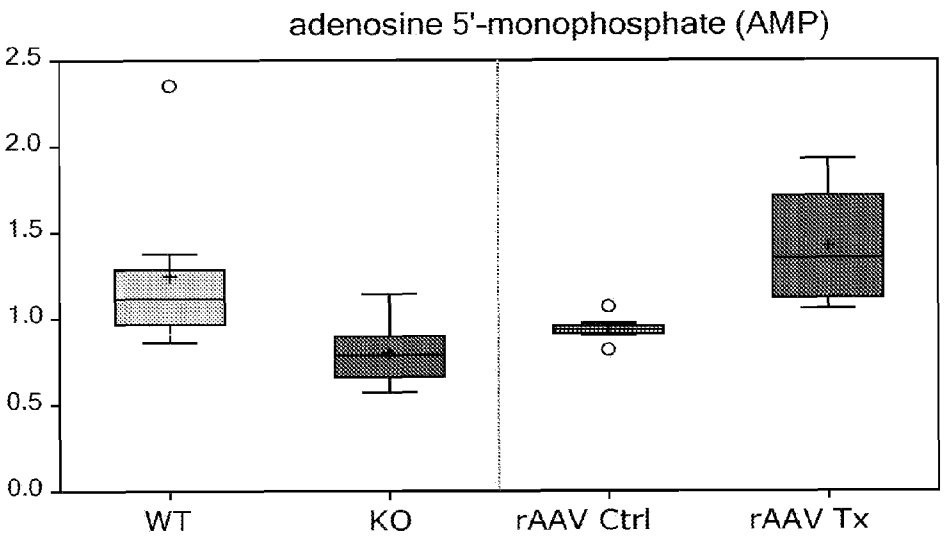
adenosine 5'-monophosphate (AMP)
2.5
2.0
1.5
1.0
0.5
0.0
WT
KO
rAAV Ctrl
rAAV Tx

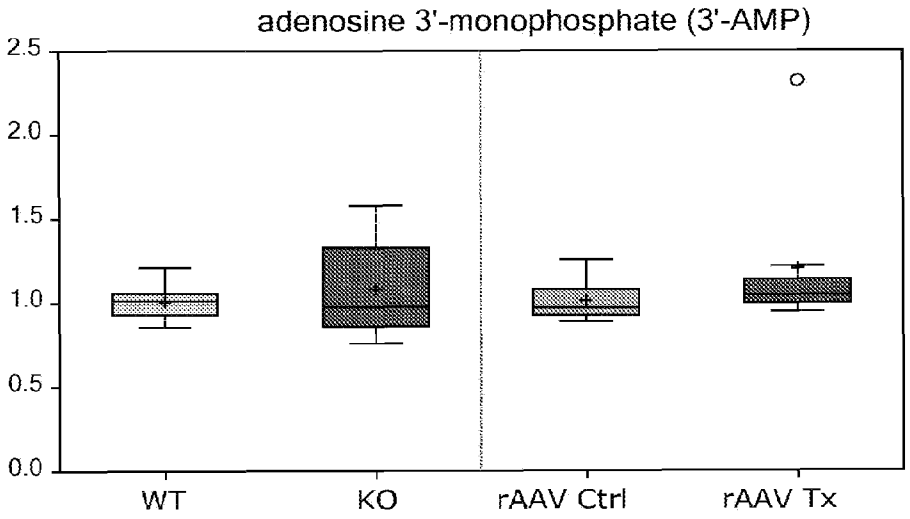
adenosine 3'-monophosphate (3'-AMP)
2.5
2.0
1.5
1.0
0.5
0.0
WT
KO
rAAV Ctrl
rAAV Tx

FIG. 57 cont.

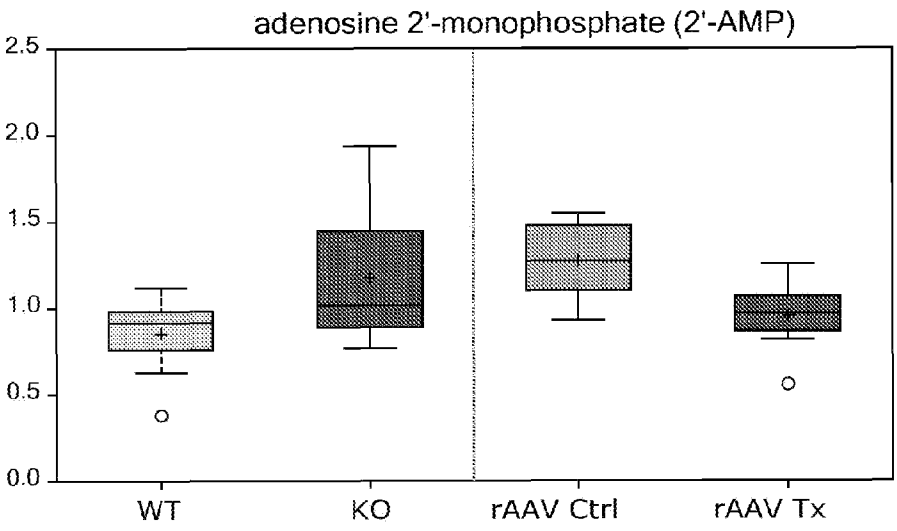
adenosine 2'-monophosphate (2'-AMP)
2.5
2.0
1.5
1.0
0.5
0.0
WT
KO
rAAV Ctrl
rAAV Tx

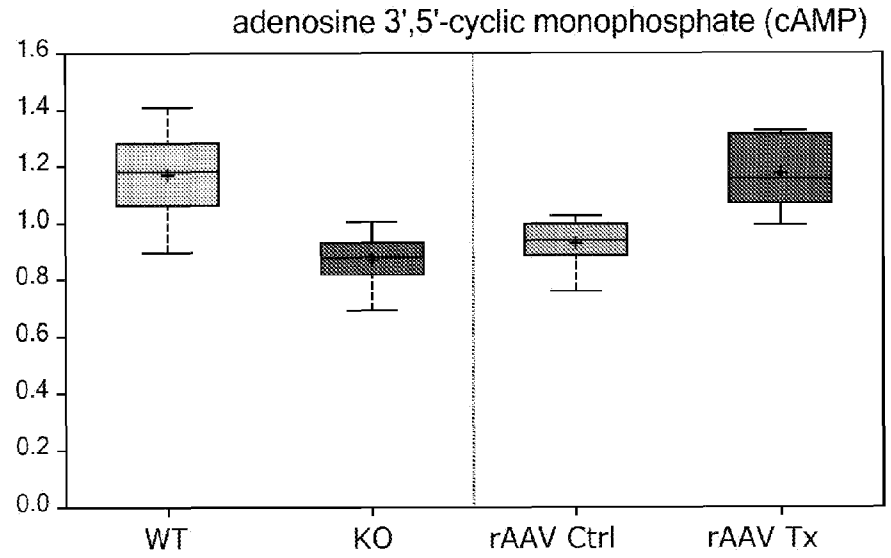
adenosine 3',5'-cyclic monophosphate (cAMP)
1.6
1.4
1.2
1.0
0.8
0.6
0.4
0.2
0.0
WT
KO
rAAV Ctrl
rAAV Tx

FIG. 57 cont.

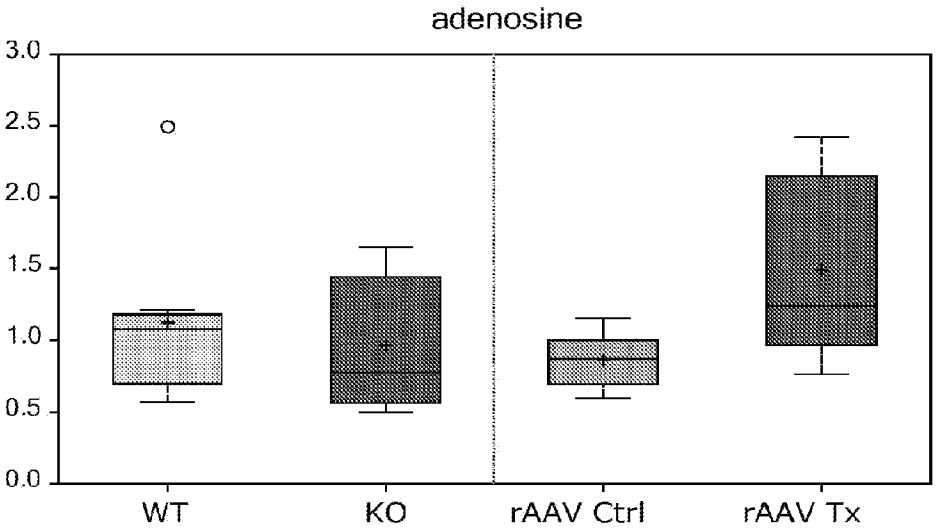
adenosine
3.0
2.5
2.0
1.5
1.0
0.5
0.0
WT
KO
rAAV Ctrl
rAAV Tx

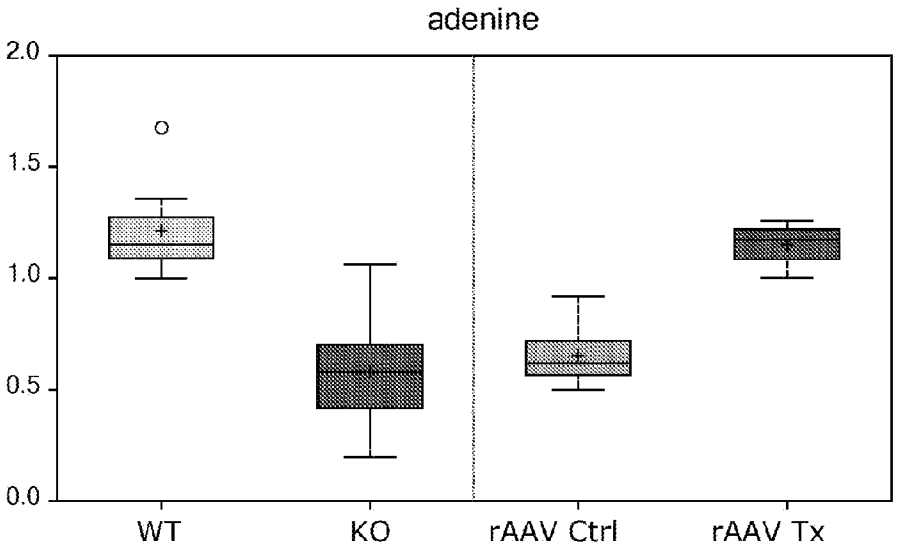
adenine
2.0
1.5
1.0
0.5
0.0
WT
KO
rAAV Ctrl
rAAV Tx

FIG. 57 cont.

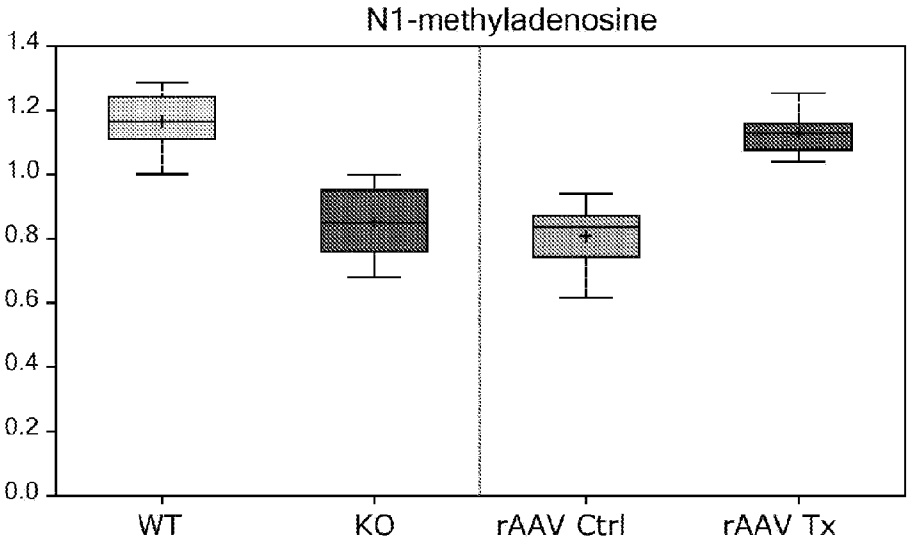
N1-methyladenosine
1.4
1.2
1.0
0.8
0.6
0.4
0.2
0.0
WT
KO
rAAV Ctrl
rAAV Tx

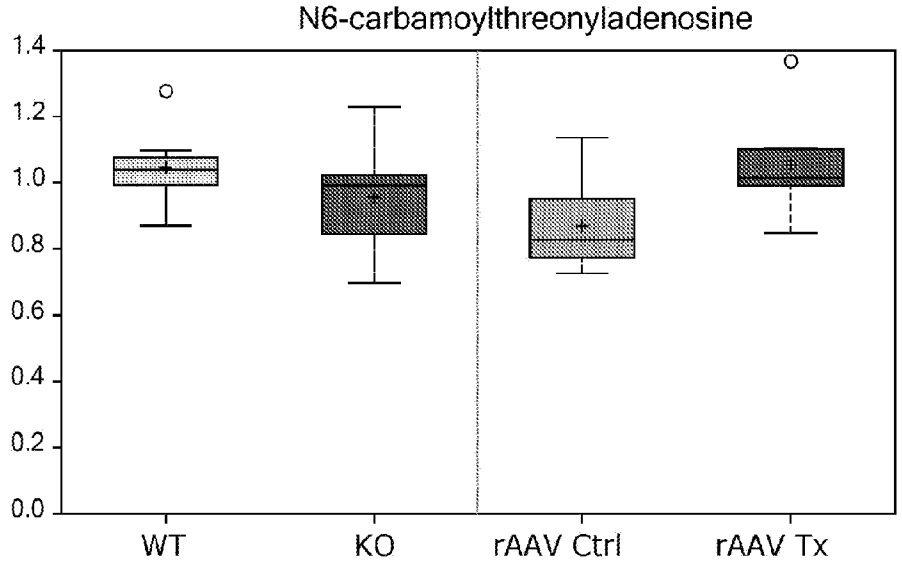
N6-carbamoylthreonyladenosine
1.4
1.2
1.0
0.8
0.6
0.4
0.2
0.0
WT
KO
rAAV Ctrl
rAAV Tx

FIG. 57 cont.

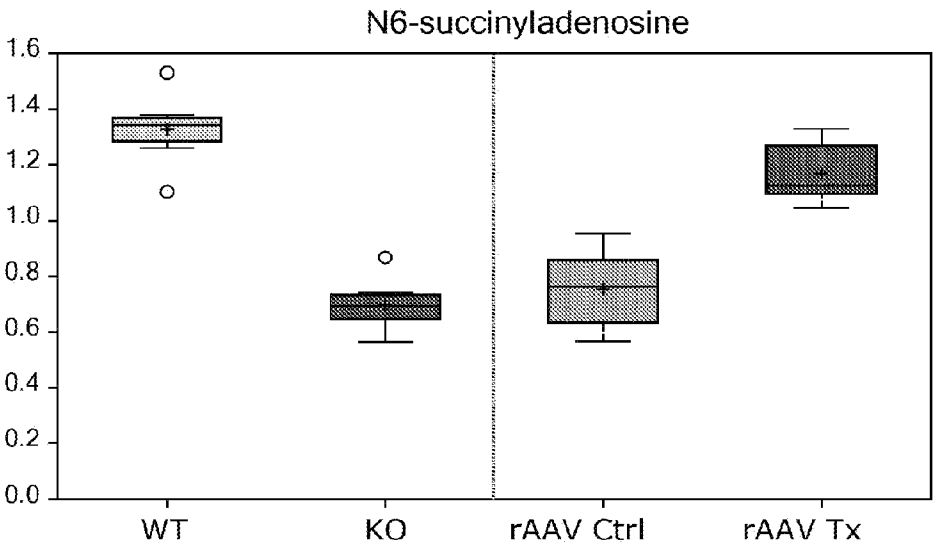
N6-succinyladenosine
1.6
1.4
1.2
1.0
0.8
0.6
0.4
0.2
0.0
WT
KO
rAAV Ctrl
rAAV Tx

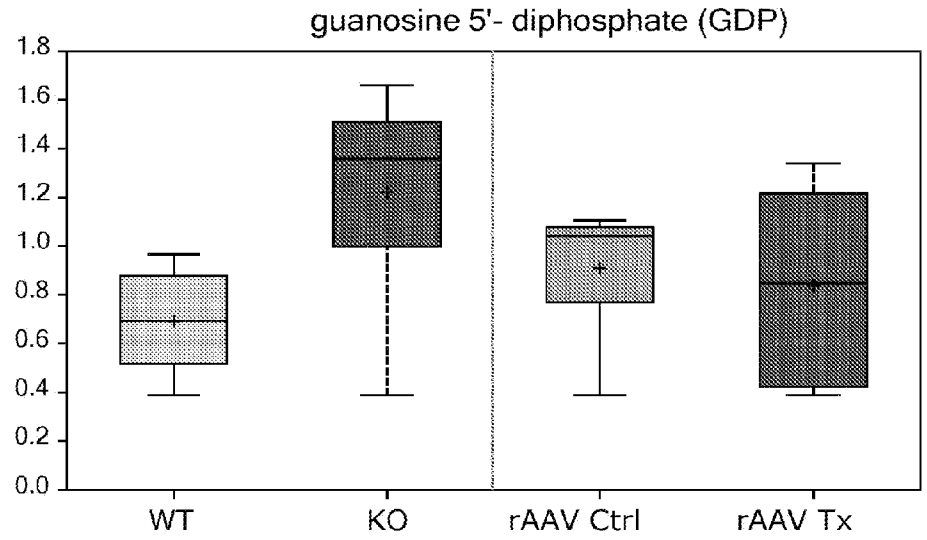
guanosine 5'- diphosphate (GDP)
1.8
1.6
1.4
1.2
1.0
0.8
0.6
0.4
0.2
0.0
WT
KO
rAAV Ctrl
rAAV Tx

FIG. 57 cont.

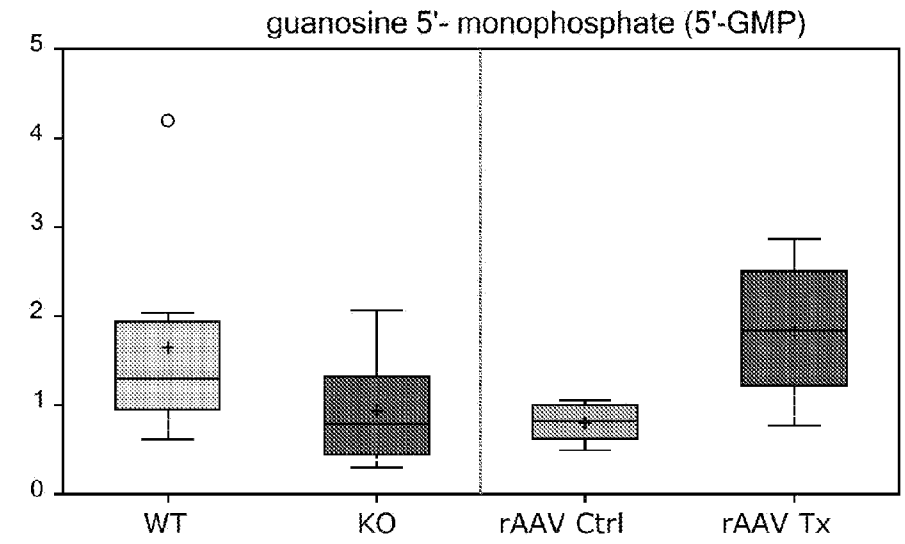
guanosine 5'- monophosphate (5'-GMP)
5
4
3
2
1
0
WT
KO
rAAV Ctrl
rAAV Tx

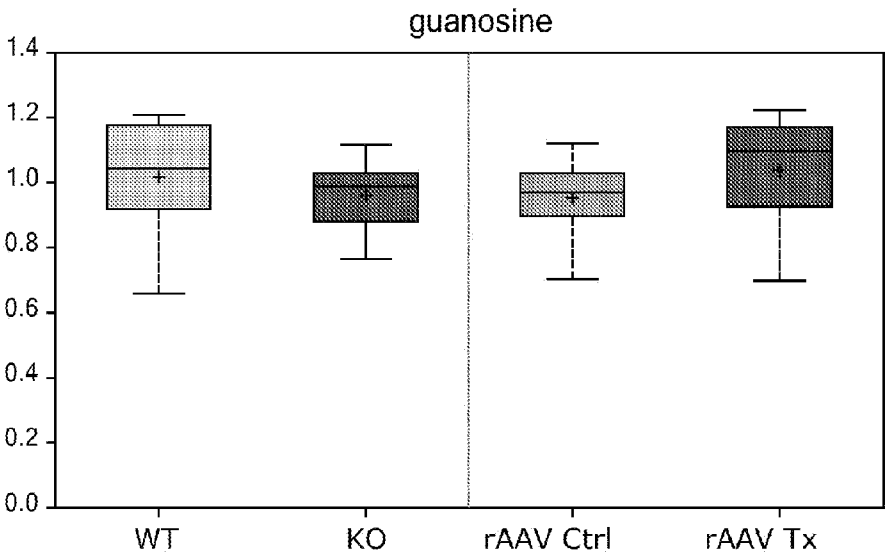
guanosine
1.4
1.2
1.0
0.8
0.6
0.4
0.2
0.0
WT
KO
rAAV Ctrl
rAAV Tx

FIG. 57 cont.

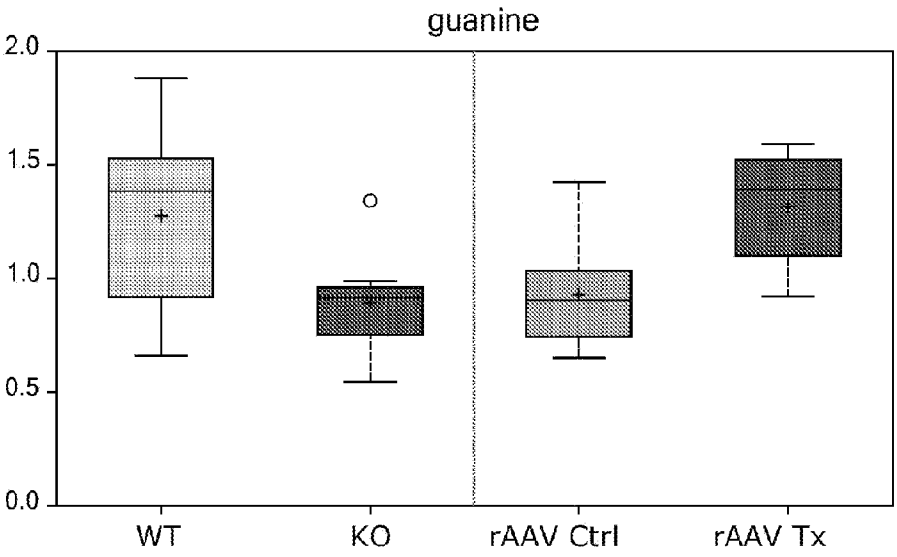
guanine
2.0
1.5
1.0
0.5
0.0
WT
KO
rAAV Ctrl
rAAV Tx

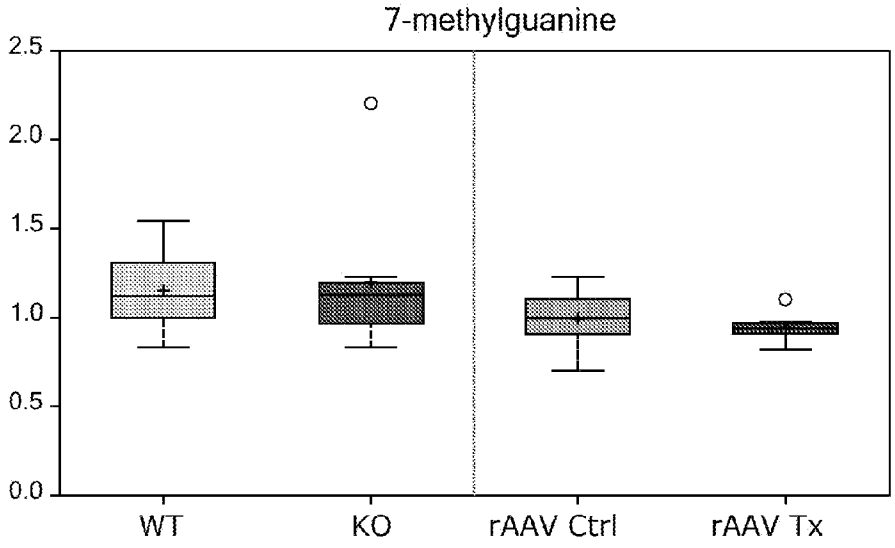
7-methylguanine
2.5
2.0
1.5
1.0
0.5
0.0
WT
KO
rAAV Ctrl
rAAV Tx

FIG. 57 cont.

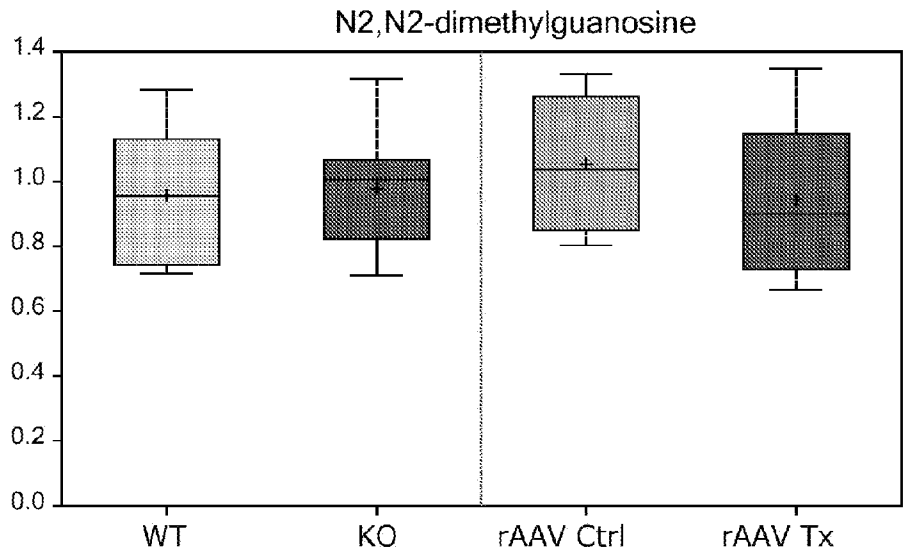
N2,N2-dimethylguanosine
1.4
1.2
1.0
0.8
0.6
0.4
0.2
0.0
WT
KO
rAAV Ctrl
rAAV Tx

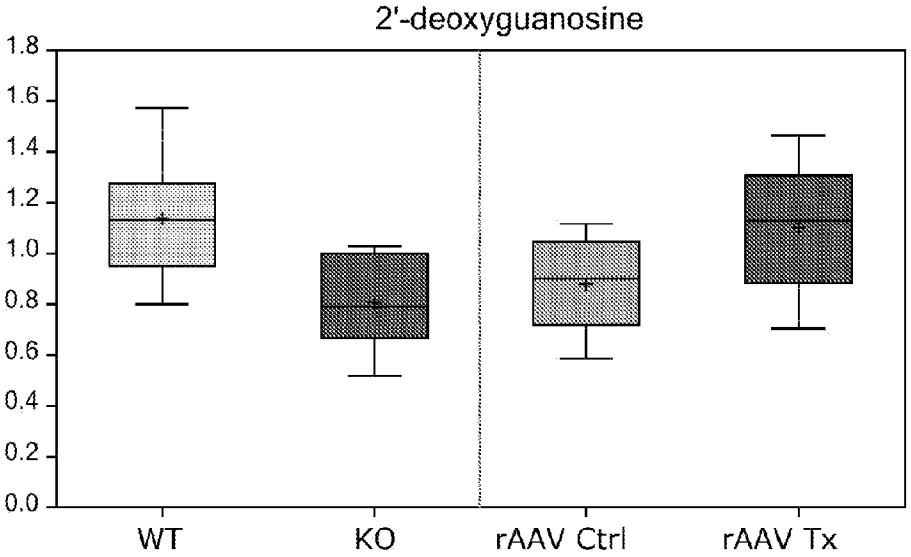
2'-deoxyguanosine
1.8
1.6
1.4
1.2
1.0
0.8
0.6
0.4
0.2
0.0
WT
KO
rAAV Ctrl
rAAV Tx

FIG. 57 cont.

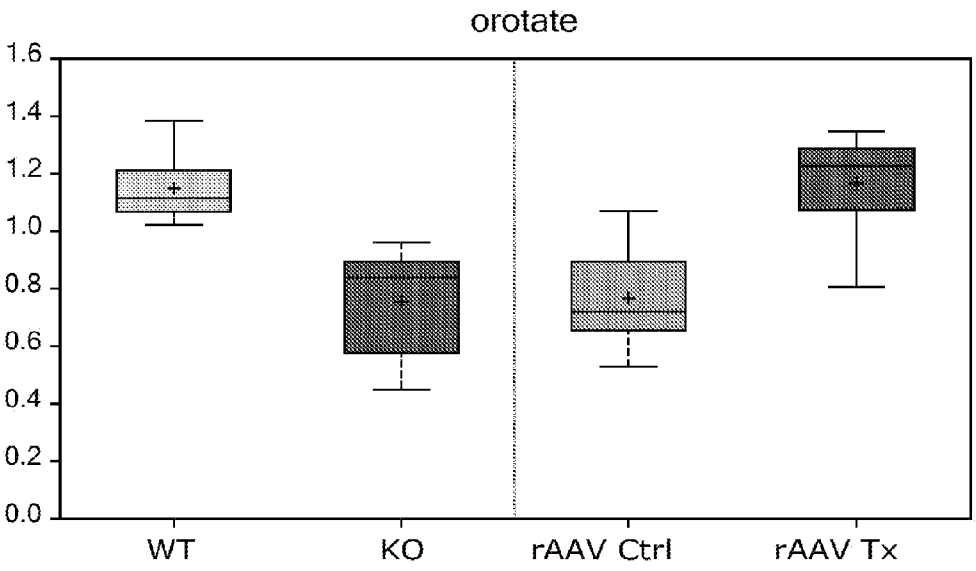
orotate
1.6
1.4
1.2
1.0
0.8
0.6
0.4
0.2
0.0
WT
KO
rAAV Ctrl
rAAV Tx

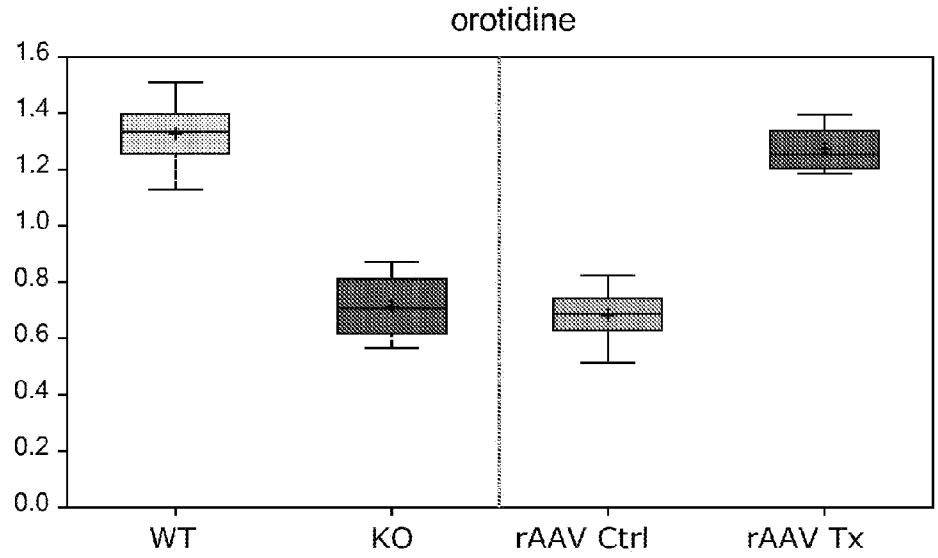
orotidine
1.6
1.4
1.2
1.0
0.8
0.6
0.4
0.2
0.0
WT
KO
rAAV Ctrl
rAAV Tx

FIG. 57 cont.

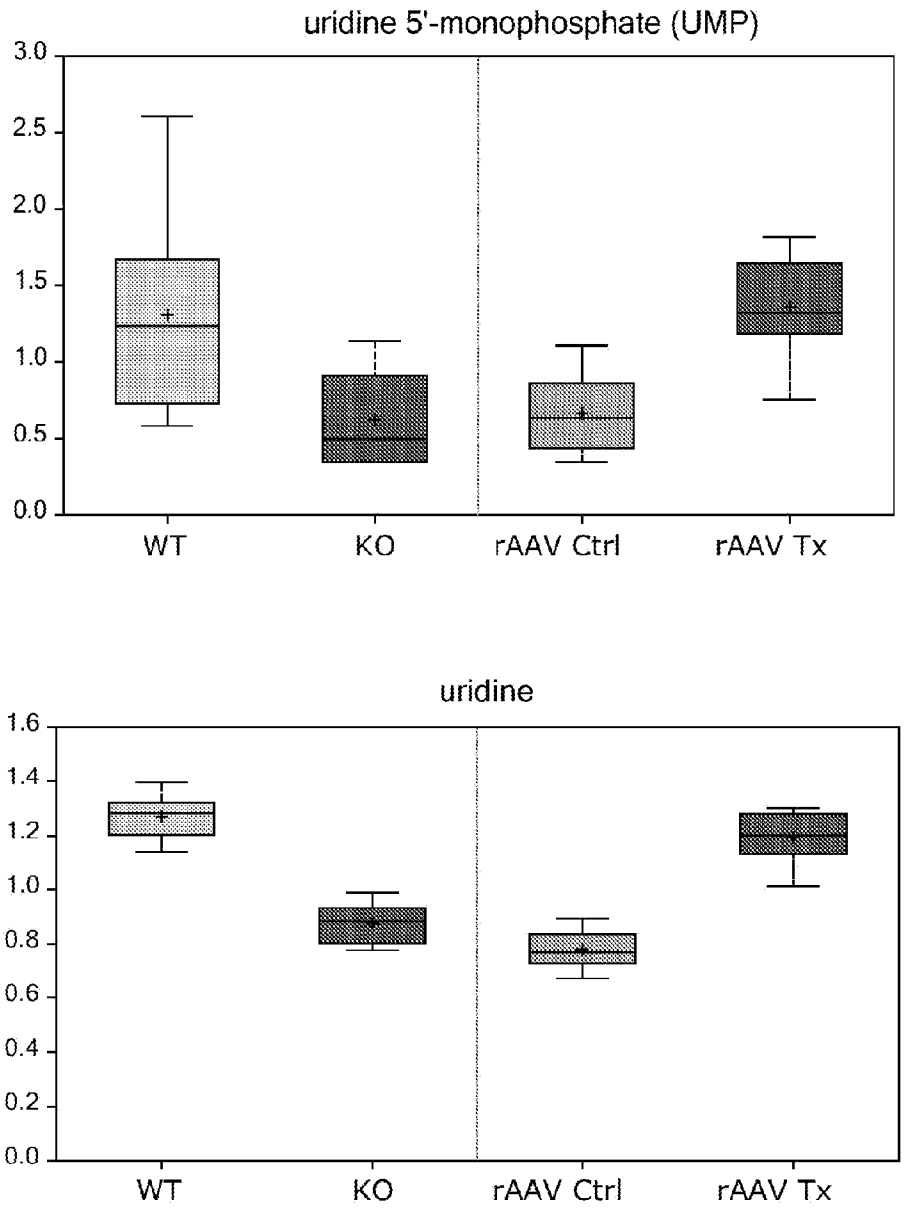
uridine 5'-monophosphate (UMP)
3.0
2.5
2.0
1.5
1.0
0.5
0.0
WT
KO
rAAV Ctrl
rAAV Tx
uridine
1.6
1.4
1.2
1.0
0.8
0.6
0.4
0.2
0.0
WT
KO
rAAV Ctrl
rAAV Tx

FIG. 57 cont.

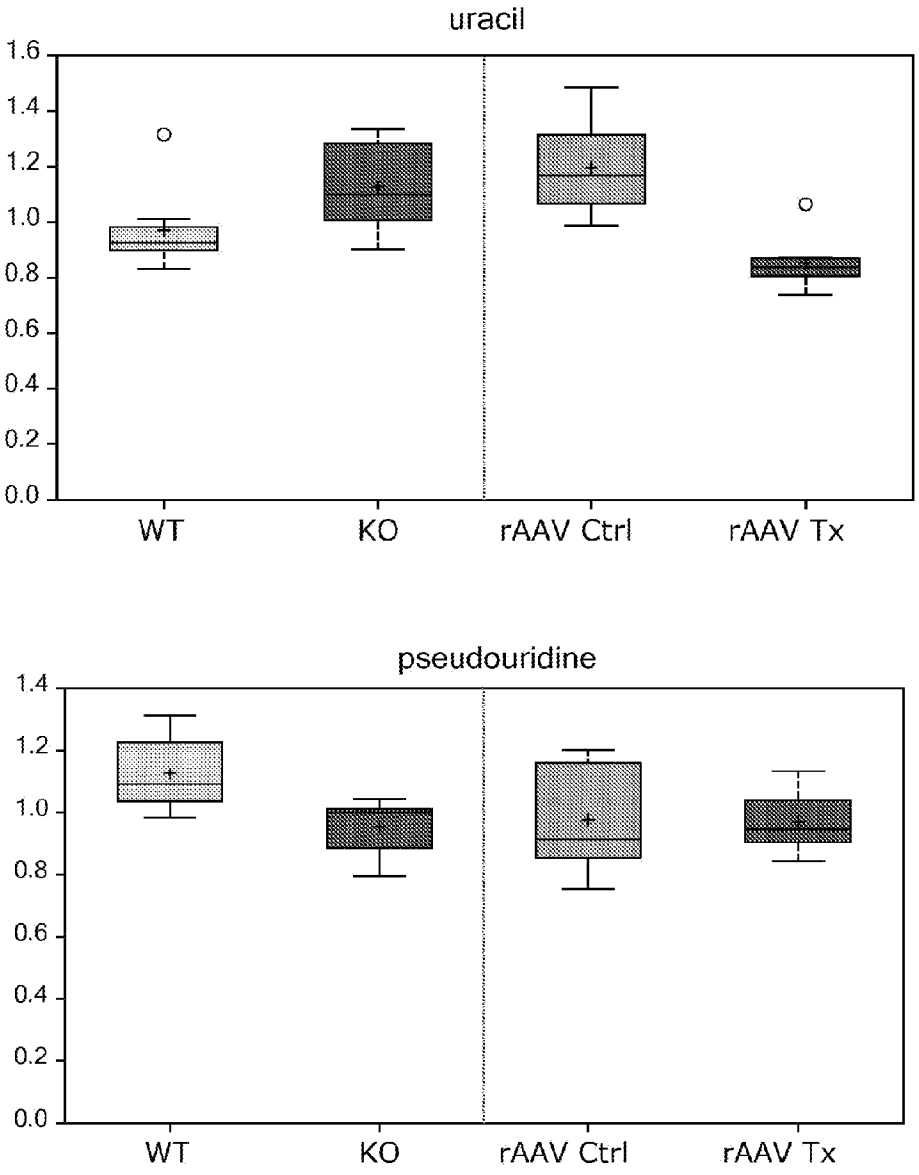
uracil
1.6
1.4
1.2
1.0
0.8
0.6
0.4
0.2
0.0
WT
KO
rAAV Ctrl
rAAV Tx
pseudouridine
1.4
1.2
1.0
0.8
0.6
0.4
0.2
0.0
WT
KO
rAAV Ctrl
rAAV Tx

FIG. 57 cont.

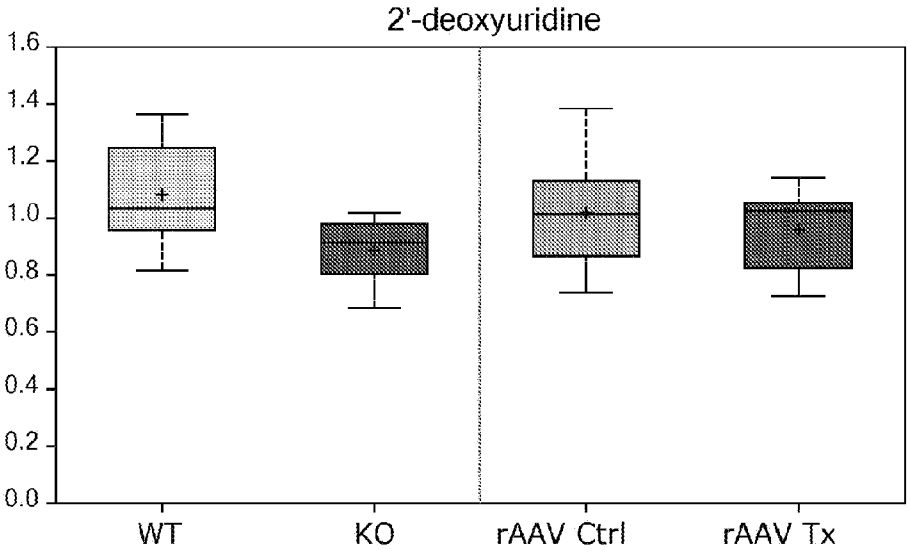
2'-deoxyuridine
1.6
1.4
1.2
1.0
0.8
0.6
0.4
0.2
0.0
WT
KO
rAAV Ctrl
rAAV Tx

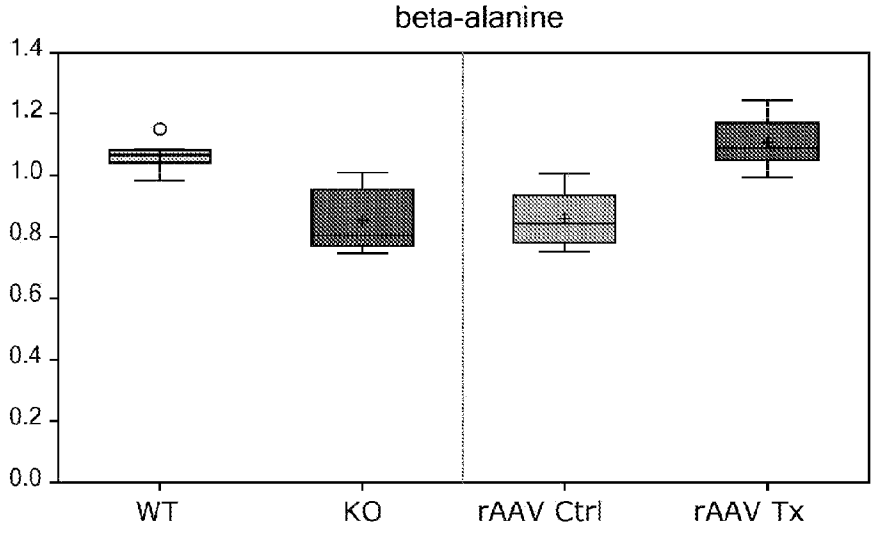
beta-alanine
1.4
1.2
1.0
0.8
0.6
0.4
0.2
0.0
WT
KO
rAAV Ctrl
rAAV Tx

FIG. 57 cont.

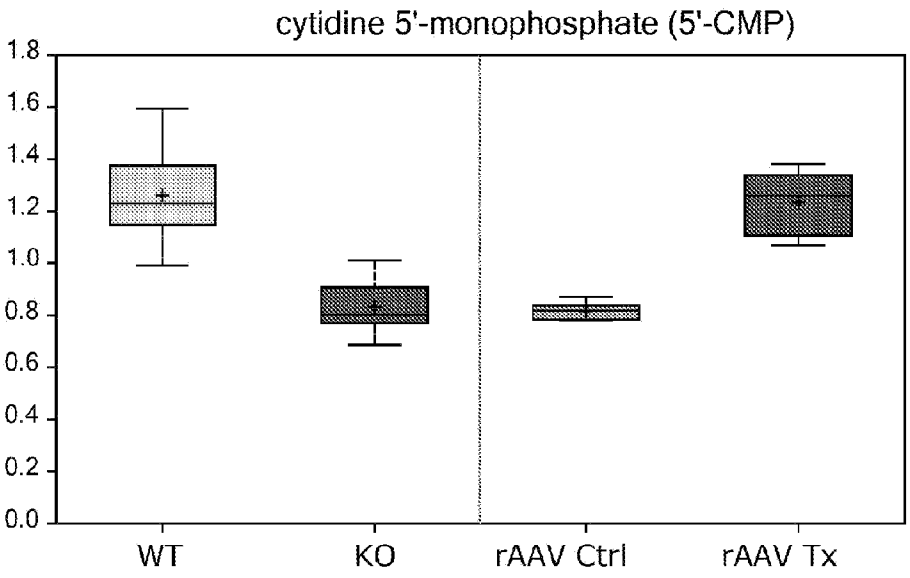
cytidine 5'-monophosphate (5'-CMP)
1.8
1.6
1.4
1.2
1.0
0.8
0.6
0.4
0.2
0.0
WT
KO
rAAV Ctrl
rAAV Tx

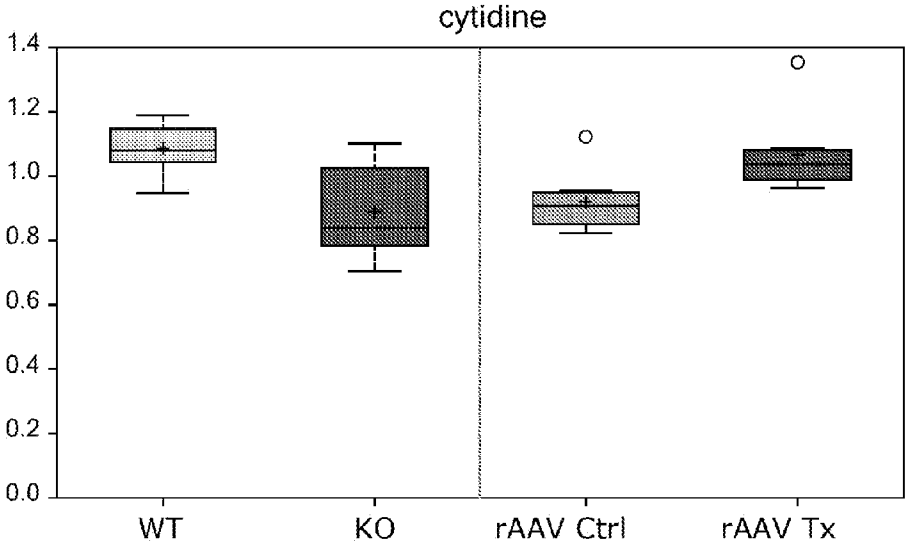
cytidine
1.4
1.2
1.0
0.8
0.6
0.4
0.2
0.0
WT
KO
rAAV Ctrl
rAAV Tx

FIG. 57 cont.

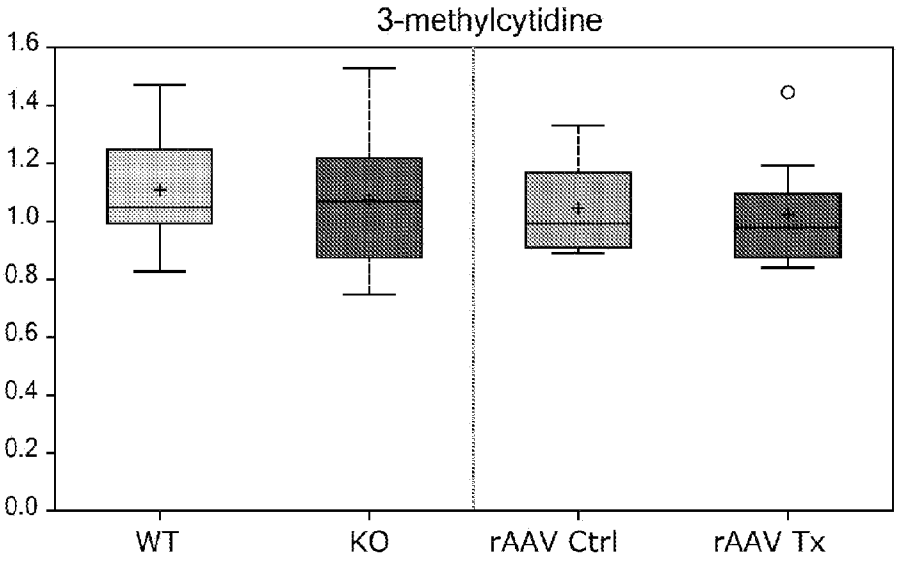
3-methylcytidine
1.6
1.4
1.2
1.0
0.8
0.6
0.4
0.2
0.0
WT
KO
rAAV Ctrl
rAAV Tx

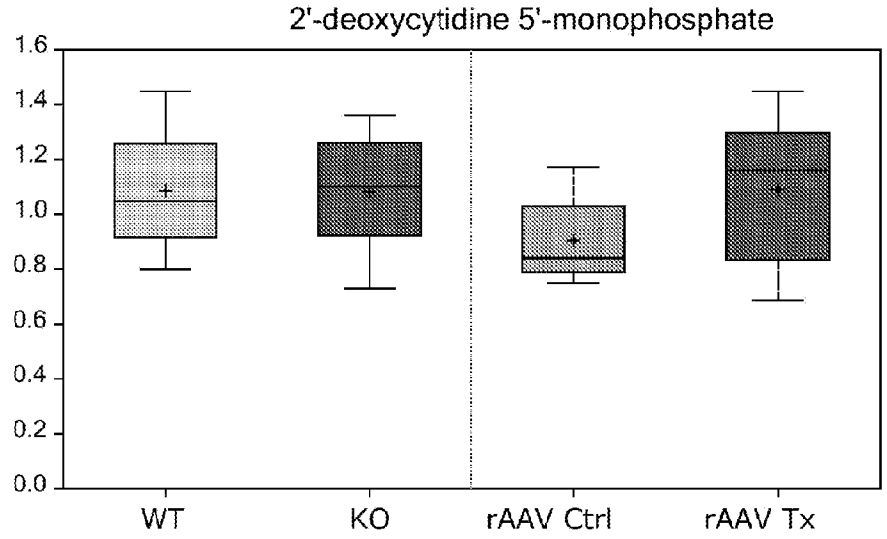
2'-deoxycytidine 5'-monophosphate
1.6
1.4
1.2
1.0
0.8
0.6
0.4
0.2
0.0
WT
KO
rAAV Ctrl
rAAV Tx

FIG. 57 cont.

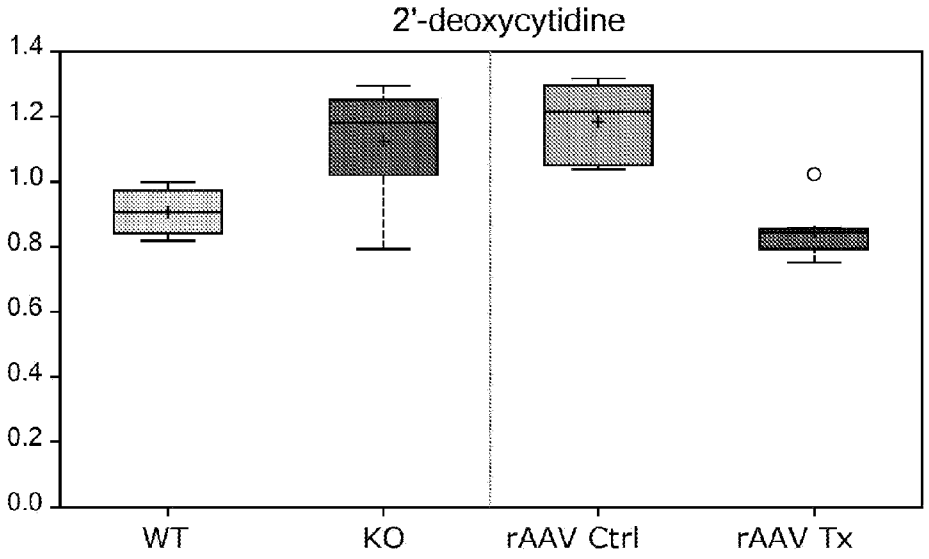
2'-deoxycytidine
1.4
1.2
1.0
0.8
0.6
0.4
0.2
0.0
WT
KO
rAAV Ctrl
rAAV Tx

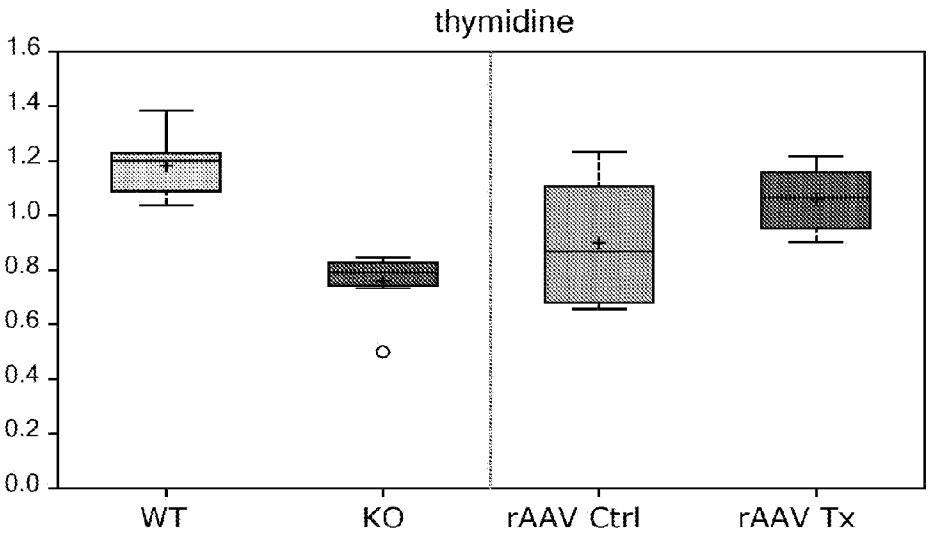
thymidine
1.6
1.4
1.2
1.0
0.8
0.6
0.4
0.2
0.0
WT
KO
rAAV Ctrl
rAAV Tx

FIG. 57 cont.

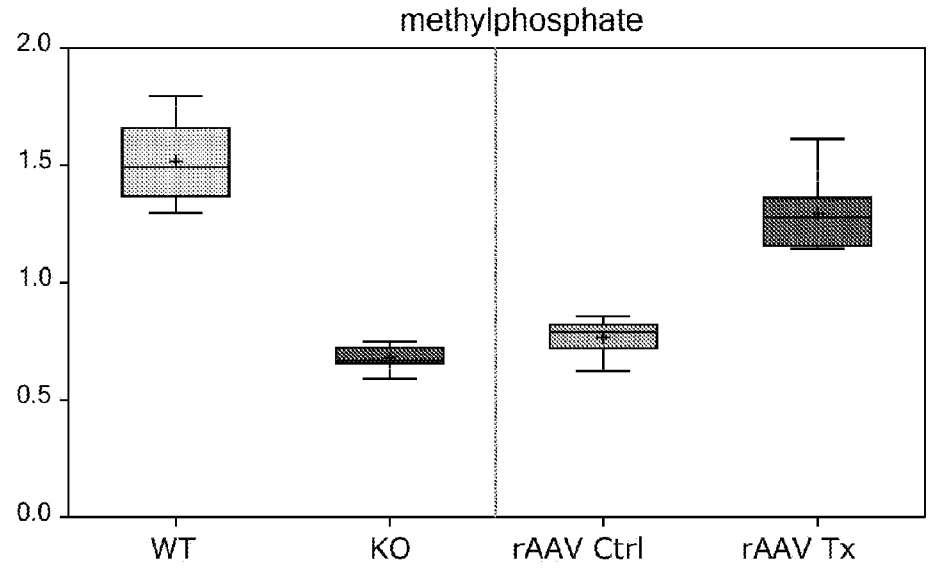
methylphosphate
2.0
1.5
1.0
0.5
0.0
WT
KO
rAAV Ctrl
rAAV Tx

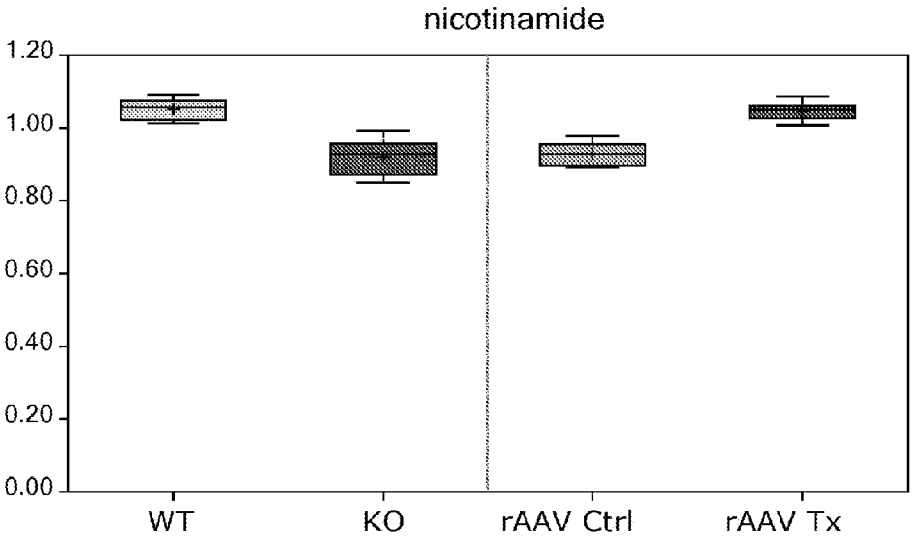
nicotinamide
1.20
1.00
0.80
0.60
0.40
0.20
0.00
WT
KO
rAAV Ctrl
rAAV Tx

FIG. 57 cont.

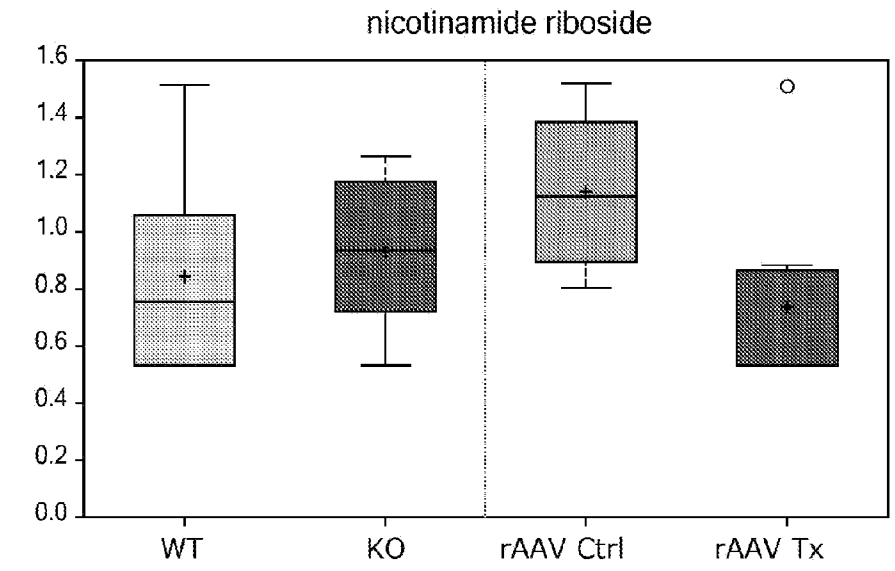
nicotinamide riboside
1.6
1.4
1.2
1.0
0.8
0.6
0.4
0.2
0.0
WT
KO
rAAV Ctrl
rAAV Tx

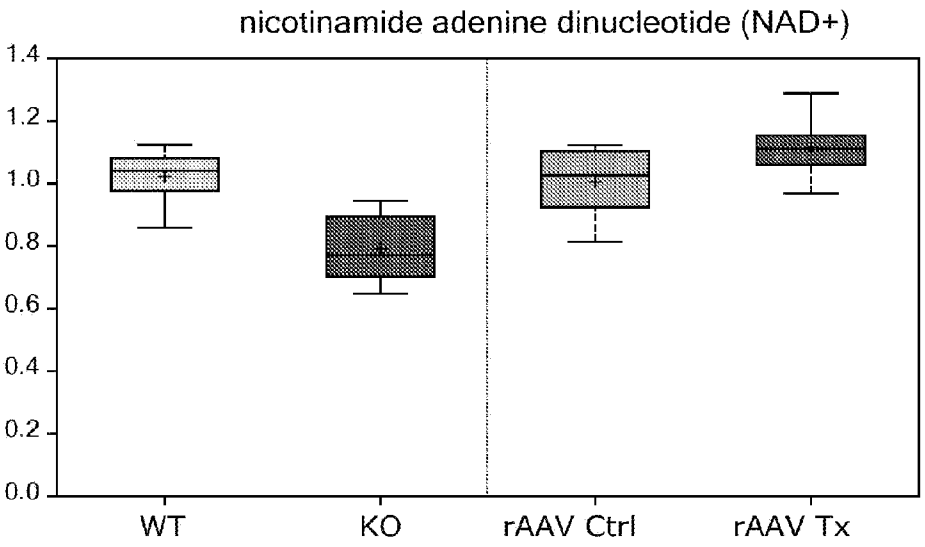
nicotinamide adenine dinucleotide (NAD+)
1.4
1.2
1.0
0.8
0.6
0.4
0.2
0.0
WT
KO
rAAV Ctrl
rAAV Tx

FIG. 57 cont.

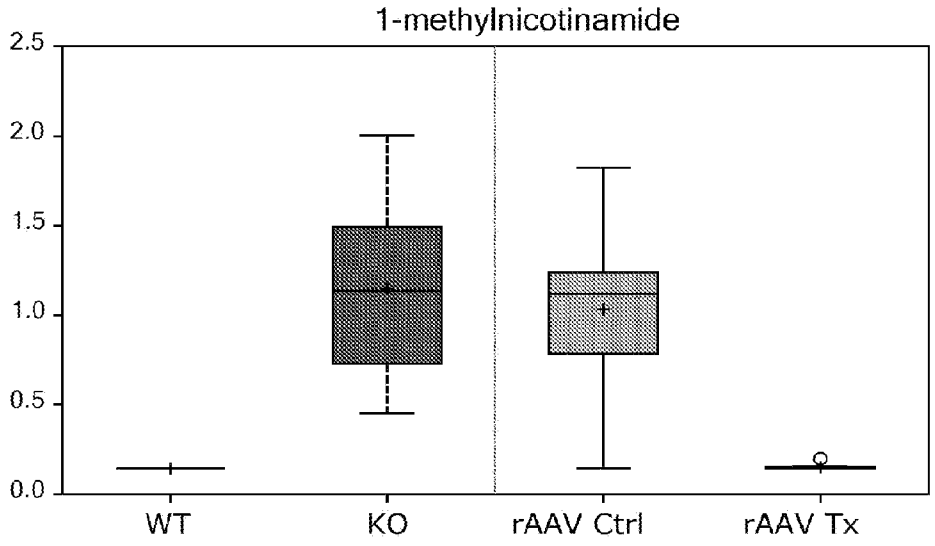
1-methylnicotinamide
2.5
2.0
1.5
1.0
0.5
0.0
WT
KO
rAAV Ctrl
rAAV Tx

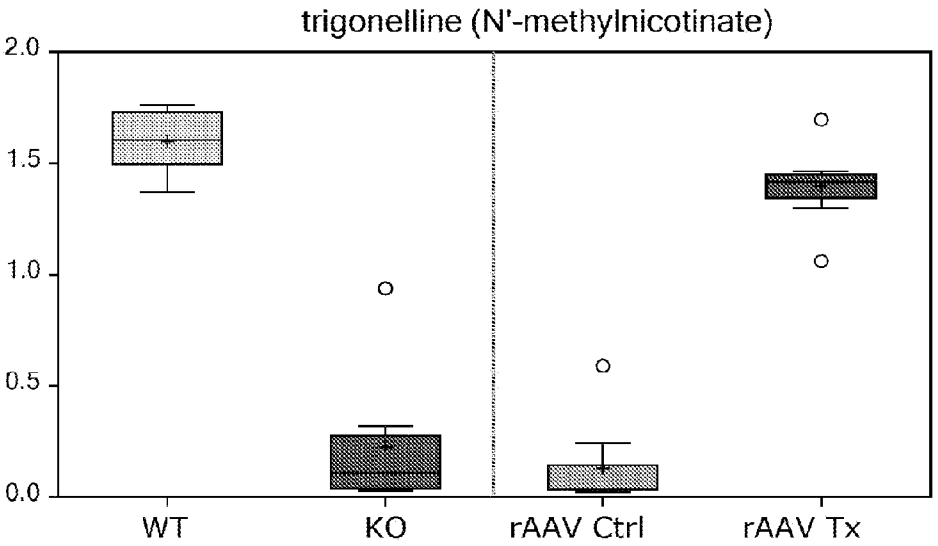
trigonelline (N'-methylnicotinate)
2.0
1.5
1.0
0.5
0.0
WT
KO
rAAV Ctrl
rAAV Tx

FIG. 57 cont.

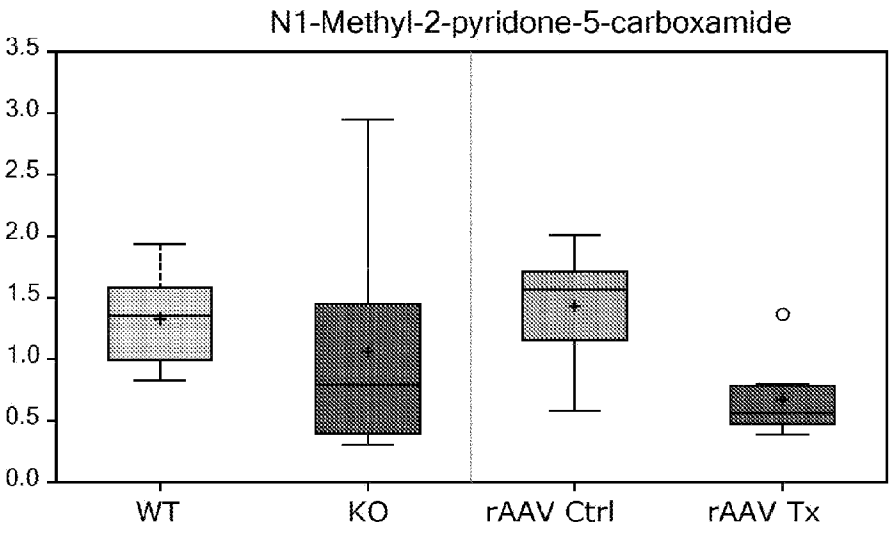
N1-Methyl-2-pyridone-5-carboxamide
3.5
3.0
2.5
2.0
1.5
1.0
0.5
0.0
WT
KO
rAAV Ctrl
rAAV Tx

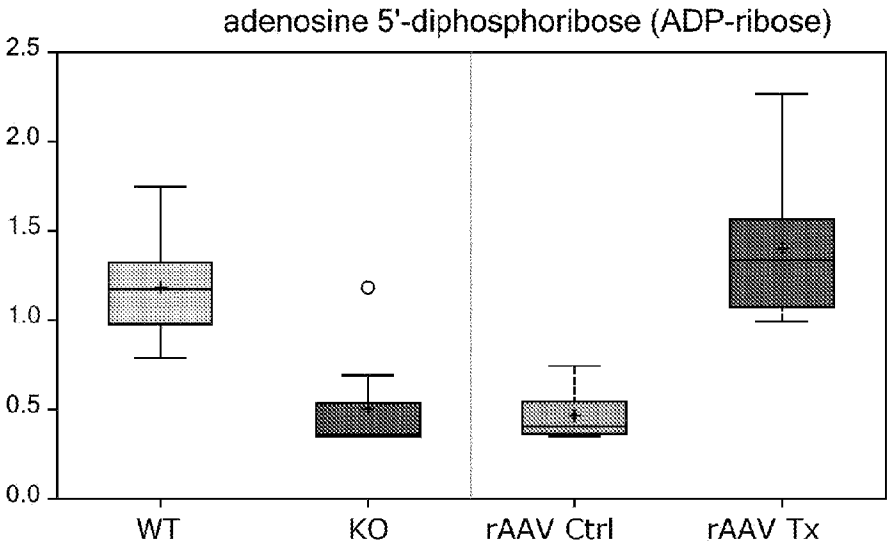
adenosine 5'-diphosphoribose (ADP-ribose)
2.5
2.0
1.5
1.0
0.5
0.0
WT
KO
rAAV Ctrl
rAAV Tx

FIG. 57 cont.

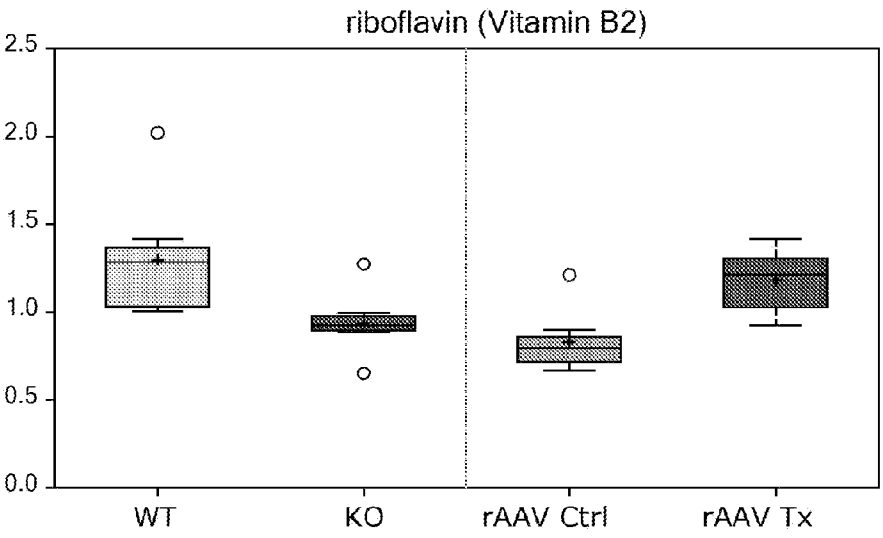
riboflavin (Vitamin B2)
2.5
2.0
1.5
1.0
0.5
0.0
WT
KO
rAAV Ctrl
rAAV Tx

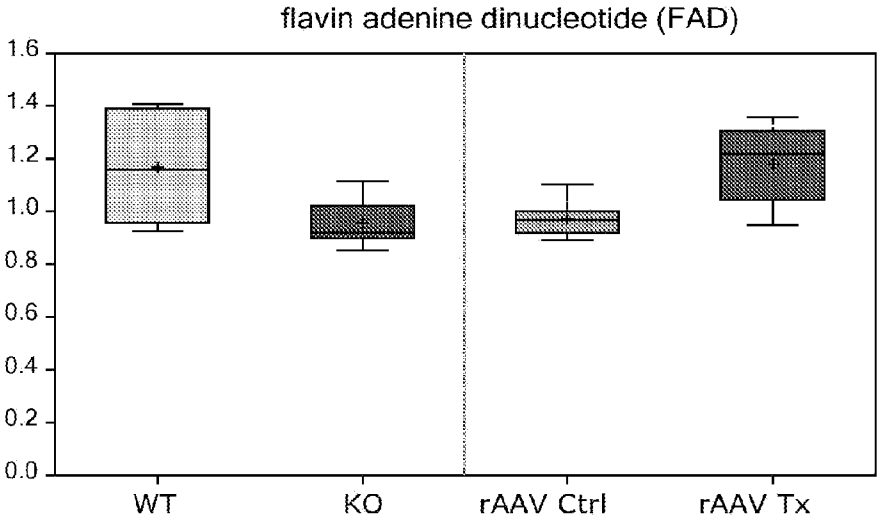
flavin adenine dinucleotide (FAD)
1.6
1.4
1.2
1.0
0.8
0.6
0.4
0.2
0.0
WT
KO
rAAV Ctrl
rAAV Tx

FIG. 57 cont.

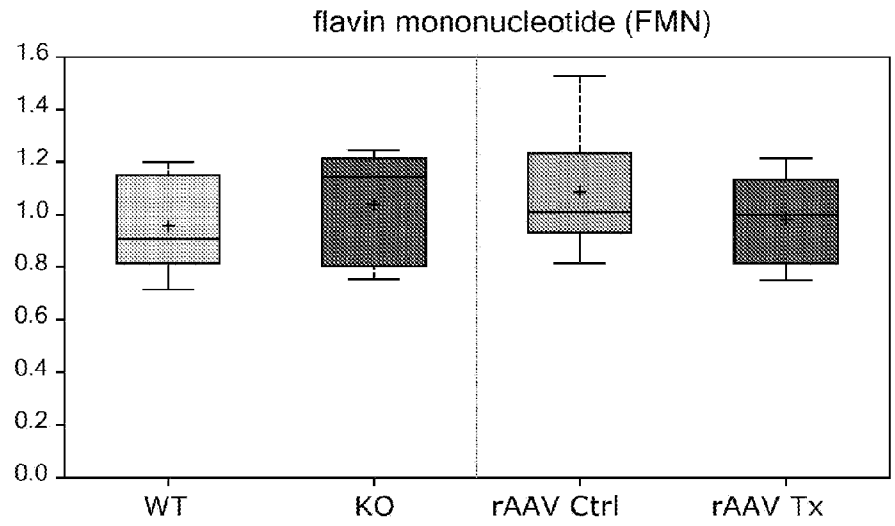
flavin mononucleotide (FMN)
1.6
1.4
1.2
1.0
0.8
0.6
0.4
0.2
0.0
WT
KO
rAAV Ctrl
rAAV Tx

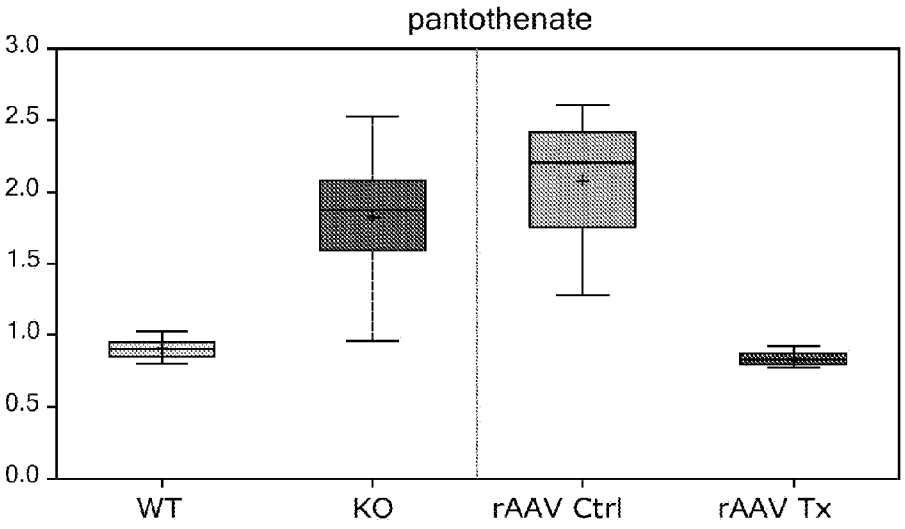
pantothenate
3.0
2.5
2.0
1.5
1.0
0.5
0.0
WT
KO
rAAV Ctrl
rAAV Tx

FIG. 57 cont.

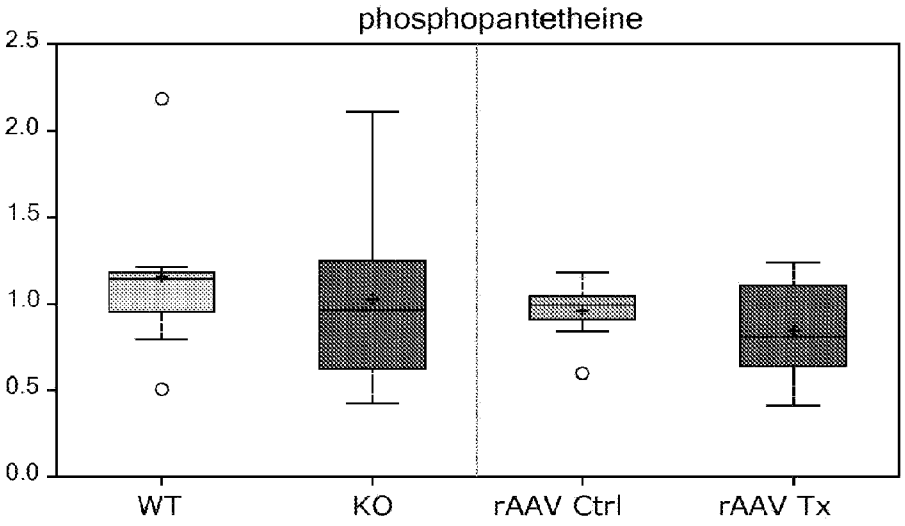
phosphopantetheine
2.5
2.0
1.5
1.0
0.5
0.0
WT
KO
rAAV Ctrl
rAAV Tx

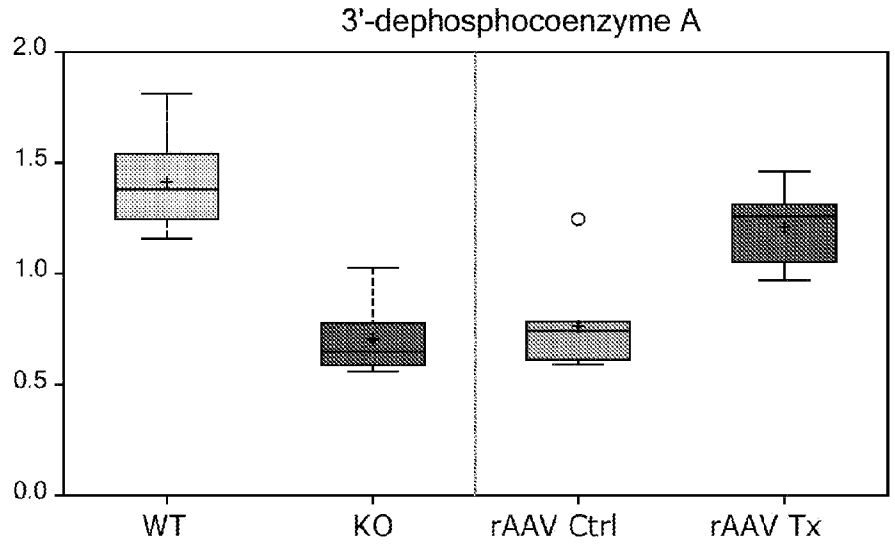
3'-dephosphocoenzyme A
2.0
1.5
1.0
0.5
0.0
WT
KO
rAAV Ctrl
rAAV Tx

FIG. 57 cont.

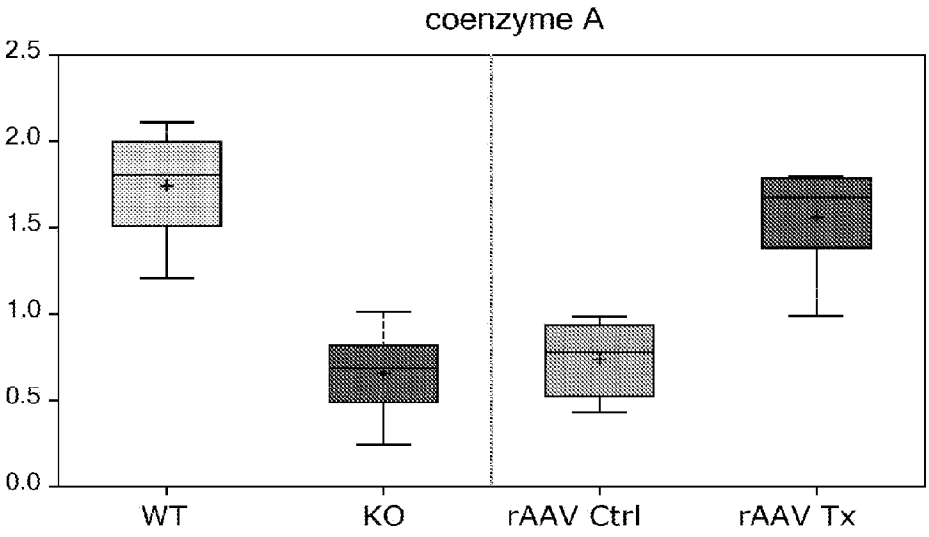
coenzyme A
2.5
2.0
1.5
1.0
0.5
0.0
WT
KO
rAAV Ctrl
rAAV Tx

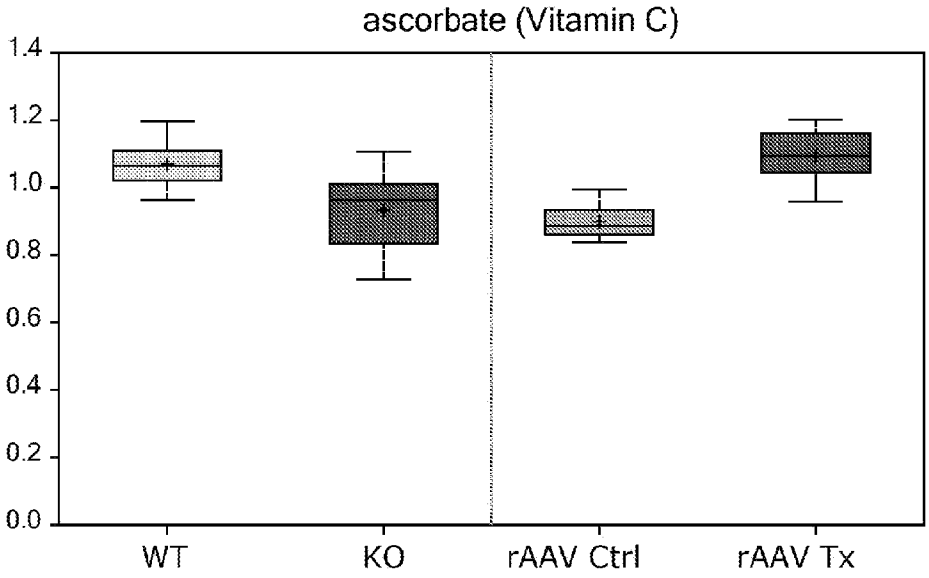
ascorbate (Vitamin C)
1.4
1.2
1.0
0.8
0.6
0.4
0.2
0.0
WT
KO
rAAV Ctrl
rAAV Tx

FIG. 57 cont.

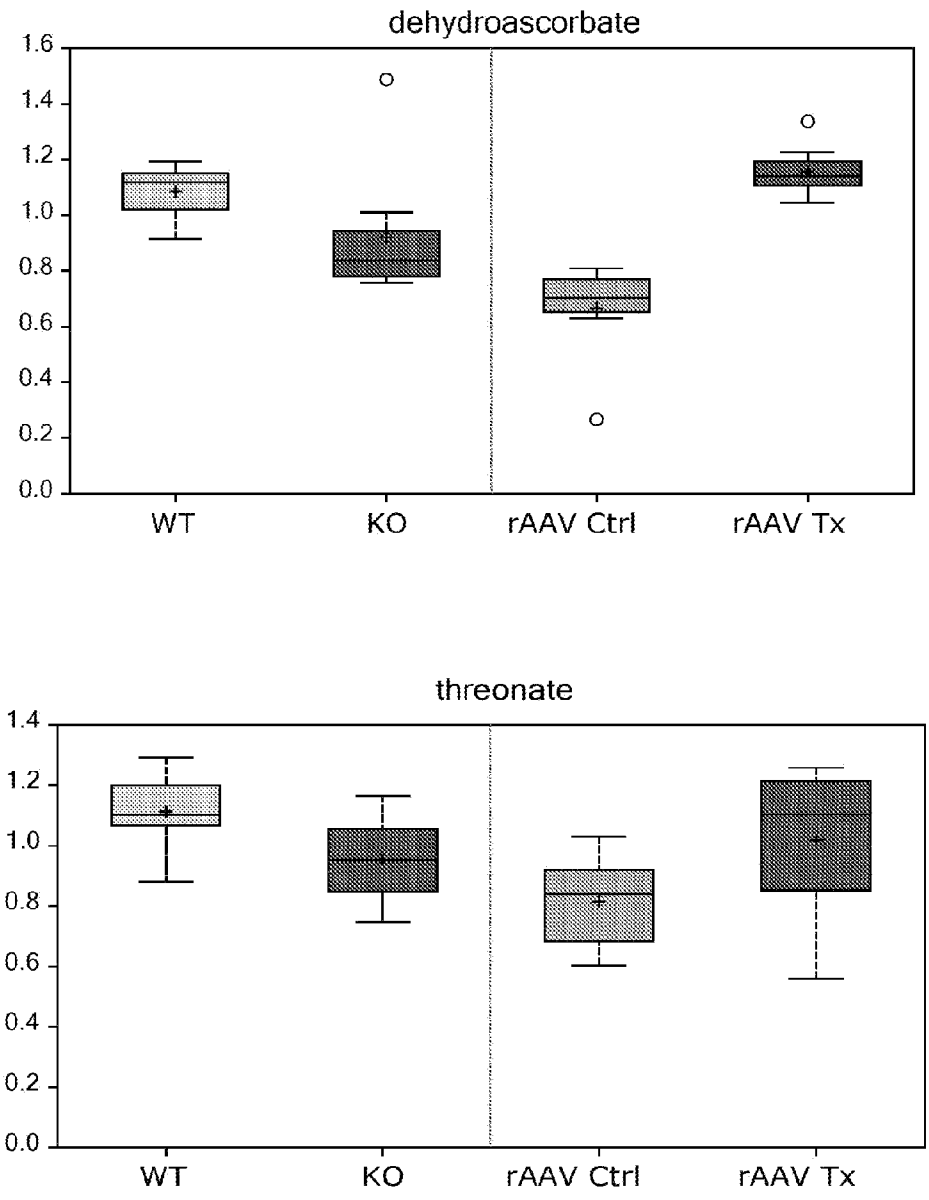
dehydroascorbate
1.6
1.4
1.2
1.0
0.8
0.6
0.4
0.2
0.0
WT
KO
rAAV Ctrl
rAAV Tx
threonate
1.4
1.2
1.0
0.8
0.6
0.4
0.2
0.0
WT
KO
rAAV Ctrl
rAAV Tx

FIG. 57 cont.

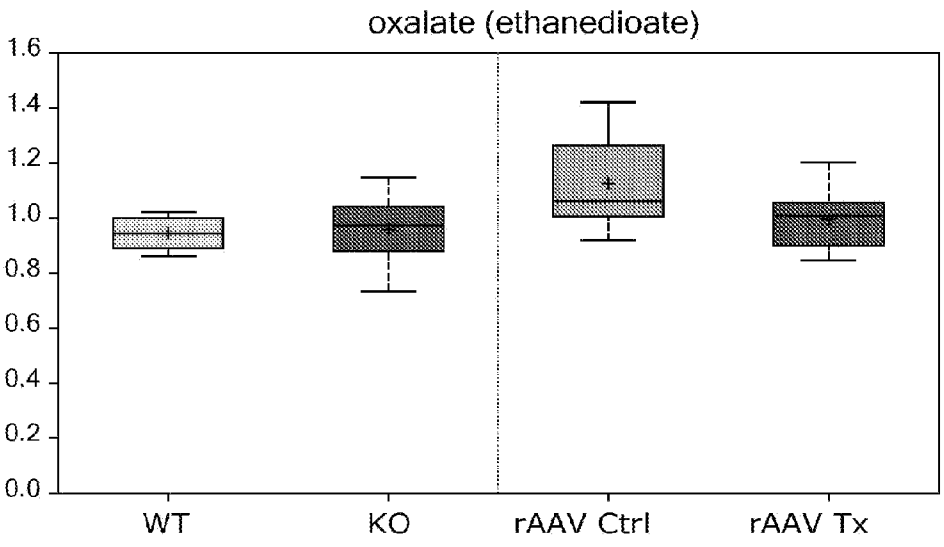
oxalate (ethanedioate)
1.6
1.4
1.2
1.0
0.8
0.6
0.4
0.2
0.0
WT
KO
rAAV Ctrl
rAAV Tx

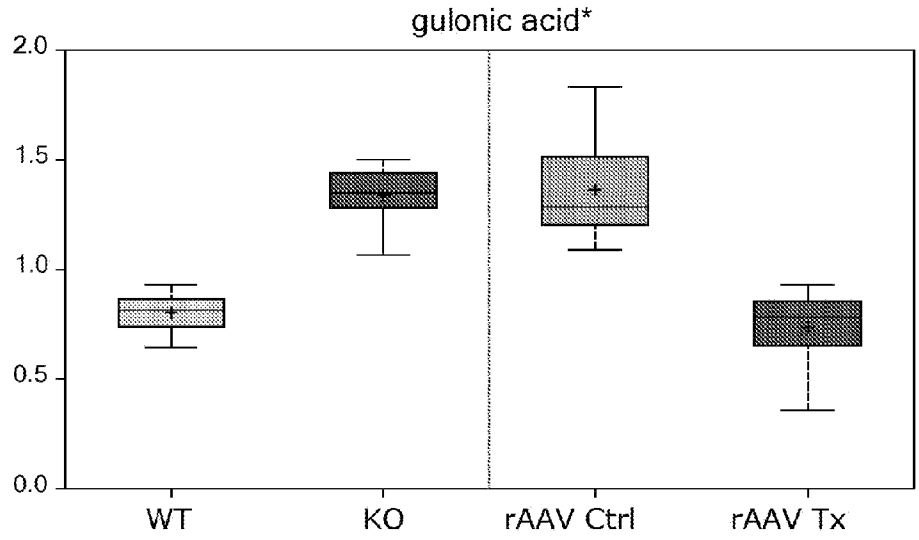
gulonic acid*
2.0
1.5
1.0
0.5
0.0
WT
KO
rAAV Ctrl
rAAV Tx

FIG. 57 cont.

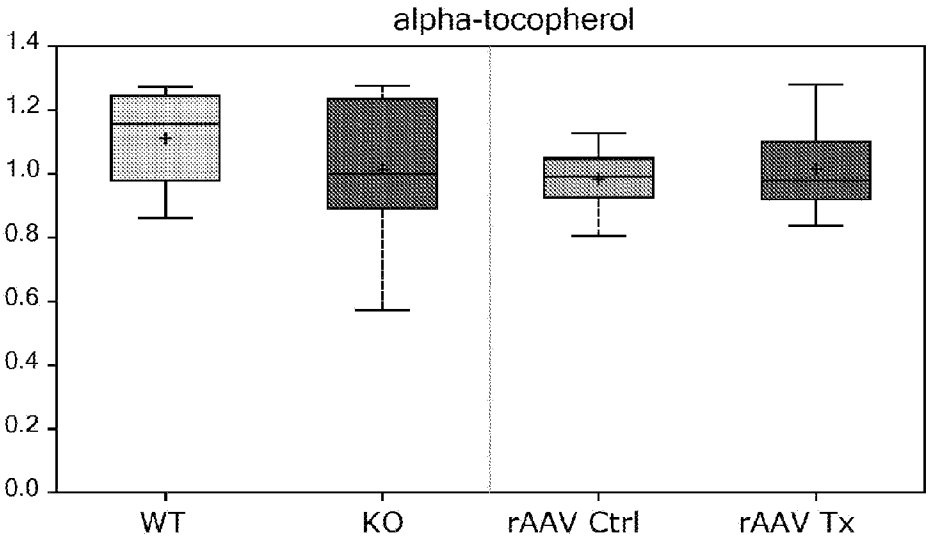
alpha-tocopherol
1.4
1.2
1.0
0.8
0.6
0.4
0.2
0.0
WT
KO
rAAV Ctrl
rAAV Tx

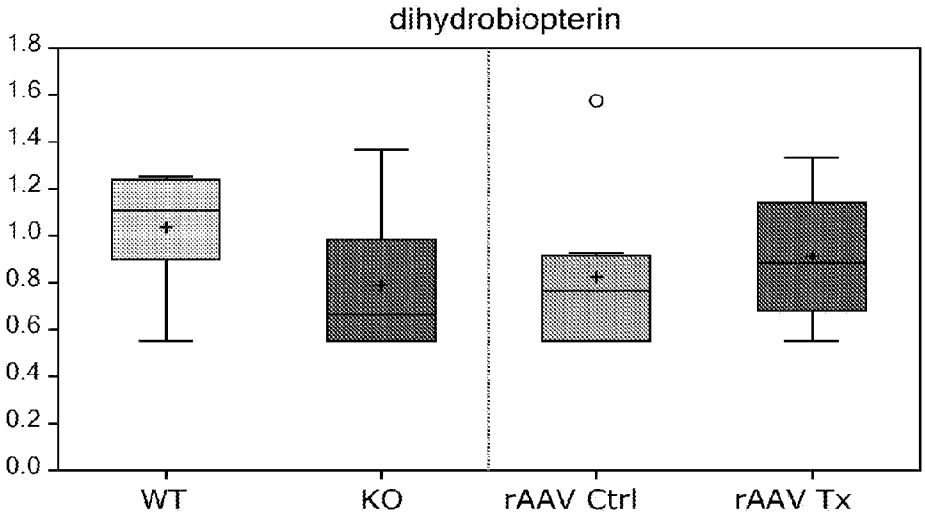
dihydrobiopterin
1.8
1.6
1.4
1.2
1.0
0.8
0.6
0.4
0.2
0.0
WT
KO
rAAV Ctrl
rAAV Tx

FIG. 57 cont.

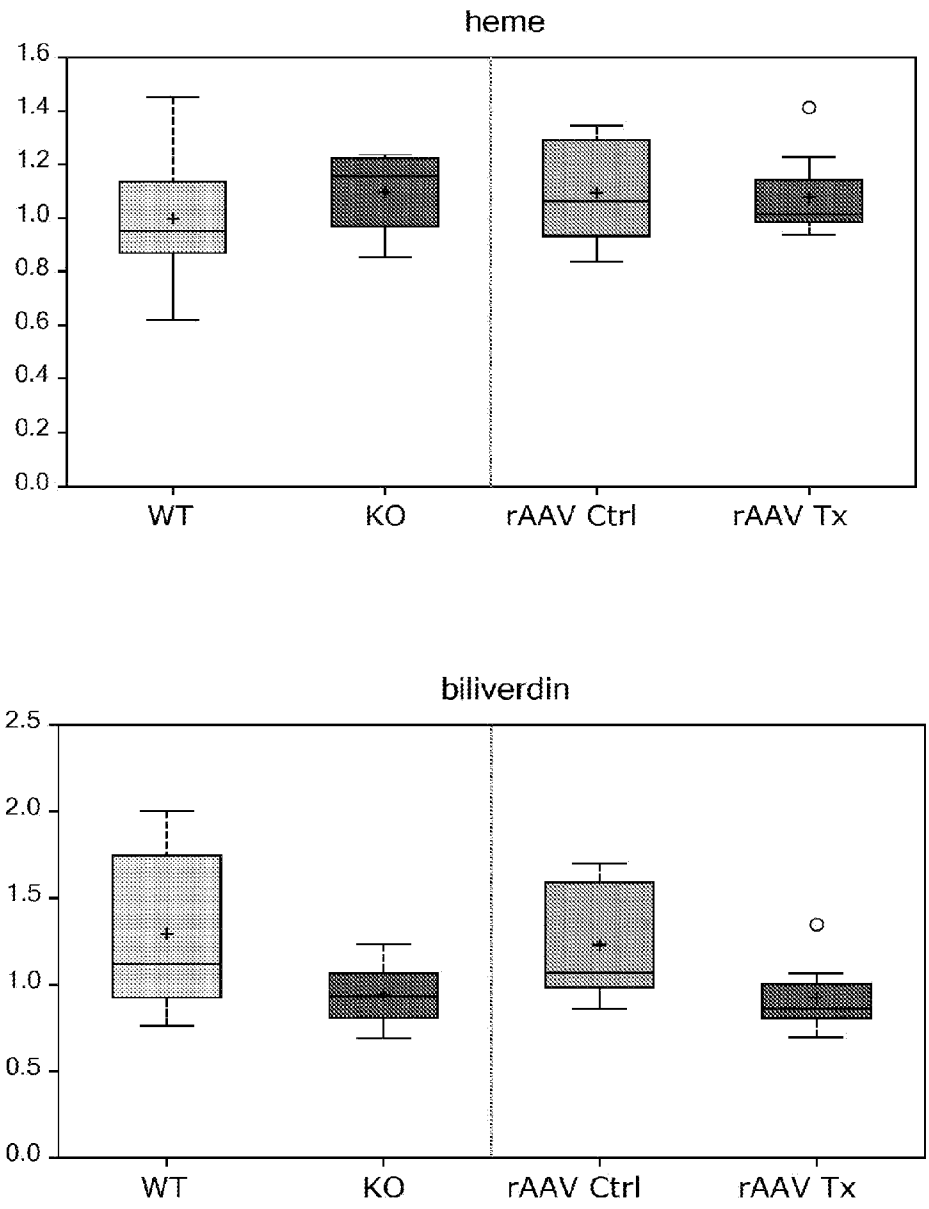
heme
1.6
1.4
1.2
1.0
0.8
0.6
0.4
0.2
0.0
WT
KO
rAAV Ctrl
rAAV Tx
biliverdin
2.5
2.0
1.5
1.0
0.5
0.0
WT
KO
rAAV Ctrl
rAAV Tx

FIG. 57 cont.

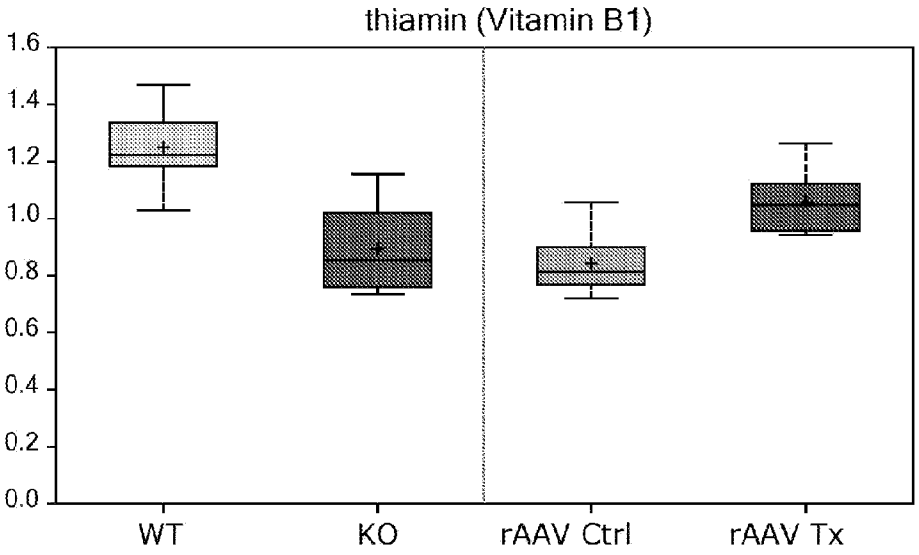
thiamin (Vitamin B1)
1.6
1.4
1.2
1.0
0.8
0.6
0.4
0.2
0.0
WT
KO
rAAV Ctrl
rAAV Tx

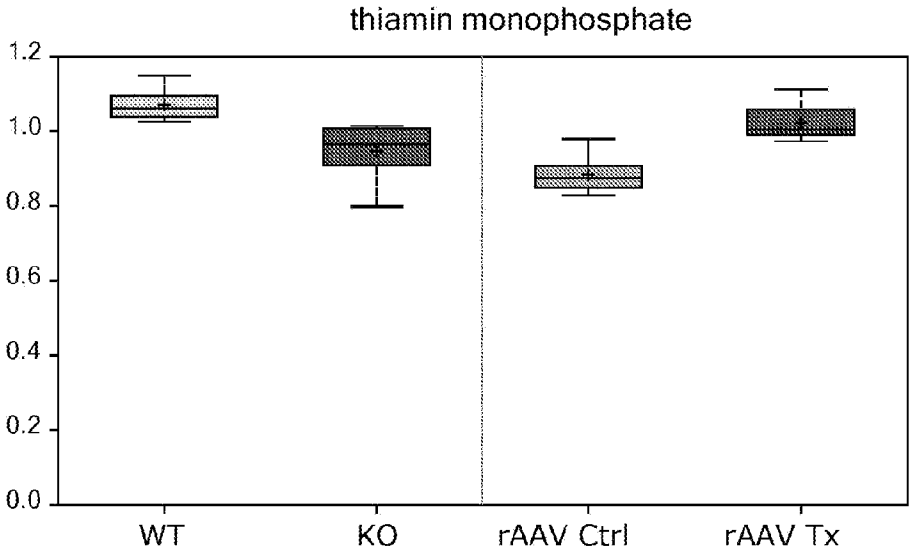
thiamin monophosphate
1.2
1.0
0.8
0.6
0.4
0.2
0.0
WT
KO
rAAV Ctrl
rAAV Tx

FIG. 57 cont.

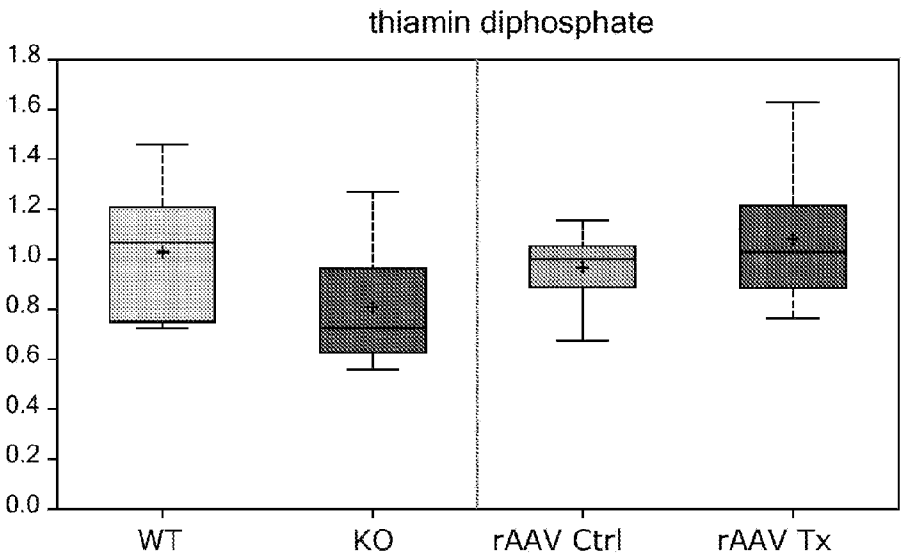
thiamin diphosphate
1.8
1.6
1.4
1.2
1.0
0.8
0.6
0.4
0.2
0.0
WT
KO
rAAV Ctrl
rAAV Tx

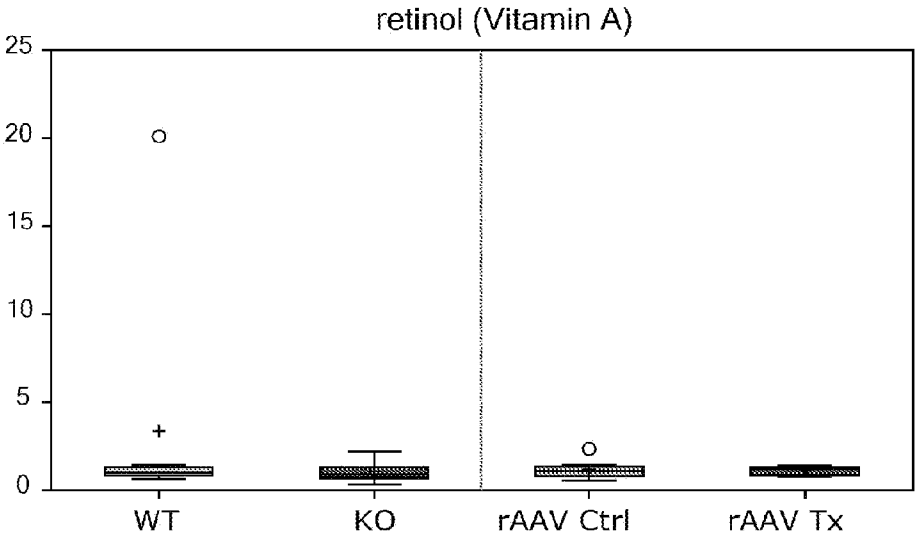
retinol (Vitamin A)
25
20
15
10
5
0
WT
KO
rAAV Ctrl
rAAV Tx

FIG. 57 cont.

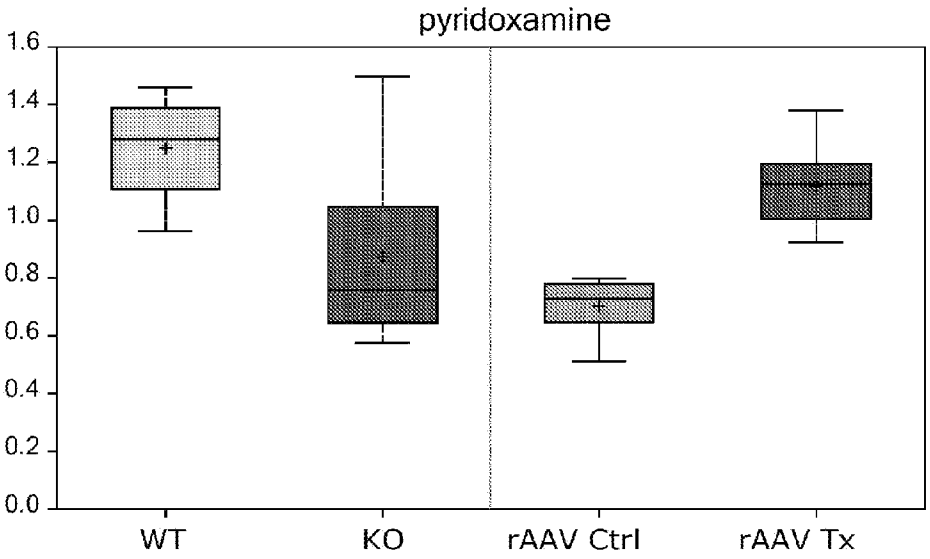
pyridoxamine
1.6
1.4
1.2
1.0
0.8
0.6
0.4
0.2
0.0
WT
KO
rAAV Ctrl
rAAV Tx

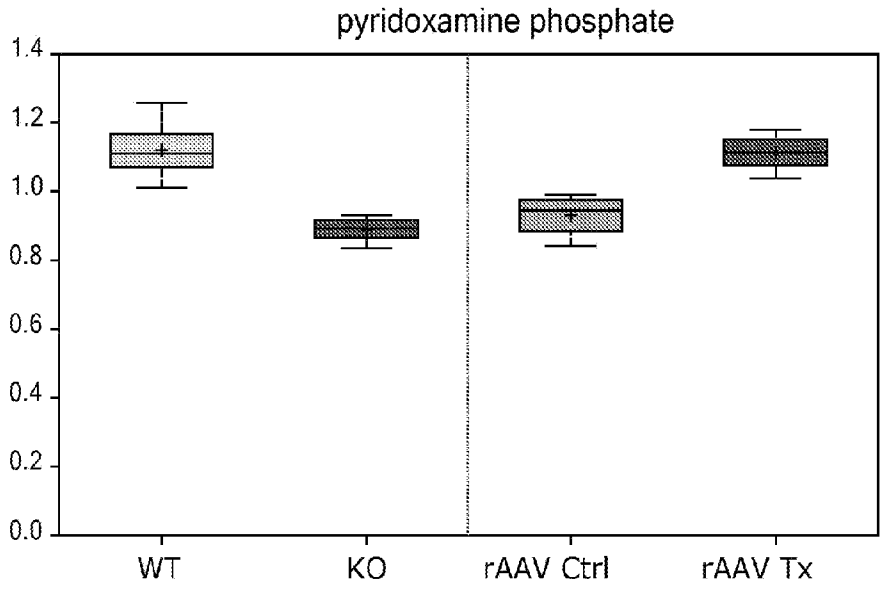
pyridoxamine phosphate
1.4
1.2
1.0
0.8
0.6
0.4
0.2
0.0
WT
KO
rAAV Ctrl
rAAV Tx

FIG. 57 cont.

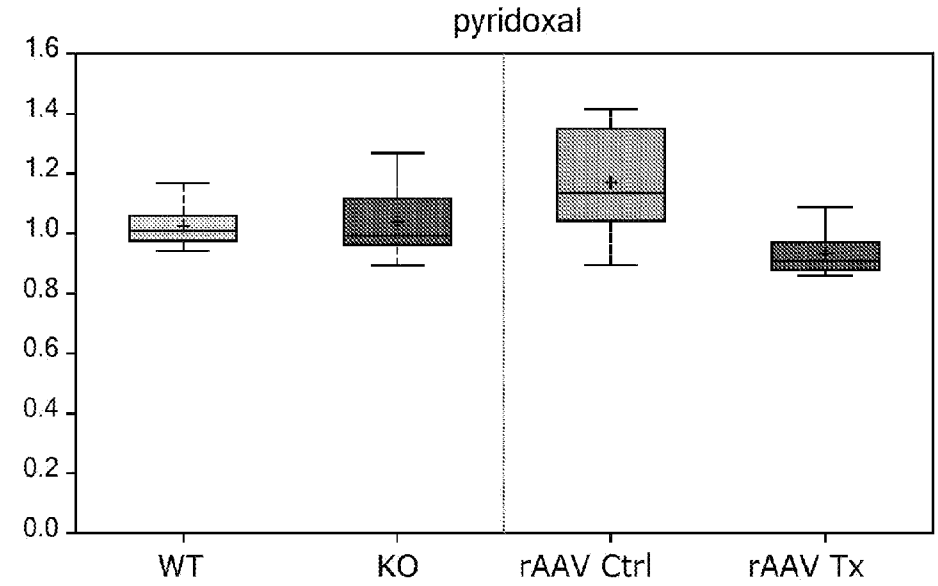
pyridoxal
1.6
1.4
1.2
1.0
0.8
0.6
0.4
0.2
0.0
WT
KO
rAAV Ctrl
rAAV Tx

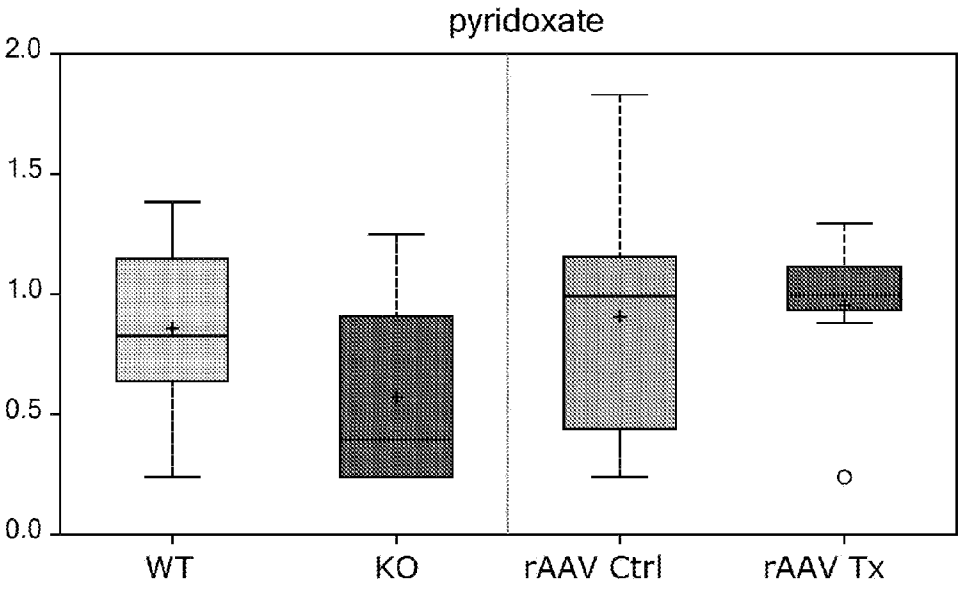
pyridoxate
2.0
1.5
1.0
0.5
0.0
WT
KO
rAAV Ctrl
rAAV Tx

FIG. 57 cont.

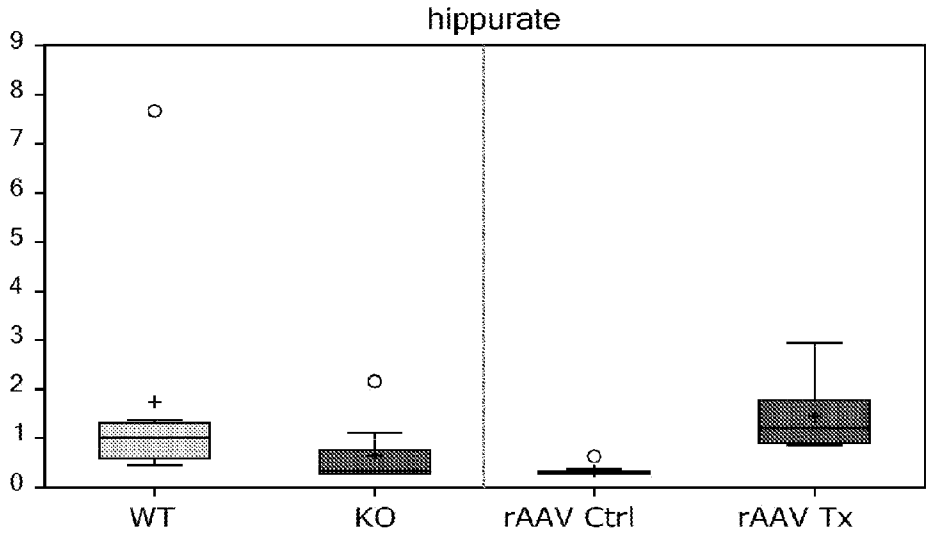
hippurate
9
8
7
6
5
4
3
2
1
0
WT
KO
rAAV Ctrl
rAAV Tx

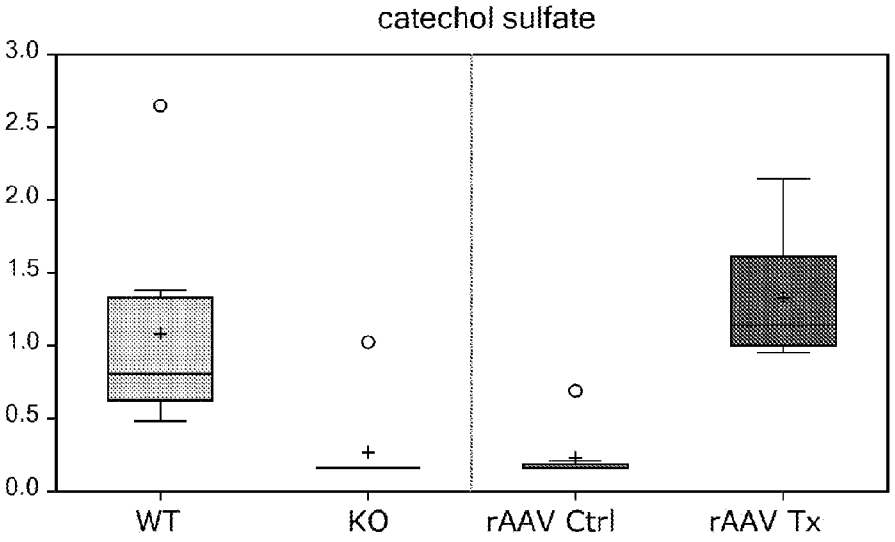
catechol sulfate
3.0
2.5
2.0
1.5
1.0
0.5
0.0
WT
KO
rAAV Ctrl
rAAV Tx

FIG. 57 cont.

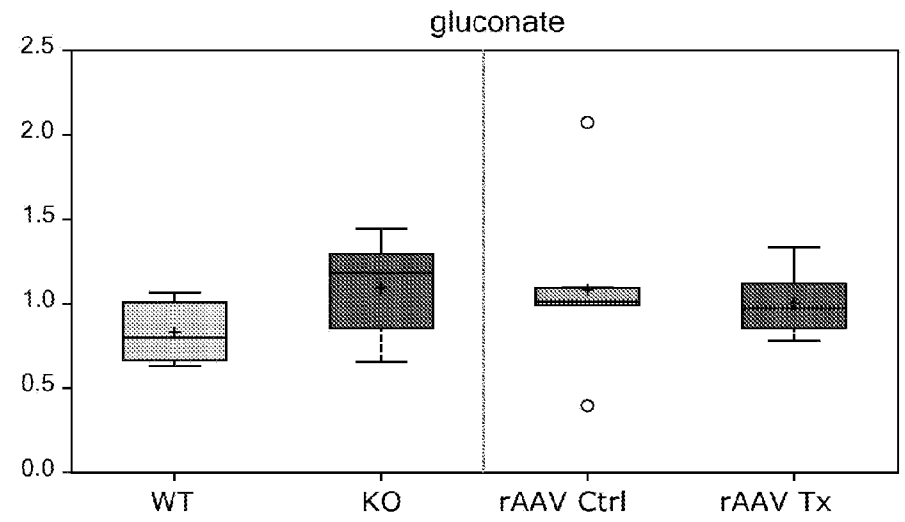
gluconate
2.5
2.0
1.5
1.0
0.5
0.0
WT
KO
rAAV Ctrl
rAAV Tx

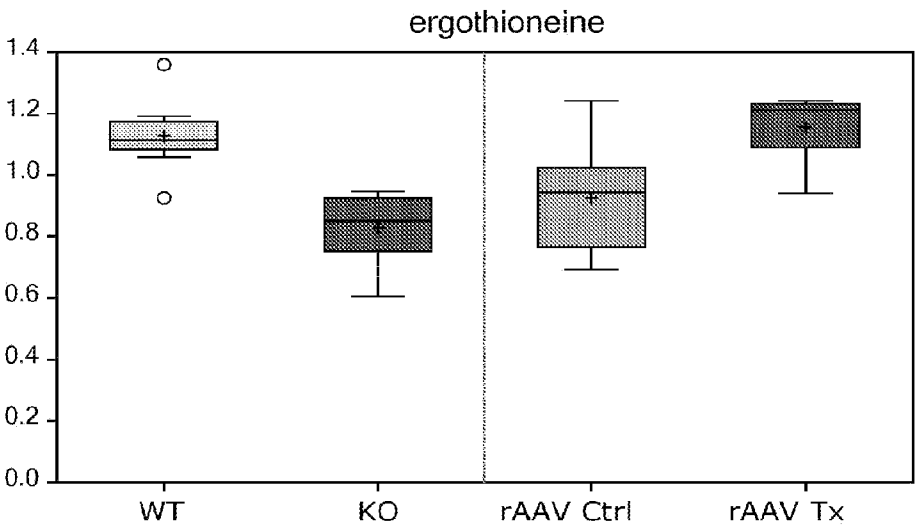
ergothioneine
1.4
1.2
1.0
0.8
0.6
0.4
0.2
0.0
WT
KO
rAAV Ctrl
rAAV Tx

FIG. 57 cont.

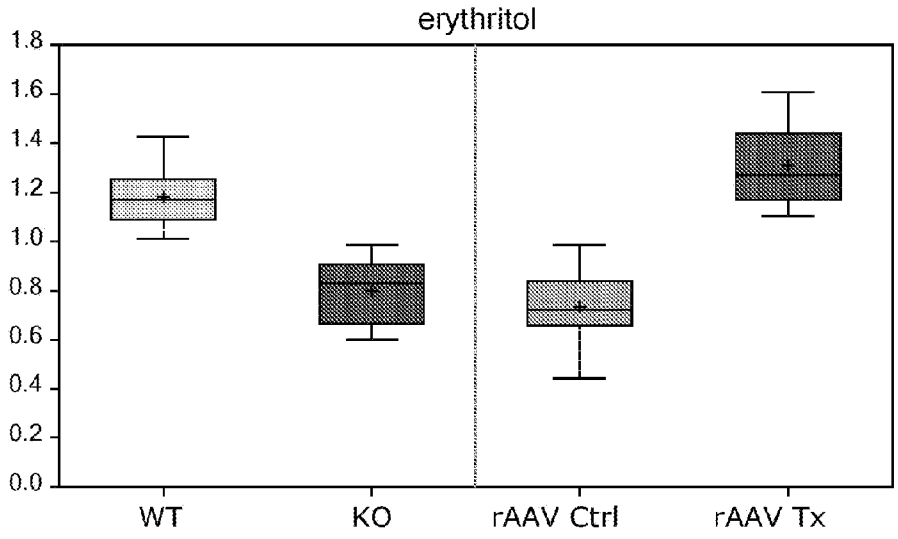
erythritol
1.8
1.6
1.4
1.2
1.0
0.8
0.6
0.4
0.2
0.0
WT
KO
rAAV Ctrl
rAAV Tx

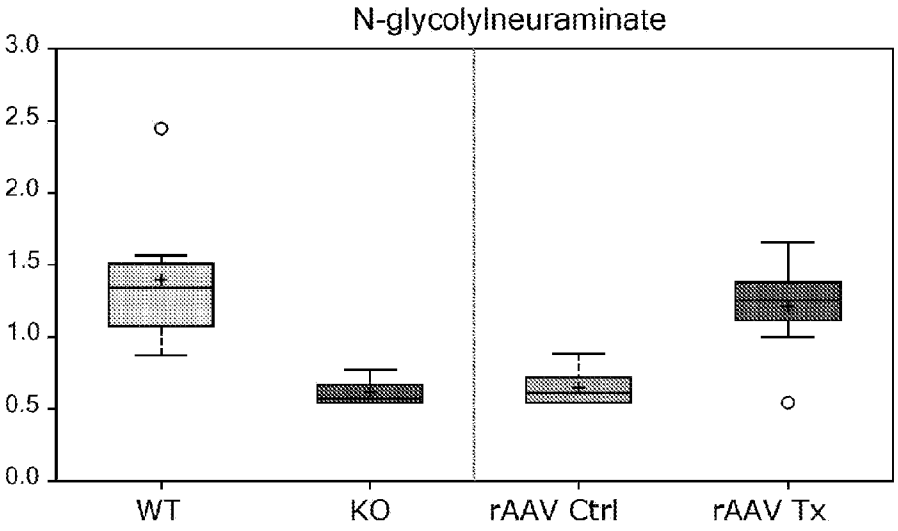
N-glycolylneuraminate
3.0
2.5
2.0
1.5
1.0
0.5
0.0
WT
KO
rAAV Ctrl
rAAV Tx

FIG. 57 cont.

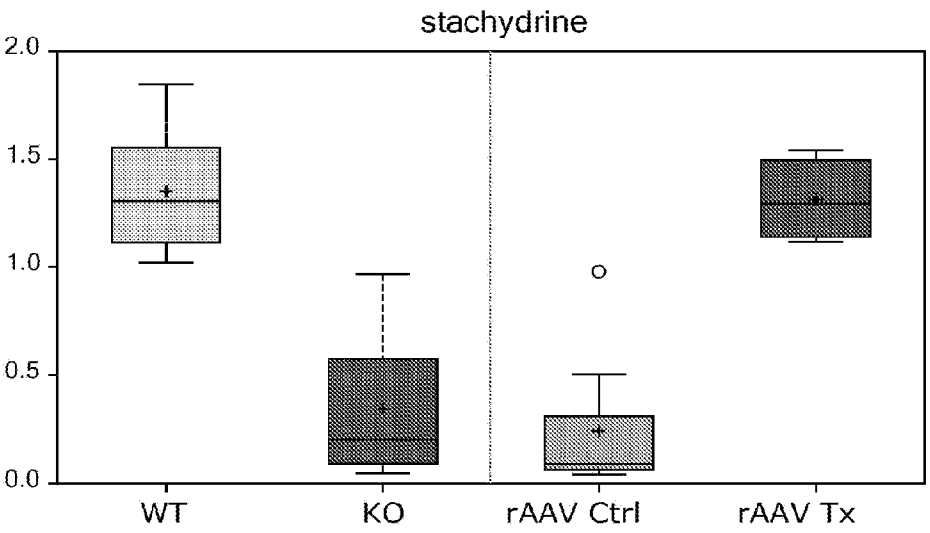
stachydrine
2.0
1.5
1.0
0.5
0.0
WT
KO
rAAV Ctrl
rAAV Tx

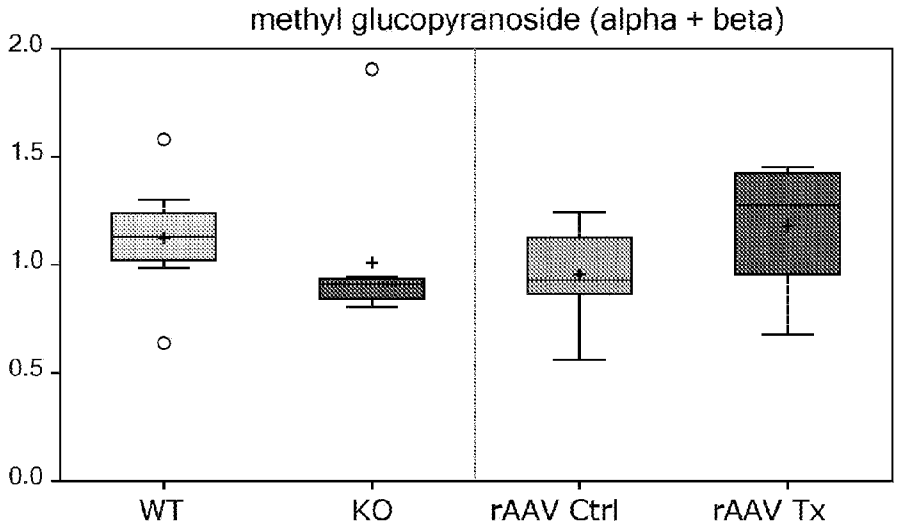
methyl glucopyranoside (alpha + beta)
2.0
1.5
1.0
0.5
0.0
WT
KO
rAAV Ctrl
rAAV Tx

FIG. 57 cont.

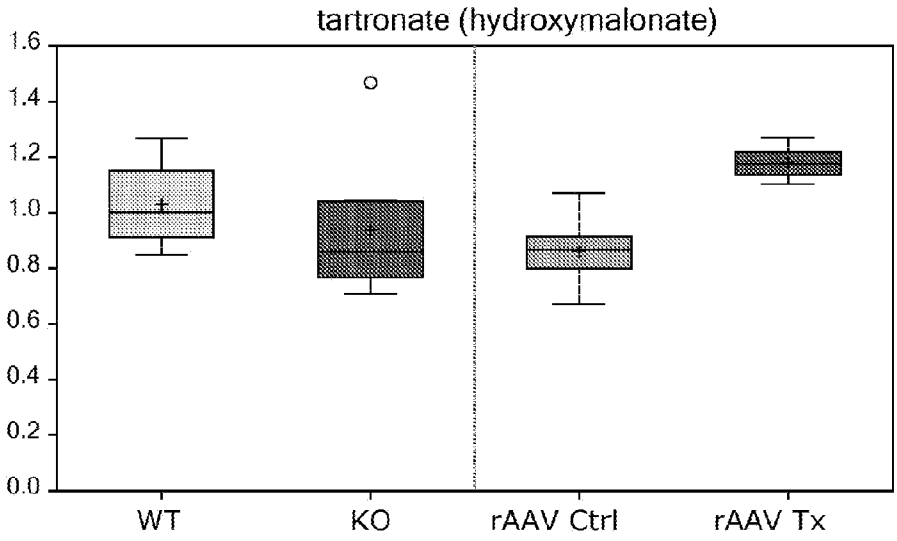
tartronate (hydroxymalonate)
1.6
1.4
1.2
1.0
0.8
0.6
0.4
0.2
0.0
WT
KO
rAAV Ctrl
rAAV Tx

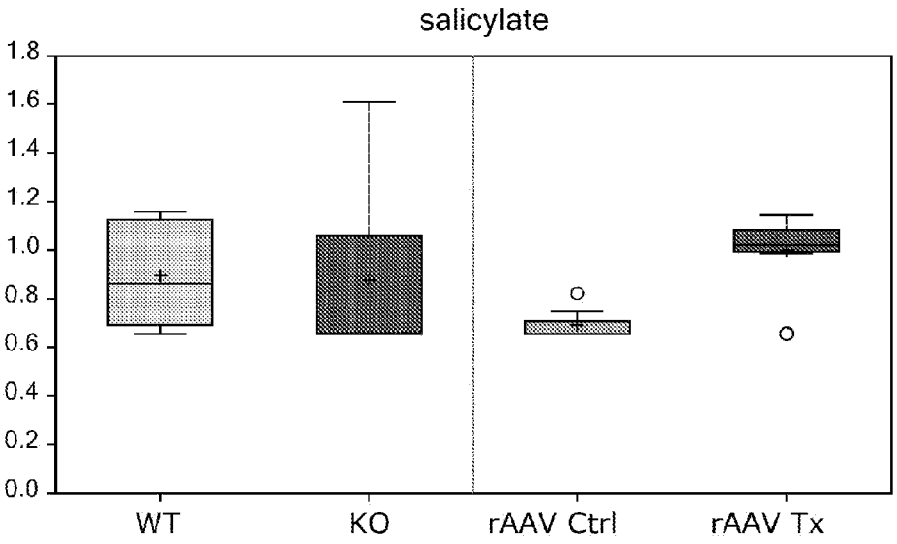
salicylate
1.8
1.6
1.4
1.2
1.0
0.8
0.6
0.4
0.2
0.0
WT
KO
rAAV Ctrl
rAAV Tx

FIG. 57 cont.

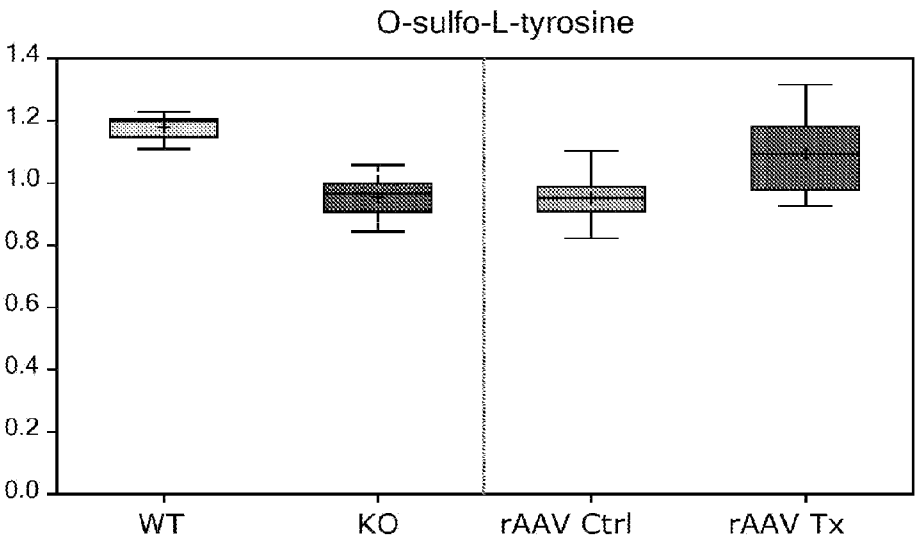
O-sulfo-L-tyrosine
1.4
1.2
1.0
0.8
0.6
0.4
0.2
0.0
WT
KO
rAAV Ctrl
rAAV Tx

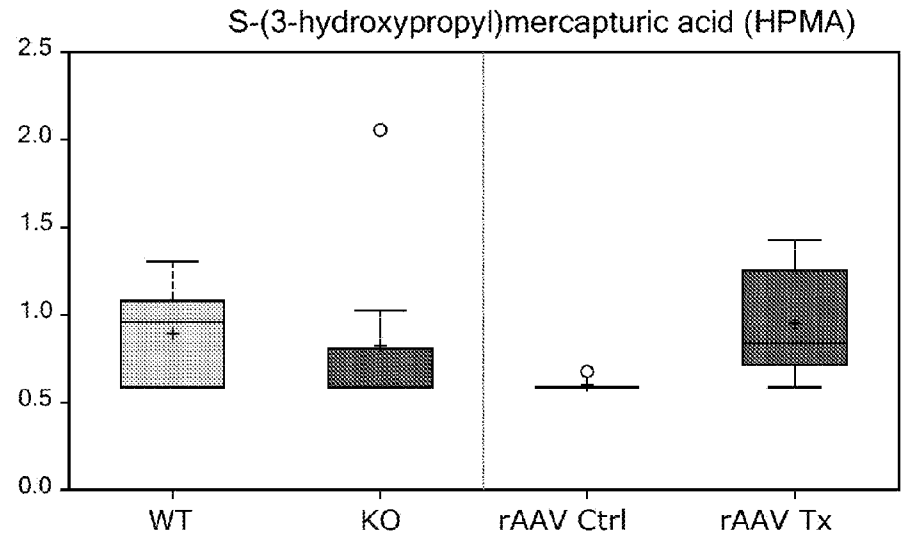
S-(3-hydroxypropyl)mercapturic acid (HPMA)
2.5
2.0
1.5
1.0
0.5
0.0
WT
KO
rAAV Ctrl
rAAV Tx

FIG. 57 cont.

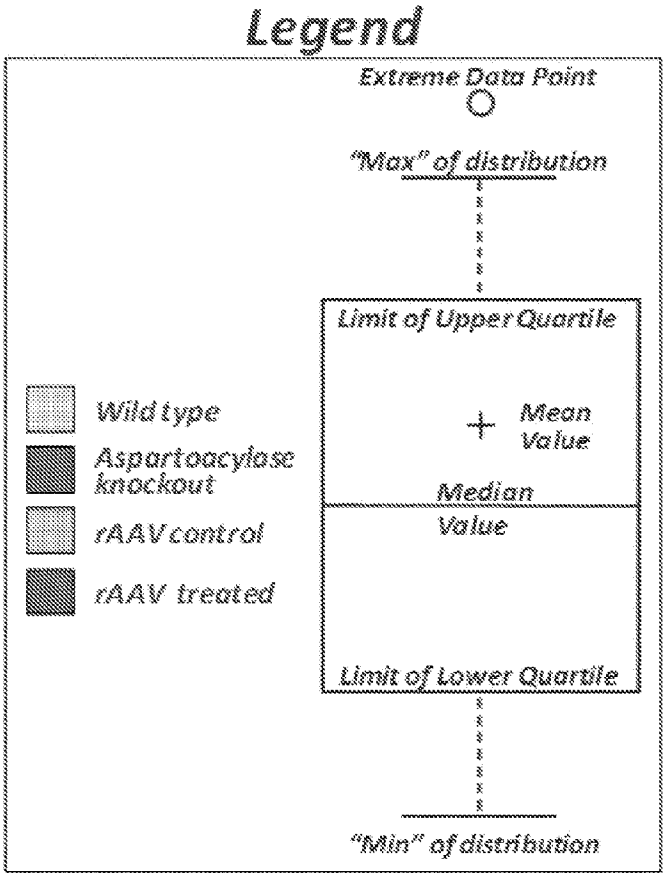
Legend
Extreme Data Point
"Max" of distribution
Limit of Upper Quartile
Mean Value
Median Value
Limit of Lower Quartile
"Min" of distribution
Wild type
Aspartoacylase knockout
rAAV control
rAAV treated

FIG. 57 cont.

SEKVENSLISTE

Sekvenslisten er udeladt af skriftet og kan hentes fra det Europæiske Patent Register.

The Sequence Listing was omitted from the document and can be downloaded from the European Patent Register.